frontiers | Research Topics

Research advances of tuberculosis vaccine and its implication on COVID-19

Edited by
Wenping Gong, Ashok Aspatwar, Jianping Xie and Hao Li

Published in
Frontiers in Immunology

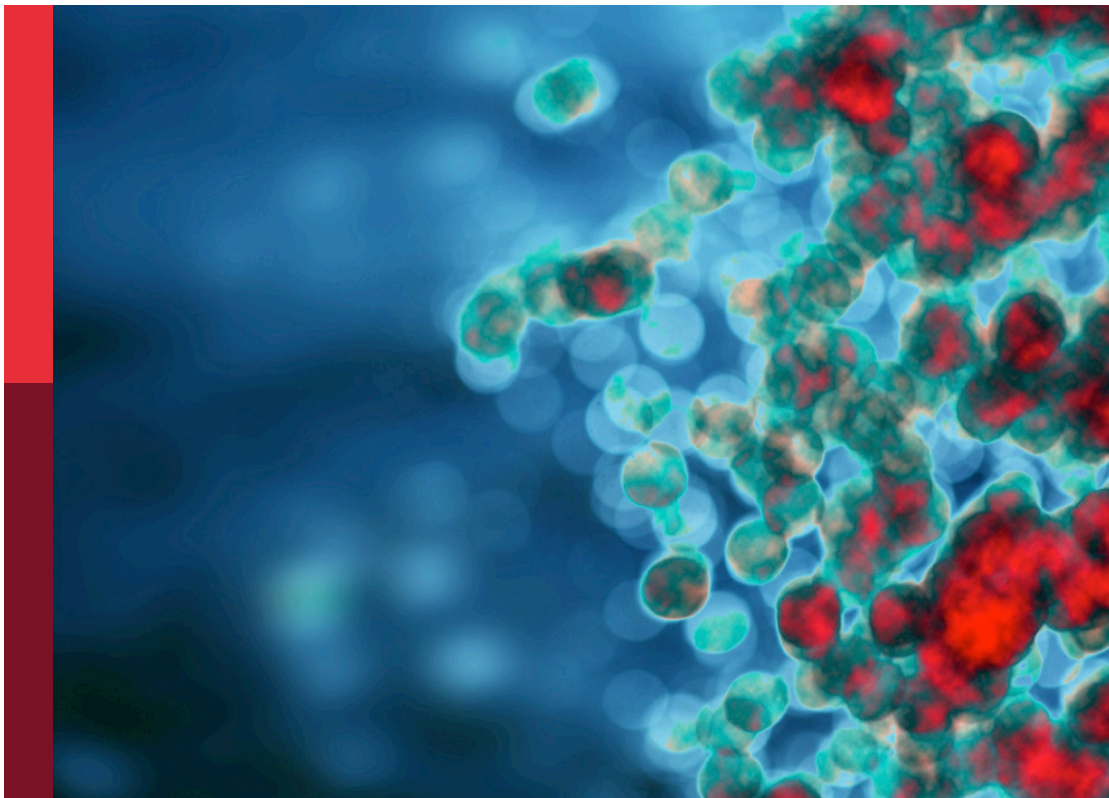

ISSN 1664-8714
ISBN 978-2-8325-5174-5
DOI 10.3389/978-2-8325-5174-5

About Frontiers

Frontiers is more than just an open access publisher of scholarly articles: it is a pioneering approach to the world of academia, radically improving the way scholarly research is managed. The grand vision of Frontiers is a world where all people have an equal opportunity to seek, share and generate knowledge. Frontiers provides immediate and permanent online open access to all its publications, but this alone is not enough to realize our grand goals.

Frontiers journal series

The Frontiers journal series is a multi-tier and interdisciplinary set of open-access, online journals, promising a paradigm shift from the current review, selection and dissemination processes in academic publishing. All Frontiers journals are driven by researchers for researchers; therefore, they constitute a service to the scholarly community. At the same time, the *Frontiers journal series* operates on a revolutionary invention, the tiered publishing system, initially addressing specific communities of scholars, and gradually climbing up to broader public understanding, thus serving the interests of the lay society, too.

Dedication to quality

Each Frontiers article is a landmark of the highest quality, thanks to genuinely collaborative interactions between authors and review editors, who include some of the world's best academicians. Research must be certified by peers before entering a stream of knowledge that may eventually reach the public - and shape society; therefore, Frontiers only applies the most rigorous and unbiased reviews. Frontiers revolutionizes research publishing by freely delivering the most outstanding research, evaluated with no bias from both the academic and social point of view. By applying the most advanced information technologies, Frontiers is catapulting scholarly publishing into a new generation.

What are Frontiers Research Topics?

Frontiers Research Topics are very popular trademarks of the *Frontiers journals series*: they are collections of at least ten articles, all centered on a particular subject. With their unique mix of varied contributions from Original Research to Review Articles, Frontiers Research Topics unify the most influential researchers, the latest key findings and historical advances in a hot research area.

Find out more on how to host your own Frontiers Research Topic or contribute to one as an author by contacting the Frontiers editorial office: frontiersin.org/about/contact

Research advances of tuberculosis vaccine and its implication on COVID-19

Topic editors

Wenping Gong — Senior Department of Tuberculosis, The 8th Medical Center of PLA General Hospital, China

Ashok Aspatwar — Tampere University, Finland

Jianping Xie — Southwest University, China

Hao Li — China Agricultural University, China

Citation

Gong, W., Aspatwar, A., Xie, J., Li, H., eds. (2024). *Research advances of tuberculosis vaccine and its implication on COVID-19*. Lausanne: Frontiers Media SA.

doi: 10.3389/978-2-8325-5174-5

Table of contents

05 Editorial: Research advances of tuberculosis vaccine and its implication on COVID-19
Wenping Gong, Jianping Xie, Hao Li and Ashok Aspatwar

08 Peptide-Based Vaccines for Tuberculosis
Wenping Gong, Chao Pan, Peng Cheng, Jie Wang, Guangyu Zhao and Xueqiong Wu

49 Efficacy and Safety of BCG Revaccination With *M. bovis* BCG Moscow to Prevent COVID-19 Infection in Health Care Workers: A Randomized Phase II Clinical Trial
Laura Raniere Borges dos Anjos, Adeliane Castro da Costa, Amanda da Rocha Oliveira Cardoso, Rafael Alves Guimarães, Roberta Luiza Rodrigues, Kaio Mota Ribeiro, Kellen Christina Malheiros Borges, Ana Carolina de Oliveira Carvalho, Carla Iré Schnier Dias, Aline de Oliveira Rezende, Carine de Castro Souza, Renato Rodney Mota Ferreira, Guylherme Saraiva, Lilia Cristina de Souza Barbosa, Tayro da Silva Vieira, Marcus Barreto Conte, Marcelo Fouad Rabahi, André Kipnis and Ana Paula Junqueira-Kipnis

67 Optimizing the Boosting Schedule of Subunit Vaccines Consisting of BCG and "Non-BCG" Antigens to Induce Long-Term Immune Memory
Wei Lv, Pu He, Yanlin Ma, Daquan Tan, Fei Li, Tao Xie, Jiangyuan Han, Juan Wang, Youjun Mi, Hongxia Niu and Bingdong Zhu

81 Immunotherapeutic Effects of Different Doses of *Mycobacterium tuberculosis ag85a/b* DNA Vaccine Delivered by Electroporation
Yan Liang, Lei Cui, Li Xiao, Xiao Liu, Yourong Yang, Yanbo Ling, Tong Wang, Lan Wang, Jie Wang and Xueqiong Wu

91 Research Advances for Virus-vectored Tuberculosis Vaccines and Latest Findings on Tuberculosis Vaccine Development
Zhidong Hu, Shui-Hua Lu, Douglas B. Lowrie and Xiao-Yong Fan

107 The Natural Effect of BCG Vaccination on COVID-19: The Debate Continues
Wenping Gong, Huiru An, Jie Wang, Peng Cheng and Yong Qi

114 Progressive Host-Directed Strategies to Potentiate BCG Vaccination Against Tuberculosis
Kriti Negi, Ashima Bhaskar and Ved Prakash Dwivedi

134 EST12 regulates Myc expression and enhances anti-mycobacterial inflammatory response *via* RACK1-JNK-AP1-Myc immune pathway
Jian Wu, Feng-Ling Luo, Yan Xie, Huan Xiong, Yadong Gao, Guanghui Liu and Xiao-Lian Zhang

152 Cyclic di-AMP as endogenous adjuvant enhanced BCG-induced trained immunity and protection against *Mycobacterium tuberculosis* in mice

Huanhuan Ning, Jian Kang, Yanzhi Lu, Xuan Liang, Jie Zhou, Rui Ren, Shan Zhou, Yong Zhao, Yanling Xie, Lu Bai, Linna Zhang, Yali Kang, Xiaojing Gao, Mingze Xu, Yanling Ma, Fanglin Zhang and Yinlan Bai

170 Recombinant BCG expressing the LTAK63 adjuvant improves a short-term chemotherapy schedule in the control of tuberculosis in mice

Monalisa Martins Trentini, Alex Issamu Kanno, Dunia Rodriguez, Lazaro Moreira Marques-Neto, Silas Fernandes Eto, Ana Marisa Chudzinki-Tavassi and Luciana Cezar de Cerqueira Leite

182 B21 DNA vaccine expressing ag85b, rv2029c, and rv1738 confers a robust therapeutic effect against latent *Mycobacterium tuberculosis* infection

Shufeng Weng, Jinyi Zhang, Huixia Ma, Jingyu Zhou, Liqiu Jia, Yanmin Wan, Peng Cui, Qiaoling Ruan, Lingyun Shao, Jing Wu, Honghai Wang, Wenhong Zhang and Ying Xu

195 Pam2CSK4-adjuvanted SARS-CoV-2 RBD nanoparticle vaccine induces robust humoral and cellular immune responses

Yidan Qiao, Yikang Zhan, Yongli Zhang, Jieyi Deng, Achun Chen, Bingfeng Liu, Yiwen Zhang, Ting Pan, Wangjian Zhang, Hui Zhang and Xin He

frontiers | Frontiers in Immunology

TYPE Editorial
PUBLISHED 09 February 2023
DOI 10.3389/fimmu.2023.1147704

OPEN ACCESS

EDITED AND REVIEWED BY
Denise L. Doolan,
James Cook University, Australia

*CORRESPONDENCE
Wenping Gong
gwp891015@whu.edu.cn

SPECIALTY SECTION
This article was submitted to Vaccines and Molecular Therapeutics, a section of the journal Frontiers in Immunology

RECEIVED 19 January 2023
ACCEPTED 26 January 2023
PUBLISHED 09 February 2023

CITATION
Gong W, Xie J, Li H and Aspatwar A (2023) Editorial: Research advances of tuberculosis vaccine and its implication on COVID-19. *Front. Immunol.* 14:1147704. doi: 10.3389/fimmu.2023.1147704

Editorial: Research advances of tuberculosis vaccine and its implication on COVID-19

Wenping Gong[1]*, Jianping Xie[2], Hao Li[3] and Ashok Aspatwar[4]

[1]Tuberculosis Prevention and Control Key Laboratory/Beijing Key Laboratory of New Techniques of Tuberculosis Diagnosis and Treatment, Senior Department of Tuberculosis, The 8Medical Center of PLA General Hospital, Beijing, China, [2]Institute of Modern Biopharmaceuticals, State Key Laboratory Breeding Base of Eco-Environment and Bio-Resource of the Three Gorges Area, Key Laboratory of Eco-environments in Three Gorges Reservoir Region, Ministry of Education, School of Life Sciences, Southwest University, Chongqing, China, [3]College of Veterinary Medicine, China Agricultural University, Beijing, China, [4]Faculty of Medicine and Health Technology, Tampere University, Tampere, Finland

KEYWORDS

***Mycobacterium tuberculosis*, vaccine, immune response, peptide, mechanism**

Editorial on the Research Topic:
Research advances of tuberculosis vaccine and its implication on COVID-19

Introduction

Tuberculosis (TB) caused by *Mycobacterium tuberculosis* (*M. tuberculosis*) remains a global public health threat. As an aged disease, TB remains the leading cause of human death in 2021 from a single pathogen (https://www.who.int/news-room/fact-sheets/detail/tuberculosis). However, it is reported that the protective efficacy of BCG is highly variable and ranges between 0% and 80%, and its protection lasts only for 10 to 15 years (1). Therefore, developing a new effective TB vaccine is pressing and challenging for governments and scientists to end TB. Against this background, we launched a Research Topic in Frontiers in Immunology entitled "Research Advances of Tuberculosis Vaccine and its Implication on COVID-19". This Research Topic published high-quality research articles that provide insight into the innate and adaptive immune responses during *M. tuberculosis* infection, trained immunity and protective efficacy induced by BCG or recombinant BCG (rBCG) vaccine, the potential role of the BCG vaccine on the prevention of COVID-19, and the latest progress of novel TB vaccines.

BCG: Old tree sprouts new buds

Although BCG vaccination can effectively protect infants and young children from *M. tuberculosis* infection, especially in the prevention of severe TB diseases such as disseminated tuberculosis and tuberculous meningitis (TBM), its efficacy in adult pulmonary tuberculosis (PTB) is not satisfactory (2, 3). In recent years, with the rapid development of molecular biology, it has become possible to improve the efficacy of BCG by genetic modification. Recombinant BCG (rBCG) strains are developed by expressing foreign antigens, human cytokines, and pro-apoptotic factors. In this Research Topic, two studies developed new rBCG strains and investigated their efficacy in animal models. Based on previous findings that

a recombinant BCG expressing the LTAK63 adjuvant (rBCG-LTAK63) can protect mice from *M. tuberculosis* infection based on increased early and long-term immune responses (4, 5), Trentini et al. evaluated the effect of rBCG-LTAK63 in the treatment of mice infected by *M. tuberculosis*. They found that both the bacterial burden and the area of inflammation in the lungs of mice treated with rBCG-LTAK63 were less than those of the BCG control group. Similarly, Ning et al. further evaluated the protection efficiency of the rBCG-DisA vaccine in mice infected with *M. tuberculosis*. Their data demonstrated that the rBCG-DisA vaccine induced robust trained and adaptive immunities and showed an excellent performance in the prime-boost strategy against *M. tuberculosis* infection in mice. Currently, three rBCG vaccines (VPM1002, rBCG30, and AERAS-422) have been evaluated in clinical trials, but the rBCG30 and AERAS-422 trials were stopped due to safety concerns (6, 7). Therefore, attention must be paid to the safety of the rBCG vaccine when designing a novel rBCG strain.

In addition to improving the BCG strains by genetic engineering, BCG's prime-boost strategy is also a rational way to develop new TB vaccines. Lv et al. primed C57BL/6 mice with BCG followed by two or three booster immunizations with MH (Mtb10.4-HspX) or EC (ESAT6-CFP10) subunit vaccine. The results showed that two booster doses of MH at 12 and 24 weeks or three booster doses of EC at 12, 16, and 24 weeks after BCG primary immunization could induce significantly high levels of long-term memory T cells and improve the protective efficiency of the subunit vaccines. Negi et al. reviewed progress in BCG vaccination programs, including BCG vaccination in children and potential strategies to enhance BCG-induced protection in adults.

BCG and COVID-19: More evidence is needed

Trained immunity is defined as the ability of innate immune cells to generate heterologous memory in response to specific exogenous exposures (8). Previous ecological, analytical, and animal studies demonstrate that the trained immunity induced by the BCG vaccine might protect against infections of various respiratory pathogens other than *M. tuberculosis*, including SARS-CoV-2 (9). In this Research Topic, Anjos et al. conducted a randomized Phase II clinical trial to evaluate the efficacy and safety of BCG to prevent SARS-CoV-2 infection in health care workers. They found that revaccination with BCG produced using Moscow strain was safe and resulted in a lower, but not statistically significant, incidence of COVID-19 positivity. Furthermore, Gong et al. published an opinion article to discuss the natural effect of BCG vaccination on COVID-19. They discussed the non-specific immune response induced by the BCG, analyzed early findings from the ecological and analytical studies, and pointed out that the heterogeneity of these findings might originate from some confounding factors. In addition to exploring the potential roles of BCG vaccine in the prevention and controlling of COVID-19, a study has evaluated the role of a TLR2/6 agonist, Pam2CSK4, in COVID-19 vaccine (Qiao et al.). Qiao et al. used Pam2CSK4 to enhance the immune responses induced by a nanoparticle vaccine against COVID-19, they found that with the help of TLR2/6 agonist Pam2CSK4, the nanoparticle vaccine could induce a significantly higher levels of antigen-specific neutralizing antibodies and Th1-biased immune response by upregulating genes involved in the migration, activation, and proliferation of leukocytes. These results suggest that Pam2CSK4 might be a promising adjuvant for the nanoparticle vaccine, which highlights a new tool to enhance the immunogenicity of TB vaccines.

New TB vaccines: A potential new force to end TB

The growing evidence indicate that humoral immune responses play important roles against *M. tuberculosis* infection, which suggests that the humoral responses as well as the cellular immune responses elicited by the vaccines shall be factored into new vaccines design (3, 10–12). Wu et al. found a secreted Rv1579c (EST12) protein from the *M. tuberculosis* region of deletion 3 (RD3) could promote Myc binding to the promoters of IL-6 and TNF-α cytokines, nitric oxide (NO), and inducible nitric oxide synthase (iNOS) *via* activating JNK-AP1-Myc signaling pathway, which facilitates host clearance of *M. tuberculosis*. This study provides new insight into the mechanism of interaction between *M. tuberculosis* and the host, as well as potential target for developing new TB vaccines.

A viral vector is a newly discovered vaccine vector that relies on molecular biology techniques to integrate the gene of the target antigen of *M. tuberculosis* into its genome and deliver it to the host cell for expression of the target antigen to induce an immune response (13). Hu et al. reviewed the research progress of virus-vectored TB vaccines, especially those that have been in clinical trials and those that are still in preclinical research stage but most promising, they also provided an update on the latest tools and concepts that facilitate TB vaccine research and development.

Furthermore, DNA vaccines against TB have been investigated in this Research Topic. Liang et al. constructed an *M. tuberculosis ag85a/b* chimeric DNA vaccine and evaluated and compared its immunotherapeutic effects under different immunization doses and routes. They demonstrated that the *ag85a/b* chimeric DNA vaccine killed *M. tuberculosis* and eliminated by inducing a Th1-type cellular immune response. Weng et al. constructed four DNA vaccines (A39, B37, B31, and B21) and found that the B21 DNA vaccine could induce effector memory and central memory T cells and produce the strongest Th1/Th17 and $CD8^+$ cytotoxic T lymphocyte responses to reduce mycobacterial loads in the mice with latent *M. tuberculosis* infection (LTBI), suggesting that the B21 DNA vaccine can enhance T cell responses and control the LTBI infection.

Different from the above vaccines, peptide-based TB vaccines have emerged based on the rapidly developing bioinformatics and immunoinformatics technologies in recent years. Gong et al. provided the first detailed and comprehensive review of the peptide-based TB vaccine. They summarized the development of bioinformatics tools used in the identification of potential antigens of *M. tuberculosis*, prediction of T cell and B cell epitopes, analysis of epitope immunogenicity, antigenicity, allergenicity, and toxicity, and construction of peptide-based vaccines.

Where to go: Challenges and opportunities

Since the only TB vaccine, BCG, was developed more than a hundred years ago, no new TB vaccine has been approved for use to prevent and control TB. Although 14 TB vaccines have entered the clinical trial stage, the final protection efficiency of the highly anticipated M72/AS01$_E$ vaccine after 36 months of follow-up is only 49.7% (14), which makes the research of TB vaccine enter the darkest moment. A better understanding of the pathogenic mechanism of *M. tuberculosis* and the host's immune protection mechanism would help solve the current stagnation of TB vaccine development. To overcome these difficulties, future research should focus on the following aspects: 1) Novel discovery and theory on the pathogenic mechanism of *M. tuberculosis* and the immune protection mechanism of the host; 2) The trained immunity induced by BCG vaccine and the rBCG vaccine development; 3) Protective immune responses induced by the immunotherapeutic vaccines; 4) Novel TB vaccines and their protective mechanisms in pre-clinical and clinical studies, especially the vaccines based on new technologies or antigens; 5) New technologies such as bioinformatics, immunoinformatics, and reverse vaccinology in the design and construction of novel TB vaccines; 6) Animal models that more accurately predict the heterogeneity of the immune response against *M. tuberculosis* in humans; 7) Vaccine immunization strategies, such as adjuvants, immunization routes, doses, and times; 8) Therapeutic vaccines to prevent relapse following cure or adjunctive treatment of TB and passive immunization such as antibodies directed against *M. tuberculosis* antigens.

In summary, the collection of papers published in this Research Topic (Volume 1) demonstrates the current status of the research and development in the areas of TB vaccines. In the second volume, we will continue to focus on the above eight future research directions, showcase the achievements of TB vaccine research and the latest immunization strategies from different perspectives, and contribute to the vision of ending TB by 2035 formulated by the WHO.

Author contributions

All authors listed have made a substantial, direct, and intellectual contribution to the work and approved it for publication.

Funding

This study was funded by the Beijing Municipal Science & Technology Commission (Grant No. 7212103 and L192065), the National Natural Science Foundation of China (Grant No. 81801643, and No. 32070937), and the National key research and development program of China (grant number 2022YFA1303500-003), Finnish Cultural Foundation, and Tampere Tuberculosis Foundation (AA)

Conflict of interest

The authors declare that the research was conducted in the absence of any commercial or financial relationships that could be construed as a potential conflict of interest.

Publisher's note

References

1. Andersen P, Doherty TM. The success and failure of BCG - implications for a novel tuberculosis vaccine. *Nat Rev Microbiol* (2005) 3:656–62. doi: 10.1038/nrmicro1211

2. Gong W, Liang Y, Wu X. The current status, challenges, and future developments of new tuberculosis vaccines. *Hum Vaccin Immunother* (2018) 14:1697–716. doi: 10.1080/21645515.2018.1458806

3. Qu M, Zhou X, Li H. BCG Vaccination strategies against tuberculosis: updates and perspectives. *Hum Vaccin Immunother* (2021) 17:5284–95. doi: 10.1080/21645515.2021.2007711

4. Nascimento IP, Rodriguez D, Santos CC, Amaral EP, Rofatto HK, Junqueira-Kipnis AP, et al. Recombinant BCG expressing LTAK63 adjuvant induces superior protection against mycobacterium tuberculosis. *Sci Rep* (2017) 7:2109. doi: 10.1038/s41598-017-02003-9

5. Carvalho Dos Santos C, Rodriguez D, Kanno Issamu A, Cezar De Cerqueira Leite L, Pereira Nascimento I. Recombinant BCG expressing the LTAK63 adjuvant induces increased early and long-term immune responses against mycobacteria. *Hum Vaccin Immunother* (2020) 16:673–83. doi: 10.1080/21645515.2019.1669414

6. Da CA, Nogueira SV, Kipnis A, Junqueirakipnis AP. Recombinant BCG: Innovations on an old vaccine. scope of BCG strains and strategies to improve long-lasting memory. *Front Immunol* (2014) 5:152. doi: 10.3389/fimmu.2014.00152

7. Hoft DF, Blazevic A, Selimovic A, Turan A, Tennant J, Abate G, et al. Safety and immunogenicity of the recombinant BCG vaccine AERAS-422 in healthy BCG-naive adults: A randomized, active-controlled, first-in-human phase 1 trial. *EBioMedicine* (2016) 7:278–86. doi: 10.1016/j.ebiom.2016.04.010

8. Bannister S, Kim B, Domínguez-Andrés J, Kilic G, Ansell BRE, Neeland MR, et al. Neonatal BCG vaccination is associated with a long-term DNA methylation signature in circulating monocytes. *Sci Adv* (2022) 8:eabn4002. doi: 10.1126/sciadv.abn4002

9. Gong W, Mao Y, Li Y, Qi Y. BCG Vaccination: A potential tool against COVID-19 and COVID-19-like black swan incidents. *Int Immunopharmacol* (2022) 108:108870. doi: 10.1016/j.intimp.2022.108870

10. Li H, Javid B. Antibodies and tuberculosis: Finally coming of age? *Nat Rev Immunol* (2018) 18:591–6. doi: 10.1038/s41577-018-0028-0

11. Li H, Wang XX, Wang B, Fu L, Liu G, Lu Y, et al. Latently and uninfected healthcare workers exposed to TB make protective antibodies against mycobacterium tuberculosis. *Proc Natl Acad Sci USA* (2017) 114:5023–8. doi: 10.1073/pnas.1611776114

12. Watson A, Li H, Ma B, Weiss R, Bendayan D, Abramovitz L, et al. Human antibodies targeting a mycobacterium transporter protein mediate protection against tuberculosis. *Nat Commun* (2021) 12:602. doi: 10.1038/s41467-021-20930-0

13. McCann N, O'Connor D, Lambe T, Pollard AJ. Viral vector vaccines. *Curr Opin Immunol* (2022) 77:102210. doi: 10.1016/j.coi.2022.102210

14. Tait DR, Hatherill M, van der Meeren O, Ginsberg AM, Van Brakel E, Salaun B, et al. Final analysis of a trial of M72/AS01(E) vaccine to prevent tuberculosis. *N Engl J Med* (2019) 381:2429–39. doi: 10.1056/NEJMoa1909953

frontiers in Immunology

REVIEW
published: 31 January 2022
doi: 10.3389/fimmu.2022.830497

Peptide-Based Vaccines for Tuberculosis

Wenping Gong[1†], Chao Pan[2†], Peng Cheng[1,3], Jie Wang[1], Guangyu Zhao[4] and Xueqiong Wu[1*]*

[1] Tuberculosis Prevention and Control Key Laboratory/Beijing Key Laboratory of New Techniques of Tuberculosis Diagnosis and Treatment, Senior Department of Tuberculosis, The 8th Medical Center of PLA General Hospital, Beijing, China, [2] State Key Laboratory of Pathogen and Biosecurity, Beijing Institute of Biotechnology, Beijing, China, [3] Hebei North University, Zhangjiakou City, China, [4] State Key Laboratory of Pathogen and Biosecurity, Beijing Institute of Microbiology and Epidemiology, Beijing, China

Tuberculosis (TB) is an infectious disease caused by *Mycobacterium tuberculosis*. As a result of the coronavirus disease 2019 (COVID-19) pandemic, the global TB mortality rate in 2020 is rising, making TB prevention and control more challenging. Vaccination has been considered the best approach to reduce the TB burden. Unfortunately, BCG, the only TB vaccine currently approved for use, offers some protection against childhood TB but is less effective in adults. Therefore, it is urgent to develop new TB vaccines that are more effective than BCG. Accumulating data indicated that peptides or epitopes play essential roles in bridging innate and adaptive immunity and triggering adaptive immunity. Furthermore, innovations in bioinformatics, immunoinformatics, synthetic technologies, new materials, and transgenic animal models have put wings on the research of peptide-based vaccines for TB. Hence, this review seeks to give an overview of current tools that can be used to design a peptide-based vaccine, the research status of peptide-based vaccines for TB, protein-based bacterial vaccine delivery systems, and animal models for the peptide-based vaccines. These explorations will provide approaches and strategies for developing safer and more effective peptide-based vaccines and contribute to achieving the WHO's End TB Strategy.

Keywords: tuberculosis (TB), peptide-based vaccine, epitope, bioinformatics, immunity, adjuvants, animal models

OPEN ACCESS

Edited by:
Stephanie Yanow, University of Alberta, Canada

Reviewed by:
Ved Prakash Dwivedi, International Centre for Genetic Engineering and Biotechnology, India
Sandeep Kumar Dhanda, St. Jude Children's Research Hospital, United States

***Correspondence:**
Xueqiong Wu
xueqiongwu@139.com
Guangyu Zhao
guangyu0525@163.com

[†]These authors have contributed equally to this work

Specialty section:
This article was submitted to Vaccines and Molecular Therapeutics, a section of the journal Frontiers in Immunology

Received: *07 December 2021*
Accepted: *10 January 2022*
Published: *31 January 2022*

Citation:
Gong W, Pan C, Cheng P, Wang J, Zhao G and Wu X (2022) Peptide-Based Vaccines for Tuberculosis. Front. Immunol. 13:830497. doi: 10.3389/fimmu.2022.830497

1 INTRODUCTION

As an ancient infectious disease, tuberculosis (TB) has followed the footsteps of humanity for thousands of years (1, 2). *Mycobacterium tuberculosis* is the pathogen that causes TB. The war between humans and *M. tuberculosis* has never stopped from ancient times to modern society. Even today, TB remains a serious health threat. It has been reported that there were almost 1.3 million TB deaths among the human immunodeficiency virus (HIV) negative population in 2020 globally, up from 1.2 million in 2019 (3). These data indicated that the coronavirus disease 2019 (COVID-19) pandemic had disturbed years of global progress in reducing TB deaths, pushing the total number of TB deaths in 2020 back to the 2017 level (3). Furthermore, the emergence of drug-resistant and multidrug-resistant TB (MDR-TB) and the lack of effective methods for differential diagnosis of latent TB infection (LTBI) pose many challenges to TB prevention and treatment (4, 5).

Vaccination is the most effective way to control TB. The only licensed TB vaccine is Bacille Calmette-Guérin (BCG), which has been used for more than 100 years (6, 7). Previous studies have reported that BCG can protect children from severe TB and miliary TB. Therefore, BCG has been recommended by the World Health Organization (WHO) for widespread use in childhood immunization programmes in 154 countries in 2020 (3). However, a growing number of studies have reported that BCG is protective for only 10 - 20 years (8). This may be the reason why the defensive efficiency of BCG in adult pulmonary TB ranges from 0% to 80% (1, 9). According to the report released by WHO, there are 14 TB vaccine candidates in clinical trials, including AEC/BC02, Ad5 Ag85A, and ChAdOx185A-MVA85A vaccines in Phase I, MTBVAC, ID93 + GLA-SE, TB/FLU-04L, and GamTBvac vaccines in Phase IIa, DAR-901 booster, H56: IC31, M72/AS01$_E$, BCG revaccination, and RUTI® vaccines in Phase IIb, VPM1002 and MIP/Immuvac vaccines in Phase III (10). These TB novel vaccines can be divided into four categories: Viral vector vaccines, subunit vaccines, attenuated live mycobacterial vaccines, and inactivated vaccines (10). The most promising of these vaccines is M72/AS01$_E$. It has been reported that the M72/AS01$_E$ vaccine had good protection in healthy adults (11, 12), HIV infected adults in Switzerland (13), and healthy infants in Gambia (14). Consequently, M72 has been selected for further vaccine development. In 2018, a Phase IIb controlled trial of the M72/AS01$_E$ vaccine showed that the protective efficacy of the vaccine against active pulmonary TB in adults was 54.0%, and there was no obvious safety problem (15). One year later, after three years of follow-up, the New England journal of medicine (NEJM) published the final results of this Phase IIb clinical trial of the M72/AS01$_E$ vaccine. It was found that the total effectiveness was 49.7% after 36 months of follow-up, and the evaluation of vaccine efficacy increased throughout the study period, with vaccine effectiveness of 27.4% in the first year, 55.2% in the second year and 60.2% in the third year (16). However, it needs to be recognized that even if M72/AS01$_E$ vaccine is proven to be reliable in larger populations, TB control cannot be based on the M72/AS01$_E$ vaccine alone. We should develop more effective and safer vaccines to prevent and control TB.

The biggest obstacle to developing a TB vaccine is the lack of understanding of the pathogenesis of *M. tuberculosis* and host immune protective mechanism. The innate and adaptive immunity of the host plays a vital role in the elimination or killing of *M. tuberculosis* (**Figure 1**). Innate immune cells, such as macrophages, dendritic cells (DCs), and natural killer (NK) cells, are the front-line to resist *M. tuberculosis* invasion. As the most important antigen presenting cells (APCs), macrophages and DCs play an essential role in phagocytosing *M. tuberculosis*. DCs activated by *M. tuberculosis* migrate to lymph nodes to display peptides of mycobacteria on their surface, which will be recognized by CD4$^+$ T cells and CD8$^+$ T cells through major histocompatibility complex (MHC) II and MHC I molecules, respectively (5, 17). Interestingly, the recognition between T cells and APCs is based on peptides rather than full-length protein (**Figure 1**). Therefore, the selection of vaccine candidate antigens and the prediction and screening of these immunodominant peptides are the key to designing a new generation of TB vaccine, known as peptide-

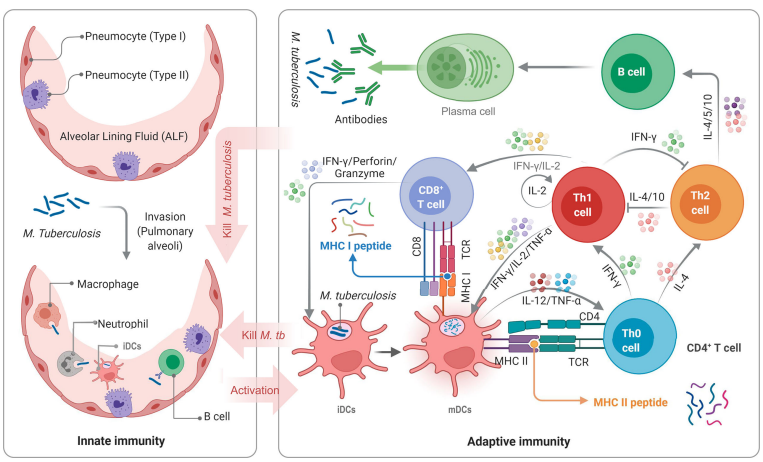

FIGURE 1 | Schematic diagram of TB infection and anti-TB immunity of the host. APCs, such as DCs, macrophages, neutrophils, and even B cells, not only play the role of innate immune cells but also serve as a bridge between innate and adaptive immunity. DCs are the most important APCs, and their antigen presenting ability *in vitro* is 10-100 times that of other APCs. *M. tuberculosis* bacilli invading host's pulmonary alveoli are first recognized and swallowed by APCs. Then, immature dendritic cells (iDCs) take up *M. tuberculosis* antigens and migrate to lymph nodes. During this process, the expression of MHC molecules on the surface is up-regulated, the antigen presentation function and the ability to activate T cells are also enhanced, and iDCs are transformed into mature dendritic cells (mDCs). mDCs can secrete interleukin-12 (IL-12), tumor necrosis factor-α (TNF-α), and interferon-α (IFN-α) to act on native CD4$^+$ T cells (Th0 cells) to differentiate into Th1 cells. IFN-γ, IL-2, and TNF-α produced by Th1 cells can effectively activate CD8$^+$ T cells and macrophages to eliminate intracellular *M. tuberculosis* by perforin, granzyme, reactive oxygen, and reactive nitrogen. Furthermore, mDCs produce IL-4, making Th0 cells differentiate into Th2 cells. The function of the Th2 response and IL-4 in the anti-tuberculosis immune response remains unclear. It is generally believed that Th2 cells will affect B lymphocytes by secreting IL-4, IL-5, and IL-10, mediating humoral immune response.

based vaccine. The most significant advantage of peptide-based vaccines is the aggregation of immunodominant epitopes, which improves the immunogenicity of the vaccine and reduces its side effects (2).

This study reviewed the latest bioinformatics tools, linkers, and adjuvants used in designing peptide-based vaccines, the research status of peptide-based vaccines for TB, the protein-based bacterial vaccine delivery system, and animal models for peptide-based vaccines. To our knowledge, this is the first detailed and comprehensive review to report peptide-based vaccines for TB. We hope that through this review, we can provide practical tools and methods for designing peptide-based vaccines and contribute new ideas to developing novel TB vaccines.

2 THE DEVELOPMENT OF BIOINFORMATICS TECHNOLOGY HAS LAID THE FOUNDATION FOR THE RISE OF PEPTIDE-BASED VACCINES FOR TB

The rapid development of bioinformatics technology makes it possible to predict and design a peptide-based vaccine with computers in advance. Compared with conditional vaccines, peptide-based vaccines have many advantages: more straightforward and faster production, more stable and convenient transportation and storage, lower cost, and decreased side effects (18). Despite these benefits of peptide-based vaccines, the following tasks must be done to design a peptide-based vaccine successfully: identification of potential antigens, prediction of T cell and B cell epitopes, analysis of epitope immunogenicity, antigenicity, allergenicity, and toxicity, selection of linkers and adjuvant peptides, construction and optimization of final vaccine, and analysis of the characteristics of the final vaccines. A list of databases or servers used to construct a peptide-based vaccine has been shown in **Table 1**.

2.1 Epitope Prediction

2.1.1 Determination of Protective Antigens and the Coverage of MHC Alleles

Before predicting T cell or B cell epitopes, it is necessary to determine the protective antigens for vaccine construction and the coverage of MHC alleles in specific populations. Protective antigens should be selected from previous studies, and these antigens must have been proven to have significantly higher protective efficacy in animal models or clinical trials. Amino acid sequences of protective antigens can be obtained from National Center of Biotechnology Information (NCBI, https://www.ncbi.nlm.nih.gov/protein), Target-Pathogen database (http://target.sbg.qb.fcen.uba.ar/patho), Uniprot protein database (https://beta.uniprot.org/), and GeneDB database (http://www.genedb.org/Homepage) (19, 21–23).

Fortunately, with the rapid development of bioinformatics technology, a growing number of TB specific databases or servers have been developed for TB vaccine construction, such as Mycobrowser (20), MtbVeb (24), MycobacRV (26), and PeMtb (25). These novel tools provide powerful support for designing peptide-based vaccines for TB. Mycobrowser (https://mycobrowser.epfl.ch/) is a comprehensive genomic and proteomic database for ten pathogenic mycobacteria species, including *M. tuberculosis* H37Rv, *M. tuberculosis* 18b, *M. smegmatis* MC^2-155, *M. orygis* 51145, *M. marinum* M, *M. lepromatosis* Mx1-22A, *M. leprae* TN, *M. haemophilum* DSM_44634/ATCC_29548, *M. bovis* AF2122/97, and *M. abscessus* ATCC_19977. The Mycobrowser knowledge base provides general annotation, gene or protein summary information, orthologues, and cross-references to the UniProt, Gene Ontology, SWISS-MODEL, and TB database (20). MtbVeb (http://crdd.osdd.net/raghava/mtbveb/) is a database developed by scientists from Institute of Microbial Technology in India for designing TB vaccines by using three approaches, such as strain, antigen, and epitope based vaccines (24). This database maintains integrated genomic information of 59 mycobacterium strains and provides comprehensive information for the antigenicity of potential vaccine candidates (24). MycobacRV database (http://mycobacteriarv.igib.res.in), developed by scientists from CSIR-Institute of Genomics and Integrative Biology in India, includes whole-genome sequences of 22 pathogenic mycobacterium species and one non-pathogenic mycobacterium H37Ra strain, and a set of 233 most probable vaccine candidates (26). Recently, a database of MHC antigenic peptide of *M. tuberculosis* named PeMtb has been developed to assist scientists in more efficient selection of epitopes that can be used for peptide-based vaccine construction (25). PeMtb is a free platform for predicting potential antigenic peptides of *M. tuberculosis*, which has unique advantages in epitopes prediction for TB vaccines development.

Furthermore, the most significant difference between peptide-based vaccines and traditional vaccines is that the former has MHC restriction. Human MHC molecules are also known as human leukocyte antigen (HLA). The HLA gene is located at the end of the short arm of human chromosome 6 and is divided into three regions: HLA Class I, HLA Class II, and HLA Class III (101). HLA genes with antigen presentation function are classic HLA genes located in HLA class I and HLA class II regions. The classic HLA I genes are divided into three categories: HLA-A, HLA-B, and HLA-C, and the classic HLA II genes are divided into three categories: HLA-DP, HLA-DQ, and HLA-DR (102). Therefore, selecting peptides with different MHC binding specificities will increase the coverage of the target population of peptide-based vaccines. However, due to the polymorphism of MHC molecules in other races, the design of peptide-based vaccines has become more complicated. Therefore, the coverage of MHC alleles in the vaccinated population must be considered when constructing a peptide-based vaccine. To overcome this issue, some databases and resources have been developed, including the Allele Frequency Net Database (http://www.allelefrequencies.net/pops.asp) and population coverage submodule of Immune Epitope Database and Analysis Resource (IEDB, www.iedb.org) (103). The Allele Frequency database provides allele frequencies for 115 countries and 21 different ethnicities grouped into 16 other geographical areas (28). IEDB is a popular database for providing information on immune epitopes. There are two components in the IEDB

TABLE 1 | A list of databases or servers used to construct a peptide-based vaccine for TB.

Items	Subitems	Databases or servers	Web site	Remark	References
Protein sequence and functional information	Universal databases	NCBI	https://www.ncbi.nlm.nih.gov/protein	–	(19)
		Uniprot protein database	https://beta.uniprot.org/	–	(20, 21)
		GeneDB database	http://www.genedb.org/Homepage	–	(21, 22)
		Target-Pathogen database	http://target.sbg.qb.fcen.uba.ar/patho	Designed and developed as an online resource that allows the integration and weighting of protein information.	(23)
	Databases for *M. tuberculosis*	Mycobrowser database	https://mycobrowser.epfl.ch/	A comprehensive genomic and proteomic database for pathogenic mycobacteria	(20)
		MtbVeb	http://crdd.osdd.net/raghava/mtbveb/	A web portal for *M. tuberculosis* vaccines	(24)
		PeMtb	http://www.pemtb-amu.org	A practical platform for trial and computational analyses of antigenic peptides for *M. tuberculosis*	(25)
		MycobacRV	http://mycobacteriarv.igib.res.in	An immunoinformatics database of known and predicted mycobacterial vaccine candidates	(26)
MHC alleles	Population Coverage	Allele Frequency Net Database	http://www.allelefrequencies.net/pops.asp	–	(27)
		IEDB population coverage	http://tools.iedb.org/population/	–	(28)
T Cell epitope prediction tools	Epitope binding to MHC class II molecules (HTL epitope)	IEDB database	http://tools.immuneepitope.org/mhcii/	A small numbered adjusted percentile rank indicates high affinity, peptides with IC50 values <50 nM are considered high affinity	(29)
		RANKPEP server	http://imed.med.ucm.es/Tools/rankpep.HTML	Threshold 1.0: 49.5% sensitivity, 76.0% specificity; Threshold 0.5: 59.4% sensitivity, 69.4% specificity (Default); Threshold 0.0: 68.3% sensitivity, 60.9% specificity	(30)
		MetaMHCIIpan	http://datamining-iip.fudan.edu.cn/MetaMHCpan/index.php/pages/view/info	Peptides with IC50 less than 500 nm can be deemed as a binder.	(31)
		ProPred	http://www.imtech.res.in/raghava/propred/	The peptides predicted to bind > 50% HLA-DR alleles included in the ProPred were considered promiscuous for binding predictions.	(32, 33)
		NetMHCIIpan-4.0	https://services.healthtech.dtu.dk/service.php?NetMHCIIpan-4.0	The output of the model is a prediction score for the likelihood of a peptide to be naturally presented by and MHC II receptor of choice.	(34, 35)
		NetMHCIIpan 3.2	https://services.healthtech.dtu.dk/service.php?NetMHCIIpan-3.2	The prediction values are given in IC50 values and as %Rank, a lower % Rank value indicates a stronger binding peptide	(36)
	Epitope binding to MHC class I molecules (CTL epitope)	IEDB database	http://tools.immuneepitope.org/mhci/	A small numbered adjusted percentile rank indicates high affinity, peptides with IC50 values <50 nM are considered high affinity	(37)
		NetCTL-1.2	https://services.healthtech.dtu.dk/service.php?NetCTL-1.2	Different thresholds for the integrated score can be translated into sensitivity/specificity values.	(38)
		RANKPEP server	http://imed.med.ucm.es/Tools/rankpep.HTML	Threshold 1.0: 49.5% sensitivity, 76.0% specificity; Threshold 0.5: 59.4% sensitivity, 69.4% specificity (Default); Threshold 0.0: 68.3% sensitivity, 60.9% specificity	(30)
		ProPred1	http://www.imtech.res.in/raghava/propred1/	Mirror site of this server is available at http://bioinformatics.uams.edu/mirror/propred1/	(39)
		NetMHCpan-4.1	https://services.healthtech.dtu.dk/service.php?NetMHCpan-4.1	The peptide will be identified as a strong binder if it is found among the top x% predicted peptides, where x% is the specified threshold for strong binders (by default 0.5%).	(34)
		MetaMHCIpan	http://datamining-iip.fudan.edu.cn/MetaMHCpan/index.php/pages/view/info	Peptides with IC50 less than 500 nm can be deemed as a binder.	(31)
		NetMHC4.0	http://www.cbs.dtu.dk/services/NetMHC/	A default threshold value of 0.5% for strong binders and 2% for weak binders is recommended in NetMHC4.0	(40)
		MHCpred 2.0			(41)

(Continued)

TABLE 1 | Continued

Items	Subitems	Databases or servers	Web site	Remark	References
			http://www.ddg-pharmfac.net/mhcpred/MHCPred/	Suggested IC50 values are between 0.01 to 5000 nM. If the value is above 5000, then the peptide is unlikely to bind MHC molecules.	
		EpiJen	http://www.ddg-pharmfac.net/epijen/EpiJen/EpiJen.htm	–	(42)
		CTLPred	http://www.imtech.res.in/raghava/ctlpred/index.html	A SVM and ANN based CTL epitope prediction	(43)
B Cell epitope prediction tools	Linear B cell epitopes	ABCpred	http://www.imtech.res.in/raghava/abcpred	Sensitivity = 67.14%, specificity = 64.71%, and accuracy = 66.41%.	(44, 45)
		IEDB Antibody Epitope Prediction	http://tools.iedb.org/bcell/	A collection of 7 methods to predict linear B cell epitopes based on sequence characteristics of the antigen using amino acid scales and HMMs.	(46–52)
		BCPred	http://ailab-projects1.ist.psu.edu:8080/bcpred/predict.html	AUC = 0.758, accuracy = 65.89%	(53, 54; a)
		BepiPred 2.0	https://services.healthtech.dtu.dk/service.php?BepiPred-2.0	AUC = 0.620	(52)
		APCpred	http:/ccb.bmi.ac.cn/APCpred/	AUC = 0.748 and accuracy = 68.43%	(55)
		SVMTriP	http://sysbio.unl.edu/SVMTriP/	Sensitivity = 80.1%, AUC = 0.702, and a precision of 55.2%	(56)
	Conformational B cell epitopes	DiscoTope-2.0	https://services.healthtech.dtu.dk/service.php?DiscoTope-2.0	AUC = 0.824 or 0.748 on the benchmark or Discotope dataset, respectively.	(57)
		BEpro (formerly known as PEPITO)	http://pepito.proteomics.ics.uci.edu/	AUC = 0.754 or 0.683 on the Discotope or Epitome dataset, respectively.	(58)
		ElliPro	http://tools.iedb.org/ellipro/	AUC = 0.732 on the benchmark dataset	(59)
		SEPPA	http://www.badd-cao.net/seppa3/index.html	AUC = 0.742 and a successful pick-up rate of 96.64%	(60)
		Epitopia	http://epitopia.tau.ac.il	AUC = 0.600	(61)
		EPCES	http://sysbio.unl.edu/EPCES/	Sensitivity = 47.8%, specificity = 69.5%, and AUC = 0.632.	(62)
		EPSVR	http://sysbio.unl.edu/EPSVR/	AUC = 0.597	(63)
		EPMeta	http://sysbio.unl.edu/EPMeta/	AUC = 0.638	(63)
Epitope Screening tools	Inducing MHC II binders' prediction	IFNepitope	http://crdd.osdd.net/raghava/ifnepitope/index.php	Maximum prediction accuracy of 82.10% with MCC of 0.62 on main dataset	(64)
		IL4pred	https://webs.iiitd.edu.in/raghava/il4pred/index.php	Maximum accuracy of 75.76% and MCC of 0.51	(65)
		IL-10pred	https://webs.iiitd.edu.in/raghava/il10pred/predict3.php	MCC = 0.59 with an accuracy of 81.24%	(66)
	Immunogenicity	IEDB MHC I immunogenicity	http://tools.iedb.org/immunogenicity/	The higher score indicates a greater probability of eliciting an immune response	(67)
		IEDB MHC II immunogenicity	http://tools.iedb.org/CD4episcore/	predict the allele independent CD4 T cell immunogenicity at population level	(68)
		MARIA	https://maria.stanford.edu/	An integrated tool to predict how likely a peptide to be presented by HLA-II complexes on cell surface.	(69)
		PopCover-2.0	https://services.healthtech.dtu.dk/service.php?PopCover-2.0	An effective method for rational selection of peptide subsets with broad HLA and pathogen coverage	(70)
		BciPep	http://www.imtech.res.in/raghava/bcipep	A database of experimentally determined linear B-cell epitopes of varying immunogenicity	(71)
	Antigenicity	VaxiJen 2.0	http://www.ddg-pharmfac.net/vaxijen/VaxiJen/VaxiJen.html	The result will be showed as a statement of protective antigen or non-antigen	(72)

(Continued)

TABLE 1 | Continued

Items	Subitems	Databases or servers	Web site	Remark	References
		ANTIGENpro	http://scratch.Proteomics.ics.uci.edu/	Correctly classifies 82% of the known protective antigens, accuracy on the combined dataset is estimated at 76%	(73)
	Allergenicity	AllerTOP v 2.0	http://www.ddg-pharmfac.net/AllerTOP/	The result will be showed as a statement of allergen or non-allergen	(74)
		AllergenFP v.1.0	http://ddg-pharmfac.net/AllergenFP/	The recognition accuracy was 88% and the Matthews correlation coefficient was 0.759.	(75)
		AlgPred 2.0	https://webs.iiitd.edu.in/raghava/algpred2/	The result will be showed as a statement of allergen or non-allergen	(76)
		Allermatch™	http://allermatch.org	The amino acid sequence of a protein of interest can be compared with sequences of allergenic proteins.	(77)
	Toxicity	ToxinPred	http://crdd.osdd.net/raghava/toxinpred/	The performance of dipeptide-based model in terms of accuracy was 94.50% with MCC 0.88	(78)
		T3DB	http://www.t3db.ca/biodb/search/target_bonds/sequence	Currently there are 3543 small molecule toxins (<1500 Da) and 136 peptide or protein toxins (>1500 Da) in T3DB	(79)
	Epitope Cluster Analysis	IEDB Clusters with Similar Sequences	http://tools.iedb.org/cluster/	This tool groups epitopes into clusters based on sequence identity	(80)
	Proinflammatory peptides	PIP-EL	http://www.thegleelab.org/PIP-EL/	MCC of 0.435 in a 5-fold cross-validation test	(81)
	Anti-inflammatory peptides	PreAIP	http://kurata14.bio.kyutech.ac.jp/PreAIP/	AUC = 0.833 in the training dataset *via* 10-fold cross-validation test, Score ≥ 0.468, Sensitivity = 63.22%; Specificity = 90.30%	(82)
Codon optimization and in silico cloning	Codon optimization	Java Codon Optimization Tool (JCat)	http://www.jcat.de/	The best CAI value is 1.0, while > 0.8 is regard a good score	(83)
	In silico clone	SnapGene software	https://www.snapgene.com/try-snapgene/		(84)
	Solubility prediction	Protein–Sol server	https://protein-sol.manchester.ac.uk/	Solubility value greater than 0.45 is predicted to have a higher solubility	(85)
Structure and function prediction	TCR-pMHC Binding Model	PAComplex	http://pacomplex.life.nctu.edu.tw./	Investigating and visualizing both TCR-peptide/peptide-MHC interfaces	(86)
		HADDOCK 2.2	http://haddock.science.uu.nl/services/HADDOCK/haddockserver-guru.html	Achieved success rate is 34.1%	(87)
		ClusPro server	https://cluspro.org	Achieved success rate is 27.3%	(88)
		LightDock	https://life.bsc.es/pid/lightdock/	Achieved success rate is 6.8%	(89)
		ZDOCK	http://zlab.bu.edu/~rong/dock	Achieved success rate is 15.9%	(90)
		iMOD	https://bio3d.colorado.edu/imod/paper/	NMA analysis of refined complexes	(91)
	Secondary structure prediction	PDBsum	http://www.ebi.ac.uk/thornton-srv/databases/pdbsum/		(92)
		SSpro8	http://scratch.proteomics.ics.uci.edu/	Can predict 8-class secondary structure of a protein	(93)
		GOR V server	https://abs.cit.nih.gov/gor/	Accuracy of prediction Q3 of 73.5%.	(94)
		SOPMA	http://npsa-pbil.ibcp.fr/cgi-bin/npsa_automat.pl?page=npsa_sopma.html		(95)
	Tertiary structure prediction	GalaxyWEB	http://galaxy.seoklab.org/cgi-bin/submit.cgi?type=REFINE	Protein structure prediction and refinement	(96)
		CABS-Flex 2.0	http://biocomp.chem.uw.edu.pl/CABSflex/	Predicts the structural flexibility of a protein/peptide	(97)
		3Dpro	http://scratch.proteomics.ics.uci.edu/	Predict tertiary structure of a protein	(98)
		Phyre2			(99)

(Continued)

TABLE 1 | Continued

Items	Subitems	Databases or servers	Web site	Remark	References
			http://www.sbg.bio.ic.ac.uk/phyre2	A typical structure prediction will be returned between 30 min and 2 h after submission	
		SWISS-MODEL	http://swissmodel.expasy.org		(100)

AUC, area under the curve; CTL, cytotoxic T lymphocyte; HTL, helper T lymphocyte; IEDB, Immune Epitope Database and Analysis Resource; MCC, Matthews' correlation coefficient; MHC, major histocompatibility complex; NCBI, National Center for Biotechnology Information; pMHCs, major histocompatibility complex presented antigenic peptides; PI, Protrusion Index.

database, including the home page search and Analysis Resource. The home page search is designed to simplify the search process for many commonly queries such as Epitope (Linear peptide, discontinuous peptide, non-peptidic, and Any), Assay (T cell, B cell, and MHC ligand), Epitope Source (Organism and Antigen), MHC Restriction (Class I, Class II, Non-classical, and Any), hosts (humans, non-human primates, and other animal species), and Disease. The Analysis Resource component provides a set of tools for predicting and analyzing immune epitopes, which can be divided into three categories: (1) T Cell Epitope Prediction Tools: Peptide binding to MHC class I or II molecules (29, 37), peptide processing predictions and immunogenicity predictions (67, 104–106), TCRmatch (107), and structure tools such as LYRA (Lymphocyte Receptor Automated Modelling) (108), SCEptRe (Structural Complexes of Epitope Receptor) (109), and Docktope (109); (2) B Cell Epitope Prediction Tools: Prediction of linear epitopes from protein sequence including Chou & Fasman Beta-Turn Prediction, Emini Surface Accessibility Prediction, Karplus & Schulz Flexibility Prediction, Kolaskar & Tongaonkar Antigenicity, Parker Hydrophilicity Prediction, Bepipred Linear Epitope Prediction, and Bepipred Linear Epitope Prediction 2.0 (46–52); Discotope (110), ElliPro (59), methods for modeling and docking of antibody and protein 3D structures (111), LYRA server (108), and SCEptRe (109); (3) Analysis tools: Population Coverage (28), Epitope Conservancy Analysis (112), Epitope Cluster Analysis (80), Computational Methods for Mapping Mimotopes to Protein Antigens (http://tools.iedb.org/main/analysis-tools/mapping-mimotopes/), RATE (Restrictor Analysis Tool for Epitopes) (113), and ImmunomeBrowser (114). The components of the IEDB database related to peptide-based vaccine development are described in detail below.

2.1.2 T Cell Epitope Prediction Tools

MHC molecules, expressed on the surface of APCs, are responsible for presenting antigenic peptides to T cells, making them irreplaceable in activating adaptive immunity (34). MHC molecules can be divided into two sets, MHC Class I (MHC I) and MHC Class II (MHC II), which primarily presents intracellular and extracellular peptides, respectively. Hence, identifying peptides binding to MHC I and II molecules is crucial for activating $CD8^+$ and $CD4^+$ T lymphocytes. Furthermore, recent studies have reported that engaging both helper T lymphocytes (HTL) epitopes binding to MHC II molecule and cytotoxic T lymphocytes (CTL) epitopes binding to MHC I molecule is desirable for inducing a robust immune response against *M. tuberculosis* (115, 116). Therefore, accurate computational prediction of HTL and CTL epitopes is the cornerstone for successfully constructing a peptide-based vaccine.

Currently, a growing number of bioinformatics technologies are available for HTL and CTL epitopes prediction, such as the IEDB database (29), RANKPEP server (30), MetaMHCIIpan (31), ProPred (32, 33), NetMHCIIpan-4.0 (34, 35), NetMHCIIpan 3.2 (36), NetCTL-1.2 (38), RANKPEP server (30), ProPred1 (39), NetMHCpan-4.1 (34), MetaMHCIpan (31), NetMHC4.0 (40), MHCpred 2.0 (41), EpiJen (42), and CTLPred (43) (**Table 1**). Three of these servers or databases can predict both HTL and CTL epitopes, including RANKPEP server, MetaMHCpan, and MHCPred. RANKPEP server predicts HTL and CTL epitopes from protein sequence using Position Specific Scoring Matrices (PSSMs) (30). MetaMHCpan has two parts: MetaMHCIpan and MetaMHCIIpan, for predicting CTL and HTL epitopes, respectively. MetaMHCIpan is based on two existing predictors (MHC2SKpan and LApan), while MetaMHCIIpan is based on four existing predictors (TEPITOPEpan, MHC2SKpan, LApan, and MHC2MIL) (31). MHCPred was developed to predict both HTL and CTL epitopes based on an Allele specific Quantitative Structure Activity Relationship (QSAR) model generated using partial least squares (PLS). MHCPred 2.0 covers 11 HLA class I, three human HLA class II, and three mouse MHC class I models (41). Furthermore, MHCPred 2.0 has multiple significant merits, such as incorporating a binding model for human transporter associated with antigen processing (TAP) that offers additional evidence, comprising a tool for designing heteroclitic peptides, and providing a confidence percentage for every peptide prediction (41).

As the most popular epitope prediction database, IEDB has unique advantages in HTL and CTL epitopes prediction. For MHC II epitopes prediction, nine methods are implemented, including IEDB recommended, Consensus method (117), Combinatorial library, NN-align-2.3 (netMHCII-2.3) (36), NN-align-2.2 (netMHCII-2.2) (118), SMM-align (netMHCII-1.1) (119), Sturniolo (120), NetMHCIIpan-3.1 (121), and NetMHCIIpan-3.2 (36). IEDB Recommended, selected as the default method, uses the best possible scenario for a given MHC molecule based on the following rules: the Consensus approach (a combination of any three of NN-align, SMM-align, CombLib, and Sturniolo) will be used if any corresponding predictor is available for the antigen. Otherwise, NetMHCIIpan is used. The performance of the MHC class II binding predictions has been

evaluated in two studies based on over 10,000 binding affinities (117) and 40,000 binding affinities (29), and one study comparing pan-specific methods (122). For MHC I epitopes prediction, ten methods are implemented, including IEDB recommended 2020.09 (NetMHCpan EL4.1), Artificial neural network (ANN) (40), Stabilized matrix method (SMM) (123), SMM with a Peptide: MHC Binding Energy Covariance matrix (SMMPMBEC), Scoring Matrices derived from Combinatorial Peptide Libraries (Comblib_Sidney2008) (124), Consensus (125), NetMHCpan (126), NetMHCcons (127), PickPocket (128) and NetMHCstabpan (129). Similarly, IEDB recommended NetMHCpan EL 4.1 is selected as the default method and used across all alleles.

2.1.3 B Cell Epitope Prediction Tools

More and more attention has been paid to the role of B cells in *M. tuberculosis* infection. B cells secrete antigen-specific antibodies to fight against *M. tuberculosis* invasion. Antigenic peptides are critical triggers for B cell antibody recognition. Therefore, the prediction of B cell epitopes is helpful to study the mechanism of the host's self-protection system and design a peptide-based vaccine. Unlike T cell epitopes, B cell epitopes have both continuous (also known as linear epitopes) and discontinuous (also known as conceptual epitopes). A linear epitope is a continuous fragment from an antigen sequence. In contrast, a conformational epitope comprises several fragments distributed in an antigen sequence that form a structural domain-like interface in three dimensions.

At present, most of the available methods for predicting B cell epitopes are focused on continuous epitopes, such as ABCpred (44, 45), IEDB B-cell epitope tools (46–52), BCPred (53, 54; a), BepiPred 2.0 (52), APCpred (55), and SVMTriP (56). These methods are based on antigen amino acid sequence, and the operation method is simple and easy to study. Overall, the sensitivity and specificity of these methods for predicting linear B cell epitopes ranged from 60% to 70%, and the area under the curve (AUC) ranged from 0.6 to 0.8 (**Table 1**). Compared with other methods, IEDB Antibody Epitope Prediction is a collection of seven methods to predict continuous B cell epitopes based on antigen sequence using amino acid scales and machine learning algorithm Hidden Markov Model (HMM), including Bepipred Linear Epitope Prediction 2.0, Bepipred Linear Epitope Prediction, Chou & Fasman Beta-Turn Prediction, Emini Surface Accessibility Prediction, Karplus & Schulz Flexibility Prediction, Kolaskar & Tongaonkar Antigenicity, and Parker Hydrophilicity Prediction (46–52). These seven methods of IEDB predict linear B cell epitopes based on specific characteristics of an antigen sequence, such as hydrophilicity, accessibility, flexibility, turns, polarity, exposed surface, and antigenic propensity.

Previous studies have shown that up to 90% of B cell epitopes are discontinuous in nature, but most predictions have focused on linear epitopes, which may be related to the tertiary structure of proteins required for B cell conformational epitopes prediction. Despite the rapid development of single-crystal X-ray diffraction (SCXRD), nuclear magnetic resonance (NMR) spectroscopy, and X-ray crystallography, many tertiary structures of biological macromolecules have been elucidated, but accurate prediction of B cell epitopes remains challenging (58). Currently, several methods have been used for predicting conformational B cell epitopes, including DiscoTope-2.0 (57), BEpro (formerly known as PEPITO) (58), ElliPro (59), SEPPA (60), Epitopia (61), EPCES (62), EPSVR (63), EPMeta (63). A previous study compared the performance of DiscoTope-2.0 to the PEPITO, ElliPro, SEPPA, Epitopia, EPCES and EPSVR methods. The results indicated that the AUC value of DiscoTope-2.0 was observably higher than that of ElliPro but comparable to PEPITO. Furthermore, DiscoTope-2.0 revealed an enhanced AUC value compared to that of SEPPA (0.720 vs 0.711), EPCES (0.733 vs 0.695), Epitopia (0.727 vs 0.652) and EPSVR (0.746 vs 0.588) based on benchmark dataset (57).

2.1.4 Peptide Analysis and Screening Tools

As shown in **Figure 1**, the IFN-γ and IL-4 cytokines secreted by APCs play an essential role in promoting the differentiation of native $CD4^+$ T cells into Th1 and Th2 cells, which is the principal arm for controlling and killing intracellular *M. tuberculosis* (130). Three methods have been developed to predict the IFN-γ, IL-4, and IL-10 inducers by bioinformatics technologies, including IFNepitope (64), IL4pred (65), and IL-10pred (66). IFNepitope is an online prediction server that can predict the epitopes that can induce $CD4^+$ T cells to secrete IFN-γ based on the protein sequence. It can help immunologists select and design IFN-γ-induced MHC Class II binding epitopes from proteins of interest, which is essential for designing better and more effective peptide-based vaccines (64). IL4pred and IL-10pred were developed to predict IL-4 and IL-10 inducing MHC II binding epitopes, respectively. The algorithm of the three servers relies on the following three models: Motif based model, Support Vector Machine (SVM) based model, and/or Hybrid approach (a combination of Motif and SVM). The maximum prediction accuracy of the three servers is 82.10%, 75.76%, and 81.24%, and the Matthew's correlation coefficient (MCC) is 0.62, 0.51, and 0.59, respectively (64–66).

In the design of peptide-based vaccines, in addition to considering those mentioned cytokine-induced epitopes, it is also necessary to assess the immunogenicity, antigenicity, allergenicity, and toxicity of the epitopes. Previous studies have shown that these characteristics vary significantly among epitopes (67, 72, 74, 78). Therefore, how to choose epitopes with strong immunogenicity and antigenicity but low toxicity and allergenicity is a challenge for peptide-based vaccine design. To overcome these obstacles, some new algorithms, models or servers have been developed, including IEDB MHC I immunogenicity, IEDB CD4 T cell immunogenicity prediction, MARIA, BciPep, and PopCover-2.0 for immunogenicity (67–71), VaxiJen 2.0 and ANTIGENpro for antigenicity (72, 73), AllerTOP v 2.0, AllergenFP v.1.0, AlgPred 2.0, and Allermatch™ for allergenicity (74–77), ToxinPred and T3DB for toxicity (78, 79). In addition, other useful tools have been developed to help scientists design more effective peptide-based vaccines, such as IEDB Clusters with Similar Sequences for epitope cluster analysis (80), PIP-EL for proinflammatory peptides prediction (81), and PreAIP for anti-inflammatory peptides prediction (82).

2.2 Construction of Peptide-Based Vaccines

The most potential immunodominant epitopes are short peptides composed of dozens of amino acid residues and quickly degrade at the inoculation site. In order to overcome this shortcoming, it is necessary to use appropriate linkers and/or additional helper peptides (adjuvant peptides and agonists used in constructing a peptide-base vaccine) to fuse these dispersed epitopes to improve the efficiency of the vaccine.

2.2.1 Linkers

Linkers are short amino acid sequences of natural origin that separate multiple domains in proteins (131). The selection of suitable linkers to link protein domains together is always complicated, but it is often overlooked in the design of peptide-based vaccines. If there are no linkers, a direct fusion of immunodominant epitopes may lead to many undesirable results, including misfolding of peptide-based vaccine (132), low vaccine yields (133), and impaired biological activity (134). Therefore, the selection and rational design of linkers connecting dominant epitopes is a crucial but undeveloped field in developing peptide-based vaccines.

According to the characteristics of linkers, they can be divided into three categories: flexible linkers, rigid linkers, and cleavable linkers. (1) Flexible linkers are usually used to connect protein domains that need mobility and interaction. They contain some polar or nonpolar amino acids with small molecular weight, which provides flexibility for the movement and interaction between protein domains (135). The commonly used flexible linkers include $(GGGGS)_n$ (135), $(Gly)_8$ (136), $(Gly)_6$ (137), GSAGSAAGSGEF (138), KESGSVSSEQLAQFRSLD and EGKSSGSGSESKST (139). The GSAGSAAGSGEF linker is better than the $(GGGGS)_4$ linker due to its better hydrophilicity and no-repeats (140). Providing flexibility for the movement and interaction between protein domains is the advantage of flexible linkers, but the lack of rigidity may lead to inefficient expression of recombinant proteins or loss of biological activity (133, 141). (2) Rigid linkers are usually used to maintain the distance between protein domains, effectively separating different protein domains and reducing the interaction and influence between the domains. Common rigid linkers are (EAAAK)n, $A(EAAAK)_nA$ (n = 2-5), PAPAP, $(Ala\text{-}Pro)_n$ (132, 140, 142, 143). The rigid linker exhibits a relatively rigid structure by adopting an α-helical structure, and they separate protein domains more effectively than flexible linkers. Furthermore, the length of the rigid linker can be easily adjusted by changing the number of copies to achieve the best distance between domains. Therefore, rigid linkers are chosen when the spatial separation of domains is essential to maintain the stability or biological activity of the fusion protein. (3) Cleavage linkers are usually used to separate domains or peptides from protein or vaccine to achieve the biological functions of a single domain or peptide. These linkers can reduce steric hindrance, improve biological activity, and realize the independent function/metabolism of a single domain of the recombinant fusion protein after the linker is cut. However, the design of cleavable linkers for recombinant fusion proteins *in vivo* is a very challenging subject. Hence, cleavage linkers are rarely used in the design of peptide-based vaccines. Linkers used in peptide-based vaccine construction can be found in **Table 2**.

2.2.2 TLR Agonists and Helper Peptides

Like other subunit vaccines, weak immunogenicity is one of the disadvantages of peptide-based vaccines. Covalent conjugation of helper peptides to peptide-based vaccines appears to be a powerful strategy for improving the immunogenicity and protective efficiency of peptide-based vaccines. Currently, two kinds of adjuvants have been used in peptide-based vaccine construction to enhance its protective efficacy: Toll-like receptor (TLR) agonists and helper peptides. TLRs are important protein molecules involved in innate immunity and serve as a bridge between innate and adaptive immunity (168). There are ten common TLRs, of which, TLR1, TLR2 (a heterodimer of TLR1 and TLR6), TLR4, TLR5, TLR6 and TLR10 are located on the cell membrane, while TLR3, TLR7, TLR8, and TLR9 are located on the membrane of the endosome (**Figure 2**). Among these TLRs, TLR10 is an orphan receptor whose ligand, signaling pathway and biological function are still unknown (**Figure 2**).

Previous studies have reported that TLR2-, TLR4-, and TLR9-mediated immune responses are critical for host defense against *M. tuberculosis* infection (169, 170). TLR9, expressed by human B cells and DCs, play an essential role in recognizing the CpG DNA in bacterial rather than in not mammalian, which induces the differentiation, maturation, and proliferation of macrophages, NK cells, monocytes, T cells, and B cells, and enhances the production of Th1 type cytokines, such as IFN-γ, TNF-α, and IL-12 (171). More currently, there are three kinds of CpG oligonucleotides (ODN) that have been used as TLR-9 agonists, 1) Type A CpG ODN is consist of a phosphodiester/phosphothioate backbone, a palindrome sequence containing CpG dinucleotide, and poly G tail at the 3' and 5' terminals, which can activate the plasmacytoid dendritic cells (pDCs) to produce IFN-α (172); Type B CpG ODN is composed of multiple CpG motifs, which has solid immunostimulatory activity against B cells, but cannot activate pDCs (173); Type C CpG ODN is composed of whole phosphorothioate and palindromic CpG motifs, has the activity of both type A and type B CpG-ODNs, and can activate B cells and pDCs (174). TLR2 and TLR4 activate DCs by recognizing with the pathogen associated molecular patterns (PAMPs), and the activated DCs will produce kinds of cytokines to kill *M. tuberculosis via* TLR2-MyD88-NK-κB/IRFs-IFN-I/γ signaling pathway and TLR4-MyD88/TRIF-NK-κB/IRFs-IFN-I/γ signaling pathway (**Figure 2**) (175). Therefore, enhancing host immune responses with TLR2 and TLR4 agonists may be the option for constructing an ideal peptide-based vaccine in future. At present, some TLR2 and TLR4 agonists have been used in peptide-based vaccines against infectious diseases, including TB, such as TLR2 agonists ESAT6 (144), phenol-soluble modulin α4 (PSMα4) (145), dipalmitoyl-S-glyceryl cysteine (Pam2Cys) (115, 146), and PorB (147, 148), TLR4 agonists RpfE (Rv2450c) (149), 50S ribosomal protein L7/L12 (RplL) (22, 150–155), heparin binding hemagglutinin (HBHA) (156), cholera toxin subunit B

TABLE 2 | Linkers and helper peptides used in peptide-based vaccine construction.

Reference	Helper peptides	Sequence of helper peptides	Linker for helper peptides	Linkers for epitopes			Diseases or pathogen
				CTL	HTL	B cell	
(144)	TLR2 agonist ESAT6	MTEQQWNFAGIEAAASAIQGNVTSIHSLLDEGKQSLTKLAAAWGGSGS EAYQGVQQKWDATATELNNALQNLARTISEAGQAMASTEGNVTGMFA	EAAAK	AAY	–	–	TB
(145)	TLR2 agonist PSMα4	MAIVGTIIKIIKAIIDIFAK	EAAAK	Alternately linked by GPGPG and AAY	–	–	TB
(115, 146)	TLR-2 agonist Pam2Cys	FNNFTVSFWLRVPKVSASHLE	NA	NA	NA	NA	TB
(147)	TLR2 agonist PorB	IALTLAALPVAAMADVTLYGTIKAGVETSRSVAHNGAQAASVETGTG IVDLGSKIGFKGQEDLGNGLKAIWQVEQ KASIAGTDSGWGNRQSFIGLKGGFGK	EAAAK	AAY	GPGPG	–	*Streptococcus pneumoniae*
(148)	TLR2 agonist PorB and helper epitope PADRE	PorB (IALTLAALPVAAMADVTLYGTIKAGVETSRSVAHNGAQAAS VETGTGIVDLGSKIGFKGQEDLGNGLKAIWQVEQ KASIAGTDSGWGNRQSFIG LKGGFGK), and PADRE (AGLFQRHGEGTKATVGEPV)	EAAAK	GPGPG	AAY	–	*Neisseria meningitidis*
(149)	TLR4 agonist RpfE (Rv2450c)	LKNARTTLIAAAIAGTLVTTSPAGIANADDAGLDPNAAAGPDAVGFDPNL PPAPDAAPVDTPPAPEDAGFDPNLPPPLAPDFLSPPAEEAPPVPVAYS VNWDAIAQCESGGNWSINTGNGYYGGLRFTAGTWRANGGSGSAANA SREEQIRVAENVLRSQGIRAWPVCGRRG	EAAAK	AAY	GPGPG	KK	TB
(150)	TLR4 agonist RplL	MAKLSTDELLDAFKEMTLLELSDFVKKFEETFEVTAAAPVAVAAAGAAPAGAAVEAAEEQ SEFDVILEAAGDKKIGVIKVVREIVSGLGLKEAKDLVDGAPKPLLEKVAKEAADEAKAKLEAAGATVTVK	EAAAK	AAY	GPGPG	KK	TB
(151)	TLR4 agonist RplL and PADRE	RplL (MAKLSTDELLDAFKEMTLLELSDFVKKFEETFEVTAAAPVAVAAAGAAPAGAAVEAAEEQSEF DVILEAAGDKKIGVIKVVREIVSGLGLKEAKDLVDGAPKPLLEKVAKEAADEAKAKLEAAGATVTVK), PADRE (AGLFQRHGEGTKATVGEPV)	EAAAK	GPGPG	HEYGAEALERAG	–	*Schistosoma mansoni*
(152)	TLR4 agonist RplL	MAKLSTDELLDAFKEMTLLELSDFVKKFEETFEVTAAAPVAVAAAGAAPAGAAVEAAEE QSEFDVILEAAGDKKIGVIKVVREIVSGLGLKEAKDLVDGAPKPLLEKVAKEAADEAKAKLEAAGATVTVK	EAAAK	AAY	GPGPG	KK	*Staphylococcus aureus*
(153)	TLR4 agonist RplL	MAKLSTDELLDAFKEMTLLELSDFVKKFEETFEVTAAAPVAVAAAGAAPAGAAVEAAEEQSEFD VILEAAGDKKIGVIKVVREIVSGLGLKEAKDLVDGAPKPLLEKVAKEAADEAKAKLEAAGATVTVK	EAAAK	AAY	GPGPG	–	*Helicobacter pylori*
(154)	TLR4 agonist RplL	MAKLSTDELLDAFKEMTLLELSDFVKKFEETFEVTAAAPVAVAAAGAAPAGAAVEAAEEQSEFDVILE AAGDKKIGVIKVVREIVSGLGLKEAKDLVDGAPKPLLEKVAKEAADEAKAKLEAAGATVTVK	EAAAK	AAY	GPGPG	KK	*Leishmania parasite*
(155)	TLR4 agonist RplL	MAKLSTDELLDAFKEMTLLELSDFVKKFEETFEVTAAAPVAVAAAGAA PAGAAVEAAEEQSEFDVILEAAGDKKIGVIKVVREIVSGLGLKEAKDLV DGAPKPLLEKVAKEAADEAKAKLEAAGATVTVK	EAAAK	AAY	GPGPG	–	*Onchocerca volvulus*
(22)	TLR4 agonist RplL	MAKLSTDELLDAFKEMTLLELSDFVKKFEETFEVTAAAPVAVAAAGAAPAGAAVEAAEEQSEFDVILEA AGDKKIGVIKVVREIVSGLGLKEAKDLVDGAPKPLLEKVAKEAADEAKAKLEAAGATVTVK	EAAAK	GPGPG	AAY	–	*Schistosoma mansoni*
(156)	TLR4 agonist HBHA and helper epitope PADRE	HBHA (MAENSNIDDIKAPLLAALGAADLALATVNELITNLRERAEETRTDTRSRVEESRARLTKL QEDLPEQLTELREKFTAEELRKAAEGYLEAATSRYNELVERGEAALERLRSQQSFEEVSARAE GYVDQAVELTQEALGTVASQTRAVGERAAKLVGIEL), PADRE (AGLFQRHGEGTKATVGEPV)	EAAAK	GPGPG	GPGPG	–	Melanoma
(157)	TLR4 agonist CTB	MTPQNITDLCAEYHNTQIYTLNDKIFSYTESLAGKREMAIITFKNGAIFQVEVPGSQHID QKKAIERMKDTLRIAYLTEAKVEKLCVWNNKTPHAIAAISMAN	EAAAK	GPGPG			Brucellosis
(158)	TLR4 agonist CTB	MTPQNITDLCAEYHNTQIYTLNDKIFSYTESLAGKREMAIITFKNGAIFQVEVPG SQHIDSQKKAIERMKDTLRIAYLTEAKVEKLCVWNNKTPHAIAAISMAN	EAAAK	–	GPGPG	–	*Vibrio cholerae*
(159)	TLR4 agonist CTB	MTPQNITDLCAEYHNTQIHTLNDKIFSYTESLAGKREMAIITFKNGATFQVEV PGSQHIDSQKKAIERMKDTLRIAYLTEAKVEKLCVWNNKTPHAIAAISMAN	GPGPG	GPGPG	GPGPG	KK	*Helicobacter pylori*
(160)	TLR-4 agonist RS-09	APPHALS	EAAAK	AAY	GPGPG	–	TB

(Continued)

TABLE 2 | Continued

Reference	Helper peptides	Sequence of helper peptides	Linker for helper peptides	Linkers for epitopes			Diseases or pathogen
				CTL	HTL	B cell	
(161)	Hsp70, TR-433, and TLR-4 agonist RS-09	Hsp70 (NTTIPTKRSETFTTADDNQPSVQIQVYQGEREIAAHNKFDIDANGIVHVTAKKDKGTGKENTAHA EEDRKRREEADVRNQAKFVKEQREAEGGSKV), TR-433 (NLKQMSEFSVFLSLRNLIYL), and RS-09 (APPHALS)	EAAAK	AAY	GPGPG	KK	SARS-CoV-2
(162)	HBD-1	MRTSYLLLFTLCLLLSEMASGGNFLTGLGHRSDHYNCVSSGGQCLYSACPIFTKIQGTCYRGKAKCCK	EAAAK	AAY	GPGPG	KK	SARS-CoV-2
(163)	HBD-2	MRVLYLLFSFLFIFLMPLPGVFGGIGDPVTCLKSGAICHPVFCPRRYKQIGTCGLPGTKCCKKP	EAAAK	GPGPG	–	–	HIV
(164)	HBD-3	GIINTLQKYYCRVRGGRCAVLSCLPKEEQIGKCSTRGRKCCRRKK	EAAAK	AAY	GPGPG	–	Zika virus
(165)	HBD-3	GIINTLQKYYCRVRGGRCAVLSCLPKEEQIGKCSTRGRKCCRRKK	EAAAK	AAY	GGGS	KK	Chandipura virus
(166)	HBD-3	GIINTLQKYYCRVRGGRCAVLSCLPKEEQIGKCSTRGRKCCRRKK	EAAAK	AAY	GPGPG	–	SARS-CoV-2
(167)	HBD-3	GIINTLQKYYCRVRGGRCAVLSCLPKEEQIGKCSTRGRKCCRRKK	EAAAK	GGGS	–	–	SARS-CoV-2
(19)	HBD-3	GIINTLQKYYCRVRGGRCAVLSCLPKEEQIGKCSTRGRKCCRRKK	EAAAK	AAY	GPGPG	KK	SARS-CoV-2
(84)	Griselimycin	VPSLPLVPLG	EAAAK	AAY	GPGPG	GPGPG	TB

CTB, Cholera toxin subunit B; HBHA, Heparin Binding Hemagglutinin; HDB, human β-defensin; PADRE, Pan human leukocyte antigen-DR reactive epitope; PSMα4, Phenol-soluble modulin α4; RplL, 50S ribosomal protein L7/L12; TLR: Toll-like receptor.

FIGURE 2 | Toll-like receptors and their agonists. TLRs play an essential role in innate immunity and serve as a bridge between innate and adaptive immunity. TLR1, TLR2 (a heterodimer of TLR1 and TLR6), TLR4, TLR5, TLR6, and TLR10 are located on the cell membrane, while TLR3, TLR7, TLR8, and TLR9 are located on the membrane of the endosome. It has been reported that TLR2, TLR4, and TLR9 are critical for host defense against *M. tuberculosis* infection. In addition, the agonists of TLR2, TLR4, and TLR9 can enhance the immunogenicity and protective efficacy of peptide-based vaccines *via* TLR2- MyD88-NK-κB/IRFs-IFN-I/γ signaling pathway and TLR4-MyD88/TRIF-NK-κB/IRFs-IFN-I/γ signaling pathway. TLR10 is an orphan receptor without confirmed ligands, signalling pathway and biological function.

(CTB) (157–159), and RS-09 (160, 161). In addition, helper peptides and antimicrobial peptides are also used to construct peptide-based vaccines to enhance their immune effects, such as PADRE (148) (151) (156), Hsp70 (161), TR-433 (161), human β-defensin 1 (HBD-1) (162), HBD-2 (163), HBD-3 (19, 164–167), and Griselimycin (84). The amino acid sequences of the mentioned helper peptides can be found in **Table 2**.

2.2.3 Codon Optimization and Prediction of Structure and Function of Peptide-Based Vaccines

After the prediction and screening of dominant epitopes and the use of linkers and helper peptides (or adjuvants), a preliminary peptide-based vaccine was constructed. However, this native vaccine needs further optimization to become a mature peptide vaccine, including codon optimization, cloning and expression evaluation, and solubility prediction. Codon optimization is essential because the degeneracy of the genetic code allows one amino acid to be encoded by multiple codons (84). Java Codon Adaptation Tool (JCat) is the most popular tool for codon adaptation (**Table 1**). Compared with previous tools, JCat has superiorities in avoiding unnecessary cleavage sites for restriction endonuclease and Rho-independent transcription terminators and defining highly expressed genes as more intelligent, faster, and more accessible (83). Codon Adaptation Index (CAI) values are used to evaluate codon optimization. The best CAI value is 1.0, while CAI > 0.8 is regarded as a good score (83). Then, the sequence of the final vaccine optimized with JCat should be inserted into an appropriate plasmid vector using

SnapGene software (84). Finally, the solubility of the final vaccine should be predicted by bioinformatics methods such as Protein-Sol server (85).

TCR and MHC are the bridges connecting APCs, T lymphocytes and peptide-based vaccines. Accurate recognition of TCR and major histocompatibility complex presented antigenic peptides (pMHC) triggers adoptive immune responses to kill *M. tuberculosis*. In the past, the crystallization and structural resolution of TCR-pMHC complexes were expensive and took a lot of time. However, with the development of computational technology, some valuable models or algorithms have been developed to study the TCR-pMHC interaction at the molecular level, such as PAComplex (86), ZDOCK (90), LightDock (89), ClusPro (88), HADDOCK (87) and iMOD (91). Furthermore, a recent study compared the ability of four standard tools (including ZDOCK, LightDock, ClusPro, and HADDOCK) to perform accurate molecular docking of the TCR-pMHC based on an expanded benchmark set of 44 TCR-pMHC docking cases (176). It was suggested that achieved success rates of HADDOCK, ClusPro, ZDOCK, and LightDock are 34.1%, 27.3%, 15.9% and 6.8%, respectively, indicating that HADDOCK is the best performer. At present, HADDOCK has been updated to version 2.2, which provides some new characteristics such as additional experimental restraints, support for mixed molecule types, improved protocols, and a more friendly interface (87).

The epitope prediction is based on the amino acid sequence of the protein. However, the immunological function of the peptide-based vaccine depends not only on the amino acid sequence but also on the secondary structure and tertiary structure of the vaccine candidate (177). Recently, some bioinformatics approaches and immunoinformatics technologies have been widely used in predicting the secondary structure and tertiary structure of peptide-based vaccines, including PDBsum (92), SSpro8 (93), GOR V server (94), and SOPMA (95) for secondary structure prediction, GalaxyWEB (96), CABS-Flex 2.0 (97), 3Dpro (98), Phyre2 (99), and SWISS-MODEL (100) for tertiary structure prediction.

3 RESEARCH STATUS OF TB PEPTIDE-BASED VACCINES

Peptide-based vaccines are subunit vaccines and are new vaccines with unique advantages. Compared with traditional subunit vaccines, peptide-based vaccines are more precise and accurate in design (178). As mentioned above, the construction of peptide-based vaccines involves the identification of potential antigens, prediction and screening of dominant epitopes, comparison of MHC affinity, the addition of adjuvants or helper peptides, codon optimization, and prediction of structure and function. These tedious but indispensable processes enable peptide-based vaccines to efficiently cluster dominant epitopes together to induce a more robust immune response in the recipient, improving the efficiency and reducing side effects by excluding unwanted material from a full-length protein or whole pathogen (179).

The first peptide-based vaccine was reported and developed to fight against *Plasmodium falciparum* by Etlinger HM et al. in 1988 (180). This peptide-based vaccine consisted of a synthetic peptide [Ac-Cys-(NANP)3] and a tetanus toxoid protein. The immunological parameters of this vaccine were evaluated in a mouse model. To determine the research process of peptide-based vaccine for TB, we searched the PubMed database with terms of "peptide, epitope, and tuberculosis" (**Figure 3A**). Analyzing these results showed that the research of peptide-based vaccines for TB can be traced back to around 1990, but due to the lack of bioinformatics technology, the research progress is slow. Around 2010, with the rapid development of bioinformatics technology, the research of peptide-based vaccines for TB began to enter the fast lane. Especially in 2020, with the rise of COVID-19 peptide-based vaccines, the investigation of peptide-based vaccines for TB has also been extensively developed (red bubbles in **Figure 3A**).

Further analysis indicated that 150 studies involved in the peptide or epitope for TB, including 76 studies in epitope screening and prediction, 45 studies in evaluating immunogenicity, 8 studies in peptide-based vaccine construction, and 21 studies in assessing vaccine efficacy in animal models (**Figure 3B** and **Table S1**). Among these 150 articles, we found that 14 teams had published at least 3 articles in these four areas of TB epitopes or peptides, including six studies on epitope screening and prediction (181–186) and three studies on immunogenicity (187–189) from Pro. Markus J Maeurer's team; seven studies on epitope screening and prediction from Pro. Abu Salim Mustafa's team (190–196); one study on epitope screening and prediction (197) and two studies on immunogenicity (197, 198) from Pro. Anne S De Groot's team; two studies on epitope screening and prediction (199, 200), one study on immunogenicity (201), and two studies on protective efficacy (202, 203) from Pro. Annemieke Geluk's team; one study on epitope screening and prediction (204) and two studies on immunogenicity (205, 206) from Pro. Dora P. A. J. Fonseca's team; three studies on epitope screening and prediction from Pro. Harald G Wiker's team (207–209); four studies on protective efficacy from Pro. Javed Naim Agrewala's team (115, 146, 210, 211); one study on epitope screening and prediction (212) and three studies on immunogenicity (212–214) from Pro. Juraj Ivanyi's team; three studies on epitope screening and prediction from Pro. Kris Huygen's team (215–217); two studies on epitope screening and prediction (218, 219) and one study on immunogenicity (220) from Pro. Marisol Ocampo's team; one study on epitope screening and prediction (221) and two studies on protective efficacy (222, 223) from Pro. Peter Andersen's team; four studies on epitope screening and prediction from Pro. R Nayak's team (224–227); two studies on epitope screening and prediction (228, 229) and one study on protective efficacy (230) from Pro. Tom H. M. Ottenhoff's team; three studies on epitope screening and prediction from Pro. Yanfeng Gao's team (231–233). The works from these teams and the efforts of other scientists have laid the foundation for the development of peptide-based TB vaccines.

The detailed information of TB peptide-based vaccines in the stage of prediction, construction, and immunogenicity can be found in **Tables 2**, **S1**. Therefore, the following sections will focus on TB peptide-based vaccines in the stage of efficacy evaluation (**Table 3**).

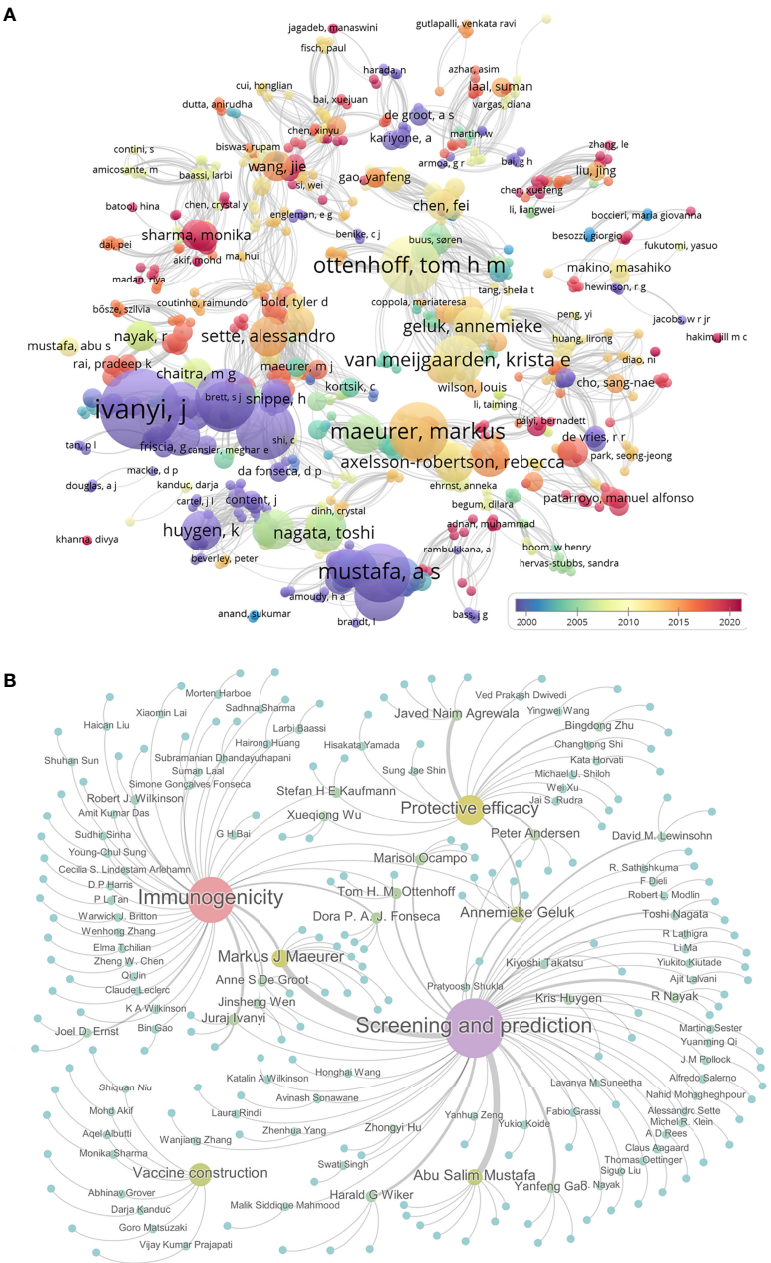

FIGURE 3 | The progress in peptide-based vaccines for TB. The PubMed database was used to search the literature related to the peptide-based vaccine for TB using "peptide, epitope, and tuberculosis". Their relationships were shown as bubble charts based on publication year and association strength by using VOSviewer software **(A)**. Furthermore, the relationships among 150 pieces of literature related to peptides or epitopes for TB were shown by using Gephi software. These literatures were divided into four categories: epitope screening and prediction, vaccine construction, immunogenicity, and protective efficacy. Gephi software was used to show 150 articles under corresponding authors. Each bubble represents a study, the size of which is proportional to the number of papers the author has published, and the color from blue to purple indicates the level of activity **(B)**.

3.1 Peptide-Based TB Vaccines Evaluated for Immunogenicity

As early as 2004, Mollenkopf HJ et al. identified 36 DNA vaccine candidates preselected by comparative proteomic and found that BCG prime-Rv3407 encoding DNA vaccine boost vaccination induced significantly higher protection compared to BCG alone (234). Then, the putative MHC I epitopes of Rv3407 were predicted by computational method and determined by enzyme-linked immunospot assay (ELISPOT). It was found that Rv3407 $_{64\text{-}72}$ (IPARRPQNL) and Rv3407 $_{68\text{-}76}$ (RPQNLLDVT) peptides stimulated splenocytes collected from BALB/c mice immunized with Rv3407 DNA vaccine secreting significantly higher

TABLE 3 | A list of TB peptide-based vaccines evaluated for immunogenicity and protection in animal models.

Reference	Protein and peptide (sequences)	Formulation (likers or adjuvant)	Host organism	Dose/route	Adjuvant	Challenge	Efficacy
(234)	Rv3407 $_{64-72}$ (IPARRPQNL), and Rv3407 $_{68-76}$ (RPQNLLDVT)	–	Splenocytes from vaccinated BALB/c mice	10^5 splenocytes per well were stimulated with 10 μg of peptide	–	-	These peptides stimulated splenocytes collected from vaccine immunized mice secreting significantly higher IFN-γ
(197)	15 peptides† from Rv0203, Rv3106, Rv2223c, Rv3201c, Rv3296, Rv1242, Rv1184c, Rv3207c, Rv1157c, Rv1158c, Rv1291c, Rv1860, Rv2190c, Rv333c, Rv0309	–	PBMCs	–	–	-	15 peptides stimulated IFN-γ response, and eight peptides stimulated lymphocyte proliferation *in vitro*.
(235)	pcDNA3-M-38 vaccine, MPT64 $_{190-198}$ (FAVTNDGVI) and 38 kDa proteins $_{166-175}$ (IAALNPGVNL)	pcDNA3 vector + MPT64 $_{190-198}$ (FAVTNDGVI) + 38 kDa proteins $_{166-175}$ (IAALNPGVNL)	C57BL/6 (H-2b) mice	100μg of DNA per mouse/ i.m., 3 times at intervals of 21 days	–	–	DNA immunization with p3-M-38 vaccine could induce epitope-specific $CD8^+$ CTL response but not antibodies
(236)	Ag85B $_{96–111}$ (QDAYNAAGGHNAVFN) and Ag85B $_{241–256}$ (PAFEWYYQSGLSIVMP)	Rv1886c $_{96-111}$ or Rv1886c $_{241-256}$ + RVG peptide (YTIWMPENPRPGTPCDIFTNSR)	C57BL/6 mice	10μg of peptides (RVG, Rv1886c $_{96-111}$ or Rv1886c $_{241-256}$)/s.c. or i.n., 3 times at 14days apart	–	–	Higher levels of IL-12, IFN-γ, IL-2, and TNF-α
(237)	Rv0934 $_{169-405}$ and Rv0934 $_{802-1119}$	Rv0934 $_{169-405}$ + Rv0934 $_{802-1119}$ + His-tag	BALB/c mice	Triplicate over a 2-week interval/s.c.	DDA/poly (I: C)	–	Elicited higher IgG and IFN-γ, IL-2
(198)	TB 001 DNA multi epitope vaccine, 24 peptides from Antigen 85 complex, MPT 64, MPB/MPT 70, MPT 63, the 38 kDa, 14-kDa, 16-kDa, 19-kDa, and 32-kDa Mtb	24 peptides linked with GPGPG linker	HLA-DR B*0101 transgenic mice	100 μg of DNA vaccine/ i.m., 3 times at intervals of 14 days	rIL-15	-	Epitope-specific T cell responses were observed to eight of the 24 epitopes contained in the DNA construct
(223)	ESAT-6 (Rv3875) $_{1–15}$ (MTEQQWNFAGIEAAA)	ESAT-6 or Δ15ESAT-6 (lack the immunodominant ESAT-6 $_{1–15}$) + CAF01 adjuvant	CB6F1 mice	5 μg of ESAT-6 or Δ15-ESAT with a 200μl CAF01/ s.c., 3 times, with a 2-week interval	CAF01	*Mtb* Erdman strain (20-50 CFUs/ aerosol)	Both vaccines reduced CFUs at the early time point, only the Δ15ESAT-6-based vaccine gave significant levels of protection (0.9 log10 reduction of CFU)
(222)	ESAT-6 (Rv3875) $_{51–70}$ (YQGVQQKWDATATELNNALQ)	DDA/MPLA/IL2 emulsion	B6CBAF1 mice	10μg peptide with a mixture	DDA and TLR4	*Mtb* H37Rv strain	ESAT-$6_{51–70}$ epitope

(Continued)

TABLE 3 | Continued

Reference	Protein and peptide (sequences)	Formulation (likers or adjuvant)	Host organism	Dose/route	Adjuvant	Challenge	Efficacy
				of 25μg MPLA, and 100 ng recombinant mouse IL-2/ i.p. or i.m., 3 times, with a 2-week interval	agonist MPLA	(5×10^4 CFUs/i.v. or 250 CFUs/ aerosol)	promoted significant levels of protective immunity (equivalent to BCG and ESAT-6).
(238)	ESAT-6 (Rv3875) $_{4-18}$ (QQWNFAGIEAAASAI), ESAT-6 $_{22-36}$ (VTSIHSLLDEGKQSL) and ESAT-6 $_{56-70}$ (QKWDATATELNNALQ)	pIRES + FL + ESAT-6 $_{4-18}$ +AAY + ESAT-6 $_{22-36}$ + AAY + ESAT-6 $_{56-70}$ + HIS	C57BL/6 mice	100 μg plasmid DNA per mouse/ i.m., two boosters at the interval of 3 weeks	–	*Mtb* H37Rv strain (5×10^5 CFUs/ intratracheal instillation)	DNA vaccine and boosted with the peptides increased IFN-γ and IL-12, the number of IFN-γ^+ T cells and activities of CTL as well as IgG, enhanced protection challenge.
(239)	Ag85B (Rv1886c) $_{10-27}$ (AWGRRLMIGTAAAVVLPG), Ag85B $_{19-36}$ (TAAAVVLPGLVGLAGGAA), Ag85B $_{91-108}$ (WDINTPAFEWYYQSGLSI), ESAT6 (Rv3875) $_{33-47}$ (KQSLTKLAAAWGGSG), ESAT6 $_{37-51}$ (TKLAAAWGGSGSEAY), ESAT6 $_{29-43}$ (LDEGKQSLTKLAAAW), ESAT6 $_{72-95}$ (LARTISEAGQAMASTEGNVTGMEA)	1 mL of vaccine mixture contains 10 μg of each peptide, 100 μg of Pam3Cys-SK-4, and 10 μg of CpG ODN	C57BL/6 mice	50 μl per mouse per dose	TLR9 agonist CpG ODN	*Mtb* H37Rv strain (150 CFUs/ aerosol)	Enhanced BCG protective efficacy, induced Th1 and Th17 responses
(116)	Ag85B (Rv1886c) $_{239-247}$ (KLVANNTRL), IniB (Rv0341) $_{33-45}$ (GLIDIAPHQISSV) and PPE68 (Rv3873) $_{127-136}$ (FFGINTIPIA)	Branched chain palmitoyl-peptide conjugate on Tuftsin (TKPKG) carrier, A/P/I mix, A(P)I, and Pal-A(P)I.	CB6F1 mice	50 μg vaccine in 100 μl PBS were injected s.c. three times, two weeks apart.	–	*Mtb* H37Rv strain (2×10^5 CFUs/i.p.)	Significantly lower number of bacteria in the spleen after i.p. challenge with Mtb.
(240)	TB10.4 (Rv0288) $_{4–11}$ (IMYNYPAM) and Ag85B (Rv1886c) $_{280–294}$ (FQDAYNAAGGHNAVF)	TB10.4-KFE8 nanofibers or TB85B-KFE8 nanofibers with KFE8 (FKFEFKFE) + Pam2Cys adjuvant	C57BL6 mice	1×10^6 CFU of BCG/s.c. prime followed by 25 μl of nanofiber formulations and boosted with 15 μl 30 or 90 days later	Pam2Cys	*Mtb* H37Rv strain (100 CFUs/ aerosol)	Induced a 8-fold expansion in multifunctional CD8+ T cell populations and 1.3 log10 CFU reduction in lung bacterial burden.
(241)	Ag85A (Rv3804c) $_{141-160}$	Recombinant (Ag85A) BCG Tokyo or Ag85A DNA vaccine with Ag85A peptide boosting	Guinea pigs	1. Recombinant (Ag85A) BCG: 5×10^6 CFUs/ s.c. boosted by 500 mg of Ag85A (141–160)/s.c. at 3 weeks later. 2. Ag85A DNA: 50 mg/ i.m., 2 times at intervals of 3 weeks, boosted by	–	*Mtb* Kurono strain (150 CFUs/ aerosol)	Peptide boosting is important for the induction of higher protective efficacy by recombinant BCG Tokyo or a tuberculosis DNA vaccine

(Continued)

TABLE 3 | Continued

Reference	Protein and peptide (sequences)	Formulation (likers or adjuvant)	Host organism	Dose/route	Adjuvant	Challenge	Efficacy
				500 mg of Ag85A (141–160)/s.c. in IFA.			
(242)	Acr (Hsp16.3, Rv2031c) $_{91–104}$ (SEFAYGSFVRTVSL)	Hsp16.3 $_{91–104}$ peptide mixed with DDA-MPLA (TLR4 agonist) or IFA	BALB/c mice	25μg synthetic peptide with DDA-MPLA/ mouse/s.c., 3 times, with a 2-week interval	250μg DDA + 25μg MPLA, or 100μl IFA	*Mtb* H37Rv strain (1×10^5 CFUs/i.v.)	Induced significantly stronger specific antibodies but lower IFN-γ than BCG, the protection was equivalent to BCG
(210)	Acr (Rv2031c) $_{91–110}$ (SEFAYGSFVRTVSLPVGADE)	Peptide + Pam2Cys	BALB/c mice or Duncan-Hartley guinea pigs	20 nmol per mouse or 100 nmol per guinea pig/i.p., 21 days later a booster (10 nmol per mouse and 50 nmol per guinea pig)	–	*Mtb* H37Rv strain (100 CFUs per mouse or 30 CFUs per guinea pigs, aerosol)	Enhanced activation of DCs, rousted Th1 immune response, and harbored significantly lower CFUs in the lungs
(146)	Acr (Rv2031c) $_{91–110}$ (SEFAYGSFVRTVSLPVGADE)	L91 vaccine, 1 HTL (SEFAYGSFVRTVSLPVGADE) + TLR-2 agonist (Pam2Cys)	BALB/c mice	Danish strain of BCG (10^6 CFU/animal), 21 days later, two boosters with L91 (20 nmol) at the interval of 2 weeks	–	*Mtb* H37Rv strain (100 CFUs/ aerosol)	L91 booster significantly enhanced Th1 cells and Th17 cells and reduced the mycobacterial burden
(115)	Acr (Rv2031c) $_{91–110}$ (SEFAYGSFVRTVSLPVGADE), TB10.4 (Rv0288) $_{20-28}$ (GYAGTLQSL)	L4.8 vaccine, 1 HTL (SEFAYGSFVRTVSLPVGADE) + 1 CTL (GYAGTLQSL) + TLR-2 agonist (Pam2Cys)	BALB/c mice	Danish strain of BCG (10^6 CFU/animal), 21 days later, two boosters with L4.8 (20 nmol) at the interval of 2 weeks	–	*Mtb* H37Rv strain (100 CFUs/ aerosol)	Significantly elicited both CD8 T cells and CD4 T cells immunity, and the BCG-L4.8 prime boost strategy imparts a better protection against TB than the BCG alone.
(211)	TB10.4 (Rv0288) $_{1-13}$ (MSQIMYNYPAMLG), TB10.4 (Rv0288) $_{78-94}$ (ANTMAMMARDTAEAAKW), Rv0476 $_{1-19}$ (MLVLLVAVLVTAVYAFVHA), CFP10 (Rv3874) $_{71-90}$ (EISTNIRQAGVQYSRADEEQ), Acr (Rv2031c) $_{91-110}$ (SEFAYGSFVRTVSLPVGADE), and Acr $_{21-40}$ (LFAAFPSFAGLRPTFDTRLM)	All six peptide sequences aligned in duplicates were attached by protease-sensitive linker sequence with N terminal secretory signal of human growth hormone	C57BL/6 mice	100 μg per mouse/s.c. Two boosters at the interval of 2 weeks	–	*Mtb* H37Rv strain (100 CFUs/ aerosol)	Significant reduction in the *Mtb* burden and enhanced IFN-γ and TNF-α cytokine release.
(202)	Hsp65 (Rv0440) $_{3–13}$ (KTIAYDEEARR), Ag85B (Rv1886c) $_{56–64}$ (PSMGRDIKV), 19 kDa (Rv3763) $_{51–61}$ (KVVIDGKDQNV), Acr (Hsp16.3, Rv2031c) $_{31–50}$ (LRPTFDTRLMRLEDEMKEGR) and Rv1733c $_{63–77}$ (AGTAVQDSRSHVYAH)	Recombinant polyepitope with CpG ODN1826 adjuvant	HLA-DR3 transgenic mice	25 μg peptide vaccine with 50 μg CpG in 200 μl PBS were injected s.c. three	50 μg TLR9 agonist CpG (ODN1826)	*Mtb* H37Rv strain (1×10^5 CFUs/i.n.)	High IgG levels and polyfunctional CD4(+) T-cells producing IFN-γ, TNF and IL-

(Continued)

TABLE 3 | Continued

Reference	Protein and peptide (sequences)	Formulation (likers or adjuvant)	Host organism	Dose/route	Adjuvant	Challenge	Efficacy
				times, two weeks apart.			2, and reduce CFUs in lungs
(243)	Four Th1 peptides ESAT-6 $_{1–20}$ (MTEQQWNFAGIEAAASAIQG), Ag85B $_{241–255}$ (VANNTRLWVYCGNGT), PE19 (Rv1791) $_{4–18}$ (VTTQPEALAAAAANL), PPE25 (Rv1787) $_{241–255}$ (AQFFASIAQQLTFGP), and 1 CTL peptide MTB10.4 (Rv0288) $_{3–11}$ (QIMYNYPAM)	HSP65 scaffold + ESAT-6 $_{1–20}$ + Ag85B $_{241–255}$ + MTB10.4 $_{3–11}$ + AAY + PPE25 $_{241–255}$ + PE19 $_{4–18}$	C57BL/6 mice	Four doses of 50 μg DNA vaccine per mouse/i.m.	–	Intranasally inoculated with 1×10^7 CFUs BCG in 100 μL PBS under anesthesia	Induce higher IFN-γ^+ T cell response, granzyme B^+ CTL and IL-2^+ $CD8^+$ T cell responses, and significantly improved protection
(244)	21 conserved PE/PPE peptides ‡	PE peptide + ESAT-6 (PE-ESAT-6), PPE peptide + ESAT-6 (PPE-ESAT-6), and PE + PPE peptide + ESAT-6 (PE/PPE-ESAT-6)	C57BL/6J mice	2 mg per mouse/s.c. Two boosters at the interval of 3 weeks	GLA-SE (5mg/mouse)	*Mtb* Beijing strain HN878 (100 CFUs/aerosol)	Enhanced IL-2^+IFN-γ^+ $CD4^+$ T cells, lower CFUs
(2)	Mtb8.4 (Rv1174c) $_{69-83}$ (LRNFLAAPPPQRAAM), PPE18 $_{115-129}$ (RAELMILIATNLLGQ), PPE18 (Rv1196) $_{149-163}$ (AAAMFGYAAATATAT), PPE68 (Rv3873) $_{138-152}$ (DYFIRMWNQAALAME), RpfA (Rv0867c) $_{377-391}$ (AYTKKLWQAIRAQDV), and TB10.4 (Rv0288) $_{21-35}$ (YAGTLQSLGAEIAVE)	TrxA-tag +6 HTL (GGGGS) + His-tag	Humanized C57BL/6 mice and wild- C57BL/6 mice	30 μg MP3RT per mouse/s.c. Two booster (20 μg) at the interval of 2 weeks	TLR9 agonist CpG-ODN2395	*Mtb* H37Rv strain (2 × 10^5 CFUs/tail vein injection)	Inducing protection characterized by high levels of IFN-γ and $CD3^+$IFN-γ^+ T lymphocytes
(245)	MPT64 (Rv1980c) $_{190-198}$ (FAVTNDGVI)	AMM (Ag85B-Mpt64 $_{190-198}$ -Mtb8.4)	C57BL/6 mice	5×10^5 CFU of BCG prime followed by 20 μg of AMM plus 250 μg of DDA and 30 μg of BCG PSN/s.c. Boosting twice at weeks 8 and 10	250 μg of DDA and 30 μg of BCG PSN	*Mtb* H37Rv strain (1×10^6 CFUs/i.v.)	AMM induced stronger humoral and cell-mediated immune responses than Ag85B alone and could boost BCG-primed immunity and lead to a better protection than BCG alone or BCG-prime followed by Ag85B-boost.
(246)	MPT64 (Rv1980c) $_{190-198}$ (FAVTNDGVI)	AMH (Ag85B-Mpt64$_{190-198}$ -HspX) AMM (Ag85B-Mpt64 $_{190-198}$ -Mtb8.4)	C57BL/6 mice	5×10^5 CFU of BCG prime followed by 10 μg of AMM and 10 μg of AMH plus 250 μg of DDA and 30 μg of BCG PSN/s.c. Boosting twice at weeks 8 and 10	250 μg of DDA and 30 μg of BCG PSN	*Mtb* H37Rv strain (1×10^6 CFUs/i.v.)	Boosted with AMM + AMH had significantly lower bacterial count in the lungs than those receiving BCG, whereas mice boosted with AMH or AMM did not.
(247)	MPT64 (Rv1980c) $_{190-198}$ (FAVTNDGVI)	ESAT6 + Ag85B + MPT64$_{(190–198)}$ + Mtb8.4-Rv2626c	C57BL/6 mice	13 μg/dose/mouse, s.c., 3 times at 2-week intervals	250 μg DDA and 50 μg TLR3 agonist Poly (I:C)	*Mtb* H37Rv strain (50-100 CFUs/aerosol)	Generated strong antigen-specific humoral and cell-mediated immunity, and induced higher protective

(Continued)

TABLE 3 | Continued

Reference	Protein and peptide (sequences)	Formulation (likers or adjuvant)	Host organism	Dose/route	Adjuvant	Challenge	Efficacy
(203)	Rv1733c $_{57–84}$ (IPFAAAAGTAVQDSRSHVYAHQAQTRHP)	Synthetic long peptide (SLP) with CpG ODN1826 adjuvant	HLA -DRB1*0301/ DRA transgenic mice	25μg Rv1733c p63-77, or Rv1733c p57-84 peptide with CpG/ mouse/s.c., 3 times, with a 2-week interval	TLR9 agonist CpG ODN1826	*Mtb* H37Rv strain ($1×10^6$ CFUs/i.n.)	efficacy than BCG Had the highest reduction (0.92 log) in bacterial load in their lungs (from 3.6 × 10^5 to 0.44 × 10^5) compared to mice vaccinated only with BCG.

AcMNPV, Autographa californica multicapsid nucleopolyherovirus; BCG PSN, BCG polysaccharide nucleic acid; DDA, N, N'-dimethyl-N, N'-dioctadecylammonium bromide; FL, fms-like tyrosine kinase 3 ligand; IFA, Incomplete Freund's Adjuvant; RVG, Rabies Virus Glycoprotein; MPLA, Monophosphoryl lipid A; Pam2Cys, lipid moiety S-[2,3-bis(palmitoyloxy)propyl] cysteine; PBMC, Peripheral blood mononuclear cells; p.i., postinfection; Poly (I: C), polyribocytidylic acid; s.c., subcutaneous injection; i.m., intramuscular injection; i.v., intravenous injection; i.n., intranasally; i.p., intraperitoneal injection; †: Rv0203 (TRRRLLAVLIAL), Rv3106 (GHRRMVFRFLTSPIEI), Rv2223c (WRRRPLSSALLSFGLLLGGLPL), Rv3201c (GQLLRRVRSRLARL), Rv3296 (RVILHSPYGLRVHGPLAL), Rv1242 (FLRIATSARVLAAPLPT), Rv1184c (LVPVNHLPLTLPL), Rv3207c (QGGLAPVMMQQTFST), Rv1157c (TQLLMAAASA), Rv1158c (GVNAPIPGI), Rv1291c (FTRRFAASMVG), Rv1860 (RKGRLAALAIA), Rv2190c (ARVIMRSAIG), Rv333c (VMRLYPVRLTTTMTR), Rv0309 (SVVMGVNKAK); ‡These 21 PE/PPE peptides can be found at https://doi.org/10.1016/j.bbrc.2018.06.017.

IFN-γ (234). Similarly, a year later, McMurry J et al. also identified 15 MHC II binding epitopes by bioinformatics tools and ELISPOT, these peptides from 15 antigens of *M. tuberculosis* could stimulate the PBMCs obtained from healthy or asymptomatic tuberculin skin test-positive donors producing high levels of IFN-γ (197). Although both studies simply validated potential peptides *in vitro*, they provide new insights into the development of peptide-based vaccines.

With the deepening of the understanding of epitopes, studies on evaluating the immunogenicity of peptides began to shift from *in vitro* experiments to *in vivo* experiments. Wang QM et al. constructed a pcDNA3-M-38 vaccine consisting of a pcDNA3 vector and two MHC II binding peptides MPT64 $_{190-198}$ (FAVTNDGVI) and 38 kDa proteins $_{166-175}$ (IAALNPGVNL). The results showed that immunization with the p3-M-38 vaccine could induce epitope-specific $CD8^+$ CTL response in C57BL/6 (H-2b) mice (235). Recently, a study constructed a new peptide-based vaccine, PstS1p, which consists of PstS1 $_{169-405}$ and PstS1 $_{802-1119}$ peptides (237). The immunity and immunogenicity of the PstS1p vaccine and PstS1 (Rv0934) protein were evaluated in BALB/c mice. The results showed that both vaccines elicited remarkably higher levels of IgG antibodies and IFN-γ as well as IL-2 Th1-type cytokines (237). Interestingly, the PstS1p peptide-based vaccine showed more potent immunogenicity than the PstS1 vaccine, indicating that the peptide-based vaccine has better prospects than the traditional subunit vaccine.

These studies indicate an excellent method to construct peptide-based vaccines using bioinformatics technology to predict the dominant epitopes and ELSPOT technology for *in vitro* validation and screening. However, the immunogenicity of peptide-based vaccines containing only dominant epitopes is not ideal, and the addition of adjuvants or helper peptides can significantly improve the immunogenicity of peptide-based vaccines. Garnica O et al. used RVG peptide (YTIWMPENPRPGTPCDIFTNSR) to enhance the immunogenicity of Ag85B $_{96–111}$ (QDAYNAAGGHNAVFN) and Ag85B $_{241–256}$ (PAFEWYYQSGLSIVMP) peptides (236). They observed that stimulation with RVG peptide fused Ag85B $_{96–111}$ or Ag85B $_{241–256}$ peptide can improve the antigen presentation ability of mouse bone marrow derived DCs (BMDCs) and human THP-1 macrophages. Furthermore, the number of IFN-γ, IL-2, and TNF-α producing cells were significantly higher in mice immunized with RVG peptide fused Ag85B 241–256 peptide than in mice immunized with Ag85B $_{241–256}$ peptide only (236). These results reveal that helper peptide RVG may be a promising adjuvant to developing effective peptide-based TB vaccines. The limitation of these studies is that the animal models used were wild-type mice. Still, the MHC molecules of mice and humans are significantly different, which may result in the failure of a peptide-based vaccine in clinical trials, which has been proved to have an excellent protective effect in the mouse model (2). To overcome this disadvantage, De Groot AS et al. developed HLA-DR B*0101 transgenic mice to evaluate the immunogenicity of a DNA multi-epitope vaccine that contains 24 epitopes derived from Antigen 85 complex, MPT 64, MPB/MPT 70, MPT 63, the 38 kDa, 14-kDa, 16-kDa, 19-kDa, and 32-kDa Mtb proteins (198). The results found that 8 of the 24 epitopes induced immune responses in these HLA-DR B*0101 transgenic mice.

3.2 Peptide-Based TB Vaccines Evaluated for Protective Efficacy in Animal Models

Previous studies on TB subunit vaccines have provided a large number of vaccine candidate antigens for peptide-based vaccines development, such as Ag85A (Rv3804c) (241), Ag85B (Rv1886c) (116, 202, 239, 240), 6-kDa early secretory antigenic target (ESAT-6, Rv3875) (222, 223, 238, 239), heat shock protein HspX (also known as Hsp16.3, Acr, and 14 kDa antigen, Rv2031c) (115, 146, 202, 210, 211, 242), TB10.4 (Rv0288) (2, 115, 211, 240), Rv0476 (211), Hsp65 (202), 19-kDa lipoprotein (Rv3763) (202), Rv1733c (202, 203), PE/PPE proteins (2, 243, 244, 248), MPT64 (Rv1980c) (246, 247), Mtb8.4 (2), and

resuscitation-promoting factors (Rpfs) (2, 228). These antigens have been reported to be attractive vaccine candidates for preventing and controlling TB. Herein, we will summarize the peptide-based vaccines developed from these protective antigens.

3.2.1 Peptide-Based Vaccines Derived From ESAT-6 Family Proteins

ESAT-6 family antigens are low-mass fractions of culture filtrates of *M. tuberculosis* (249). Previous studies reported that ESAT-6, CFP10, and TB10.4 antigens belong to ESAT-6 family members, they play an essential role in TB pathogenesis and induced significantly enhanced humoral and cellular responses in animal models or clinical trials (250–256). This evidence lay the foundation for constructing peptide-based vaccines based on ESAT-6 family antigens. Aagaard CS et al. identified an immunodominant peptide ESAT-6 (Rv3875) $_{1-15}$ (MTEQQWNFAGIEAAA) that can be recognized by the splenocytes of CB6F1 mice and triggered a significant release of IFN-γ (223). To further investigate the role of ESAT-6 $_{1-15}$ epitope in ESAT-6 full-length antigen, they compared the protective efficacy of a full-length ESAT-6 vaccine and a Δ15ESAT-6 vaccine with the absence of ESAT-6 $_{1-15}$ epitope. Surprisingly, although both vaccines decreased bacterial numbers of the lung at the early time point, only the Δ15ESAT-6 vaccine revealed significant protection at the long time point (223). These data suggest that the ESAT-6 $_{1-15}$ immunodominant epitope may negatively affect the full-length ESAT-6 vaccine, reminding that excluding some epitopes may be a potential approach to construct a more protective vaccine. Besides ESAT-6 $_{1-15}$ epitope, other immunodominant epitopes of ESAT-6 antigen were also determined by different studies. Olsen AW et al. investigated the vaccine potential of two peptides, ESAT-6 $_{1-20}$ (MTEQQWNFAGIEAAASAIQG) and ESAT-6 $_{51-70}$ (YQGVQQKWDATATELNNALQ), in B6CBAF1 (H-2b,k) mice. The results showed that both peptides were recognized by $CD4^+$ T cells and induced a significantly higher IFN-γ release, but only the vaccine based on the ESAT-6 $_{51-70}$ peptide promoted significant protection against *M. tuberculosis* infection (222).

More recently, Jiang Q et al. constructed a recombinant DNA vaccine (pIRES-epitope-peptide-FL) encoding three T cell peptides of ESAT-6 antigen, including ESAT-6 $_{4-18}$ (QQWNFAGIEAAASAI), ESAT-6 $_{22-36}$ (VTSIHSLLDEGKQSL), and ESAT-6 $_{56-70}$ (QKWDATATELNNALQ) peptides (238). Results revealed that pIRES-epitope-peptide-FL vaccination increased the proliferation of IFN-γ^+ T cells, induced significantly higher levels of IFN-γ and IL-12 but relatively lower levels of IL-4 and IL-10, and enhanced protection from *M. tuberculosis* challenge in C57BL/6 mice (238). The results of the above studies suggest that there is competition between ESAT-6 $_{1-15}$ or ESAT-6 $_{1-20}$ epitope and other epitopes of ESAT-6 antigen, and ESAT-6 $_{1-15}$ and ESAT-6 $_{1-20}$ epitopes may weaken the recognition ability of other epitopes to MHC molecule (222). It may explain why the Δ15ESAT-6 vaccine or ESAT-6 51–70 peptide vaccine is more protective than the ESAT-6 vaccine or ESAT-6 $_{1-20}$ peptide vaccine. These results provide a new strategy that synthetic long peptides (SLPs) in peptide-based vaccine design may attenuate the adverse effects of some epitopes and improve the immunogenicity and vaccine efficacy (116). Furthermore, ESAT-6 is a virulence factor secreted by *M. tuberculosis*, the safety of this protein and their peptides should be considered in designing a peptide-based vaccine.

3.2.2 Peptide-Based Vaccines Derived From Ag85A and Ag85B Proteins

M. tuberculosis Ag85 complex consists of three homologous proteins, including Ag85A (Rv3804c), Ag85B (Rv1886c), and Ag85C (Rv0129c), which induce strong humoral and cellular immune responses (257). They play critical roles in virulence, preventing the formation of phagolysosomes and drug-resistant TB of the pathogen (258). Therefore, Ag85 complex proteins have been utilized by scientists to construct TB vaccines, such asrBCG30 (259), AERAS-422 (rBCG::Ag85A-Ag85B-Rv3407) (260), MVA85A (AERAS-485) (261), Ad35/AERAS-402 (262), Ad5Ag85A (262), ChAdOx1.85A (263), and AEC/BC02 (264). Previous studies have shown that Ag85A and Ag85B proteins are rich in epitope resources, giving them a distinct advantage in constructing peptide-based vaccines (257, 265). Kumar S et al. generated a vaccine mixture (peptide-TLR agonist-liposomes, abbreviation for PTL), consisting of three Ag85B peptides, four ESAT-6 peptides, TLR2 agonist Pam3Cys-SK-4, and TLR9 agonist CpG ODN (**Table 3**) (239). Interestingly, the BCG-PTL coimmunization enhanced the proportion of vaccine-induced Tcm cells and polyfunctional cytokine responses and increased the defensive efficiency against TB compared with BCG vaccination (239). Linear T cell epitopes are usually short and therefore less immunogenic and stable *in vivo*. It is an effective strategy to enhance the immunogenicity and presentation of epitopes by using conjugation and palmitoylation approaches. To investigate this strategy, Horváti K et al. developed three peptide-based vaccines termed A/P/I mix, A(P)I, and Pal-A(P)I, respectively (116). The similarity of the three vaccines is that they consist of Ag85B $_{239-247}$ (KLVANNTRL), isoniazid inductible gene protein IniB (Rv0341) $_{33-45}$ (GLIDIAPHQISSV), and PPE68 (Rv3873) $_{127-136}$ (FFGINTIPIA) peptides. The difference is that A/P/I mix is a mixture of three peptides, A(P)I is a conjugation of three peptides separated with a tuftsin sequence (TKPKG), and Pal-A(P)I is the palmitoylated A(P)I. As expected, the internalization rates of A(P)I and Pal-A(P)I vaccines were higher than these of A/P/I mix in human murine bone marrow-derived macrophages (BMDMs) or MonoMac6 human monocytes (MM6), especially the Pal-A(P)I vaccine. Immunization with Pal-A(P)I vaccine induced significantly higher levels of splenocytes proliferation and Th1-type cytokines, and lower numbers of bacteria in the lung or spleen of mice. This exploration suggests that conjugation and palmitoylation are a promising route to enhance the immunogenicity and protective efficacy of peptide-based vaccine.

In addition to the conjugation and palmitoylation routes described above, other novel vaccination strategies have been developed to design peptide-based vaccines. Recently, Chesson

CB et al. reported a vaccination strategy based on self-assembling peptide-nanofibers to present TB10.4 (Rv0288) $_{4–11}$ (IMYNYPAM) and Ag85B (Rv1886c) $_{280–294}$ (FQDAYNAAGGHNAVF) peptides (240). It was found that intranasal immunization with self-assembling peptide-nanofibers induced an 8-fold expansion in multifunctional $CD8^+$ T cell populations and bacterial loads in the lungs of mice primed with BCG and boosted intranasally with co-assembled nanofibers of TB10.4 $_{4–11}$ peptide and Pam2Cys adjuvant showed a 1.3 log10 CFUs reduction compared to naïve mice (240). Thus, the utilization of new materials or adjuvants can significantly improve the immunogenicity and protection efficiency of peptide-based vaccines. Furthermore, the BCG prime-boost strategy can also considerably enhance the protection efficiency of peptide-based vaccines. Sugawara I et al. confirmed the prime-boost strategy by developing a recombinant (Ag85A) BCG vaccine, an Ag85A DNA vaccine, and an Ag85A (Rv3804c) $_{141\text{-}160}$ peptide (241). The results presented that the recombinant BCG Tokyo (Ag85A) or Ag85A DNA vaccination boosted with Ag85A $_{141\text{-}160}$ peptide could remarkably reduce pathological lesions and CFUs burden in the lung of guinea pigs.

3.2.3 Peptide-Based Vaccines Derived From 16-kDa Alpha-Crystallin (Acr, Rv2031c) Protein

Acr, also known as HspX and Hsp16.3, is a heat shock protein localized in the inner membrane. This protein plays an essential role in maintaining the long-term survival during latent or asymptomatic infection and slowing the growth of *M. tuberculosis* in the early stage of active disease (266, 267). Previous study has suggested it as a subunit vaccine candidate (268). Currently, three peptides from Acr protein have been used to develop peptide-based vaccines, including Acr $_{31–50}$ (LRPTFDTRLMRLEDEMKEGR), Acr $_{91–104}$ (SEFAYGSFVRTVSL), and Acr $_{91–110}$ (SEFAYGSFVRTVSLPVGADE) peptides (**Table 3**). Shi C et al. compared the immune responses and protection of Acr protein vaccine and its peptide Acr $_{91–104}$ mixed with TLR4 agonist DDA-MPLA (N, N'-dimethyl-N, N'-dioctadecylammonium bromide-Monophosphoryl lipid A) on BALB/c mice. They observed that, compared to the BCG vaccine, both vaccines induced significantly higher levels of antibodies, splenolymphocyte proliferation, lower levels of IFN-γ, and equivalent protection (242). Two previous studies constructed a peptide-based vaccine termed L91 by linking Acr $_{91–110}$ (SEFAYGSFVRTVSLPVGADE) peptide to TLR-2 agonist Pam2Cys. Both studies found similar results that L91 vaccination stimulated significantly higher levels of Th1 and Th17 immune responses and induced significantly lower CFUs in the lungs of BALB/c mice or Duncan-Hartley guinea pigs than BCG vaccine (146, 210). The possible immune protective mechanism of the L91 vaccine is to reduce the inhibitory effect of *M. tuberculosis* on APCs by enhancing the expression of NF-κB and iNOS (146, 269). Interestingly, to achieve better protection, Rai, PK et al. improved the L91 vaccine by incorporating a CD8 T cell epitope TB10.4 $_{20\text{-}28}$ (GYAGTLQSL), and the new peptide-based vaccine was named as L4.8 (115). The results showed that the L4.8 vaccination elicited significantly higher levels of $CD4^+$ and $CD8^+$ T cells immunity, and the BCG-L4.8 prime-boost strategy resulted in better protection against *M. tuberculosis* infection than L91 and BCG vaccines. It can be seen from the above studies that peptide-based vaccines using both HTL and CTL peptides as well as agonists or helper peptides can induce stronger $CD4^+$ and $CD8^+$ T cell immunity to improve their protective effect (115, 270).

Furthermore, two additional studies were performed to improve the immunogenicity and protection of Acr $_{91\text{-}110}$ peptide by adding other peptides, such as TB10.4 $_{1\text{-}13}$ (MSQIMYNYPAMLG), TB10.4 $_{78\text{-}94}$ (ANTMAMMARDTAEAAKW), Rv0476 $_{1\text{-}19}$ (MLVLLVAVL VTAVYAFVHA), CFP10 (Rv3874) $_{71\text{-}90}$ (EISTNIRQAGVQ YSRADEEQ), Acr $_{21\text{-}40}$ (LFAAFPSFAGLRPTFDTRLM), Hsp65 (Rv0440) $_{3–13}$ (KTIAYDEEARR), Ag85B (Rv1886c) $_{56–64}$ (PSMGRDIKV), 19 kDa (Rv3763) $_{51–61}$ (KVVIDGKDQNV), Acr $_{31–50}$ (LRPTFDTRLMRLEDEMKEGR) and Rv1733c $_{63–77}$ (AGTAVQDSRSHVYAH) (202, 203). As expected, the results revealed that peptide-based vaccine with multi-peptides could induce significantly higher levels of IgG antibodies, IFN-γ, TNF, and IL-2 cytokines, and lower CFUs in lungs of C57BL/6 mice (211) or HLA-DR3 transgenic mice (202).

3.2.4 Peptide-Based Vaccines Derived From PE/PPE Family Proteins

In *M. tuberculosis*, PE/PPE family has up to 167 members, most of which are located on the surface of *M. tuberculosis* or secreted out of the bacteria and can be well recognized by the host immune system. Despite the function of most PE/PPE family members is still unknown, accumulating studies indicate that PE/PPE family members related to the ESAT6 family are considered as "immunogenicity islands" due to their high immunogenicity and immunopathogenic (271; 248). This evidence suggests that PE/PPE proteins may be promising candidates for the design of peptide-based vaccines. Wu M et al. designed a multi-epitope DNA vaccine termed as pPES by grafting four Th1 epitopes ESAT-6 $_{1–20}$ (MTEQQWNFAGIEAAASAIQG), Ag85B $_{241–255}$ (VANNTRL WVYCGNGT), PE19 (Rv1791) $_{4–18}$ (VTTQPEALAAAAANL), PPE25 (Rv1787) $_{241–255}$ (AQFFASIAQQLTFGP), and a CTL epitope MTB10.4 (Rv0288) $_{3–11}$ (QIMYNYPAM) into Hsp65 (Rv0440) scaffold protein (243)**.** pPES vaccination generated HSP65-specific antibodies, induced higher levels of IFN-γ^+CD4^+ T cell response, multi-functional $CD4^+$ T cell response, cytotoxic $CD8^+$ T cell response, and lower bacterial loads in lungs and spleens of mice (243). These data indicated that epitope grafting did not reduce the immunogenicity of HSP65 protein, and epitope grafting strategy may be a potential method to construct peptide-based vaccines. A study identified 21 immunodominant peptides from 167 proteins of the PE/PPE family and constructed three peptide-based vaccines by fusing these peptides to ESAT-6 protein, including PE peptides + ESAT-6 (shorten as PE-ESAT-6), PPE peptides + ESAT-6 (PPE-ESAT-6), and PE + PPE peptides + ESAT-6 (PE/PPE-ESAT-6) (244). The results showed that, compared to control, PE/PPE-ESAT-6 immunization induced significantly higher levels of IFN-γ, multifunctional $CD4^+CD44^+CD62L^-$ T cells, and lower CFUs loads in lungs and/or spleens of C57BL/6J mice.

We recently developed a novel peptide-based vaccine termed as MP3RT (2). This vaccine is made up of six immunogenicity HTL

peptides, including Mtb8.4 (Rv1174c) $_{69-83}$ (LRNFLAAPPPQRAAM), PPE18 $_{115-129}$ (RAELMILIATNLLGQ), PPE18 (Rv1196) $_{149-163}$ (AAAMFGYAAATATAT), PPE68 (Rv3873) $_{138-152}$ (DYFIRMWNQAALAME), RpfA (Rv0867c) $_{377-391}$ (AYTKKLWQAIRAQDV), and TB10.4 (Rv0288) $_{21-35}$ (YAGTLQSLGAEIAVE). To evaluate the effect of epitope MHC restriction on the immunogenicity and protective efficiency of the MP3RT vaccine, humanized C57BL/6 mice and wild- C57BL/6 mice were used. Our results showed that MP3RT induced significantly higher levels of IFN-γ and $CD3^+IFN\text{-}\gamma^+$ T lymphocytes and lower CFUs in the lungs and spleens of humanized mice rather than wild-type mice (2). The same method was used to evaluate other peptide-based vaccine named as ACP that only contains three peptides Ag85B (Rv1886c) $_{12-26}$ (GRRLMIGTAAAVVLP), CFP21 (Rv1984c) $_{12-26}$ (VVVATT LALVSAPAG), and PPE18 (Rv1196) $_{149-163}$ (AAAMFGYAAATA TAT) (9). We found that although ACP induced significant humoral and cellular immune responses in humanized mice, its protective efficiency was not significantly better than that of the phosphate buffer solution (PBS) control. Taken together, these data once again demonstrated that grafting or fusion of multiple immunodominant epitopes on the protective antigen skeleton could significantly improve the immunogenicity and protection efficiency of the antigen, and these findings provide new ideas for the construction of peptide-based vaccines for TB.

3.2.5 Peptide-Based Vaccines Derived From MPT64 (Rv1980c) Protein

The MPT64 protein is an immunogenic protein initially isolated from the culture filtrate of the BCG Tokyo strain (272). Previous studies have shown that MPT64 protein contains T or B cell epitopes, inducing strong humoral or cellular immune responses (273). Therefore, MPT64 protein is a promising candidate for constructing a peptide-based vaccine. Peptide MPT64 $_{190-198}$ (FAVTNDGVI) has received more attention in recent years. Professor Zhu BD et al. developed a peptide-based vaccine Ag85B-MPT64(190-198)-Mtb8.4 (named as AMM). They investigated its immunogenicity and capacity to boost BCG-primed immunity in a DDA-BCG PSN adjuvant (dimethyl-dioctyldecyl ammonium bromide and BCG polysaccharide nucleic acid). They found that BCG-AMM prime-boost vaccination induced significantly higher levels of immune responses and better protection than BCG or AMM vaccination alone (245). Subsequently, they further confirmed this vaccine and developed a novel vaccine named AMH that consists of Ag85B-MPT64(190-198)- HspX (246). Compared with the mice receiving BCG only, the mice boosted with AMH, AMM, or their combination (AMH+AMM) showed significantly higher levels of specific antibodies and IFN-γ^+ T cells. In addition, the mice boosted with the combination of AMM and AMH had substantially lower bacterial counts in the lungs, whereas mice boosted with AMH or AMM did not. Heterogeneity of protective effect of AMM vaccine in both studies may be related to vaccine dose. Analysis of the two studies showed that all parameters were identical except the vaccine dose. In their first study, they used 20 μg of the AMM vaccine, but in the second study, the vaccine dose was reduced to 10 μg. It indicates that vaccine dose significantly affects its protection efficiency, suggesting that future studies should select an appropriate vaccine dose to immunize mice to avoid vaccine failure due to this factor.

More recently, Zhu's team modified and upgraded the AMM vaccine and constructed a new peptide-based vaccine called LT70, which consists of ESAT6-Ag85B-MPT64(190-198)-Mtb8.4-Rv2626c (247). They observed that LT70 was well recognized by T cells obtained from TB patients and LTBI volunteers and induced dramatically higher levels of cellular and humoral immunity as well as protective efficacy compared to BCG vaccine or PBS control in C57BL/6 mice. There were significant differences in experimental design between this study and the previous two studies. For example, the vaccine dose was adjusted to 13 μg, BCG-PSN adjuvant was replaced by Poly (I:C) adjuvant, and the route of the challenge was changed from intravenous injection to respiratory aerosol inhalation. These optimizations and improvements have contributed to the improved immune protection efficiency of the LT70 vaccine.

3.2.6 Peptide-Based Vaccines Derived From Rv1733c Protein

Rv1733c is a probably conserved transmembrane protein of *M. tuberculosis* and belongs to dormancy survival regulon antigens (DosRs) related to LTBI (5). Rv1733c protein has been considered an immunopotent T cell candidate of the 45 top-ranking antigens (274). Black GF et al. compared the immunogenicity of 51 DosR regulon-encoded *M. tuberculosis* recombinant proteins among 131 individuals from Uganda, Gambia, and South Africa. They found that of the 51 DosRs, Rv1733c is one of the most frequently recognized DosRs in all three population groups (275). Furthermore, it has been shown that Rv1733c also induces strong IFN-γ response in T cells collected from tuberculin skin test positive (TST^+) individuals (276) and a Rv1733c DNA prime followed by boosting with Rv1733c protein increased T cell proliferation and IFN-γ secretion in mice (277).

Thus, it can be seen that Rv1733c has good immunogenicity and is expected to be a new vaccine candidate for fighting against LTBI. Coppola M et al. investigated an SLP Rv1733c $_{57–84}$ (IPFAAAAGTAVQDSRSHVYAHQAQTRHP) derived from Rv1733c protein and assessed its immunogenicity and protective capacity in HLA-DRB1*0301/DRA transgenic mice (203). After three times' immunization, the mice vaccinated with Rv1733c SLP and TLR9 agonist CpG ODN1826 showed significantly higher levels of IFN-γ^+ TNF^+ and IFN-γ^+ $CD4^+$ T cells and Rv1733c protein-specific antibodies. Interestingly, compared with mice vaccinated with BCG only, the mice primed with BCG and boosted with Rv1733c SLP revealed the highest reduction in CFUs burdens in lungs (203). Furthermore, Geluk A et al. also evaluated the immunogenicity of another peptide Rv1733c $_{63–77}$ (AGTAVQDSRSHVYAH) in HLA-DRB1*03:01/DRA transgenic mice. It was found that Rv1733c $_{63–77}$ stimulated significantly higher levels of IFN-γ in splenocytes harvested from HLA-DR3 mice infected with *M. tuberculosis* and

showed higher levels of IFN-γ^+, TNF^+, or IL-2^+ $CD4^+$ T cells (202). These data suggest that Rv1733c SLP may be a potential booster vaccine for TB.

4 PROTEIN-BASED BACTERIAL VACCINE DELIVERY SYSTEM

In recent years, subunit vaccines, especially peptide-based vaccines with more single and safer components, have gradually become new vaccine forms. However, their weak immunogenicity makes it difficult to induce an adequate immune response and thus often need adding additional adjuvants. With the development of immunology, the delivery system, which aims to enhance antigens targeting secondary lymphoid organs and the activation of APCs, is continuously developed and applied in the vaccine design. Although many potential delivery systems have been widely explored in therapeutic vaccines, there have not been thoroughly studied in prophylactic vaccines because of the higher requirements for the safety of the materials usually applied in healthy people, even the elderly and children. With that in mind, more compatible and safer protein-based delivery vectors have great potential in prophylactic vaccine research (**Table 4**).

4.1 Self-Assembled Proteinaceous Nanoparticles

Some proteins can assemble into particles of a specific size under natural conditions and have been developed as great delivery systems. One kind is virus-like particles (VLPs) which are artificial nanostructures that self-assembled after the expression of viral capsid protein. It has been reported that poly (ribosylribitolphosphate) (PRP) polysaccharide of Hib was connected to Hepatitis B virus surface antigen (HBsAg) VLP *via* an adipic acid dihydrazide (ADH) spacer, and stronger IgG antibodies to both the PRP were induced than a commercial conjugate vaccine in mice (279). Similar, VLPs (e.g., Qβ and HBsAg) could also chemically load S. pneumonia capsular polysaccharide. The VLP vaccines could induce serotype-specific IgG antibodies. With synthetic biology and protein glycosylation system development, a new and simpler coupling method between polysaccharide antigens and protein has been explored. Li X. et al. successfully prepared the Shigella conjugate vaccine by using bacterial *in vivo* protein glycosylation reaction to couple the complete pathogenic bacterial polysaccharide to VLP (AP205) for the first time (281, 364). This VLP based conjugate vaccine showed better immune and protective effects in mice than the conventional vector. Besides, flock house virus VLP and bacteriophage T4 nanoparticle vaccine were explored and exhibited good protection against the challenge (282, 283). Designable self-assembled nanoparticle is another kind of self-assembled proteinaceous delivery vector used in pathogenic bacterial vaccines. Due to its modular design, it is a promising protein vector, which has shown good development potential in the development of vaccines such as viruses, but it seems to have just begun in the field of bacteria. Pan et al. developed a Nano-B5 system to produce self-assembled nano vaccines by fusion expression of bacterial B5 toxin and trimeric peptide and connected polysaccharide antigen through glycosylation in the pathogenic host (284). This particle was about 25 nm, which prolonged retention in draining lymph nodes and could stimulate strong cellular and humoral immune responses. Further, the system could be introduced into a modified *E. coli* host to prepare exogenous pathogenic bacteria, such as *Klebsiella pneumoniae*, nano-scaled conjugate vaccine and protect mice from systemic and pulmonary infection (285). Polysaccharide conjugate vaccine is considered the most successful bacterial vaccine at present. Although immunogenicity of carbohydrate antigen itself is very weak, it could be significantly improved by conjugating them (either synthetic short sugar chain or natural polysaccharide) with proteinaceous nanoparticles. Thus, self-assembled proteinaceous has excellent potential to enhance weak antigen immunogenicity and be used in the bacterial vaccine.

4.2 Viral Vector

Vaccines consist of a non-replicating virus that contains certain genetic material from the pathogen that needs to be immunized. It seems to be an ideal vaccine delivery system because of its natural viral structure, which can be well recognized by the immune system (365). The adenovirus vector is widely used (366) to develop a bacterial vaccine. Other viral vectors (e.g. influenza viral and semliki forest virus) have also been explored. McConnell M J et al. described a replication-incompetent adenovirus expressing domain 4 (D4) of *B. anthracis* protective antigen (PA) (Ad.D4), which could induce a more robust humoral and cellular immune responses than anthrax vaccine absorbed (AVA) (the only one FDA-approved anthrax vaccine which needs to be vaccinated six times within 18 months and enhanced once each year) (367) and provide complete protection against lethal spore challenge in single immunized mice (286). However, pre-existing immunity to Ad in humans may inhibit subsequent immunization-induced antibody responses. Influenza viral vectors may be another promising one for human use because of the lack of pre-existing immunity, safety and immunogenicity, which have been demonstrated in various models (chickens, ferrets and rhesus macaques and humans) (368–370). Tabynov K et al. developed recombinant influenza A viruses of the subtypes H5N1 and H1N1 expressing *Brucella* protective antigen (ribosomal protein L7/L12 or Omp16) and strong cellular immune response and protection effect were induced (291). Moreover, these vaccines with adjuvant could provide long term protection for cattle and induced good cross-protection against *B. melitensis* infection in pregnant heifers and even sheep and goats (371–375). However, influenza viruses expressing *B. anthracis* PA unable to induced *in vitro* anthrax toxin neutralization activity antibodies, although the titers against PA were high (287, 376). Interesting, this situation could be solved by heterologous prime/boost immunization strategy, which may be attributed to the B-cell affinity maturation and Ig gene high-frequency mutation in germinal centres by combining different heterologous vectors. Moreover, antigen epitopes ($PA_{232–247}$ and $PA_{628–637}$) also could be expressed in a plant-virus Tobacco Mosaic Virus (TMV).

TABLE 4 | Protein-based bacterial vaccine delivery systems.

Delivery systems	Antigens	Targeted pathogens	Adjuvant	References
Self-assembled proteinaceous nanoparticles				
VLP				
HBsAg	Capsular polysaccharide 33F	*S. pneumoniae*	—	(278)
	PRP polysaccharide	*H. influenzae type b*	—	(279)
	Vi polysaccharide	*S. typhi*	—	(279)
Qβ	TS3 and TS14 (capsular polysaccharides repeated units)	*S. pneumoniae*	—	(280)
AP205	O-polysaccharide	Shigella	—	(281)
Flock house virus	PA	*B. anthracis*	—	(282)
T4 Bacteriophage	PA	*B. anthracis*	—	(283)
	Mutated capsular antigen F1 and low-calcium-response V antigen	*Y. pestis*	—	(282)
Designable self-assembled nanoparticle				
	O-polysaccharide	Shigella	—	(284)
	O-polysaccharide	*S. Paratyphi A*	—	(284)
	O-polysaccharide	*K. pneumoniae*	—	(285)
Live viral vector				
	PAD4; PA	*B. anthracis*	—	(286–288)
	Cu-Zn SOD; IF3; L7/L12; Omp16; Omp19	Brucella	—	(289–292)
	D2 domain of FnbpB	*S. aureus*	—	(293)
Bacterial vectors				
Probiotics	PsaA; PspA; PspA5; PppA; PspC	*S. pneumoniae*	—	(294–300)
	Fusion of ST and LTB; F41; K99 fimbriae; β-Intimin fragment; Fusion of K99, K88 fimbriae; FaeG; FaeG with DC-targeting peptide; EspA and the Tir central domain; PapG	*E. coli*	Without, or LTB mutated LTA and LTB	(301–311)
	CTB	*V. cholerae*	—	(312)
	FliC or fusion of FilC and SipC	*S. enterica serovar Enteritidis*	—	(313, 314)
	PA; PA with DC-targeting peptide	*B. anthracis*	—	(315–319)
	L7/L12, Cu-Zn SOD, Omp31	Brucella	—	(320–322)
	ClfA and FnbpA; B-cell epitope, D3(22–33), from FnbpA	*S. aureus*	Without or Freund's adjuvant	(323, 324)
	Hp0410; Urease B subunit	*H. pylori*	—	(325, 326)
	LcrV	*Y. pestis*	—	(327)
GEM	PppA; IgA1p; PpmA; SlrA	*S. pneumoniae*	—	(299, 328)
	PTd, FHA, and PRN	*B. pertussis*	—	(329)
	CUE	*H. pylori*	—	(330, 331)
	Omp31	Brucella	—	(322)
S. enterica	PA, PAD1 and 4, and PAD4	*B. anthracis*	—	(332)
Attenuated *S. typhimurium*	L7/L12; Fusion of L7/L12 and BLS	Brucella	—	(333, 334)
	SaEsxA and SaEsxB	*S. aureus*	—	(335)
Ochrobactrum anthropi	Cu-Zn SOD	Brucella	CpG	(336)
OMV				
	OMV components	*K. pneumoniae*	—	(337)
	OMV components	*B. pertussis*	—	(338–340)
	OMV components	*E. coli*	—	(341)
	OMV components	Shigella	Without or Alhydrogel	(342–345)
	OMV components	*V. cholerae*	—	(346, 347)
	OMV components	*S. typhimurium*	—	(348)
	OMV components	*S. typhi and paratyphi A*	—	(349)
	HlaH35L, LukE and extracellular vesicle (EV) components	*S. aureus*	—	(350, 351)
	OMV components	*H. pylori*	—	(352)

(Continued)

TABLE 4 | Continued

Delivery systems	Antigens	Targeted pathogens	Adjuvant	References
	OMV components	*Y. pestis*	—	(353)
Modified OMV				
Deposited onto bovine serum albumin nanoparticles	OMV components	*K. pneumoniae*	—	(354)
Lipid A-meditation	OMV components	*B. pertussis*	—	(355)
OMVs+Chitosan+Eudragit L-100	OMV components	*E. coli*	—	(356)
Encapsulated in polyanhydride nanoparticles	OMV components	Shigella	—	(357, 358)
Encapsulated in chitosan-tripolyphosphate particles and Eudragit L-100	OMV components	Shigella	—	(359)
Encapsulated in indocyanine green (ICG)-loaded magnetic mesoporous silica nanoparticles	EVs components	*S. aureus*	—	(360)
E. coli OMV	Glycan antigens (Polysialic acid (PSA) and T antigen)	Neisseria meningitidis group B	—	(361)
	HlaH35L, SpAKKAA, FhuD2, Csa1A, and LukE; SAcoagulase	*S. aureus*	—	(362, 363)

However, immunized mice showed almost no protection (377). Possible reasons may be the too weak immunogenicity of short epitopes or plant virus self, and a prime/boost immunization strategy can be tried.

4.3 Lactic Acid Bacteria Vector

Lactic acid bacteria are commonly used as delivery vehicles because they are safe and human friendliness and can stimulate mucosal and systemic immune responses through mucosal pathways. Many kinds of lactic acid bacteria (e.g. *L. reuteri*, *L. casei*, *L. plantarum* and *L. plantarum*) have been used as delivery vectors, of which *L. casei* is the most studied (378). Lactic acid bacteria are generally applied for the vaccine design against intestinal and respiratory infection, and there are main two strategies for antigen delivery. One is to express antigen *in vivo* directly. Studies have shown that an oral vaccine expressing *E.coli* F41 in *L. casei* can stimulate strong systemic and local mucosal immune responses simultaneously and protect mice from the lethal challenge, even still achieving more than 80% protection nine weeks after the last immunization (303, 304). In addition, Yu M et al. found that when the antigen was co-expressed with B5 toxins (such as LTB), it induced a more robust mucosal immune response and provided 100% protection (311). Moreover, even some capsular polysaccharides, such as type 3 and type 14 of *S. pneumonia*, have been successfully expressed in *L. lactis*, and the immune response of type 3 vaccine was detected, showing that *L. lactis* is a potential host for capsule vaccine antigens (379). Another strategy is using a non-genetically modified gram-positive enhancer matrix (GEM) particle for antigen delivery. The particles were prepared from living bacteria and had no nucleic acid and cytoplasmic components while maintaining the size and cell wall components of the bacteria. Multiple *S. pneumonia* protein antigens (e.g., PppA, PpmA, SlrA and IgA1p) have been anchored on the particles by a lactococcal peptidoglycan binding domain and shown to be efficacious against pneumococci in animal models (299, 328, 380). In addition, GEM loading epitope antigens also showed a significant effect. For example, when the *H. pylori* multi-epitope vaccine (CUE) (based on CTB fusing with T and B cell epitopes from *H. pylori* urease A and B subunits) was displayed on the surface of GEM, these prophylactic and therapeutic effects in orally immunized mice could further enhanced by inducing mucosal specific antibody responses and local Th1/Th17 cell-mediated immune response (330, 331), which was an optimal immunity type against *H. pylori* infection (381, 382).

4.4 Outer Membrane Vesicles (OMVs)

A large number of gram-negative bacteria naturally could produce extracellular OMVs, which is from 50 to 250 nm in diameter, suitable for targeting and being phagocytized by APCs (383). OMV contains many components, such as outer membrane proteins (OMPs) and lipoproteins, which are conducive to immune response and various immunogenic antigens. At present, the use of OMVs has become a very promising vaccination strategy. OMVs from many pathogenic bacteria (e.g. Klebsiella pneumoniae, *B. pertussis, E. coli, Shigella, Vibrio cholerae, Salmonella*, *Helicobacter pylori* and *Neisseria meningitidi*s group B) has been proved to have the ability to stimulate humoral and cellular immune responses and provide good protective effect after immunization (337, 384–386).

Because natural OMVs often contains toxic components like LPS, which could induce host inflammatory responses, many studies have focused on reducing the toxicity of OMVs by deleting the lipid A related genes (e.g. *msbB, htrB*, *pagP, lpxL*, or pagL) (355, 387–390) or toxin genes (391, 392). For example, Kim S H et al. generated OMVs from *E. coli* O157:H7 with the mutation of *msbB* (encoding an acyltransferase catalyzing the final myristoylation step during lipid A biosynthesis) and Shiga toxin A StxA. The reduced toxicity OMVs were immunized by eyedrop in BALB/c mice and showed that it was safe and could induce both humoral and mucosal immune (tear, saliva, and fecal) responses, which is enough to protect the vaccinated animal from the challenge of the lethal HUS-causative agent (wtOMVs) (341). Another example was that the knocking out of *lpxL*, which is involved in

lipid A biosynthesis, in *N. meningitidis* could result in at least a 200-fold decrease in pyrogenicity than wild-type OMV. The protective effect can be largely restored by adding adjuvants used in humans (393). In addition, Sinha R et al. reported that the OMV-mediated toxicity could be significantly reduced by being pre-treated with all-trans retinoic acid (ATRA), active metabolites of vitamin A, which are anti-inflammatory and mucosal adjuvant properties, and the immunity was enhanced (394). Fredriksen J H et al. produced a group B *N. meningitidis* OMV vaccines by including an additional step of detergent extraction (395). The detergent extracted outer membrane vesicles contain much fewer LPS (5–8%) and have been helpful in several countries (396). Moreover, a hydroquinone non-pathogenic OMV from *E. coli* was developed as delivery vehicles by expressing group B glycan antigens (361). However, most bacterial capsular polysaccharides in gram-positive bacteria are difficult to express in gram-negative bacteria *E. coli* efficiently. The difference of membrane structure and the polysaccharide gene cluster is relatively large (mostly more than 10 kbp), making it difficult for cloning.

OMVs were usually combined with other delivery systems to meet some specific requirements. For example, to solve the problems of the poor size uniformity and low stability of OMV, Wu, G. et al. produced a 70-90 nm sized OMV (from *K. pneumoniae*) based nanovaccine by depositing the hollow-structured OMVs onto bovine serum albumin nanoparticles. As a result, the OMV could be reinforced from the core-shell structure. The protecting effect against carbapenem-resistant K. pneumoniae (CRKP) was significantly improved after vaccination (354). Camacho A I et al. found that when *Shigella* OMVs were encapsulated in polyanhydride nanoparticles, a stronger Th1 immune response, which was more needed against intracellular bacteria, was induced (357, 397). OMVs also be encapsulated in biopolymer chitosan, which was used to prepare nanogel particles by ionotropic gelation with tripolyphosphate. After being coated with an enteric polymer, mice were administrated orally and showed better protection against infection after 78 days of immunization, whereas free OMVs have no protection (359). Therefore, although OMV as a delivery carrier faces some problems, it can achieve the expected effect through further optimization and transformation.

4.5 Liposome

The liposome is a kind of phospholipid bilayer sphere formed *via* self-assembly in water and proved to be a safe and effective delivery system. Although liposomes do not belong to protein delivery carriers, we will still review their application in vaccine design, especially for peptide-based vaccines, because of their wide use (398). The versatility and plasticity characteristics of liposomes make them designable according to different parameter requirements, such as lipid composition, charge, size, entrapment and location (399). Besides loading various antigens in a liposome, adjuvants and/or functional molecules could also be loaded quickly to enhance further the immune effect (400). For peptide antigens, they were usually coupled to liposomes *via* lipid core peptide technology, which consists of an oligomeric polylysine core conjugated to a series of lipoamino acids for anchoring of the antigen (401, 402), and this strategy has been frequently utilized in Group A Streptococcal (GAS) vaccine studies (403–405). Ghaffar et al. developed a cationic liposome through the film hydration method with dimethyldioctadecylammonium bromide (DDAB). Lipopeptides antigens, entrapped by the liposome, could induce both mucosal and systemic response for a long time in intranasally immunized mice (403). In addition, the high-level antibody reaction was further confirmed in various sizes (70 nm to 1000 nm) of the carriers (406). In addition, some polymer, such as polyethylenimine (PEI), which could attach to the cells' surface and deliver cargo into endosomal and cytosolic compartments, was introduced in the lipopeptide-based vaccine design. PEI incorporated in liposome peptide vaccine could induce significant specific mucosal and systemic antibodies, which effectively opsonize multiple isolates of clinically isolated GAS (407). Further, they found that the ratio of PEI, rather than molecular weight, present in the liposome vaccines impact immune response (408). Besides, the addition of some functional elements can realize the immune enhancement of vaccines. For example, Yang et al. designed a cell-penetrating peptides (CPPs)-liposome delivery system on the liposomal nanoparticles, in which CPP could enhance both cellular and humoral immune responses through direct delivery of antigen into the cytoplasm and from the endocytic pathway (409–411). Nasal immunization of the vaccine in mice could induce antibodies that showed high opsonic activity against clinically isolated GAS strains (412). Liposomes have also been used in the study of TB vaccines. Dimethyldioctadecylammonium (DDA) could self-assemble into closed vesicular bilayers in water similar to liposomes and was known as an effective adjuvant for eliciting cellular and humoral responses (413, 414). However, the physical instability of the DDA liposomes limits its application. To solve this problem, Davidsen et al. incorporated a glycolipid trehalose 6,6′-dibehenate (TDB), comprising a 6,6′-diester of α,α′-trehalose with two long 22-carbon acyl chains, into the DDA liposome bilayers. By loading tuberculosis vaccine antigen Ag85B–ESAT-6 fusion protein and immunization of mice, a robust specific Th1 type immune response was induced (415). The post-challenge bacterial growth of *M. bovis* BCG was reduced in adult or neonatal murine (416), suggesting the increase of adjuvant efficacy of DDA liposomes. In conclusion, the characteristics of liposomes endow them with more designability, and some deficiencies can be solved by further transformation and optimization so that liposomes have great potential in peptide vaccine delivery design.

5 ANIMAL MODELS FOR PEPTIDE-BASED VACCINES

Many animal models have been utilized to develop TB vaccines, ranging from expensive none-human primates (NHPs) to small non-mammals such as zebrafish. In comparison, NHP, which can well reflect the human immune response and susceptibility to TB, has been used in many preclinical experiments. At the same time, smaller animal models such as mice, rats, guinea pigs, rabbits and zebrafish are generally more suitable for studying narrower aspects of the immune response to Mycobacterium tuberculosis, such as granuloma formation, susceptibility to different strains, or immunogenicity of vaccine candidates.

NHP represents one of the most frequently used and most important models when testing vaccines against *M. tuberculosis* infection. This model has significant similarities in human physiology, genome, and immune response (417, 418). Rhesus macaques and cynomolgus are the most commonly used NHPs in TB infections for vaccine evaluation (417, 419–421). Today, the NHP models have become indispensable for the preclinical evaluation of vaccine effects. However, some of the difficulties in using NHP models to evaluate anti-tuberculosis vaccines are the considerable investment requirements for the maintenance and use of BLS-3 biosafety facilities, the lack of commercial molecular and immune reagents, and the timely availability of sufficient animals. Compared with the NHP model, the advantages of using the mouse model include the availability of genetically modified strains, more common molecular and immunological reagents on the market, and lower cost of feeding and specialized containment facilities. These characteristics ensure that the mouse model is always the first choice for TB vaccine research, especially for exploratory studies on vaccines before preclinical evaluation using NHP models. Although common mouse strains exampled as C57BL/6 and BALB/c are often not susceptible to tuberculosis infection, they are still widely used in vaccine research. To date, most *M. tuberculosis* peptides are discovered in the C57BL/6 model (**Table 3**).

The use of mice is ubiquitous in scientific research. Still, the experimental results obtained on rodents, and primarily murine, in reality, are often very different from the clinical immune response of humans. Moreover, this difference in immune response has a certain relationship with the species differences between animals and humans, causing the development of many novel vaccines and drugs to stagnate or even fail to continue when they reach clinical trial phase I/II. Therefore, the development of small animal models that can more accurately reflect the characteristics of human immune response is a problem that deserves special attention.

MHC is one of the gene groups with the most polymorphism in humans and mammals. It induces and regulates innate immunity and adaptive immune response and participates in the development and maturation of T lymphocytes, the presentation of exogenous/endogenous antigens and immune signals, as well as the establishment of central immune tolerance (422). At the same time, MHC is closely related to the occurrence and progression of many autoimmune diseases and chronic diseases and has essential biological functions and significance. For example, the HLA-A11 subtype is closely associated with the occurrence of many infectious diseases, such as familial otosclerosis (423, 424), TB (425), leprosy (426), epilepsy and cytomegalovirus infection (427), etc. In addition, increased specific expression of the HLA-A11 gene was found in patients with upper laryngeal cancer (428) and osteosarcoma (429). Furthermore, HLA-A11, DR3 and DR4 subtypes played a synergistic role in the occurrence of autoimmune hepatitis (430). In addition to HLA-A11, other individual MHC subtypes also play a significant role in the disease process after HIV-1 infection (431–435). In recent years, how to use and exert the biological functions of HLA through animal models has gradually become a research hotspot in animal models, and the first is the development of new vaccines based on MHC-restricted CTL and HTL epitopes.

Mice and humans share more than 95% of genes and about 80% of genetic material. As small animal models, mice are widely used in vaccines and drugs preclinical trials (436). Although the MHC of the mouse (H-2) and human (HLA) are very similar in structure and function, there are still significant differences in the presentation of antigens (437), and the dominant antigen peptides presented also have different structural characteristics. Therefore, the MHC humanized mouse has become an essential model for epitope research and the development and evaluation of epitope vaccines.

In recent years, MHC humanized mouse models have played a vital role in developing and evaluating disease immune pathogenic mechanisms, vaccines, and drugs. This mouse model has also undergone a continuous development and progress stage. In the first stage, the whole HLA molecule is usually directly transferred into the mouse genome, such as HLA-B27 mice (438), HLA-B7 mice (439), HLA-A2 mice (440), HLA-Cw3 mice (441) and other early developed models. However, the binding force between the α3 functional region in the human HLA molecule and the mouse CD8 is weak (442–444). At the same time, the presence of mouse MHC (H-2) leads to competitive inhibition of mouse H-2-I restricted immune response to human HLA-I restricted immune response (445). In this stage, the mouse immune response is still dominant in the model, which cannot reflect the function and role of human HLA molecules alone in the immune response. Studies have shown that when H-2 is present in mice, the expression of HLA transgenic molecules on the surface of mouse lymphocytes is significantly reduced (446). In the second stage, the scientists improved the MHC humanized mouse model through two methods. One is to transfer the gene fragment encoding human $CD4^+$ or $CD8^+$ into the mouse genome so that the mouse can express both murine and human $CD4^+$ or $CD8^+$ molecules (447), which can effectively improve the binding efficiency of HLA and CD4 or CD8 accessory molecules, and efficiently start the second signal of antigen presentation. Another method is to optimize the structure of HLA transgenic molecules, replace the transmembrane α3 functional region with murine α3 functional region, and construct a chimeric HLA molecule (HHM). The murine α3 structure can promote HLA and mouse CD4 or mouse CD8. Representative mouse models include the HLA-B27 (HHM) mice model (448, 449). After optimization of the above two methods, the mouse model can produce a certain HLA-restriction-specific response. However, most cellular immune response is still regulated by mouse H-2 molecules. In the third stage, the researchers adopted a new construction strategy to design transgenic vectors and constructed a chimeric transgenic vector (HHD) (450) of HLA and H-2, including the promoter of HLA-I, light chain β2m, and heavy chain. The α1 and α2 functional regions, the α3 functional region and the transmembrane region of H-2-Db, and the important components β2m and IAβ of mouse H-2 are also knocked out. For example, in the HLA-A11 humanized mouse model (451), the α3 functional area of mouse H-2 is used to replace the α3 functional area of human HLA-A11, which effectively enhances the binding force between the human HLA-A11 molecule and the mouse CD8 and avoids the complexity of transferring human CD8 into the mouse genome. At the same time, knock out the important components β2m and IAβ (the β chain of the IA molecule) of the mouse-derived

H-2 I and II molecules, and replace them with fragments larger than the originals. Such pseudogene fragments of the gene achieving the purpose of silencing the expression of mouse H-2 molecules. Therefore, in this type of HLA-I humanized mice, the competitive inhibition of the H-2-I restricted reaction is eliminated, and only the HLA-I restricted immune response can be produced. The humanized mouse model of HLA-II was also constructed using the same strategy. The resulting HLA-I/II humanized mouse model was replaced with human HLA molecules at the level of MHC-I and II molecules. HLA exerts a restrictive function in antigen presentation, regulates the immune response in mice, and enables MHC mice to be "humanized" to a greater extent, which can more effectively simulate human immune response at the HLA level. The representative HLA-A2/DR1 and HLA-A11/DR1 transgenic mouse models have been well applied in HIV、EBOV and SARS-CoV-2 epitope screenings (451–453). Encouragingly, the MHC humanized mouse model has been well used for TB peptide-based vaccine research (2, 9, 198, 202, 203).

Although the MHC humanized mouse model can effectively simulate the human immune restriction and affect the immune function. However, as a better model for epitope vaccine research and evaluation, MHC humanized mouse models have two problems that need to be optimized in future development. On the one hand, it makes MHC humanized mouse models sensitive to pathogens. On the other hand, mice are not susceptible to many human pathogens or cannot be infected due to differences in receptors. For example, regular mice are not sensitive to SARS-CoV-2, SARS-CoV, MERS-CoV, and many subtypes of influenza viruses. Therefore, it requires changing the virus (constructing a mouse-adapted strain) or changing the animal (pathogen-receptor humanized mouse) to obtain a sensitive mouse model. Another aspect is to combine MHC humanized mice with immunodeficient mice for better humanized immune reconstitution. At present, although NOD/SCID mice have played a critical role in the research fields of immune transplantation and tumor immunity, the transplanted human-derived cells have undergone development and differentiation in the mouse thymus. However, the MHC obtained restriction is still restricted by mouse H-2, and it is impossible to carry out research on specific HLA-restricted CTL and Th immune responses. Therefore, through the combination of MHC humanized mice and immunodeficient mice, immune reconstitution can be humanized, and a more real humanized immune system can be realized.

6 CONCLUSIONS AND FUTURE PERSPECTIVES

Vaccination has been considered as the most effective strategy to eliminate TB infection. Accumulating studies have showed that peptide-based vaccines are promising vaccine candidates for preventing and controlling TB due to their advantages, such as aggregation of immunodominant epitopes, preservation of peptide structure, good stability, easy to store and transport, lower cost, and decreased side effects. Furthermore, the rapid development of bioinformatics technology provides a tool for predicting and constructing peptide-based vaccines, which dramatically saves time and reduces the cost of peptide-based vaccine research. Herein, we give a detailed description of how to design a peptide vaccine using an immunoinformatics approach, including determination of protective antigens, T and B cell epitope prediction, screening of immunodominant epitopes, and selection of selection linkers, adjuvant or helper peptides, codon optimization, and in *silico* analysis. We further reviewed the peptide-based vaccine candidates worldwide based on this basic knowledge. We found that 150 previous articles related to peptide-based vaccines for TB are being investigated in pre-clinical studies, including 76 studies in epitope screening and prediction, 45 studies in evaluating immunogenicity, 8 studies in peptide-based vaccine construction, and 21 in assessing vaccine efficacy in animal models. However, some drawbacks of peptide-based vaccines should not be ignored, such as weak immunogenicity for a single peptide, MHC restriction, and high requirements for animal models.

In the future, these disadvantages can be solved by the following strategies: (1) a detailed understanding of the potential cellular and molecular mechanisms involved in peptide-based vaccine immunity is the key to improving its immunogenicity and protective efficiency (454); (2) improving the vaccine construction techniques, including broad antigen repertoire, SLPs, conjugation and palmitoylation of peptides, grafting epitopes into a protective antigen; (3) using appropriate linkers, helper peptides, TLR agonists, adjuvants, and potential delivery systems to enhance the immunogenicity; (4) primed with BCG and boosted with peptide-based vaccines; (5) employing transgenic animal models with human HLA molecules to evaluate peptide-based vaccines.

AUTHOR CONTRIBUTIONS

Conceptualization: XW and WG. Data curation: WG, CP, PC, JW, and GZ. Formal analysis: WG. Funding acquisition: WG. Methodology: WG, CP, PC, JW, and GZ. Software: WG. Writing - original draft: WG, CP, and GZ. Writing - review & editing: WG and XW. All authors contributed to the article and approved the submitted version.

FUNDING

This study was funded by the National Natural Science Foundation of China (Grant No. 81801643), Beijing Municipal Science & Technology Commission (Grant No. 19L2152), and Chinese PLA General Hospital (Grant No. QNC19047).

SUPPLEMENTARY MATERIAL

The Supplementary Material for this article can be found online at: https://www.frontiersin.org/articles/10.3389/fimmu.2022.830497/full#supplementary-material

Supplementary Table S1 | Summary of studies related with peptide or epitope candidates against Mycobacterium tuberculosis.

REFERENCES

1. Gong W, Liang Y, Wu X. The Current Status, Challenges, and Future Developments of New Tuberculosis Vaccines. *Hum Vaccin Immunother* (2018) 14(7):1697–716. doi: 10.1080/21645515.2018.1458806
2. Gong W, Liang Y, Mi J, Jia Z, Xue Y, Wang J, et al. Peptides-Based Vaccine MP3RT Induced Protective Immunity Against Mycobacterium Tuberculosis Infection in a Humanized Mouse Model. *Front Immunol* (2021) 12:666290 (1393). doi: 10.3389/fimmu.2021.666290
3. WHO. *Global Tuberculosis Report 2021*. Geneva: Genevapp: World Health Organization (2021).
4. Allué-Guardia A, García JI, Torrelles JB. Evolution of Drug-Resistant Mycobacterium Tuberculosis Strains and Their Adaptation to the Human Lung Environment. *Front Microbiol* (2021) 12:612675. doi: 10.3389/fmicb.2021.612675
5. Gong W, Wu X. Differential Diagnosis of Latent Tuberculosis Infection and Active Tuberculosis: A Key to a Successful Tuberculosis Control Strategy. *Front Microbiol* (2021) 12:745592(3126). doi: 10.3389/fmicb.2021.745592
6. Aspatwar A, Gong W, Wang S, Wu X, Parkkila S. Tuberculosis Vaccine BCG: The Magical Effect of the Old Vaccine in the Fight Against the COVID-19 Pandemic. *Int Rev Immunol* (2021) 2021:1–14. doi: 10.1080/08830185.2021.1922685 Published online first.
7. Gong W, Aspatwar A, Wang S, Parkkila S, Wu X. COVID-19 Pandemic: SARS-CoV-2 Specific Vaccines and Challenges, Protection via BCG Trained Immunity, and Clinical Trials. *Expert Rev Vaccines* (2021) 20(7):857–80. doi: 10.1080/14760584.2021.1938550
8. Andersen P, Doherty TM. The Success and Failure of BCG - Implications for a Novel Tuberculosis Vaccine. *Nat Rev Microbiol* (2005) 3(8):656–62. doi: 10.1038/nrmicro1211
9. Gong W, Liang Y, Mi J, Xue Y, Wang J, Wang L, et al. A Peptide-Based Vaccine ACP Derived From Antigens of Mycobacterium Tuberculosis Induced Th1 Response But Failed to Enhance the Protective Efficacy of BCG in Mice. *Indian J Tuberculosis* (2021). doi: 10.1016/j.ijtb.2021.08.016 In Press.
10. WHO. *Global Tuberculosis Report 2020*. Geneva: Genevapp: World Health Organization (2020).
11. Day CL, Tameris M, Mansoor N, van Rooyen M, de Kock M, Geldenhuys H, et al. Induction and Regulation of T-Cell Immunity by the Novel Tuberculosis Vaccine M72/AS01 in South African Adults. *Am J Respir Crit Care Med* (2013) 188(4):492–502. doi: 10.1164/rccm.201208-1385OC
12. Montoya J, Solon JA, Cunanan SR, Acosta L, Bollaerts A, Moris P, et al. A Randomized, Controlled Dose-Finding Phase II Study of the M72/AS01 Candidate Tuberculosis Vaccine in Healthy PPD-Positive Adults. *J Clin Immunol* (2013) 33(8):1360–75. doi: 10.1007/s10875-013-9949-3
13. Thacher EG, Cavassini M, Audran R, Thierry AC, Bollaerts A, Cohen J, et al. Safety and Immunogenicity of the M72/AS01 Candidate Tuberculosis Vaccine in HIV-Infected Adults on Combination Antiretroviral Therapy: A Phase I/II, Randomized Trial. *Aids* (2014) 28(12):1769–81. doi: 10.1097/qad.0000000000000343
14. Idoko OT, Owolabi OA, Owiafe PK, Moris P, Odutola A, Bollaerts A, et al. Safety and Immunogenicity of the M72/AS01 Candidate Tuberculosis Vaccine When Given as a Booster to BCG in Gambian Infants: An Open-Label Randomized Controlled Trial. *Tuberculosis (Edinb)* (2014) 94(6):564–78. doi: 10.1016/j.tube.2014.07.001
15. Van Der Meeren O, Hatherill M, Nduba V, Wilkinson RJ, Muyoyeta M, Van Brakel E, et al. Phase 2b Controlled Trial of M72/AS01(E) Vaccine to Prevent Tuberculosis. *N Engl J Med* (2018) 379(17):1621–34. doi: 10.1056/NEJMoa1803484
16. Tait DR, Hatherill M, van der Meeren O, Ginsberg AM, Van Brakel E, Salaun B, et al. Final Analysis of a Trial of M72/AS01(E) Vaccine to Prevent Tuberculosis. *N Engl J Med* (2019) 381(25):2429–39. doi: 10.1056/NEJMoa1909953
17. Ernst JD. Mechanisms of M. Tuberculosis Immune Evasion as Challenges to TB Vaccine Design. *Cell Host Microbe* (2018) 24(1):34–42. doi: 10.1016/j.chom.2018.06.004
18. Bellini C, Horváti K. Recent Advances in the Development of Protein- and Peptide-Based Subunit Vaccines Against Tuberculosis. *Cells* (2020) 9 (12):2673. doi: 10.3390/cells9122673
19. Dong R, Chu Z, Yu F, Zha Y. Contriving Multi-Epitope Subunit of Vaccine for COVID-19: Immunoinformatics Approaches. *Front Immunol* (2020) 11:1784. doi: 10.3389/fimmu.2020.01784
20. Kapopoulou A, Lew JM, Cole ST. The MycoBrowser Portal: A Comprehensive and Manually Annotated Resource for Mycobacterial Genomes. *Tuberculosis (Edinb)* (2011) 91(1):8–13. doi: 10.1016/j.tube.2010.09.006
21. Consortium U. UniProt: A Worldwide Hub of Protein Knowledge. *Nucleic Acids Res* (2019) 47(D1):D506–15. doi: 10.1093/nar/gky1049
22. Sanches RCO, Tiwari S, Ferreira LCG, Oliveira FM, Lopes MD, Passos MJF, et al. Immunoinformatics Design of Multi-Epitope Peptide-Based Vaccine Against Schistosoma Mansoni Using Transmembrane Proteins as a Target. *Front Immunol* (2021) 12:621706. doi: 10.3389/fimmu.2021.621706
23. Sosa EJ, Burguener G, Lanzarotti E, Defelipe L, Radusky L, Pardo AM, et al. Target-Pathogen: A Structural Bioinformatic Approach to Prioritize Drug Targets in Pathogens. *Nucleic Acids Res* (2018) 46(D1):D413–d418. doi: 10.1093/nar/gkx1015
24. Dhanda SK, Vir P, Singla D, Gupta S, Kumar S, Raghava GP. A Web-Based Platform for Designing Vaccines Against Existing and Emerging Strains of Mycobacterium Tuberculosis. *PloS One* (2016) 11(4):e0153771. doi: 10.1371/journal.pone.0153771
25. Zia Q, Azhar A, Ahmad S, Afsar M, Hasan Z, Owais M, et al. PeMtb: A Database of MHC Antigenic Peptide of Mycobacterium Tuberculosis. *Curr Pharm Biotechnol* (2017) 18(8):648–52. doi: 10.2174/1389201018666170914150115
26. Chaudhuri R, Kulshreshtha D, Raghunandanan MV, Ramachandran S. Integrative Immunoinformatics for Mycobacterial Diseases in R Platform. *Syst Synth Biol* (2014) 8(1):27–39. doi: 10.1007/s11693-014-9135-9
27. Gonzalez-Galarza FF, McCabe A, Santos E, Jones J, Takeshita L, Ortega-Rivera ND, et al. Allele Frequency Net Database (AFND) 2020 Update: Gold-Standard Data Classification, Open Access Genotype Data and New Query Tools. *Nucleic Acids Res* (2020) 48(D1):D783–8. doi: 10.1093/nar/gkz1029
28. Bui HH, Sidney J, Dinh K, Southwood S, Newman MJ, Sette A. Predicting Population Coverage of T-Cell Epitope-Based Diagnostics and Vaccines. *BMC Bioinf* (2006) 7:153. doi: 10.1186/1471-2105-7-153
29. Wang P, Sidney J, Kim Y, Sette A, Lund O, Nielsen M, et al. Peptide Binding Predictions for HLA DR, DP and DQ Molecules. *BMC Bioinf* (2010) 11:568. doi: 10.1186/1471-2105-11-568
30. Reche PA, Glutting JP, Zhang H, Reinherz EL. Enhancement to the RANKPEP Resource for the Prediction of Peptide Binding to MHC Molecules Using Profiles. *Immunogenetics* (2004) 56(6):405–19. doi: 10.1007/s00251-004-0709-7
31. Xu Y, Luo C, Mamitsuka H, Zhu S. MetaMHCpan, A Meta Approach for Pan-Specific MHC Peptide Binding Prediction. *Methods Mol Biol* (2016) 1404:753–60. doi: 10.1007/978-1-4939-3389-1_49
32. Singh H, Raghava GP. ProPred: Prediction of HLA-DR Binding Sites. *Bioinformatics* (2001) 17(12):1236–7. doi: 10.1093/bioinformatics/17.12.1236
33. Mustafa AS, Shaban FA. ProPred Analysis and Experimental Evaluation of Promiscuous T-Cell Epitopes of Three Major Secreted Antigens of Mycobacterium Tuberculosis. *Tuberculosis (Edinb)* (2006) 86(2):115–24. doi: 10.1016/j.tube.2005.05.001
34. Reynisson B, Alvarez B, Paul S, Peters B, Nielsen M. NetMHCpan-4.1 and NetMHCIIpan-4.0: Improved Predictions of MHC Antigen Presentation by Concurrent Motif Deconvolution and Integration of MS MHC Eluted Ligand Data. *Nucleic Acids Res* (2020) 48(W1):W449–w454. doi: 10.1093/nar/gkaa379
35. Reynisson B, Barra C, Kaabinejadian S, Hildebrand WH, Peters B, Nielsen M. Improved Prediction of MHC II Antigen Presentation Through Integration and Motif Deconvolution of Mass Spectrometry MHC Eluted Ligand Data. *J Proteome Res* (2020) 19(6):2304–15. doi: 10.1021/acs.jproteome.9b00874
36. Jensen KK, Andreatta M, Marcatili P, Buus S, Greenbaum JA, Yan Z, et al. Improved Methods for Predicting Peptide Binding Affinity to MHC Class II Molecules. *Immunology* (2018) 154(3):394–406. doi: 10.1111/imm.12889
37. Andreatta M, Nielsen M. Gapped Sequence Alignment Using Artificial Neural Networks: Application to the MHC Class I System. *Bioinformatics* (2016) 32(4):511–7. doi: 10.1093/bioinformatics/btv639

38. Larsen MV, Lundegaard C, Lamberth K, Buus S, Lund O, Nielsen M. Large-Scale Validation of Methods for Cytotoxic T-Lymphocyte Epitope Prediction. *BMC Bioinf* (2007) 8:424. doi: 10.1186/1471-2105-8-424
39. Singh H, Raghava GP. ProPred1: Prediction of Promiscuous MHC Class-I Binding Sites. *Bioinformatics* (2003) 19(8):1009–14. doi: 10.1093/bioinformatics/btg108
40. Nielsen M, Lundegaard C, Worning P, Lauemøller SL, Lamberth K, Buus S, et al. Reliable Prediction of T-Cell Epitopes Using Neural Networks With Novel Sequence Representations. *Protein Sci* (2003) 12(5):1007–17. doi: 10.1110/ps.0239403
41. Guan P, Hattotuwagama CK, Doytchinova IA, Flower DR. MHCPred 2.0: An Updated Quantitative T-Cell Epitope Prediction Server. *Appl Bioinf* (2006) 5(1):55–61. doi: 10.2165/00822942-200605010-00008
42. Doytchinova IA, Guan P, Flower DR. EpiJen: A Server for Multistep T Cell Epitope Prediction. *BMC Bioinf* (2006) 7:131. doi: 10.1186/1471-2105-7-131
43. Srivastava VK, Kaushik S, Bhargava G, Jain A, Saxena J, Jyoti A. A Bioinformatics Approach for the Prediction of Immunogenic Properties and Structure of the SARS-COV-2 B.1.617.1 Variant Spike Protein. *BioMed Res Int* (2021) 2021:7251119. doi: 10.1155/2021/7251119
44. Saha S, Raghava GP. Prediction of Continuous B-Cell Epitopes in an Antigen Using Recurrent Neural Network. *Proteins* (2006) 65(1):40–8. doi: 10.1002/prot.21078
45. Khanna D, Rana PS. Improvement in Prediction of Antigenic Epitopes Using Stacked Generalisation: An Ensemble Approach. *IET Syst Biol* (2020) 14(1):1–7. doi: 10.1049/iet-syb.2018.5083
46. Chou PY, Fasman GD. Prediction of the Secondary Structure of Proteins From Their Amino Acid Sequence. *Adv Enzymol Relat Areas Mol Biol* (1978) 47:45–148. doi: 10.1002/9780470122921.ch2
47. Emini EA, Hughes JV, Perlow DS, Boger J. Induction of Hepatitis A Virus-Neutralizing Antibody by a Virus-Specific Synthetic Peptide. *J Virol* (1985) 55(3):836–9. doi: 10.1128/jvi.55.3.836-839.1985
48. PA K, GE S. Prediction of Chain Flexibility in Proteins - A Tool for the Selection of Peptide Antigens. *Naturwissenschafren* (1985) 72:212–3. doi: 10.1007/BF01195768
49. Parker JM, Guo D, Hodges RS. New Hydrophilicity Scale Derived From High-Performance Liquid Chromatography Peptide Retention Data: Correlation of Predicted Surface Residues With Antigenicity and X-Ray-Derived Accessible Sites. *Biochemistry* (1986) 25(19):5425–32. doi: 10.1021/bi00367a013
50. Kolaskar AS, Tongaonkar PC. A Semi-Empirical Method for Prediction of Antigenic Determinants on Protein Antigens. *FEBS Lett* (1990) 276(1-2):172–4. doi: 10.1016/0014-5793(90)80535-q
51. Larsen JE, Lund O, Nielsen M. Improved Method for Predicting Linear B-Cell Epitopes. *Immunome Res* (2006) 2:2. doi: 10.1186/1745-7580-2-2
52. Jespersen MC, Peters B, Nielsen M, Marcatili P. BepiPred-2.0: Improving Sequence-Based B-Cell Epitope Prediction Using Conformational Epitopes. *Nucleic Acids Res* (2017) 45(W1):W24–9. doi: 10.1093/nar/gkx346
53. Chen J, Liu H, Yang J, Chou KC. Prediction of Linear B-Cell Epitopes Using Amino Acid Pair Antigenicity Scale. *Amino Acids* (2007) 33(3):423–8. doi: 10.1007/s00726-006-0485-9
54. El-Manzalawy Y, Dobbs D, Honavar V. Predicting Linear B-Cell Epitopes Using String Kernels. *J Mol Recognit* (2008) 21(4):243–55. doi: 10.1002/jmr.893
55. Shen W, Cao Y, Cha L, Zhang X, Ying X, Zhang W, et al. Predicting Linear B-Cell Epitopes Using Amino Acid Anchoring Pair Composition. *BioData Min* (2015) 8:14. doi: 10.1186/s13040-015-0047-3
56. Yao B, Zhang L, Liang S, Zhang C. SVMTriP: A Method to Predict Antigenic Epitopes Using Support Vector Machine to Integrate Tri-Peptide Similarity and Propensity. *PloS One* (2012) 7(9):e45152. doi: 10.1371/journal.pone.0045152
57. Kringelum JV, Lundegaard C, Lund O, Nielsen M. Reliable B Cell Epitope Predictions: Impacts of Method Development and Improved Benchmarking. *PloS Comput Biol* (2012) 8(12):e1002829. doi: 10.1371/journal.pcbi.1002829
58. Sweredoski MJ, Baldi P. PEPITO: Improved Discontinuous B-Cell Epitope Prediction Using Multiple Distance Thresholds and Half Sphere Exposure. *Bioinformatics* (2008) 24(12):1459–60. doi: 10.1093/bioinformatics/btn199
59. Ponomarenko J, Bui HH, Li W, Fusseder N, Bourne PE, Sette A, et al. ElliPro: A New Structure-Based Tool for the Prediction of Antibody Epitopes. *BMC Bioinf* (2008) 9:514. doi: 10.1186/1471-2105-9-514
60. Zhou C, Chen Z, Zhang L, Yan D, Mao T, Tang K, et al. SEPPA 3.0-Enhanced Spatial Epitope Prediction Enabling Glycoprotein Antigens. *Nucleic Acids Res* (2019) 47(W1):W388–w394. doi: 10.1093/nar/gkz413
61. Rubinstein ND, Mayrose I, Martz E, Pupko T. Epitopia: A Web-Server for Predicting B-Cell Epitopes. *BMC Bioinf* (2009) 10:287. doi: 10.1186/1471-2105-10-287
62. Liang S, Zheng D, Zhang C, Zacharias M. Prediction of Antigenic Epitopes on Protein Surfaces by Consensus Scoring. *BMC Bioinf* (2009) 10:302. doi: 10.1186/1471-2105-10-302
63. Liang S, Zheng D, Standley DM, Yao B, Zacharias M, Zhang C. EPSVR and EPMeta: Prediction of Antigenic Epitopes Using Support Vector Regression and Multiple Server Results. *BMC Bioinf* (2010) 11:381. doi: 10.1186/1471-2105-11-381
64. Dhanda SK, Vir P, Raghava GP. Designing of Interferon-Gamma Inducing MHC Class-II Binders. *Biol Direct* (2013) 8:30. doi: 10.1186/1745-6150-8-30
65. Dhanda SK, Gupta S, Vir P, Raghava GP. Prediction of IL4 Inducing Peptides. *Clin Dev Immunol* (2013) 2013:263952. doi: 10.1155/2013/263952
66. Nagpal G, Usmani SS, Dhanda SK, Kaur H, Singh S, Sharma M, et al. Computer-Aided Designing of Immunosuppressive Peptides Based on IL-10 Inducing Potential. *Sci Rep* (2017) 7:42851. doi: 10.1038/srep42851
67. Calis JJ, Maybeno M, Greenbaum JA, Weiskopf D, De Silva AD, Sette A, et al. Properties of MHC Class I Presented Peptides That Enhance Immunogenicity. *PloS Comput Biol* (2013) 9(10):e1003266. doi: 10.1371/journal.pcbi.1003266
68. Dhanda SK, Karosiene E, Edwards L, Grifoni A, Paul S, Andreatta M, et al. Predicting HLA CD4 Immunogenicity in Human Populations. *Front Immunol* (2018) 9:1369. doi: 10.3389/fimmu.2018.01369
69. Chen B, Khodadoust MS, Olsson N, Wagar LE, Fast E, Liu CL, et al. Predicting HLA Class II Antigen Presentation Through Integrated Deep Learning. *Nat Biotechnol* (2019) 37(11):1332–43. doi: 10.1038/s41587-019-0280-2
70. Nilsson JB, Grifoni A, Tarke A, Sette A, Nielsen M. PopCover-2.0. Improved Selection of Peptide Sets With Optimal HLA and Pathogen Diversity Coverage. *Front Immunol* (2021) 12:728936. doi: 10.3389/fimmu.2021.728936
71. Saha S, Raghava GP. Searching and Mapping of B-Cell Epitopes in Bcipep Database. *Methods Mol Biol* (2007) 409:113–24. doi: 10.1007/978-1-60327-118-9_7
72. Doytchinova IA, Flower DR. VaxiJen: A Server for Prediction of Protective Antigens, Tumour Antigens and Subunit Vaccines. *BMC Bioinf* (2007) 8 (1):4. doi: 10.1186/1471-2105-8-4
73. Magnan CN, Zeller M, Kayala MA, Vigil A, Randall A, Felgner PL, et al. High-Throughput Prediction of Protein Antigenicity Using Protein Microarray Data. *Bioinformatics* (2010) 26(23):2936–43. doi: 10.1093/bioinformatics/btq551
74. Anand R, Biswal S, Bhatt R, Tiwary BN. Computational Perspectives Revealed Prospective Vaccine Candidates From Five Structural Proteins of Novel SARS Corona Virus 2019 (SARS-CoV-2). *PeerJ* (2020) 8:e9855. doi: 10.7717/peerj.9855
75. Dimitrov I, Naneva L, Doytchinova I, Bangov I. AllergenFP: Allergenicity Prediction by Descriptor Fingerprints. *Bioinformatics* (2014) 30(6):846–51. doi: 10.1093/bioinformatics/btt619
76. Sharma N, Patiyal S, Dhall A, Pande A, Arora C, Raghava GPS. AlgPred 2.0: An Improved Method for Predicting Allergenic Proteins and Mapping of IgE Epitopes. *Brief Bioinform* (2021) 22(4):bbaa294. doi: 10.1093/bib/bbaa294
77. Fiers MW, Kleter GA, Nijland H, Peijnenburg AA, Nap JP, van Ham RC. Allermatch, a Webtool for the Prediction of Potential Allergenicity According to Current FAO/WHO Codex Alimentarius Guidelines. *BMC Bioinf* (2004) 5:133. doi: 10.1186/1471-2105-5-133
78. Gupta S, Kapoor P, Chaudhary K, Gautam A, Kumar R, Raghava GP. In Silico Approach for Predicting Toxicity of Peptides and Proteins. *PloS One* (2013) 8(9):e73957. doi: 10.1371/journal.pone.0073957
79. Wishart D, Arndt D, Pon A, Sajed T, Guo AC, Djoumbou Y, et al. (2015). doi: 10.1093/nar/gku1004
80. Dhanda SK, Vaughan K, Schulten V, Grifoni A, Weiskopf D, Sidney J, et al. Development of a Novel Clustering Tool for Linear Peptide Sequences. *Immunology* (2018) 155(3):331–45. doi: 10.1111/imm.12984
81. Manavalan B, Shin TH, Kim MO, Lee G. PIP-EL: A New Ensemble Learning Method for Improved Proinflammatory Peptide Predictions. *Front Immunol* (2018) 9:1783. doi: 10.3389/fimmu.2018.01783

82. Khatun MS, Hasan MM, Kurata H. PreAIP: Computational Prediction of Anti-Inflammatory Peptides by Integrating Multiple Complementary Features. *Front Genet* (2019) 10:129. doi: 10.3389/fgene.2019.00129
83. Grote A, Hiller K, Scheer M, Münch R, Nörtemann B, Hempel DC, et al. JCat: A Novel Tool to Adapt Codon Usage of a Target Gene to its Potential Expression Host. *Nucleic Acids Res* (2005) 33(Web Server issue):W526–531. doi: 10.1093/nar/gki376
84. Bibi S, Ullah I, Zhu B, Adnan M, Liaqat R, Kong WB, et al. In Silico Analysis of Epitope-Based Vaccine Candidate Against Tuberculosis Using Reverse Vaccinology. *Sci Rep* (2021) 11(1):1249. doi: 10.1038/s41598-020-80899-6
85. Hebditch M, Carballo-Amador MA, Charonis S, Curtis R, Warwicker J. Protein-Sol: A Web Tool for Predicting Protein Solubility From Sequence. *Bioinformatics* (2017) 33(19):3098–100. doi: 10.1093/bioinformatics/btx345
86. Liu IH, Lo YS, Yang JM. PAComplex: A Web Server to Infer Peptide Antigen Families and Binding Models From TCR-pMHC Complexes. *Nucleic Acids Res* (2011) 39(Web Server issue):W254–260. doi: 10.1093/nar/gkr434
87. van Zundert GCP, Rodrigues J, Trellet M, Schmitz C, Kastritis PL, Karaca E, et al. The HADDOCK2.2 Web Server: User-Friendly Integrative Modeling of Biomolecular Complexes. *J Mol Biol* (2016) 428(4):720–5. doi: 10.1016/j.jmb.2015.09.014
88. Kozakov D, Hall DR, Xia B, Porter KA, Padhorny D, Yueh C, et al. The ClusPro Web Server for Protein-Protein Docking. *Nat Protoc* (2017) 12 (2):255–78. doi: 10.1038/nprot.2016.169
89. Jiménez-García B, Roel-Touris J, Romero-Durana M, Vidal M, Jiménez-González D, Fernández-Recio J. LightDock: A New Multi-Scale Approach to Protein-Protein Docking. *Bioinformatics* (2018) 34(1):49–55. doi: 10.1093/bioinformatics/btx555
90. Chen R, Li L, Weng Z. ZDOCK: An Initial-Stage Protein-Docking Algorithm. *Proteins* (2003) 52(1):80–7. doi: 10.1002/prot.10389
91. Kremer JR, Mastronarde DN, McIntosh JR. Computer Visualization of Three-Dimensional Image Data Using IMOD. *J Struct Biol* (1996) 116 (1):71–6. doi: 10.1006/jsbi.1996.0013
92. Laskowski RA, Jabłońska J, Pravda L, Vařeková RS, Thornton JM. PDBsum: Structural Summaries of PDB Entries. *Protein Sci* (2018) 27(1):129–34. doi: 10.1002/pro.3289
93. Pollastri G, Przybylski D, Rost B, Baldi P. Improving the Prediction of Protein Secondary Structure in Three and Eight Classes Using Recurrent Neural Networks and Profiles. *Proteins* (2002) 47(2):228–35. doi: 10.1002/prot.10082
94. Sen TZ, Jernigan RL, Garnier J, Kloczkowski A. GOR V Server for Protein Secondary Structure Prediction. *Bioinformatics* (2005) 21(11):2787–8. doi: 10.1093/bioinformatics/bti408
95. Geourjon C, Deléage G. SOPMA: Significant Improvements in Protein Secondary Structure Prediction by Consensus Prediction From Multiple Alignments. *Comput Appl Biosci* (1995) 11(6):681–4. doi: 10.1093/bioinformatics/11.6.681
96. Ko J, Park H, Heo L, Seok C. GalaxyWEB Server for Protein Structure Prediction and Refinement. *Nucleic Acids Res* (2012) 40(Web Server issue): W294–297. doi: 10.1093/nar/gks493
97. Kuriata A, Gierut AM, Oleniecki T, Ciemny MP, Kolinski A, Kurcinski M, et al. CABS-Flex 2.0: A Web Server for Fast Simulations of Flexibility of Protein Structures. *Nucleic Acids Res* (2018) 46(W1):W338–w343. doi: 10.1093/nar/gky356
98. Cheng J, Randall AZ, Sweredoski MJ, Baldi P. SCRATCH: A Protein Structure and Structural Feature Prediction Server. *Nucleic Acids Res* (2005) 33(Web Server issue):W72–76. doi: 10.1093/nar/gki396
99. Kelley LA, Mezulis S, Yates CM, Wass MN, Sternberg MJ. The Phyre2 Web Portal for Protein Modeling, Prediction and Analysis. *Nat Protoc* (2015) 10 (6):845–58. doi: 10.1038/nprot.2015.053
100. Waterhouse A, Bertoni M, Bienert S, Studer G, Tauriello G, Gumienny R, et al. SWISS-MODEL: Homology Modelling of Protein Structures and Complexes. *Nucleic Acids Res* (2018) 46(W1):W296–w303. doi: 10.1093/nar/gky427
101. Seedat F, James I, Loubser S, Waja Z, Mallal SA, Hoffmann C, et al. Human Leukocyte Antigen Associations With Protection Against Tuberculosis Infection and Disease in Human Immunodeficiency Virus-1 Infected Individuals, Despite Household Tuberculosis Exposure and Immune Suppression. *Tuberculosis (Edinb)* (2021) 126:102023. doi: 10.1016/j.tube.2020.102023
102. Malkova A, Starshinova A, Zinchenko Y, Basantsova N, Mayevskaya V, Yablonskiy P, et al. The Opposite Effect of Human Leukocyte Antigen Genotypes in Sarcoidosis and Tuberculosis: A Narrative Review of the Literature. *ERJ Open Res* (2020) 6(3):00155–2020. doi: 10.1183/23120541.00155-2020
103. Vita R, Mahajan S, Overton JA, Dhanda SK, Martini S, Cantrell JR, et al. The Immune Epitope Database (IEDB): 2018 Update. *Nucleic Acids Res* (2019) 47 (D1):D339–d343. doi: 10.1093/nar/gky1006
104. Nielsen M, Lundegaard C, Lund O, Keşmir C. The Role of the Proteasome in Generating Cytotoxic T-Cell Epitopes: Insights Obtained From Improved Predictions of Proteasomal Cleavage. *Immunogenetics* (2005) 57(1-2):33–41. doi: 10.1007/s00251-005-0781-7
105. Tenzer S, Peters B, Bulik S, Schoor O, Lemmel C, Schatz MM, et al. Modeling the MHC Class I Pathway by Combining Predictions of Proteasomal Cleavage, TAP Transport and MHC Class I Binding. *Cell Mol Life Sci* (2005) 62(9):1025–37. doi: 10.1007/s00018-005-4528-2
106. Giguère S, Drouin A, Lacoste A, Marchand M, Corbeil J, Laviolette F. MHC-NP: Predicting Peptides Naturally Processed by the MHC. *J Immunol Methods* (2013)400–1:307–36. doi: 10.1016/j.jim.2013.10.003 30-36.
107. Chronister WD, Crinklaw A, Mahajan S, Vita R, Koşaloğlu-Yalçın Z, Yan Z, et al. TCRMatch: Predicting T-Cell Receptor Specificity Based on Sequence Similarity to Previously Characterized Receptors. *Front Immunol* (2021) 12:640725. doi: 10.3389/fimmu.2021.640725
108. Klausen MS, Anderson MV, Jespersen MC, Nielsen M, Marcatili P. LYRA, a Webserver for Lymphocyte Receptor Structural Modeling. *Nucleic Acids Res* (2015) 43(W1):W349–355. doi: 10.1093/nar/gkv535
109. Mahajan S, Yan Z, Jespersen MC, Jensen KK, Marcatili P, Nielsen M, et al. Benchmark Datasets of Immune Receptor-Epitope Structural Complexes. *BMC Bioinf* (2019) 20(1):490. doi: 10.1186/s12859-019-3109-6
110. Haste Andersen P, Nielsen M, Lund O. Prediction of Residues in Discontinuous B-Cell Epitopes Using Protein 3D Structures. *Protein Sci* (2006) 15(11):2558–67. doi: 10.1110/ps.062405906
111. Kuroda D, Shirai H, Jacobson MP, Nakamura H. Computer-Aided Antibody Design. *Protein Eng Des Sel* (2012) 25(10):507–21. doi: 10.1093/protein/gzs024
112. Bui HH, Sidney J, Li W, Fusseder N, Sette A. Development of an Epitope Conservancy Analysis Tool to Facilitate the Design of Epitope-Based Diagnostics and Vaccines. *BMC Bioinf* (2007) 8:361. doi: 10.1186/1471-2105-8-361
113. Paul S, Arlehamn CSL, Schulten V, Westernberg L, Sidney J, Peters B, et al. Experimental Validation of the RATE Tool for Inferring HLA Restrictions of T Cell Epitopes. *BMC Immunol* (2017) 18(Suppl 1):20. doi: 10.1186/s12865-017-0204-1
114. Dhanda SK, Vita R, Ha B, Grifoni A, Peters B, Sette A. ImmunomeBrowser: A Tool to Aggregate and Visualize Complex and Heterogeneous Epitopes in Reference Proteins. *Bioinformatics* (2018) 34(22):3931–3. doi: 10.1093/bioinformatics/bty463
115. Rai PK, Chodisetti SB, Maurya SK, Nadeem S, Zeng W, Janmeja AK, et al. A Lipidated Bi-Epitope Vaccine Comprising of MHC-I and MHC-II Binder Peptides Elicits Protective CD4 T Cell and CD8 T Cell Immunity Against Mycobacterium Tuberculosis. *J Transl Med* (2018) 16(1):279. doi: 10.1186/s12967-018-1653-x
116. Horváti K, Pályi B, Henczkó J, Balka G, Szabó E, Farkas V, et al. A Convenient Synthetic Method to Improve Immunogenicity of Mycobacterium Tuberculosis Related T-Cell Epitope Peptides. *Vaccines (Basel)* (2019) 7(3):101. doi: 10.3390/vaccines7030101
117. Wang P, Sidney J, Dow C, Mothé B, Sette A, Peters B. A Systematic Assessment of MHC Class II Peptide Binding Predictions and Evaluation of a Consensus Approach. *PloS Comput Biol* (2008) 4(4):e1000048. doi: 10.1371/journal.pcbi.1000048
118. Nielsen M, Lund O. NN-Align. An Artificial Neural Network-Based Alignment Algorithm for MHC Class II Peptide Binding Prediction. *BMC Bioinf* (2009) 10:296. doi: 10.1186/1471-2105-10-296
119. Nielsen M, Lundegaard C, Lund O. Prediction of MHC Class II Binding Affinity Using SMM-Align, a Novel Stabilization Matrix Alignment Method. *BMC Bioinf* (2007) 8:238. doi: 10.1186/1471-2105-8-238
120. Sturniolo T, Bono E, Ding J, Raddrizzani L, Tuereci O, Sahin U, et al. Generation of Tissue-Specific and Promiscuous HLA Ligand Databases

Using DNA Microarrays and Virtual HLA Class II Matrices. *Nat Biotechnol* (1999) 17(6):555–61. doi: 10.1038/9858
121. Nielsen M, Lundegaard C, Blicher T, Peters B, Sette A, Justesen S, et al. Quantitative Predictions of Peptide Binding to Any HLA-DR Molecule of Known Sequence: NetMHCIIpan. *PloS Comput Biol* (2008) 4(7):e1000107. doi: 10.1371/journal.pcbi.1000107
122. Zhang L, Udaka K, Mamitsuka H, Zhu S. Toward More Accurate Pan-Specific MHC-Peptide Binding Prediction: A Review of Current Methods and Tools. *Brief Bioinform* (2012) 13(3):350–64. doi: 10.1093/bib/bbr060
123. Peters B, Sette A. Generating Quantitative Models Describing the Sequence Specificity of Biological Processes With the Stabilized Matrix Method. *BMC Bioinf* (2005) 6:132. doi: 10.1186/1471-2105-6-132
124. Sidney J, Assarsson E, Moore C, Ngo S, Pinilla C, Sette A, et al. Quantitative Peptide Binding Motifs for 19 Human and Mouse MHC Class I Molecules Derived Using Positional Scanning Combinatorial Peptide Libraries. *Immunome Res* (2008) 4:2. doi: 10.1186/1745-7580-4-2
125. Moutaftsi M, Peters B, Pasquetto V, Tscharke DC, Sidney J, Bui HH, et al. A Consensus Epitope Prediction Approach Identifies the Breadth of Murine T (CD8+)-Cell Responses to Vaccinia Virus. *Nat Biotechnol* (2006) 24(7):817–9. doi: 10.1038/nbt1215
126. Hoof I, Peters B, Sidney J, Pedersen LE, Sette A, Lund O, et al. NetMHCpan, a Method for MHC Class I Binding Prediction Beyond Humans. *Immunogenetics* (2009) 61(1):1–13. doi: 10.1007/s00251-008-0341-z
127. Karosiene E, Lundegaard C, Lund O, Nielsen M. NetMHCcons: A Consensus Method for the Major Histocompatibility Complex Class I Predictions. *Immunogenetics* (2012) 64(3):177–86. doi: 10.1007/s00251-011-0579-8
128. Zhang H, Lund O, Nielsen M. The PickPocket Method for Predicting Binding Specificities for Receptors Based on Receptor Pocket Similarities: Application to MHC-Peptide Binding. *Bioinformatics* (2009) 25(10):1293–9. doi: 10.1093/bioinformatics/btp137
129. Rasmussen M, Fenoy E, Harndahl M, Kristensen AB, Nielsen IK, Nielsen M, et al. Pan-Specific Prediction of Peptide-MHC Class I Complex Stability, a Correlate of T Cell Immunogenicity. *J Immunol* (2016) 197(4):1517–24. doi: 10.4049/jimmunol.1600582
130. Abebe F. Synergy Between Th1 and Th2 Responses During Mycobacterium Tuberculosis Infection: A Review of Current Understanding. *Int Rev Immunol* (2019) 38(4):172–9. doi: 10.1080/08830185.2019.1632842
131. Reddy Chichili VP, Kumar V, Sivaraman J. Linkers in the Structural Biology of Protein-Protein Interactions. *Protein Sci* (2013) 22(2):153–67. doi: 10.1002/pro.2206
132. Zhao HL, Yao XQ, Xue C, Wang Y, Xiong XH, Liu ZM. Increasing the Homogeneity, Stability and Activity of Human Serum Albumin and Interferon-Alpha2b Fusion Protein by Linker Engineering. *Protein Expr Purif* (2008) 61(1):73–7. doi: 10.1016/j.pep.2008.04.013
133. Amet N, Lee HF, Shen WC. Insertion of the Designed Helical Linker Led to Increased Expression of Tf-Based Fusion Proteins. *Pharm Res* (2009) 26 (3):523–8. doi: 10.1007/s11095-008-9767-0
134. Bai Y, Shen WC. Improving the Oral Efficacy of Recombinant Granulocyte Colony-Stimulating Factor and Transferrin Fusion Protein by Spacer Optimization. *Pharm Res* (2006) 23(9):2116–21. doi: 10.1007/s11095-006-9059-5
135. Argos P. An Investigation of Oligopeptides Linking Domains in Protein Tertiary Structures and Possible Candidates for General Gene Fusion. *J Mol Biol* (1990) 211(4):943–58. doi: 10.1016/0022-2836(90)90085-z
136. Sabourin M, Tuzon CT, Fisher TS, Zakian VA. A Flexible Protein Linker Improves the Function of Epitope-Tagged Proteins in Saccharomyces Cerevisiae. *Yeast* (2007) 24(1):39–45. doi: 10.1002/yea.1431
137. de Bold MK, Sheffield WP, Martinuk A, Bhakta V, Eltringham-Smith L, de Bold AJ. Characterization of a Long-Acting Recombinant Human Serum Albumin-Atrial Natriuretic Factor (ANF) Expressed in Pichia Pastoris. *Regul Pept* (2012) 175(1-3):7–10. doi: 10.1016/j.regpep.2012.01.005
138. Waldo GS, Standish BM, Berendzen J, Terwilliger TC. Rapid Protein-Folding Assay Using Green Fluorescent Protein. *Nat Biotechnol* (1999) 17(7):691–5. doi: 10.1038/10904
139. Bird RE, Hardman KD, Jacobson JW, Johnson S, Kaufman BM, Lee SM, et al. Single-Chain Antigen-Binding Proteins. *Science* (1988) 242(4877):423–6. doi: 10.1126/science.3140379
140. Chen X, Zaro JL, Shen WC. Fusion Protein Linkers: Property, Design and Functionality. *Adv Drug Delivery Rev* (2013) 65(10):1357–69. doi: 10.1016/j.addr.2012.09.039
141. Maeda Y, Ueda H, Kazami J, Kawano G, Suzuki E, Nagamune T. Engineering of Functional Chimeric Protein G-Vargula Luciferase. *Anal Biochem* (1997) 249(2):147–52. doi: 10.1006/abio.1997.2181
142. Ulrich JT, Cieplak W, Paczkowski NJ, Taylor SM, Sanderson SD. Induction of an Antigen-Specific CTL Response by a Conformationally Biased Agonist of Human C5a Anaphylatoxin as a Molecular Adjuvant. *J Immunol* (2000) 164(10):5492–8. doi: 10.4049/jimmunol.164.10.5492
143. McCormick AL, Thomas MS, Heath AW. Immunization With an Interferon-Gamma-Gp120 Fusion Protein Induces Enhanced Immune Responses to Human Immunodeficiency Virus Gp120. *J Infect Dis* (2001) 184(11):1423–30. doi: 10.1086/324371
144. Medha P, Sharma S, Sharma M. Design of a Peptide-Based Vaccine From Late Stage Specific Immunogenic Cross-Reactive Antigens of PE/PPE Proteins of Mycobacterium Tuberculosis. *Eur J Pharm Sci* (2021) 168:106051. doi: 10.1016/j.ejps.2021.106051
145. Shiraz M, Lata S, Kumar P, Shankar UN, Akif M. Immunoinformatics Analysis of Antigenic Epitopes and Designing of a Multi-Epitope Peptide Vaccine From Putative Nitro-Reductases of Mycobacterium Tuberculosis DosR. *Infect Genet Evol* (2021) 94:105017. doi: 10.1016/j.meegid.2021.105017
146. Rai PK, Chodisetti SB, Zeng W, Nadeem S, Maurya SK, Pahari S, et al. A Lipidated Peptide of Mycobacterium Tuberculosis Resuscitates the Protective Efficacy of BCG Vaccine by Evoking Memory T Cell Immunity. *J Transl Med* (2017) 15(1):201. doi: 10.1186/s12967-017-1301-x
147. Dorosti H, Eslami M, Negahdaripour M, Ghoshoon MB, Gholami A, Heidari R, et al. Vaccinomics Approach for Developing Multi-Epitope Peptide Pneumococcal Vaccine. *J Biomol Struct Dyn* (2019) 37(13):3524–35. doi: 10.1080/07391102.2018.1519460
148. Rostamtabar M, Rahmani A, Baee M, Karkhah A, Prajapati VK, Ebrahimpour S, et al. Development a Multi-Epitope Driven Subunit Vaccine for Immune Response Reinforcement Against Serogroup B of Neisseria Meningitidis Using Comprehensive Immunoinformatics Approaches. *Infect Genet Evol* (2019) 75:103992. doi: 10.1016/j.meegid.2019.103992
149. Sharma R, Rajput VS, Jamal S, Grover A, Grover S. An Immunoinformatics Approach to Design a Multi-Epitope Vaccine Against Mycobacterium Tuberculosis Exploiting Secreted Exosome Proteins. *Sci Rep* (2021) 11 (1):13836. doi: 10.1038/s41598-021-93266-w
150. Chatterjee N, Ojha R, Khatoon N, Prajapati VK. Scrutinizing Mycobacterium Tuberculosis Membrane and Secretory Proteins to Formulate Multiepitope Subunit Vaccine Against Pulmonary Tuberculosis by Utilizing Immunoinformatic Approaches. *Int J Biol Macromol* (2018) 118(Pt A):180–8. doi: 10.1016/j.ijbiomac.2018.06.080
151. Rahmani A, Baee M, Rostamtabar M, Karkhah A, Alizadeh S, Tourani M, et al. Development of a Conserved Chimeric Vaccine Based on Helper T-Cell and CTL Epitopes for Induction of Strong Immune Response Against Schistosoma Mansoni Using Immunoinformatics Approaches. *Int J Biol Macromol* (2019) 141:125–36. doi: 10.1016/j.ijbiomac.2019.08.259
152. Tahir Ul Qamar M, Ahmad S, Fatima I, Ahmad F, Shahid F, Naz A, et al. Designing Multi-Epitope Vaccine Against Staphylococcus Aureus by Employing Subtractive Proteomics, Reverse Vaccinology and Immuno-Informatics Approaches. *Comput Biol Med* (2021) 132:104389. doi: 10.1016/j.compbiomed.2021.104389
153. Ghosh P, Bhakta S, Bhattacharya M, Sharma AR, Sharma G, Lee SS, et al. A Novel Multi-Epitopic Peptide Vaccine Candidate Against Helicobacter Pylori: In-Silico Identification, Design, Cloning and Validation Through Molecular Dynamics. *Int J Pept Res Ther* (2021) 27:1–18. doi: 10.1007/s10989-020-10157-w
154. Yadav S, Prakash J, Shukla H, Das KC, Tripathi T, Dubey VK. Design of a Multi-Epitope Subunit Vaccine for Immune-Protection Against Leishmania Parasite. *Pathog Glob Health* (2020) 114(8):471–81. doi: 10.1080/20477724.2020.1842976
155. Shey RA, Ghogomu SM, Esoh KK, Nebangwa ND, Shintouo CM, Nongley NF, et al. In-Silico Design of a Multi-Epitope Vaccine Candidate Against

Onchocerciasis and Related Filarial Diseases. *Sci Rep* (2019) 9(1):4409. doi: 10.1038/s41598-019-40833-x
156. Yazdani Z, Rafiei A, Irannejad H, Yazdani M, Valadan R. Designing a Novel Multiepitope Peptide Vaccine Against Melanoma Using Immunoinformatics Approach. *J Biomol Struct Dyn* (2020) 2020:1–13. doi: 10.1080/07391102.2020.1846625
157. Saadi M, Karkhah A, Nouri HR. Development of a Multi-Epitope Peptide Vaccine Inducing Robust T Cell Responses Against Brucellosis Using Immunoinformatics Based Approaches. *Infect Genet Evol* (2017) 51:227–34. doi: 10.1016/j.meegid.2017.04.009
158. Nezafat N, Karimi Z, Eslami M, Mohkam M, Zandian S, Ghasemi Y. Designing an Efficient Multi-Epitope Peptide Vaccine Against Vibrio Cholerae via Combined Immunoinformatics and Protein Interaction Based Approaches. *Comput Biol Chem* (2016) 62:82–95. doi: 10.1016/j.compbiolchem.2016.04.006
159. Meza B, Ascencio F, Sierra-Beltrán AP, Torres J, Angulo C. A Novel Design of a Multi-Antigenic, Multistage and Multi-Epitope Vaccine Against Helicobacter Pylori: An in Silico Approach. *Infect Genet Evol* (2017) 49:309–17. doi: 10.1016/j.meegid.2017.02.007
160. Albutti A. An Integrated Computational Framework to Design a Multi-Epitopes Vaccine Against Mycobacterium Tuberculosis. *Sci Rep* (2021) 11 (1):21929. doi: 10.1038/s41598-021-01283-6
161. Mitra D, Pandey J, Jain A, Swaroop S. In Silico Design of Multi-Epitope-Based Peptide Vaccine Against SARS-CoV-2 Using its Spike Protein. *J Biomol Struct Dyn* (2021) 2020:1–14. doi: 10.1080/07391102.2020.1869092
162. Kalita P, Padhi AK, Zhang KYJ, Tripathi T. Design of a Peptide-Based Subunit Vaccine Against Novel Coronavirus SARS-CoV-2. *Microb Pathog* (2020) 145:104236. doi: 10.1016/j.micpath.2020.104236
163. Abdulla F, Adhikari UK, Uddin MK. Exploring T & B-Cell Epitopes and Designing Multi-Epitope Subunit Vaccine Targeting Integration Step of HIV-1 Lifecycle Using Immunoinformatics Approach. *Microb Pathog* (2019) 137:103791. doi: 10.1016/j.micpath.2019.103791
164. Shahid F, Ashfaq UA, Javaid A, Khalid H. Immunoinformatics Guided Rational Design of a Next Generation Multi Epitope Based Peptide (MEBP) Vaccine by Exploring Zika Virus Proteome. *Infect Genet Evol* (2020) 80:104199. doi: 10.1016/j.meegid.2020.104199
165. Pavitrakar DV, Atre NM, Tripathy AS, Shil P. Design of a Multi-Epitope Peptide Vaccine Candidate Against Chandipura Virus: An Immuno-Informatics Study. *J Biomol Struct Dyn* (2020) 2020:1–12. doi: 10.1080/07391102.2020.1816493
166. Saha R, Ghosh P, Burra V. Designing a Next Generation Multi-Epitope Based Peptide Vaccine Candidate Against SARS-CoV-2 Using Computational Approaches. *3 Biotech* (2021) 11(2):47. doi: 10.1007/s13205-020-02574-x
167. Jakhar R, Kaushik S, Gakhar SK. 3CL Hydrolase-Based Multiepitope Peptide Vaccine Against SARS-CoV-2 Using Immunoinformatics. *J Med Virol* (2020) 92(10):2114–23. doi: 10.1002/jmv.25993
168. Schurz H, Daya M, Möller M, Hoal EG, Salie M. TLR1, 2, 4, 6 and 9 Variants Associated With Tuberculosis Susceptibility: A Systematic Review and Meta-Analysis. *PloS One* (2015) 10(10):e0139711. doi: 10.1371/journal.pone.0139711
169. Gopalakrishnan A, Dietzold J, Salgame P. Vaccine-Mediated Immunity to Experimental Mycobacterium Tuberculosis is Not Impaired in the Absence of Toll-Like Receptor 9. *Cell Immunol* (2016) 302:11–8. doi: 10.1016/j.cellimm.2015.12.009
170. Wani BA, Shehjar F, Shah S, Koul A, Yusuf A, Farooq M, et al. Role of Genetic Variants of Vitamin D Receptor, Toll-Like Receptor 2 and Toll-Like Receptor 4 in Extrapulmonary Tuberculosis. *Microb Pathog* (2021) 156:104911. doi: 10.1016/j.micpath.2021.104911
171. Hemmi H, Takeuchi O, Kawai T, Kaisho T, Sato S, Sanjo H, et al. A Toll-Like Receptor Recognizes Bacterial DNA. *Nature* (2000) 408(6813):740–5. doi: 10.1038/35047123
172. Krug A, Rothenfusser S, Hornung V, Jahrsdörfer B, Blackwell S, Ballas ZK, et al. Identification of CpG Oligonucleotide Sequences With High Induction of IFN-Alpha/Beta in Plasmacytoid Dendritic Cells. *Eur J Immunol* (2001) 31(7):2154–63. doi: 10.1002/1521-4141(200107)31:7<2154::aid-immu2154>3.0.co;2-u
173. Steinhagen F, Kinjo T, Bode C, Klinman DM. TLR-Based Immune Adjuvants. *Vaccine* (2011) 29(17):3341–55. doi: 10.1016/j.vaccine.2010.08.002
174. Vollmer J, Weeratna R, Payette P, Jurk M, Schetter C, Laucht M, et al. Characterization of Three CpG Oligodeoxynucleotide Classes With Distinct Immunostimulatory Activities. *Eur J Immunol* (2004) 34(1):251–62. doi: 10.1002/eji.200324032
175. Akira S, Uematsu S, Takeuchi O. Pathogen Recognition and Innate Immunity. *Cell* (2006) 124(4):783–801. doi: 10.1016/j.cell.2006.02.015
176. Peacock T, Chain B. Information-Driven Docking for TCR-pMHC Complex Prediction. *Front Immunol* (2021) 12:686127. doi: 10.3389/fimmu.2021.686127
177. Akıl M, Aykur M, Karakavuk M, Can H, Döşkaya M. Construction of a Multiepitope Vaccine Candidate Against Fasciola Hepatica: An in Silico Design Using Various Immunogenic Excretory/Secretory Antigens. *Expert Rev Vaccines* (2021) 2021:1–14. doi: 10.1080/14760584.2022.1996233
178. Malonis RJ, Lai JR, Vergnolle O. Peptide-Based Vaccines: Current Progress and Future Challenges. *Chem Rev* (2020) 120(6):3210–29. doi: 10.1021/acs.chemrev.9b00472
179. Andersen P, Scriba TJ. Moving Tuberculosis Vaccines From Theory to Practice. *Nat Rev Immunol* (2019) 19(9):550–62. doi: 10.1038/s41577-019-0174-z
180. Etlinger HM, Heimer EP, Trzeciak A, Felix AM, Gillessen D. Assessment in Mice of a Synthetic Peptide-Based Vaccine Against the Sporozoite Stage of the Human Malaria Parasite, P. Falciparum. *Immunology* (1988) 64(3):551–8.
181. Weichold FF, Mueller S, Kortsik C, Hitzler WE, Wulf MJ, Hone DM, et al. Impact of MHC Class I Alleles on the M. Tuberculosis Antigen-Specific CD8 + T-Cell Response in Patients With Pulmonary Tuberculosis. *Genes Immun* (2007) 8(4):334–43. doi: 10.1038/sj.gene.6364392
182. Gaseitsiwe S, Valentini D, Mahdavifar S, Magalhaes I, Hoft DF, Zerweck J, et al. Pattern Recognition in Pulmonary Tuberculosis Defined by High Content Peptide Microarray Chip Analysis Representing 61 Proteins From M. Tuberculosis. *PloS One* (2008) 3(12):e3840. doi: 10.1371/journal.pone.0003840
183. Axelsson-Robertson R, Weichold F, Sizemore D, Wulf M, Skeiky YA, Sadoff J, et al. Extensive Major Histocompatibility Complex Class I Binding Promiscuity for Mycobacterium Tuberculosis TB10.4 Peptides and Immune Dominance of Human Leucocyte Antigen (HLA)-B*0702 and HLA-B*0801 Alleles in TB10.4 CD8 T-Cell Responses. *Immunology* (2010) 129(4):496–505. doi: 10.1111/j.1365-2567.2009.03201.x
184. Gaseitsiwe S, Valentini D, Mahdavifar S, Reilly M, Ehrnst A, Maeurer M. Peptide Microarray-Based Identification of Mycobacterium Tuberculosis Epitope Binding to HLA-DRB1*0101, DRB1*1501, and DRB1*0401. *Clin Vaccine Immunol* (2010) 17(1):168–75. doi: 10.1128/cvi.00208-09
185. Axelsson-Robertson R, Ahmed RK, Weichold FF, Ehlers MM, Kock MM, Sizemore D, et al. Human Leukocyte Antigens A*3001 and A*3002 Show Distinct Peptide-Binding Patterns of the Mycobacterium Tuberculosis Protein TB10.4: Consequences for Immune Recognition. *Clin Vaccine Immunol* (2011) 18(1):125–34. doi: 10.1128/cvi.00302-10
186. Valentini D, Rao M, Ferrara G, Perkins M, Dodoo E, Zumla A, et al. Immune Recognition Surface Construction of Mycobacterium Tuberculosis Epitope-Specific Antibody Responses in Tuberculosis Patients Identified by Peptide Microarrays. *Int J Infect Dis* (2017) 56:155–66. doi: 10.1016/j.ijid.2017.01.015
187. Höhn H, Kortsik C, Nilges K, Necker A, Freitag K, Tully G, et al. Human Leucocyte Antigen-A2 Restricted and Mycobacterium Tuberculosis 19-kDa Antigen-Specific CD8+ T-Cell Responses are Oligoclonal and Exhibit a T-Cell Cytotoxic Type 2 Response Cytokine-Secretion Pattern. *Immunology* (2001) 104(3):278–88. doi: 10.1046/j.1365-2567.2001.01307.x
188. Höhn H, Kortsik C, Tully G, Nilges K, Necker A, Freitag K, et al. Longitudinal Analysis of Mycobacterium Tuberculosis 19-kDa Antigen-Specific T Cells in Patients With Pulmonary Tuberculosis: Association With Disease Activity and Cross-Reactivity to a Peptide From HIVenv Gp120. *Eur J Immunol* (2003) 33(6):1613–23. doi: 10.1002/eji.200323480
189. Tully G, Kortsik C, Höhn H, Zehbe I, Hitzler WE, Neukirch C, et al. Highly Focused T Cell Responses in Latent Human Pulmonary Mycobacterium Tuberculosis Infection. *J Immunol* (2005) 174(4):2174–84. doi: 10.4049/jimmunol.174.4.2174
190. Oftung F, Mustafa AS, Shinnick TM, Houghten RA, Kvalheim G, Degre M, et al. Epitopes of the Mycobacterium Tuberculosis 65-Kilodalton Protein Antigen as Recognized by Human T Cells. *J Immunol* (1988) 141(8):2749–54.

191. Mustafa AS, Oftung F, Amoudy HA, Madi NM, Abal AT, Shaban F, et al. Multiple Epitopes From the Mycobacterium Tuberculosis ESAT-6 Antigen are Recognized by Antigen-Specific Human T Cell Lines. *Clin Infect Dis* (2000) 30 Suppl 3:S201–205. doi: 10.1086/313862
192. Mustafa AS, Shaban FA, Abal AT, Al-Attiyah R, Wiker HG, Lundin KE, et al. Identification and HLA Restriction of Naturally Derived Th1-Cell Epitopes From the Secreted Mycobacterium Tuberculosis Antigen 85B Recognized by Antigen-Specific Human CD4(+) T-Cell Lines. *Infect Immun* (2000) 68 (7):3933–40. doi: 10.1128/iai.68.7.3933-3940.2000
193. Mustafa AS, Shaban FA, Al-Attiyah R, Abal AT, El-Shamy AM, Andersen P, et al. Human Th1 Cell Lines Recognize the Mycobacterium Tuberculosis ESAT-6 Antigen and its Peptides in Association With Frequently Expressed HLA Class II Molecules. *Scand J Immunol* (2003) 57(2):125–34. doi: 10.1046/j.1365-3083.2003.01204.x
194. Mustafa AS, Al-Attiyah R, Hanif SN, Shaban FA. Efficient Testing of Large Pools of Mycobacterium Tuberculosis RD1 Peptides and Identification of Major Antigens and Immunodominant Peptides Recognized by Human Th1 Cells. *Clin Vaccine Immunol* (2008) 15(6):916–24. doi: 10.1128/cvi.00056-08
195. Mustafa AS, Shaban F. Mapping of Th1-Cell Epitope Regions of Mycobacterium Tuberculosis Protein MPT64 (Rv1980c) Using Synthetic Peptides and T-Cell Lines From M. Tuberculosis-Infected Healthy Humans. *Med Princ Pract* (2010) 19(2):122–8. doi: 10.1159/000273073
196. Mustafa AS. Characterization of a Cross-Reactive, Immunodominant and HLA-Promiscuous Epitope of Mycobacterium Tuberculosis-Specific Major Antigenic Protein PPE68. *PloS One* (2014) 9(8):e103679. doi: 10.1371/journal.pone.0103679
197. McMurry J, Sbai H, Gennaro ML, Carter EJ, Martin W, De Groot AS. Analyzing Mycobacterium Tuberculosis Proteomes for Candidate Vaccine Epitopes. *Tuberculosis (Edinb)* (2005) 85(1-2):95–105. doi: 10.1016/j.tube.2004.09.005
198. De Groot AS, McMurry J, Marcon L, Franco J, Rivera D, Kutzler M, et al. Developing an Epitope-Driven Tuberculosis (TB) Vaccine. *Vaccine* (2005) 23(17-18):2121–31. doi: 10.1016/j.vaccine.2005.01.059
199. Geluk A, van Meijgaarden KE, de Vries RR, Sette A, Ottenhoff TH. A DR17-Restricted T Cell Epitope From a Secreted Mycobacterium Tuberculosis Antigen Only Binds to DR17 Molecules at Neutral pH. *Eur J Immunol* (1997) 27(4):842–7. doi: 10.1002/eji.1830270406
200. Geluk A, Taneja V, van Meijgaarden KE, Zanelli E, Abou-Zeid C, Thole JE, et al. Identification of HLA Class II-Restricted Determinants of Mycobacterium Tuberculosis-Derived Proteins by Using HLA-Transgenic, Class II-Deficient Mice. *Proc Natl Acad Sci USA* (1998) 95(18):10797–802. doi: 10.1073/pnas.95.18.10797
201. Commandeur S, van den Eeden SJ, Dijkman K, Clark SO, van Meijgaarden KE, Wilson L, et al. The In Vivo Expressed Mycobacterium Tuberculosis (IVE-TB) Antigen Rv2034 Induces $CD4^+$ T-Cells That Protect Against Pulmonary Infection in HLA-DR Transgenic Mice and Guinea Pigs. *Vaccine* (2014) 32(29):3580–8. doi: 10.1016/j.vaccine.2014.05.005
202. Geluk A, van den Eeden SJ, van Meijgaarden KE, Dijkman K, Franken KL, Ottenhoff TH. A Multistage-Polyepitope Vaccine Protects Against Mycobacterium Tuberculosis Infection in HLA-DR3 Transgenic Mice. *Vaccine* (2012) 30(52):7513–21. doi: 10.1016/j.vaccine.2012.10.045
203. Coppola M, van den Eeden SJ, Wilson L, Franken KL, Ottenhoff TH, Geluk A. Synthetic Long Peptide Derived From Mycobacterium Tuberculosis Latency Antigen Rv1733c Protects Against Tuberculosis. *Clin Vaccine Immunol* (2015) 22(9):1060–9. doi: 10.1128/CVI.00271-15
204. da Fonseca DP, Joosten D, van der Zee R, Jue DL, Singh M, Vordermeier HM, et al. Identification of New Cytotoxic T-Cell Epitopes on the 38-Kilodalton Lipoglycoprotein of Mycobacterium Tuberculosis by Using Lipopeptides. *Infect Immun* (1998) 66(7):3190–7. doi: 10.1128/iai.66.7.3190-3197.1998
205. da Fonseca DP, Frerichs J, Singh M, Snippe H, Verheul AF. Induction of Antibody and T-Cell Responses by Immunization With ISCOMS Containing the 38-Kilodalton Protein of Mycobacterium Tuberculosis. *Vaccine* (2000) 19(1):122–31. doi: 10.1016/s0264-410x(00)00102-x
206. Fonseca DP, Benaissa-Trouw B, van Engelen M, Kraaijeveld CA, Snippe H, Verheul AF. Induction of Cell-Mediated Immunity Against Mycobacterium Tuberculosis Using DNA Vaccines Encoding Cytotoxic and Helper T-Cell Epitopes of the 38-Kilodalton Protein. *Infect Immun* (2001) 69(8):4839–45. doi: 10.1128/iai.69.8.4839-4845.2001
207. Harboe M, Christensen A, Ahmad S, Ulvund G, Harkness RE, Mustafa AS, et al. Cross-Reaction Between Mammalian Cell Entry (Mce) Proteins of Mycobacterium Tuberculosis. *Scand J Immunol* (2002) 56(6):580–7. doi: 10.1046/j.1365-3083.2002.01172.x
208. Das AK, Mitra D, Harboe M, Nandi B, Harkness RE, Das D, et al. Predicted Molecular Structure of the Mammalian Cell Entry Protein Mce1A of Mycobacterium Tuberculosis. *Biochem Biophys Res Commun* (2003) 302 (3):442–7. doi: 10.1016/s0006-291x(03)00116-5
209. Harboe M, Das AK, Mitra D, Ulvund G, Ahmad S, Harkness RE, et al. Immunodominant B-Cell Epitope in the Mce1A Mammalian Cell Entry Protein of Mycobacterium Tuberculosis Cross-Reacting With Glutathione S-Transferase. *Scand J Immunol* (2004) 59(2):190–7. doi: 10.1111/j.0300-9475.2004.01383.x
210. Gowthaman U, Singh V, Zeng W, Jain S, Siddiqui KF, Chodisetti SB, et al. Promiscuous Peptide of 16 kDa Antigen Linked to Pam2Cys Protects Against Mycobacterium Tuberculosis by Evoking Enduring Memory T-Cell Response. *J Infect Dis* (2011) 204(9):1328–38. doi: 10.1093/infdis/jir548
211. Maurya SK, Aqdas M, Das DK, Singh S, Nadeem S, Kaur G, et al. A Multiple T Cell Epitope Comprising DNA Vaccine Boosts the Protective Efficacy of Bacillus Calmette-Guérin (BCG) Against Mycobacterium Tuberculosis. *BMC Infect Dis* (2020) 20(1):677. doi: 10.1186/s12879-020-05372-1
212. Harris DP, Vordermeier HM, Roman E, Lathigra R, Brett SJ, Moreno C, et al. Murine T Cell-Stimulatory Peptides From the 19-kDa Antigen of Mycobacterium Tuberculosis. Epitope-Restricted Homology With the 28-kDa Protein of Mycobacterium Leprae. *J Immunol* (1991) 147(8):2706–12.
213. Vordermeier HM, Harris DP, Friscia G, Román E, Surcel HM, Moreno C, et al. T Cell Repertoire in Tuberculosis: Selective Anergy to an Immunodominant Epitope of the 38-kDa Antigen in Patients With Active Disease. *Eur J Immunol* (1992) 22(10):2631–7. doi: 10.1002/eji.1830221024
214. Vordermeier HM, Harris DP, Mehrotra PK, Roman E, Elsaghier A, Moreno C, et al. M. Tuberculosis-Complex Specific T-Cell Stimulation and DTH Reactions Induced With a Peptide From the 38-kDa Protein. *Scand J Immunol* (1992) 35(6):711–8. doi: 10.1111/j.1365-3083.1992.tb02979.x
215. Launois P, DeLeys R, Niang MN, Drowart A, Andrien M, Dierckx P, et al. T-Cell-Epitope Mapping of the Major Secreted Mycobacterial Antigen Ag85A in Tuberculosis and Leprosy. *Infect Immun* (1994) 62(9):3679–87. doi: 10.1128/iai.62.9.3679-3687.1994
216. Denis O, Tanghe A, Palfliet K, Jurion F, van den Berg TP, Vanonckelen A, et al. Vaccination With Plasmid DNA Encoding Mycobacterial Antigen 85A Stimulates a CD4+ and CD8+ T-Cell Epitopic Repertoire Broader Than That Stimulated by Mycobacterium Tuberculosis H37Rv Infection. *Infect Immun* (1998) 66(4):1527–33. doi: 10.1128/iai.66.4.1527-1533.1998
217. Romano M, Denis O, D'Souza S, Wang XM, Ottenhoff TH, Brulet JM, et al. Induction of In Vivo Functional Db-Restricted Cytolytic T Cell Activity Against a Putative Phosphate Transport Receptor of Mycobacterium Tuberculosis. *J Immunol* (2004) 172(11):6913–21. doi: 10.4049/jimmunol.172.11.6913
218. Sánchez-Barinas CD, Ocampo M, Vanegas M, Castañeda-Ramirez JJ, Patarroyo MA, Patarroyo ME. Mycobacterium Tuberculosis H37Rv LpqG Protein Peptides Can Inhibit Mycobacterial Entry Through Specific Interactions. *Molecules* (2018) 23(3):526. doi: 10.3390/molecules23030526
219. Sánchez-Barinas CD, Ocampo M, Tabares L, Bermúdez M, Patarroyo MA, Patarroyo ME. Specific Binding Peptides From Rv3632: A Strategy for Blocking Mycobacterium Tuberculosis Entry to Target Cells? *BioMed Res Int* (2019) 2019:8680935. doi: 10.1155/2019/8680935
220. Ocampo M, Curtidor H, Vanegas M, Patarroyo MA, Patarroyo ME. Specific Interaction Between Mycobacterium Tuberculosis Lipoprotein-Derived Peptides and Target Cells Inhibits Mycobacterial Entry In Vitro. *Chem Biol Drug Des* (2014) 84(6):626–41. doi: 10.1111/cbdd.12365
221. Brandt L, Oettinger T, Holm A, Andersen AB, Andersen P. Key Epitopes on the ESAT-6 Antigen Recognized in Mice During the Recall of Protective Immunity to Mycobacterium Tuberculosis. *J Immunol* (1996) 157(8):3527–33. doi: 10.1016/S0165-2478(97)86823-X
222. Olsen AW, Hansen PR, Holm A, Andersen P. Efficient Protection Against Mycobacterium Tuberculosis by Vaccination With a Single Subdominant

Epitope From the ESAT-6 Antigen. *Eur J Immunol* (2000) 30(6):1724–32. doi: 10.1002/1521-4141(200006)30:6<1724::aid-immu1724>3.0.co;2-a

223. Aagaard CS, Hoang TT, Vingsbo-Lundberg C, Dietrich J, Andersen P. Quality and Vaccine Efficacy of CD4+ T Cell Responses Directed to Dominant and Subdominant Epitopes in ESAT-6 From Mycobacterium Tuberculosis. *J Immunol* (2009) 183(4):2659–68. doi: 10.4049/jimmunol.0900947
224. Chaitra MG, Hariharaputran S, Chandra NR, Shaila MS, Nayak R. Defining Putative T Cell Epitopes From PE and PPE Families of Proteins of Mycobacterium Tuberculosis With Vaccine Potential. *Vaccine* (2005) 23 (10):1265–72. doi: 10.1016/j.vaccine.2004.08.046
225. Chaitra MG, Shaila MS, Nayak R. Evaluation of T-Cell Responses to Peptides With MHC Class I-Binding Motifs Derived From PE_PGRS 33 Protein of Mycobacterium Tuberculosis. *J Med Microbiol* (2007) 56(Pt 4):466–74. doi: 10.1099/jmm.0.46928-0
226. Chaitra MG, Shaila MS, Chandra NR, Nayak R. HLA-A*0201-Restricted Cytotoxic T-Cell Epitopes in Three PE/PPE Family Proteins of Mycobacterium Tuberculosis. *Scand J Immunol* (2008) 67(4):411–7. doi: 10.1111/j.1365-3083.2008.02078.x
227. Chaitra MG, Shaila MS, Nayak R. Characterization of T-Cell Immunogenicity of Two PE/PPE Proteins of Mycobacterium Tuberculosis. *J Med Microbiol* (2008) 57(Pt 9):1079–86. doi: 10.1099/jmm.0.47565-0
228. Commandeur S, van Meijgaarden KE, Lin MY, Franken KL, Friggen AH, Drijfhout JW, et al. Identification of Human T-Cell Responses to Mycobacterium Tuberculosis Resuscitation-Promoting Factors in Long-Term Latently Infected Individuals. *Clin Vaccine Immunol* (2011) 18 (4):676–83. doi: 10.1128/cvi.00492-10
229. Tang ST, van Meijgaarden KE, Caccamo N, Guggino G, Klein MR, van Weeren P, et al. Genome-Based in Silico Identification of New Mycobacterium Tuberculosis Antigens Activating Polyfunctional CD8+ T Cells in Human Tuberculosis. *J Immunol* (2011) 186(2):1068–80. doi: 10.4049/jimmunol.1002212
230. Commandeur S, Coppola M, Dijkman K, Friggen AH, van Meijgaarden KE, van den Eeden SJ, et al. Clonal Analysis of the T-Cell Response to In Vivo Expressed Mycobacterium Tuberculosis Protein Rv2034, Using a CD154 Expression Based T-Cell Cloning Method. *PloS One* (2014) 9(6):e99203. doi: 10.1371/journal.pone.0099203
231. Zhu YH, Gao YF, Chen F, Liu W, Zhai MX, Zhai WJ, et al. Identification of Novel T Cell Epitopes From Efflux Pumps of Mycobacterium Tuberculosis. *Immunol Lett* (2011) 140(1-2):68–73. doi: 10.1016/j.imlet.2011.06.009
232. Chen F, Zhai MX, Zhu YH, Qi YM, Zhai WJ, Gao YF. In Vitro and In Vivo Identification of a Novel Cytotoxic T Lymphocyte Epitope From Rv3425 of Mycobacterium Tuberculosis. *Microbiol Immunol* (2012) 56(8):548–53. doi: 10.1111/j.1348-0421.2012.00470.x
233. Li D, Dou Z, Wu Y, Qi Y, Chen J, Gao Y. Identification of Novel Cytotoxic T Lymphocyte Epitopes of Drug- Resistance Related Protein InhA From Mycobacterium Tuberculosis. *Protein Pept Lett* (2020) 27(11):1141–50. doi: 10.2174/0929866527666200505215346
234. Mollenkopf HJ, Grode L, Mattow J, Stein M, Mann P, Knapp B, et al. Application of Mycobacterial Proteomics to Vaccine Design: Improved Protection by Mycobacterium Bovis BCG Prime-Rv3407 DNA Boost Vaccination Against Tuberculosis. *Infect Immun* (2004) 72(11):6471–9. doi: 10.1128/iai.72.11.6471-6479.2004
235. Wang QM, Sun SH, Hu ZL, Zhou FJ, Yin M, Xiao CJ, et al. Epitope DNA Vaccines Against Tuberculosis: Spacers and Ubiquitin Modulates Cellular Immune Responses Elicited by Epitope DNA Vaccine. *Scand J Immunol* (2004) 60(3):219–25. doi: 10.1111/j.0300-9475.2004.01442.x
236. Garnica O, Das K, Devasundaram S, Dhandayuthapani S. Enhanced Delivery of Mycobacterium Tuberculosis Antigens to Antigen Presenting Cells Using RVG Peptide. *Tuberculosis (Edinb)* (2019) 116s:S34–s41. doi: 10.1016/j.tube.2019.04.009
237. Fan X, Li X, Wan K, Zhao X, Deng Y, Chen Z, et al. Construction and Immunogenicity of a T Cell Epitope-Based Subunit Vaccine Candidate Against Mycobacterium Tuberculosis. *Vaccine* (2021) 39(47):6860–5. doi: 10.1016/j.vaccine.2021.10.034
238. Jiang Q, Zhang J, Chen X, Xia M, Lu Y, Qiu W, et al. A Novel Recombinant DNA Vaccine Encoding Mycobacterium Tuberculosis ESAT-6 and FL Protects Against Mycobacterium Tuberculosis Challenge in Mice. *J BioMed Res* (2013) 27(5):406–20. doi: 10.7555/jbr.27.20120114
239. Kumar S, Bhaskar A, Patnaik G, Sharma C, Singh DK, Kaushik SR, et al. Intranasal Immunization With Peptide-Based Immunogenic Complex Enhances BCG Vaccine Efficacy in a Murine Model of Tuberculosis. *JCI Insight* (2021) 6(4):e145228. doi: 10.1172/jci.insight.145228
240. Chesson CB, Huante M, Nusbaum RJ, Walker AG, Clover TM, Chinnaswamy J, et al. Nanoscale Peptide Self-Assemblies Boost BCG-Primed Cellular Immunity Against Mycobacterium Tuberculosis. *Sci Rep* (2018) 8(1):12519. doi: 10.1038/s41598-018-31089-y
241. Sugawara I, Udagawa T, Taniyama T. Protective Efficacy of Recombinant (Ag85A) BCG Tokyo With Ag85A Peptide Boosting Against Mycobacterium Tuberculosis-Infected Guinea Pigs in Comparison With That of DNA Vaccine Encoding Ag85A. *Tuberculosis (Edinb)* (2007) 87(2):94–101. doi: 10.1016/j.tube.2006.05.001
242. Shi C, Zhang H, Zhang T, Wang X, Bai B, Zhao Y, et al. New Alternative Vaccine Component Against Mycobacterium Tuberculosis–Heat Shock Protein 16.3 or its T-Cell Epitope. *Scand J Immunol* (2009) 70(5):465–74. doi: 10.1111/j.1365-3083.2009.02325.x
243. Wu M, Li M, Yue Y, Xu W. DNA Vaccine With Discontinuous T-Cell Epitope Insertions Into HSP65 Scaffold as a Potential Means to Improve Immunogenicity of Multi-Epitope Mycobacterium Tuberculosis Vaccine. *Microbiol Immunol* (2016) 60(9):634–45. doi: 10.1111/1348-0421.12410
244. Choi SY, Kwon KW, Kim H, Choi HH, Shin SJ. Vaccine Potential of ESAT-6 Protein Fused With Consensus CD4(+) T-Cell Epitopes of PE/PPE Proteins Against Highly Pathogenic Mycobacterium Tuberculosis Strain HN878. *Biochem Biophys Res Commun* (2018) 503(4):2195–201. doi: 10.1016/j.bbrc.2018.06.017
245. Luo Y, Wang B, Hu L, Yu H, Da Z, Jiang W, et al. Fusion Protein Ag85B-MPT64(190-198)-Mtb8.4 has Higher Immunogenicity Than Ag85B With Capacity to Boost BCG-Primed Immunity Against Mycobacterium Tuberculosis in Mice. *Vaccine* (2009) 27(44):6179–85. doi: 10.1016/j.vaccine.2009.08.018
246. Li Q, Yu H, Zhang Y, Wang B, Jiang W, Da Z, et al. Immunogenicity and Protective Efficacy of a Fusion Protein Vaccine Consisting of Antigen Ag85B and HspX Against Mycobacterium Tuberculosis Infection in Mice. *Scand J Immunol* (2011) 73(6):568–76. doi: 10.1111/j.1365-3083.2011.02531.x
247. Liu X, Peng J, Hu L, Luo Y, Niu H, Bai C, et al. A Multistage Mycobacterium Tuberculosis Subunit Vaccine LT70 Including Latency Antigen Rv2626c Induces Long-Term Protection Against Tuberculosis. *Hum Vaccin Immunother* (2016) 12(7):1670–7. doi: 10.1080/21645515.2016.1141159
248. Qian J, Chen R, Wang H, Zhang X. Role of the PE/PPE Family in Host-Pathogen Interactions and Prospects for Anti-Tuberculosis Vaccine and Diagnostic Tool Design. *Front Cell Infect Microbiol* (2020) 10:594288. doi: 10.3389/fcimb.2020.594288
249. Sørensen AL, Nagai S, Houen G, Andersen P, Andersen AB. Purification and Characterization of a Low-Molecular-Mass T-Cell Antigen Secreted by Mycobacterium Tuberculosis. *Infect Immun* (1995) 63(5):1710–7. doi: 10.1128/iai.63.5.1710-1717.1995
250. Skjøt RL, Oettinger T, Rosenkrands I, Ravn P, Brock I, Jacobsen S, et al. Comparative Evaluation of Low-Molecular-Mass Proteins From Mycobacterium Tuberculosis Identifies Members of the ESAT-6 Family as Immunodominant T-Cell Antigens. *Infect Immun* (2000) 68(1):214–20. doi: 10.1128/iai.68.1.214-220.2000
251. Hoang T, Aagaard C, Dietrich J, Cassidy JP, Dolganov G, Schoolnik GK, et al. ESAT-6 (EsxA) and TB10.4 (EsxH) Based Vaccines for Pre- and Post-Exposure Tuberculosis Vaccination. *PloS One* (2013) 8(12):e80579. doi: 10.1371/journal.pone.0080579
252. Yang E, Lu Y, Xu Y, Liang Q, Wang C, Wang H, et al. Recombinant BCG Coexpressing Ag85B, ESAT-6 and Rv3620c Elicits Specific Th1 Immune Responses in C57BL/6 Mice. *Microb Pathog* (2014) 69-70:53–9. doi: 10.1016/j.micpath.2014.03.011
253. Li W, Li M, Deng G, Zhao L, Liu X, Wang Y. Prime-Boost Vaccination With Bacillus Calmette Guerin and a Recombinant Adenovirus Co-Expressing CFP10, ESAT6, Ag85A and Ag85B of Mycobacterium Tuberculosis Induces Robust Antigen-Specific Immune Responses in Mice. *Mol Med Rep* (2015) 12 (2):3073–80. doi: 10.3892/mmr.2015.3770

254. Liang Y, Bai X, Zhang J, Song J, Yang Y, Yu Q, et al. Ag85A/ESAT-6 Chimeric DNA Vaccine Induces an Adverse Response in Tuberculosis-Infected Mice. *Mol Med Rep* (2016) 14(2):1146–52. doi: 10.3892/mmr.2016.5364
255. Yu W, Hu T. Conjugation With an Inulin-Chitosan Adjuvant Markedly Improves the Immunogenicity of Mycobacterium Tuberculosis CFP10-TB10.4 Fusion Protein. *Mol Pharm* (2016) 13(11):3626–35. doi: 10.1021/acs.molpharmaceut.6b00138
256. Wang C, Lu J, Du W, Wang G, Li X, Shen X, et al. Ag85b/ESAT6-CFP10 Adjuvanted With Aluminum/Poly-IC Effectively Protects Guinea Pigs From Latent Mycobacterium Tuberculosis Infection. *Vaccine* (2019) 37(32):4477–84. doi: 10.1016/j.vaccine.2019.06.078
257. Karbalaei Zadeh Babaki M, Soleimanpour S, Rezaee SA. Antigen 85 Complex as a Powerful Mycobacterium Tuberculosis Immunogene: Biology, Immune-Pathogenicity, Applications in Diagnosis, and Vaccine Design. *Microb Pathog* (2017) 112:20–9. doi: 10.1016/j.micpath.2017.08.040
258. Adewumi AT, Elrashedy A, Soremekun OS, Ajadi MB, Soliman MES. Weak Spots Inhibition in the Mycobacterium Tuberculosis Antigen 85C Target for Antitubercular Drug Design Through Selective Irreversible Covalent Inhibitor-SER124. *J Biomol Struct Dyn* (2020) 2020:1–21. doi: 10.1080/07391102.2020.1844061
259. Hoft DF, Blazevic A, Abate G, Hanekom WA, Kaplan G, Soler JH, et al. A New Recombinant Bacille Calmette-Guerin Vaccine Safely Induces Significantly Enhanced Tuberculosis-Specific Immunity in Human Volunteers. *J Infect Dis* (2008) 198(10):1491–501. doi: 10.1086/592450
260. Hoft DF, Blazevic A, Selimovic A, Turan A, Tennant J, Abate G, et al. Safety and Immunogenicity of the Recombinant BCG Vaccine AERAS-422 in Healthy BCG-Naive Adults: A Randomized, Active-Controlled, First-In-Human Phase 1 Trial. *EBioMedicine* (2016) 7(C):278–86. doi: 10.1016/j.ebiom.2016.04.010
261. Hawkridge T, Scriba TJ, Gelderbloem S, Smit E, Tameris M, Moyo S, et al. Safety and Immunogenicity of a New Tuberculosis Vaccine, MVA85A, in Healthy Adults in South Africa. *J Infect Dis* (2008) 198(4):544–52. doi: 10.1086/590185
262. Kaufmann SH, Weiner J, von Reyn CF. Novel Approaches to Tuberculosis Vaccine Development. *Int J Infect Dis* (2017) 56(C):263–7. doi: 10.1016/j.ijid.2016.10.018
263. Stylianou E, Griffiths KL, Poyntz HC, Harrington-Kandt R, Dicks MD, Stockdale L, et al. Improvement of BCG Protective Efficacy With a Novel Chimpanzee Adenovirus and a Modified Vaccinia Ankara Virus Both Expressing Ag85A. *Vaccine* (2015) 33(48):6800–8. doi: 10.1016/j.vaccine.2015.10.017
264. Lu JB, Chen BW, Wang GZ, Fu LL, Shen XB, Su C, et al. Recombinant Tuberculosis Vaccine AEC/BC02 Induces Antigen-Specific Cellular Responses in Mice and Protects Guinea Pigs in a Model of Latent Infection. *J Microbiol Immunol Infect* (2015) 48(6):597–603. doi: 10.1016/j.jmii.2014.03.005
265. Viljoen A, Alsteens D, Dufrêne Y. Mechanical Forces Between Mycobacterial Antigen 85 Complex and Fibronectin. *Cells* (2020) 9(3):716. doi: 10.3390/cells9030716
266. Yuan Y, Crane DD, Simpson RM, Zhu YQ, Hickey MJ, Sherman DR, et al. The 16-kDa Alpha-Crystallin (Acr) Protein of Mycobacterium Tuberculosis Is Required for Growth in Macrophages. *Proc Natl Acad Sci USA* (1998) 95(16):9578–83. doi: 10.1073/pnas.95.16.9578
267. Hu Y, Movahedzadeh F, Stoker NG, Coates AR. Deletion of the Mycobacterium Tuberculosis Alpha-Crystallin-Like hspX Gene Causes Increased Bacterial Growth In Vivo. *Infect Immun* (2006) 74(2):861–8. doi: 10.1128/iai.74.2.861-868.2006
268. Wieczorek AE, Troudt JL, Knabenbauer P, Taylor J, Pavlicek RL, Karls R, et al. HspX Vaccination and Role in Virulence in the Guinea Pig Model of Tuberculosis. *Pathog Dis* (2014) 71(3):315–25. doi: 10.1111/2049-632x.12147
269. Siddiqui KF, Amir M, Gurram RK, Khan N, Arora A, Rajagopal K, et al. Latency-Associated Protein Acr1 Impairs Dendritic Cell Maturation and Functionality: A Possible Mechanism of Immune Evasion by Mycobacterium Tuberculosis. *J Infect Dis* (2014) 209(9):1436–45. doi: 10.1093/infdis/jit595
270. Woodworth JS, Behar SM. Mycobacterium Tuberculosis-Specific CD8+ T Cells and Their Role in Immunity. *Crit Rev Immunol* (2006) 26(4):317–52. doi: 10.1615/critrevimmunol.v26.i4.30
271. Vordermeier HM, Hewinson RG, Wilkinson RJ, Wilkinson KA, Gideon HP, Young DB, et al. Conserved Immune Recognition Hierarchy of Mycobacterial PE/PPE Proteins During Infection in Natural Hosts. *PloS One* (2012) 7(8):e40890. doi: 10.1371/journal.pone.0040890
272. Geisbrecht BV, Nikonenko B, Samala R, Nakamura R, Nacy CA, Sacksteder KA. Design and Optimization of a Recombinant System for Large-Scale Production of the MPT64 Antigen From Mycobacterium Tuberculosis. *Protein Expr Purif* (2006) 46(1):64–72. doi: 10.1016/j.pep.2005.08.011
273. Goyal B, Kumar K, Gupta D, Agarwal R, Latawa R, Sheikh JA, et al. Utility of B-Cell Epitopes Based Peptides of RD1 and RD2 Antigens for Immunodiagnosis of Pulmonary Tuberculosis. *Diagn Microbiol Infect Dis* (2014) 78(4):391–7. doi: 10.1016/j.diagmicrobio.2013.12.018
274. Zvi A, Ariel N, Fulkerson J, Sadoff JC, Shafferman A. Whole Genome Identification of Mycobacterium Tuberculosis Vaccine Candidates by Comprehensive Data Mining and Bioinformatic Analyses. *BMC Med Genomics* (2008) 1:18. doi: 10.1186/1755-8794-1-18
275. Black GF, Thiel BA, Ota MO, Parida SK, Adegbola R, Boom WH, et al. Immunogenicity of Novel DosR Regulon-Encoded Candidate Antigens of Mycobacterium Tuberculosis in Three High-Burden Populations in Africa. *Clin Vaccine Immunol* (2009) 16(8):1203–12. doi: 10.1128/cvi.00111-09
276. Leyten EM, Lin MY, Franken KL, Friggen AH, Prins C, van Meijgaarden KE, et al. Human T-Cell Responses to 25 Novel Antigens Encoded by Genes of the Dormancy Regulon of Mycobacterium Tuberculosis. *Microbes Infect* (2006) 8(8):2052–60. doi: 10.1016/j.micinf.2006.03.018
277. Bivas-Benita M, Lin MY, Bal SM, van Meijgaarden KE, Franken KL, Friggen AH, et al. Pulmonary Delivery of DNA Encoding Mycobacterium Tuberculosis Latency Antigen Rv1733c Associated to PLGA-PEI Nanoparticles Enhances T Cell Responses in a DNA Prime/Protein Boost Vaccination Regimen in Mice. *Vaccine* (2009) 27(30):4010–7. doi: 10.1016/j.vaccine.2009.04.033
278. Qian W, Huang Z, Chen Y, Yang J, Wang L, Wu K, et al. Elicitation of Integrated Immunity in Mice by a Novel Pneumococcal Polysaccharide Vaccine Conjugated With HBV Surface Antigen. *Sci Rep* (2020) 10(1):6470. doi: 10.1038/s41598-020-62185-7
279. An SJ, Woo JS, Chae MH, Kothari S, Carbis R. Preparation and Testing of a Haemophilus Influenzae Type B/Hepatitis B Surface Antigen Conjugate Vaccine. *Vaccine* (2015) 33(13):1614–9. doi: 10.1016/j.vaccine.2015.01.061
280. Polonskaya Z, Deng S, Sarkar A, Kain L, Comellas-Aragones M, McKay CS, et al. T Cells Control the Generation of Nanomolar-Affinity Anti-Glycan Antibodies. *J Clin Invest* (2017) 127(4):1491–504. doi: 10.1172/JCI91192
281. Li X, Pan C, Sun P, Peng Z, Feng E, Wu J, et al. Orthogonal Modular Biosynthesis of Nanoscale Conjugate Vaccines for Vaccination Against Infection. *Nano Res* (2021) 2021:1–9. doi: 10.1007/s12274-021-3713-4
282. Manayani DJ, Thomas D, Dryden KA, Reddy V, Siladi ME, Marlett JM, et al. A Viral Nanoparticle With Dual Function as an Anthrax Antitoxin and Vaccine. *PloS Pathog* (2007) 3(10):1422–31. doi: 10.1371/journal.ppat.0030142
283. Tao P, Mahalingam M, Zhu J, Moayeri M, Sha J, Lawrence WS, et al. A Bacteriophage T4 Nanoparticle-Based Dual Vaccine Against Anthrax and Plague. *mBio* (2018) 9(5):e01926–18. doi: 10.1128/mBio.01926-18
284. Pan C, Wu J, Qing S, Zhang X, Zhang L, Yue H, et al. Biosynthesis of Self-Assembled Proteinaceous Nanoparticles for Vaccination. *Adv Mater* (2020) 32(42):e2002940. doi: 10.1002/adma.202002940
285. Peng Z, Wu J, Wang K, Li X, Sun P, Zhang L, et al. Production of a Promising Biosynthetic Self-Assembled Nanoconjugate Vaccine Against Klebsiella Pneumoniae Serotype O2 in a General Escherichia Coli Host. *Adv Sci (Weinh)* (2021) 8(14):e2100549. doi: 10.1002/advs.202100549
286. McConnell MJ, Hanna PC, Imperiale MJ. Adenovirus-Based Prime-Boost Immunization for Rapid Vaccination Against Anthrax. *Mol Ther* (2007) 15(1):203–10. doi: 10.1038/sj.mt.6300034
287. Langley WA, Bradley KC, Li ZN, Smith ME, Schnell MJ, Steinhauer DA. Induction of Neutralizing Antibody Responses to Anthrax Protective Antigen by Using Influenza Virus Vectors: Implications for Disparate Immune System Priming Pathways. *J Virol* (2010) 84(16):8300–7. doi: 10.1128/JVI.00183-10
288. Wang HC, An HJ, Yu YZ, Xu Q. Potentiation of Anthrax Vaccines Using Protective Antigen-Expressing Viral Replicon Vectors. *Immunol Lett* (2015) 163(2):206–13. doi: 10.1016/j.imlet.2014.07.012

289. Onate AA, Donoso G, Moraga-Cid G, Folch H, Cespedes S, Andrews E. An RNA Vaccine Based on Recombinant Semliki Forest Virus Particles Expressing the Cu,Zn Superoxide Dismutase Protein of Brucella Abortus Induces Protective Immunity in BALB/c Mice. *Infect Immun* (2005) 73 (6):3294–300. doi: 10.1128/IAI.73.6.3294-3300.2005
290. Cabrera A, Saez D, Cespedes S, Andrews E, Onate A. Vaccination With Recombinant Semliki Forest Virus Particles Expressing Translation Initiation Factor 3 of Brucella Abortus Induces Protective Immunity in BALB/c Mice. *Immunobiology* (2009) 214(6):467–74. doi: 10.1016/j.imbio.2008.11.016
291. Tabynov K, Sansyzbay A, Kydyrbayev Z, Yespembetov B, Ryskeldinova S, Zinina N, et al. Influenza Viral Vectors Expressing the Brucella OMP16 or L7/L12 Proteins as Vaccines Against B. Abortus Infection. *Virol J* (2014) 11:69. doi: 10.1186/1743-422X-11-69
292. Bugybayeva D, Kydyrbayev Z, Zinina N, Assanzhanova N, Yespembetov B, Kozhamkulov Y, et al. A New Candidate Vaccine for Human Brucellosis Based on Influenza Viral Vectors: A Preliminary Investigation for the Development of an Immunization Schedule in a Guinea Pig Model. *Infect Dis Poverty* (2021) 10(1):13. doi: 10.1186/s40249-021-00801-y
293. Brennan FR, Bellaby T, Helliwell SM, Jones TD, Kamstrup S, Dalsgaard K, et al. Chimeric Plant Virus Particles Administered Nasally or Orally Induce Systemic and Mucosal Immune Responses in Mice. *J Virol* (1999) 73(2):930–8. doi: 10.1128/JVI.73.2.930-938.1999
294. Oliveira ML, Areas AP, Campos IB, Monedero V, Perez-Martinez G, Miyaji EN, et al. Induction of Systemic and Mucosal Immune Response and Decrease in Streptococcus Pneumoniae Colonization by Nasal Inoculation of Mice With Recombinant Lactic Acid Bacteria Expressing Pneumococcal Surface Antigen A. *Microbes Infect* (2006) 8(4):1016–24. doi: 10.1016/j.micinf.2005.10.020
295. Hanniffy SB, Carter AT, Hitchin E, Wells JM. Mucosal Delivery of a Pneumococcal Vaccine Using Lactococcus Lactis Affords Protection Against Respiratory Infection. *J Infect Dis* (2007) 195(2):185–93. doi: 10.1086/509807
296. Campos IB, Darrieux M, Ferreira DM, Miyaji EN, Silva DA, Areas AP, et al. Nasal Immunization of Mice With Lactobacillus Casei Expressing the Pneumococcal Surface Protein A: Induction of Antibodies, Complement Deposition and Partial Protection Against Streptococcus Pneumoniae Challenge. *Microbes Infect* (2008) 10(5):481–8. doi: 10.1016/j.micinf.2008.01.007
297. Medina M, Villena J, Vintini E, Hebert EM, Raya R, Alvarez S. Nasal Immunization With Lactococcus Lactis Expressing the Pneumococcal Protective Protein A Induces Protective Immunity in Mice. *Infect Immun* (2008) 76(6):2696–705. doi: 10.1128/IAI.00119-08
298. Ferreira DM, Darrieux M, Silva DA, Leite LC, Ferreira JM Jr, Ho PL, et al. Characterization of Protective Mucosal and Systemic Immune Responses Elicited by Pneumococcal Surface Protein PspA and PspC Nasal Vaccines Against a Respiratory Pneumococcal Challenge in Mice. *Clin Vaccine Immunol* (2009) 16(5):636–45. doi: 10.1128/CVI.00395-08
299. Vintini E, Villena J, Alvarez S, Medina M. Administration of a Probiotic Associated With Nasal Vaccination With Inactivated Lactococcus Lactis-PppA Induces Effective Protection Against Pneumoccocal Infection in Young Mice. *Clin Exp Immunol* (2010) 159(3):351–62. doi: 10.1111/j.1365-2249.2009.04056.x
300. Hernani Mde L, Ferreira PC, Ferreira DM, Miyaji EN, Ho PL, Oliveira ML. Nasal Immunization of Mice With Lactobacillus Casei Expressing the Pneumococcal Surface Protein C Primes the Immune System and Decreases Pneumococcal Nasopharyngeal Colonization in Mice. *FEMS Immunol Med Microbiol* (2011) 62(3):263–72. doi: 10.1111/j.1574-695X.2011.00809.x
301. Chu H, Kang S, Ha S, Cho K, Park SM, Han KH, et al. Lactobacillus Acidophilus Expressing Recombinant K99 Adhesive Fimbriae has an Inhibitory Effect on Adhesion of Enterotoxigenic Escherichia Coli. *Microbiol Immunol* (2005) 49(11):941–8. doi: 10.1111/j.1348-0421.2005.tb03687.x
302. Wu CM, Chung TC. Mice Protected by Oral Immunization With Lactobacillus Reuteri Secreting Fusion Protein of Escherichia Coli Enterotoxin Subunit Protein. *FEMS Immunol Med Microbiol* (2007) 50 (3):354–65. doi: 10.1111/j.1574-695X.2007.00255.x
303. Liu JK, Hou XL, Wei CH, Yu LY, He XJ, Wang GH, et al. Induction of Immune Responses in Mice After Oral Immunization With Recombinant Lactobacillus Casei Strains Expressing Enterotoxigenic Escherichia Coli F41 Fimbrial Protein. *Appl Environ Microbiol* (2009) 75(13):4491–7. doi: 10.1128/AEM.02672-08
304. Wei CH, Liu JK, Hou XL, Yu LY, Lee JS, Kim CJ. Immunogenicity and Protective Efficacy of Orally or Intranasally Administered Recombinant Lactobacillus Casei Expressing ETEC K99. *Vaccine* (2010) 28(24):4113–8. doi: 10.1016/j.vaccine.2009.05.088
305. Ferreira PC, da Silva JB, Piazza RM, Eckmann L, Ho PL, Oliveira ML. Immunization of Mice With Lactobacillus Casei Expressing a Beta-Intimin Fragment Reduces Intestinal Colonization by Citrobacter Rodentium. *Clin Vaccine Immunol* (2011) 18(11):1823–33. doi: 10.1128/CVI.05262-11
306. Wen LJ, Hou XL, Wang GH, Yu LY, Wei XM, Liu JK, et al. Immunization With Recombinant Lactobacillus Casei Strains Producing K99, K88 Fimbrial Protein Protects Mice Against Enterotoxigenic Escherichia Coli. *Vaccine* (2012) 30(22):3339–49. doi: 10.1016/j.vaccine.2011.08.036
307. Liu JK, Wei CH, Hou XL, Yu LY. Passive Protection of Mice Pups Through Oral or Intranasal Immunization of Dams With Recombinant Lactobacillus Casei Vaccine Against ETEC F41. *Res Vet Sci* (2014) 96(2):283–7. doi: 10.1016/j.rvsc.2014.01.010
308. Ashrafi F, Fallah Mehrabadi J, Siadat SD, Aghasadeghi MR. Expression and Purification of the Uropathogenic Escherichia Coli PapG Protein and its Surface Absorption on Lactobacillus Reuteri: Implications for Surface Display System Vaccines. *Jundishapur J Microbiol* (2015) 8(9):e25595. doi: 10.5812/jjm.25595
309. Lin R, Zhang Y, Long B, Li Y, Wu Y, Duan S, et al. Oral Immunization With Recombinant Lactobacillus Acidophilus Expressing espA-Tir-M Confers Protection Against Enterohemorrhagic Escherichia Coli O157:H7 Challenge in Mice. *Front Microbiol* (2017) 8:417. doi: 10.3389/fmicb.2017.00417
310. Yang G, Jiang Y, Tong P, Li C, Yang W, Hu J, et al. Alleviation of Enterotoxigenic Escherichia Coli Challenge by Recombinant Lactobacillus Plantarum Expressing a FaeG- and DC-Targeting Peptide Fusion Protein. *Benef Microbes* (2017) 8(3):379–91. doi: 10.3920/BM2016.0116
311. Yu M, Qi R, Chen C, Yin J, Ma S, Shi W, et al. Immunogenicity of Recombinant Lactobacillus Casei-Expressing F4 (K88) Fimbrial Adhesin FaeG in Conjunction With a Heat-Labile Enterotoxin A (LTAK63) and Heat-Labile Enterotoxin B (LTB) of Enterotoxigenic Escherichia Coli as an Oral Adjuvant in Mice. *J Appl Microbiol* (2017) 122(2):506–15. doi: 10.1111/jam.13352
312. Okuno T, Kashige N, Satho T, Irie K, Hiramatsu Y, Sharmin T, et al. Expression and Secretion of Cholera Toxin B Subunit in Lactobacilli. *Biol Pharm Bull* (2013) 36(6):952–8. doi: 10.1248/bpb.b12-01021
313. Kajikawa A, Satoh E, Leer RJ, Yamamoto S, Igimi S. Intragastric Immunization With Recombinant Lactobacillus Casei Expressing Flagellar Antigen Confers Antibody-Independent Protective Immunity Against Salmonella Enterica Serovar Enteritidis. *Vaccine* (2007) 25(18):3599–605. doi: 10.1016/j.vaccine.2007.01.055
314. Kajikawa A, Igimi S. Innate and Acquired Immune Responses Induced by Recombinant Lactobacillus Casei Displaying Flagellin-Fusion Antigen on the Cell-Surface. *Vaccine* (2010) 28(19):3409–15. doi: 10.1016/j.vaccine.2010.02.077
315. Zegers ND, Kluter E, van der Stap H, van Dura E, van Dalen P, Shaw M, et al. Expression of the Protective Antigen of Bacillus Anthracis by Lactobacillus Casei: Towards the Development of an Oral Vaccine Against Anthrax. *J Appl Microbiol* (1999) 87(2):309–14. doi: 10.1046/j.1365-2672.1999.00900.x
316. Mohamadzadeh M, Duong T, Sandwick SJ, Hoover T, Klaenhammer TR. Dendritic Cell Targeting of Bacillus Anthracis Protective Antigen Expressed by Lactobacillus Acidophilus Protects Mice From Lethal Challenge. *Proc Natl Acad Sci USA* (2009) 106(11):4331–6. doi: 10.1073/pnas.0900029106
317. Mohamadzadeh M, Durmaz E, Zadeh M, Pakanati KC, Gramarossa M, Cohran V, et al. Targeted Expression of Anthrax Protective Antigen by Lactobacillus Gasseri as an Anthrax Vaccine. *Future Microbiol* (2010) 5 (8):1289–96. doi: 10.2217/fmb.10.78
318. Kathania M, Zadeh M, Lightfoot YL, Roman RM, Sahay B, Abbott JR, et al. Colonic Immune Stimulation by Targeted Oral Vaccine. *PloS One* (2013) 8 (1):e55143. doi: 10.1371/journal.pone.0055143

319. O'Flaherty S, Klaenhammer TR. Multivalent Chromosomal Expression of the Clostridium Botulinum Serotype A Neurotoxin Heavy-Chain Antigen and the Bacillus Anthracis Protective Antigen in Lactobacillus Acidophilus. *Appl Environ Microbiol* (2016) 82(20):6091–101. doi: 10.1128/AEM.01533-16
320. Pontes DS, Dorella FA, Ribeiro LA, Miyoshi A, Le Loir Y, Gruss A, et al. Induction of Partial Protection in Mice After Oral Administration of Lactococcus Lactis Producing Brucella Abortus L7/L12 Antigen. *J Drug Target* (2003) 11(8-10):489–93. doi: 10.1080/10611860410001670035
321. Saez D, Fernandez P, Rivera A, Andrews E, Onate A. Oral Immunization of Mice With Recombinant Lactococcus Lactis Expressing Cu,Zn Superoxide Dismutase of Brucella Abortus Triggers Protective Immunity. *Vaccine* (2012) 30(7):1283–90. doi: 10.1016/j.vaccine.2011.12.088
322. Shirdast H, Ebrahimzadeh F, Taromchi AH, Mortazavi Y, Esmaeilzadeh A, Sekhavati MH, et al. Recombinant Lactococcus Lactis Displaying Omp31 Antigen of Brucella Melitensis Can Induce an Immunogenic Response in BALB/c Mice. *Probiotics Antimicrob Proteins* (2021) 13(1):80–9. doi: 10.1007/s12602-020-09684-1
323. Veloso TR, Mancini S, Giddey M, Vouillamoz J, Que YA, Moreillon P, et al. Vaccination Against Staphylococcus Aureus Experimental Endocarditis Using Recombinant Lactococcus Lactis Expressing ClfA or FnbpA. *Vaccine* (2015) 33(30):3512–7. doi: 10.1016/j.vaccine.2015.05.060
324. Clow F, Peterken K, Pearson V, Proft T, Radcliff FJ. PilVax, a Novel Lactococcus Lactis-Based Mucosal Vaccine Platform, Stimulates Systemic and Mucosal Immune Responses to Staphylococcus Aureus. *Immunol Cell Biol* (2020) 98(5):369–81. doi: 10.1111/imcb.12325
325. Corthesy B, Boris S, Isler P, Grangette C, Mercenier A. Oral Immunization of Mice With Lactic Acid Bacteria Producing Helicobacter Pylori Urease B Subunit Partially Protects Against Challenge With Helicobacter Felis. *J Infect Dis* (2005) 192(8):1441–9. doi: 10.1086/444425
326. Hongying F, Xianbo W, Fang Y, Yang B, Beiguo L. Oral Immunization With Recombinant Lactobacillus Acidophilus Expressing the Adhesin Hp0410 of Helicobacter Pylori Induces Mucosal and Systemic Immune Responses. *Clin Vaccine Immunol* (2014) 21(2):126–32. doi: 10.1128/CVI.00434-13
327. del Rio B, Fuente JL, Neves V, Dattwyler R, Seegers JF, Gomes-Solecki M. Platform Technology to Deliver Prophylactic Molecules Orally: An Example Using the Class A Select Agent Yersinia Pestis. *Vaccine* (2010) 28(41):6714–22. doi: 10.1016/j.vaccine.2010.07.084
328. Audouy SA, van Selm S, van Roosmalen ML, Post E, Kanninga R, Neef J, et al. Development of Lactococcal GEM-Based Pneumococcal Vaccines. *Vaccine* (2007) 25(13):2497–506. doi: 10.1016/j.vaccine.2006.09.026
329. Shi W, Kou Y, Jiang H, Gao F, Kong W, Su W, et al. Novel Intranasal Pertussis Vaccine Based on Bacterium-Like Particles as a Mucosal Adjuvant. *Immunol Lett* (2018) 198:26–32. doi: 10.1016/j.imlet.2018.03.012
330. Liu W, Tan Z, Xue J, Luo W, Song H, Lv X, et al. Therapeutic Efficacy of Oral Immunization With a non-Genetically Modified Lactococcus Lactis-Based Vaccine CUE-GEM Induces Local Immunity Against Helicobacter Pylori Infection. *Appl Microbiol Biotechnol* (2016) 100(14):6219–29. doi: 10.1007/s00253-016-7333-y
331. Liu W, Tan Z, Liu H, Zeng Z, Luo S, Yang H, et al. Nongenetically Modified Lactococcus Lactis-Adjuvanted Vaccination Enhanced Innate Immunity Against Helicobacter Pylori. *Helicobacter* (2017) 22(5):e12426. doi: 10.1111/hel.12426
332. Stokes MG, Titball RW, Neeson BN, Galen JE, Walker NJ, Stagg AJ, et al. Oral Administration of a Salmonella Enterica-Based Vaccine Expressing Bacillus Anthracis Protective Antigen Confers Protection Against Aerosolized B. Anthracis. *Infect Immun* (2007) 75(4):1827–34. doi: 10.1128/IAI.01242-06
333. Zhao Z, Li M, Luo D, Xing L, Wu S, Duan Y, et al. Protection of Mice From Brucella Infection by Immunization With Attenuated Salmonella Enterica Serovar Typhimurium Expressing A L7/L12 and BLS Fusion Antigen of Brucella. *Vaccine* (2009) 27(38):5214–9. doi: 10.1016/j.vaccine.2009.06.075
334. Senevirathne A, Hewawaduge C, Lee JH. Live Vaccine Consisting of Attenuated Salmonella Secreting and Delivering Brucella Ribosomal Protein L7/L12 Induces Humoral and Cellular Immune Responses and Protects Mice Against Virulent Brucella Abortus 544 Challenge. *Vet Res* (2020) 51(1):6. doi: 10.1186/s13567-020-0735-y
335. Xu C, Zhang BZ, Lin Q, Deng J, Yu B, Arya S, et al. Live Attenuated Salmonella Typhimurium Vaccines Delivering SaEsxA and SaEsxB via Type III Secretion System Confer Protection Against Staphylococcus Aureus Infection. *BMC Infect Dis* (2018) 18(1):195. doi: 10.1186/s12879-018-3104-y
336. He Y, Vemulapalli R, Schurig GG. Recombinant Ochrobactrum Anthropi Expressing Brucella Abortus Cu,Zn Superoxide Dismutase Protects Mice Against B. Abortus Infection Only After Switching of Immune Responses to Th1 Type. *Infect Immun* (2002) 70(5):2535–43. doi: 10.1128/iai.70.5.2535-2543.2002
337. Lee WH, Choi HI, Hong SW, Kim KS, Gho YS, Jeon SG. Vaccination With Klebsiella Pneumoniae-Derived Extracellular Vesicles Protects Against Bacteria-Induced Lethality via Both Humoral and Cellular Immunity. *Exp Mol Med* (2015) 47:e183. doi: 10.1038/emm.2015.59
338. Roberts R, Moreno G, Bottero D, Gaillard ME, Fingermann M, Graieb A, et al. Outer Membrane Vesicles as Acellular Vaccine Against Pertussis. *Vaccine* (2008) 26(36):4639–46. doi: 10.1016/j.vaccine.2008.07.004
339. Bottero D, Gaillard ME, Errea A, Moreno G, Zurita E, Pianciola L, et al. Outer Membrane Vesicles Derived From Bordetella Parapertussis as an Acellular Vaccine Against Bordetella Parapertussis and Bordetella Pertussis Infection. *Vaccine* (2013) 31(45):5262–8. doi: 10.1016/j.vaccine.2013.08.059
340. Raeven RHM, Brummelman J, Pennings JLA, van der Maas L, Helm K, Tilstra W, et al. Molecular and Cellular Signatures Underlying Superior Immunity Against Bordetella Pertussis Upon Pulmonary Vaccination. *Mucosal Immunol* (2018) 11(3):1009. doi: 10.1038/mi.2017.110
341. Choi KS, Kim SH, Kim ED, Lee SH, Han SJ, Yoon S, et al. Protection From Hemolytic Uremic Syndrome by Eyedrop Vaccination With Modified Enterohemorrhagic E. Coli Outer Membrane Vesicles. *PloS One* (2014) 9 (7):e100229. doi: 10.1371/journal.pone.0100229
342. Mitra S, Chakrabarti MK, Koley H. Multi-Serotype Outer Membrane Vesicles of Shigellae Confer Passive Protection to the Neonatal Mice Against Shigellosis. *Vaccine* (2013) 31(31):3163–73. doi: 10.1016/j.vaccine.2013.05.001
343. Gerke C, Colucci AM, Giannelli C, Sanzone S, Vitali CG, Sollai L, et al. Production of a Shigella Sonnei Vaccine Based on Generalized Modules for Membrane Antigens (GMMA), 1790gahb. *PloS One* (2015) 10(8):e0134478. doi: 10.1371/journal.pone.0134478
344. Obiero CW, Ndiaye AGW, Scire AS, Kaunyangi BM, Marchetti E, Gone AM, et al. A Phase 2a Randomized Study to Evaluate the Safety and Immunogenicity of the 1790GAHB Generalized Modules for Membrane Antigen Vaccine Against Shigella Sonnei Administered Intramuscularly to Adults From a Shigellosis-Endemic Country. *Front Immunol* (2017) 8:1884. doi: 10.3389/fimmu.2017.01884
345. Raso MM, Gasperini G, Alfini R, Schiavo F, Aruta MG, Carducci M, et al. GMMA and Glycoconjugate Approaches Compared in Mice for the Development of a Vaccine Against Shigella Flexneri Serotype 6. *Vaccines (Basel)* (2020) 8(2):160. doi: 10.3390/vaccines8020160
346. Schild S, Nelson EJ, Camilli A. Immunization With Vibrio Cholerae Outer Membrane Vesicles Induces Protective Immunity in Mice. *Infect Immun* (2008) 76(10):4554–63. doi: 10.1128/IAI.00532-08
347. Roy N, Barman S, Ghosh A, Pal A, Chakraborty K, Das SS, et al. Immunogenicity and Protective Efficacy of Vibrio Cholerae Outer Membrane Vesicles in Rabbit Model. *FEMS Immunol Med Microbiol* (2010) 60(1):18–27. doi: 10.1111/j.1574-695X.2010.00692.x
348. Alaniz RC, Deatherage BL, Lara JC, Cookson BT. Membrane Vesicles are Immunogenic Facsimiles of Salmonella Typhimurium That Potently Activate Dendritic Cells, Prime B and T Cell Responses, and Stimulate Protective Immunity *In Vivo*. *J Immunol* (2007) 179(11):7692–701. doi: 10.4049/jimmunol.179.11.7692
349. Howlader DR, Koley H, Sinha R, Maiti S, Bhaumik U, Mukherjee P, et al. Development of a Novel S. Typhi and Paratyphi A Outer Membrane Vesicles Based Bivalent Vaccine Against Enteric Fever. *PloS One* (2018) 13(9): e0203631. doi: 10.1371/journal.pone.0203631
350. Wang X, Thompson CD, Weidenmaier C, Lee JC. Release of Staphylococcus Aureus Extracellular Vesicles and Their Application as a Vaccine Platform. *Nat Commun* (2018) 9(1):1379. doi: 10.1038/s41467-018-03847-z
351. Fan X, Wang F, Zhou X, Chen B, Chen G. Size-Dependent Antibacterial Immunity of Staphylococcus Aureus Protoplast-Derived Particulate Vaccines. *Int J Nanomed* (2020) 15:10321–30. doi: 10.2147/IJN.S285895
352. Liu Q, Li X, Zhang Y, Song Z, Li R, Ruan H, et al. Orally-Administered Outer-Membrane Vesicles From Helicobacter Pylori Reduce H. Pylori

Infection via Th2-Biased Immune Responses in Mice. *Pathog Dis* (2019) 77 (5):ftz050. doi: 10.1093/femspd/ftz050
353. Wang X, Singh AK, Zhang X, Sun W. Induction of Protective Antiplague Immune Responses by Self-Adjuvanting Bionanoparticles Derived From Engineered Yersinia Pestis. *Infect Immun* (2020) 88(5):e00081–20. doi: 10.1128/IAI.00081-20
354. Wu G, Ji H, Guo X, Li Y, Ren T, Dong H, et al. Nanoparticle Reinforced Bacterial Outer-Membrane Vesicles Effectively Prevent Fatal Infection of Carbapenem-Resistant Klebsiella Pneumoniae. *Nanomedicine* (2020) 24:102148. doi: 10.1016/j.nano.2019.102148
355. Asensio CJ, Gaillard ME, Moreno G, Bottero D, Zurita E, Rumbo M, et al. Outer Membrane Vesicles Obtained From Bordetella Pertussis Tohama Expressing the Lipid A Deacylase PagL as a Novel Acellular Vaccine Candidate. *Vaccine* (2011) 29(8):1649–56. doi: 10.1016/j.vaccine.2010.12.068
356. Noroozi N, Gargari SLM, Nazarian S, Sarvary S, Adriani RR. Immunogenicity of Enterotoxigenic Escherichia Coli Outer Membrane Vesicles Encapsulated in Chitosan Nanoparticles. *Iran J Basic Med Sci* (2018) 21(3):284–91. doi: 10.22038/ijbms.2018.25886.6371
357. Camacho AI, de Souza J, Sanchez-Gomez S, Pardo-Ros M, Irache JM, Gamazo C. Mucosal Immunization With Shigella Flexneri Outer Membrane Vesicles Induced Protection in Mice. *Vaccine* (2011) 29 (46):8222–9. doi: 10.1016/j.vaccine.2011.08.121
358. Camacho AI, Irache JM, de Souza J, Sanchez-Gomez S, Gamazo C. Nanoparticle-Based Vaccine for Mucosal Protection Against Shigella Flexneri in Mice. *Vaccine* (2013) 31(32):3288–94. doi: 10.1016/j.vaccine.2013.05.020
359. Sarvary S, Gargari SLM, Nazarian S, Adriani RR, Noroozi N. Immunogenicity of Shigella Sonnei Outer Membrane Vesicles Extracted in Different Environmental Conditions. *Biologia* (2021) 76):721–8. doi: 10.2478/s11756-020-00606-8
360. Chen G, Bai Y, Li Z, Wang F, Fan X, Zhou X. Bacterial Extracellular Vesicle-Coated Multi-Antigenic Nanovaccines Protect Against Drug-Resistant Staphylococcus Aureus Infection by Modulating Antigen Processing and Presentation Pathways. *Theranostics* (2020) 10(16):7131–49. doi: 10.7150/thno.44564
361. Valentine JL, Chen L, Perregaux EC, Weyant KB, Rosenthal JA, Heiss C, et al. Immunization With Outer Membrane Vesicles Displaying Designer Glycotopes Yields Class-Switched, Glycan-Specific Antibodies. *Cell Chem Biol* (2016) 23(6):655–65. doi: 10.1016/j.chembiol.2016.05.014
362. Kim OY, Choi SJ, Jang SC, Park KS, Kim SR, Choi JP, et al. Bacterial Protoplast-Derived Nanovesicles as Vaccine Delivery System Against Bacterial Infection. *Nano Lett* (2015) 15(1):266–74. doi: 10.1021/nl503508h
363. Irene C, Fantappie L, Caproni E, Zerbini F, Anesi A, Tomasi M, et al. Bacterial Outer Membrane Vesicles Engineered With Lipidated Antigens as a Platform for Staphylococcus Aureus Vaccine. *Proc Natl Acad Sci USA* (2019) 116(43):21780–8. doi: 10.1073/pnas.1905112116
364. Pan C, Sun P, Liu B, Liang H, Peng Z, Dong Y, et al. Biosynthesis of Conjugate Vaccines Using an O-Linked Glycosylation System. *MBio* (2016) 7(2):e00443–00416. doi: 10.1128/mBio.00443-16
365. Peek LJ, Middaugh CR, Berkland C. Nanotechnology in Vaccine Delivery. *Adv Drug Delivery Rev* (2008) 60(8):915–28. doi: 10.1016/j.addr.2007.05.017
366. Zhang J, Tarbet EB, Toro H, Tang DC. Adenovirus-Vectored Drug-Vaccine Duo as a Potential Driver for Conferring Mass Protection Against Infectious Diseases. *Expert Rev Vaccines* (2011) 10(11):1539–52. doi: 10.1586/erv.11.141
367. Shi Z, Zeng M, Yang G, Siegel F, Cain LJ, van Kampen KR, et al. Protection Against Tetanus by Needle-Free Inoculation of Adenovirus-Vectored Nasal and Epicutaneous Vaccines. *J Virol* (2001) 75(23):11474–82. doi: 10.1128/JVI.75.23.11474-11482.2001
368. Hien TT, de Jong M, Farrar J. Avian Influenza–a Challenge to Global Health Care Structures. *N Engl J Med* (2004) 351(23):2363–5. doi: 10.1056/NEJMp048267
369. Romanova J, Krenn BM, Wolschek M, Ferko B, Romanovskaja-Romanko E, Morokutti A, et al. Preclinical Evaluation of a Replication-Deficient Intranasal DeltaNS1 H5N1 Influenza Vaccine. *PloS One* (2009) 4(6):e5984. doi: 10.1371/journal.pone.0005984
370. Wacheck V, Egorov A, Groiss F, Pfeiffer A, Fuereder T, Hoeflmayer D, et al. A Novel Type of Influenza Vaccine: Safety and Immunogenicity of Replication-Deficient Influenza Virus Created by Deletion of the Interferon Antagonist NS1. *J Infect Dis* (2010) 201(3):354–62. doi: 10.1086/649428
371. Tabynov K, Ryskeldinova S, Sansyzbay A. An Influenza Viral Vector Brucella Abortus Vaccine Induces Good Cross-Protection Against Brucella Melitensis Infection in Pregnant Heifers. *Vaccine* (2015) 33(31):3619–23. doi: 10.1016/j.vaccine.2015.06.045
372. Tabynov K, Yespembetov B, Matikhan N, Ryskeldinova S, Zinina N, Kydyrbayev Z, et al. First Evaluation of an Influenza Viral Vector Based Brucella Abortus Vaccine in Sheep and Goats: Assessment of Safety, Immunogenicity and Protective Efficacy Against Brucella Melitensis Infection. *Vet Microbiol* (2016) 197:15–20. doi: 10.1016/j.vetmic.2016.11.001
373. Tabynov K, Yespembetov B, Ryskeldinova S, Zinina N, Kydyrbayev Z, Kozhamkulov Y, et al. Prime-Booster Vaccination of Cattle With an Influenza Viral Vector Brucella Abortus Vaccine Induces a Long-Term Protective Immune Response Against Brucella Abortus Infection. *Vaccine* (2016) 34(4):438–44. doi: 10.1016/j.vaccine.2015.12.028
374. Mailybayeva A, Yespembetov B, Ryskeldinova S, Zinina N, Sansyzbay A, Renukaradhya GJ, et al. Improved Influenza Viral Vector Based Brucella Abortus Vaccine Induces Robust B and T-Cell Responses and Protection Against Brucella Melitensis Infection in Pregnant Sheep and Goats. *PloS One* (2017) 12(10):e0186484. doi: 10.1371/journal.pone.0186484
375. Mailybayeva A, Ryskeldinova S, Zinina N, Zhou EM, Renukaradhya GJ, Tabynov K. Evaluation of Duration of Immunogenicity and Protective Efficacy of Improved Influenza Viral Vector-Based Brucella Abortus Vaccine Against Brucella Melitensis Infection in Sheep and Goats. *Front Vet Sci* (2020) 7:58. doi: 10.3389/fvets.2020.00058
376. Smith ME, Koser M, Xiao S, Siler C, McGettigan JP, Calkins C, et al. Rabies Virus Glycoprotein as a Carrier for Anthrax Protective Antigen. *Virology* (2006) 353(2):344–56. doi: 10.1016/j.virol.2006.05.010
377. McComb RC, Ho CL, Bradley KA, Grill LK, Martchenko M. Presentation of Peptides From Bacillus Anthracis Protective Antigen on Tobacco Mosaic Virus as an Epitope Targeted Anthrax Vaccine. *Vaccine* (2015) 33(48):6745–51. doi: 10.1016/j.vaccine.2015.10.075
378. LeCureux JS, Dean GA. Lactobacillus Mucosal Vaccine Vectors: Immune Responses Against Bacterial and Viral Antigens. *mSphere* (2018) 3(3): e00061–18. doi: 10.1128/mSphere.00061-18
379. Gilbert C, Robinson K, Le Page RW, Wells JM. Heterologous Expression of an Immunogenic Pneumococcal Type 3 Capsular Polysaccharide in Lactococcus Lactis. *Infect Immun* (2000) 68(6):3251–60. doi: 10.1128/iai.68.6.3251-3260.2000
380. Audouy SA, van Roosmalen ML, Neef J, Kanninga R, Post E, van Deemter M, et al. Lactococcus Lactis GEM Particles Displaying Pneumococcal Antigens Induce Local and Systemic Immune Responses Following Intranasal Immunization. *Vaccine* (2006) 24(26):5434–41. doi: 10.1016/j.vaccine.2006.03.054
381. Ermak TH, Giannasca PJ, Nichols R, Myers GA, Nedrud J, Weltzin R, et al. Immunization of Mice With Urease Vaccine Affords Protection Against Helicobacter Pylori Infection in the Absence of Antibodies and is Mediated by MHC Class II-Restricted Responses. *J Exp Med* (1998) 188(12):2277–88. doi: 10.1084/jem.188.12.2277
382. Kao JY, Zhang M, Miller MJ, Mills JC, Wang B, Liu M, et al. Helicobacter Pylori Immune Escape is Mediated by Dendritic Cell-Induced Treg Skewing and Th17 Suppression in Mice. *Gastroenterology* (2010) 138(3):1046–54. doi: 10.1053/j.gastro.2009.11.043
383. Mashburn-Warren LM, Whiteley M. Special Delivery: Vesicle Trafficking in Prokaryotes. *Mol Microbiol* (2006) 61(4):839–46. doi: 10.1111/j.1365-2958.2006.05272.x
384. Lee JC, Lee EJ, Lee JH, Jun SH, Choi CW, Kim SI, et al. Klebsiella Pneumoniae Secretes Outer Membrane Vesicles That Induce the Innate Immune Response. *FEMS Microbiol Lett* (2012) 331(1):17–24. doi: 10.1111/j.1574-6968.2012.02549.x
385. Raeven RH, Brummelman J, Pennings JL, van der Maas L, Tilstra W, Helm K, et al. Bordetella Pertussis Outer Membrane Vesicle Vaccine Confers Equal Efficacy in Mice With Milder Inflammatory Responses Compared to a Whole-Cell Vaccine. *Sci Rep* (2016) 6:38240. doi: 10.1038/srep38240
386. Song Z, Li B, Zhang Y, Li R, Ruan H, Wu J, et al. Outer Membrane Vesicles of Helicobacter Pylori 7.13 as Adjuvants Promote Protective Efficacy Against

Helicobacter Pylori Infection. *Front Microbiol* (2020) 11:1340. doi: 10.3389/fmicb.2020.01340
387. Lee SR, Kim SH, Jeong KJ, Kim KS, Kim YH, Kim SJ, et al. Multi-Immunogenic Outer Membrane Vesicles Derived From an MsbB-Deficient Salmonella Enterica Serovar Typhimurium Mutant. *J Microbiol Biotechnol* (2009) 19(10):1271–9. doi: 10.4014/jmb.0901.0055
388. Leitner DR, Feichter S, Schild-Prufert K, Rechberger GN, Reidl J, Schild S. Lipopolysaccharide Modifications of a Cholera Vaccine Candidate Based on Outer Membrane Vesicles Reduce Endotoxicity and Reveal the Major Protective Antigen. *Infect Immun* (2013) 81(7):2379–93. doi: 10.1128/IAI.01382-12
389. Rossi O, Caboni M, Negrea A, Necchi F, Alfini R, Micoli F, et al. Toll-Like Receptor Activation by Generalized Modules for Membrane Antigens From Lipid A Mutants of Salmonella Enterica Serovars Typhimurium and Enteritidis. *Clin Vaccine Immunol* (2016) 23(4):304–14. doi: 10.1128/CVI.00023-16
390. De Benedetto G, Alfini R, Cescutti P, Caboni M, Lanzilao L, Necchi F, et al. Characterization of O-Antigen Delivered by Generalized Modules for Membrane Antigens (GMMA) Vaccine Candidates Against Nontyphoidal Salmonella. *Vaccine* (2017) 35(3):419–26. doi: 10.1016/j.vaccine.2016.11.089
391. Kim SH, Kim KS, Lee SR, Kim E, Kim MS, Lee EY, et al. Structural Modifications of Outer Membrane Vesicles to Refine Them as Vaccine Delivery Vehicles. *Biochim Biophys Acta* (2009) 1788(10):2150–9. doi: 10.1016/j.bbamem.2009.08.001
392. Kim SH, Lee SR, Kim KS, Ko A, Kim E, Kim YH, et al. Shiga Toxin A Subunit Mutant of Escherichia Coli O157:H7 Releases Outer Membrane Vesicles Containing the B-Pentameric Complex. *FEMS Immunol Med Microbiol* (2010) 58(3):412–20. doi: 10.1111/j.1574-695X.2010.00654.x
393. Fisseha M, Chen P, Brandt B, Kijek T, Moran E, Zollinger W. Characterization of Native Outer Membrane Vesicles From lpxL Mutant Strains of Neisseria Meningitidis for Use in Parenteral Vaccination. *Infect Immun* (2005) 73(7):4070–80. doi: 10.1128/IAI.73.7.4070-4080.2005
394. Sinha R, Howlader DR, Ta A, Mitra S, Das S, Koley H. Retinoic Acid Pre-Treatment Down Regulates V. Cholerae Outer Membrane Vesicles Induced Acute Inflammation and Enhances Mucosal Immunity. *Vaccine* (2017) 35(28):3534–47. doi: 10.1016/j.vaccine.2017.05.036
395. Fredriksen JH, Rosenqvist E, Wedege E, Bryn K, Bjune G, Froholm LO, et al. Production, Characterization and Control of MenB-Vaccine "Folkehelsa": An Outer Membrane Vesicle Vaccine Against Group B Meningococcal Disease. *NIPH Ann* (1991) 14(2):67–79. discussion 79-80.
396. Borrow R, Balmer P, Miller E. Meningococcal Surrogates of Protection–Serum Bactericidal Antibody Activity. *Vaccine* (2005) 23(17-18):2222–7. doi: 10.1016/j.vaccine.2005.01.051
397. Tamayo I, Irache JM, Mansilla C, Ochoa-Reparaz J, Lasarte JJ, Gamazo C. Poly(anhydride) Nanoparticles Act as Active Th1 Adjuvants Through Toll-Like Receptor Exploitation. *Clin Vaccine Immunol* (2010) 17(9):1356–62. doi: 10.1128/CVI.00164-10
398. Pan C, Yue H, Zhu L, Ma GH, Wang HL. Prophylactic Vaccine Delivery Systems Against Epidemic Infectious Diseases. *Adv Drug Delivery Rev* (2021) 176:113867. doi: 10.1016/j.addr.2021.113867
399. Schwendener RA. Liposomes as Vaccine Delivery Systems: A Review of the Recent Advances. *Ther Adv Vaccines* (2014) 2(6):159–82. doi: 10.1177/2051013614541440
400. Wang N, Chen M, Wang T. Liposomes Used as a Vaccine Adjuvant-Delivery System: From Basics to Clinical Immunization. *J Control Release* (2019) 303:130–50. doi: 10.1016/j.jconrel.2019.04.025
401. Hayman WA, Toth I, Flinn N, Scanlon M, Good MF. Enhancing the Immunogenicity and Modulating the Fine Epitope Recognition of Antisera to a Helical Group A Streptococcal Peptide Vaccine Candidate From the M Protein Using Lipid-Core Peptide Technology. *Immunol Cell Biol* (2002) 80(2):178–87. doi: 10.1046/j.1440-1711.2002.01067.x
402. Olive C, Batzloff MR, Toth I. Lipid Core Peptide Technology and Group A Streptococcal Vaccine Delivery. *Expert Rev Vaccines* (2004) 3(1):43–58. doi: 10.1586/14760584.3.1.43
403. Ghaffar KA, Marasini N, Giddam AK, Batzloff MR, Good MF, Skwarczynski M, et al. Liposome-Based Intranasal Delivery of Lipopeptide Vaccine Candidates Against Group A Streptococcus. *Acta Biomater* (2016) 41:161–8. doi: 10.1016/j.actbio.2016.04.012
404. Marasini N, Khalil ZG, Giddam AK, Ghaffar KA, Hussein WM, Capon RJ, et al. Lipid Core Peptide/Poly(Lactic-Co-Glycolic Acid) as a Highly Potent Intranasal Vaccine Delivery System Against Group A Streptococcus. *Int J Pharm* (2016) 513(1-2):410–20. doi: 10.1016/j.ijpharm.2016.09.057
405. Bartlett S, Skwarczynski M, Toth I. Lipids as Activators of Innate Immunity in Peptide Vaccine Delivery. *Curr Med Chem* (2020) 27(17):2887–901. doi: 10.2174/0929867325666181026100849
406. Ghaffar KA, Marasini N, Giddam AK, Batzloff MR, Good MF, Skwarczynski M, et al. The Role of Size in Development of Mucosal Liposome-Lipopeptide Vaccine Candidates Against Group A Streptococcus. *Med Chem* (2016) 13(1):22–7. doi: 10.2174/1573406412666160720093138
407. Dai CC, Yang J, Hussein WM, Zhao L, Wang X, Khalil ZG, et al. Polyethylenimine: An Intranasal Adjuvant for Liposomal Peptide-Based Subunit Vaccine Against Group A Streptococcus. *ACS Infect Dis* (2020) 6(9):2502–12. doi: 10.1021/acsinfecdis.0c00452
408. Dai CC, Huang W, Yang J, Hussein WM, Wang J, Khalil ZG, et al. Polyethylenimine Quantity and Molecular Weight Influence its Adjuvanting Properties in Liposomal Peptide Vaccines. *Bioorg Med Chem Lett* (2021) 40:127920. doi: 10.1016/j.bmcl.2021.127920
409. Muto K, Kamei N, Yoshida M, Takayama K, Takeda-Morishita M. Cell-Penetrating Peptide Penetratin as a Potential Tool for Developing Effective Nasal Vaccination Systems. *J Pharm Sci* (2016) 105(6):2014–7. doi: 10.1016/j.xphs.2016.03.026
410. Bahadoran A, Ebrahimi M, Yeap SK, Safi N, Moeini H, Hair-Bejo M, et al. Induction of a Robust Immune Response Against Avian Influenza Virus Following Transdermal Inoculation With H5-DNA Vaccine Formulated in Modified Dendrimer-Based Delivery System in Mouse Model. *Int J Nanomed* (2017) 12:8573–85. doi: 10.2147/IJN.S139126
411. Huang HC, Lu HF, Lai YH, Lee CP, Liu HK, Huang C. Tat-Enhanced Delivery of the C Terminus of HDAg-L Inhibits Assembly and Secretion of Hepatitis D Virus. *Antiviral Res* (2018) 150:69–78. doi: 10.1016/j.antiviral.2017.12.009
412. Yang J, Firdaus F, Azuar A, Khalil ZG, Marasini N, Capon RJ, et al. Cell-Penetrating Peptides-Based Liposomal Delivery System Enhanced Immunogenicity of Peptide-Based Vaccine Against Group A Streptococcus. *Vaccines (Basel)* (2021) 9(5):499. doi: 10.3390/vaccines9050499
413. Ribeiro AM, Chaimovich H. Preparation and Characterization of Large Dioctadecyldimethylammonium Chloride Liposomes and Comparison With Small Sonicated Vesicles. *Biochim Biophys Acta* (1983) 733(1):172–9. doi: 10.1016/0005-2736(83)90103-7
414. Carmona-Ribeiro AM, Chaimovich H. Salt-Induced Aggregation and Fusion of Dioctadecyldimethylammonium Chloride and Sodium Dihexadecylphosphate Vesicles. *Biophys J* (1986) 50(4):621–8. doi: 10.1016/S0006-3495(86)83501-9
415. Davidsen J, Rosenkrands I, Christensen D, Vangala A, Kirby D, Perrie Y, et al. Characterization of Cationic Liposomes Based on Dimethyldioctadecylammonium and Synthetic Cord Factor From M. Tuberculosis (Trehalose 6,6'-Dibehenate)-a Novel Adjuvant Inducing Both Strong CMI and Antibody Responses. *Biochim Biophys Acta* (2005) 1718(1-2):22–31. doi: 10.1016/j.bbamem.2005.10.011
416. Kamath AT, Rochat AF, Christensen D, Agger EM, Andersen P, Lambert PH, et al. A Liposome-Based Mycobacterial Vaccine Induces Potent Adult and Neonatal Multifunctional T Cells Through the Exquisite Targeting of Dendritic Cells. *PloS One* (2009) 4(6):e5771. doi: 10.1371/journal.pone.0005771
417. Kaushal D, Mehra S, Didier PJ, Lackner AA. The non-Human Primate Model of Tuberculosis. *J Med Primatol* (2012) 41(3):191–201. doi: 10.1111/j.1600-0684.2012.00536.x
418. Pena JC, Ho WZ. Non-Human Primate Models of Tuberculosis. *Microbiol Spectr* (2016) 4(4). doi: 10.1128/microbiolspec.TBTB2-0007-2016
419. McMurray DN. A Nonhuman Primate Model for Preclinical Testing of New Tuberculosis Vaccines. *Clin Infect Dis* (2000) 30:S210–212. doi: 10.1086/313885
420. Kaushal D, Foreman TW, Gautam US, Alvarez X, Adekambi T, Rangel-Moreno J, et al. Mucosal Vaccination With Attenuated Mycobacterium Tuberculosis Induces Strong Central Memory Responses and Protects Against Tuberculosis. *Nat Commun* (2015) 6:8533. doi: 10.1038/ncomms9533
421. Foreman TW, Veatch AV, LoBato DN, Didier PJ, Doyle-Meyers LA, Russell-Lodrigue KE, et al. Nonpathologic Infection of Macaques by an Attenuated Mycobacterial Vaccine Is Not Reactivated in the Setting of HIV Co-Infection. *Am J Pathol* (2017) 187(12):2811–20. doi: 10.1016/j.ajpath.2017.08.014

422. Goldberg AC, Rizzo LV. MHC Structure and Function - Antigen Presentation. Part 1. *Einstein (Sao Paulo Brazil)* (2015) 13(1):153–6. doi: 10.1590/s1679-45082015rb3122
423. Gregoriadis S, Zervas J, Varletzidis E, Toubis M, Pantazopoulos P, Fessas P. HLA Antigens and Otosclerosis. A Possible New Genetic Factor. *Arch Otolaryngol (Chicago Ill: 1960)* (1982) 108(12):769–71. doi: 10.1001/archotol.1982.00790600013004
424. Singhal SK, Mann SB, Datta U, Panda NK, Gupta AK. Genetic Correlation in Otosclerosis. *Am J Otolaryngol* (1999) 20(2):102–5. doi: 10.1016/s0196-0709(99)90019-4
425. Xu XP, Li SB, Wang CY, Li QH. Study on the Association of HLA With Pulmonary Tuberculosis. *Immunol Investigat* (1986) 15(4):327–32. doi: 10.3109/08820138609052951
426. Kim SJ, Choi IH, Dahlberg S, Nisperos B, Kim JD, Hansen JA. HLA and Leprosy in Koreans. *Tissue Antigens* (1987) 29(3):146–53. doi: 10.1111/j.1399-0039.1987.tb01567.x
427. Iannetti P, Morellini M, Raucci U, Cappellacci S. HLA Antigens, Epilepsy and Cytomegalovirus Infection. *Brain Dev* (1988) 10(4):256–8. doi: 10.1016/s0387-7604(88)80008-1
428. Konieczna A, Turowski G. HLA-ABC Antigens in Supraglottic Cancer Patients and Their Relationship With Incidence and Survival. Materia Medica Polona. *Polish J Med Pharm* (1993) 25(2):73–9.
429. Barona P, Sierrasesumaga L, Antillon F, Villa-Elizaga I. Study of HLA Antigens in Patients With Osteosarcoma. *Hum Hered* (1993) 43(5):311–4. doi: 10.1159/000154149
430. Marcos Y, Fainboim HA, Capucchio M, Findor J, Daruich J, Reyes B, et al. Two-Locus Involvement in the Association of Human Leukocyte Antigen With the Extrahepatic Manifestations of Autoimmune Chronic Active Hepatitis. *Hepatol (Baltimore Md)* (1994) 19(6):1371–4. doi: 10.1016/0270-9139(94)90230-5
431. Kaslow RA, Carrington M, Apple R, Park L, Munoz A, Saah AJ, et al. Influence of Combinations of Human Major Histocompatibility Complex Genes on the Course of HIV-1 Infection. *Nat Med* (1996) 2(4):405–11. doi: 10.1038/nm0496-405
432. Carrington M, O'Brien SJ. The Influence of HLA Genotype on AIDS. *Annu Rev Med* (2003) 54:535–51. doi: 10.1146/annurev.med.54.101601.152346
433. Zhang YH, Peng YC, Yan HP, Xu KY, Saito M, Wu H, et al. Multilayered Defense in HLA-B51-Associated HIV Viral Control. *J Immunol* (2011) 187(2):684–91. doi: 10.4049/jimmunol.1100316
434. Apps R, Qi Y, Carlson JM, Chen HY, Gao XJ, Thomas R, et al. Influence of HLA-C Expression Level on HIV Control. *Science* (2013) 340(6128):87–91. doi: 10.1126/science.1232685
435. Zhang H, Zhao B, Han XX, Wang Z, Liu BG, Lu CM, et al. Associations of HLA Class I Antigen Specificities and Haplotypes With Disease Progression in HIV-1-Infected Hans in Northern China. *Hum Immunol* (2013) 74(12):1636–42. doi: 10.1016/j.humimm.2013.08.287
436. Taneja V, David CS. HLA Transgenic Mice as Humanized Mouse Models of Disease and Immunity. *J Clin Invest* (1998) 101(5):921–6. doi: 10.1172/jci2860
437. Pascolo S. HLA Class I Transgenic Mice: Development, Utilisation and Improvement. *Expert Opin Biol Ther* (2005) 5(7):919–38. doi: 10.1517/14712598.5.7.919
438. Kievits F, Ivanyi P, Krimpenfort P, Berns A, Ploegh HL. HLA-Restricted Recognition of Viral Antigens in HLA Transgenic Mice. *Nature* (1987) 329(6138):447–9. doi: 10.1038/329447a0
439. Chamberlain JW, Nolan JA, Gromkowski SH, Kelley KA, Eisenstadt JM, Herrup K, et al. Cell Surface Expression and Alloantigenic Function of a Human Class I MHC Heavy Chain Gene (HLA-B7) in Transgenic Mice. *J Immunol (Baltimore Md: 1950)* (1988) 140(4):1285–92. doi: 10.0000/PMID3125253
440. Bernhard EJ, Le AX, Barbosa JA, Lacy E, Engelhard VH. Cytotoxic T Lymphocytes From HLA-A2 Transgenic Mice Specific for HLA-A2 Expressed on Human Cells. *J Exp Med* (1988) 168(3):1157–62. doi: 10.1084/jem.168.3.1157
441. Dill O, Kievits F, Koch S, Ivanyi P, Hammerling GJ. Immunological Function of HLA-C Antigens in HLA-Cw3 Transgenic Mice. *Proc Natl Acad Sci USA* (1988) 85(15):5664–8. doi: 10.1073/pnas.85.15.5664
442. Connolly JM, Potter TA, Wormstall EM, Hansen TH. The Lyt-2 Molecule Recognizes Residues in the Class I Alpha 3 Domain in Allogeneic Cytotoxic T Cell Responses. *J Exp Med* (1988) 168(1):325–41. doi: 10.1084/jem.168.1.325
443. Irwin MJ, Heath WR, Sherman LA. Species-Restricted Interactions Between CD8 and the Alpha 3 Domain of Class I Influence the Magnitude of the Xenogeneic Response. *J Exp Med* (1989) 170(4):1091–101. doi: 10.1084/jem.170.4.1091
444. Engelhard VH, Lacy E, Ridge JP. Influenza A-Specific, HLA-A2.1-Restricted Cytotoxic T Lymphocytes From HLA-A2.1 Transgenic Mice Recognize Fragments of the M1 Protein. *J Immunol (Baltimore Md* (1991) 1950) 146(4):1226–32.
445. Barra C, Gournier H, Garcia Z, Marche PN, Jouvin-Marche E, Briand P, et al. Abrogation of H-2-Restricted CTL Responses and Efficient Recognition of HLA-A3 Molecules in DBA/2 HLA/A24 Responder Mice. *J Immunol (Baltimore Md: 1950)* (1993) 150(9):3681–9.
446. Boucherma R, Kridane-Miledi H, Bouziat R, Rasmussen M, Gatard T, Langa-Vives F, et al. HLA-A*01:03, HLA-A*24:02, HLA-B*08:01, HLA-B*27:05, HLA-B*35:01, HLA-B*44:02, and HLA-C*07:01 Monochain Transgenic/H-2 Class I Null Mice: Novel Versatile Preclinical Models of Human T Cell Responses. *J Immunol* (2013) 191(2):583–93. doi: 10.4049/jimmunol.1300483
447. LaFace DM, Vestberg M, Yang Y, Srivastava R, DiSanto J, Flomenberg N, et al. Human CD8 Transgene Regulation of HLA Recognition by Murine T Cells. *J Exp Med* (1995) 182(5):1315–25. doi: 10.1084/jem.182.5.1315
448. Kalinke U, Arnold B, Hammerling GJ. Strong Xenogeneic HLA Response in Transgenic Mice After Introducing an Alpha 3 Domain Into HLA B27. *Nature* (1990) 348(6302):642–4. doi: 10.1038/348642a0
449. Vitiello A, Marchesini D, Furze J, Sherman LA, Chesnut RW. Analysis of the HLA-Restricted Influenza-Specific Cytotoxic T Lymphocyte Response in Transgenic Mice Carrying a Chimeric Human-Mouse Class I Major Histocompatibility Complex. *J Exp Med* (1991) 173(4):1007–15. doi: 10.1084/jem.173.4.1007
450. Pascolo S, Bervas N, Ure JM, Smith AG, Lemonnier FA, Perarnau B. HLA-A2.1-Restricted Education and Cytolytic Activity of CD8(+) T Lymphocytes From Beta2 Microglobulin (Beta2m) HLA-A2.1 Monochain Transgenic H-2Db Beta2m Double Knockout Mice. *J Exp Med* (1997) 185(12):2043–51. doi: 10.1084/jem.185.12.2043
451. Zeng Y, Gao TT, Zhao GY, Jiang YT, Yang Y, Yu H, et al. Generation of Human MHC (HLA-A11/DR1) Transgenic Mice for Vaccine Evaluation. *Hum Vaccines Immunother* (2016) 12(3):829–36. doi: 10.1080/21645515.2015.1103405
452. Li D, Li P, Song NP, Jiang YT, Zeng Y, Zhao GY, et al. Identification of Novel HLA-A11-Restricted T-Cell Epitopes in the Ebola Virus Nucleoprotein. *Microbes Infection* (2019) 21(1):56–62. doi: 10.1016/j.micinf.2018.04.005
453. Jin XX, Ding Y, Sun SH, Wang XY, Zhou ZN, Liu XT, et al. Screening HLA-A-Restricted T Cell Epitopes of SARS-CoV-2 and the Induction of CD8(+) T Cell Responses in HLA-A Transgenic Mice. *Cell Mol Immunol* (2021) 18(12):2588–608. doi: 10.1038/s41423-021-00784-8
454. Sabatino D. Medicinal Chemistry and Methodological Advances in the Development of Peptide-Based Vaccines. *J Med Chem* (2020) 63(23):14184–96. doi: 10.1021/acs.jmedchem.0c00848

Conflict of Interest: The authors declare that the research was conducted in the absence of any commercial or financial relationships that could be construed as a potential conflict of interest.

GLOSSARY

ADH	adipic acid dihydrazide
ATRA	all-trans retinoic acid
ANN	Artificial neural network
APCs	antigen presenting cells
AUCs	areas under the curve
BCG	Bacillus Calmette-Guérin
BMDCs	bone marrow derived DCs
BMDMs	bone marrow-derived macrophages
CAI	Codon Adaptation Index
CFP-10	culture filtrate protein 10
CRKP	carbapenem-resistant K. pneumoniae
CTB	cholera toxin subunit B
CTL	cytotoxic T-lymphocytes
COVID-19	coronavirus disease 2019
DCs	dendritic cells
DosRs	dormancy survival regulon antigens
ELISpot	enzyme-linked immunospot
ESAT-6	early secreted antigenic target 6
GEM	gram-positive enhancer matrix
HBD	human β-defensin;
HBHA	heparin binding hemagglutinin
HBsAg	Hepatitis B virus surface antigen
HTL	helper T lymphocytes
HIV	human immunodeficiency virus
HLA	human leukocyte antigen
HMM	Hidden Markov Model
IEDB	Immune Epitope Database and Analysis Resource
IFN-γ	interferon-γ
IL	Interleukin
IP-10	interferon gamma inducible protein 10
LTBI	latent TB infection
MCC	Matthew's correlation coefficient
MDR-TB	drug-resistant and multidrug-resistant TB
MM6	MonoMac6 human monocytes
MHC	major histocompatibility complex
NCBI	National Center of Biotechnology Information
NMR	nuclear magnetic resonance
NK	natural killer
ODN	oligonucleotides
OMVs	Outer membrane vesicles
Pam2Cys	dipalmitoyl-S-glyceryl cysteine
PA	protective antigen
PAMPs	pathogen associated molecular patterns
PBS	phosphate buffer solution
pDCs	plasmacytoid dendritic cells
PLS	partial least squares
pMHC	major histocompatibility complex presented antigenic peptides
PRP	ribosylribitolphosphate
PSMα4	phenol-soluble modulin α4
QSAR	Quantitative Structure Activity Relationship
RD	region of difference
Rpfs	resuscitation-promoting factors
RplL	50S ribosomal protein L7/L12
SCXRD	single-crystal X-ray diffraction
SLPs	synthetic long peptides
SMM	Stabilized matrix method
SVM	Support Vector Machine
TB	tuberculosis
Th	helper T-lymphocytes
TLR	toll-like receptor
TMV	Tobacco Mosaic Virus
TNF-α	tumor necrosis factor-α
TST	tuberculin skin test
VLPs	virus-like particles
WHO	World Health Organization

frontiers in Immunology

ORIGINAL RESEARCH
published: 22 March 2022
doi: 10.3389/fimmu.2022.841868

Efficacy and Safety of BCG Revaccination With *M. bovis* BCG Moscow to Prevent COVID-19 Infection in Health Care Workers: A Randomized Phase II Clinical Trial

*Laura Raniere Borges dos Anjos[1], Adeliane Castro da Costa[2], Amanda da Rocha Oliveira Cardoso[3], Rafael Alves Guimarães[1,4], Roberta Luiza Rodrigues[3], Kaio Mota Ribeiro[5], Kellen Christina Malheiros Borges[5,6], Ana Carolina de Oliveira Carvalho[5], Carla Iré Schnier Dias[2], Aline de Oliveira Rezende[7], Carine de Castro Souza[5], Renato Rodney Mota Ferreira[3], Guylherme Saraiva[3], Lilia Cristina de Souza Barbosa[1,5], Tayro da Silva Vieira[3], Marcus Barreto Conte[8], Marcelo Fouad Rabahi[3], André Kipnis[1] and Ana Paula Junqueira-Kipnis[5]**

[1] Laboratório de Bacteriologia Molecular, Instituto de Patologia Tropical e Saúde Pública, Universidade Federal de Goiás, Goiânia, Brazil, [2] Departamento de Biomedicina, Faculdade Estácio de Sá de Goiás, Goiânia, Brazil, [3] Faculdade de Medicina, Universidade Federal de Goiás, Goiânia, Brazil, [4] Faculdade de Enfermagem, Universidade Federal de Goiás, Goiânia, Brazil, [5] Laboratório de Imunopatologia das Doenças Infecciosas, Instituto de Patologia Tropical e Saúde Pública, Universidade Federal de Goiás, Goiânia, Brazil, [6] Departamento de Áreas Acadêmicas, Instituto Federal de Goiás, Anápolis, Brazil, [7] Programa de Pós-graduação em Ciências da Saúde, Universidade Federal do Maranhão, São Luís, Brazil, [8] Departamento de Pesquisa Clínica, Faculdade de Medicina de Petrópolis, Petrópolis, Brazil

The Bacillus Calmette-Guérin (BCG) vaccine, which is widely used to protect children against tuberculosis, can also improve immune response against viral infections. This unicentric, randomized-controlled clinical trial assessed the efficacy and safety of revaccination with BCG Moscow in reducing the positivity and symptoms of COVID-19 in health care workers (HCWs) during the COVID-19 pandemic. HCWs who had negative COVID-19 IgM and IgG and who dedicated at least eight hours per week in facilities that attended to individuals suspected of having COVID-19 were included in the study and were followed for 7, 15, 30, 60, and 180 days by telemedicine. The HCWs were randomly allocated to a revaccinated with BCG group, which received the BCG vaccine, or an unvaccinated group. Revaccination with BCG Moscow was found to be safe, and its efficacy ranged from 30.0% (95.0%CI -78.0 to 72.0%) to 31.0% (95.0%CI -74.0 to 74.0%). *Mycobacterium bovis* BCG Moscow did not induce NK cell activation at 15–20 days post-revaccination. As hypothesized, revaccination with BCG Moscow was associated with a lower incidence of COVID-19 positivity, though the results did not reach statistical significance. Further studies should be carried out to assess whether revaccination with BCG is able to protect HCWs against COVID-19. The protocol of this clinical trial was registered on August 5th, 2020, at REBEC (Registro Brasileiro de Ensaios

OPEN ACCESS

Edited by:
Wenping Gong,
The 8th Medical Center of PLA General Hospital, China

Reviewed by:
Christine Benn,
Statens Serum Institut (SSI), Denmark
Jun Jiao,
Beijing Institute of Microbiology and Epidemiology, China

***Correspondence:**
Ana Paula Junqueira-Kipnis
ana_kipnis@ufg.br

Specialty section:
This article was submitted to Vaccines and Molecular Therapeutics, a section of the journal Frontiers in Immunology

Received: *22 December 2021*
Accepted: *28 February 2022*
Published: *22 March 2022*

Citation:
dos Anjos LRB, da Costa AC, Cardoso ARO, Guimarães RA, Rodrigues RL, Ribeiro KM, Borges KCM, Carvalho ACO, Dias CIS, Rezende AO, Souza CC, Ferreira RRM, Saraiva G, Barbosa LCS, Vieira TS, Conte MB, Rabahi MF, Kipnis A and Junqueira-Kipnis AP (2022) Efficacy and Safety of BCG Revaccination With M. bovis BCG Moscow to Prevent COVID-19 Infection in Health Care Workers: A Randomized Phase II Clinical Trial. Front. Immunol. 13:841868. doi: 10.3389/fimmu.2022.841868

Clínicos, RBR-4kjqtg - ensaiosclinicos.gov.br/rg/RBR-4kjqtg/1) and the WHO (# U1111-1256-3892). The clinical trial protocol was approved by the Comissão Nacional de ética de pesquisa- CONEP (CAAE 31783720.0.0000.5078).

Keywords: NK cells, innate response, cross protection, respiratory infection, symptoms

INTRODUCTION

On March 11, 2020, the World Health Organization (WHO) declared the Coronavirus Disease 2019 (COVID-19), caused by severe acute respiratory syndrome coronavirus 2 (SARS-CoV-2), as a pandemic (1). This disease has caused high morbidity, mortality, and direct and indirect costs for society in general and for countries' economies, representing a serious public health and socioeconomic problem. Currently, to our knowledge, there is no effective pharmacologic prophylaxis and thus vaccination is the best preventive strategy (2). Despite the rapid advance in the immunization of the world population against COVID-19, the production and acquisition of immunizing agents are still lower than the demand, especially in developing countries like Brazil (3). In addition, new variants (e.g. B.1.1.7 [alpha], B.1.351 [beta], P.1. [gamma], B.1.617.1 [kappa], B.1.617.2 [delta]) and B.1.1.529 [omicron] of SARS-CoV-2 have emerged that may increase the pathogenic potential of the virus (4, 5).

The Bacillus Calmette-Guérin (BCG) vaccine has been safely and widely used in newborns and children for 100 years. Composed of attenuated *Mycobacterium bovis*, this vaccine prevents disseminated childhood tuberculosis (TB) and meningitis (6). Previous epidemiological studies have shown that BCG vaccination was associated to reduced child mortality from all causes (7, 8). Other studies proved that the vaccination with BCG could confer immunity against viral respiratory tract infections in children (9). Later, immunological studies demonstrated that the administration of the BCG vaccine provided a non-specific immunomodulatory effect, called trained immunity, that was associated with cross-protection against other infections (10). Trained immunity is mediated by the epigenetic, transcriptional, and functional reprogramming of innate immune cells (monocytes, macrophages, and natural killer [NK] cells), potentially increasing the production of cytokines (10, 11). Shortly after, a meta-analysis of three trials reinforced that early administration of BCG in low weight infants was associated with major reductions in mortality rate (12). It has recently been demonstrated that the vaccination with BCG can confer immunity against viral respiratory tract infections in elderly (13, 14).

The mild manifestations of COVID-19 among children, seen in ecological studies performed in the early stages of the pandemic, were associated with trained immunity generated using vaccines such as BCG (15). However, these studies were heavily criticized for not systematically correcting confounding variables such as socioeconomic differences, demographic structure, time of arrival of the COVID-19 pandemic, population comorbidities, testing capacity, and control strategies between countries (16, 17). To our knowledge, studies that evaluated BCG vaccine efficacy against COVID-19 in health care workers (HCWs) are scarce or are still ongoing. Thus, this prompted us to design a randomized clinical trial to evaluate the efficacy and safety of BCG revaccination among HCWs at a high risk for COVID-19 infection to prevent disease or decrease symptoms and to improve innate immune response.

METHODS

Trial Design

This study was a unicentric, parallel, randomized, phase II clinical trial conducted among HCWs with no prior COVID-19 infection. The study was conducted at the Federal University of Goiás (UFG), Brazil, between August 20th, 2020, and August 31st, 2021. The protocol of this clinical trial was registered on August 5th, 2020, at REBEC (Registro Brasileiro de Ensaios Clínicos, RBR-4kjqtg- ensaiosclinicos.gov.br/rg/RBR-4kjqtg/1) and the WHO (# U1111-1256-3892). The clinical trial protocol was approved by the Comissão Nacional de ética em pesquisa-CONEP (CAAE 31783720.0.0000.5078). The detailed study protocol was published as appendix data in a previous publication (18). This study complied with guidelines outlined under the Consolidated Standards of Reporting Trials (CONSORT) (19).

Participants

The HCWs were recruited at Hospital das Clínicas (HC/UFG) or Hospital Estadual Geral de Goiânia Dr. Alberto Rassi (HGG), or by independently completing an online recruitment form. Inclusion and exclusion criteria were described previously (18) and are described next. Inclusion criteria: Eligible individuals were HCWs working at least eight hours per week in a medical facility attending to confirmed or suspected COVID-19 patients, aged 18 years or older, with a history of previous BCG vaccination and with no history of COVID-19. Potential study volunteers underwent a screening evaluation that included an explanation of the study and an invitation to take part in it. After signing the informed consent form, sociodemographics, comorbidities, lifestyle habits, use of medications, information about contacts with people with COVID-19 were collected. In addition, all HCWs were asked about their previous history of vaccination with BCG, and the region of the deltoid muscle on the upper external surface of the right arm was observed to verify the presence of a BCG vaccine scar. Exclusion criteria: Subjects with prior known reaction to the BCG vaccine, fever in the previous 24 hours, pregnant or breastfeeding women, suspected or confirmed viral infection including COVID-19 or bacterial

infection, previous diagnosis of tuberculosis, vaccination in the previous four weeks, medical diagnosis of immunosuppressive diseases, such as human immunodeficiency virus (HIV), and/or cancer in the previous two years and/or autoimmune disease and/or use of corticosteroids and/or antibiotics and/or chemotherapy were not eligible to participate in the study. Also, at enrollment, subjects with positive IgM and/or IgG for COVID-19 and/or neutrophil counts bellow 500/mm^3 were not enrolled in the study. Participants were randomized to one of two arms: a revaccination with *M. bovis* BCG Moscow arm or an unvaccinated arm (no placebo vaccine was used). This study was conducted in accordance with the requirements for Good Clinical Practice ICH E6 (R2).

Blood samples from all included HCWs were processed and serum, plasma, PBMCs, and total blood were stored for immunological assays. Initially, enrolled subjects were subsequently excluded if they received a COVID-19-positive test on day 15 after randomization. However, the study protocol was modified and participants who tested positive for COVID-19 within the first 15 days after randomization were kept in the study. This alteration was approved by the Comissão Nacional de Ética em Pesquisa- CONEP and did not affect the integrity of the interpretation of the results obtained and allowed for the assessment of the maximum accurate description of the efficacy of the BCG vaccine since its administration.

Definitions, Intervention, and Follow-Up

Flu-like syndrome symptoms according to the recommendations of the Brazilian Ministry of Health were defined as: dry or productive cough, hemoptysis, fever, sore throat, night sweats, shortness of breath, reduced sense of smell or taste, lack of appetite, diarrhea, headache, rhinorrhea, nasal congestion, asthenia/fatigue, and/or myalgia (20).

COVID-19 was considered for an individual presenting an IgM/IgG test or RT-PCR positive test. Any participant that presented symptoms related to flu-like syndrome or symptoms associated to COVID-19 were oriented to perform an RT-PCR test. The severity of COVID-19 was classified according to the WHO guidelines (21) as follows. (1) Asymptomatic: without any symptoms or signs, but with a laboratory diagnosis; (2) Mild/moderate condition: dry cough, fever (regardless of temperature), headache, mild difficulty in breathing defined by a respiratory rate up to 30 breaths per minute and oxygen saturation measured by digital oximetry that was greater than or equal to 90% in ambient air; (3) Severe: signs of pneumonia (fever, cough, dyspnea, tachypnea) and one of the following: respiratory rate > 30 bpm; acute respiratory distress syndrome; SaO2 < 90% in ambient air; (4) Critical condition: admission to the ICU, need for ventilatory support (NIV, HNFA, IMV), use of vasoactive drugs.

Enrolled subjects either received or did not receive a single dose of BCG Moscow vaccine *via* intradermal administration. All participants were followed and evaluated through telemedicine on days 7, 15, 30, 60, and 180. An assessment tool designed for this study to evaluate signs of flu-like syndrome symptoms (20) and possible adverse events (AEs) was used (22). Also, participants were able to contact the medical team, if needed, to report a clinical sign and/or symptom and/or confirmation of COVID-19 diagnosis and/or for medical assistance. Participants suspected of contamination with SARS-CoV-2 were invited to submit to serological and/or molecular tests and clinical evaluation. Participants diagnosed with COVID-19 were referred for treatment to accredited health facilities for the care of COVID-19 cases. Fifteen days after randomization, a new blood sample was collected from the randomized HCWs for COVID-19 testing and immune response evaluation. After 180 days of inclusion, all HCWs were contacted for final blood collection for COVID-19 testing. At the end of the study, the results of the BCG-vaccinated and unvaccinated groups were unblinded and compared according to primary and secondary outcomes.

Interventions After Initiation of Specific Vaccination Against COVID-19

Although not envisioned in the trial design, specific vaccines against COVID-19 were approved during the trial in Brazil and were made available for the vaccination of priority groups, which included HCWs. To avoid any bias in data interpretation, all HCWs included in this clinical trial who did not develop symptomatic COVID-19 were invited to submit to a third blood draw for COVID-19 serological testing before their COVID-19-specific vaccination or within 14 days thereafter. This additional information as well as the COVID-19 vaccine types was recorded, and these participants were followed by telemedicine for the diagnosis of COVID-19 for 180 days.

Outcomes

Primary: Reduction of positivity for COVID-19 through serological and molecular tests and clinical evaluation among individuals vaccinated with BCG. Reduction of COVID-19 symptoms among HCWs revaccinated with BCG was verified by telemedicine and clinical evaluation during follow-up for 180 days.

Secondary: Innate immune activation among individuals in the BCG-vaccinated group was verified by NK cell population activation analysis after 15–20 days post-randomization compared to day 1 (the day of inclusion in the study).

Safety Evaluation

Adverse events (AEs) and serious adverse events (SAEs) were reported from baseline until the last patient's evaluation for all included participants. SAEs and all other AEs were reported according to NIH and FDA guidelines (23, 24). An adverse event was defined as any reaction that was not present before the start of the study (exposure to study vaccination) or any pre-existing reaction that worsened in intensity and frequency after exposure. In this study, SAEs were defined as events that were life-threatening, resulted in initial or prolonged hospitalization, caused irreversible, persistent, or significant disability and/or incapacity, required intervention to prevent harm, or had other medically serious consequences. All other AEs were reported as non-severe. All AEs were graded as grade I (transient and well-tolerated by the patient), grade II (causing discomfort and causing disability), grade III (affecting the usual activities to an important degree and causing disability) while SAEs

were classified as grade IV, indicating a potentially life-threatening event.

BCG vaccine-related AEs (adverse reactions) were questioned to all trial participants. As this study did not use a placebo vaccine, only participants allocated to the BCG-vaccinated group reported any vaccine-related AE. Therefore, vaccine-related AEs were measured in analysis only for the intervention group. According to the Brazilian Ministry of Health (22), severe local AEs related to BCG vaccination (severe adverse reactions) are local abscess keloid, cutaneous skin lesions, and lymphadenitis suppuration, while possible severe systemic AEs related to BCG vaccination are osteitis, disseminated BCG, and immune reconstitution syndrome.

Randomization

Randomization of 400 consecutive numbers was performed on the online platform Randomization.com (http://www.jerrydallal.com/random/permute.htm) in blocks of 20 (see **Supplementary Materials** for detailed information). In order to randomly allocate recruited individuals to the vaccination or unvaccinated groups and, at the same time, optimize the use of the BCG vaccine, which could not be stored for more than six hours after the vaccine vial was opened. 400 consecutive numbers ranging from BCG001 to BCG400 were inserted on the online platform Randomization.com (http://www.jerrydallal.com/random/permute.htm) with the permutable treatment labels "BCG vaccination" and "No vaccination" to designate whether the individual would be vaccinated or not, respectively. The total number of subjects was set to 400, and the randomization was divided into blocks of 20 with 20 subjects each. A collaborator who was not involved with the recruitment manipulated the randomization output. Four hundred envelopes externally labeled with the consecutive numbers BCG001 to BCG400 received the respective randomization output printed on a piece of paper with the same BCG number and the result "BCG vaccination" or "No vaccination" generated by the computer software. All 400 envelopes were sealed and ready as of day 1 of the subjects' recruitment. On the day of recruitment, a consecutive BCG number was assigned to each individual included in the study and a sealed envelope with the exact same BCG number was opened in front of the participant, at which point both the participant and the study staff learned whether the individual was allocated to the vaccination group or not. If allocated to the vaccination group, the individual was transported to the vaccination site; if not, the individual was informed once more about the importance of the unvaccinated group for the trial and their contribution in continuing to participate in the project until the end.

At the vaccination site, a new vial of BCG Moscow was suspended with 1 mL of the accompanying diluent and maintained at 4–8°C in a cooler until use. For each participant assigned to be vaccinated, a nurse with ample experience with BCG vaccination retrieved 100 µL of the vaccine immediately prior to vaccination and injected the whole volume intradermally in the region of the upper right arm. The individual received a flyer with possible AEs of the BCG vaccine and a physician contact telephone number in case of any additional concerns. Inquiries about AEs related to BCG vaccination began at seven days post-randomization or were spontaneously reported if the participant contacted the physician with any concern regarding the vaccination.

Blinding

The study was blinded to laboratory researchers, to those who evaluated the results, and to those who performed the statistical analyses. In this case, only the participant's identification number was made available. There was no blinding for health professionals participating in this trial. The statistician first had access to data coded only by the participant's ID, and only after the conclusion of the study and approval by the Data and Safety Monitoring Board were the data unmasked and analyzed accordingly. The data remained blinded to the researchers.

Innate Immune Response After BCG Vaccination

Heparinized total blood was withdrawn from the participants on the day of inclusion and 15–20 days after randomization. Five hundred microliters of blood were aliquoted in cryogenic tubes containing 500 µL of freezing solution composed of 20% DMSO and 80% bovine serum albumin (BSA). All blood samples were kept at -80°C until their cell preparations for cytometry. Using a 37°C water bath, the cells were quickly thawed and distributed in 50 mL tubes or 48-well plates. NK cell staining was performed according to a protocol standardized in our laboratory. In detail, on the day of the cell analyses, two samples of blood from each participant were processed, one collected on the day of recruitment, and one collected at 15–20 days post-randomization. To evaluate NK cell activation, 500 µL of the cell suspensions were transferred to 50 mL conical tubes and erythrocytes were lysed with lysis buffer (0.15 M NH4Cl, 10 mM KHCO3). After washing the cells with saline, the cell pellet was resuspended with 800 µL of complete RPMI (cRPMI; GIBCO, Invitrogen Corporation Grand Island, NY, USA) containing glutamine (200 mM; Sigma–Aldrich-Brazil, São Paulo), pyruvate (10 nM; Sigma–Aldrich-Brazil, São Paulo), non-essential amino acids (2 mM; Sigma–Aldrich-Brazil, São Paulo), 50 µg/mL of penicillin/streptomycin (1.000 U/mL GIBCO) and 10% BSA. The cells were counted and adjusted to 10^6 cells/mL and distributed in 96-well culture plates (200 µL/well). Cells were stimulated with medium or with culture filtrate proteins (CFPs) from BCG (0.5 µg/µL) after resting for two hours at 37°C in a 5% CO_2 incubator. Then, the cells were incubated for 17 hours, and monensin (3 mM; eBioscience) was added to the cultures, which were further incubated for 5 hours. After this period, the plates were centrifuged at 2000 xg for 15 minutes at 10°C and the cells were resuspended and treated with 20 µL of mouse sera to block FC receptors. After 10 minutes of incubation at 4–8°C, the cells were incubated for 30 minutes at the same temperature with monoclonal antibodies against surface markers diluted according to a previous standardization. According to the analysis that was to be performed, a combination of the following antibodies were used: mouse anti-human CD16-FITC, CD314-PerCP-eFluor™ 710, TCR-PE-Cyanine7, CD57-eFluor 660, CD27-APC, CD3-Alexa Fluor 700, and CD56

APC-eFluor 780 (all antibodies were from eBioscience; the clones of all antibodies used in this study are presented in **Table 1**). Next, the cells were incubated for 20 minutes with Perm Fix (100 µL), followed by the addition of 100 µL of Perm wash for a further 20 minutes. After centrifuging the plates at the established conditions, the antibodies against intracellular cytokines were added diluted in Perm wash solution (BD Pharmingen, San Jose, CA, EUA) and the plates were incubated for 30 minutes at 4–8°C. For this purpose, mouse anti-human IFN-γ-PE and TNF-α-PE were used. Then, the plates were centrifuged, and the pellet was resuspended in 400 µL of 0.05% sodium azide PBS containing 0.05% sodium azide. The paired samples corresponding to day 1 and 15 for each participant were always processed and analyzed concomitantly. The cells were immediately acquired using Attune™ NxT (ThermoFisher). To evaluate NK cells, at least 50,000 events were acquired and analyzed. The data were evaluated using FlowJo Version 7.0 software (FlowJo™). All cells were gated to exclude doublets using FCS-A and FCS-H parameters. After this, using granularity and size, lymphocytes were gated and cells $CD16^+CD56^+$ were selected. These cells were analyzed for CD3 expression, and cells $CD16^+CD56^+$ $CD3^-$ were considered NK cells.

Sample Size

The sample size calculation, which was already published (18), was performed according to the formula outlined by Hulley et al. (25). Thus, 197 HCWs would be allocated to each intervention group. As mentioned above, with the initiation of COVID-19-specific vaccination of HCWs, the study was unmasked in September 2021, before reaching the target numbers but without compromising the analysis, since most of HCWs became vaccinated against COVID19. This, a new sample size calculation was performed based on new publication of COVID-19 which evaluated the effectiveness of BCG revaccination in individuals at risk (26). Thus, considering a statistical power of 80%, significance level of 5%, equal allocation rate between groups and a proportion of the primary outcome (development of COVID-19) in the control group of 51.5% and in the intervention group of 25.9%, effect size of 50.0%, drop rate of 68% and clinically acceptable margin of 0.15, the minimum necessary sample size was estimated at 104 patients (52 in the unvaccinated group and 52 in the intervention group).

Statistical Methods

Baseline Comparison

The unvaccinated and BCG groups had their demographic, clinical, and behavioral characteristics analyzed and compared. Pearson's chi-squared test with Yates' continuity correction or Fisher's exact tests were used to compare the proportions of categorical variables. A Student's t-test (normal distribution) or a Mann-Whitney U test with continuity correction (non-normal distribution) was used to compare the means or distributions of continuous variables. The analysis of the normality of continuous variables was performed using the Kolmogorov-Smirnov test with Lilliefors correction. Parametric quantitative variables were evaluated using a paired t-test or a Wilcoxon test; for non-parametric quantitative variables.

Vaccine Efficacy (VE)

Population analysis was performed to estimate VE in the prevention of COVID-19. VE was calculated by two statistical methods: a Poisson regression model and a Cox proportional regression model. A Poisson regression model was used to estimate the incidence rate ratio (IRR) (27). The terms included in the model (explanatory variables) were the study group (BCG group versus control group), age at randomization, and sex. Even with a balance between groups, age was included in the model due to its potential influence on the adjusted measures in VE studies; sex was also included due to a *P*-value <0.10 observed in group comparisons. Also, the log of the risk period to

TABLE 1 | Antibodies used in this study (all from eBioscience™).

Fluorochrome	Marker	Catalog #	Channel	Clone
FITC	CD16	11-0168-42	BL1	eBioCB16 (CB16)
PE	CD49d	12-0499-42	BL-2	9F10
PE	IFN-γ	12-7319-42	BL-2	4S.B3
PE	TNF-α	12-7349-82	BL-2	MAb11
PercP	CD63	MA110269	BL-3	MEM-259
PerCP-eFluor™ 710	CD314 (NKG2D)	46-5878-42	BL-3	1D11
PE-Cyanine7	CD15	25-0159-42	BL-4	HI98
PE-Cyanine7	TCR V alpha 24 J alpha 18	25-5806-42	BL4	6B11
eFluor® 660	CD57	50-0577-42	RL-1	TB01 (TBO1)
APC	CD27	17-0279-42	RL-1	O323
APC	LAP	17-9829-42	RL-1	FNLAP
APC	CD66	17-0668-42	RL-1	CD66a-B1.1
Alexa Fluor 700	CD3	56-0038-42	RL-2	UCHT1
Alexa Fluor 700	ARGINASE	56-3697-82	RL-2	A1exF5
Alexa Fluor 700	CD14	56-0149-42	RL-2	61D3
APC-eFluor® 780	CD56 (NCAM)	47-0452-82	RL-3	RA3-6B2
APC-eFluor® 780	CD123	47-1239-42	RL-3	6H6
APC-eFluor® 780	CD16	47-0168-42	RL-3	eBioCB16 (CB16)

LAP, latency-associated peptide.

the primary outcome was used as the model's offset variable to adjust for participants with different study follow-up times. A Cox proportional regression model was used to estimate the hazard ratio (HR). The terms included in this model (explanatory variables) were the study group (BCG group versus control group), age at randomization, and sex. VE was defined as the percentage reduction in the IRR or HR for the primary outcome and was calculated as 1-aIRR (Poisson model) or 1-HR (Cox model), accompanied by the respective 95% CI. Cumulative incidences of cases were presented using the Kaplan-Meier method.

The first vaccine against COVID-19 was approved for use in Brazil in January 2021, during the follow-up of participants in this clinical trial. Thus, two analyses were performed for VE at endpoints. In the first scenario, entitled "without censoring for COVID-19 vaccination", we included all cases of COVID-19 until the end of the follow-up, regardless of the participant's COVID-19 vaccination status. In this case, the time of the event was from the date of inclusion to the date of development of the primary outcome; the participant was censored when (i) follow-up was missed or (ii) 180 days of follow-up had been completed. In the second scenario, entitled "with censoring for COVID-19 vaccination", individuals were censored from the analysis after 14 days of the subject's first dose of COVID-19 vaccination, independent of the producing laboratory. In this scenario, the participant was censored when (i) the follow-up was missed (ii) after 14 days of the first vaccine dose (if the participant received the COVID-19 vaccine), or (iii) 180 days of follow-up had been completed (if the participant did not receive the COVID-19 vaccine). Similarly, vaccine efficacies were evaluated according to symptomatic COVID-19 cases.

Registration and Protocol

The protocol was registered on August 5th, 2020, at REBEC (Registro Brasileiro de Ensaios Clínicos, RBR-4kjqtg) and the WHO (# U1111-1256-3892). The clinical trial protocol was approved by the Brazilian Ethics Committee (CAAE 31783720.0.0000.5078).

This study complied with guidelines outlined under the Consolidated Standards of Reporting Trials (CONSORT).

RESULTS

Recruitment and Participants

This clinical trial recruited 592 HCWs, of whom 454 were ineligible (141 for not meeting inclusion criteria, 294 for declining to participate spontaneously, and 19 for other reasons) and 138 were randomized, as summarized in **Figure 1**. Of the randomized HCWs, 68 were allocated to the revaccinated with BCG group and 70 to the unvaccinated group. In the revaccinated-BCG group, two participants were excluded from analysis due to false information about COVID-19 status on the day of inclusion, and two participants were excluded from analysis because they were working remotely. Thus, 64 participants were considered for analysis. In the group unvaccinated with BCG, one participant was excluded from analysis due to false information about COVID-19 status on the day of inclusion, one participant was excluded from analysis because he was working remotely, and one participant revaccinated with BCG on their own. Thus, 67 participants were considered for analysis (**Figure 1**). The sample consisted of HCWs categorized as administrative staff (n = 13; 9.9%), nurse staff (n = 48; 36.6%), dental professionals (n = 9; 6.9%), laboratory staff (n = 12; 9.2%), nutritionists (n = 4; 3.1%), community health agents (n = 6; 4.6%), paramedics (nurses) (n = 18; 13.7%), medical staff (n = 10; 7.6%), and other HCWs (n = 11; 8.4%).

The baseline characteristics of participants according to allocated group (unvaccinated and revaccinated with BCG) are shown in **Table 2**. The results indicated that all sociodemographic and clinical variables, use of medications, and baseline laboratory values were balanced between the unvaccinated and revaccinated with BCG groups, with no statistically significant difference ($P > 0.05$). In addition, all HCWs included in the study reported a previous history of BCG vaccination and there was no statistically significant difference between the percentage of individuals with and without a scar from previous BCG vaccination between the BCG-revaccinated and unvaccinated groups.

Vaccine Efficacy to Prevent COVID-19 Infection and Symptomatic COVID-19

As detailed in methods, during the trial period, specific COVID-19 vaccines became available to HCWs, thus the VE is presented in two scenarios (**Figure 2**; **Table 3**). The Kaplan-Meier cumulative incidence curves of the primary endpoint for the scenarios without censoring for COVID-19 vaccination (**Figure 2A**) and with censoring for COVID-19 vaccination (**Figure 2B**) are shown in **Figure 2**. Although the COVID-19 cumulative cases were smaller in the revaccinated with BCG group than in the unvaccinated group, no differences were observed between the curves (**Figure 2A**). Similarly, considering censoring for COVID-19 vaccination, no differences were observed between the cumulative incidence curves (**Figure 2B**). The general VE based on the Cox proportional model was 30.0% (95.0% CI: -78.0 to 72.0%) and, based on the Poisson model, 31.0% (95.0% CI: -74.0 to 74.0%) (**Table 3**). In this scenario (n = 115. 87.8%), nine COVID-19 cases were detected in the unvaccinated group and seven in the revaccinated with BCG group. Thus, the VE based on the Cox proportional model in this scenario was 26.0% (95.0% CI: -107.0 to 73.0%) and, based on the Poisson model, 32.0% (95.0% CI: -89.0 to 77.0%) (**Table 3**).

The Kaplan-Meier cumulative incidences of symptomatic COVID-19 were evaluated for the scenarios without censoring for COVID-19 vaccination (**Figure 2C**) and with censoring for COVID-19 vaccination (**Figure 2D**). No differences were observed between the curves in both scenarios. The VE result for this outcome based on the Cox proportional model was 28.0% (95.0% CI: -98.0 to 74.0%) and, based on the Poisson model, 30.0% (95.0% CI: -93.0 to 76.0%), since nine cases of COVID-19 were observed in the unvaccinated group and seven

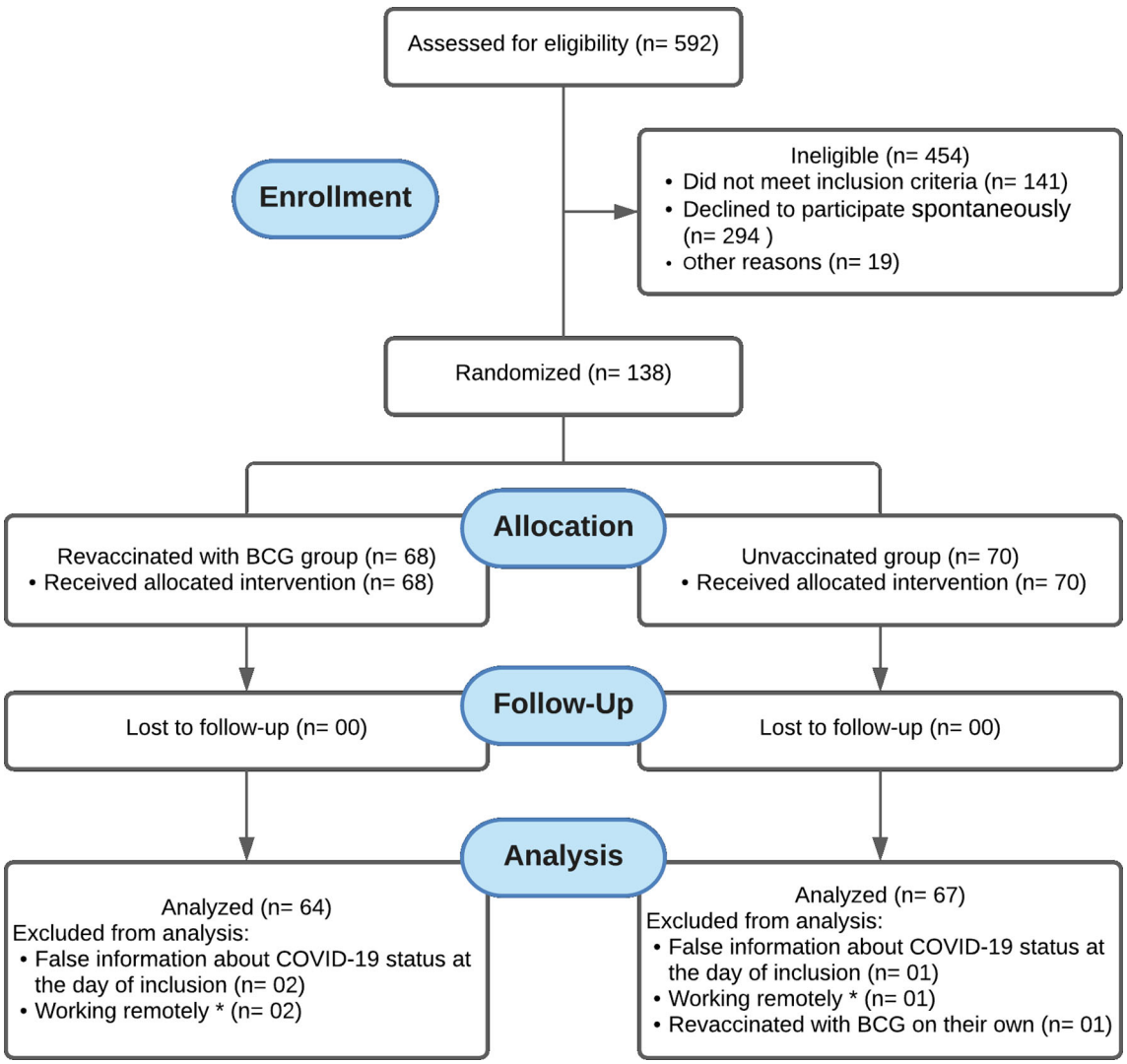

FIGURE 1 | Flow diagram showing that 592 HCWs were recruited, of whom 454 were ineligible (141 did not meet the inclusion criteria, 294 declined to participate, and 19 were excluded for other reasons) and 138 were randomized. Of the randomized HCWs, 68 were allocated to the revaccinated with BCG group and 70 to the unvaccinated group. There was no loss to follow-up in neither group. In the revaccinated BCG group, two participants were excluded from analysis due to false information about COVID-19 status on the day of inclusion, and another two were excluded for working remotely, remaining 64 participants for analysis. In the unvaccinated group, one participant was excluded from analysis due to false information about COVID-19 status on the day of inclusion, another one was excluded for working remotely, and one was excluded for having been vaccinated with BCG on their own, leaving 67 participants for analysis. * Health care workers in remote jobs refers to HCWs who were not working for at least eight hours per week under exposure to those suspected of being infected with COVID-19.

in the revaccinated with BCG group (**Table 4**). In the scenario with COVID-19-specific vaccination, the VE for symptomatic COVID-19 was 8.0% (95.0% CI: -173.0 to 69.0%) based on the Cox proportional model and based on the Poisson model, 16.0% (95.0% CI: -155.0 to 72.0%) (**Table 4**).

Additionally, the efficacies calculated considering only HCWs that presented previous BCG scar showed no significant differences between the groups that were revaccinated with BCG or unvaccinated (VE varied from 20.0 to 24.0; **Table S1**). In this study, 31 men were included (11 in the unvaccinated group and 20 in the revaccinated group). Five COVID-19 positive cases were seen among male HCWs, most of them occurred among individuals revaccinated with BCG (4/20; 20%). One hundred females were enrolled and evaluated, among them, 14 COVID-19 positives were observed. Most of the positive cases happened among HCW females unvaccinated with BCG (10/56; 17.9%; **Table S2**). In female HCWs, VE based on Cox analysis was 52.0% (95.0% CI: -52.0 to 85.0%). While our data showed that females were protected for COVID-19 and males presented a negative VE (-132.0, 95% CI: -2,040.0-75.0), the analysis did not show statistically significant difference (**Table S2**).

Comparing the symptoms presented by HCWs that had symptomatic COVID-19, no significant differences between the revaccinated with BCG group and the unvaccinated group was

TABLE 2 | Baseline characteristics according to allocated group (Unvaccinated or revaccinated with BCG).

Variables	All (n = 131)	Unvaccinated (n = 67)	Revaccinated with BCG (n = 64)	*P* -value
Age (years), mean (SD)	43.0 (11.2)	44.2 (11.3)	41.8 (11.0)	0.23*
Age distribution (years), n (%)				
18-59	119 (90.8)	60 (89.6)	59 (92.2)	0.60†
≥ 60	12 (9.2)	7 (10.4)	5 (7.8)	
Sex, n (%)				
Female	100 (76.3)	56 (83.6)	44 (68.8)	0.07†
Male	31 (23.7)	11 (16.4)	20 (31.3)	
Economic class, n (%)‖				
A or B	37 (28.2)	20 (29.9)	17 (27.0)	0.79†
C	62 (47.7)	30 (44.8)	32 (50.8)	
D or E	31 (23.8)	17 (25.4)	14 (22.2)	
Number of contacts with suspected COVID-19 patients, median (IQR)	20.0 (8.0-50.0)	20.0 (7.5-50.0)	17.5 (8.0-40.0)	0.78§
BMI (Kg/m^2), mean (SD)	27.0 (5.0)	27.3 (4.9)	26.7 (5.0)	0.49*
Obesity, n (%)	31 (23.7)	18 (26.9)	13 (20.3)	0.50†
Comorbidity, n (%)	25 (19.1)	14 (20.9)	11 (17.2)	0.75†
Comorbidities, n (%)				
Hypertension	19 (14.5)	10 (14.9)	9 (14.1)	1.00†
Diabetes	4 (3.1)	4 (2.0)	0	0.12‡
Cardiac insufficiency	4 (3.1)	2 (3.0)	2 (3.1)	1.00‡
Renal insufficiency	0	0	0	N/A
Current smoking, n (%)	3 (2.3)	1 (1.5)	2 (3.1)	0.61‡
Alcohol addiction, n (%)	8 (6.1)	3 (4.5)	5 (7.8)	0.49‡
BCG vaccine scar*, n (%)	113 (86.3)	57 (85.1)	56 (87.5)	0.88†
Medication use, n (%)				
Antihypertensive	19 (14.5)	11 (16.4)	8 (12.5)	0.70†
Antiarrhythmic	4 (3.1)	2 (3.0)	2 (3.1)	1.00‡
Insulin	1 (0.8)	1 (1.5)	0	1.00‡
Antibiotic	0	0	0	N/A
Anticoagulant	0	0	0	N/A
Vitamin supplement	43 (32.8)	24 (35.8)	19 (29.7)	0.58†
Ivermectin	4 (3.1)	2 (3.0)	2 (3.1)	1.00‡
Hydroxychloroquine	0	0	0	N/A
Hematological parameters				
Red cells (tera/L), median (IQR)	4.7 (4.4-5.0)	4.7 (4.4-5.0)	4.8 (4.4-5.1)	0.46§
Hematocrit (%), median (IQR)	42.7 (41.9-45.6)	42.6 (40.8-45.6)	43.1 (41.3-45.2)	0.46§
Hemoglobin (g/dL), mean (SD)	14.1 (1.5)	14.1 (1.4)	14.2 (1.5)	0.58*
MCV (IL), median (IQR)	91.2 (88.6-93.6)	91.4 (88.9-94.6)	91.4 (88.6-93.1)	0.50§
MCH, median (IQR)	29.7 (28.7-30.8)	29.7 (28.8-31.0)	29.6 (28.4-30.5)	0.58§
CHCM (g/dL), mean (SD)	32.6 (0.9)	32.6 (1.0)	32.6 (0.9)	0.83*
RDW (%), median (IQR)	12.2 (11.8-12.7)	12.2 (11.8-12.7)	12.3 (11.9-12.8)	0.50§
WBC (x10^9/L), mean (SD)	6.1 (1.5)	6.0 (1.4)	6.2 (1.7)	0.51*
Neutrophils (x10^9/L), median (IQR)	3.2 (2.6-4.0)	3.3 (2.7-3.9)	3.2 (2.5-4.2)	1.00§
Lymphocytes (x10^9/L), mean (SD)	2.2 (0.7)	2.2 (0.6)	2.3 (0.8)	0.25*
Monocytes (x10^9/L), median (IQR)	0.3 (0.2-0.4)	0.3 (0.2-0.4)	0.3 (0.2-0.4)	0.38§
Platelets (x10^9/L), median (IQR)	245.0 (209.5-283.0)	250.0 (215.5-286.5)	244.0 (204.0-280.5)	0.64§

*SD, standard deviation; BCG, Bacilli de Calmette and Guérin; COVID-19, coronavirus disease 2019; IQR, interquartile range; BMI, body mass index; MCH, mean corpuscular hemoglobin; MCV, mean corpuscular volume; CHCM, mean corpuscular hemoglobin concentration; N/A, not applicable; RDW, red cell distribution width; WBC, white blood cells; *Student's t-test for independent samples; †Pearson's chi-squared test with Yate' continuity correction; ‡Fisher's exact test; §Mann-Whitney U test with continuity correction; ‖Missing data=1. *The BCG vaccine scar was verified at the time of inclusion of the HCW in the study.*

observed (**Table S3**). For this analysis purposes, the signs and symptoms reported were grouped into: (i) systemic: night sweats, fever, myalgia, fatigue and, arthralgia;(ii) high respiratory: sore throat, runny nose and, nasal congestion; (iii) low respiratory: cough and dyspnea; (iv) gastrointestinal: nausea, vomiting, and diarrhea; (v) neurological: headache, anosmia, and ageusia; (vi) flu syndrome.

The comparison of general symptoms reported by HCWs included in the unvaccinated and revaccinated with BCG groups is described in **Table S4**. The results indicated that clinical symptoms were similar between the HCWs included in BCG and unvaccinated groups during the follow up, with no statistically significant difference ($P > 0.05$).

The SARS-CoV-2 exposure profile and risk of COVID-19 infection among included HCWs who had COVID-19 according to their occupation is described in **Table S5**. The results indicated that the number of COVID-19 cases, despite being higher among HCWs directly exposed to SARS-CoV-2 and at greater risk for COVID-19 infection (physicians, nurses, paramedic nurses), is similar among those HCWs included in BCG revaccinated or unvaccinated groups, regardless of occupation (**Table S5**).

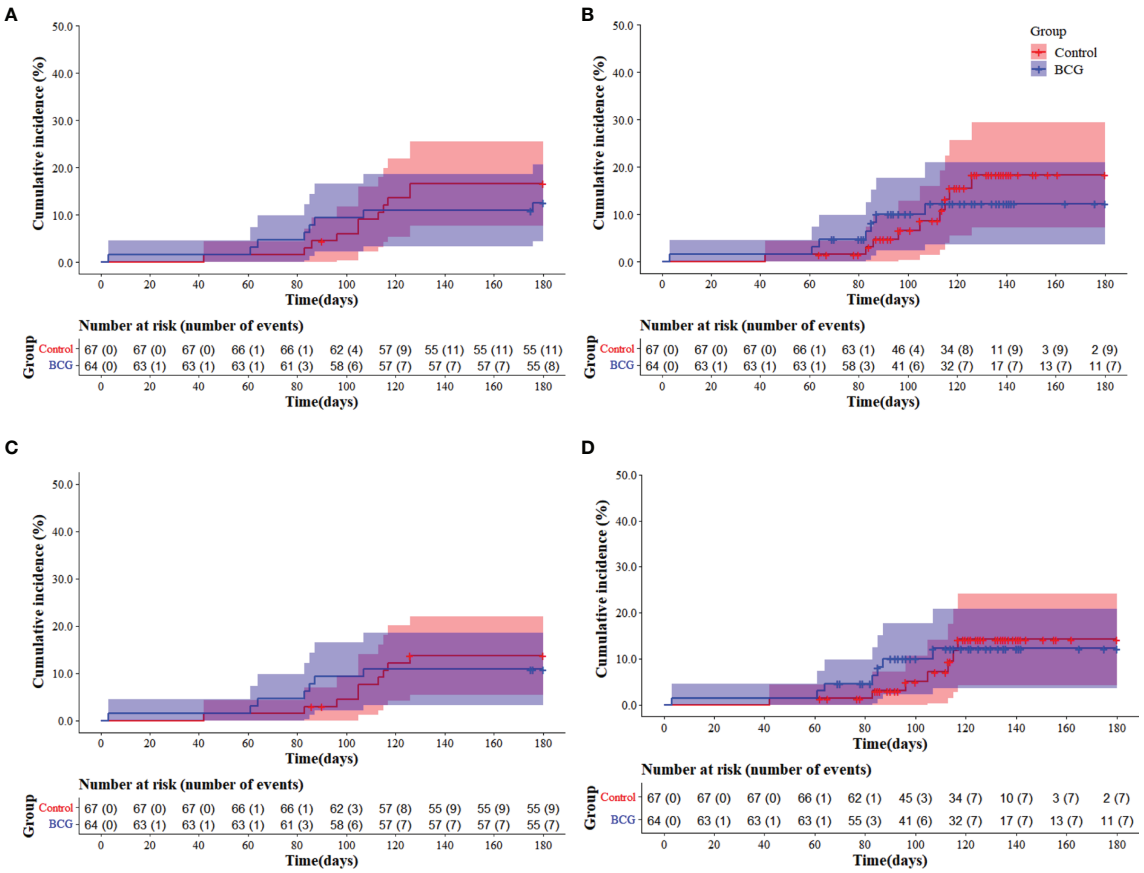

FIGURE 2 | Cumulative incidence Kaplan-Meier curves of COVID-19 cases (laboratory-confirmed COVID-19) in two scenarios: without censoring for COVID-19 vaccination **(A)** and with censoring for COVID-19 vaccination **(B)**. The cumulative incidence Kaplan-Meier curves of symptomatic COVID-19 cases are also shown in two scenarios: without censoring for COVID-19 vaccination **(C)** and with censoring for COVID-19 vaccination **(D)**. Blue lines and shadings represent the revaccinated with BCG group (BCG) cumulative incidence of cases and 95% CI, respectively. Red lines and shadings represent the unvaccinated group (Control, unvaccinated) cumulative incidence of cases and 95% CI, respectively.

TABLE 3 | Vaccine efficacy based on COVID-19 infection in both scenarios: without censoring for COVID-19 vaccination and with censoring for COVID-19 vaccination.

Scenario	All	Unvaccinated	Revaccinated with BCG
COVID-19 – without censoring for COVID-19 vaccination			
Number of COVID-19 cases, n	19	11	8
Cumulative incidence, n/total (%)	19/131 (14.5)	11/67 (16.4)	8/64 (12.5)
Number censored, n (%)	112 (85.5)	56 (83.6)	56 (87.5)
VE based on HR (95.0% CI)*			30.0 (-78.0 to 72.0)
Person-Years	59.8	30.4	29.4
IR per 100 Person-Years (95.0% CI)	31.8 (19.1-49.6)	36.2 (18.1-64.7)	27.2 (11.7-53.6)
VE based on IRR (95.0% CI) †			31.0 (-74.0 to 74.0)
COVID-19 – with censoring for COVID-19 vaccination			
Number of COVID-19 cases, n	16	9	7
Cumulative incidence, n/total (%)	16/131 (12.2)	9/67 (13.4)	7/64 (10.9)
Number censored, n (%)	115 (87.8)	58 (86.6)	57 (89.1)
VE based on HR (95.0% CI)*			26.0 (-107.0 to 73.0)
Person-Years	42.2	21.2	21.0
IR per 100 Person-Years (95.0% CI)	37.9 (21.7-61.6)	42.5 (19.4-80.6)	33.3 (13.4-68.7)
VE based on IRR (95.0% CI)†			32.0 (-89.0 to 77.0)

The primary endpoint was COVID-19 defined as the presence of positivity by RT-PCR or IGM or IgG serology defined as presented in methods.
*IRR, incidence rate ratio; HR=hazard ratio; VE, vaccine efficacy; CI, confidence interval. *Vaccine efficacy based on 1-HR obtained in Cox proportional model adjusted for age and sex.*
†Vaccine efficacy based on 1-IRR obtained in Poisson model adjusted for age and sex, with the natural logarithm (log[n]) of time at risk as offset variable.

TABLE 4 | Vaccine efficacy based on symptomatic COVID-19 infection in both scenarios: without censoring for COVID-19 vaccination and with censoring for COVID-19 vaccination.

Scenario	All	Unvaccinated	Revaccinated with BCG
COVID-19 – without censoring for COVID-19 vaccination			
Number of COVID-19 cases, n	16	9	7
Cumulative incidence. n/total (%)	16/131 (12.2)	9/67 (13.4)	7/64 (10.9)
Number censored, n (%)	115 (87.8)	58 (86.6)	57 (89.1)
VE based on HR (95.0% CI)*			28.0 (-98.0 to 74.0)
Person-Years	59.8	30.4	29.4
IR per 100 Person-Years (95.0% CI)	26.8 (15.3-43.4)	29.6 (13.5-56.2)	23.8 (9.6-49.1)
VE based on IRR (95.0% CI)†			30.0 (-93.0 to 76.0)
COVID-19 – with censoring for COVID-19 vaccination			
Number of COVID-19 cases, n	14	7	7
Cumulative incidence, n/total (%)	14/131 (10.7)	7/67 (10.4)	7/64 (10.9)
Number censored, n (%)	117 (89.3)	60 (89.6)	57 (89.1)
VE based on HR (95.0% CI)*			8.0 (-173.0 to 69.0)
Person-Years	42.2	21.2	21.0
IR per 100 Person-Years (95.0% CI)	33.2 (18.1-55.7)	33.0 (13.3-68.0)	33.3 (13.4-68.7)
VE based on IRR (95.0% CI)†			16.0 (-155.0 to 72.0)

*Symptomatic COVID-19 defined as the presence of RT-PCR or IgM or IgG serology positive test and presence of flu-like symptoms. IRR, incidence rate ratio; HR=hazard ratio; VE, vaccine efficacy; CI, confidence interval. *Vaccine efficacy based on 1-HR obtained in Cox proportional model adjusted for age and sex; †Vaccine efficacy based on 1-IRR obtained in Poisson model adjusted for age and sex, with the natural logarithm (log[n]) of time at risk as offset variable.*

Safety

The local reactogenicity of the BCG vaccine was evaluated for all groups, revaccinated or unvaccinated. The HCWs revaccinated with BCG reported some vaccine-related AEs. However, as expected, the non-revaccinated group, for which no placebo was used, did not report BCG vaccine-related AEs. Of the total number of individuals (64), sixty-three (98.4%) had local adverse events related to BCG, the three most frequent of which were erythema (n=60; 93.8%), papule (n=50; 78.1%), and crust (n=45; 54.7%). The median number of local AEs related to BCG vaccination was five (IQR=4–6) (**Table 5**). AEs not associated with BCG were reported by 21 HCWs, being more frequent in the revaccinated with BCG group, as reported by 15 HCWs. No participant in the unvaccinated group had severe adverse event (SAE), while three participants in the BCG group (4.7%) had, one of which was related to COVID-19 (**Table 6**) and the other two were not related to BCG vaccination (leg cellulitis and diverticulitis).

TABLE 5 | Reactogenicity of the BCG vaccine.

Variables, n (%)*	
Any local AE	63 (98.4)
Grade I	
Erythema	60 (93.8)
Macula	3 (4.7)
Papule	50 (78.1)
Pustule	31 (48.4)
Softening in the center of the lesion	4 (6.3)
Crust	45 (54.7)
Scar	39 (60.9)
Itching	16 (25.0)
Local pain	18 (28.1)
Local heat	6 (9.4)
Local desquamation	4 (6.3)
Grade II	
Exudation	3 (4.7)
Total number of local AE	308
Median (IQR)	5 (4-6)

**Percentages are based on the number of participants in the BCG group. AE, adverse event; IQR, interquartile range.*

Innate Immune Response After BCG Revaccination

To verify the responsiveness of NK IFN-γ- or TNF-α-positive cells, total blood was stimulated with BCG Moscow culture filtrate proteins (CFPs). It was possible to observe that the unvaccinated and revaccinated with BCG groups had similar levels of NK IFN-γ- or TNF-α-positive cells, on both day 1 and day 15 (**Table 7**; $P > 0.05$). The immune response results presented high variability; thus, the fold of increase of these cell populations was evaluated, comparing day 15 relative to day 1 post-randomization. As shown, no differences were observed when the fold of increase of activated cells was evaluated (**Table 7**; $P > 0.05$).

BCG vaccinations were hypothesized as inductors of NK responses that could reduce SARS-COV-2 cell propagation and therefore reduce COVID-19 symptoms. Although no differences were observed in the evaluated immune responses, it was questioned whether previously activated NK cells could have an impact on the symptoms associated with COVID-19. Participants who had a higher fold of increase of NK IFN-γ in the 15–20 days after randomization presented fewer incidences of fever and dyspnea (**Table 8**; $P < 0.05$), indicating a possible role for NK cells that requires further study. No differences were observed when analyzing the other symptoms. Furthermore, the fold of increase analysis of NK TNF-α-positive cells showed no differences between symptomatic and non-symptomatic individuals (**Table 9**; $P > 0.05$).

The positivity for COVID-19 or the development of flu-like syndrome symptoms during the trial was analyzed with the fold of increase of NK IFN-γ cells. It was observed that COVID-19-positive individuals or those that presented flu-like symptoms had a lower fold of increase of NK IFN-γ-positive cells when

TABLE 6 | Distribution of adverse event during 180 days of follow-up according to the allocation groups†.

Variables	All (n = 131)	Unvaccinated (n = 67)	Revaccinated with BCG (n = 64)	*P* -value*
HCWs reporting any AE not related to BCG	21 (16.0)	6 (9.0)	15 (23.4)	**0.03**
Number of AEs	23	4	19	N/A
Grade I or II AE, n (%)	20	4	15	0.06
Grade III AE, n (%)				
Anemia	1 (0.8)	0	1 (1.6)	0.49
Severe AE, n (%)	3 (2.3)	0	3 (4.7)	0.11
Hospitalization due to diverticulitis (CID-10 K57.0)	1 (0.8)	0	1 (1.6)	0.49
Hospitalization due to cellulitis with surgical drainage (CID-10 L03.8)	1 (0.8)	0	1 (1.6)	0.49
Hospitalization due to COVID-19 (CID-10 U07.1)	1 (0.8)	0	1 (1.6)	0.49

†*Adverse reaction (AE) is defined as any event that was not present before the start of the study (exposure to study vaccination) or any pre-existing event that worsens in intensity and frequency after exposure. Percentages are based on the number of participants in the trial. N/A, not applicable; *Fisher's exact test.*

compared to COVID-19-negative individuals or those that presented flu-like syndrome, respectively (**Figures 3A, C**; $P < 0.05$). No differences were observed when the fold of increase of NK TNF-α-positive cells was evaluated (**Figures 3B, D**; $P > 0.05$).

DISCUSSION

This randomized clinical trial was properly structured to assess the potential of BCG revaccination in protecting against or reducing the severity of COVID-19 among HCWs. The target population were HCWs who, according to the WHO (28), are comprehensively defined as all those engaged in health promotion and maintenance actions, whether in transport, admission, or direct patient care. Here, BCG revaccination has not been shown to be effective in reducing the rate of COVID-19, symptoms or improving innate NK immune response. The study was ended prematurely because a national immunization campaign initiated using specific vaccines for the prevention of COVID-19. One of the campaign's priority groups was HCWs, discouraging them from participating in this study and, the majority of recruited HCWs had previous COVID-19, one of the study exclusion criteria. As a matter of fact, the national immunization campaign hampered recruitment to achieve the anticipated sample size, introduced a confounding factor and may have limited the findings and conclusions of this study. Nonetheless, to our knowledge, studies using BCG - Moscow strain as well as with HCWs at Brazil had never been analyzed, thus this work contribute to the field and may aid other studies. After the introduction of COVID-19 specific vaccine immunization at Brazil and with the consequent rapid decline of subject's inclusion in the study, a new theoretical analysis was performed for sample size calculation based on a recent release of COVID-19 incidences among HCWs (26). This assured to ask DSMB to analyze a request for study unmasking, which was consented in August of 2021.

The pandemic is demonstrating that most SARS-CoV-2-infected individuals develop COVID-19 in its asymptomatic form or as a mild form of respiratory infection. However, approximately 20% of cases evolve to its severe form and require specialized care (29). As a result, the rate of hospitalization for complications from COVID-19 has grown exponentially and overloaded health systems. The decision to consider HCWs as a target population was made because the world's population was isolated in their homes to contain the spread of the SARS-CoV-2 virus, while frontline HCWs were exposed to long and exhausting workdays, often accentuated by insufficient protective equipment, inefficient infection control measures, and accompanying risk of contamination by SARS-CoV-2 (30–35).

In the first half of the pandemic, Gómez-Ochoa et al. (36) demonstrated that 10.1% of COVID-19 cases, registered in 11 countries, involved HCWs. In Brazil, there are no official estimates of the number of HCWs who were contaminated with SARS-CoV-2 or died from complications of COVID-19. However, in public hospitals in Rio de Janeiro, it was reported that 25% of HCWs had COVID-19 in the initial phase of the pandemic, which exceeded the rate recorded by Italy (11%), which was one of the epicenters of COVID-19 in Europe (37, 38).

TABLE 7 | NK responses to *M. bovis*-CFP stimulation in BCG and unvaccinated groups.

Immune responses†	Total (n = 121)	Unvaccinated (n = 61)	Revaccinated with BCG (n = 60)	*P* -value*
NK IFN - γ^+ cells				
Day 1	3.08 (1.70-4.66)	3.08 (1.42-4.60)	3.07 (1.76-5.02)	0.63
Day 15	4.00 (2.48-7.56)	3.87 (2.52-6.59)	4.08 (2.20-8.52)	0.74
NK TNF - α^+ cells				
Day 1	8.14 (2.84-14.35)	7.90 (2.68-13.79)	8.33 (2.83-15.66)	0.60
Day 15	8.50 (2.69-16.97)	9.24 (2.57-17.32)	8.42 (2.80-16.32)	0.90
IFN fold of increase	1.48 (0.70-2.93)	1.44 (0.70-3.10)	1.52 (0.51-2.86)	0.83
TNF fold of increase	0.94 (0.52-1.86)	0.86 (0.44-1.70)	1.01 (0.60-1.99)	0.26

**Mann-Whitney U test;* †*Results are presented as median (IQR).*

TABLE 8 | Fold of increase of NK IFN- γ^+ cells after *M. bovis* CFP stimulation according to the different symptoms.

Symptoms†	No	Yes	*P* -value*
Cough	1.60 (0.71-3.02)	0.73 (0.43-1.43)	0.06
Fever	1.56 (0.75-3.03)	0.59 (0.52-1.54)	0.02
Sore throat	1.53 (0.70-2.98)	0.44 (0.74-2.05)	0.14
Night sweats	1.46 (0.70-2.88)	N/A	0.45
Dyspnea	1.51 (0.70-2.98)	0.30 (0.2-N/A)	0.05
Anosmia	1.53 (0.70-2.98)	0.70 (0.37-1.69)	0.12
Diarrhea	1.51 (0.71-3.00)	0.58 (0.44-2.33)	0.18
Headache	1.52 (0.70-2.87)	1.32 (066-3.32)	0.86
Runny nose	1.53 (0.71-2.96)	0.77 (0.57-3.64)	0.45
Nasal congestion	1.48 (0.70-2.86)	1.99 (0.57-11.24)	0.48
Ageusia	1.52 (0.71-2.96)	0.59 (0.33-1.99)	0.11
Fatigue	1.46 (0.68-2.87)	1.54 (0.77-3.32)	0.51
Myalgia	1.46 (0.70-2.79)	1.54 (0.58-4.40)	0.63
Arthralgia	1.48 (0.70-2.89)	1.80 (0.28-N/A)	0.76
Nausea	1.46 (0.70-2.95)	N/A	0.51
Vomiting	1.46 (0.70-2.95)	N/A	0.51

**Mann-Whitney U test. †Data are presented as median (IQR); N/A, not applicable.*

These records worried the entire population, considering that HCWs are essential for the care of patients diagnosed with COVID-19. As a result, HCWs were soon included in the COVID-19 risk group worldwide (32, 39). The HCWs included in this clinical trial were residents of the metropolitan region of Goiânia, which is in the Center-West region of Brazil, where the highest incidence of COVID-19/100 thousand inhabitants was recorded at the time of this writing (40). Most of these HCWs were nurse staff, paramedics (nurses), and medical staff, all of whom were inserted in an environment of high exposure to the SARS-CoV-2 virus, presenting, on average, contact with 20 patients suspected or confirmed for COVID-19 per week. As expected, this group of HCWs, who provided direct patient care, had the highest incidence of COVID-19 during the study (**Table S5** and **Table 2**).

It should be noted that the study did not use a placebo for HCWs allocated to the unvaccinated group because a mock vaccine that provokes similar reactions as the BCG vaccine was not available and, furthermore, the HCWs would easily determine that they were in the placebo group. Other randomized studies have already evaluated the effect of the BCG vaccine in protecting against other diseases without the use of a placebo in the control group. Some of these studies showed results supporting the efficacy and induction of the immune response generated by vaccination with BCG, whereas others did not (7, 41–44). This indicates that the absence of a placebo in the control group does not interfere with the conclusions obtained. However, it should be noted that HCWs not vaccinated with BCG may have been disappointed with the result of randomization and changed their behavior regarding the reporting of health conditions to the telemedicine team, as has already occurred in other studies (45).

On the other hand, once vaccinated with BCG, HCWs were subject to the occurrence of AEs. The reactogenicity provoked by the different strains of BCG is variable and can be influenced by the route of administration (46). The results shown here in this clinical trial revealed that the main reactions reported by HCWs vaccinated with BCG Moscow intradermally were erythema,

TABLE 9 | Fold of increase of NK TNF-α^+ cells after *M. bovis* CFP stimulation according to the different symptoms.

Symptoms†	No	Yes	*P* -value*
Cough	0.98 (0.50-1.90)	0.85 (0.65-1.52)	0.69
Fever	0.99 (0.50-1.89)	0.85 (0.60-1.75)	0.79
Sore throat	0.93 (0.53-1.83)	1.44 (0.42-2.06)	0.53
Night sweats	0.95 (0.53-1.87)	N/A	0.23
Dyspnea	0.94 (0.53-1.88)	0.84 (0.00- N/A)	0.52
Anosmia	0.99 (0.54-1.91)	0.61 (0.21-1.05)	0.16
Diarrhea	0.97 (0.52-1.90)	0.74 (0.44-1.47)	0.55
Headache	0.95 (0.50-1.94)	0.84 (0.66-1.50)	0.93
Runny nose	0.93 (0.47-1.90)	1.41 (0.81-1.63)	0.27
Nasal congestion	0.94 (0.50-1.89)	1.26 (0.67-2.85)	0.56
Ageusia	0.99 (0.53-1.90)	0.85 (0.30-1.26)	0.26
Fatigue	0.95 (0.50-1.89)	0.84 (0.60-1.68)	0.83
Myalgia	0.99 (0.53-1.92)	0.66 (0.28-1.44)	0.36
Arthralgia	0.97 (0.50-1.89)	0.75 (0.66- N/A)	0.61
Nausea	0.95 (0.51-1.87)	N/A	0.94
Vomiting	0.95 (0.51-1.87)	N/A	0.94

**Mann-Whitney U test. †Data are presented as median (IQR). N/A, not applicable.*

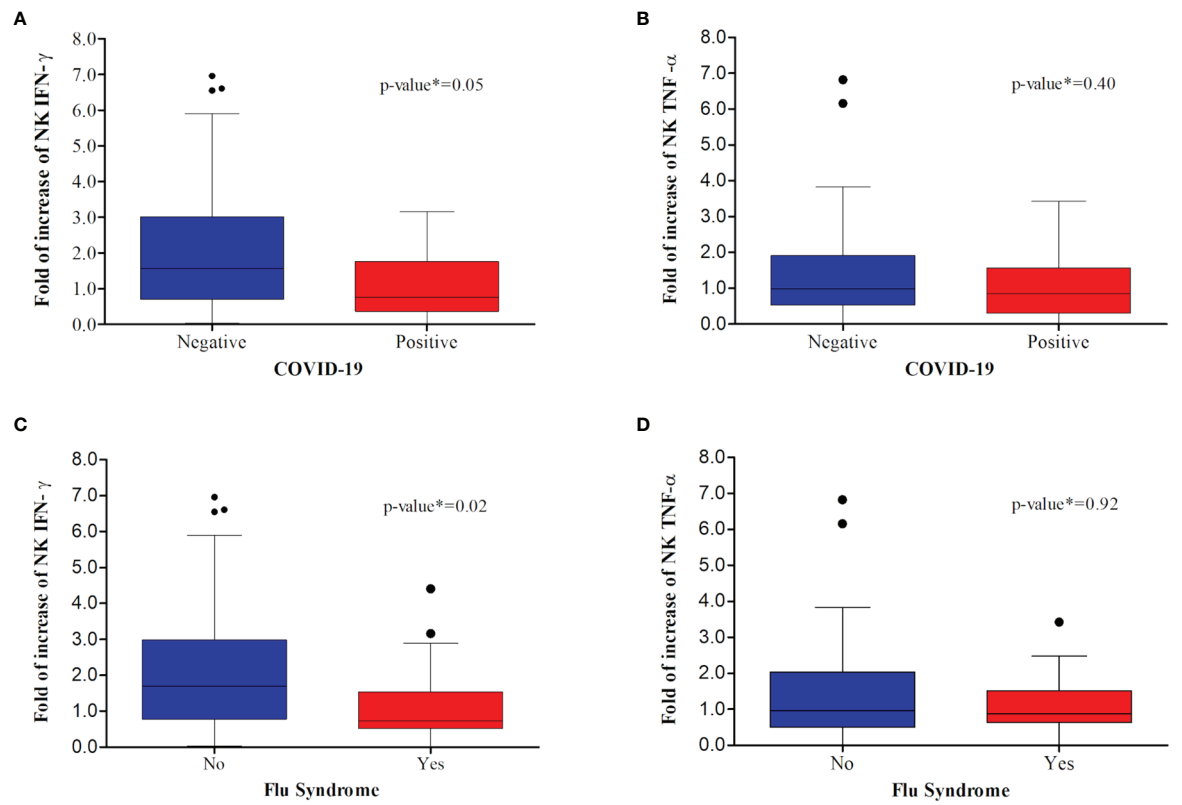

FIGURE 3 | Comparative analysis between confirmed COVID-19 and immunological markers: **(A, C)** fold increase of day 15 relative to day one of NK cells positive for IFN-γ; **(B, D)** fold increase of day 15 relative to day one of NK cells positive for TNF-α. Among individuals that acquired COVID-19 **(A, B)**, there was a significant decrease in the fold increase of NK IFN-γ cells. Similarly, there was a significant decrease in the fold increase of NK IFN-γ cells between those individuals that presented flu syndrome **(C, D)**.

papule, and crust. These local reactions are similar to those from primary BCG vaccination, as previously described by Hoft et al. (47) during the assessment of clinical reactogenicity of BCG vaccination (Connaught Laboratories, Swiftwater, PA) by the intradermal route. Here, in this clinical trial, AEs were resolved completely and spontaneously over the 180 days of monitoring performed by the telemedicine team, and no SAEs were attributed to BCG vaccination. Considering that approximately a quarter of the world population is infected with latent tuberculosis infection (LTBI) (48), here, in this clinical trial, hypothetical positivity for LTBI did not result in SAEs. In addition, no deaths of BCG-revaccinated or unvaccinated HCWs were reported in this clinical trial, suggesting that BCG vaccination is also not associated with risk of death. This information revealed that the revaccination of adults with BCG Moscow was well tolerated, safe, and, therefore, could be used for new applications in individuals in this age group.

A previous study by Giamarellos-Bourboulis et al. (13) found no difference in the frequency of AEs between the groups vaccinated with BCG and the control in the prevention of infectious conditions in the elderly. Despite this, there is concern regarding the potential harm that could be caused by excessive inflammation induced by the BCG vaccine in patients with COVID-19. Here, in this clinical trial, we observed a higher frequency of AEs not associated with BCG in the revaccinated group. Nonetheless, only one serious event was attributed to COVID-19. In this case, 58 days after inclusion in the clinical trial, one HCW vaccinated with BCG presented dyspnea and hypoxemia, which quickly progressed to respiratory failure unresponsive to non-invasive ventilation, resulting in hospitalization in an ICU and orotracheal intubation. According to information self-reported by the HCW, her clinical condition was characterized by extreme pulmonary involvement, reaching 75% of the organs. After 16 days of hospitalization, this HCW was discharged from the hospital, continued with post-COVID-19 respiratory physiotherapy, and, later, returned to her normal professional activities. The causes that led to the severe prognosis and need for hospitalization have not been elucidated and need further investigation. As BCG revaccination did not induce an increase in the inflammatory innate response, the SAEs observed in this individual could not be attributed to the BCG vaccine. Additionally, here we showed that individuals who developed COVID-19 had a reduced fold of increase in the number of NK IFN-γ cells (**Figure 3**). Despite this SAE, BCG revaccination did not show an increased risk of hospitalization for COVID-19.

In this study, BCG revaccinated individuals presented less COVID-19 cases than control group, although the sample size limited to reach a significant difference. The frequency of symptoms presented by HCWs in the unvaccinated group and those revaccinated with BCG were similar. Notably, this trial was planned in a context without censoring for COVID-19 vaccination. During the study, just after the regulatory agencies' approval, specific COVID-19 vaccines began to be used for elderly people and HCWs in Brazil (49). Similar findings regarding the efficacy, cumulative incidence rate of COVID-19, and symptom severity were observed even when HCWs were vaccinated against COVID-19 (**Table 4**). Similarly, Amirlak et al. (50) evaluated if BCG revaccination was able to provide COVID-19 protection. Although the study was retrospective in regard to BCG revaccination, a reduction in COVID-19 incidence among the BCG boosted HCWs was observed (50).

A retrospective study carried out by Hamiel et al. (51) compared the incidence of severe COVID-19 in a large cohort of adult Israelis who had and who had not been vaccinated with BCG (unreported strain) in childhood. The results indicated only one case of severe COVID-19 requiring ventilation or admission to the ICU in each group, and no deaths were reported. Similar to our data, the small number of COVID-19 cases in Hamiel et al.'s study could not support a statistically significant difference in the positivity rate for COVID-19, and the number of severe cases was small. Due to these inconclusive results, the authors did not support the idea that childhood BCG vaccination had a protective effect against COVID-19 in adulthood. Despite the similarities between the results, it is prudent to emphasize that Hamiel et al. (51) evaluated the potential of childhood BCG vaccination to protect against COVID-19 in adulthood, rather than recent BCG vaccination.

Interestingly, preliminary data derived from the study BCG-PRIME (NCT04537663) suggested that the BCG vaccine did not protect vulnerable elderly people from COVID-19. Although the study included and monitored more than 6,132 sixty-year-old individuals for 180 days after BCG vaccination, the results revealed that COVID-19 infection in combination with disease symptoms occurred with the same frequency in the elderly from the control group and those vaccinated with BCG. However, it is important to note that almost all individuals participating in the BCG-PRIME study received the BCG vaccine for the first time, as the Netherlands did not adopt a policy of vaccination with BCG in childhood (52).

In contrast, the double-blind, randomized trial (ACTIVATE-2) performed with Greek volunteers demonstrated that BCG revaccination resulted in a 68% risk reduction for total COVID19 diagnoses (OR 0.32. 95% CI 0.13-0.79). However, in that study, the diagnosis of COVID-19 of some participants was based on the clinical diagnosis of possible or probable COVID-19 (26). Another study, carried out with HCWs from Emirates International Hospital (United Arab Emirates) demonstrated potential effectiveness of BCG revaccination in preventing COVID-19 infections (50). Although all HCWs were tested for COVID-19 during the study period, there are two important limitations that should be considered here: the lack of understanding of any confounding factors between the BCG-revaccinated and non-BCG-revaccinated groups that eventually may have influenced the rate of transmission and infection, in addition to the discrepancy between the number of individuals in the two groups (revaccinated with BCG=71 and not revaccinated with BCG=209).

Additionally, study carried out by Rivas et al. (53) demonstrated that HCWs with a history of BCG vaccination presented lower positivity for anti-SARS-CoV-2 IgG or COVID-19 symptoms. Here, it was also observed a reduced number of COVID-19 cases among HCWs revaccinated with BCG, but no significant differences between the groups were observed. Furthermore, it should be noted that the BCG vaccination referred by Rivas et al. (53) is retrospective to the analysis, that is different from a randomized clinical trial.

The reasons why no non-specific effects attributable to BCG revaccination in protecting against or reducing the severity of COVID-19 were observed in the present clinical trial should be investigated by different aspects, including immune response. Many studies are underway to explore the immune response profile of BCG vaccination. Some studies have shown that the revaccination of elderly individuals with BCG Pasteur has contributed to the prevention of acute upper respiratory tract infection (AURTI). This vaccine contributes to an increase in plasma levels of IFN-γ and IL-10 after six months of administration (14). More recently, it was shown that elderly individuals newly vaccinated with BCG Bulgaria had a lower frequency of viral infections during the year. The stimulation of blood mononuclear cells with *Mycobacterium tuberculosis* (Mtb) resulted in an increase in IFN-γ specific to Mtb at 90 days but is not observable at 14 days after vaccination. Stimulation with non-specific components results in the production of IL-6 at 14 and 90 days after vaccination (13). In a study using the BCG SSI vaccine (Danish), it was shown that vaccination appeared to be involved in preventing fungal infections such as Candidiasis. After 14 days of immunization, it was observed that vaccination with BCG induced non-specific pro-inflammatory cytokine-secreting NK cells, such as IL-1β, IL-6, and TNF-α (54). However, in the work evaluated here, no difference in the levels of NK IFN-γ- or TNF-α-positive cells was observed after stimulation with CFPs from *M. bovis* BCG. Some works have shown that after 15–20 days post-BCG vaccination, NK cells are activated, while other studies have shown that this response is maintained for at least three months (11, 54). However, none of these studies used BCG Moscow as a vaccine. Whether the BCG strain may have contributed to the lack of NK responses and consequently to the failure to prevent SARS-CoV-2 infection is still a matter of debate.

It is known that the protection conferred by BCG against tuberculosis depends on the induction of a specific response, Th1 (55); however, this protection differs in terms of the type of strain used worldwide (56). It has been observed that the immune response also presents a different response amplitude, according to the strain used (57). This can be seen in a clinical trial carried out in Uganda (ISRCTN32849447), which tested three different

types of strains (BCG Moscow, BCG Bulgaria, and BCG Danish), verifying that both BCG Danish and BCG Bulgaria strains induced IFN-γ and IL-10 in a manner superior to that induced by BCG Moscow (58). When using the BCG vaccine to prevent various infections, such as flu infections, the same effect has been observed. Another clinical trial (ClinicalTrial.gov NCT03296423) used the revaccination of elderly individuals with BCG Bulgaria and demonstrated a reduction in the frequency of viral infections and respiratory infections, which may be related to the cross-effect induced by the BCG vaccine (13). However, in this study, which used the BCG Moscow vaccine, a reduction in the degree of infection by SARS-CoV-2 or in the symptoms presented in individuals who were vaccinated and infected was not observed. The decision to use the BCG Moscow strain in this trial was based on its use in the Brazilian National Immunization Program since 2018. Thus, further studies should be developed to evaluate its protective response against tuberculosis in Brazil.

The protection observed in a work by Giamarellos-Bourboulis et al. (13) has been related to epigenetic modifications in monocytes, which showed increased H3K27 histone acetylation at the *IL-6* and *TNF* genes and increased TNF-α, IL-1β, and IL-10 cytokine synthesis after three months of immunization. Apparently, the BCG Bulgaria vaccine induces an effective heterologous response, which may have contributed to a cross-response against other infections. Different from the results observed by Giamarellos-Bourboulis et al. (13), our work, which used the BCG Moscow strain, evaluated by flow cytometry NK ($CD16^{+}CD56dim$) cells after 14 days of immunization, which did not enhance their production of IFN-γ or TNF-α. Our work, although employing a different methodology, presented similar results as those observed by Kleinnijenhuis et al. (54). In their experiment, cytokines secreted by cultured NK cells stimulated with Mtb antigens after BCG vaccination were evaluated. Kleinnijenhuis and colleagues observed that although other cytokines were increased, neither IFN-γ nor TNF-α were significantly increased upon NK cell stimulation, 14 days after BCG vaccination.

In addition, it has been shown that sex hormones can interfere with the immune response induced by BCG Bulgaria. In the work developed by Koeken et al. (59), referring to 300BCG (NL58553.091.16) and 500FG (NL42561.091.12) studies, it was shown that the response of the BCG Bulgaria vaccine reduced systemic inflammation in vaccinated men. However, the elicited immune response evaluated by the production of IFN-γ by PBMC in response to Mtb antigens was greater in women than in men (59). In this clinical trial, women were overrepresented due to their predominance in the health workforce. Nonetheless, the incidence of COVID-19 was reduced among BCG revaccinated women compared to unvaccinated group, while revaccinated men had a higher risk of developing COVID-19. Unfortunately, due to the limited number of individuals investigated, the differences did not reach statistical significance (**Table S2**). Unfortunately, due to this low number of infected HCWs, we cannot conclude whether sex hormones interfered with the immune response induced by BCG Moscow. Despite the disappointing findings, this clinical trial provided information that should be of interest for the medical and scientific community globally and can inform further studies about how to face future challenges posed by other infectious diseases.

In conclusion, the revaccination of adults with BCG Moscow was safe but did not protect HCWs against COVID-19. BCG Moscow revaccination of HCWs did not induce NK activation.

LIMITATION

Caution is required when interpreting the findings presented in this study. One limitation was the fact that many recruited volunteers spontaneously stopped participating for various reasons, but mainly due to previous COVID-19 infection. Furthermore, during the study, just after the regulatory agencies' approval, specific COVID-19 vaccines began to be used for elderly people and HCWs in Brazil. All HCWs who were being followed and who decided to take a specific vaccine were asked to submit to blood sample collection to assess the possible presence of asymptomatic COVID-19. Even so, HCWs were tested for COVID-19 after 180 days of study enrollment, as provided for in the study design. As the results of this study were objective and were verified through serological and molecular tests or clinical assessment as recommended by the WHO, it is believed that vaccination against COVID-19 did not compromise the analyses. At the time of this trial design, data regarding COVID-19 incidence among HCWs and the population in general were scarce, especially in Brazil, so the reported European incidence rate was used to calculate the sample size. This rate was shown to be higher than that observed among Brazilian HCWs. Nonetheless, the target of 197 participants was the objective of the trial, which was not reached for two main reasons: a high rate of COVID-19 infection among the recruited HCWs, thereby barring inclusion in the study, and the introduction of COVID-19-specific vaccination among HCWs. The reduction of the sample size and the reduced cases of COVID-19 among HCWs hindered the detection of significant differences.

DATA AVAILABILITY STATEMENT

The raw data supporting the conclusions of this article will be made available by the authors, without undue reservation.

ETHICS STATEMENT

The studies involving human participants were reviewed and approved by Comissão Nacional de ética em Pesquisa -CONEP. The patients/participants provided their written informed consent to participate in this study.

AUTHOR CONTRIBUTIONS

APJK was the principal investigator and conceived and designed the trial protocol with help from AK, LRBA, ACC, AROC, MFR, and MBC. LRBA, KMR, RLR, KMCB, ACOC, CCS, RRMF, and CISD performed the recruitment. LA, KR, and CS performed the scheduling for the study participants. APJK, AK, and LRBA ensured the correct storage and use of the BCG vaccine. KMR, KB, ACOC, LSB, CCS, and LRBA assisted with the informed consent collection process and participant inclusion. APJK, ACC, AR, LRBA, and KMR performed the laboratory testing and organized the sample collection. MBC helped in the training of the team involved in conducting the clinical trial. RG was an external member who performed the data curation and statistical analyses. AROC, GS, RLR, RRMF, TV, and MFR performed the clinical follow-up with the study participants for 180 days using telemedicine and/or clinical evaluations. APJK, ACC, and LSB performed the NK experiments and analysis. LRBA, ACC, and RG wrote the original manuscript draft. APJK and AK edited and conducted the final proofreading of the text, and the authors read and approved the manuscript.

FUNDING

This trial was funded by Conselho Nacional de Desenvolvimento Científico e Tecnológico/National Council for Scientific and Technological Development (CNPq), Ministério da Ciência, Tecnologia e Inovações (MCTI)/Ministry of Science, Technology and Innovations, Grant numbers: (401206/2020-3; 303671/2019-0; 314366/2020-2). Furthermore, the BCG vaccines were kindly donated by the Brazilian Immunization Program of the Health Ministry of the Brazilian Government/Programa Nacional de Imunização, Ministério da Saúde, Brasil. Neither the funding agency nor the Brazilian Immunization Program had a role in the trial design, the conception, collection, analysis, interpretation, or conclusions, or the decision to write this manuscript. LRBA received fellowship from Coordenação de Pessoal de nível Superior (CAPES-Finance Code 001) and KMR, CCS, ACOC, and AOR received fellowship from CNPq.

ACKNOWLEDGMENTS

The authors thank the collaborators who were part of the project: "Volunteer internship in a randomized clinical trial impacting the COVID-19 pandemic." which included undergraduate students, graduate students, and professionals who assisted in promoting, through social media, the BCG-COVID19 clinical trial and were mentioned in detail in (18). Thanks to Margarida Dobler Komma Laboratory (IPTSP/UFG). represented by technicians Petain José Ferreira Neto and Luismar Pereira Cardoso, for performing the blood sampling and the hemograms of the study participants; to the National Immunization Program for supplying the BCG vaccines; to nurse Dasdores Gonçalves da Silva Oliveira and nursing technician Maria de Lourdes da Silva Borges for performing the immunizations of the participants; to biomedical professional Rogério Coutinho Neves for assisting us during the inclusion of the participants in the study; to Independent Security Data Monitoring (DSMB), represented by João Alves de Araújo Filho, Leandro do Prado Assunção, and Yves Mauro Fernandes Ternes.

SUPPLEMENTARY MATERIAL

The Supplementary Material for this article can be found online at: https://www.frontiersin.org/articles/10.3389/fimmu.2022.841868/full#supplementary-material

REFERENCES

1. World Health Organization WHO. *Timeline: Who's COVID-19 Response* (2020). Available at: www.who.int/news-room/detail/27-04-2020-who-timeline—covid-19.
2. Cascella M, Rajnik M, Aleem A, Dulebohn SC, Di Napoli R. *Features, Evaluation, and Treatment of Coronavirus (COVID-19)*. Treasure Island (FL):StatPearls (2021). Available at: www.ncbi.nlm.nih.gov/books/NBK554776/.
3. Organisation for Economic Cooperation and Development OECD. *Access to COVID-19 Vaccines: Global Approaches in a Global Crisis* (2021). Available at: www.oecd.org/coronavirus/policy-responses/access-to-covid-19-vaccines-global-approaches-in-a-global-crisis-c6a18370/.
4. Saxena SK, Kumar S, Ansari S, Paweska JT, Maurya VK, Tripathi AK, et al. Characterization of the Novel SARS-CoV-2 Omicron (B.1.1.529) Variant of Concern and Its Global Perspective. *J Med Virol* (2021) 94:1738–44. doi: 10.1002/jmv.27524
5. Khateeb J, Li Y, Zhang H. Emerging SARS-CoV-2 Variants of Concern and Potential Intervention Approaches. *Crit Care* (2021) 25(1):244. doi: 10.1186/s13054-021-03662-x
6. Abdallah AM, Behr MA. Evolution and Strain Variation in BCG. *Adv Exp Med Biol* (2017) 1019:155–69. doi: 10.1007/978-3-319-64371-7_8
7. Aaby P, Roth A, Ravn H, Napirna BM, Rodrigues A, Lisse IM, et al. Randomized Trial of BCG Vaccination at Birth to Low-Birth-Weight Children: Beneficial Nonspecific Effects in the Neonatal Period? *J Infect Dis* (2011) 204(2):245–52. doi: 10.1093/infdis/jir240
8. Biering-Sørensen S, Aaby P, Napirna BM, Roth A, Ravn H, Rodrigues A, et al. Small Randomized Trial Among Low-Birth-Weight Children Receiving Bacillus Calmette-Guérin Vaccination at First Health Center Contact. *Pediatr Infect Dis J* (2012) 31(3):306–8. doi: 10.1097/INF.0b013e3182458289
9. Stensballe LG, Nante E, Jensen IP, Kofoed PE, Poulsen A, Jensen H, et al. Acute Lower Respiratory Tract Infections and Respiratory Syncytial Virus in Infants in Guinea-Bissau: A Beneficial Effect of BCG Vaccination for Girls Community Based Case-Control Study. *Vaccine* (2005) 23(10):1251–7. doi: 10.1016/j.vaccine.2004.09.006
10. Netea MG, Domínguez-Andrés J, Barreiro LB, Chavakis T, Divangahi M, Fuchs E, et al. Defining Trained Immunity and Its Role in Health and Disease. *Nat Rev Immunol* (2020) 20(6):375–88. doi: 10.1038/s41577-020-0285-6
11. Netea MG, Joosten LA, Latz E, Mills KH, Natoli G, Stunnenberg HG, et al. Trained Immunity: A Program of Innate Immune Memory in Health and Disease. *Science* (2016) 352(6284):aaf1098. doi: 10.1126/science.aaf1098
12. Biering-Sørensen S, Aaby P, Lund N, Monteiro I, Jensen KJ, Eriksen HB, et al. Early BCG-Denmark and Neonatal Mortality Among Infants Weighing <2500 G: A Randomized Controlled Trial. *Clin Infect Dis: Off Publ Infect Dis Soc America* (2017) 65(7):1183–90. doi: 10.1093/cid/cix525

13. Giamarellos-Bourboulis EJ, Tsilika M, Moorlag S, Antonakos N, Kotsaki A, Domínguez-Andrés J, et al. Activate: Randomized Clinical Trial of BCG Vaccination Against Infection in the Elderly. *Cell* (2020) 183(2):315–23.e9. doi: 10.1016/j.cell.2020.08.051
14. Wardhana, Datau EA, Sultana A, Mandang VV, Jim E. The Efficacy of Bacillus Calmette-Guerin Vaccinations for the Prevention of Acute Upper Respiratory Tract Infection in the Elderly. *Acta Med Indonesiana* (2011) 43(3):185–90. doi: 10.1111/j.1399-3038.2010.01051.x
15. Cao Q, Chen Y-C, Chen C-L, Chiu C-H. SARS-CoV-2 Infection in Children: Transmission Dynamics and Clinical Characteristics. *J Formosan Med Assoc* (2020) 119(3):670. doi: 10.1016/j.jfma.2020.02.009
16. Hensel J, McAndrews KM, McGrail DJ, Dowlatshahi DP, LeBleu VS, Kalluri R. Protection Against SARS-CoV-2 by BCG Vaccination Is Not Supported by Epidemiological Analyses. *Sci Rep* (2020) 10(1):18377. doi: 10.1038/s41598-020-75491-x
17. Escobar LE, Molina-Cruz A, Barillas-Mury C. BCG Vaccine Protection From Severe Coronavirus Disease 2019 (COVID-19). *Proc Natl Acad Sci* (2020) 117 (30):17720–6. doi: 10.1073/pnas.2008410117
18. Junqueira-Kipnis AP, dos Anjos LRB, Barbosa L, da Costa AC, Borges KCM, Cardoso A, et al. BCG Revaccination of Health Workers in Brazil to Improve Innate Immune Responses Against COVID-19: A Structured Summary of a Study Protocol for a Randomised Controlled Trial. *Trials* (2020) 21(1):881. doi: 10.1186/s13063-020-04822-0
19. Cuschieri S. The CONSORT Statement. *Saudi J Anaesth* (2019) 13(Suppl 1): S27–s30. doi: 10.4103/sja.SJA_559_18
20. Ministério da Saúde do Brasil MS. *Portaria N° 432, 19 De Março De 2020* (2021). Available at: https://brasilsus.com.br/index.php/pdf/portaria-no-397-2/.
21. World Health Organization W. *Clinical Management of COVID-19: Interim Guidance, 27 May 2020*. Geneva: World Health Organization (2020). 2020. Report No.: Contract No.: WHO/2019-nCoV/clinical/2020.5.
22. Ministério da Saúde do Brasil MS. *Manual De Vigilância Epidemiológica De Eventos Adversos Pós-Vacinação*. Brasilia: Ministério da Saúde Brasília (2014). Available at: https://bvsms.saude.gov.br/bvs/publicacoes/manual_vigilancia_epidemiologica_eventos_adversos_pos_vacinacao.pdf.
23. National Institutes of Health NIH. *Division of AIDS: National Institute of Allergy and Infectious Diseases, National Institutes of Health, US Department of Health and Human Services*. Washington, DC: National Institute of Allergy and Infectious Diseases (2017).
24. Food and Drug Administration F. *CFR 314.80: Postmarketing Reporting of Adverse Drug Experiences* (2017). Available at: https://www.ecfr.gov/cgi-bin/text-idx?SID=db68ad73ff4f35bdb5750e78aebfd5b5&mc=true&node=se21.5.314_180&rgn=div8.(2017).
25. Hulley Sb C, Ws B, Grady D. *Designing Clinical Research: An Epidemiologic Approach* Vol. 75. City: Philadelphia: PA: Lippincott Williams & Wilkins (2013).
26. Tsilika M, Taks E, Dolianitis K, Kotsaki A, Leventogiannis K, Damoulari C, et al. ACTIVATE-2: A Double-Blind Randomized Trial of BCG Vaccination Against COVID19 in Individuals at Risk. *medRxiv* (2021). doi: 10.1101/2021.05.20.21257520
27. Zou G. A Modified Poisson Regression Approach to Prospective Studies With Binary Data. *Am J Epidemiol* (2004) 159(7):702–6. doi: 10.1093/aje/kwh090
28. World Health Organization WHO. *The World Health Report 2006: Working Together for Health*. Geneva: World Health Organization (2006). Available at: https://www.who.int/whr/2006/whr06_en.pdf.
29. Flanagan KL, Best E, Crawford NW, Giles M, Koirala A, Macartney K, et al. Progress and Pitfalls in the Quest for Effective SARS-CoV-2 (COVID-19) Vaccines. *Front Immunol* (2020) 11:579250(2410). doi: 10.3389/fimmu.2020.579250
30. Pruc M, Golik D, Szarpak L, Adam I, Smereka J. COVID-19 in Healthcare Workers. *Am J Emergency Med* (2021) 39:236. doi: 10.1016/j.ajem.2020.05.017
31. Eurosurveillance Editorial T. Updated Rapid Risk Assessment From ECDC on Coronavirus Disease 2019 (COVID-19) Pandemic: Increased Transmission in the EU/EEA and the UK. *Euro Surveill: Bull Euro Sur Les Malad Transmiss = Eur Commun Dis Bull* (2020) 25(12):121. doi: 10.2807/1560-7917.es.2020.25.12.2003261
32. Mandić-Rajčević S, Masci F, Crespi E, Franchetti S, Longo A, Bollina I, et al. Source and Symptoms of COVID-19 Among Hospital Workers in Milan. *Occup Med* (2020) 70(9):672–9. doi: 10.1093/occmed/kqaa201
33. Bielicki JA, Duval X, Gobat N, Goossens H, Koopmans M, Tacconelli E, et al. Monitoring Approaches for Health-Care Workers During the COVID-19 Pandemic. *Lancet Infect Dis* (2020) 20(10):e261–e7. doi: 10.1016/s1473-3099(20)30458-8
34. Barranco R, Ventura F. Covid-19 and Infection in Health-Care Workers: An Emerging Problem. *Medico-Legal J* (2020) 88(2):65–6. doi: 10.1177/0025817220923694
35. Mhango M, Dzobo M, Chitungo I, Dzinamarira T. COVID-19 Risk Factors Among Health Workers: A Rapid Review. *Saf Health Work* (2020) 11(3):262–5. doi: 10.1016/j.shaw.2020.06.001
36. Gómez-Ochoa SA, Franco OH, Rojas LZ, Raguindin PF, Roa-Díaz ZM, Wyssmann BM, et al. COVID-19 in Health-Care Workers: A Living Systematic Review and Meta-Analysis of Prevalence, Risk Factors, Clinical Characteristics, and Outcomes. *Am J Epidemiol* (2021) 190(1):161–75. doi: 10.1093/aje/kwaa191
37. AZEVEDO AL. *Coronavírus Atinge Até 25% De Profissionais De Saúde No Rio O Globo* (2020). Available at: https://oglobo.globo.com/saude/coronavirus/coronavirus-atinge-ate-25-dos-profissionais-de-saude-no-rio-.
38. Anelli F, Leoni G, Monaco R, Nume C, Rossi RC, Marinoni G, et al. Italian Doctors Call for Protecting Healthcare Workers and Boosting Community Surveillance During Covid-19 Outbreak. *Bmj* (2020) 368(10.1136):m1254. doi: 10.1136/bmj.m1254
39. Nguyen LH, Drew DA, Graham MS, Joshi AD, Guo C-G, Ma W, et al. Risk of COVID-19 Among Front-Line Health-Care Workers and the General Community: A Prospective Cohort Study. *Lancet Public Health* (2020) 5(9): e475–e83. doi: 10.1016/S2468-2667(20)30164-X
40. Secretaria Estadual De Saúde do Estado De Goiás SES-Go. In: *Coronavírus (COVID-19): Goiás Goiás* Goiânia, Goias Government. Available at: https://www.saude.go.gov.br/coronavirus.
41. Thøstesen LM, Kjaer HF, Pihl GT, Nissen TN, Birk NM, Kjaergaard J, et al. Neonatal BCG Has No Effect on Allergic Sensitization and Suspected Food Allergy Until 13 Months. *Pediatr Allergy Immunol* (2017) 28(6):588–96. doi: 10.1111/pai.12748
42. Nissen TN, Birk NM, Smits G, Jeppesen DL, Stensballe LG, Netea MG, et al. Bacille Calmette-Guérin (BCG) Vaccination at Birth and Antibody Responses to Childhood Vaccines. A Randomised Clinical Trial. *Vaccine* (2017) 35 (16):2084–91. doi: 10.1016/j.vaccine.2017.02.048
43. Jensen SK, Jensen TM, Birk NM, Stensballe LG, Benn CS, Jensen KJ, et al. Bacille Calmette-Guérin Vaccination at Birth and Differential White Blood Cell Count in Infancy. A Randomised Clinical Trial. *Vaccine* (2020) 38 (11):2449–55. doi: 10.1016/j.vaccine.2020.02.006
44. Walk J, de Bree LCJ, Graumans W, Stoter R, van Gemert G-J, van de Vegte-Bolmer M, et al. Outcomes of Controlled Human Malaria Infection After BCG Vaccination. *Nat Commun* (2019) 10(1):874. doi: 10.1038/s41467-019-08659-3
45. Schulz KF, Grimes DA. Blinding in Randomised Trials: Hiding Who Got What. *Lancet* (2002) 359(9307):696–700. doi: 10.1016/S0140-6736(02)07816-9
46. Roh EJ, Lee Y-K, Lee M-H, Kim M-K, Kim TE, Lee SG, et al. Investigation of Adverse Events Following Bacille Calmette-Guérin Immunization Using Immunization Safety Surveillance System in Korea Centers for Disease Control and Prevention. *Clin Exp Vaccine Res* (2020) 9(2):133–45. doi: 10.7774/cevr.2020.9.2.133
47. Hoft DF, Leonardi C, Milligan T, Nahass GT, Kemp B, Cook S, et al. Clinical Reactogenicity of Intradermal Bacille Calmette-Guerin Vaccination. *Clin Infect Dis* (1999) 28(4):785–90. doi: 10.1086/515201
48. Carranza C, Pedraza-Sanchez S, de Oyarzabal-Mendez E, Torres M. Diagnosis for Latent Tuberculosis Infection: New Alternatives. *Front Immunol* (2020) 11:2006. doi: 10.3389/fimmu.2020.02006
49. Tregoning JS, Brown ES, Cheeseman HM, Flight KE, Higham SL, Lemm N-M, et al. Vaccines for COVID-19. *Clin Exp Immunol* (2020) 202(2):162–92. doi: 10.1111/cei.13517
50. Amirlak L, Haddad R, Hardy JD, Khaled NS, Chung MH, Amirlak B. Effectiveness of Booster BCG Vaccination in Preventing Covid-19 Infection. *Hum Vaccines Immunother* (2021) 17(11):3913–5. doi: 10.1080/21645515.2021.1956228
51. Hamiel U, Kozer E, Youngster I. SARS-CoV-2 Rates in BCG-Vaccinated and Unvaccinated Young Adults. *Jama* (2020) 323(22):2340–1. doi: 10.1001/jama.2020.8189
52. Utrecht U. *Prevention Of Respiratory Tract Infection And Covid-19 Through BCG Vaccination In Vulnerable Older Adults* (2020). Available at: https://clinicaltrials.gov/ct2/show/NCT04537663.

53. Rivas MN, Ebinger JE, Wu M, Sun N, Braun J, Sobhani K, et al. BCG Vaccination History Associates With Decreased SARS-CoV-2 Seroprevalence Across a Diverse Cohort of Health Care Workers. *J Clin Invest* (2021) 131(2): e145157. doi: 10.1172/JCI145157
54. Kleinnijenhuis J, Quintin J, Preijers F, Joosten LA, Jacobs C, Xavier RJ, et al. BCG-Induced Trained Immunity in NK Cells: Role for Non-Specific Protection to Infection. *Clin Immunol* (2014) 155(2):213–9. doi: 10.1016/j.clim.2014.10.005
55. Soares AP, Scriba TJ, Joseph S, Harbacheuski R, Murray RA, Gelderbloem SJ, et al. Bacillus Calmette-Guerin Vaccination of Human Newborns Induces T Cells With Complex Cytokine and Phenotypic Profiles. *J Immunol* (2008) 180 (5):3569–77. doi: 10.4049/jimmunol.180.5.3569
56. Ritz N, Hanekom WA, Robins-Browne R, Britton WJ, Curtis N. Influence of BCG Vaccine Strain on the Immune Response and Protection Against Tuberculosis. *FEMS Microbiol Rev* (2008) 32(5):821–41. doi: 10.1111/j.1574-6976.2008.00118.x
57. Ritz N, Dutta B, Donath S, Casalaz D, Connell TG, Tebruegge M, et al. The Influence of Bacille Calmette-Guerin Vaccine Strain on the Immune Response Against Tuberculosis: A Randomized Trial. *Am J Respir Crit Care Med* (2012) 185(2):213–22. doi: 10.1164/rccm.201104-0714OC
58. Anderson EJ, Webb EL, Mawa PA, Kizza M, Lyadda N, Nampijja M, et al. The Influence of BCG Vaccine Strain on Mycobacteria-Specific and Non-Specific Immune Responses in a Prospective Cohort of Infants in Uganda. *Vaccine* (2012) 30(12):2083–9. doi: 10.1016/j.vaccine.2012.01.053
59. Koeken VA, de Bree LCJ, Mourits VP, Moorlag SJ, Walk J, Cirovic B, et al. BCG Vaccination in Humans Inhibits Systemic Inflammation in a Sex-Dependent Manner. *J Clin Invest* (2020) 130(10):5591–602. doi: 10.1172/JCI133935

Conflict of Interest: The authors declare that the research was conducted in the absence of any commercial or financial relationships that could be construed as a potential conflict of interest.

Publisher's Note: All claims expressed in this article are solely those of the authors and do not necessarily represent those of their affiliated organizations, or those of the publisher, the editors and the reviewers. Any product that may be evaluated in this article, or claim that may be made by its manufacturer, is not guaranteed or endorsed by the publisher.

frontiers | Frontiers in Immunology

ORIGINAL RESEARCH
published: 12 April 2022
doi: 10.3389/fimmu.2022.862726

Optimizing the Boosting Schedule of Subunit Vaccines Consisting of BCG and "Non-BCG" Antigens to Induce Long-Term Immune Memory

*Wei Lv[1], Pu He[1], Yanlin Ma[1], Daquan Tan[1], Fei Li[1], Tao Xie[1], Jiangyuan Han[1], Juan Wang[1], Youjun Mi[1,2], Hongxia Niu[1] and Bingdong Zhu[1,3]**

[1] Gansu Provincial Key Laboratory of Evidence Based Medicine and Clinical Translation and Lanzhou Center for Tuberculosis Research, Institute of Pathogen Biology, School of Basic Medical Sciences, Lanzhou University, Lanzhou, China, [2] Institute of Pathophysiology, School of Basic Medical Sciences, Lanzhou University, Lanzhou, China, [3] State Key Laboratory of Veterinary Etiological Biology, College of Veterinary Medicine, Lanzhou University, Lanzhou, China

OPEN ACCESS

Edited by:
Wenping Gong, The 8th Medical Center of PLA General Hospital, China

Reviewed by:
Xiaolu Xiong, Beijing Institute of Microbiology and Epidemiology, China
Alastair Copland, University of Birmingham, United Kingdom

***Correspondence:**
Bingdong Zhu
bdzhu@lzu.edu.cn

Specialty section:
This article was submitted to Vaccines and Molecular Therapeutics, a section of the journal Frontiers in Immunology

Received: *26 January 2022*
Accepted: *16 March 2022*
Published: *12 April 2022*

Citation:
Lv W, He P, Ma Y, Tan D, Li F, Xie T, Han J, Wang J, Mi Y, Niu H and Zhu B (2022) Optimizing the Boosting Schedule of Subunit Vaccines Consisting of BCG and "Non-BCG" Antigens to Induce Long-Term Immune Memory. Front. Immunol. 13:862726. doi: 10.3389/fimmu.2022.862726

Boosting Bacillus Calmette-Guérin (BCG) with subunit vaccine is expected to induce long-term protection against tuberculosis (TB). However, it is urgently needed to optimize the boosting schedule of subunit vaccines, which consists of antigens from or not from BCG, to induce long-term immune memory. To address it two subunit vaccines, Mtb10.4-HspX (MH) consisting of BCG antigens and ESAT6-CFP10 (EC) consisting of antigens from the region of difference (RD) of *Mycobacterium tuberculosis* (*M. tuberculosis*), were applied to immunize BCG-primed C57BL/6 mice twice or thrice with different intervals, respectively. The long-term antigen-specific immune responses and protective efficacy against *M. tuberculosis* H37Ra were determined. The results showed that following BCG priming, MH boosting twice at 12-24 weeks or EC immunizations thrice at 12-16-24 weeks enhanced the number and function of long-lived memory T cells with improved protection against H37Ra, while MH boosting thrice at 12-16-24 weeks or twice at 8-14 weeks and EC immunizations twice at 12-24 weeks or thrice at 8-10-14 weeks didn't induce long-term immunity. It suggests that following BCG priming, both BCG antigens MH boosting twice and "non-BCG" antigens EC immunizations thrice at suitable intervals induce long-lived memory T cell-mediated immunity.

Keywords: tuberculosis, BCG, subunit vaccine, boost schedule, immunization program

1 INTRODUCTION

Tuberculosis (TB) is a serious infectious disease mainly caused by *Mycobacterium tuberculosis* (*M. tuberculosis*) (1, 2). Bacillus Calmette-Guerin (BCG) is commonly applied in newborns and has proved to be effective in protecting children from severe tuberculosis infection (3, 4), but the protective immunity wanes and shows limited protection against tuberculosis in adults (5, 6). T cell-mediated immune responses are critical for host defense against *M. tuberculosis* infection (7–9). *M. tuberculosis* infection or vaccine immunization activates several kinds of T cells, including stem cell-like memory T cells (T_{SCM}), central memory T cells (T_{CM}), effector memory T cells (T_{EM}) and

effector T cells (T_{eff}) (10, 11). T_{SCM} and T_{CM} can be maintained for many years and have strong proliferation ability, in which T_{SCM} can live longer than T_{CM} (8, 12–14). Under secondary infection or antigen re-stimulation, T_{SCM} could differentiate into T_{CM}, which mainly secrete interleukin-2 (IL-2); T_{CM} can differentiate into T_{EM} and T_{eff}, and then secrete cytokine interferon-γ (IFN-γ) (13, 15, 16). T_{EM} can be maintained for 4 to 8 weeks and provides short-term protection (17). Therefore, long-term protection against TB depends on long-lived memory T cells such as T_{SCM} and T_{CM} cells (18, 19).

BCG mainly induces T_{EM} which may wane as the children grow up, failing to provide enough protection in adults (20). It is supposed that adjuvanted subunit vaccine had the potential to boost BCG-primed immunity. For example, ten weeks after BCG priming, BALB/c mice received ChAdOx1.85A or MVA85A vaccine twice every 4 weeks showed significantly decreased bacterial burdens in the lung when the mice were challenged with aerosolized *M. tuberculosis* 4 weeks after the last immunization ($P < 0.01$) (21). In addition, H4-IC31H vaccine boosting at 19th and 22nd week after BCG immunizations significantly reduced bacterial burdens in lung and spleen compared with BCG when the mice were challenged with *M. tuberculosis* 5 weeks after the final booster vaccination (22). Cynomolgus macaques were primed with BCG and boosted with Mtb72F/AS02A three times with 4 weeks apart induced protection superior to BCG alone when the monkeys were challenged with *M. tuberculosis* 4 weeks after the last immunization (23).

However, the above traditional short-interval subunit vaccine boosting programs usually induced T_{EM} and provided short-term protection (24, 25). It was reported that macaques vaccinated with BCG and boosted with M72 vaccine at 16 and 20 weeks did not enhance the protective efficacy of BCG when the macaques were challenged with a low dose (8–16 CFU) of *M. tuberculosis* Erdman *via* bronchoscope at 12 weeks after the final immunization (26). In a clinical trial, boosting healthy infants (aged 4-6 months) who received BCG previously with MAV85A induced modest cell-mediated immune responses without improving protective efficacy against TB (27). Besides limited antigen profile, the boosting progress was supposed to be a reason for the poor protection (28–31). Therefore, how to boost BCG-primed immune memory with subunit vaccine to induce long-lived memory T cells is urgently needed to be investigated.

It is well-known that antigen stimulation times and intervals might affect the development of T_{CM} (32, 33). As far as subunit vaccine immunization schedule was considered, our previous work found that compared with the traditional immunization program of 0-3-6 weeks, prolonging the intervals of immunization, the schedule of 0-4-12 weeks, could increase the number and function of long-lived memory T cells and improve the protective efficacy (25).

The immunization program of boosting BCG with subunit vaccine is complicated. We hypothesized that BCG antigens and "non-BCG" antigens (being absent from BCG), from RD of *M. tuberculosis*, might require different boosting programs to induce long-term immune memory. In this experiment, Mtb10.4-HspX (MH) protein was used as the representative of antigen from BCG and ESAT6-CFP10 (EC) protein was applied as the representative antigen from RD (34, 35). The optimized immunization schedules for these two types of antigens were investigated.

2 MATERIALS AND METHODS

2.1 Animals and Ethics Statement

Specific pathogen-free 6-8-week-old female C57BL/6J mice were purchased from Gansu University of Chinese Medicine (Lanzhou, China). Animals received free access to water and standard mouse chow throughout the study. All animal experiments were carried out under the guidelines of the Council on Animal Care and Use, and the protocols were reviewed and approved by the Institutional Animal Care and Use Committee of Lanzhou University.

2.2 Preparation of H37Ra, BCG and Antigen Proteins

M. tuberculosis H37Ra (ATCC25177) and BCG (Danish strain) bacteria were cultured in Sauton's medium. The fusion proteins MH and EC were prepared as previously reported (35, 36). In brief, MH fusion antigen without tag was purified by hydrophobic interaction chromatography using butyl-sepherose high performance (Butyl HP) column and ion-exchange chromatography using Q-sepharose high performance (Q HP) column (35). The fusion antigen EC without tag was purified by ion-exchange chromatography using Q HP column (36). Single mycobacterial proteins heat shock protein X (HspX), 10 kDa culture filtrate protein (CFP10) and 6 kDa early secreted antigen target (ESAT6) with His tag were purified by Ni-NTA His column (Novagen) (37, 38). The endotoxin concentrations of fusion protein were tested by Limulus amebocyte lysate (LAL) (Xiamen bioendo technology co., ltd, Xiamen, China). The purified protein derivative (PPD) of tuberculin was extracted from BCG, which contained a variety of proteins with different molecular weights.

2.3 Vaccine Immunization Program

2.3.1 Long Interval Immunization Schedule

The mice were primed subcutaneously with BCG (5×10^5 CFU in 100 μl per mouse). The purified protein MH or EC (10μg/dose) was emulsified in an adjuvant being composed of N, N′-dimethyl-N, N′-dioctadecyl ammonium bromide (DDA) (250μg/dose) (Anhui Super chemical technology Co., Ltd., China) and polyinosinic-polycytidylic acid (Poly I: C) (50μg/dose) (Kaiping Genuine Biochemical Pharmaceutical Co., Ltd., Guangdong, China) to construct subunit vaccine (39). To observe the long-term immune memory and protective efficacy, the BCG-primed mice were boosted with MH and EC twice or thrice subcutaneously with a long interval: MH/EC immunizations at 12-24 weeks groups; MH/EC immunizations

at 12-16-24 weeks groups. The number of mice per group was 30. The BCG-primed mice were revaccinated subcutaneously with BCG (5×10^5 CFU in 100 μl per mouse) at 24 weeks to be consistent with other boosters on immunoassays. BCG is a live attenuated tuberculosis vaccine and is usually boosted once when considering re-vaccination (40). PBS and BCG without boosting groups were used as control (**Figure 1A**). The immune memory was evaluated at 12 weeks and 28 weeks after the last immunization. The long-term protective efficacy was detected by H37Ra (5×10^6 CFU in 50 μl per mouse) intranasal challenge at 19 weeks after the last immunization.

2.3.2 Short Interval Immunization Schedule

Based on the results from the long interval immunization schedule, the protective efficacy of subunit vaccine boosting with a shortened interval was observed. The BCG-immunized mice were boosted with MH at 8-14 weeks or EC at 8-10-14 weeks subcutaneously (*SC*). The number of mice per group was 10. PBS and BCG without boosting groups were used as control (**Figure 1B**). The immune responses were detected by flow cytometry at 12 weeks after the last immunization. The long-term protective efficacy was detected by H37Ra intranasal challenge at 17 weeks after the last immunization.

2.4 Flow Cytometry and Intracellular Cytokine Staining (ICS)

2.4.1 IFN-γ and IL-2 Secretion Following Antigen Stimulation *In Vitro*

Lymphocytes were isolated from spleen or bone marrow of mice by using Mouse 1 × Lymphocyte Separation Medium (Dakewe Biotech Company Limited, China) and cultured in media containing RPMI-1640, 10% fetal bovine serum (FBS), 100 U/ml Penicillin-Streptomycin Solution. Then the lymphocytes were inoculated in 24 well plates at the number of 5×10^6 cells/well. The lymphocytes were stimulated with PPD (4 ug/ml) or mixed antigens PHEC including PPD (4 ug/ml), HspX (2ug/ml), ESAT6 (2ug/ml) and CFP10 (2ug/ml) at 37°C, 5% CO_2. To keep experiments consistent, the same stimulus (PHEC) was used to observe the immune responses induced by the different vaccines. After 4 hours of stimulation, the cells were incubated for 7-8h with BD GolgiPlug™ (containing brefeldin A) at 37°C, 5% CO_2. At last, the cells were collected and stained with anti-CD4-FITC (RM4-5, eBioscience) and anti-CD8-PerCP-Cy5.5 (53-6.7, eBioscience). Lymphocytes were permeabilized using the BD Cytofix/Cytoperm kit according to the manufacturer's instructions and stained with anti-IFN-γ-APC (XMG1.2, eBioscience) and anti-IL-2-PE (JES6-5H4, BD). Lymphocytes

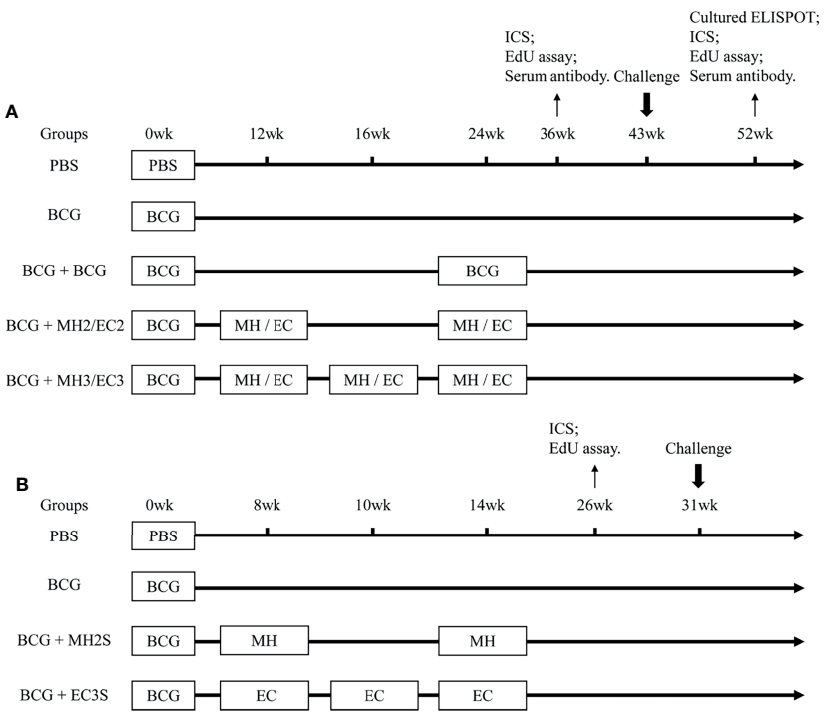

FIGURE 1 | Immunization Schedule. **(A)** Long interval immunization schedule: C57BL/6 mice were primed with BCG and boosted with MH/EC at 12-24 weeks and 12-16-24 weeks respectively. Then, the function of memory T cells was evaluated at 12 weeks and 28 weeks after the last immunization. At 19 weeks after the last immunization, the mice were challenged intranasally with H37Ra, and lung tissues were collected for CFU counting 3 weeks after the challenge. **(B)** Short interval immunization schedule: C57BL/6 mice were primed with BCG and immunized with MH at 8-14 weeks or EC at 8-10-14 weeks respectively. The immune response of memory T cells was evaluated at 12 weeks after the last immunization. At 17 weeks after the last immunization, mice were challenged intranasally with H37Ra, and lung tissues were collected for CFU counting 3 weeks after the challenge. ICS, intracellular cytokine staining.

from individual mice were analyzed on a NovoCyte flow cytometer (ACEA Biosciences). Flow cytometry gating strategy was shown in **Supplementary Figure 1A**. The spleen or bone marrow lymphocytes were first gated by the parameters SSC-H and FSC-H (lymphocytes), and then single cells were gated by the parameters FSC-H and FSC-A (single cells). Finally, $CD4^+$ IFN-γ^+ T cells, $CD4^+$ IL-2^+ T cells, $CD8^+$ IFN-γ^+ T cells, $CD8^+$ IL-2^+ T cells or $CD8^+$ IFN-γ^+ IL-2^+ T cells were analyzed by flow cytometric. The analyzed cytokine-producing T-cells were either represented as percentages among total number of spleen lymphocytes or described as actual counts of cytokine-producing cells as bar graphs.

2.4.2 IFN-γ Secretion Following Re-Stimulation With Antigens *In Vivo* and *In Vitro*

Our previous experiment showed that at 25 weeks following subunit vaccine immunization, once antigen stimulation could not induce cytokines production (41), which suggests that T_{EM} cells wane at that time (42). Therefore, at 28 weeks after vaccination only long-lived memory T cells (T_{SCM} and T_{CM}) exist. Since the percentage of antigen-specific long-lived memory T cells was too few to be detected directly by the surface markers of central memory T cells (CCR7, CD62L, CD44, and CD127) (17). Upon antigen stimulation antigen-specific T_{SCM} and T_{CM} cells proliferate and differentiate into T_{EM} and T_{eff} cells, and then produce cytokine IFN-γ (32, 43, 44). Based on the principle, in our previous studies we detected the role long-lived memory T cells through analyzing IFN-γ production following stimulation with same antigen twice every 9 days (25, 41).

At 28 weeks after last immunization, the vaccine-immunized mice were injected subcutaneously with mixed of antigens of PPD (4 ug/mouse), HspX, EAST6, CFP10 (2 ug/mouse of each protein) *in vivo*. The long-lived memory T cells were supposed to be activated and differentiated into T_{EM} or T_{eff} cells (32). Subsequently, the spleen lymphocytes were separated at 3 days later and stimulated with the same mixed antigens of PPD (4 ug/ml), HspX, EAST6, CFP10 (2 ug/ml of each protein) for 12 hours *in vitro*, during that time T_{EM} cells could differentiate into T_{eff} cells and produce IFN-γ. The intracellular cytokine staining was analyzed by flow cytometry to indirectly reflect the function of long-lived memory T cells (25, 45).

2.5 Cultured IFN-γ ELISPOT Assay

A cultured IFN-γ enzyme-linked immunospot (ELISPOT) assay was also used to evaluate the immune responses of long-lived memory T cells (43, 44). Twenty-eight weeks after the last immunization, spleen lymphocytes were suspended in RPMI-1640 medium supplemented with 10% fetal bovine serum, 100U/ml Penicillin-Streptomycin Solution, 2 mM L-glutamine, 25 mM HEPES buffer, 1% sodium pyruvate, and 50 mM 2-mercaptoethanol. Spleen lymphocytes (5×10^6 cells/ml/well) were stimulated with mixed antigens of PHEC containing PPD (4 μg/ml) and HspX, ESAT-6, CFP10 (2 μg/ml of each protein). Spleen lymphocytes were incubated at 37°C and 5% CO_2 with half culture media containing recombinant human IL-2 (rhIL-2) 100 U/ml, which were replaced on days 3 and 7, allowing expansion of antigen-specific T cells. On day 9, the cultured cells were harvested and antigen-presenting cells (APCs) were added. Then, cultured cells were plated (1×10^6 cells/well) and re-stimulated with PHEC for an additional 20 hours in the presence of APCs in anti-IFN-γ coated ELISPOT plates (Dakewe Biotech Company Limited, China). The spot-forming cells (SFCs) were counted by an ELISPOT reader (Dakewe Biotech Company Limited, China).

2.6 EdU Proliferation Assay for Long-Lived Memory T Cells

5-Ethynyl-2'-deoxyuridine (EdU) is to be infiltrated into the deoxyribonucleic acid (DNA) of T cells as the cells proliferate, and it can be detected following proliferation and division of memory T cells. Spleen lymphocytes (5×10^6 cells/well) were stimulated with the mixed antigens PHEC for 7 days in 24-well plates. Three days after antigen stimulation, when T_{SCM} and T_{CM} were to be activated into T_{EM}, EdU (Click-iT™ EdU Flow Cytometry Assay Kit, Invitrogen™, OR, USA) was added at a final concentration of 30 μM and the lymphocytes were continued to be cultured for 4 days. On day 7, cells were harvested, fixed, permeabilized, and incubated with Click-iT reaction buffer according to the manufacturer's instructions of the Click-iT™ EdU Flow Cytometry Assay Kit. Subsequently, cells were stained with anti-CD4-APC (RM4-5, eBioscience). Finally, a flow cytometry assay was performed to evaluate the proliferating capability of $CD4^+$ T cells. Spleen lymphocytes were first gated by the parameters SSC-H and FSC-H (lymphocytes), and then single cells were gated by the parameters FSC-H and FSC-A (single cells). Flow cytometry gating strategy was shown in **Supplementary Figure 1B**.

2.7 Detection of Antigen-Specific Antibodies in Mouse Sera by ELISA

At 12 and 28 weeks after the last immunization, antigen-specific immunoglobulin IgG, IgG1, and IgG2c in sera were detected by enzyme-linked immunosorbent assay (ELISA). Firstly, 0.5 μg/well of PPD, HspX, and ESAT6 were separately added into the plate at 4°C overnight. Secondly, the plates were blocked with 5% skimmed milk powder, then incubated with the double-diluted serum at 37°C for an hour. And then the plates were washed and added 100 μL of goat anti-mouse IgG (Solarbio, Beijing, China) and rabbit anti-mouse IgG1 and IgG2c (Rockland Immunochemicals Inc., Montgomery, PA, USA) The 3,3′,5,5′-tetramethylbenzidine (TMB) substrate was added at 200 μL/well and incubated at room temperature for 5 min. The reaction was then stopped by diluted sulfuric acid (1 mol/L) at 50 μL/well. The color was quantified at 450 nm. The serum in the PBS group was used as the negative control. The antibody titer was evaluated as a reciprocal of each endpoint dilution.

2.8 Quantification of CFU of *Mycobacterium tuberculosis* H37Ra in Lung Tissue

The mice received intraperitoneal anesthesia with 1% sodium pentobarbital at a concentration of 50 mg/kg. Mice from each group were challenged through intranasal route (*i.n.*) with 5 ×

10^6 CFU of H37Ra. Lungs of infected animals were harvested three weeks after the H37Ra intranasal challenge. Organs were ground and resuspended in PBS. The dilutions were plated in Middlebrook 7H10 plates (BD) containing oleic acid/albumin/dextrose/catalase (OADC). The colony-forming units (CFU) were counted.

2.9 Statistical Analysis

The experimental data were expressed as Mean ± SD. The data were evaluated by GraphPad Prism 8.0 software with unpaired two-tailed Student's *t*-tests to compare two groups and one-way analysis of variance (ANOVA) followed by a Tukey *post hoc* test to compare multiple groups. Among them, $P < 0.05$ was considered statistically significant.

3 RESULTS

3.1 Longitudinal Changes of Immune Responses Induced by BCG Vaccination

To observe the longitudinal changes of immune responses induced by BCG, lymphocytes in spleen and bone marrow were stimulated with PPD antigen for 12 hours *in vitro* at different times after BCG immunization, and flow cytometry was used to quantify IFN-γ producing $CD4^+$ T cells. In spleen lymphocytes, the frequency of IFN-γ producing $CD4^+$ T cells peaked at 4 weeks, slightly decreased at 9 weeks, and the immune responses reduced to a low level at 12 weeks (**Supplementary Figures 2A, C**). In bone marrow, the frequency of IFN-γ producing $CD4^+$ T cells increased at 4 weeks, reached the highest level at 9 weeks and decreased at 12 weeks (**Supplementary Figures 2B, D**). It indicated that the immune response induced by effector memory T cells decreased at the 12th week after BCG vaccination, which should be an optimal time for boosting (46–49).

3.2 Boosting BCG With Subunit Vaccines With Suitable Schedules Induced Long-Lived Memory T Cells

3.2.1 Cytokines Production by Memory T Cells at 12 Weeks After Last Vaccine Immunization

The fusion proteins MH and EC and single proteins ESAT6, CFP-10 and HspX were prepared (**Supplementary Figure 3**). At the concentration of MH and EC (1mg/ml of each protein), the endotoxin levels were 0.009031EU/μg and 0.00985 EU/μg, respectively (**Supplementary Table 1**). According to above results, the mice were boosted with the subunit vaccine at 12 weeks after BCG immunization. Fusion protein EC consisting of RD antigen ("non-BCG" antigen) and MH consisting of BCG antigen were administered twice at 12-24 weeks and thrice at 12-16-24 weeks respectively to investigate which immunization programs could induce long-term immune memory to prolong BCG-primed immune responses (**Figure 1A**).

To assess the frequency of vaccine-induced antigen-specific memory T cells at 12 weeks after last immunization, cytokines production in the splenocytes following specific antigens PHEC stimulation for 12 hours *in vitro* was analyzed by flow cytometry. The results showed that compared with MH boosting at 12-16-24 weeks group (0.82 ± 0.46) and EC immunizations at 12-24 weeks group (0.61 ± 0.21), MH boosting at 12-24 weeks group produced a higher frequency of IFN-γ producing $CD4^+$ T cells (1.97 ± 0.70, $P < 0.05$; **Figures 2A, B**). Compared with PBS group (0.23 ± 0.12) and BCG revaccination group (0.36 ± 0.15), MH boosting at 12-24 weeks group (0.88 ± 0.32) and EC immunizations at 12-16-24 weeks group (1.33 ± 0.56) produced a higher frequency of IFN-γ producing $CD8^+$ T cells ($P < 0.05$; **Figures 2A, B**). Compared with PBS (1.89 ± 0.95) group and BCG group (2.67 ± 0.7), EC immunizations at 12-16-24 weeks group (5.84 ± 1.41) increased frequency of IL-2 producing $CD4^+$ T cells (**Figures 2A, B**). Furthermore, compared with MH boosting at 12-16-24 weeks group, the EC immunizations at 12-16-24 weeks group had a higher number of IFN-γ/IL-2 producing $CD4^+$ and $CD8^+$ T cells ($P < 0.05$; **Figure 2C**). Moreover, compared with MH boosting twice or EC immunizations thrice groups, MH boosting at 12-24 weeks and EC immunizations at 12-16-24 weeks improved the proportion of IFN-γ^+ and IL-2^+ double-positive $CD8^+$ T cells (**Supplementary Figure 4**). The results indicated that MH boosting at 12-24 weeks and EC immunizations at 12-16-24 weeks induced strong memory T cell-mediated immune response compared with the EC immunizations at 12-24 weeks and MH boosting at 12-16-24 weeks.

3.2.2 Antigen-Specific Cytokines Production by Long-Lived Memory T Cells at 28 Weeks After the Last Vaccine Immunization

At 28 weeks after vaccine immunization, the antigen-specific effector memory T cells would fade away, so the vaccine-induced long-lived memory T cells were analyzed (41). The immune responses following antigen stimulation to monitor the number and function of vaccine-induced long-lived memory T cells indirectly by two methods as follow (25, 41).

First, the cultured ELISPOT was used to investigate the function and number of antigen-specific long-lived memory T cells (43). The results showed that compared with the group of EC immunizations at 12-24 weeks (86.2 ± 33.7 SFCs/5 × 10^6 cells), MH boosting at 12-24 weeks group induced an increasing number of antigen-specific IFN-γ producing T cells (166 ± 22.4 SFCs/5 × 10^6 cells, $P < 0.05$; **Figures 5A, B**). In addition, compared with the group of MH boosting at 12-16-24 weeks (73 ± 52 SFCs/5 × 10^6 cells), the group of EC immunizations at 12-16-24 weeks (162.25 ± 18.3 SFCs/5 × 10^6 cells) significantly elevated numbers of antigen-specific IFN-γ secreting T cells ($P < 0.05$; **Figures 3A, B**). The results indicated that both MH boosting at 12-24 weeks and EC immunizations at 12-16-24 weeks might induce a great number of long-lived memory T cells.

Second, according to the principle of cultured ELISPOT, flow cytometry assay was used to detect the immune responses of long-lived memory T cells under repeated antigen stimulation (25, 43). The immunized mice were stimulated subcutaneously with PHEC antigens *in vivo* 3 days prior to immunoassay. It was supposed that the long-lived memory T cells activated and

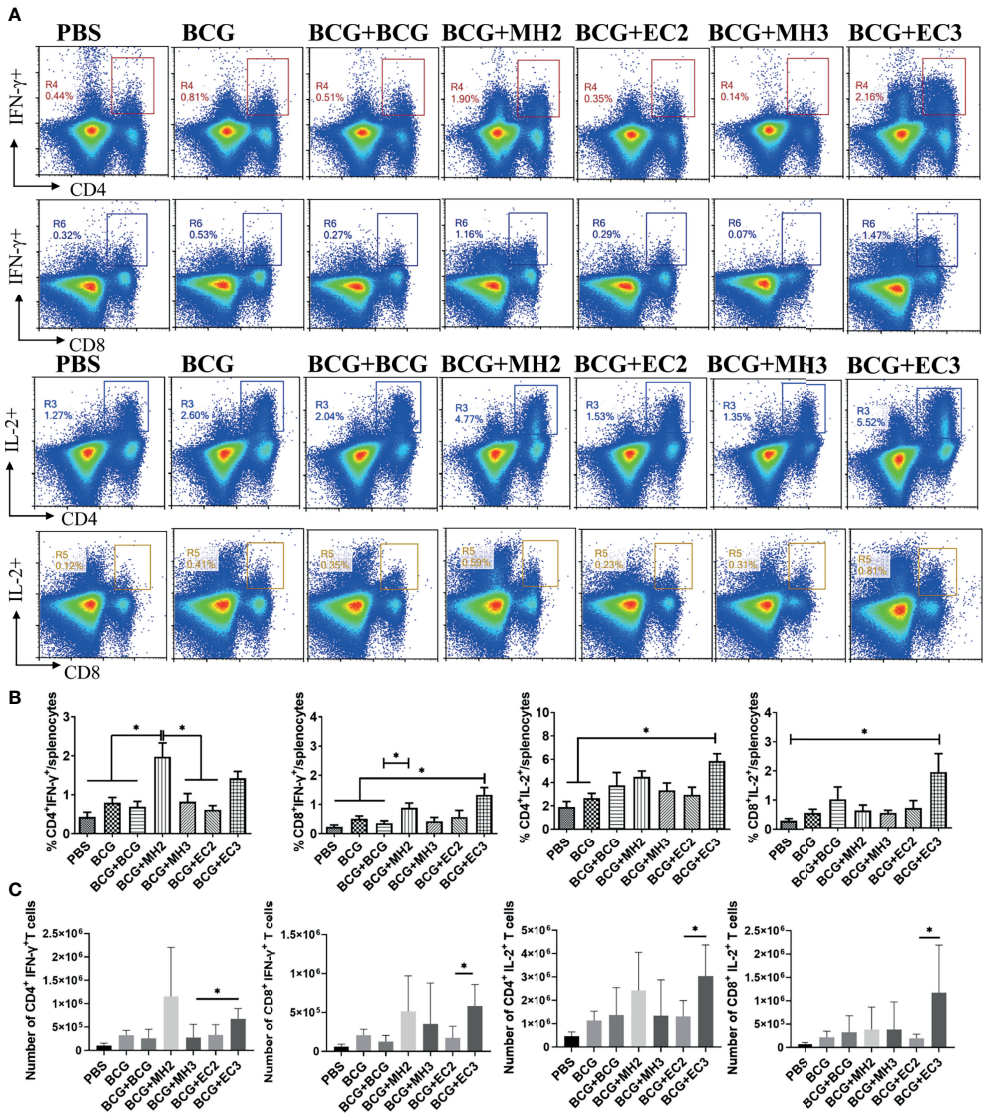

FIGURE 2 | The ratio and number of IFN-γ and IL-2 producing T cells following antigen stimulation. At 12 weeks after the last immunization, the splenic lymphocytes were separated and stimulated with mixed antigens of PPD, ESAT-6, CFP10 and HspX (PHEC) *in vitro* for 12 hours. The intracellular cytokines staining was analyzed using flow cytometry. **(A)** Flow cytometric analysis of IFN-γ and IL-2 producing $CD4^+$ T cells and $CD8^+$ T cells. **(B)** Statistical analysis of the proportion of IFN-γ and IL-2 producing $CD4^+$ T cells and $CD8^+$ T cells. **(C)** Statistical analysis of the number of IFN-γ and IL-2 producing $CD4^+$ T cells and $CD8^+$ T cells among total spleen lymphocytes from each immunized group. Results are presented as means ± SD, $n = 4 \sim 5$. The data were evaluated with unpaired two-tailed Student's *t*-tests to compare two groups and one-way analysis of variance (ANOVA) followed by a Tukey *post hoc* test to compare multiple groups. *$P < 0.05$.

developed into T_{EM} or T_{eff}. Three days later, spleen lymphocytes were isolated and stimulated with PHEC antigens for 12 hours *in vitro*, during that time the T_{EM} developed into T_{eff} and secreted cytokine IFN-γ. Then the secretion of cytokines IFN-γ was detected by intracellular cytokine staining. This method indirectly reflected the functions of vaccine-induced long-lived memory T cells (11, 25). The results showed that compared with PBS group (1.29 ± 0.17), BCG group (1.91 ± 0.53), and the groups of EC immunizations twice at 12-24 weeks (1.59 ± 0.34) and MH boosting thrice at 12-16-24 weeks (1.00 ± 0.38), MH boosting twice at 12-24 weeks group (3.58 ± 0.37) produced high frequencies of IFN-γ producing $CD4^+$ T cells ($P < 0.05$; **Figures 3C, D**). Compared with the group of MH boosting thrice at 12-16-24 weeks (1.00 ± 0.38), EC immunizations thrice at 12-16-24 weeks group produced higher frequencies of IFN-γ producing $CD4^+$ T cells (3.27 ± 1.21, $P < 0.05$; **Figures 3C, D**). The MH boosting at 12-24 weeks group had a higher number of IFN-γ producing $CD4^+$ T cells compared with EC immunizations at 12-24 weeks group ($P < 0.05$; **Figure 3E**). The EC immunizations at 12-16-24 weeks group had more IFN-γ producing $CD4^+$ T cells compared with EC immunizations at 12-24 weeks group ($P < 0.05$; **Figure 3E**). The above results

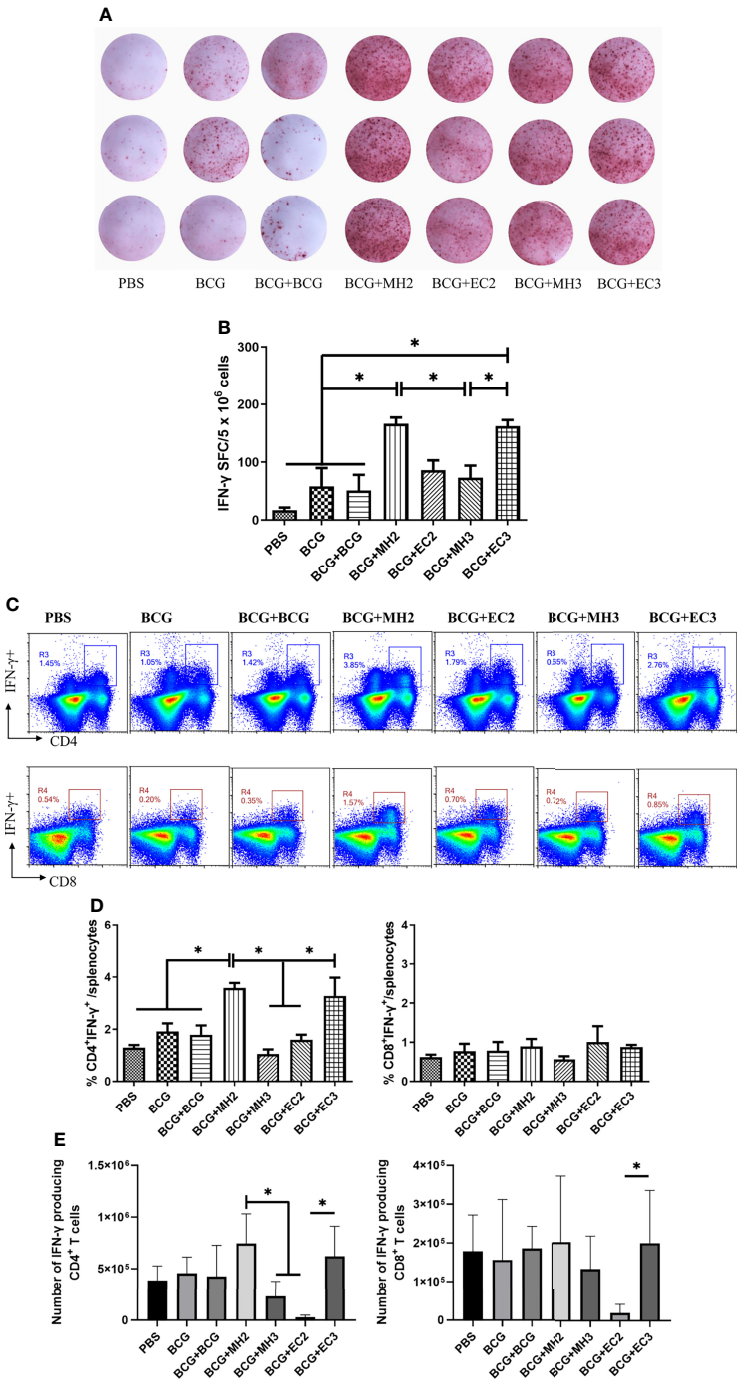

FIGURE 3 | IFN-γ production by long-lived memory T cells. At 28 weeks after the last immunization, spleen lymphocytes were cultured with or without mixed antigens of PPD, HspX, ESAT-6, and CFP10 for 9 days and then the cells were harvested and restimulated with the same antigens for 20 hours in the presence of APCs in anti-IFN-γ coated ELISPOT plates. At 28 weeks after the last immunization, mice were injected subcutaneously with mixed antigens of PPD, ESAT-6, CFP10 and HspX (PHEC) for 3 days. Then, mice were euthanized and spleen lymphocytes were isolated and stimulated with mixed antigens PHEC for 12 hours *in vitro* and analyzed by Flow cytometry. **(A)** Representative images of IFN-γ ELISPOT wells from long-term cultured IFN-γ ELISPOT assays. **(B)** Statistical analysis of the cultured IFN-γ ELISPOT assay. Results are presented as means ± SD, $n = 4$. $^*P < 0.05$. **(C)** Flow cytometric analysis of IFN-γ producing $CD4^+$ and $CD8^+$ T cells. **(D)** Statistical analysis of the proportion of IFN-γ producing $CD4^+$ T cells and $CD8^+$ T cells. **(E)** Statistical analysis of the actual number of IFN-γ producing T cells among total spleen lymphocytes from each immunized group. Results are presented as means ± SD, $n = 4 \sim 5$. The data were evaluated with unpaired two-tailed Student's *t*-tests to compare two groups and one-way analysis of variance (ANOVA) followed by a Tukey *post hoc* test to compare multiple groups. $^*P < 0.05$.

indicated that MH boosting twice at 12-24 weeks and EC immunizations thrice at 12-16-24 weeks increased the immune responses of long-lived memory T cells.

3.2.3 The Proliferation Capability of Long-Lived Memory T Cells

To verify the proliferative capacity of T cells induced by different boosting programs, the proliferation capacity of long-lived memory T cells was analyzed by the EdU method at 12 weeks and 28 weeks after the last immunization, respectively. At 12 weeks after the last immunization, compared with PBS group (0.95 ± 0.46), BCG group (1.28 ± 0.46), and BCG revaccination group (1.17 ± 0.45), the proportion of EdU^+ cells in the MH boosting twice at 12-24 weeks group (2.18 ± 0.32) increased significantly ($P < 0.05$). The proportion of EdU^+ cells in MH boosting twice at 12-24 weeks group (2.18 ± 0.32) and EC immunizations thrice at 12-16-24 weeks group (2.00 ± 0.36) were significantly higher than MH boosting thrice at 12-16-24 weeks group (1.42 ± 0.63) ($P < 0.05$; **Figures 4A, C**). At 28 weeks after the last immunization, compared with the PBS group (0.67 ± 0.31), BCG group (0.98 ± 0.40) and BCG revaccination group (0.71 ± 0.57), the proportion of EdU^+ cells in MH boosting twice at 12-24 weeks group (2.83 ± 0.57) and EC immunizations thrice at 12-16-24 weeks group (3.33 ± 0.39) increased significantly ($P < 0.05$; **Figures 4B, D**). Compared with the MH boosting thrice at 12-16-24 weeks group (1.20 ± 0.78), and EC immunizations twice at 12-24 weeks group (1.89 ± 0.82), the proportion of EdU^+ cells in MH boosting twice at 12-24 weeks group (2.83 ± 0.57) increased significantly ($P < 0.05$; **Figures 4B, D**). Taken together, both MH boosting twice at 12-24 weeks group and EC immunizations thrice at 12-16-24 weeks group enhanced the proliferative capacity of $CD4^+$ T cells.

3.3 BCG-Prime and MH/EC-Boost Induced Durable Humoral Immune Response

At 12 weeks and 28 weeks after the last immunization, the IgG, IgG1 and IgG2c against HspX, ESAT6 and PPD in serum were measured by ELISA. The results demonstrated that compared with BCG and BCG revaccination groups, MH/EC-boosting groups produced long-durable higher levels of antibody titers

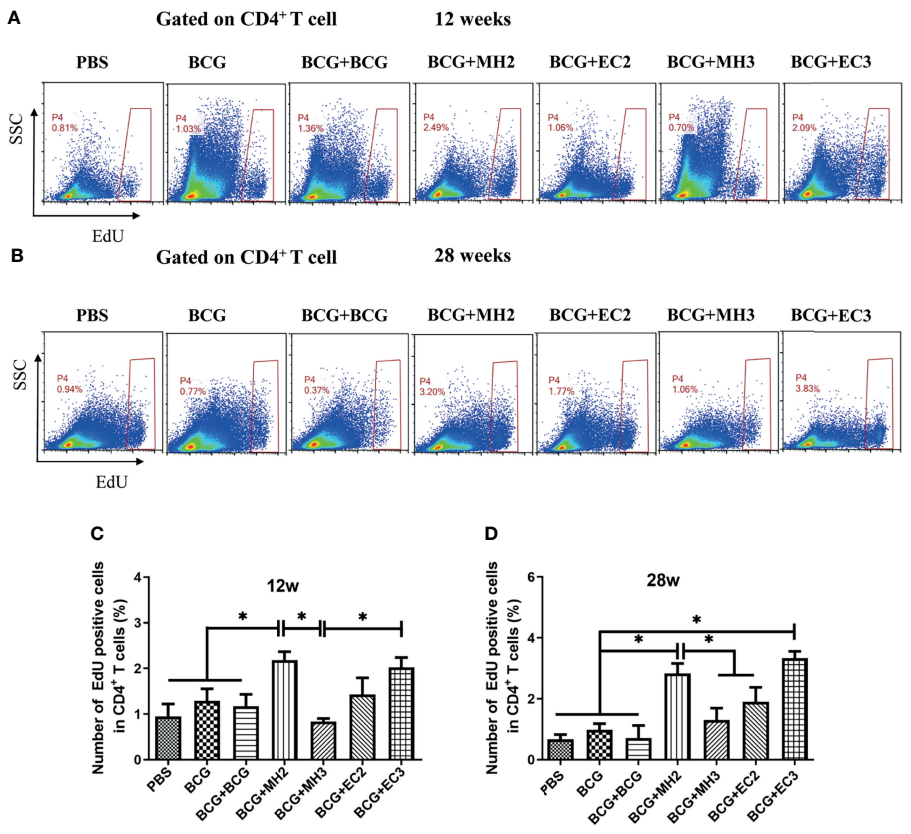

FIGURE 4 | $CD4^+$ T cell proliferation detected by EdU assay. At 12 weeks and 28 weeks after the last immunization, splenic lymphocytes (5×10^6 cells/well) were stimulated with mixture antigens of PPD, ESAT-6, CFP10 and HspX *in vitro* for 7 days. Three days after antigen stimulation, EdU was added at a final concentration of 30 μM, continued to culture for 4 days and was determined using flow cytometry. **(A, B)** Representative experiments of flow cytometric analysis of $CD4^+$ T cells proliferation. **(C)** Statistical analysis of $CD4^+$ T cell proliferation at 12 weeks after the last immunization. **(D)** Statistical analysis of $CD4^+$ T cell proliferation at 28 weeks after the last immunization. Results are presented as means ± SD, $n = 4 \sim 5$. The data were evaluated with unpaired two-tailed Student's *t*-tests to compare two groups and one-way analysis of variance (ANOVA) followed by a Tukey *post hoc* test to compare multiple groups. $^*P < 0.05$.

($P < 0.05$; **Table 1**). Furthermore, MH/EC boosting at 12-16-24 weeks group produced significantly higher levels of HspX/ESAT6-specific IgG, IgG1, and IgG2c than MH/EC boosting at 12-24 weeks group ($P < 0.05$; **Table 1**). The results indicated that MH/EC vaccine boosting induced durable strong serum antibodies.

3.4 The Protective Efficacy of BCG-Prime and MH/EC Boosting at Different Schedules

Furthermore, we observed the long-term protective effect induced by MH boosting twice at 12-24 weeks and EC immunizations at 12-16-24 weeks. The attenuated *M. tuberculosis* H37Ra, which expresses all single proteins of Mtb10.4/HspX and ESAT-6/CFP-10 (50), was used to challenge the immunized mice. ESAT-6 expression in H37Ra was further confirmed by western blotting (**Supplementary Figure 5**). Considering H37Ra was an attenuated strain and could be cleared in mice around 4 weeks, the mice were challenged with high doses of H37Ra and determined the bacteria load in lung tissue at 3 weeks after the challenge. The immunized mice were challenged intranasally with avirulent *M. tuberculosis* H37Ra at 19 weeks after the last immunization. The results demonstrated that BCG group, MH and EC immunizations groups induced a significant reduction of mycobacterial loads in the lungs compared with PBS controls ($P < 0.01$). The groups of MH boosting at 12-24 weeks and EC immunizations at 12-16-24 weeks reduced bacteria load in lung tissues, declining approximately 0.1 $\log_{10}$ CFU compared with the BCG control group ($P < 0.05$) (**Figure 5A**). It showed that the schemes of MH boosting twice at 12-24 weeks and EC immunizations thrice at 12-16-24 weeks promoted long-lived memory T cells and improved protective efficacy.

Based on the results from the long interval immunizing schedule, shorten interval schedules were designed, and the protective efficacy and immune responses were analyzed. Following BCG priming, mice were immunized with MH/DP twice at 8-14 weeks and the EC/DP thrice at 8-10-14 weeks (**Figure 1B**). At 12 weeks after the last vaccine immunization, the immune response and T cell proliferation were detected by flow cytometry. At 17 weeks after the last vaccine immunization, the protective efficacy was detected by H37Ra challenge. The results showed that MH/DP boosting twice at 8-14 weeks and the EC/DP immunizing thrice at 8-10-14 weeks did not improve T cell proliferative capacity and BCG-primed immune protection, although an increased IFN-γ production following antigen stimulation was observed (**Figure 5B**; **Supplementary Figure 6**). The results suggest that subunit vaccines need suitable boosting schedules to induce long-term immune memory.

4 DISCUSSION

In this study, we investigated the long-term immune memory induced by BCG priming and MH/EC vaccine boosting with different regimens. We found that MH boosting at 12-24 weeks and EC immunizations at 12-16-24 weeks enhanced the long-lived memory T cell-mediated immunity and improved protection efficiency of BCG, while MH boosting at 8-14 weeks and EC immunizations at 8-10-14 weeks reduced the long-term protective efficacy compared with BCG without boosting.

BCG vaccination mainly activates effector memory T cells, which cannot be maintained for a long time. In this experiment, T cell immune responses following BCG immunization declined at 9-12 weeks, which were consistent with the results in our laboratory's previous work (25, 51). Besides, kinetics of BCG induced immune responses in the spleen of BALB/c mice at weeks 3, 6, and 10 found that T cell activation peaked at week 3 and gradually declined thereafter (52). In the C57BL/6 mouse model, the immune response of T lymphocytes collected for retro-orbital blood was peaked at 3 weeks and weakened at 5 weeks following BCG vaccination (53). Furthermore, in BCG-vaccinated mice, anti-mycobacterial T cell responses persisted for long period, peaked at 12-32 weeks, and waned gradually thereafter (54, 55). These studies suggest that the mouse strain, BCG vaccine strain,

TABLE 1 | The production of antigen-specific IgG, IgG1, and IgG2c.

	Groups	12weeks				28weeks			
		IgG	IgG1	IgG2c	IgG2c/IgG1	IgG	IgG1	IgG2c	IgG2c/IgG1
Anti-HspX	**BCG**	2.31 ± 0.19	2.33 ± 1.03	1.34 ± 0.41	0.57 ± 0.17	2.19 ± 0.12	0.74 ± 0.53	0.62 ± 0.3	0.92 ± 0.37
	BCG+BCG	2.28 ± 0.11	2.50 ± 0.17	1.27 ± 0.26	0.50 ± 0.1	1.84 ± 0.49	0.87 ± 0.59	0.80 ± 0.29	0.84 ± 0.45
	BCG+MH2	2.93 ± 0.27*	4.39 ± 0.67*	3.48 ± 0.31*	0.79 ± 0.07	2.91 ± 0.46*	3.12 ± 0.81*	2.83 ± 0.3*	0.90 ± 0.1
	BCG+MH3	4.00 ± 0.17*#	5.74 ± 0.7*#	4.84 ± 0.81*#	0.84 ± 0.14	3.78 ± 0.42*#	3.93 ± 0.44*#	3.6 ± 0.39*#	0.93 ± 0.1
Anti-PPD	**BCG**	3.00 ± 0.25	2.20 ± 0.13	2.67 ± 0.12	1.21 ± 0.05	2.28 ± 0.41	1.52 ± 0.1	1.66 ± 0.16	1.09 ± 0.1
	BCG+BCG	2.80 ± 0.51	2.30 ± 0.17	2.73 ± 0.1	1.18 ± 0.04	2.26 ± 0.32	1.47 ± 0.34	1.89 ± 0.35	1.28 ± 0.24
	BCG+MH2	3.20 ± 0.11*	3.71 ± 0.49*	3.96 ± 0.32*	1.10 ± 0.06	3.01 ± 0.4*	2.01 ± 0.32*	2.98 ± 0.37*	1.48 ± 0.18
	BCG+MH3	4.27 ± 0.37*#	5.40 ± 0.31*#	5.71 ± 0.54*#	1.07 ± 0.1	3.92 ± 0.9*#	5.13 ± 1.65*#	3.76 ± 0.44*#	0.73 ± 0.08
Anti-ESAT6	**BCG**	2.17 ± 0.32	1.96 ± 0.41	2.00 ± 0.31	0.84 ± 0.08	2.15 ± 0.14	1.00 ± 0.56	2.10 ± 0.37	2.18 ± 0.27
	BCG+BCG	2.19 ± 0.11	2.31 ± 0.18	1.94 ± 0.2	1.02 ± 0.16	2.05 ± 0.28	1.00 ± 0.37	1.98 ± 0.05	1.98 ± 0.05
	BCG+EC2	2.57 ± 0.19*	4.93 ± 0.78*	2.14 ± 0.75	0.43 ± 0.15	2.61 ± 0.06*	2.15 ± 0.63*	2.92 ± 0.53*	1.34 ± 0.28
	BCG+EC3	3.11 ± 0.35*$	5.63 ± 0.69*	2.57 ± 0.48	0.45 ± 0.08	2.83 ± 0.15*$	2.65 ± 0.51*	3.30 ± 0.11*	1.24 ± 0.04

*At 12 weeks and 28 weeks after the last immunization, the IgG, IgG1 and IgG2c against HspX, PPD and ESAT6 in serum were measured by ELISA. Data are expressed as means ± standard deviation (SD) (n = 4). Antibody titers are presented as the means of log10 antibody titers ± SD. The statistical significance of data was determined using the unpaired two-tailed Student's t-test. *P < 0.05 vs. BCG plus BCG + BCG; #P < 0.05 vs. BCG+MH2; and $P < 0.05 vs. BCG+EC2.*

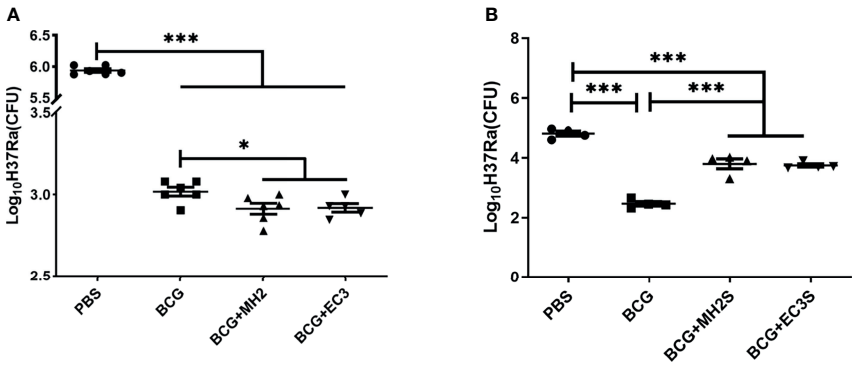

FIGURE 5 | Bacterial burden at necropsy. **(A)** In the long interval immunization schedules, at 19 weeks after the last immunization, the immunized mice were challenged intranasally with *M. tuberculosis* H37Ra. **(B)** In the short interval immunization schedules, at 17 weeks after the last immunization, the immunized mice were challenged intranasally with *M. tuberculosis* H37Ra. At 3 weeks after challenge, mice were euthanized and the bacterial burden was measured in the lungs. Data were presented as $\log_{10}$ CFU ± SD from groups of 5-6 mice. The data were evaluated with unpaired two-tailed Student's *t*-tests to compare two groups and one-way analysis of variance (ANOVA) followed by a Tukey *post hoc* test to compare multiple groups. $^{*}P < 0.05$, $^{***}P < 0.001$.

and antigen(s) used for *in vitro* stimulations might lead to the differences of T cell-mediated immune responses.

Boosting BCG-primed immune responses with subunit vaccines is expected to induce long-lived memory T cells. T_{SCM} and T_{CM} provide long-term immune protection against *M. tuberculosis* infection (8, 56–58). Treating BCG-immunized mice with Suplatast tosylate and D4476, inhibitor of T help 2 and regulatory T cells, favored the development of T_{CM} over T_{EM}. Adoptively transfer of T_{CM} cells generated by treatment with immunomodulators during BCG vaccination conferred protective efficiency against *M. tuberculosis* infection (59). To improve the access of BCG antigens to MHC I pathway, a urease C-deficient recombinant BCG ΔureC::hly (rBCG ΔureC::hly), which secreted pore-forming listeriolysin (Hly) was constructed (60, 61). rBCG ΔureC::hly immunization produced greater expansion of T_{CM} than BCG (62). Transfer of antigen-specific T_{CM} distinctly provided protection against *M. tuberculosis* infection (62). The Ag85B-ESAT-6/CAF01 subunit vaccines could promote long-term protective immune responses characterized by high levels of multifunctional T cells with proliferative potential (63). Mice immunized with ID93/GLA-SE exhibited a significant reduction of *M. tuberculosis* and elicited sustained antigen-specific multifunctional IFN-γ, tumor necrosis factor alpha (TNF-α), and IL-2 co-producing $CD4^+$ T cells (64). A novel Sendai virus vectored TB vaccine (SeV85AB) induced antigen-specific T_{CM} cells and enhanced BCG-primed immune protection (65).

It is well-known that T_{eff} is apoptotic at 1-2 weeks after immunization or infection (66), T_{EM} cells wane around 90 days (42), T_{CM} and T_{SCM} cells live for a long time after formation (67, 68). In our previous study we found that at 25 weeks after the last immunization, the immune responses of T_{EM} were undetectable, but the immune response of long-lived memory T cells, including T_{CM} and T_{SCM}, could be detected by restimulation with antigen (41). At 12 weeks after vaccination T cell subsets in spleen could include T_{EM}, T_{CM} and T_{SCM} cells, but only T_{CM} and T_{SCM} cells could maintain up to 28 weeks. In this study, the vaccine-induced immune responses at 12 and 28 weeks after MH/EC boosting were detected. At 12 weeks after last immunization, EC immunizations thrice at 12-16-24 weeks group produced high numbers of IL-2 producing $CD4^+$ and $CD8^+$ T cells. MH boosting twice at 12-24 weeks produced more IFN-γ producing $CD4^+$ T cells than MH boosting thrice at 12-16-24 weeks and EC immunizations twice at 12-24 weeks. As same as the results of cytokines production, the results of memory T cells proliferation showed that both programs of MH boosting at 12-24 weeks and EC immunizations at 12-16-24 weeks improved the proliferation of long-lived memory T cells. At 28 weeks after last immunization, proliferation assay, cultured ELISPOT assay, detection of IFN-γ production following antigen restimulation *in vivo* and *in vitro* were applied for the detection of vaccine-induced long-lived memory T cells. The results showed that both MH boosting at 12-24 weeks and EC immunizations at 12-16-24 weeks enhanced the number and function of long-lived memory T cells. In the protection efficiency against *M. tuberculosis* H37Ra, these two regiments of MH boosting at 12-24 weeks and EC immunizations at 12-16-24 weeks prolonged BCG-primed protective efficacy, consisting with the assumption that vaccine-generated memory T cells were essential for preventing or limiting *M. tuberculosis* infections (69).

The times of antigen stimulations affect the development of memory T cells (70–73). It was reported that the expansion and survival of memory T cell populations were impaired if antigens were stimulated more times (33, 74). The decreasing-potential model for generating effector and memory T cell heterogeneity suggests that repetitive stimulation with antigen and other signals drive greater effector cell proliferation and terminal differentiation (32). Our experiments found that following BCG priming, the RD antigen EC immunizations thrice at 12-16-24 weeks induced long-term immune protection. Claus Aagaard et al. reported that the *M. tuberculosis*-specific (or "non-BCG") vaccine ESX-1-associated antigens (H74) boosting

BCG-primed mice three times at 2-week intervals added significantly to the BCG-induced protection (75). BCG expresses the antigen of Mtb10.4 and HspX. In the program of MH boosting twice, Mtb10.4 and HspX actually encountered three times, which was as same times as that of ESAT6 and CFP10 encountered in the EC immunizations thrice program. BCG-prime and MH boosting twice induced more long-lived memory T cells than MH boosting thrice. In a clinical trial in which BCG-vaccinated participants received varying doses of ID93 + GLA-SE at 0-28-112 days, the vaccination-induced Th1 cellular responses peaked after two administrations rather than after the third administration (74). It suggests that the immune schedule including vaccination times and intervals be related to the production of memory T cells, and should be investigated for different vaccines respectively.

In our study, MH boosting at 8-14 weeks and EC immunizations at 8-10-14 weeks after BCG priming decreased the long-term protective efficiency. The interval of vaccination affected the generation of T_{CM} (25). Subunit vaccine boosting at short intervals might produce abundant Teff/T_{EM} cells, which wane several weeks (47) and are poised for immediate protection at the expense of forming stable long-term memory (24). Therefore, in the case of vaccine boosting, a suitable long interval played an important role in inducing long-term immune memory.

As far as humoral immune responses were considered, BCG-prime and subunit vaccine MH/EC immunizations improved the production of durable antigen-specific antibodies, while BCG revaccination did not stimulate the production of durable antibodies. The same results were also observed in clinical trials on H4:IC31 and H56:IC31. In the BCG-primed population, H4:IC31 and H56:IC31 vaccine boosting significantly increased the IgG level, while BCG revaccination did not (76). In addition, BCG revaccination of cattle did not increase the level of antigen-specific antibodies (77). Mounting data showed that the subunit vaccines such as ID93 + GLA-SE (74, 78) and M72/AS01 (79, 80) vaccination increased antigen-specific IgG responses significantly in the animal experiments and clinical trials. The role of antibodies in immune protection against *M. tuberculosis* infection needs further investigation (81, 82).

In this study, H37Ra was used to preliminarily evaluate the protective efficacy induced by fusion proteins MH and EC in adjuvant DP with different boosting schedules. Our study suggests that both BCG and "non-BCG" antigens require different schedules to boost BCG-primed immune responses so as to induce long-term immune protection against TB. Although H37Ra has some limitations, it still has been used to preliminarily evaluate the protective efficacy of vaccines (83). However, H37Ra was an attenuated strain and could not persist in mice for a long time as virulent strain. For this reason, we only detected bacterial load in lung of the mice after intranasal challenge. The whole lungs of each mouse were used for bacteria counting and the pathological lesion was not analyzed. In future, virulent *M. tuberculosis* strain H37Rv will be required to evaluate the protective efficacy induced by BCG-prime and different subunit vaccines-boost with different strategies.

5 CONCLUSION

Following BCG priming, MH boosting twice at 12-24 weeks, and EC immunizations thrice at 12-16-24 weeks could produce long-term immune responses and improved the BCG-primed protective efficiency. MH represents the antigens from BCG, while EC represents the antigens from RD. It suggests that following BCG-priming BCG antigen MH boosted twice or "non-BCG" antigens EC immunized thrice at suitable intervals tend to induce long-lived memory T cells. This finding will be helpful for optimizing subunit vaccine boosting schedules to prolong BCG-primed immune protection. Following BCG vaccination, the expression and persistence of antigens *in vivo* can vary, therefore the boosting schedules of different subunit vaccines should be investigated respectively to induce durable immunity against *M. tuberculosis* infection.

DATA AVAILABILITY STATEMENT

The original contributions presented in the study are included in the article/**Supplementary Material**. Further inquiries can be directed to the corresponding author.

ETHICS STATEMENT

The animal study was reviewed and approved by Institutional Animal Care and Use Committee of Lanzhou University.

AUTHOR CONTRIBUTIONS

BZ designed experiments. WL, PH, YLM, DT, FL, TX, JH, JW, YJM, and HN performed experiments. WL and BZ wrote and revised the manuscript. All authors have read and agreed to the published version of the manuscript.

FUNDING

The work was funded by National Key Research and Development Program of China (2021YFC2301503), National Science and Technology Major Projects of China (2018ZX10302302-002-003), Gansu Science and Technology Project (21JR7RA534) and National Science Foundation of China (31470895).

SUPPLEMENTARY MATERIAL

The Supplementary Material for this article can be found online at: https://www.frontiersin.org/articles/10.3389/fimmu.2022.862726/full#supplementary-material

REFERENCES

1. Furin J, Cox H, Pai M. Tuberculosis. *Lancet* (2019) 393(10181):1642–56. doi: 10.1016/S0140-6736(19)30308-3
2. Nathavitharana RR, Friedland JS. A Tale of Two Global Emergencies: Tuberculosis Control Efforts Can Learn From the Ebola Outbreak. *Eur Respir J* (2015) 46(2):293–6. doi: 10.1183/13993003.00436-2015
3. Zwerling A, Behr MA, Verma A, Brewer TF, Menzies D, Pai M. The BCG World Atlas: A Database of Global BCG Vaccination Policies and Practices. *PloS Med* (2011) 8(3):e1001012. doi: 10.1371/journal.pmed.1001012
4. Roy A, Eisenhut M, Harris RJ, Rodrigues LC, Sridhar S, Habermann S, et al. Effect of BCG Vaccination Against Mycobacterium Tuberculosis Infection in Children: Systematic Review and Meta-Analysis. *BMJ* (2014) 349:g4643. doi: 10.1136/bmj.g4643
5. Mangtani P, Abubakar I, Ariti C, Beynon R, Pimpin L, Fine PE, et al. Protection by BCG Vaccine Against Tuberculosis: A Systematic Review of Randomized Controlled Trials. *Clin Infect Dis* (2014) 58(4):470–80. doi: 10.1093/cid/cit790
6. Andersen P, Doherty TM. The Success and Failure of BCG — Implications for a Novel Tuberculosis Vaccine. *Nat Rev Microbiol* (2005) 3(8):656–62. doi: 10.1038/nrmicro1211
7. Luke D, Jasenosky 1, T.J.S., Hanekom WA, Goldfeld AE. T Cells and Adaptive Immunity to Mycobacterium Tuberculosis in Humans. *Immunol Rev* (2015) 264(1):74–87. doi: 10.1111/imr.12274
8. Counoupas C, Triccas JA. The Generation of T-Cell Memory to Protect Against Tuberculosis. *Immunol Cell Biol* (2019) 97(7):656–63. doi: 10.1111/imcb.12275
9. Moguche AO, Musvosvi M, Penn-Nicholson A, Plumlee CR, Mearns H, Geldenhuys H, et al. Antigen Availability Shapes T Cell Differentiation and Function During Tuberculosis. *Cell Host Microbe* (2017) 21(6):695–706.e5. doi: 10.1016/j.chom.2017.05.012
10. Fuertes Marraco SA, Soneson C, Cagnon L, Gannon PO, Allard M, Abed Maillard S, et al. Long-Lasting Stem Cell-Like Memory CD8+ T Cells With a Naïve-Like Profile Upon Yellow Fever Vaccination. *Sci Transl Med* (2015) 7 (282):282ra48. doi: 10.1126/scitranslmed.aaa3700
11. Andersen P, Scriba TJ. Moving Tuberculosis Vaccines From Theory to Practice. *Nat Rev Immunol* (2019) 19(9):550–62. doi: 10.1038/s41577-019-0174-z
12. Sallusto F, Geginat J, Lanzavecchia A. Central Memory and Effector Memory T Cell Subsets: Function, Generation, and Maintenance. *Annu Rev Immunol* (2004) 22:745–63. doi: 10.1146/annurev.immunol.22.012703.104702
13. Gattinoni L, Lugli E, Ji Y, Pos Z, Paulos CM, Quigley MF, et al. A Human Memory T Cell Subset With Stem Cell-Like Properties. *Nat Med* (2011) 17 (10):1290–7. doi: 10.1038/nm.2446
14. Gattinoni L, Speiser DE, Lichterfeld M, Bonini C. T Memory Stem Cells in Health and Disease. *Nat Med* (2017) 23(1):18–27. doi: 10.1038/nm.4241
15. Kaech SM, Wherry EJ, Ahmed R. Effector and Memory T-Cell Differentiation: Implications for Vaccine Development. *Nat Rev Immunol* (2002) 2(4):251–62. doi: 10.1038/nri778
16. Obar JJ, Lefrançois L. Memory CD8+ T Cell Differentiation. *Ann N Y Acad Sci* (2010) 1183:251–66. doi: 10.1111/j.1749-6632.2009.05126.x
17. Masopust D, Vezys V, Marzo AL, Lefrançois L. Preferential Localization of Effector Memory Cells in Nonlymphoid Tissue. *Science* (2001) 291 (5512):2413–7. doi: 10.1126/science.1058867
18. Klebanoff CA, Gattinoni L, Torabi-Parizi P, Kerstann K, Cardones AR, Finkelstein SE, et al. Central Memory Self/Tumor-Reactive CD8+ T Cells Confer Superior Antitumor Immunity Compared With Effector Memory T Cells. *Proc Natl Acad Sci USA* (2005) 102(27):9571–6. doi: 10.1073/pnas.0503726102
19. Mpande CAM, Dintwe OB, Musvosvi M, Mabwe S, Bilek N, Hatherill M, et al. Functional, Antigen-Specific Stem Cell Memory (T(SCM)) CD4(+) T Cells Are Induced by Human Mycobacterium Tuberculosis Infection. *Front Immunol* (2018) 9:324. doi: 10.3389/fimmu.2018.00324
20. Kaveh DA, Garcia-Pelayo MC, Hogarth PJ. Persistent BCG Bacilli Perpetuate CD4 T Effector Memory and Optimal Protection Against Tuberculosis. *Vaccine* (2014) 32(51):6911–8. doi: 10.1016/j.vaccine.2014.10.041
21. Stylianou E, Griffiths KL, Poyntz HC, Harrington-Kandt R, Dicks MD, Stockdale L, et al. Improvement of BCG Protective Efficacy With a Novel Chimpanzee Adenovirus and a Modified Vaccinia Ankara Virus Both Expressing Ag85A. *Vaccine* (2015) 33(48):6800–8. doi: 10.1016/j.vaccine.2015.10.017
22. Billeskov R, Elvang TT, Andersen PL, Dietrich J. The HyVac4 Subunit Vaccine Efficiently Boosts BCG-Primed Anti-Mycobacterial Protective Immunity. *PloS One* (2012) 7(6):e39909. doi: 10.1371/journal.pone.0039909
23. Reed SG, Coler RN, Dalemans W, Tan EV, DeLa Cruz EC, Basaraba RJ, et al. Defined Tuberculosis Vaccine, Mtb72F/AS02A, Evidence of Protection in Cynomolgus Monkeys. *Proc Natl Acad Sci USA* (2009) 106(7):2301–6. doi: 10.1073/pnas.0712077106
24. Thompson EA, Beura LK, Nelson CE, Anderson KG, Vezys V. Shortened Intervals During Heterologous Boosting Preserve Memory CD8 T Cell Function But Compromise Longevity. *J Immunol* (2016) 196(7):3054–63. doi: 10.4049/jimmunol.1501797
25. Bai C, He J, Niu H, Hu L, Luo Y, Liu X, et al. Prolonged Intervals During Mycobacterium Tuberculosis Subunit Vaccine Boosting Contributes to Eliciting Immunity Mediated by Central Memory-Like T Cells. *Tuberc (Edinb)* (2018) 110:104–11. doi: 10.1016/j.tube.2018.04.006
26. Darrah PA, DiFazio RM, Maiello P, Gideon HP, Myers AJ, Rodgers MA, et al. Boosting BCG With Proteins or Rad5 Does Not Enhance Protection Against Tuberculosis in Rhesus Macaques. *NPJ Vaccines* (2019) 4:21. doi: 10.1038/s41541-019-0113-9
27. Tameris MD, Hatherill M, Landry BS, Scriba TJ, Snowden MA, Lockhart S, et al. Safety and Efficacy of MVA85A, a New Tuberculosis Vaccine, in Infants Previously Vaccinated With BCG: A Randomised, Placebo-Controlled Phase 2b Trial. *Lancet* (2013) 381(9871):1021–8. doi: 10.1016/S0140-6736(13)60177-4
28. Khademi F, Derakhshan M, Yousefi-Avarvand A, Tafaghodi M, Soleimanpour S. Multi-Stage Subunit Vaccines Against Mycobacterium Tuberculosis: An Alternative to the BCG Vaccine or a BCG-Prime Boost? *Expert Rev Vaccines* (2018) 17(1):31–44. doi: 10.1080/14760584.2018.1406309
29. Esser MT, Marchese RD, Kierstead LS, Tussey LG, Wang F, Chirmule N, et al. Memory T Cells and Vaccines. *Vaccine* (2003) 21(5-6):419–30. doi: 10.1016/S0264-410X(02)00407-3
30. Andersen P, Woodworth JS. Tuberculosis Vaccines–Rethinking the Current Paradigm. *Trends Immunol* (2014) 35(8):387–95. doi: 10.1016/j.it.2014.04.006
31. Fatima S, Kumari A, Das G, Dwivedi VP. Tuberculosis Vaccine: A Journey From BCG to Present. *Life Sci* (2020) 252:117594. doi: 10.1016/j.lfs.2020.117594
32. Kaech SM, Cui W. Transcriptional Control of Effector and Memory CD8+ T Cell Differentiation. *Nat Rev Immunol* (2012) 12(11):749–61. doi: 10.1038/nri3307
33. Rai D, Martin MD, Badovinac VP. The Longevity of Memory CD8 T Cell Responses After Repetitive Antigen Stimulations. *J Immunol* (2014) 192 (12):5652–9. doi: 10.4049/jimmunol.1301063
34. Maue AC, Waters WR, Palmer MV, Nonnecke BJ, Minion FC, Brown WC, et al. An ESAT-6:CFP10 DNA Vaccine Administered in Conjunction With Mycobacterium Bovis BCG Confers Protection to Cattle Challenged With Virulent M. Bovis. *Vaccine* (2007) 25(24):4735–46. doi: 10.1016/j.vaccine.2007.03.052
35. Niu H, Hu L, Li Q, Da Z, Wang B, Tang K, et al. Construction and Evaluation of a Multistage Mycobacterium Tuberculosis Subunit Vaccine Candidate Mtb10.4-HspX. *Vaccine* (2011) 29(51):9451–8. doi: 10.1016/j.vaccine.2011.10.032
36. Weixin D, Baowen C, Xiaobing S, Guozhi W. Clone Expression in E. Coli and Efficiency Measurement of Recombinant CFP10-ESAT6 Fusion Proteins From Mycobacterium Turberculosis(in Chinese). *Chin J Antituberculosis* (2006) 2006(04):221–4. doi: 10.3969/j.issn.1000-6621.2006.04.008.
37. Xin Q, Niu H, Li Z, Zhang G, Hu L, Wang B, et al. Subunit Vaccine Consisting of Multi-Stage Antigens has High Protective Efficacy Against Mycobacterium Tuberculosis Infection in Mice. *PloS One* (2013) 8(8):e72745. doi: 10.1371/journal.pone.0072745
38. Bai Y, Xue Y, Gao H, Wang L, Ding T, Bai W, et al. Expression and Purification of Mycobacterium Tuberculosis ESAT-6 and MPT64 Fusion Protein and its Immunoprophylactic Potential in Mouse Model. *Protein Expr Purif* (2008) 59(2):189–96. doi: 10.1016/j.pep.2007.11.016
39. Liu X, Da Z, Wang Y, Niu H, Li R, Yu H, et al. A Novel Liposome Adjuvant DPC Mediates Mycobacterium Tuberculosis Subunit Vaccine Well to Induce

Cell-Mediated Immunity and High Protective Efficacy in Mice. *Vaccine* (2016) 34(11):1370–8. doi: 10.1016/j.vaccine.2016.01.049
40. Nemes E, Geldenhuys H, Rozot V, Rutkowski KT, Ratangee F, Bilek N, et al. Prevention of M. Tuberculosis Infection With H4:IC31 Vaccine or BCG Revaccination. *N Engl J Med* (2018) 379(2):138–49. doi: 10.1056/NEJMoa1714021
41. Han J, Ma Y, Ma L, Tan D, Niu H, Bai C, et al. Id3 and Bcl6 Promote the Development of Long-Term Immune Memory Induced by Tuberculosis Subunit Vaccine. *Vaccines (Basel)* (2021) 9(2):126. doi: 10.3390/vaccines9020126
42. Martin MD, Kim MT, Shan Q, Sompallae R, Xue HH, Harty JT, et al. Phenotypic and Functional Alterations in Circulating Memory CD8 T Cells With Time After Primary Infection. *PloS Pathog* (2015) 11(10):e1005219. doi: 10.1371/journal.ppat.1005219
43. Todryk SM, Pathan AA, Keating S, Porter DW, Berthoud T, Thompson F, et al. The Relationship Between Human Effector and Memory T Cells Measured by Ex Vivo and Cultured ELISPOT Following Recent and Distal Priming. *Immunology* (2009) 128(1):83–91. doi: 10.1111/j.1365-2567.2009.03073.x
44. Maggioli MF, Palmer MV, Thacker TC, Vordermeier HM, Waters WR. Characterization of Effector and Memory T Cell Subsets in the Immune Response to Bovine Tuberculosis in Cattle. *PloS One* (2015) 10(4):e0122571. doi: 10.1371/journal.pone.0122571
45. Swain SL, Agrewala JN, Brown DM, Jelley-Gibbs DM, Golech S, Huston G, et al. CD4+ T-Cell Memory: Generation and Multi-Faceted Roles for CD4+ T Cells in Protective Immunity to Influenza. *Immunol Rev* (2006) 211:8–22. doi: 10.1111/j.0105-2896.2006.00388.x
46. Dogra P, Ghoneim HE, Abdelsamed HA, Youngblood B. Generating Long-Lived CD8+T-Cell Memory: Insights From Epigenetic Programs. *Eur J Immunol* (2016) 46(7):1548–62. doi: 10.1002/eji.201545550
47. Sallusto F, Lanzavecchia A, Araki K, Ahmed R. From Vaccines to Memory and Back. *Immunity* (2010) 33(4):451–63. doi: 10.1016/j.immuni.2010.10.008
48. Wherry EJ, Barber DL, Kaech SM, Blattman JN, Ahmed R. Antigen-Independent Memory CD8 T Cells do Not Develop During Chronic Viral Infection. *Proc Natl Acad Sci U.S.A.* (2004) 101(45):16004–9. doi: 10.1073/pnas.0407192101
49. Nandakumar S, Kannanganat S, Dobos KM, Lucas M, Spencer JS, Amara RR, et al. Boosting BCG-Primed Responses With a Subunit Apa Vaccine During the Waning Phase Improves Immunity and Imparts Protection Against Mycobacterium Tuberculosis. *Sci Rep* (2016) 6:25837. doi: 10.1038/srep25837
50. Mostowy S, Cleto C, Sherman DR, Behr MA. The Mycobacterium Tuberculosis Complex Transcriptome of Attenuation. *Tuberc (Edinb)* (2004) 84(3-4):197–204. doi: 10.1016/j.tube.2004.02.002
51. Niu H, Peng J, Bai C, Liu X, Hu L, Luo Y, et al. Multi-Stage Tuberculosis Subunit Vaccine Candidate LT69 Provides High Protection Against Mycobacterium Tuberculosis Infection in Mice. *PloS One* (2015) 10(6):e0130641. doi: 10.1371/journal.pone.0130641
52. Chen L, Wang J, Zganiacz A, Xing Z. Single Intranasal Mucosal Mycobacterium Bovis BCG Vaccination Confers Improved Protection Compared to Subcutaneous Vaccination Against Pulmonary Tuberculosis. *Infect Immun* (2004) 72(1):238–46. doi: 10.1128/IAI.72.1.238-246.2004
53. Hart BE, Lee S. Overexpression of a Mycobacterium Ulcerans Ag85B-EsxH Fusion Protein in Recombinant BCG Improves Experimental Buruli Ulcer Vaccine Efficacy. *PloS Negl Trop Dis* (2016) 10(12):e0005229. doi: 10.1371/journal.pntd.0005229
54. Goonetilleke NP, McShane H, Hannan CM, Anderson RJ, Brookes RH, Hill AV. Enhanced Immunogenicity and Protective Efficacy Against Mycobacterium Tuberculosis of Bacille Calmette-Guérin Vaccine Using Mucosal Administration and Boosting With a Recombinant Modified Vaccinia Virus Ankara. *J Immunol* (2003) 171(3):1602–9. doi: 10.4049/jimmunol.171.3.1602
55. Nandakumar S, Kannanganat S, Dobos KM, Lucas M, Spencer JS, Fang S, et al. O-Mannosylation of the Mycobacterium Tuberculosis Adhesin Apa is Crucial for T Cell Antigenicity During Infection But Is Expendable for Protection. *PloS Pathog* (2013) 9(10):e1003705. doi: 10.1371/journal.ppat.1003705
56. Ahmad S, Bhattacharya D, Gupta N, Rawat V, Tousif S, Van Kaer L, et al. Clofazimine Enhances the Efficacy of BCG Revaccination via Stem Cell-Like Memory T Cells. *PloS Pathog* (2020) 16(5):e1008356. doi: 10.1371/journal.ppat.1008356
57. Tonaco MM, Moreira JD, Nunes FFC, Loures CMG, Souza LR, Martins JM, et al. Evaluation of Profile and Functionality of Memory T Cells in Pulmonary Tuberculosis. *Immunol Lett* (2017) 192:52–60. doi: 10.1016/j.imlet.2017.10.014
58. Lindenstrøm T, Knudsen NP, Agger EM, Andersen P. Control of Chronic Mycobacterium Tuberculosis Infection by CD4 KLRG1- IL-2-Secreting Central Memory Cells. *J Immunol* (2013) 190(12):6311–9. doi: 10.4049/jimmunol.1300248
59. Bhattacharya D, Dwivedi VP, Kumar S, Reddy MC, Van Kaer L, Moodley P, et al. Simultaneous Inhibition of T Helper 2 and T Regulatory Cell Differentiation by Small Molecules Enhances Bacillus Calmette-Guerin Vaccine Efficacy Against Tuberculosis. *J Biol Chem* (2014) 289(48):33404–11. doi: 10.1074/jbc.M114.600452
60. Grode L, Seiler P, Baumann S, Hess J, Brinkmann V, Nasser Eddine A, et al. Increased Vaccine Efficacy Against Tuberculosis of Recombinant Mycobacterium Bovis Bacille Calmette-Guérin Mutants That Secrete Listeriolysin. *J Clin Invest* (2005) 115(9):2472–9. doi: 10.1172/JCI24617
61. Reyrat JM, Berthet FX, Gicquel B. The Urease Locus of Mycobacterium Tuberculosis and its Utilization for the Demonstration of Allelic Exchange in Mycobacterium Bovis Bacillus Calmette-Guérin. *Proc Natl Acad Sci USA* (1995) 92(19):8768–72. doi: 10.1073/pnas.92.19.8768
62. Vogelzang A, Perdomo C, Zedler U, Kuhlmann S, Hurwitz R, Gengenbacher M, et al. Central Memory CD4+ T Cells are Responsible for the Recombinant Bacillus Calmette-Guérin Δurec::Hly Vaccine's Superior Protection Against Tuberculosis. *J Infect Dis* (2014) 210(12):1928–37. doi: 10.1093/infdis/jiu347
63. Lindenstrøm T, Agger EM, Korsholm KS, Darrah PA, Aagaard C, Seder RA, et al. Tuberculosis Subunit Vaccination Provides Long-Term Protective Immunity Characterized by Multifunctional CD4 Memory T Cells. *J Immunol* (2009) 182(12):8047–55. doi: 10.4049/jimmunol.0801592
64. Cha SB, Kim WS, Kim JS, Kim H, Kwon KW, Han SJ, et al. Pulmonary Immunity and Durable Protection Induced by the ID93/GLA-SE Vaccine Candidate Against the Hyper-Virulent Korean Beijing Mycobacterium Tuberculosis Strain K. *Vaccine* (2016) 34(19):2179–87. doi: 10.1016/j.vaccine.2016.03.029
65. Hu Z, Gu L, Li CL, Shu T, Lowrie DB, Fan XY. The Profile of T Cell Responses in Bacille Calmette-Guérin-Primed Mice Boosted by a Novel Sendai Virus Vectored Anti-Tuberculosis Vaccine. *Front Immunol* (2018) 9:1796. doi: 10.3389/fimmu.2018.01796
66. Badovinac VP, Porter BB, Harty JT. Programmed Contraction of CD8(+) T Cells After Infection. *Nat Immunol* (2002) 3(7):619–26. doi: 10.1038/ni804
67. Grassmann S, Mihatsch L, Mir J, Kazeroonian A, Rahimi R, Flommersfeld S, et al. Early Emergence of T Central Memory Precursors Programs Clonal Dominance During Chronic Viral Infection. *Nat Immunol* (2020) 21(12):1563–73. doi: 10.1038/s41590-020-00807-y
68. Costa Del Amo P, Lahoz-Beneytez J, Boelen L, Ahmed R, Miners KL, Zhang Y, et al. Human TSCM Cell Dynamics In Vivo are Compatible With Long-Lived Immunological Memory and Stemness. *PloS Biol* (2018) 16(6):e2005523. doi: 10.1371/journal.pbio.2005523
69. Woodworth JS, Behar SM. Mycobacterium Tuberculosis-Specific CD8+ T Cells and Their Role in Immunity. *Crit Rev Immunol* (2006) 26(4):317–52. doi: 10.1615/CritRevImmunol.v26.i4.30
70. Martin MD, Shan Q, Xue HH, Badovinac VP. Time and Antigen-Stimulation History Influence Memory CD8 T Cell Bystander Responses. *Front Immunol* (2017) 8:634. doi: 10.3389/fimmu.2017.00634
71. Martin MD, Badovinac VP. Influence of Time and Number of Antigen Encounters on Memory CD8 T Cell Development. *Immunol Res* (2014) 59(1-3):35–44. doi: 10.1007/s12026-014-8522-3
72. Masopust D, Ha SJ, Vezys V, Ahmed R. Stimulation History Dictates Memory CD8 T Cell Phenotype: Implications for Prime-Boost Vaccination. *J Immunol* (2006) 177(2):831–9. doi: 10.4049/jimmunol.177.2.831
73. Wirth TC, Xue HH, Rai D, Sabel JT, Bair T, Harty JT, et al. Repetitive Antigen Stimulation Induces Stepwise Transcriptome Diversification But Preserves a Core Signature of Memory CD8(+) T Cell Differentiation. *Immunity* (2010) 33(1):128–40. doi: 10.1016/j.immuni.2010.06.014
74. Penn-Nicholson A, Tameris M, Smit E, Day TA, Musvosvi M, Jayashankar L, et al. Safety and Immunogenicity of the Novel Tuberculosis Vaccine ID93 + GLA-SE in BCG-Vaccinated Healthy Adults in South Africa: A Randomised, Double-Blind, Placebo-Controlled Phase 1 Trial. *Lancet Respir Med* (2018) 6(4):287–98. doi: 10.1016/S2213-2600(18)30077-8

75. Aagaard C, Knudsen NPH, Sohn I, Izzo AA, Kim H, Kristiansen EH, et al. Immunization With Mycobacterium Tuberculosis-Specific Antigens Bypasses T Cell Differentiation From Prior Bacillus Calmette-Guérin Vaccination and Improves Protection in Mice. *J Immunol* (2020) 205(8):2146–55. doi: 10.4049/jimmunol.2000563
76. Bekker LG, Dintwe O, Fiore-Gartland A, Middelkoop K, Hutter J, Williams A, et al. A Phase 1b Randomized Study of the Safety and Immunological Responses to Vaccination With H4:IC31, H56:IC31, and BCG Revaccination in Mycobacterium Tuberculosis-Uninfected Adolescents in Cape Town, South Africa. *EClinicalMedicine* (2020) 21:100313. doi: 10.1016/j.eclinm.2020.100313
77. Parlane NA, Shu D, Subharat S, Wedlock DN, Rehm BH, de Lisle GW, et al. Revaccination of Cattle With Bacille Calmette-Guérin Two Years After First Vaccination When Immunity has Waned, Boosted Protection Against Challenge With Mycobacterium Bovis. *PloS One* (2014) 9(9):e106519. doi: 10.1371/journal.pone.0106519
78. Kwon KW, Lee A, Larsen SE, Baldwin SL, Coler RN, Reed SG, et al. Long-Term Protective Efficacy With a BCG-Prime ID93/GLA-SE Boost Regimen Against the Hyper-Virulent Mycobacterium Tuberculosis Strain K in a Mouse Model. *Sci Rep* (2019) 9(1):15560. doi: 10.1038/s41598-019-52146-0
79. Idoko OT, Owolabi OA, Owiafe PK, Moris P, Odutola A, Bollaerts A, et al. Safety and Immunogenicity of the M72/AS01 Candidate Tuberculosis Vaccine When Given as a Booster to BCG in Gambian Infants: An Open-Label Randomized Controlled Trial. *Tuberc (Edinb)* (2014) 94(6):564–78. doi: 10.1016/j.tube.2014.07.001
80. Thacher EG, Cavassini M, Audran R, Thierry AC, Bollaerts A, Cohen J, et al. Safety and Immunogenicity of the M72/AS01 Candidate Tuberculosis Vaccine in HIV-Infected Adults on Combination Antiretroviral Therapy: A Phase I/II, Randomized Trial. *Aids* (2014) 28(12):1769–81. doi: 10.1097/QAD.0000000000000343
81. Achkar JM, Prados-Rosales R. Updates on Antibody Functions in Mycobacterium Tuberculosis Infection and Their Relevance for Developing a Vaccine Against Tuberculosis. *Curr Opin Immunol* (2018) 53:30–7. doi: 10.1016/j.coi.2018.04.004
82. Lu LL, Chung AW, Rosebrock TR, Ghebremichael M, Yu WH, Grace PS, et al. A Functional Role for Antibodies in Tuberculosis. *Cell* (2016) 167(2):433–43.e14. doi: 10.1016/j.cell.2016.08.072
83. Fatma F, Tripathi DK, Srivastava M, Srivastava KK, Arora A. Immunological Characterization of Chimeras of High Specificity Antigens From Mycobacterium Tuberculosis H37Rv. *Tuberc (Edinb)* (2021) 127:102054. doi: 10.1016/j.tube.2021.102054

Conflict of Interest: The authors declare that the research was conducted in the absence of any commercial or financial relationships that could be construed as a potential conflict of interest.

Publisher's Note: All claims expressed in this article are solely those of the authors and do not necessarily represent those of their affiliated organizations, or those of the publisher, the editors and the reviewers. Any product that may be evaluated in this article, or claim that may be made by its manufacturer, is not guaranteed or endorsed by the publisher.

frontiers | Frontiers in Immunology

ORIGINAL RESEARCH
published: 04 May 2022
doi: 10.3389/fimmu.2022.876579

Immunotherapeutic Effects of Different Doses of *Mycobacterium tuberculosis ag85a/b* DNA Vaccine Delivered by Electroporation

*Yan Liang†, Lei Cui†, Li Xiao†, Xiao Liu, Yourong Yang, Yanbo Ling, Tong Wang, Lan Wang, Jie Wang and Xueqiong Wu**

Tuberculosis Prevention and Control Key Laboratory, Beijing Key Laboratory of New Techniques of Tuberculosis Diagnosis and Treatment, Senior Department of Tuberculosis, The Eighth Medical Center of PLA General Hospital, Beijing, China

OPEN ACCESS

Edited by:
Jianping Xie,
Southwest University, China

Reviewed by:
Bingdong Zhu,
Lanzhou University, China
Mohd Saqib,
Albany Medical College, United States
Limei Wang,
Fourth Military Medical University, China
Vicente Larraga,
Spanish National Research Council (CSIC), Spain
Angelo Izzo,
Royal Prince Alfred Hospital, Australia

***Correspondence:**
Xueqiong Wu
xueqiongwu@139.com

†These authors have contributed equally to this work

Specialty section:
This article was submitted to Vaccines and Molecular Therapeutics, a section of the journal Frontiers in Immunology

Received: *15 February 2022*
Accepted: *05 April 2022*
Published: *04 May 2022*

Citation:
Liang Y, Cui L, Xiao L, Liu X, Yang Y, Ling Y, Wang T, Wang L, Wang J and Wu X (2022) Immunotherapeutic Effects of Different Doses of Mycobacterium tuberculosis ag85a/b DNA Vaccine Delivered by Electroporation. Front. Immunol. 13:876579. doi: 10.3389/fimmu.2022.876579

Background: Tuberculosis (TB) is a major global public health problem. New treatment methods on TB are urgently demanded.

Methods: Ninety-six female BALB/c mice were challenged with 2×10^4 colony-forming units (CFUs) of MTB $H_{37}Rv$ through tail vein injection, then was treated with 10μg, 50μg, 100μg, and 200μg of *Mycobacterium tuberculosis* (MTB) *ag85a/b* chimeric DNA vaccine delivered by intramuscular injection (IM) and electroporation (EP), respectively. The immunotherapeutic effects were evaluated immunologically, bacteriologically, and pathologically.

Results: Compared with the phosphate-buffered saline (PBS) group, the $CD4^+IFN\text{-}\gamma^+$ T cells% in whole blood from 200 μg DNA IM group and four DNA EP groups increased significantly ($P<0.05$), $CD8^+IFN\text{-}\gamma^+$ T cells% (in 200 μg DNA EP group), $CD4^+IL\text{-}4^+$ T cells% (50 μg DNA IM group) and $CD8^+IL\text{-}4^+$ T cells% (50 μg and 100 μg DNA IM group, 100 μg and 200 μg DNA EP group) increased significantly only in a few DNA groups ($P< 0.05$). The $CD4^+CD25^+$ Treg cells% decreased significantly in all DNA vaccine groups ($P<0.01$). Except for the 10 μg DNA IM group, the lung and spleen colony-forming units (CFUs) of the other seven DNA immunization groups decreased significantly ($P<0.001$, $P<0.01$), especially the 100 μg DNA IM group and 50 μg DNA EP group significantly reduced the pulmonary bacterial loads and lung lesions than the other DNA groups.

Conclusions: An MTB *ag85a/b* chimeric DNA vaccine could induce Th1-type cellular immune reactions. DNA immunization by EP could improve the immunogenicity of the low-dose DNA vaccine, reduce DNA dose, and produce good immunotherapeutic effects on the mouse TB model, to provide the basis for the future human clinical trial of MTB *ag85a/b* chimeric DNA vaccine.

Keywords: DNA vaccine, ag85a/b DNA, immunotherapy, *Mycobacterium tuberculosis*, electroporation

INTRODUCTION

Tuberculosis (TB) remains one of the major infectious diseases leading to death. In 2021, there were 10 million incident cases and 1.28 million deaths (1). The epidemic of TB presents a new challenge to the control of tuberculosis. *Mycobacterium bovis* Bacillus Calmette-Guérin (BCG) is an effective vaccine protecting from TB in childhood, but its efficacy against adult pulmonary TB remains controversial (2). Thus, new, safe, and effective TB vaccines are needed. DNA vaccine, one of the latest biotechnological breakthroughs, is the beginning of a new chapter in the vaccine field. DNA vaccines have performed well in clinical trials for diseases such as cancer, human acquired immunodeficiency syndrome (AIDS), malaria, hepatitis B, influenza, allergies, and autoimmunity diseases, demonstrating their potential for disease prevention and immunotherapy (3, 4). DNA vaccines have some advantages, for example, they are more stable, cost-efficient, safe in handling, and easy to produce, transport and store. They can induce comprehensive immune responses including antibody immunity, helper T cell immunity, cytotoxic T cell immunity (5). Although DNA vaccine has strong immunogenicity in small animal models, DNA vaccine has poor performance in large animal and human clinical trials, especially the results in human trials are regret, and it requires very high doses, which creates a barrier to its clinical application (6–10). The main reason for the relatively low immunogenicity of DNA vaccines in large animals and humans is that the amount of antigen expressed by plasmid DNA is insufficient to induce a strong immune responses. Therefore, enhancing the immune effect of DNA vaccine has become a hotspot in this field (11, 12). Strategies for optimizing DNA vaccines include carrier and gene optimization, new adjuvants, and more efficient gene delivery pathways (13–17). In recent years, the development of vaccine delivery technologies such as gene gun, liposome, microparticle, nanoparticle, and electroporation (EP) *in vivo* has significantly improved the delivery efficiency of DNA vaccine (15–19). *In vivo* EP, as an effective route of DNA vaccine delivery, can significantly enhance the immune effect of DNA vaccine for cancer, AIDS, malaria, hepatitis B, influenza, Ebola, dengue fever, and autoimmunity diseases in small animals, even in large animals, including humans (10, 12, 20–22). It has the advantages of high transfection efficiency, simple operation, strong repeatability, high safety, and wide application for mammalian *in vivo* gene transfer (11). Under the action of the electric field, a "hole" is opened instantly on the cell membrane, which can improve the probability of the target gene entering the cell and thus improve the expression efficiency. The slight tissue damage caused by EP also promotes the recruitment of pro-inflammatory cells to the inoculation site and induces the local secretion of cytokines and lymphocyte infiltration to improve antigen presentation and enhance the body's immune responses (23–28).

In previous studies, the *Mycobacterium tuberculosis* (MTB) *ag85a/b* DNA vaccine had good immunotherapeutic effects (29). At present, *in vivo* EP, as an effective route of TB DNA vaccine delivery, is in the pre-clinical research stage. Our research and others had shown that EP was a safe, effective, and non-toxic side effect, which can significantly enhance the immune effect of DNA vaccine (30–34). Although the IM/EP delivery method has been applied to various disease models, anti-TB immunity mainly depends on cellular immune responses, the effect of IM/EP delivery on the dose-efficacy relationship of the tuberculosis DNA vaccine will also be different from other diseases. Therefore, in this study, we firstly used intramuscular injection (IM) and EP technology to deliver different doses of the MTB *ag85a/b* DNA vaccine and compared their immunotherapeutic effects on the mouse TB model, to provide a basis for improving the immunotherapeutic effects of MTB *ag85a/b* DNA vaccine in future human clinical trials and reducing the dosage of DNA vaccine.

MATERIALS AND METHODS

Ethics Statement

All of the experiments involving animals were approved and conducted by the Animal Ethical Committee of the Eighth Medical Center of the Chinese PLA General Hospital. Mouse care met the standards of the Experimental Animal Regulation Ordinances defined by the China National Science and Technology Commission.

Mice

Ninety-six 6-8 week age of the specific pathogen-free (SPF) female BALB/c mice were purchased from Beijing Vital River Laboratory Animal Technology Company Limited, China, maintained under infection barrier conditions in a negative pressure animal room in the Eighth Medical Center of the Chinese PLA General Hospital, Beijing, China. They fed a sterile commercial mouse diet (Beijing KeAoXieLi Company Limited, China).

MTB Strain

MTB $H_{37}Rv$ was provided by National Institutes for Food and Drug Control, Beijing, China.

The MTB $H_{37}Rv$ strain was inoculated on a Lowenstein-Jensen medium (Baso Biotechnology Co., LTD., Zhuhai, Guangdong province, China) and incubated at 37°C for three weeks. Bacterial colonies were collected, weighed, and homogenized in 0.5% Tween 80-saline, then 0.1mg/ml bacterial suspension was prepared and stored at -20°C. Before use, the frozen bacterial suspension was thawed, diluted to 0.5mg/ml, and then further serially diluted 10-fold. 0.1 ml of each dilution was plated in duplicate onto Lowenstein-Jensen plates and incubated at 37°C for 4 weeks. The MTB colonies on each plate were enumerated. The 0.05mg/ml MTB $H_{37}Rv$ suspension contained 5×10^4 CFUs/ml, each mouse was injected with 0.4 ml through tail vein. In this study, one mouse was challenged with 2×10^4 CFUs of MTB $H_{37}Rv$ through tail vein injection.

MTB *ag85a/b* Chimeric DNA and Recombinant Ag85AB Chimeric Protein

The method of constructing MTB *ag85a/b* chimeric DNA was described previously (29). Briefly, the DNA encoding amino acids

125-282 in the Ag85B protein of MTB $H_{37}Rv$ were amplified by PCR with specific oligonucleotide primers containing the site of endonuclease enzyme Acc I. PCR product was purified and then inserted into the endonuclease enzyme Acc I site of the *ag85a* gene that was cloned into eukaryotic expression vector pVAX1 (Invitrogen Life Technologies Corporation, Carlsbad, CA, USA). The length of gene sequence encoding for strong immunogen Ag85A was 888 bp, and the Ag85B was 474 bp. MTB *ag85a/b* chimeric DNA vaccine was thus constructed by inserting the sequence encoding amino acids 125-282 of Ag85B protein into nucleotide 430-435 (endonuclease enzyme Acc I site) of Ag85A DNA vaccine. In this study, the MTB *ag85a/b* chimeric DNA was produced and purified by Guangzhou Baiyunhan Baidi Biological Medicine Co.Ltd (Guangdong province, China).

Treatment of MTB-Infected Mice

The flow chart of DNA vaccine treatment on the mouse TB model is shown in **Figure 1**. Ninety-six female BALB/c mice were challenged with 2×10^4 colony-forming units (CFUs) of MTB $H_{37}Rv$ through tail vein injection, randomly divided into nine groups as follow: (1) PBS as a negative control (100 μl); (2) 10 μg *ag85a/b* DNA intramuscular injection (IM) (10 μg in 100 μl PBS); (3) 50 μg *ag85a/b* DNA IM (50 μg in 100 μl PBS); (4) 100 μg *ag85a/b* DNA IM (100 μg in 100 μl PBS); (5) 200 μg *ag85a/b* DNA IM (200 μg in 100 μl PBS);(6) 10 μg *ag85a/b* DNA IM +EP (10 μg in 100 μl PBS); (7) 50 μg *ag85a/b* DNA IM +EP (50 μg in 100 μl PBS); (8) 100 μg *ag85a/b* DNA IM +EP (100 μg in 100 μl PBS); (9) 200 μg *ag85a/b* DNA IM +EP (200 μg in 100 μl PBS). On the third day after infection, the mice in groups 1 to 5 were immunized intramuscularly, and in groups 6 to 9 were medicated by EP three times at two-week intervals, respectively. EP was performed using a TERESA Gene Delivery Device (TERESA Health Technology Co., LTD, Shanghai, China), set at 36 Voltage and 25 Hz, and six pulses of 10 ms in 3mm depth of thigh muscle of the hind leg of a mouse.

Determination of $CD4^+$ and $CD8^+$ T Cell Subsets Expressing Intracellular IFN-γ or IL-4

The operation procedure was described previously (35). 500 μl of whole blood was stimulated by adding phorbol 12-myristate 13-acetate (PMA, Cat. No. 8139, BD Biosciences, San Jose, Ca, USA) and ionomycin (Cas.10634, Sigma Chemical Co., St.Louis, Mo, USA) as a positive control or by adding 10μl of 1mg/ml Ag85AB protein and then incubating with 5% CO_2 at 37°C for 4 h in the presence of inhibitor brefeldin A (Cat. No. 347688, BD Biosciences, San Jose, Ca, USA). Samples incubated with brefeldin A alone were used as non-stimulated controls (as a negative control). 200μl of blood was then pipetted directly into a 12 × 75 mm fluorescence-activated cell sorting (FACS) tube containing FITC Hamster Anti-Mouse CD3e (Cat. No. 553061, Clone: 145-2C11, BD Biosciences, San Jose, Ca, USA) and PerCP-Cy™5.5 Rat Anti-Mouse CD8a (Cat. No. 551162, Clone: 53-6.7, BD Biosciences, San Jose, Ca, USA), and incubated at room temperature in the dark for 15 min. Then 60 μl of 1 × permeabilizing solution A (BD IntraSure kit, Cat. No.641776, BD Biosciences, San Jose, Ca, USA) was added into the tube and incubated at room temperature in the dark for 5 min. The erythrocytes were then lysed using 2 ml of 1 × FACS lysing solution (Cat. No. 349202, BD Biosciences, San Jose, Ca, USA) for 12 min before centrifugation at 1500 rpm for 5 min.

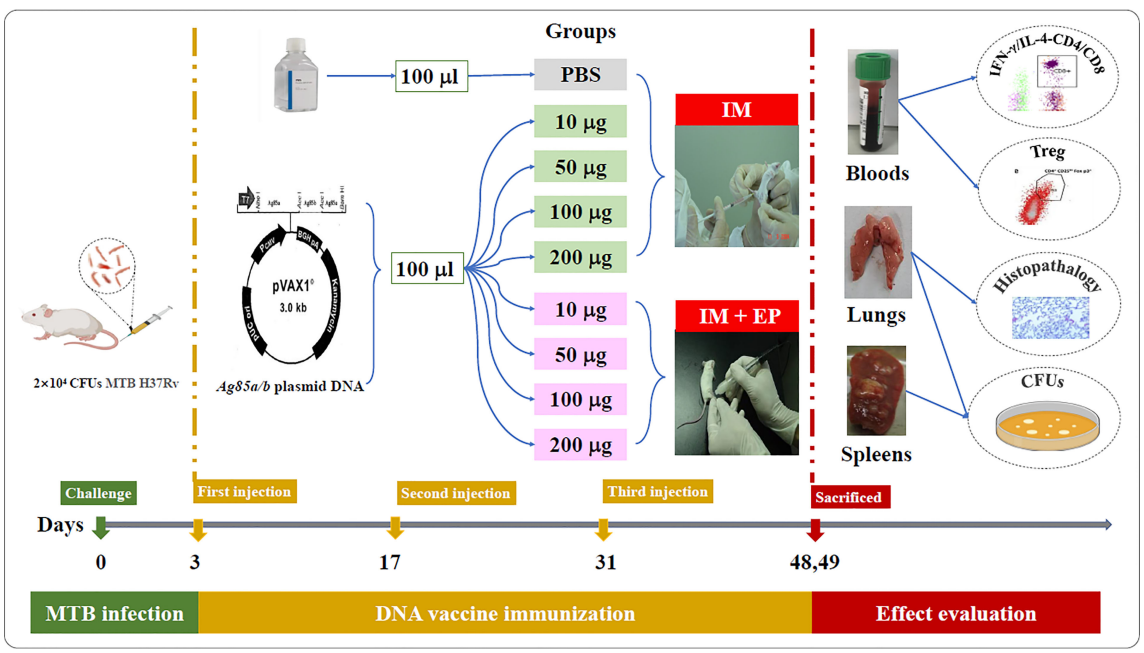

FIGURE 1 | The flow chart of DNA vaccine treatment on the mouse TB model. IM, intramuscular injection; EP, electroporation.

Thesupernatant was aspirated and 30 μl of 1 × permeabilizing solution B (BD IntraSure kit, Cat. No.641776, BD Biosciences, San Jose, Ca, USA) and 5 μl of APC Rat Anti-Mouse IFN-γ (Cat. No. 554413, Clone: XMG1.2, BD Biosciences, San Jose, Ca, USA) 5 μl of PE Rat Anti-Mouse IL-4 (Cat. No. 554435, Clone: 11B11, BD Biosciences, San Jose, Ca, USA) were added into the sample tube, 5 μl of APC Rat IgG1 κ isotype control (Cat. No. 554886, Clone: R3-34, BD Biosciences, San Jose, Ca, USA), 5 μl of PE Rat IgG1 κisotype control (Cat. No. 554885, Clone: R3-34, BD Biosciences, San Jose, Ca, USA), respectively, and incubated at room temperature in the dark for 20 min. 1 ml of PBS containing 2% fetal bovine serum (FBS) was added before centrifugation at 1500 rpm for 5 min. The supernatant was aspirated, 500 μl PBS was added, and the cell suspension was transferred into 12 × 75 mm FACS tubes and analyzed within 1 h by flow cytometry. $CD4^+IFN\text{-}\gamma^+$ T cell, $CD4^+IL\text{-}4^+$ T cell, $CD8^+IFN\text{-}\gamma^+$ T cell, and $CD8^+IL\text{-}4^+$ T cell responding to recombinant Ag85AB proteins were calculated. Cells expressing IFN-γ and IL-4 were presented as a percentage of the total population of $CD3^+$ cells. The data were collected using the FACS Calibur flow cytometer (BD Pharmingen) and analyzed using CellQuest software. The representing FACS figures with gating method and representing flow cytometry dot plot were shown in **Supplementary Figure 1**.

Assay of $CD4^+CD25^+$ Treg and $CD4^+CD25^+FoxP3^+$ Treg Cell Subsets

The blood (100 μl) with Heparin sodium anticoagulant from seven mice per group was pipetted directly into second 12×75 mm FACS tube containing 2 μl of FITC Rat Anti-Mouse CD4 (Cat. No. 553046, Clone: RM4.5, BD Biosciences, San Jose, Ca, USA) and 5 μl of APC Rat Anti-Mouse CD25 (Cat. No. 557192, Clone: PC61, BD Biosciences, San Jose, Ca, USA) and incubated at room temperature in the dark for 15 minutes. Red blood cells were lysed using 1 ml of 1×FACS lysing solution (Cat. No. 349202, BD Biosciences, San Jose, Ca, USA) for 30 minutes before centrifugation at 1200 rpm for 5 minutes. 1 ml of PBS was added into the tube before centrifugation at 1200 rpm for 5 minutes, the supernatant was aspirated, and 1×fixation/permeabilization concentrate (Foxp3/Transcription factor staining buffer set Cat. No. 00-5523, eBioscience, San Diego, Ca, USA) was added into the tube and incubated for 15 minutes at 4°Cin the dark. 1 ml of PBS was added into the tube before centrifugation at 1200 rpm for 5 minutes, the supernatant was aspirated, and 2 ml of 1× permeabilization buffer (FoxP3/Transcription factor staining buffer set Cat. No. 00-5523, eBioscience, San Diego, Ca, USA)was added into the tube before centrifugation at 1200 rpm for 5 minutes. The supernatant was aspirated, and 2 μl normal rat serum was added into the tube and incubated for 15 minutes at room temperature in the dark. 5 μl of PE Anti-Mouse/Rat FoxP3 (Cat. No. 12-5773, Clone: FJK-16s, eBioscience, San Diego, Ca, USA), 2.5 μl of APC Rat IgG1 λ Isotype control (Cat. No. 550884, BD Biosciences, San Jose, Ca, USA) 2.5 μl of PE Rat IgG2a κ isotype (Cat. No. 12-4321, eBiosciences, San Diego, Ca, USA) were added into the tube and incubated for 40 minutes at 4°C in the dark. 2 ml of permeabilization buffer was added into the tube before centrifugation at 1200 rpm for 5 minutes. The supernatant was aspirated, 300 μl of PBS was added into the tube, and the cell suspension was transferred into 12×75 mm FACS tubes and analyzed in an hour by FACS Calibur flow cytometry (BD Pharmingen) and analyzed using CellQuest software. The FACS figures with gating method and representing flow cytometry dot plot were shown in **Supplementary Figure 2**.

Bacterium Counts

The mice were sacrificed by cervical dislocation under anesthetic with 5ml dethylether (Beijing Chemical Reagents Company, Beijing, China) at 17-18 days after the third immunization. The tissue suspensions of mouse lungs and spleens were serially diluted 10-fold, and 100 μL suspension dilution was inoculated in duplicate on Lowenstein-Jensen medium plates and cultured at 37°C for four weeks. MTB colonies on the medium were counted, and the results were shown as CFUs per organ.

Lung Histopathological Examination

The mouse lungs tissues paraffin-embedded were sliced into 3-μm thick tissue sections, which were dyed with hematoxylin and eosin, and then examined by a certified and veteran pathologist.

Statistical Analyses

Data are shown as means and standard deviations. Statistical analyses were performed using one-way ANOVA followed by Dunnett's multiple comparison test and two factors factorial design ANOVA followed by compared with t-test using SAS 9.1 software, and a *P*-value of <0.05 was considered to be statistically significant.

RESULTS

Immunological Evaluation

The results of immunological evaluation on mouse TB model immunized with different doses of MTB *ag85a/b* DNA vaccine by IM and EP were shown in **Figures 2**, **3**. The proportion of $CD4^+$ T cells expressing IFN-γ in response to recombinant Ag85AB chimeric protein in the whole blood from all DNA groups were higher than that in the PBS group by flow cytometry, but there was a significant difference among those only in the 200 μg DNA IM group and 10 μg, 50 μg, 100 μg, 200 μg DNA EP groups ($P<0.05$, $P<0.0001$, **Figure 2A**). There was no significant difference among those in the four doses of DNA IM groups or the DNA EP group ($P>0.05$). The proportion of $CD4^+$ T cells expressing IL-4 in the blood only from the 50μg DNA IM group was significantly higher than that of the PBS group ($P<0.05$, **Figure 2B**).

The proportion of $CD8^+$ T cells expressing IFN-γ in response to recombinant Ag85AB chimeric protein in the whole blood from all DNA groups were higher than that of the PBS group, but only the 200 μg DNA EP group was significantly higher than that of the PBS group ($P<0.01$, **Figure 2C**). The proportion of $CD8^+IFN\text{-}\gamma^+$ T cells in the 10μg, or 100 μg or 200 μg DNA EP group was significantly higher than that in the 10 μg or 100 μg or 200 μg DNA IM group ($P<0.05$), the proportion of $CD8^+IFN\text{-}\gamma^+$

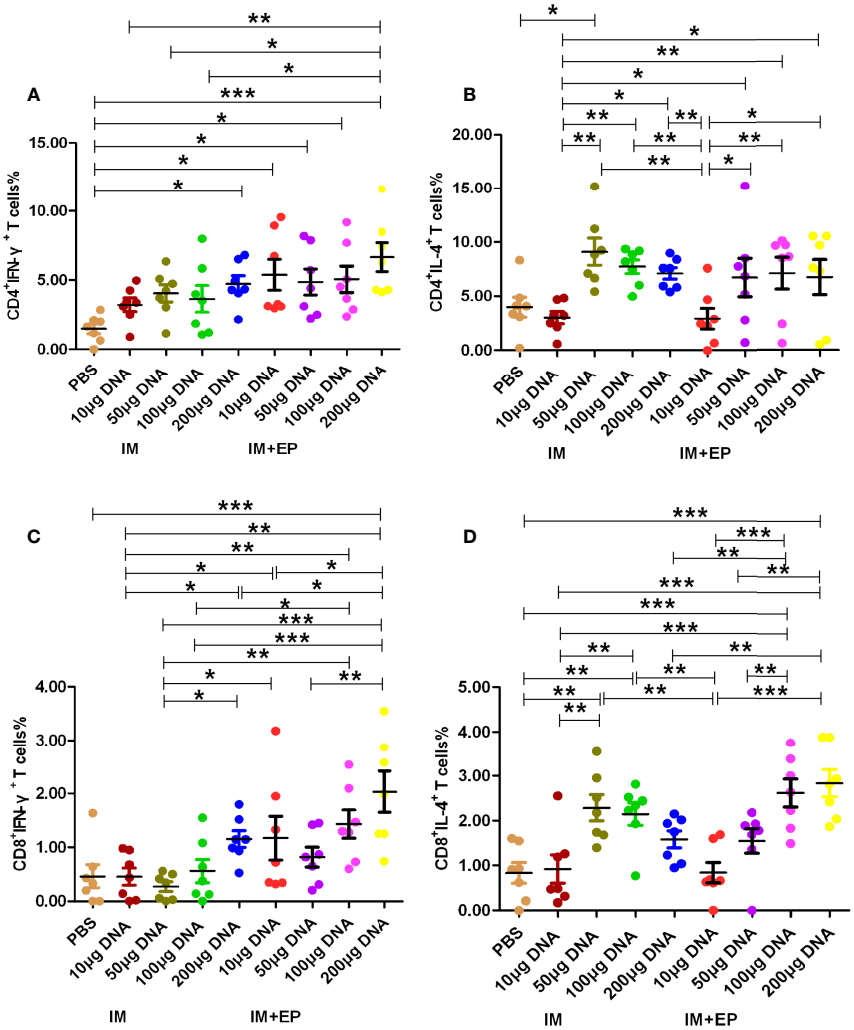

FIGURE 2 | Frequencies of $CD4^+$ and $CD8^+$ T cell subsets in whole blood were assessed by flow cytometry. At 17-18 days after the third immunization, the data are expressed as the mean% ± standard deviation (n = 7) from 7 mice in each group. **(A)** $CD4^+$ T cells expressing IFN-γ (IFN-γ-FITC); **(B)** $CD4^+$ T cells expressing IL-4 (IL-4-PE); **(C)** $CD8^+$ T cells expressing IFN-γ (IFN-γ-FITC); **(D)** $CD8^+$ T cells expressing IL-4 (IL-4-PE). IM, intramuscular injection; EP, electroporation. $^*P<0.05$, $^{**}P < 0.01$, $^{***}P < 0.0001$.

T cells in the 50μg DNA EP group was higher than that in the 50 μg DNA IM group, but there was no significant difference among them ($P>0.05$). The proportion of $CD8^+$ T cells expressing IL-4 in the blood from the 50 μg, 100 μg DNA IM groups and 100 μg, 200 μg DNA EP groups were significantly higher than that in the PBS group ($P<0.01$, $P<0.0001$, **Figure 2D**). The proportion of $CD8^+IL\text{-}4^+$ T cells in the 50μg and 100 μg DNA IM group was significantly higher than those in the 10 μg DNA IM group and 10 μg DNA EP groups ($P<0.01$, $P<0.0001$). The proportion of $CD8^+IL\text{-}4^+$ T cells in the 100 μg and 200 μg DNA EP group was higher than that in the 10 μg,and 200 μg DNA IM, 10μg and 50μg DNA EP groups ($P<0.01$, $P<0.0001$), but there was no significant difference between them ($P>0.05$).

The proportion of $CD4^+CD25^+$ Treg cells in the whole blood from all DNA groups was significantly lower than that of the PBS group by flow cytometry ($P<0.01$, $P<0.0001$, **Figure 3A**), but there was no significant difference in the proportion of $CD4^+CD25^+$ $FoxP3^+$ Treg of all groups ($P>0.05$, **Figure 3B**). The proportion of $CD4^+CD25^+$ Treg cells in the 10 μg DNA EP group was higher than that in the 10 μg DNA IM group ($P<0.001$); the proportion of $CD4^+CD25^+$ Treg cells in the 100 μg and 200 μg DNA EP group were significantly lower than those in the same doses of DNA IM group ($P<0.05$, $P<0.0001$). The proportion of $CD4^+CD25^+$ Treg cells in the 100 μg DNA IM group was significantly higher than those in the 10 μg DNA IM group and 50 μg, 100 μg, 200 μg DNA EP groups ($P<0.05$, $P<0.001$, $P<0.0001$), but was lower than that in the 200 μg DNA IM group ($P>0.05$). The proportion of $CD4^+CD25^+$ Treg cells in the 50 μg DNA EP group was significantly lower than those in the 10 μg DNA EP group and 100 μg, 200 μg DNA IM groups

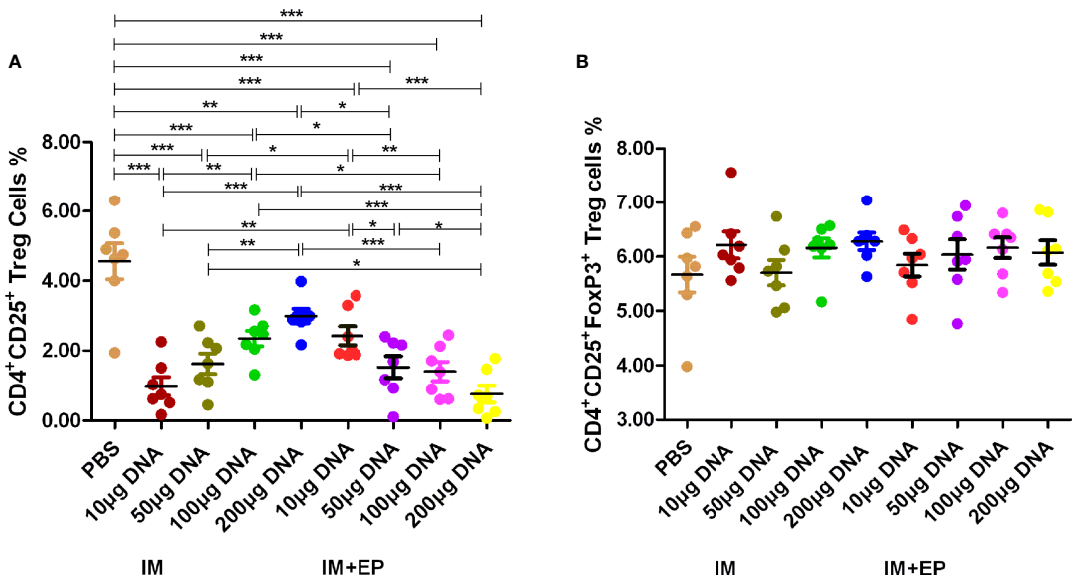

FIGURE 3 | Frequencies of $CD4^+$ and $CD25^+$ Treg cell subsets in whole blood were assessed by flow cytometry. At 17-18 days after the third immunization, the data are expressed as the mean% ± standard deviation (n = 7) from 7 mice in each group. **(A)** Frequencies of $CD4^+$ $CD25^+$ Treg cells; **(B)** Frequencies of $CD4^+CD25^+Foxp3^+$ Treg cells. IM, intramuscular injection; EP, electroporation. $^*P < 0.05$, $^{**}P < 0.01$, $^{***}P < 0.0001$.

(P<0.05, P<0.001), but was significantly higher than that in the 200 μg DNA EP group (P<0.05).

Bacterial Counts in the Lungs and Spleens

The live bacteria in mouse lungs and spleens were determined at 17-18 days after the third immunotherapy (shown in **Figure 4**). Compared with the PBS group, except the 10 μg DNA IM. group, the CFUs of mouse lungs and spleens in other doses of DNA vaccine groups delivered by IM and EP decreased significantly (P<0.0001, P<0.01, P<0.05). The CFUs of mouse lungs and spleens in10 μg and 50 μg DNA EP groups were significantly lower than those in the same doses of the DNA IM group (P<0.0001, P<0.01, P<0.05). However, the CFUs of mouse lungs and spleens in the 100μg DNA EP group was higher than that in the 100 μg DNA IM. group (P< 0.01, P< 0.0001), and in the 200μg DNA EP group were slightly higher than that in the 200 μg DNA IM group, but there was no significant difference (P>0.05). There was no significant difference in lung CFUs between the 100 μg DNA IM group and the 50μg DNA EP group (P>0.05). These two groups were significantly lower than those in other groups (P<0.01, P<0.0001). The spleen CFU in the 50μg DNA EP group was significantly higher than that in the 100 μg DNA IM group (P<0.01), but lower than other groups, especially significantly lower than the 10 μg and 50 μg DNA IM group (P<0.05, P<0.0001). As a result, the 100 μg DNA IM group and 50 μg DNA EP group had a better therapeutic effect on the mouse TB model.

Histopathological Changes

In the PBS group, the alveolar wall was severely thickened, a large number of lymphocytes infiltrated under the bronchioles mucosa, and large granuloma nodules were formed locally, its percentage of lung lesion area was (65 ± 23)%. In the 10 μ g DNA IM group, the lesions were similar to that in the PBS group, and more granuloma nodules were formed locally, its percentage of lung lesion area was (58 ± 28)%. In the 50 μg, 200 μg DNA IM group, and in the 10 μ g, 100 μg, 200 μg DNA EP groups, the lesions were lighter, the alveolar wall was slightly thickened, small granulomatous nodules were formed locally, with a small amount of lymphocyte infiltration, and the area of the lesions was reduced at different agree, their percentages of lung lesion area were (54 ± 27)%, (52 ± 25)%, (51 ± 27)%, (52 ± 23)% and (55 ± 27)%, respectively. The lesions in the 100 μg DNA IM group and 50 μg DNA EP group were the lightest, and most of the alveolar was relatively clear and had typical structures, their percentage of lung lesion areas were perspectively (39 ± 25)% and (39 ± 33)%, which were significantly lower than that in the PBS group (P<0.05). Representative histopathological changes of nine groups were shown in **Figure 5**.

DISCUSSION

EP of muscle has proven to be efficient in enhancing gene delivery, transgene expression, and the immunogenicity of DNA vaccines encoding antigens in both small and large animals (36). More plasmids were delivered into the muscle cells by EP, and then antigen expression in muscle is improved 100- to 1000-fold compared to antigen expression from intracellular uptake of plasmids by naked DNA injection (37). Zucchelli et al. (38) constructed a DNA vaccine encoding HCV E2 glycoprotein, the gene expression increased by 10 times in mouse tissues and

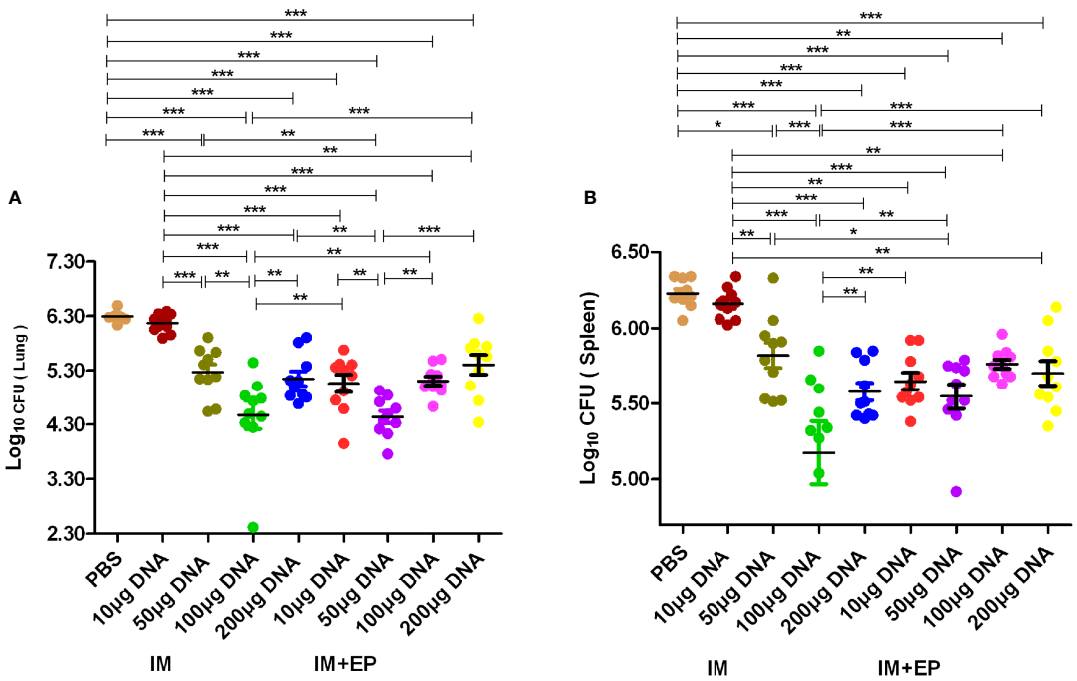

FIGURE 4 | The numbers of live bacteria in lungs **(A)** and spleens **(B)** at 17-18days after the third immunization. The data are expressed as the mean% ± standard deviation (n = 10) from 10 mice in each group. IM, intramuscular injection; EP, electroporation. *$P < 0.05$, **$P < 0.01$, ***$P < 0.0001$.

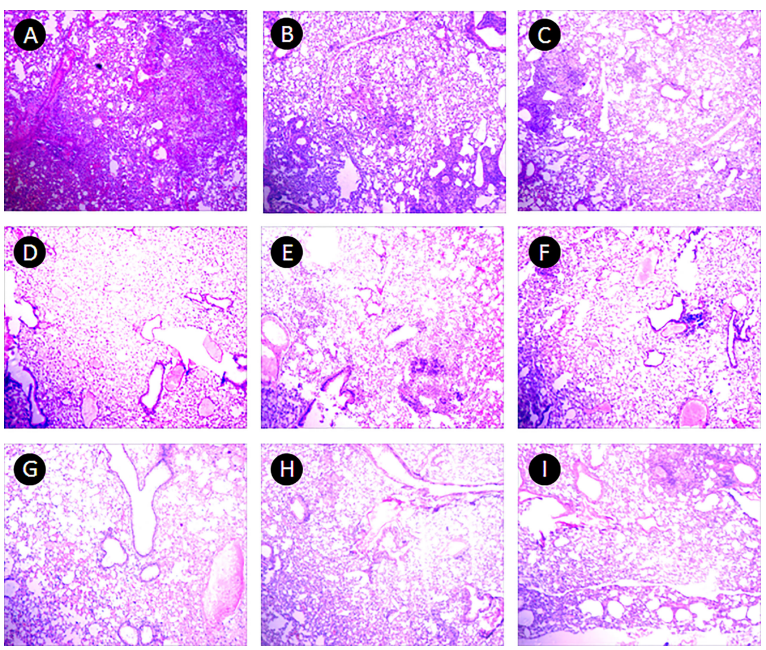

FIGURE 5 | Pulmonary histopathological changes. This figure shows representative photomicrographs (H and E, 40×) of lung tissue obtained from mice each group at 17-18 days after the third immunization. **(A)** PBS group. **(B–E)**, 10 μg, 50 μg, 100 μg and 200 μg *ag85a/b* DNA IM groups. **(F–I)**, 10 μg, 50 μg, 100 μg and 200 μg *ag85a/b* DNA EP groups. IM, intramuscular injection; EP, electroporation.

antibody levels increased 10-30 times in BALB/c mice, CD rats, and New Zealand rabbits by EP, respectively. Li Dingfeng et al. (39) applied EP technology to enhance the immunogenicity of HIV Gag DNA, the specific antibody levels increased by 28 times, but the cellular immune response did not enhance. Anti-tuberculosis immunity is primarily a cell-mediated immune response. The combination of suitable novel prominent TB antigens was incorporated into DNA vaccines could drive both a CD4 and CD8 T cell-mediated immune response, which has emerged as a promising approach (40). Therefore, in this study, we compared the immunotherapeutic of different doses of MTB *ag85a/b* chimeric DNA vaccine delivered by intramuscular injection and EP technology on the mouse TB model, to improve DNA immunogenicity, reduce DNA dosage, and achieve the same therapeutic effect by EP.

Inducing a strong Th1-type immune response can induce anti-TB protection. Inhibition of Th2-type immune response can also produce beneficial intervention effects (41, 42). Therefore, the detection of Th1-/Th2-type immune responses and their cytokines has become an important evaluation index for the immunogenicity of the TB vaccine. Th1-type cells produce cytokines such as IFN-γ. IFN-γ is mainly produced by activated $CD4^+$, $CD8^+$ T cells, and natural killer cell, and play a wide range of anti-TB immune effects. Th2-type cells mainly secrete cytokines such as IL-4. IL-4 can inhibit the proliferation and differentiation of Th1 cells and induce a humoral immune response. Treg cells are a subset of T cells that express CD4 and CD25 molecules. $CD4^+CD25^+$ Treg cells account for 5% - 10% of $CD4^+$ T cells. Its main function is to inhibit the activation of other effector T cells, induce immune tolerance and play an immunomodulatory role (43). Foxp3 T cells are a subset of $CD4^+CD25^+$ Treg cells, express CD45RO subtype, GITC and CD152 molecules on the surface, and Foxp3 transcription factor in the nucleus. $CD4^+CD25^+Foxp3^+$ Treg cells can inhibit anti-TB immune function or release anti-inflammatory factors IL-10 and TGF-β,effectively down-regulate Th1-typeimmune function and promote the latency and proliferation of MTB (44, 45). Tollefsen S et al. immunized mice with 120 μg *ag85a* DNA, 100 μg PAP lacZ DNA and 100 μg *ag85b* DNA by electroporation, the number of antigen-specific $CD4^+$ and $CD8^+$ T cells detected by ELISPOT assay increased 3 to 6 times compared with the mice without electroporation (46). In this study, compared with the PBS group, the $CD4^+IFN\text{-}\gamma^+$ T cells% in 200 μg DNA IM group and four DNA EP groups increased significantly ($P< 0.05$), in 10 μg, 50 μg and 100 μg DNA IM group also higher than that in the PBS group, but there was no significant difference; the $CD4^+IFN\text{-}\gamma^+$ T cells% in four DNA EP groups were higher than those of four DNA IM groups. The detection of flow cytometry in this study used comparative counting method, the $CD4^+IFN\text{-}\gamma^+$ T cells% increased in DNA vaccine groups, so that $CD8^+IFN\text{-}\gamma^+$ T cells% (in 200 μg DNA EP group), $CD4^+IL\text{-}4^+$ T cells% (50μg DNA IM group) and $CD8^+IL\text{-}4^+$ T cells% (50 μg and 100 μg DNA IM groups, 100 μg and 200 μg DNA EP groups) increased significantly only in a few DNA groups ($P< 0.05$).The $CD4^+CD25^+$ Treg cells% decreased significantly in all DNA vaccine groups, and $CD4^+CD25^+Foxp3^+$ Treg cells had no significant difference. These results suggest that MTB *ag85a/b* chimeric DNA vaccines a strong inducer of $CD4^+IFN\text{-}\gamma^+$ T cells, and EP could further enhance Th1-type immune response. Treg cells decreased or remained unchanged, indicating the ratio between these two types of cells can balance protection and lung injury (30, 47). Therefore, EP immunization can enhance the immune response of low-dose DNA vaccines, and a small amount of DNA vaccine can produce strong immunogenicity.

The bacterial organ load is one of the essential indicators to evaluate curative effects on animal TB experiments (48). Compared with the PBS group, the lung and spleen CFUs of the other seven DNA immunization groups except for the 10 μg DNA IM group decreased significantly, especially 50 μg DNA EP group and 100 μg DNA IM group significantly reduced the pulmonary bacterial loads than the other DNA groups, which were consistent with its lightest lung lesions. Similarly, Sallberg et al. reported a transient reduction in viral load (0.6 $\log_{10}$ to 2.4 $\log_{10}$) in patients infected with chronic hepatitis C vaccinated with an NS3/4a based DNA vaccine delivered *via* EP (49). There were dose-dependent effects in the 10 μg, 50 μg, and 100 μg IM groups, 10 μg and 50 μg DNA EP groups, which is in agreement with our previous studies (29, 30, 50). The appropriate amount of DNA delivered by IM or EP can express sufficient protein *in vivo* to induce an effective cellular immune response and protect mice against MTB invasion. Compared with the antigen expression of plasmid ingested by naked DNA injection, EP can deliver more plasmids to muscle cells and improve the antigen expression in muscle. The less DNA delivered by EP can achieve the immunotherapeutic effect of 100 μg DNA IM on the mouse TB model. Delivering too much DNA would induce a Th2-type immune response. For example, the effect of the 100 μg DNA EP group was significantly lower than the 50 μg DNA EP group, which is consistent with our previous studies (51). Overall, the protective immune response induced was consistent with the bacterial lung load and lesion range. These results suggest that DNA immunization by EP could improve the immunogenicity of the low-dose DNA groups, which is lower than the effective dose of intramuscular injection, reduce the number of bacteria and the range of lesions, so that the 50 μg DNA EP group could achieve the immunotherapeutic effects of the 100 DNA IM group on the mouse TB model. The clinical trials from Yan J et al. showed that the main adverse effect (grade 1/2) related to the EP procedure was temporary pain, which quickly subsided within 25-30 minutes (52), indicating that EP had no apparent side effects. The characteristics of EP to improve immunogenicity may lead to the progress of delivery technology. When DNA vaccine is applied to larger animals or humans in the future, it is essential to determine the optimal DNA dose.

CONCLUSION

An MTB *ag85a/b* chimeric DNA vaccine could induce Th1-type cellular immune reactions. DNA immunization by EP could improve the DNA immunogenicity of the low-dose DNA vaccine, reduce DNA dose, produce sound immunotherapeutic effects on TB, and provide the basis for the future human clinical trial of MTB *ag85a/b* chimeric DNA vaccine.

DATA AVAILABILITY STATEMENT

The original contributions presented in the study are included in the article/**Supplementary Material**. Further inquiries can be directed to the corresponding author.

ETHICS STATEMENT

The animal study was reviewed and approved by The Animal Ethical Committee of the 8th Medical Center of the Chinese PLA General Hospital.

AUTHOR CONTRIBUTIONS

Conceptualization: XW and YL. Methodology: YL, LC, LX, XL, YY, YBL, TW, LW, and JW. Data analysis: YL. Wrote original manuscript: YL. Review and revise manuscript: XW and YL. All authors contributed to the article and approved the submitted version.

FUNDING

This project was supported by the grant from the Serious Infectious Diseases Special Foundation (2012ZX10003008-002, 2018ZX10731301-005), the Special Key Project of the Medical Innovation Project of China (18CXZ028).

ACKNOWLEDGMENTS

The authors would like to acknowledge Dr. Ning Li and Dr.Wen Chen from the Department of the pathology of the Eighth Medical Center of Chinese PLA General Hospital to prepare pathological sections.

SUPPLEMENTARY MATERIAL

The Supplementary Material for this article can be found online at: https://www.frontiersin.org/articles/10.3389/fimmu.2022.876579/full#supplementary-material

REFERENCES

1. World Health Organization. *Global Tuberculosis Report 2021*. Available at: https://www.who.int/teams/global-tuberculosis-programme/tb-reports (Accessed Oct 14 2021).
2. Kaufmann SH. Envisioning Future Strategies for Vaccination Against Tuberculosis. *Nat Rev Immunol* (2006) 6:699–704. doi: 10.1038/nri1920
3. Donnelly JJ, Ulmer JB, Shiver JW, Liu MA. DNA Vaccines. *Annu Rev Immunol* (1997) 15:617–48. doi: 10.1146/annurev.immunol.15.1.617
4. Liu MA, Ulmer JB. Human Clinical Trials of Plasmid DNA Vaccines. *Adv Genet* (2005) 55:25–40. doi: 10.1016/S0065-2660(05)55002-8
5. Prazeres DMF, Monteiro GA. Plasmid Biopharmaceuticals. *Microbiol Spectr* (2014) 2:PLAS-0022-2014. doi: 10.1128/microbiolspec.PLAS-0022-2014
6. MacGregor RR, Boyer JD, Ugen KE, Lacy KE, Gluckman SJ, Bagarazzi ML, et al. First Human Trial of a DNA Based Vaccine for Treatment of Human Immunodeficiency Virus Type 1 Infection: Safety and Host Response. *J Infect Dis* (1998) 178:92–100. doi: 10.1086/515613
7. Liu MA, McClements W, Ulmer JB, Shiver J, Donnelly J. Immunization of Non- Human Primates With DNA Vaccine. *Vaccine* (1997) 15:909–12. doi: 10.1016/S0264-410X(96)00280-0
8. Tacket CO, Roy MJ, Widera G, Swain WF, Broome S, Edelman R. Phase 1 Safety and Immune Response Studies of a DNA Vaccine Encoding Hepatitis B Surface Antigen Delivered by a Gene Delivery Device. *Vaccine* (1999) 17:2826–29. doi: 10.1016/S0264-410X(99)00094-8
9. Cohen J. Disappointing Data Scuttle Plans for Large-Scale AIDS Vaccine Trial. *Science* (2002) 295:1616–17. doi: 10.1126/science.295.5560.1616
10. Babiuk S, Baca-Estrada ME, Foldvari M, Storms M, Rabussay D. Electroporation Improve the Efficacy of DNA Vaccines in Large Animals. *Vaccine* (2002) 20:3399–408. doi: 10.1016/S0264-410X(02)00269-4
11. Gurunathan S, Klinman DM, Seder RA. DNA Vaccines: Immunology, Application, and Optimization. *Ann Rev Immunol* (2000) 18:927–74. doi: 10.1146/annurev.immunol.18.1.927
12. Sardesai NY, Weiner DB. Electroporation Delivery of DNA Vaccines: Prospects for Success. *Curr Opin Immunol* (2011) 23:421–9. doi: 10.1016/j.coi.2011.03.008
13. Mu J, Jeyanathan M, Small CL, Zhang X, Feng X, Chong D, et al. Immunization With a Bivalent Adenovirus Vectored Tuberculosis Vaccine Provides Markedly Improved Protection Over Its Monovalent Counterpart Against Pulmonary Tuberculosis. *Mol Ther* (2009) 17:1093–100. doi: 10.1038/mt.2009.60
14. Hobernik D, Bros M. DNA Vaccines–How Far From Clinical Use? *Int J Mol Sci* (2018) 19:3605. doi: 10.3390/ijms19113605
15. Pasquini S, Xiang Z, Wang Y, He Z, Deng H, Blaszczyk-Thurin M, et al. Cytokines and Costimulatory Molecules as Genetic Adjuvants. *Immunol Cell Biol* (1997) 75:397–401. doi: 10.1038/icb.1997.62
16. Cui Z, Mumper RJ. Microparticles and Nanopartides Delivery Systems for DNA Vaccines. *Crit Rey Ther Drug Carrier Syst* (2003) 20:103–37. doi: 10.1615/CritRevTherDrugCarrierSyst.v20.i23.10
17. Klenchin VA, Sukharev SI, Serov SM, Chernomordik LV, Yua C. Electrically Induced DNA Uptake by Cells Is a Fast Process Involving DNA Electrophoresis. *Biophys J* (1991) 60:804–11. doi: 10.1016/S0006-3495(91)82115-4
18. Kim HJ, Jung BK, Lee JJ, Pyo KH, Chai JY. CD8 T-Cell Activation in Mice Injected With a Plasmid DNA Vaccine Encoding AMA-1 of the Reemerging Korean Plasmodium Vivax. *Korean J Parasitol* (2011) 49:85–90. doi: 10.3347/kjp.2011.49.1.85
19. Gregoriadis G, Saffie R, deSouza JB. Liposome-Mediated DNA Vaccination. *FEBS Lett* (1997) 402:107–10. doi: 10.1016/S0014-5793(96)01507-4
20. Suschak JJ, Bagley K, Shoemaker CJ, Carolyn S, Steven K, Dupuy LC, et al. The Genetic Adjuvants Interleukin-12 and Granulocyte-Macrophage Colony Stimulating Factor Enhance the Immunogenicity of an Ebola Virus Deoxyribonucleic Acid Vaccine in Mice. *J Infect Dis* (2018) 218:S519–S27. doi: 10.1093/infdis/jiy378
21. Sheng Z, Chen H, Feng K, Gao N, Wang R, Wang P, et al. Electroporation-Mediated Immunization of a Candidate DNA Vaccine Expressing Dengue Virus Serotype 4 prM-E Antigen Confers Long-Term Protection in Mice. *Virol Sin* (2019) 34:88–96. doi: 10.1007/s12250-019-00090-8
22. Luxembourg A, Hannaman D, Ellefsen B, Nakamura G, Bernard R. Enhancement of Immune Responses to an HBV DNA Vaccine by Electroporation. *Vaccine* (2006) 24:4490–3. doi: 10.1016/j.vaccine.2005.08.014
23. Luckay A, Sidhu MK, Kjeken R, Megati S, Chong SY, Roopchand V, et al. Effect of Plasmid DNA Vaccine Design and *In Vivo* Electroporation on the Resulting Vaccine–Specific Immune Responses In Rhesus Macaques. *J Virol* (2007) 81:5257–69. doi: 10.1128/JVI.00055-07
24. Kalat M, Küpcü Z, Schüller S, Zalusky D, Zehetner M, Paster W, et al. *In Vivo* Plasmid Electroporation Induces Tumor Antigen-Specific $CD8^+$ T-cell Responses and Delays Tumor Growth in a Syngeneic Mouse Melanoma Model. *Can Res* (2002) 62:5489–94. doi: 10.1097/00002820-200210000-00012
25. Shirota H, Petrenko L, Hong C, Klinman DM. Potential of Transfected Muscle Cells to Contribute to DNA Vaccine Immunogenicity. *J Immunol* (2007) 179:329–36. doi: 10.4049/jimmunol.179.1.329

26. Zupanic A, Corovic S, Miklavcic D, Pavlin M. Numerical Optimization of Gene Electrotransfer Into Muscle Tissue. *BioMed Eng Online* (2010) 9:66. doi: 10.1186/1475-925X-9-66
27. Liu KH, Ascenzi MA, Bellezza CA, Bezuidenhout AJ, Cote PJ, Gonzalez-Aseguinolaza G, et al. Electroporation Enhances Immunogenicity of a DNA Vaccine Expressing Woodchuck Hepatitis Virus Surface Antigen in Woodchucks. *J Virol* (2011) 85:4853–62. doi: 10.1128/JVI.02437-10
28. Barbon CM, Baker L, Lajoie C, Ramstedt U, Hedley ML, Luby TM. *In Vivo* Electroporation Enhances the Potency of Poly-Lactide Co-Glycolide (PLG) Plasmid DNA Immunization. *Vaccine* (2010) 28:7852–64. doi: 10.1016/j.vaccine.2010.09.078
29. Liang Y, Wu X, Zhang J, Xiao L, Yang Y, Bai X, et al. Immunogenicity and Therapeutic Effects of Ag85A/B Chimeric DNA Vaccine in Mice Infected With *Mycobacterium Tuberculosis*. *FEMS Immunol Med Microbiol* (2012) 66:419–26. doi: 10.1111/1574-695X.12008
30. Liang Y, Li X, Bai XJ, Gao Y, Yang Y, Zhang X, et al. Immunogenicity of Different Dosage DNA Vaccine From *Mycobacterium Tuberculosis* Medicated by Electroporation. *Chin J Antituberc* (2014) 36:424–8. doi: 10.3969/j.issn.1000-6621.2014.06.004
31. Tang J, Cai Y, Liang J, Tan Z, Tang X, Chi Z, et al. *In Vivo* Electroporation of a Codon-Optimized BER (Opt) DNA Vaccine Protect Mice From Pathogenic *Mycobacterium Tuberculosis* Aerosol Challenge. *Tuberculosis (Edinb)* (2018) 113:65–75. doi: 10.1016/j.tube.2018.07.003
32. Tollefsen S, Vordermeier M, Olsen I, Storset AK, Reitan LJ, Clifford D, et al. DNA Injection Combination With Electroporation: A Novel Method for Vaccination of Farmed Ruminants. *Scand J Immunol* (2003) 57:229–38. doi: 10.1046/j.1365-3083.2003.01218.x
33. Li Z, Zhang H, Fan X, Zhang Y, Huang J, Liu Q, et al. DNA Electroporation Prime and Protein Boost Strategy Enhances Humoral Immunity of Tuberculosis DNA Vaccines in Mice and Non-Human Primates. *Vaccine* (2006) 24:4565–8. doi: 10.1016/j.vaccine.2005.08.021
34. Zhang X, Divangahi M, Ngai P, Santosuosso M, Millar J, Zganiacz A, et al. Intramuscular Immunization With a Monogenic Plasmid DNA Tuberculosis Vaccine: Enhanced Immunogenicity by Electroporation and Co-Expression of GM-CSF Transgene. *Vaccine* (2007) 25:1342–52. doi: 10.1016/j.vaccine.2006.09.089
35. Liang Y, Zhang X, Xiao L, Bai X, Wang X, Yang Y, et al. Immunogenicity and Therapeutic Effects of Pvax1- *Rv1419* DNA From Mycobacterium Tuberculosis. *Curr Gene Ther* (2016) 16:249–55. doi: 10.2174/1566523216666161102170123
36. Lin F, Shen X, McCoy JR, Mendoza JM, Yan J, Kemmerrer SV, et al. A Novel Prototype Device for Electroporation-Enhanced DNA Vaccine Delivery Simultaneously to Both Skin and Muscle. *Vaccine* (2011) 29:6771–80. doi: 10.1016/j.vaccine.2010.12.057
37. Villarreal DO, Talbott KT, Choo DK, Shedlock DJ, Weiner DB. Synthetic DNA Vaccine Strategies Against Persistent Viral Infections. *Expert Rev Vaccines* (2013) 12:537–54. doi: 10.1586/erv.13.33
38. Zucchelli S, Capone S, Fattori E, Folgori A, Marco AD, Casimiro D, et al. Enhancing and T Cell Immune Response to a Hepatitis C Virus E2 DNA Vaccine by Intramuscular Electrical Gene Transfer. *J Virol* (2000) 74:11598–607. doi: 10.1128/JVI.74.24.11598-11607.2000
39. Feng LD, Zhang YW, Li HS, Fan WL, Sun MS, Liu Y, et al. Effects of Vivo Electroporation on Reporter Gene Expression and Immune Responses Induced by DNA Vaccination. *Chin J Microbiol Immunol* (2006) 26:1038–41. doi: 10.3760/j:issn:0254-5101.2006.11.019
40. Villarreal DO, Walters J, Laddy DJ, Yan J, Weiner DB. Multivalent TB Vaccines Targeting the Esx Gene Family Generate Potent and Broad Cell-Mediated Immune Responses Superior to BCG. *Hum Vaccin Immunother* (2014) 10:2188–98. doi: 10.4161/hv.29574
41. Winslow GM, Cooper A, Reiley W, Chatterjee M, Woodland DL. Early T-Cell Responses in Tuberculosis Immunity. *Immunol Rev* (2008) 225(1):284–99. doi: 10.1111/j.1600-065X.2008.00693.x
42. Roy E, Brennan J, Jolles S, Lowrie DB. Beneficial Effect of Anti-Interleukin-4 Antibody When Administered in a Murine Model of Tuberculosis Infection. *Tuberculosis (Edinb)* (2008) 88(3):197–202. doi: 10.1016/j.tube.2007.11.005
43. Cardona P, Cardona PJ. Regulatory T Cells in *Mycobacterium Tuberculosis* Infection. *Front Immunol* (2019) 10:2139. doi: 10.3389/fimmu.2019.02139
44. Belkaid Y, Piccirillo CA, Mendez S, Shevach EM, Sacks DL. $CD4^+CD25^+$ Regulatory T Cells Control Leishmania Major Persistence and Immunity. *Nature* (2002) 420(6915):502–7. doi: 10.1038/nature01152
45. Belkaid Y, Rouse BT. Natural Regulatory T Cells in Infectious Disease. *Nat Immunol* (2005) 6(4):353–60. doi: 10.1038/ni1181
46. Tollefsen S, Tjelle TE, Joerg S, Harboe M, Wiker HG, Hewinson G, et al. Improved Cellular and Humoral Immune Responses Against *Mycobacterium Tuberculosis* Antigens After Intramuscular DNA Immunization Combined With Muscle Electroporation. *Vaccine* (2002) 20:3370–78. doi: 10.1016/S0264-410X(02)00289-X
47. Fedatto PF, Sérgio CA, Paula MOE, Gembre AF, Franco LH, Wowk PF, et al. Protection Conferred by Heterologous Vaccination Against Tuberculosis is Dependent on the Ratio of $CD4^+$/$CD4^+Foxp3^+$Cells. *Immunology* (2012) 137:239–48. doi: 10.1111/imm.12006
48. Lowrie DB, Tascon RE, Bonato VLD, Lima VMF, Faccioli LH, Stavropoulos E, et al. Therapy of Tuberculosis in Mice by DNA Vaccination. *Nature* (1999) 400:269–71. doi: 10.1038/22326
49. Weiland O, Ahlén G, Diepolder H, Jung MC, Levande S, Fons M, et al. Therapeutic DNA Vaccination Using *In Vivo* Electroporation Followed by Standard of Care Therapy in Patients With Genotype 1 Chronic Hepatitis C. *Mol Ther* (2013) 21:1796–805. doi: 10.1038/mt.2013.119
50. Wu XQ, Zheng Y, Xu YJ, Zhang JX, Lu Y, Zhang LX, et al. The Evaluation of Protective Efficacy of Tuberculosis DNA Vaccines With Different Dosage and by Codelivery of Cytokine Plasmid. *Cell Mol Immunol* (2006) 22:883–94. doi: 10.1007/s00034-004-1208-7
51. Liang Y, Li X, Zhang X, Bai XJ, Yang Y, Gao Y, et al. Evaluation of the Effects of Different Vaccinations in Muscles With DNA Vaccine Against *Mycobacterium Tuberculosis* Delivered by Electroporation. *Chin J Microbiol Immunol* (2014) 34:673–9. doi: 10.3760/cma.j.issn.0254-5101.2014.09.005
52. Yan J, Pankhong P, Shen X, Giffear M, Lee J, Harris D, et al. Phase I Safety and Immunogenicity of HPV 16 and 18 DNA Vaccines Delivered *via* Electroporation. *Mol Ther* (2010) 18:S184. doi: 10.1016/S1525-0016(16)37918-7

Conflict of Interest: The authors declare that the research was conducted in the absence of any commercial or financial relationships that could be construed as a potential conflict of interest.

frontiers | Frontiers in Immunology

REVIEW
published: 23 June 2022
doi: 10.3389/fimmu.2022.895020

Research Advances for Virus-vectored Tuberculosis Vaccines and Latest Findings on Tuberculosis Vaccine Development

Zhidong Hu[1]*, *Shui-Hua Lu*[1,2], *Douglas B. Lowrie*[2] *and Xiao-Yong Fan*[1]*

[1] Shanghai Public Health Clinical Center, Key Laboratory of Medical Molecular Virology of Ministry of Education (MOE)/ Ministry of Health (MOH), Fudan University, Shanghai, China, [2] National Medical Center for Infectious Diseases of China, Shenzhen Third People Hospital, South Science & Technology University, Shenzhen, China

Tuberculosis (TB), caused by respiratory infection with *Mycobacterium tuberculosis*, remains a major global health threat. The only licensed TB vaccine, the one-hundred-year-old Bacille Calmette-Guérin has variable efficacy and often provides poor protection against adult pulmonary TB, the transmissible form of the disease. Thus, the lack of an optimal TB vaccine is one of the key barriers to TB control. Recently, the development of highly efficacious COVID-19 vaccines within one year accelerated the vaccine development process in human use, with the notable example of mRNA vaccines and adenovirus-vectored vaccines, and increased the public acceptance of the concept of the controlled human challenge model. In the TB vaccine field, recent progress also facilitated the deployment of an effective TB vaccine. In this review, we provide an update on the current virus-vectored TB vaccine pipeline and summarize the latest findings that might facilitate TB vaccine development. In detail, on the one hand, we provide a systematic literature review of the virus-vectored TB vaccines are in clinical trials, and other promising candidate vaccines at an earlier stage of development are being evaluated in preclinical animal models. These research sharply increase the likelihood of finding a more effective TB vaccine in the near future. On the other hand, we provide an update on the latest tools and concept that facilitating TB vaccine research development. We propose that a pre-requisite for successful development may be a better understanding of both the lung-resident memory T cell-mediated mucosal immunity and the trained immunity of phagocytic cells. Such knowledge could reveal novel targets and result in the innovative vaccine designs that may be needed for a quantum leap forward in vaccine efficacy. We also summarized the research on controlled human infection and ultra-low-dose aerosol infection murine models, which may provide more realistic assessments of vaccine utility at earlier stages. In addition, we believe that the success in the ongoing efforts to identify correlates of protection would be a game-changer for streamlining the triage of multiple next-generation TB vaccine candidates. Thus, with more advanced knowledge of TB vaccine research, we remain hopeful that a more effective TB vaccine will eventually be developed in the near future.

Keywords: tuberculosis, vaccine, viral vector, mucosal immunity, trained immunity

OPEN ACCESS

Edited by:
Hao Li,
China Agricultural University, China

Reviewed by:
Joanna Kirman,
University of Otago, New Zealand
Rachel Tanner,
University of Oxford, United Kingdom

***Correspondence:**
Zhidong Hu
huzhidong@fudan.edu.cn
Xiao-Yong Fan
xyfan008@fudan.edu.cn

Specialty section:
This article was submitted to Vaccines and Molecular Therapeutics, a section of the journal Frontiers in Immunology

Received: *12 March 2022*
Accepted: *27 May 2022*
Published: *23 June 2022*

Citation:
Hu Z, Lu S-H, Lowrie DB and Fan X-Y (2022) Research Advances for Virus-vectored Tuberculosis Vaccines and Latest Findings on Tuberculosis Vaccine Development. Front. Immunol. 13:895020. doi: 10.3389/fimmu.2022.895020

1 INTRODUCTION

Among the top 10 leading causes of death worldwide and the leading cause of death by a bacterial infection, tuberculosis (TB) caused 1.5 million deaths in 2020 (1). According to the World Health Organization (WHO), a quarter of the world population is infected with *Mycobacterium tuberculosis* (*Mtb*), the cause of TB (1). The Coronavirus Disease 2019 (COVID-19) pandemic reduced access to TB diagnosis and treatment and led to an increase in TB deaths in 2020, the first time during the past decade (1). Ambitious targets for TB control have been set by WHO. The "End TB Strategy" defined milestones and targets that aim to reduce TB incidence by 90% and deaths by 95% by 2035 compared with 2015 (2). However, progress has been slow and the 2020 milestone was far from reached (1). The lack of an optimal TB vaccine is regarded as one of the key barriers for TB control, thus, WHO timelines to control the global TB epidemic require a vaccine that is more effective, particularly in adolescents and adults. In this review, we focus on the history of research and the developmental progress of virus-vectored TB vaccines that are in clinical trials, those that are in pre-clinical animal research, and the latest ancillary findings facilitating TB vaccine research and development.

2 ONE-HUNDRED-YEAR-OLD BCG: SUCCESSES AND FAILURES

Mycobacterium bovis Bacille Calmette-Guérin (BCG), a vaccine based on attenuation of a bacterium naturally causing TB in cattle, is the only licensed TB vaccine up to now. BCG was first administered to the newborn infant of a woman with TB in France in 1921, neither adverse effects nor disease developed in the subsequent 5.5 years (3). In the next several years, thousands of children in families with a history of TB received BCG at the Pasteur Institute (4). In 1928, the intradermal route was found to be more reliable compared with the oral route, and this route continues to be used today (5). In the same year, the League of Nations (the predecessor of the United Nations) declared BCG to be safe for use. Although the "Lübeck disaster", in which 72 newborn babies died from TB after BCG vaccination due to contamination with a virulent strain of *Mtb* (6), hindered the public acceptance of BCG for a long time, a resurgence of TB during World War II led to widespread BCG inoculation and public confidence in its safety was regained (7). In 1974, the WHO created the "Expanded Programme on Immunization", to ensure that mothers and children have universal access to routinely recommended neonatal vaccines, and this resulted in more than 4 billion BCG vaccinations being administered to date (8). The vaccine has probably been administered to more humans than any other vaccine. Two-thirds of those countries giving BCG vaccination are estimated to have more than 90% coverage (9) and the vaccine is still the gold standard against which new candidates are compared.

The widespread use of the BCG vaccine in infants continues, primarily because it offers protection against the aggressive childhood forms of the disease: meningeal and miliary TB (10). However, for pulmonary TB prevention in adults, clinical trials have estimated its vaccine efficacy to range from 0% in south India to 80% in the UK (11). There are many hypotheses to explain this wide variation, including age at vaccination (12, 13), exposure to environmental mycobacteria (14), gender (15), risk of TB in the study population (16), etc. However, the proposed causes of variation often remain speculative and the basis is likely to be multifactorial.

The failure of TB control indicates that BCG is insufficient. Strategies to improve TB vaccination mainly address one of two approaches: optimization of the current BCG vaccine or development of novel vaccines such as subunit, vectored, and live attenuated vaccines. In the optimization of BCG we include BCG re-vaccination, change of inoculation route, and recombinant BCG construction. Although WHO does not recommend BCG re-vaccination due to a lack of proven efficacy of repeat doses for protection against TB, the most recently completed clinical trials showed BCG re-vaccination had an efficacy of 45.4% in primary *Mtb* infection prevention, which was defined immunologically by QuantiFERON-TB Gold In-tube assay conversion (17). However, the side effects of BCG re-vaccination hinder its application in humans with immune disorders. Although intravenous BCG immunization was consigned to the history books, this approach was recently re-evaluated in the non-human primate model of TB, in which nine out of ten intravenous BCG-vaccinated macaques showed slight or even no signs of TB disease post *Mtb* infection (18). However, safety concerns will impede application in humans. One of the most promising TB vaccines may provide an alternative. The genetically modified BCG-based vaccine VPM1002, in which the gene encoding urease C was replaced by the listeriolysin encoding gene from *Listeria monocytogenes*, showed the potential to replace the current BCG vaccine and is now undergoing three phase III clinical efficacy trials (19).

Besides the optimization of the current BCG vaccine, another approach is to utilize novel TB vaccines as a booster of the BCG vaccine, since most adults who acquire TB worldwide today were BCG-vaccinated as neonates. In the past decades, several viral vector-based vaccines and protein-adjuvant vaccines were designed to enhance BCG-primed immune protection. In this review, we focus on the research and development of viral vector-based TB vaccines.

3 RECOMBINANT VIRUS-VECTORED TB VACCINES

Viruses provide some of the most widely used vaccine vectors. Recombinant virus-vectored vaccines are capable of inducing robust immune responses by mimicking the processes of pathogens invading the organism and resulting in the formation of long-lasting immune memory. Basically, most viral vaccine vectors have the following advantages: 1) they can accommodate genes encoding large antigenic fragments; 2) they have stable exogenous gene expression efficiency; 3) they can

induce high levels of both cellular and humoral immune responses; 4) the immune responses induced by the vector itself have the potential to augment the antigen-specific immune memory to some extent; 5) they do not always require the use of adjuvants; 6) they are easy to manipulate and culture; 7) the use of attenuated or replication-deficient viruses with a clear mechanism of infection provides a strong safety profile; 8) strong immune memory can generally be induced by a single immunization, and repeated vaccinations might not be required (20–24). The major disadvantages of viral-vectored vaccines includes: 1) the pre-existing neutralizing antibodies against the vector might limiting its application in humans; 2) the host-induced anti-vector immunity might limit the booster vaccination strategies; 3) some viral vectors are not appropriate for use in immunocompromised individuals.

Although it was well illustrated that Th1 $CD4^+$ T cell responses dominated anti-TB immune protection, *Mtb* can survive intracellularly for a long time after primary infection, the induction of immune responses that include high levels of cytotoxic T lymphocyte is also crucial to the clearance of intracellular *Mtb* (25–27). Cytotoxic T cells are prominent in the immune response to viruses and viruses accordingly provide one of the most widely used vector formats in the field of TB vaccines.

3.1 Mechanisms of Immune Protection Afforded by Virus-vectored Vaccines

The mechanisms of immune protection vary depending on the nature of the induction stimulus. Overall, recombinant viral-vectored vaccines carrying exogenous antigen fragments are able to invade host cells by using intrinsic viral mechanisms and undergo massive intracellular replication. The intracellular products and those secreted extracellularly induce cellular and humoral immune responses, respectively. The commonly-used attenuated or replication-deficient viruses are rapidly cleared after the host's immune response is activated, while the antigen-specific immune cells are gradually transformed into memory cells that can remain for a long time. In addition, recombinant viral-vectored vaccines are able to induce a strong co-stimulatory molecular signaling and the formation of an inflammatory microenvironment, which together act as signals 2 and 3 of the T-cell/B-cell response pathways to enhance the host's antigen-specific adaptive immunity.

3.2 Brief Introduction of the Widely Used Viral Vectors

The poxviruses are among the most widely studied viral vectors. They constitute a group of double-stranded DNA viruses that is divided into 2 subfamilies and 12 genera, among which, Orthopoxvirus, Molluscipoxvirus, Parapoxvirus, and Yatapoxvirus are known to infect humans (28, 29). Poxviruses of different genera infect different animals to cause different diseases and vaccinia virus, belonging to the genus Orthopoxvirus, although not fully non-pathogenic in human, has been a highly effective "live" vaccine against the smallpox epidemics that once ravaged humans (30). For safety reasons, most studies have chosen to use replication-deficient versions of poxviruses in vaccine vector development. The reduced immunogenicity consequent upon reduced replication can be offset by genetic modifications to knock-down molecules used by the virus to attenuate immune responses and by expression of immunostimulatory molecules in addition to the target antigens (31, 32). The types of genes encoded to enhance immune responses include: type I and type II interferons, genes regulating cytokines and chemokines, apoptosis and immunosuppression related molecules, antigen presentation signaling pathway molecules, etc. (33–35) Notable among poxvirus vaccine vectors are four strains of replication-deficient poxviruses, including modified vaccinia virus Ankara (MVA) (36), NYVAC derived from Copenhagen strain (37), ALVAC modified from canary poxvirus (38), avian poxvirus TROVAC (38), and another attenuated vaccinia strain, namely Chinese Tiantan strain poxvirus (39). The recombinant vaccine MVA85A, also known as AERAS-485, expresses *Mtb* immunodominant antigen Ag85A and was the first new TB vaccine to complete phase IIb clinical trials (40). It induced strong immune responses among Th1 and Th17 $CD4^+$ T cells, in addition to moderate $CD8^+$ T cell responses (41).

Adenovirus (Ad) is another widely used vaccine vector. About 50 human adenovirus (AdHu) serotypes have been identified, of which AdHu5 and AdHu35 are the two most widely used subtypes. Two human adenovirus-based recombinant vaccines against TB, AdAg85A (also known as AdHu5Ag85A) and AERAS-402 (also known as Crucell Ad35), in addition to ChAdOx1.85A, based on a chimpanzee adenovirus vector, are capable of inducing a strong $CD8^+$ T-cell immune response in addition to high levels of Th1-type $CD4^+$ T-cell immune response.

Other viral vectors including influenza virus, cytomegalovirus (CMV), Sendai virus (SeV), lentivirus, vesicular stomatitis virus (VSV), have also been applied to TB vaccine studies. Although these viruses infect cells by different mechanisms, most of them can induce high levels of antigen-specific Th1 $CD4^+$ and $CD8^+$ T cell immune responses as TB vaccine vectors. Among them, SeV85AB, a recombinant SeV-vectored vaccine expressing Ag85A and Ag85B, was the first viral-vectored TB vaccine found able to induce high levels of lung tissue-resident memory T cells (T_{RM})-mediated immune protection (42) and provided a new research direction for TB vaccines.

3.3 Brief History of Research and Development of Virus-vectored TB Vaccines

The recombinant poxvirus-vectored vaccine MVA85A was the first of the new TB vaccines to complete phase IIb clinical trials (40), but there are several other recombinant viral-vectored vaccines against TB in clinical and preclinical phases of evaluation. Herein, we give a brief overview of the history and the latest discoveries in the field.

3.3.1 MVA85A/AERAS-485

The MVA85A vaccine, which expresses the *Mtb* immunodominant antigen Ag85A, was developed by the University of Oxford in 2001,

researchers found that intradermal (i.d.) or intramuscular (i.m.) immunization with this vaccine was able to induce a high level of antigen-specific immune response and protective immunity against *Mtb* challenge by decreasing the bacterial loads in organs in mouse models (43–45); subsequently, the vaccine-induced protection was further validated in other animal models such as guinea pigs (46), cattle (47) and rhesus monkeys (48). In the first phase I clinical trial, published in 2004, the vaccine was inoculated i.d. and induced a strong specific T-cell immune response in adults with or without a BCG immunization history (49). In 2010, the immunogenicity and safety of this i.d. vaccine were further confirmed in children and adolescents (50). Two phase I clinical trials completed in 2012 and 2013, were conducted to optimize the immunization dose (51) and route of administration (i.m. and i.d.) (52). During this period, from 2009 to 2011, researchers recruited 2,797 BCG-immunized infants between 4 and 6 months of age and i.d. administered either MVA85A or placebo and followed them for 19 to 28 months to complete the first phase IIb clinical trial (40). Although the safety of the vaccine was strongly demonstrated, the vaccine only induced weak antigen-specific immune responses and was not protective against TB disease (40), similar with the results that MVA85A did not reduce the bacterial burden of BCG-prime mice (53). Thus, the first viral-vectored TB vaccine clinical trial was declared a failure. In a proof-of-concept phase II trial, the number of immunization times was increased to two shots in a population of HIV-infected patients, but the efficacy, which was defined by QuantiFERON-TB Gold In-Tube conversion, remained poor (54). Nonetheless, researchers have not given up their efforts. A phase I clinical trial study in 2014 reported validation of the safety of mucosal immunization with MVA85A (55), and in 2019 a phase I clinical trial showed that an aerosol prime-intradermal boost regime was well-tolerated and induced potent antigen-specific mucosal and systemic immune responses (56). Additionally, i.m. inoculation was tested in a phase II clinical trial (NCT02178748) that indicated that a change in the route of administration may be a way to improve the vaccine's protective efficacy. In 2021 a phase I trial showed that MVA85A delivered by aerosol was safe in UK adults with latent TB infection (57). Utility in a potential niche application was indicated in a phase II clinical trial that showed MVA85A vaccination in HIV-exposed newborns might be used to avoid the potential risk of BCG disease in this population (58).

Pre-clinical studies had indicated that the vaccine might work best as a booster in combination with other vaccines. To test this clinically, the vaccine was combined with the recombinant adenovirus-vectored vaccine AERAS-402 (59) with ChAdOx1.85A (currently in a phase II trial, NCT03681860) (60), with the recombinant avian poxvirus-vectored vaccine FP85A (61), or the protein adjuvant vaccine IMX313 (62), all of which had all been validated in phase I clinical trials.

Besides MVA85A, the potential of several other MVA-based recombinant TB vaccines has been indicated. For example, a multiphasic vaccine expressing 14 antigens representative of the three phases of TB infection (active, latent, and resuscitation) was subcutaneously (s.c.) immunized and induced potent multifunctional cell-mediated immunity in mice and rhesus macaque models (63). A recombinant MVA expressing α-crystallin by using i.d. route enhanced BCG-induced protection against *Mtb* infection in guinea pigs (64).

3.3.2 AdAg85A

Recombinant adenovirus vectors are widely used in the field of TB vaccine research. At least three vaccines are currently moving forward in clinical trials: AdAg85A based on AdHu5 (65, 66), AERAS-402 based on AdHu35 (67–73), and ChAdOx1.85A (60) based on a chimpanzee adenovirus vector, which would be discussed in detail below.

Recombinant AdHu5 vectored vaccine AdAg85A, was developed by McMaster University and published in 2004 (74). Similar to the MVA85A vaccine study, the safety, immunogenicity, and protective efficacy of the AdAg85A vaccine by using the aerosol and i.m. route were validated in animal models including mice (75–77), guinea pigs (78), cattle (79), goats (80), and rhesus macaques (81) before entering clinical trials. In the first clinical trial in 2013, AdAg85A was i.m. administrated in BCG-naïve and previously BCG-immunized healthy adults, and strong antigen-specific $CD4^+$ and $CD8^+$ T cell responses were observed (65). Most recently, in 2022, a phase Ib trial showed that aerosol delivery of AdAg85A was also safe and well-tolerated in previously BCG-vaccinated adults (66). A potential disadvantage of the vaccine is that substantial levels of anti-AdHu5 antibodies tend to be preexisting in humans, although the inventors of the vaccine demonstrated that AdHu5 antibodies do not affect the safety and immunogenicity of AdAg85A (65). However, a clinical trial of an AdHu5-based HIV vaccine was terminated due to the discovery that vaccinated subjects who had high titers of antibodies against adenovirus tended to have a higher incidence of HIV acquisition than those without anti-adenovirus antibodies in 2007 (82). Consequently, the role of preexisting vector-specific antibody responses remains controversial and there is currently an international preference for the use of AdHu35, the antibodies of which are largely absent from human serum. In addition, considering low sero-reactivity was observed in chimpanzee- and simian-derived adenoviral vectors compared with human-derived vectors in humans (83), several recombinant chimpanzee adenovirus-vectored TB vaccines were constructed, which will be described below. However, through a mouse model, the magnitude, quality and protective capacity of $CD8^+$ T cells elicited using simian immunodeficiency virus Gag as the target antigen were compared, AdHu5 and AdCh3 vectors conferred the best efficacy (83, 84). These studies added a layer of complexity to balancing safety and vaccine efficacy in choosing adenovirus vectors.

3.3.3 AERAS-402/Crucell Ad35

The AdHu35-based recombinant vaccine, AERAS-402, expressing Ag85A, Ag85B, and TB10.4 was developed jointly by Crucell and the Aeras organization. In 2007, it was shown that this vaccine was i.m. immunized and was able to induce a strong T-cell immune response and a strong immune-protective effect against *Mtb* in a mouse model (85). The protection afforded by AERAS-402 singly or in combination with other vaccines was

also validated in rhesus macaques (86–88). In 2010, the i.m. vaccine's safety and immunogenicity were confirmed in healthy adults in a phase I clinical trial (67). In subsequent years, through several phase I and phase II clinical trials, researchers have expanded the potential target population to include healthy infants previously vaccinated with BCG (68), healthy adults immunized with BCG (69), adults with active or previous TB (70), latently infected populations (71), and HIV-infected patients (72). A two-dose i.m. regimen was also evaluated in BCG-vaccinated adults in phase I clinical trial in 2021 (73). Several AERAS-402-based phase II clinical trials targeting different populations, including adults treated for pulmonary TB, HIV-infected/BCG-vaccinated adults, and BCG-vaccinated healthy infants, have been completed (NCT02414828, NCT01017536, and NCT01198366). The safety of i.m. AERAS-402 was confirmed through these trials.

3.3.4 ChAdOx1.85A

To minimize any effects of preexisting anti-adenovirus antibodies in humans, researchers have developed the recombinant replication-deficient chimpanzee adenovirus-vectored vaccine ChAdOx1.85A. Its i.m. immunization is capable of inducing high levels of cellular immune response in BCG-primed mice and showing protective efficacy against *Mtb* infection in combination with MVA85A (89, 90). In 2020, a phase I clinical trial demonstrated that a ChAdOx1.85A i.m.-MVA85A i.m. vaccination regimen was well tolerated and immunogenic in healthy UK adults (60). As mentioned above, this vaccine strategy is now in a phase II clinical trial (NCT03681860).

Intranasally (i.n.) immunization with a recombinant ChAdOx1 vaccine expressing Rv1039c (PPE15) instead of Ag85A conferred better protection than ChAdOx1.85A in a murine model, meriting further evaluation in clinical trials (91). Similarly, a recombinant chimpanzee adenovirus-68-vectored vaccine expressing Ag85A, namely AdCh68Ag85A, was i.n. immunized and found to be superior to AdAg85A in the induction of T-cell responses and protection against *Mtb* infection in mice that had previously been exposed to human adenovirus (92). In addition, there is evidence that this vaccine could be used as a therapeutic vaccine: Immunotherapy with a single-dose respiratory mucosal but not parenteral application of AdCh68Ag85A as an adjunct to antibiotic therapy accelerated pulmonary *Mtb* clearance, limited lung pathology, and restricted disease in mice (93).

3.3.5 TB/FLU-04L

In 2006, a recombinant influenza virus-vectored vaccine expressing ESAT-6 was shown to be able to induce a high level of Th1 $CD4^+$ T cell immune response with two i.n. injections in a mouse model (94). The protective efficacy of the vaccine was confirmed in mice and guinea pigs (95). This vaccine, named TB/FLU-04L, was aerosol immunized and completed a phase I clinical trial in 2015, but no study results have been published (NCT02501421). According to WHO reports in 2017 (96), a phase IIa clinical trial is being conducted in patients with latent TB infection. Besides TB/FLU-04L, another recombinant influenza virus-based vaccine expressing the dominant peptides of Ag85B was constructed, and robust T_{RM} responses and protective efficacy were observed in a murine model by using i.n. route (97).

3.3.6 MCMV85A and RhCMV/TB

In 2014, a recombinant murine CMV-vectored vaccine MCMV85A expressing Ag85A was developed by the University of Oxford. This vaccine was inoculated intraperitoneal (i.p.) or intravascular (i.v.), and activated NK cells to provide early nonspecific protection against *Mtb* infection, which was further potentiated by a weak 85A-specific T cell response in a murine model (98). In 2018, a rhesus monkey CMV vector vaccine RhCMV/TB was described that encoded nine proteins from three phases of *Mtb* infection: acute (Ag85A, Ag85B, ESAT-6), latency (Rv1733, Rv2626, Rv3407), and resuscitation (RpfA, RpfC, RpfD). Two doses of s.c. RhCMV/TB induced high levels of specific $CD4^+$ and $CD8^+$ T cell immune responses, and provided long-lasting vaccine-mediated immune control after highly pathogenic *Mtb* strains challenge one year after immunization in rhesus macaques, in which 41% animals showed no TB disease evaluated by computed tomography scans or necropsy (99). However, although human CMV infection only causes asymptomatic infection in the immunocompetent population, CMV is highly species-specific and systemic disease with severe complications and high mortality rate might be occurred in immunocompromised individuals (100, 101). Moreover, epidemiological studies have identified the increased human CMV infection is an important risk factor for active TB disease and latent TB infection, which was found to be associated with the magnitude of IgG, enhanced CMV-driven T-cell activation, systemic inflammation, and immune dysregulation (102, 103). Thus, more animal and clinical studies are warranted to better understand CMV-vectored immunity, to ensure its safe translation to humans, especially in active TB patients and individuals with latent TB infection.

3.3.7 SeV85AB

SeV85AB, a recombinant SeV-vectored vaccine, is the first application of a SeV vector to the TB vaccine development and it expresses *Mtb* immunodominant antigens Ag85A and Ag85B and inherently has a high safety profile. Being based upon an RNA virus, the SeV vector has no risk of integration with the human genome. Furthermore, in contrast to respiratory pathogens such as the influenza virus, the SeV does not cause human disease and there are very low antibody levels present. In 2017, using a mouse model, we validated its immunogenicity and protective efficacy against *Mtb* infection in mice and demonstrated the establishment of a high level of T_{RM}-mediated immune response in mucosal tissues by using i.n. route (42). Such memory cells can establish the first line of defense in the lung against *Mtb* invasion in the early phase of infection. In contrast, BCG vaccination usually produces a response of memory T cells in the circulatory system only after several weeks of infection. Therefore, this vaccine may be used to optimize the systemic BCG-induced immune protection against

Mtb infection (104). This immunization strategy was further optimized in combination with recombinant DNA vaccines for improved protective efficacy (105).

3.3.8 Other Viral-vectored Vaccines

Several other promising viral vectors are being explored as candidates for TB vaccine construction. In 2008, Hamamatsu University School of Medicine constructed a lentiviral vector vaccine expressing MPT51 of *Mtb*. This construct enhanced the antigen presentation efficiency of dendritic cells, and intratracheal (i.t.) immunization of mice was able to induce a $CD8^+$ T-cell immune response at the lung site and protection against *Mtb* infection (106). Recently, several other lentiviral vector-based TB vaccines have been developed, but they are at early animal model phases of investigation (107–110). Lentiviral vectors have been successfully used in the clinical trials of patients with advanced leukemia and other gene immunotherapy research (111, 112). In most of these TB vaccine studies described above, self-inactivation or non-integrating vector systems were chosen to get safe vaccines.

In 2008, researchers at McMaster University constructed a recombinant VSV-vectored vaccine VSVAg85A that expressed Ag85A and was able to induce an antigen-specific immune response and protection against *Mtb* infection but only for a short duration by using i.n. or i.m. routes. Combining the vaccination with AdAg85A in a prime-boost immunization strategy improved the protective efficacy (113); VSV-based boosting resulted in inferior protection compared with adenovirus-based boosting, and this was associated with differentially imprinted innate phagocytes at the mucosal site of immunization (114). Besides VSVAg85A, another VSV-based TB vaccine expressing Rv2660c, Rv3615c, and Mtb10.4 has generated antigen-specific T cell responses and immune protection in a BCG challenge murine model by using i.n. route (115, 116).

The use of a combination of vectors expressing the same antigen in order to enhance responses is a recurring theme. As mentioned in Section 3.3.1 above, a recombinant fowlpox virus FP9 that expressed Ag85A (FP9.Ag85A or FP85A) and boosted BCG/MVA85A-induced protective immunity in guinea pigs (46) also boosted immune responses to MVA85A in a clinical phase I trial in 2013 (61).

In 2014, a recombinant human parainfluenza type 2 virus-vectored vaccine expressing Ag85B, rhPIV2-Ag85B, was developed by the National Institute for Biomedical Innovation in Japan (117). This i.n. vaccine was able to induce a T-cell immune response and immune protection in a murine model that was subsequently found to be associated with induction of bronchus-associated lymphoid tissue (118). Similarly, a parainfluenza virus 5 vector expressing Ag85A and Ag85B has also shown immunogenicity and protective efficacy in a murine infection model by using i.n. route (119).

In 2020, different prime-boost strategies using the chimpanzee Ad3 (ChAd3) and MVA vectors expressing Ag85B, ESAT-6, Rv1733, Rv2626, and RpfD, were evaluated for immunogenicity and protective efficacy in highly susceptible rhesus macaques through different inoculation routes such as i.m., i.d., and aerosol. However, although specific immune responses were induced, none of these vaccine strategies conferred a protective effect compared to non-vaccinated controls (120).

To be noted, most of these studies used *Mtb* immunodominant antigens such as Ag85A, Ag85B, TB10.4, ESAT-6, etc., which were chosen based on their expression levels in *Mtb* and IFN-γ-inducing ability. However, the failure of MVA85A in its first phase IIb clinical trial suggest other antigens should be selected to construct a more effective vaccine. Recently, an unbiased immunopeptidomics pipeline for identifying novel antigens presented by MHC was developed, in which MHC I and MHC II complexes from BCG-infected THP-1 macrophages were immunoprecipitated and analyzed by liquid chromatography tandem mass spectrometry (121). Thus, identifying more efficient antigens by novel assays is also important in virus-vectored TB vaccine development.

Table 1 summarizes the viral vectored TB vaccine candidates that are currently in clinical trials, and **Table 2** summarizes the candidates that are currently in preclinical animal model phases. These studies of novel virus-vectored TB vaccines have been successful in developing a number of candidates that have entered the TB vaccine pipeline (https://www.tbvi.eu/what-we-do/pipeline-of-vaccines/) and are at different stages of clinical trials in humans. This may lead to newly licensed vaccines capable of replacing/supplementing the current BCG vaccine and even conferring therapeutic benefit in patients with active/latent TB.

4 LATEST FINDINGS THAT FACILITATE TB VACCINE RESEARCH DEVELOPMENT

Over the past two decades, huge progress has been achieved in the field of TB vaccine development and more than a dozen candidate vaccines including viral-vectored vaccines are in clinical trials now. However, several knowledge gaps and challenges to the successful development of a universally effective TB vaccine remain. Here we summarize the latest findings facilitating TB vaccine research development.

4.1 Controlled Human Infection Model

The immunogenicity and protective efficacy of the TB vaccines that have entered clinical trials were first repeatedly validated in animal models such as mice, guinea pigs, and rhesus macaques before trial commencement. Validation in these animal models is not only time-consuming and costly but there is also a high technical barrier in undertaking *Mtb* challenge experiments in animals (requiring prolonged use of ABSL-3 level laboratories). In addition, the failure of the phase IIb clinical trial of the MVA85A vaccine showed that the currently available animal models do not predict human immunity well. Moreover, in the clinical trials evaluating TB vaccines, the assessment of protective efficacy relies on natural exposure to *Mtb* infection and requires enrollment and follow-up of tens of thousands of people for multiple years. The limited availability of suitable human

TABLE 1 | Viral vectored TB vaccine candidates that are currently in clinical trials.

Candidate vaccines	Vectors	Antigens	Populations/animals	Clinical trial phases	Clinical trialstatus	Sponsors/inventors	References/clinical trial registry numbers
MVA85A i.d.	MVA	Ag85A	BCG-vaccinated healthy infants	IIb	Completed	Aeras, University of Oxford	37/NCT00953927
MVA85A i.d.	MVA	Ag85A	Adults infected with HIV-1	II	Completed	Aeras, University of Oxford	50/NCT01151189
MVA85A i.m.	MVA	Ag85A	BCG-vaccinated healthy adolescents	II	Completed	University of Oxford	NCT02178748
ChAdOx1.85A i.m. -MVA85A i.m.	ChAdOx1/ MVA	Ag85A	Healthy adults and adolescents	II	Active, not recruiting	University of Oxford	NCT03681860
AERAS-402 i.m.	AdHu35	Ag85A, Ag85B, TB10.4	Adults treated for pulmonary TB	II	Completed	Aeras, Crucell	NCT02414828
AERAS-402 i.m.	AdHu35	Ag85A, Ag85B, TB10.4	HIV-infected, BCG-vaccinated adults	II	Completed	Aeras, Crucell	NCT01017536
AERAS-402 i.m.	AdHu35	Ag85A, Ag85B, TB10.4	BCG-vaccinated healthy infants	II	Completed	Aeras, Crucell	NCT01198366
TB/FLU-04L aerosol	FLU-04L	ESAT-6	BCG-vaccinated healthy adults	IIa	Unknown	Research Institute for Biological Safety Problems	NCT02501421 and unkown
AdAg85A aerosol	AdHu5	Ag85A	BCG-vaccinated healthy adults	Ib	Completed	McMaster University	70/NCT02337270
AdAg85A i.m.	AdHu5	Ag85A	BCG-naïve and -vaccinated healthy adults	I	Terminated	McMaster University	69/NCT00800670
MVA85A aerosol	MVA	Ag85A	BCG-vaccinated healthy adults	I	Completed	University of Oxford	51/NCT01497769
MVA85A aerosol-MVA85A i.d.	MVA	Ag85A	BCG-vaccinated healthy adults	I	Completed	University of Oxford	52/NCT01954563
MVA85A aerosol	MVA	Ag85A	Healthy adults with latent TB infection	I	Completed	University of Oxford, University of Birmingham	53/NCT02532036
AERAS-402 i.m.-MVA85A i.d.	AdHu35/ MVA	Ag85A	BCG-vaccinated healthy adults	I	Completed	University of Oxford, Aeras, Crucell	55/NCT01683773
MVA85A i.d.-FP85A i.d.	MVA/FP9	Ag85A	BCG-vaccinated healthy adults	I	Completed	University of Oxford	57/NCT00653770
MVA85A i.d.-IMX313 i.d.	MVA/ nanoparticle	Ag85A	BCG-vaccinated healthy adults	I	Completed	University of Oxford	58/NCT01879163

i.d., intradermal; i.m., intramuscular.

populations in which this can be undertaken and the enormous cost of clinical trials further hinder the progress of TB vaccine development.

In recent years, the concept of a controlled human infection model has come under consideration to facilitate vaccine research progress. In this model, healthy volunteers are vaccinated with candidate vaccines and then are deliberately infected with the corresponding pathogen. The efficacy of the candidate vaccine is then assessed by either presence or absence of established infection or by disease progress. Recently, Vaxchora, a Cholera vaccine, was approved based on a human challenge study (122). In the field of TB, deliberately infecting healthy volunteers with virulent *Mtb* would not be ethical, since there is currently no method of anti-TB treatment that could reliably completely eradicate infection. As an alternative, Helen McShane, a co-inventor of MVA85A, described in 2012 a model in which humans are challenged with BCG (123). In this model, BCG-naive and BCG-vaccinated healthy volunteers in the UK were challenged with intradermal BCG, and the bacterial load was quantified from punch biopsies by PCR and bacterial culture (123). This model was used to assess the protective effect of MVA85A on BCG-vaccinated healthy adults (124), the data support the contention that this intradermal BCG challenge model is able to detect differences in anti-mycobacterial immunity induced by vaccination. In addition, an aerosol BCG challenge study is now underway in healthy UK adults to mimic the natural route of exposure (NCT02709278, NCT03912207).

Recently, Sarah Fortune and Eric Rubin described the development of an *Mtb* human challenge model, in which, *Mtb*'s growth is controlled by dependence on the availability of selection compounds; the bacteria are no longer viable once those compounds are removed. The study has not yet been published but was described in a commentary paper (125). This human *Mtb* infection model could substantially reduce the numbers of participants, study duration, and economic costs in TB vaccine studies.

4.2 Ultra-Low-Dose Aerosol Murine and Non-human Primate Infection Models

In general, in pre-clinical TB vaccine efficacy evaluation, animals are always infected using a single large bolus of *Mtb* that is

TABLE 2 | Viral vectored TB vaccine candidates that are currently in preclinical animal model phases.

Candidate vaccines	Vectors	Antigens	Animals	Protective efficacy[a]	Route/dose of *Mtb* challenge	Sponsors/ inventors	References
RhCMV/TB s.c.	RhCMV	Ag85A, Ag85B, ESAT-6, Rv1733, Rv2626, Rv3407, RpfA, RpfC, RpfD	Rhesus macaques	~2[b]	i.b., 25/10 CFU	Oregon Health and Science University	(99)
MVA multiphasic s.c.	MVA	RpfB, RpfD, Ag85B, TB10.4, ESAT-6, Rv2029, Rv2626, Rv1733, Rv0111, Rv0569, Rv1813, Rv3407, Rv3478, Rv1807	Rhesus macaques	N/A	N/A	Transgene, Advanced BioScience Laboratories	(63)
ChAd3-5Ag aerosol/i.m. prime, MVA-5Ag aerosol/i.d. boost	ChAd3-MVA	Ag85B, ESAT-6, Rv1733, Rv2626, and RpfD	Rhesus macaques	NS	i.b., ~15 CFU	Biomedical Primate Research Center	(120)
rMVA.acr i.d.	MVA	α-crystallin	Guinea pigs	1.27[c]	Aerosol, 5-10 CFU	University of Delhi South Campus	(64)
SeV85AB i.n.	SeV	Ag85A, Ag85B	Mice	~0.8	Aerosol, ~100 CFU	Shanghai Public Health Clinical Center, ID Pharma	(42, 104, 105)
ChAdOx1.Rv1039c i.n.	ChAdOx1	Rv1039c	Mice	~1	Aerosol, 50-100 CFU	University of Oxford	(91)
AdCh68Ag85A i.n.	AdCh68	Ag85A	Mice	~0.7	Aerosol, ~100 CFU	McMaster University	(92, 93)
PR8.p25 i.n.	H1N1 PR8	Ag85B	Mice	~0.5	Aerosol, ~100 CFU	The University of Sydney	(97)
MCMV85A i.v.	MCMV	Ag85A	Mice	~0.6	i.n., ~200 CFU	University of Oxford, Ludwig Maximilians University	(98)
MPT51 lentivirus i.t.	Lentivirus	MPT51	Mice	~1	i.t., 1.2×10^4 CFU	Hamamatsu University School of Medicine	(106)
LAR f.p.	Lentivirus	Ag85B, Rv3425	Mice	~1[c]	i.v., 1.2×10^6 CFU	Fudan University	(107)
LV vF/85A s.c./i.n.	Lentivirus	Ag85A	Mice	NS	i.n., 5×10^6 CFU[d]	University College London	(108)
A3-Len f.p.	Lentivirus	Ag85B, Rv3425	Mice	~0.3	i.v., 6.8×10^5 CFU	Fudan University, Institute Pasteur of Shanghai	(109)
LV-AEG/SVGmu f.p.	Lentivirus	Ag85A, ESAT-6	Mice	N/A	N/A	Pasteur Institute of Iran	(110)
VSVAg85A i.n./i.m.	VSV	Ag85A	Mice	~0.6/0.1	i.n., ~100 CFU	McMaster University	(113, 114)
VSV-846 i.n.	VSV	Rv2660c, Rv3615c, Mtb10.4	Mice	~1.5	i.n., 1×10^7 CFU[d]	Soochow University	(115, 116)
rhPIV2-Ag85B i.n.	hPIV2	Ag85B	Mice	~1.9	Aerosol, ~50 CFU	National Institute for Biomedical Innovation	(117, 118)
PIV5-85A/PIV5-85B i.n.	hPIV5	Ag85A/Ag85B	Mice	~1.2/0.4	Aerosol, 50-100 CFU	University of Georgia College of Veterinary Medicine	(119)

[a]*Bacterial load log reduction compared with vector-immunized/non-immunized animals in the lung.*
[b]*Log reduction in the density of culturable Mtb (CFU/g) in all lung-draining lymph nodes.*
[c]*Bacterial load log reduction of BCG prime-candidate vaccine boost group compared with BCG immunization group.*
[d]*BCG infection.*
f.p., foot pad; i.b., intrabronchial; i.d, intradermal; i.m., intramuscular; i.n., intranasal; i.p., intraperitoneal; i.t., intratracheal; i.v., intravascular; s.c., subcutaneous; N/A, not available; NS, not significant.

delivered to the lungs by intratracheal or aerosol installation. However, in natural infection most people are infected by repeated inhalation of low doses. In animal models, the evidence for the efficacy of a TB vaccine is usually accepted as significant by the demonstration of 0.5-1 $\log_{10}$ lower numbers of *Mtb* in vaccinated compared to control animals at some point after challenge infection. A wide range of experimental and cost constraints dictate that the demonstration of larger and more meaningful effects with smaller infection challenges is difficult to achieve. Consequently, vaccine development often moves forward on the basis of modest vaccine impact compared to the potency required in human clinical efficacy testing, in which at least a 60% improvement in efficacy in prevention of the disease compared to BCG alone is required (126). These divergences between laboratory models and clinical scenarios hinder TB vaccine development.

Optimization of *Mtb* challenge doses in pre-clinical TB vaccine evaluation was undertaken in non-human primate models. Recent studies tended to use a lower dose than prior vaccine studies. For instance, in 2018, in the RhCMV/TB vaccine study, the monkeys received 10 or 25 bacteria (99). In 2019, a repeated limiting-dose challenge model used an average of 1.3 bacteria implanted weekly for 8 consecutive weeks by endobronchial installation (127). In 2020, in the BCG immunization route optimization study, the monkeys were challenged by bronchoscope with 4-36 bacteria (18). These low-dose-infection non-human primate models better mimicked the natural course of TB infection in humans and allowed investigators to observe vaccine-mediated sterilizing immunity.

In 2021, a model of ultra-low-dose aerosol infection in mice was established, in which infection was initiated by only 1-3 founding bacteria, instead of the conventional ~100 CFU dose. As in human TB, highly heterogeneous bacterial burdens, immune responses, and disease manifestations were observed in this model (128). In addition, the well-circumscribed granulomas shared features with human granulomas. Thus, this ultra-low dose infection murine model more closely replicates human disease. It is also much cheaper and easier to handle than the low-dose non-human primate models, thus, it might facilitate preclinical testing of vaccine and immunotherapeutic candidates and act as a gatekeeper to determine which vaccines show promise and warrant further testing.

4.3 T_{RM}-Mediated Anti-TB Immune Protection

T_{RM} represents a distinct subset of memory T cells that was found in the past decade. Unlike other memory T cells such as central memory and effector memory T cells, T_{RM} cells colonize local tissues infected by pathogens and remain there for a long time after the pathogen has been eliminated without participating in blood circulation (129). They have been demonstrated at sites that include the intestines, skin, urogenital tract, and lung mucosa (130–133). When the pathogen invades again, T_{RM} cells immediately sense and initiate immune responses so that the pathogen can be controlled or be eliminated at the early stage of infection. This process does not depend on memory cells in the peripheral circulation and is in the first line of defense of the body as an adaptive immune response to pathogen infection (134). In 2014, Daniel L. Barber's group reported for the first time the role of lung T_{RM} in anti-TB infection in a murine model. The *Mtb*-specific $CD4^+$ T cells in lung tissues could be divided into two populations, namely, a subpopulation of T_{RM} colonizing the lung parenchyma and other memory cell subsets circulating in the vasculature; the former were identified with molecular markers as $KLRG1^-CXCR3^+$ and the latter as $KLRG1^+CX3CR1^+$ (135). The adoptive transfer of lung *Mtb*-specific T_{RM} between mice resulted in potent immune protection (135–137). Based on these observations, our investigation of the properties of circulating CD4+ T cells in patients with active TB led us to suggest that inhibition of $KLRG1^+$ expression through the incorporation of a specific inhibitor of the Akt signaling pathway in a vaccine could enhance the protective responses in immunotherapeutic and perhaps prophylactic vaccination regimens (138).

In 2016, Stefan H. E. Kaufmann's group reported for the first time T_{RM}-mediated immune protection against TB infection, which was induced by mucosal delivery of BCG (139) and we reported that SeV85AB induced high levels of lung $CD8^+$ T_{RM} by using a comprehensive intravascular staining method (42). In the same year, several TB vaccines were also reported to be able to induce T_{RM} (140–142). In fact, as early as 2010, researchers had found that treatment with FTY720 (an immunosuppressant that blocks memory cells in circulation (143)) partially counteracted the immune protection induced by the BCG vaccine (144), indirectly demonstrating that BCG possesses the ability to induce a certain level of T_{RM}-mediated immune protection. In 2020, by using an intravascular staining method in non-human primates, intravenous BCG was shown to induce higher levels of lung parenchymal $CD4^+$ T cells compared with intradermal vaccination, and this was associated with sterilizing immunity against *Mtb* challenge (18), indicating that vaccine-induced T_{RM} also conferred *Mtb* resistance in this model.

By mimicking the route of infection in vaccination, a mucosal or intravenous vaccination might be an optimal vaccination strategy, targeting the induction of immune responses at the point of entry of the bacteria. However, the role of T_{RM} in TB protection awaits further experimental confirmation; a better understanding of vaccine-induced lung T_{RM} would facilitate novel T_{RM}-targeting vaccine designs.

4.4 Role of Trained Immunity in TB Vaccine Development

Traditionally, vaccine development is mainly focused on the induction of the adaptive immune response that elicits antigen-specific long-term immune memory against infection. However, recently it has been shown that innate immunity also plays an important role in immune memory against homologous or even heterologous challenges (145, 146). Trained immunity, a *de facto* innate immune memory, has been defined as a long-term functional reprogramming of the innate immune cells that is evoked by endogenous or exogenous insults, with the cells then returning to a non-activated state and showing altered inflammatory responses against a second challenge (147, 148).

In 2020, a randomized clinical trial of BCG vaccination in the elderly showed immune protection against heterologous infections and improved survival (149). In 2021, another investigator-blind randomized controlled trial showed that BCG vaccination at birth significantly reduced all-cause infectious disease morbidity during the neonatal period (150). Trained immunity was proposed to be implicated in such BCG-induced heterologous protection. The first report of BCG-induced trained immunity showed that BCG vaccination in healthy volunteers enhanced the release of monocyte-derived cytokines in response to unrelated bacterial and fungal pathogens, and induced lymphocyte–independent protection of immunodeficiency SCID mice against disseminated candidiasis

(151). In a study of BCG-induced trained immunity against *Mtb* infection in people, a global DNA methylation analysis revealed a stable and robust differential DNA methylation pattern among the promoters of genes belonging to immune pathways in "responders" to BCG vaccination but not in non-responders. Responders were defined as having an enhanced macrophage capacity to restrict the growth of *Mtb* associated with higher levels of IL-1β production (152). In rhesus macaques, mucosal or intravenous BCG inoculation conferred better protection against *Mtb* infection and TB disease than standard intradermal vaccination, and this was associated with the induction of enhanced trained immunity (153). β-glucan-induced trained immunity also afforded protection against *Mtb* infection (154). In contrast to BCG, *Mtb* infection impairs the development of protective trained immunity through impacting IFN-I signaling (155). These data suggest that vaccines that are aimed at enhancing trained immunity might give better protection against *Mtb* infection.

In 2018, the inventors of AdAg85A reported that respiratory infection with adenovirus could induce alveolar macrophages (AMs) that had a long-lasting memory that was sustained by an enhanced trained immunity phenotype in the local mucosal sites (156). This study suggested that non-specific trained immunity induced by the virus-vectored TB vaccine might contribute to the immune protection against *Mtb* infection. In 2020, they used a murine model of TB vaccination to investigate the role of AMs in host defense against *Mtb* and showed that respiratory mucosal immunization with AdA85A provided a type of trained immunity capable of potent protection against *Mtb* in the early stage of infection (157). In 2022, they further showed that mucosal immunization is superior to intramuscular immunization for the induction of trained immunity in AMs in a murine model of the SARS-CoV-2 vaccine (158), further adding to the evidence for the importance of local induction of trained immunity.

Cumulatively, the evidence suggests that the deciding battleground is the apoptosis of *Mtb*-infected macrophages in early infection, which is mediated by AMs and is enhanced by trained immunity. However, our understanding of the relative contribution of trained immunity to viral-vectored vaccine induction of T cell-mediated immune protection against TB remains limited. In addition, it remains to be answered that whether the anti-TB immune protection induced by BCG-prime-viral vector boost strategy is associated with the trained immunity, and the effective of live viral vector boost on innate immune training by BCG prime. Unraveling the elaborate molecular mechanisms of trained immunity will be critical for devising novel approaches to optimize the exploitation of trained immunity by TB vaccines.

4.5 Lack of Validated Immune Correlates of Protection by TB Vaccines

COPs are defined as laboratory biomarkers that are associated with protection from clinical disease. In particular, vaccine-inducible COPs are expected to be transformative in developing novel vaccines as they will de-risk the selection of candidate vaccines for human efficacy studies at an early stage. They might also substantially reduce the costs of large-scale clinical trials by helping to tailor the selection of participants being enrolled and by measuring vaccine immunogenicity and potential efficacy as a supplement, or even sometimes an alternative, to assessments of disease burden (159). Once validated in efficacy trials, COPs could potentially facilitate the development and licensure of vaccines. The absence of reliable parameters that could be used as COPs for TB vaccines represents one of the greatest challenges in TB vaccine development.

The complexities of *Mtb* infection create challenges in finding predictive markers of protective efficacy. The Th1 cytokines IFN-γ, IL-2, TNF-α, the Th17 cytokine IL-17, and other cytokines are active in the immune response against *Mtb* and are used as biomarkers to determine the antigen-specific T cell responses in TB vaccine evaluation research. However, studies have found that IFN-γ accounted for only about 30% of the $CD4^+$ T cell-mediated immune protection against *Mtb* infection; and its overexpression even accelerated death in infected mice (137). More recently, close contacts of active TB patients who were persistently negative by IFN-γ release assay and tuberculin skin tests were defined as "resisters" of *Mtb* (160) and in 2019, a cohort study showed that "resisters" possess IgM and class-switched IgG antibody responses and non-IFN-γ T cell responses to *Mtb*-specific proteins (161), challenging the rationality of focus on assessing IFN-γ-based immunogenicity in TB vaccine design. In 2020, we found that T-cell activation status marker CD69 is associated with *Mtb* infection and may have the potential to distinguish latent TB infection (positive IFN-γ responses) and "resisters" (negative IFN-γ responses) (162). Based on these and similar studies, there is an urgent need to find novel molecular markers that are more correlated with immunogenicity/protective efficacy to be able to more accurately predict the protective efficacy of vaccines and to accelerate vaccine evaluation.

As mentioned above, T_{RM} showed a potential for application among novel COPs in TB vaccine research. However, validation of vaccine-induced COPs is possible only when successful placebo-controlled efficacy trials become available. Only then can compelling comparisons be made. In 2019, a phase IIb clinical trial of the subunit TB vaccine $M72/AS01_E$ showed 49.7% efficacy against progression to TB compared with placebo control. This is the first novel TB vaccine to almost reach 50% protection in the past century (163). These vaccine cohorts offered an opportunity to identify COPs of vaccine-induced immune protection against *Mtb* infection and some strategies are in place. Bill & Melinda Gates Medical Research Institute, vaccine manufacturers, sponsors of clinical trials, and trial investigators have launched an international "TB Immune Correlate Program" consortium to identify immunological COPs for TB. The first priority is informed by existing knowledge and recent findings from animal models and clinical studies, including the magnitude of mycobacteria-specific Th1/Th17 CD4 T cell responses, magnitude/subclass/avidity of mycobacteria-specific mucosal IgA or IgG antibody responses,

Fc-mediated, functional antibody activities, and trained immunity (27). However, the relatively small number of participants that reached clinical endpoints in the M72/AS01$_E$ clinical trial might restrict the statistical power of COPs discovery. Thus, larger clinical trials or the human infection model study are needed to validate the COPs that might be identified in the ongoing efforts.

5 CONCLUSION

Identified at the end of 2019, COVID-19 became a global public health threat within 3 months, it spread over the globe so rapidly that it was declared to be a "pandemic" by the WHO in March, 2020. Vaccinologists worked on the challenge immediately, leading to the development and deployment of novel vaccines within one year. Up to February of 2022, 144 and 195 COVID-19 vaccine candidates based on diverse platform technologies are being evaluated in clinical and preclinical stages, respectively, and dozens of vaccines have already been licensed to human use (164). The rapid COVID-19 vaccine development and deployment is critical for the world to return to pre-pandemic normalcy. Ironically, the only licensed TB vaccine is still the one-century-old BCG, which is inadequate. Thus, TB remains a leading cause of mortality from an infectious disease, only now surpassed by SARS-CoV-2 causing COVID-19. Considering the morbidity and mortality that is suffered from TB globally, it is time to accelerate commitment, investment, and implementation to stop the infectious disease agent that has killed more human beings than any other.

We believe that the success of COVID-19 vaccines and recent progress in TB vaccine research illustrate that the deployment of an effective TB vaccine is likely in the near future. The highly efficacious COVID-19 vaccines accelerated the vaccine development process in human use, with the notable example of mRNA vaccines and adenovirus-vectored vaccines, and increased the public acceptance of the concept of the controlled human challenge model, which might provide valuable experience on the development of TB vaccines. In this review, we have provided an update on the current viral vectored TB vaccine pipeline and summarized the latest findings that might facilitate TB vaccine developments. On the one hand, several viral vectored TB vaccines are in clinical trials, and other promising candidate vaccines at an earlier stage of development are being evaluated in preclinical animal models, and this sharply increases the likelihood of developing an effective TB vaccine in the near future, although this is far from certain. On the other hand, we propose that a better understanding of the lung-resident T_{RM}-mediated mucosal immunity, and the unique trained immunity of phagocytic cells against intracellular *Mtb* infection, could help provide novel targets for innovative and superior TB vaccine designs. Moreover, new tools, such as controlled human infection and ultra-low-dose aerosol infection murine infection models, should facilitate TB vaccine development and selection in the preclinical phase of the investigation. In addition, identification of COPs in the M72/AS01$_E$ trial and other ongoing clinical trials could be valuable in streamlining triage and evaluation of next-generation TB vaccine candidates. Allocation of resources must include the discovery and development of early pipeline candidates to increase clinical trial capacity. With more advanced knowledge, we remain hopeful that a more effective TB vaccine will be developed sooner rather than later.

AUTHOR CONTRIBUTIONS

ZH and X-YF conceived, designed and wrote the manuscript, X-YF, S-HL and DL edited the manuscript with conceptual advice. All authors contributed to the article and approved the submitted version.

FUNDING

This work was supported by National Key Research and Development Program of China (2021YFC2301503), Grants from the National Natural and Science Foundation of China (81873884, 82171815, 82171739), Shanghai Science and Technology Commission (19XD1403100, 20Y11903400), and Shanghai Municipal Medical and Health Excellent Young Talents Training Program (GWV-10.2-YQ01).

REFERENCES

1. WHO. *WHO Globlal TB Report*. (2021). https://www.who.int/teams/global-tuberculosis-programme/tbreports/global-tuberculosis-report-2021
2. Uplekar M, Weil D, Lonnroth K, Jaramillo E, Lienhardt C, Dias HM, et al. WHO's New End TB Strategy. *Lancet* (2015) 385(9979):1799–801. doi: 10.1016/S0140-6736(15)60570-0
3. Calmette A, Guérin C, Boquet A, Nègre L. La Vaccination Préventive Contre La Tuberculose Par Le" BCG," [M]. *Masson et cie* (1927).
4. Calmette A. Preventive Vaccination Against Tuberculosis With BCG. *Proc R Soc Med* (1931) 24(11):1481–90. doi: 10.1177/003591573102401109
5. Wallgren A. Intradermal Vaccinations With BCG Virus: Preliminary Note. *J Am Med Assoc* (1928) 91(24):1876–81. doi: 10.1001/jama.1928.02700240030008
6. Lange L, Pescatore H. *Bakteriologische Untersuchungen Zur Lübecker Säuglingstuberkulose. Die Säuglingstuberkulose in Lübeck*. Springer (1935) 205–305. Available at: https://link.springer.com/chapter/10.1007/978-3-642-92013-4_3
7. Fine PE, Carneiro IA, Milstien JB, Clements CJOrganization WH. *Issues Relating to the Use of BCG in Immunization Programmes: A Discussion Document*. World Health Organization (1999). Available at: https://apps.who.int/iris/bitstream/handle/10665/66120/WHO_V_B_99.23.pdf
8. Lobo N, Brooks NA, Zlotta AR, Cirillo JD, Boorjian S, Black PC, et al. 100 Years of Bacillus Calmette-Guerin Immunotherapy: From Cattle to COVID-19. *Nat Rev Urol* (2021) 18(10):611–22. doi: 10.1038/s41585-021-00481-1
9. Organization WH. *WHO-UNICEF Estimates of BCG Coverage*. (2020). https://apps.who.int/immunization_monitoring/globalsummary/timeseries/tswucoveragebcg.html

10. Trunz BB, Fine P, Dye C. Effect of BCG Vaccination on Childhood Tuberculous Meningitis and Miliary Tuberculosis Worldwide: A Meta-Analysis and Assessment of Cost-Effectiveness. *Lancet* (2006) 367 (9517):1173–80. doi: 10.1016/S0140-6736(06)68507-3
11. Mangtani P, Abubakar I, Ariti C, Beynon R, Pimpin L, Fine PE, et al. Protection by BCG Vaccine Against Tuberculosis: A Systematic Review of Randomized Controlled Trials. *Clin Infect Dis* (2014) 58(4):470–80. doi: 10.1093/cid/cit790
12. Whittaker E, Nicol MP, Zar HJ, Tena-Coki NG, Kampmann B. Age-Related Waning of Immune Responses to BCG in Healthy Children Supports the Need for a Booster Dose of BCG in TB Endemic Countries. *Sci Rep* (2018) 8 (1):15309. doi: 10.1038/s41598-018-33499-4
13. Nguipdop-Djomo P, Heldal E, Rodrigues LC, Abubakar I, Mangtani P. Duration of BCG Protection Against Tuberculosis and Change in Effectiveness With Time Since Vaccination in Norway: A Retrospective Population-Based Cohort Study. *Lancet Infect Dis* (2016) 16(2):219–26. doi: 10.1016/S1473-3099(15)00400-4
14. Abubakar I, Pimpin L, Ariti C, Beynon R, Mangtani P, Sterne JA, et al. Systematic Review and Meta-Analysis of the Current Evidence on the Duration of Protection by Bacillus Calmette-Guerin Vaccination Against Tuberculosis. *Health Technol Assess* (2013) 17(37):1–372v–vi. doi: 10.3310/hta17370
15. Rhodes SJ, Knight GM, Fielding K, Scriba TJ, Pathan AA, McShane H, et al. Individual-Level Factors Associated With Variation in Mycobacterial-Specific Immune Response: Gender and Previous BCG Vaccination Status. *Tuberculosis (Edinb)* (2016) 96:37–43. doi: 10.1016/j.tube.2015.10.002
16. Mangtani P, Nguipdop-Djomo P, Keogh RH, Trinder L, Smith PG, Fine PE, et al. Observational Study to Estimate the Changes in the Effectiveness of Bacillus Calmette-Guerin (BCG) Vaccination With Time Since Vaccination for Preventing Tuberculosis in the UK. *Health Technol Assess* (2017) 21 (39):1–54. doi: 10.3310/hta21390
17. Nemes E, Geldenhuys H, Rozot V, Rutkowski KT, Ratangee F, Bilek N, et al. Prevention of M. Tuberculosis Infection With H4:IC31 Vaccine or BCG Revaccination. *N Engl J Med* (2018) 379(2):138–49. doi: 10.1056/NEJMoa1714021
18. Darrah PA, Zeppa JJ, Maiello P, Hackney JA, Wadsworth MH2nd, Hughes TK, et al. Prevention of Tuberculosis in Macaques After Intravenous BCG Immunization. *Nature* (2020) 577(7788):95–102. doi: 10.1038/s41586-019-1817-8
19. Kaufmann SHE. Vaccine Development Against Tuberculosis Over the Last 140 Years: Failure as Part of Success. *Front Microbiol* (2021) 12:750124. doi: 10.3389/fmicb.2021.750124
20. Ura T, Okuda K, Shimada M. Developments in Viral Vector-Based Vaccines. *Vaccines (Basel)* (2014) 2(3):624–41. doi: 10.3390/vaccines2030624
21. Dalmia N, Ramsay AJ. Prime-Boost Approaches to Tuberculosis Vaccine Development. *Expert Rev Vaccines* (2012) 11(10):1221–33. doi: 10.1586/erv.12.94
22. Rollier CS, Reyes-Sandoval A, Cottingham MG, Ewer K, Hill AV. Viral Vectors as Vaccine Platforms: Deployment in Sight. *Curr Opin Immunol* (2011) 23(3):377–82. doi: 10.1016/j.coi.2011.03.006
23. Sasso E, D'Alise AM, Zambrano N, Scarselli E, Folgori A, Nicosia A. New Viral Vectors for Infectious Diseases and Cancer. *Semin Immunol* (2020) 50:101430. doi: 10.1016/j.smim.2020.101430
24. Ertl HC. Viral Vectors as Vaccine Carriers. *Curr Opin Virol* (2016) 21:1–8. doi: 10.1016/j.coviro.2016.06.001
25. Chen CY, Huang D, Wang RC, Shen L, Zeng G, Yao S, et al. A Critical Role for CD8 T Cells in a Nonhuman Primate Model of Tuberculosis. *PloS Pathog* (2009) 5(4):e1000392. doi: 10.1371/journal.ppat.1000392
26. Prezzemolo T, Guggino G, La Manna MP, Di Liberto D, Dieli F, Caccamo N. Functional Signatures of Human CD4 and CD8 T Cell Responses to Mycobacterium Tuberculosis. *Front Immunol* (2014) 5:180. doi: 10.3389/fimmu.2014.00180
27. Scriba TJ, Netea MG, Ginsberg AM. Key Recent Advances in TB Vaccine Development and Understanding of Protective Immune Responses Against Mycobacterium Tuberculosis. *Semin Immunol* (2020) 50:101431. doi: 10.1016/j.smim.2020.101431
28. Paoletti E. Poxvirus Recombinant Vaccines. *Ann N Y Acad Sci* (1990) 590:309–25. doi: 10.1111/j.1749-6632.1990.tb42239.x
29. Diven DG. An Overview of Poxviruses. *J Am Acad Dermatol* (2001) 44(1):1–16. doi: 10.1067/mjd.2001.109302
30. Copeman SM. Pathology of Vaccinia and Variola. *Br Med J* (1896) 1 (1827):7–10. doi: 10.1136/bmj.1.1827.7
31. Moss B. Genetically Engineered Poxviruses for Recombinant Gene Expression, Vaccination, and Safety. *Proc Natl Acad Sci U S A* (1996) 93 (21):11341–8. doi: 10.1073/pnas.93.21.11341
32. Kaynarcalidan O, Moreno Mascaraque S, Drexler I. Vaccinia Virus: From Crude Smallpox Vaccines to Elaborate Viral Vector Vaccine Design. *Biomedicines* (2021) 9(12):1780. doi: 10.3390/biomedicines9121780
33. Pantaleo G, Esteban M, Jacobs B, Tartaglia J. Poxvirus Vector-Based HIV Vaccines. *Curr Opin HIV AIDS* (2010) 5(5):391–6. doi: 10.1097/COH.0b013e32833d1e87
34. Gomez CE, Perdiguero B, Najera JL, Sorzano CO, Jimenez V, Gonzalez-Sanz R, et al. Removal of Vaccinia Virus Genes That Block Interferon Type I and II Pathways Improves Adaptive and Memory Responses of the HIV/AIDS Vaccine Candidate NYVAC-C in Mice. *J Virol* (2012) 86(9):5026–38. doi: 10.1128/JVI.06684-11
35. Garcia-Arriaza J, Esteban M. Enhancing Poxvirus Vectors Vaccine Immunogenicity. *Hum Vaccin Immunother* (2014) 10(8):2235–44. doi: 10.4161/hv.28974
36. Sutter G, Wyatt LS, Foley PL, Bennink JR, Moss B. A Recombinant Vector Derived From the Host Range-Restricted and Highly Attenuated MVA Strain of Vaccinia Virus Stimulates Protective Immunity in Mice to Influenza Virus. *Vaccine* (1994) 12(11):1032–40. doi: 10.1016/0264-410X(94)90341-7
37. Tartaglia J, Perkus ME, Taylor J, Norton EK, Audonnet JC, Cox WI, et al. NYVAC: A Highly Attenuated Strain of Vaccinia Virus. *Virology* (1992) 188 (1):217–32. doi: 10.1016/0042-6822(92)90752-B
38. Paoletti E, Taylor J, Meignier B, Meric C, Tartaglia J. Highly Attenuated Poxvirus Vectors: NYVAC, ALVAC and TROVAC. *Dev Biol Stand* (1995) 84:159–63.
39. Hu Z, Wang J, Wan Y, Zhu L, Ren X, Qiu S, et al. Boosting Functional Avidity of CD8+ T Cells by Vaccinia Virus Vaccination Depends on Intrinsic T-Cell MyD88 Expression But Not the Inflammatory Milieu. *J Virol* (2014) 88(10):5356–68. doi: 10.1128/JVI.03664-13
40. Tameris MD, Hatherill M, Landry BS, Scriba TJ, Snowden MA, Lockhart S, et al. Safety and Efficacy of MVA85A, a New Tuberculosis Vaccine, in Infants Previously Vaccinated With BCG: A Randomised, Placebo-Controlled Phase 2b Trial. *Lancet* (2013) 381(9871):1021–8. doi: 10.1016/S0140-6736(13)60177-4
41. Ibanga HB, Brookes RH, Hill PC, Owiafe PK, Fletcher HA, Lienhardt C, et al. Early Clinical Trials With a New Tuberculosis Vaccine, MVA85A, in Tuberculosis-Endemic Countries: Issues in Study Design. *Lancet Infect Dis* (2006) 6(8):522–8. doi: 10.1016/S1473-3099(06)70552-7
42. Hu Z, Wong KW, Zhao HM, Wen HL, Ji P, Ma H, et al. Sendai Virus Mucosal Vaccination Establishes Lung-Resident Memory CD8 T Cell Immunity and Boosts BCG-Primed Protection Against TB in Mice. *Mol Ther* (2017) 25(5):1222–33. doi: 10.1016/j.ymthe.2017.02.018
43. McShane H, Brookes R, Gilbert SC, Hill AV. Enhanced Immunogenicity of CD4(+) T-Cell Responses and Protective Efficacy of a DNA-Modified Vaccinia Virus Ankara Prime-Boost Vaccination Regimen for Murine Tuberculosis. *Infect Immun* (2001) 69(2):681–6. doi: 10.1128/IAI.69.2.681-686.2001
44. McShane H, Behboudi S, Goonetilleke N, Brookes R, Hill AV. Protective Immunity Against Mycobacterium Tuberculosis Induced by Dendritic Cells Pulsed With Both CD8(+)- and CD4(+)-T-Cell Epitopes From Antigen 85A. *Infect Immun* (2002) 70(3):1623–6. doi: 10.1128/IAI.70.3.1623-1626.2002
45. Goonetilleke NP, McShane H, Hannan CM, Anderson RJ, Brookes RH, Hill AV. Enhanced Immunogenicity and Protective Efficacy Against Mycobacterium Tuberculosis of Bacille Calmette-Guerin Vaccine Using Mucosal Administration and Boosting With a Recombinant Modified Vaccinia Virus Ankara. *J Immunol* (2003) 171(3):1602–9. doi: 10.4049/jimmunol.171.3.1602
46. Williams A, Goonetilleke NP, McShane H, Clark SO, Hatch G, Gilbert SC, et al. Boosting With Poxviruses Enhances Mycobacterium Bovis BCG Efficacy Against Tuberculosis in Guinea Pigs. *Infect Immun* (2005) 73 (6):3814–6. doi: 10.1128/IAI.73.6.3814-3816.2005

47. Vordermeier HM, Rhodes SG, Dean G, Goonetilleke N, Huygen K, Hill AV, et al. Cellular Immune Responses Induced in Cattle by Heterologous Prime-Boost Vaccination Using Recombinant Viruses and Bacille Calmette-Guerin. *Immunology* (2004) 112(3):461–70. doi: 10.1111/j.1365-2567.2004.01903.x
48. Verreck FA, Vervenne RA, Kondova I, van Kralingen KW, Remarque EJ, Braskamp G, et al. MVA.85A Boosting of BCG and an Attenuated, phoP Deficient M. Tuberculosis Vaccine Both Show Protective Efficacy Against Tuberculosis in Rhesus Macaques. *PloS One* (2009) 4(4):e5264. doi: 10.1371/journal.pone.0005264
49. McShane H, Pathan AA, Sander CR, Keating SM, Gilbert SC, Huygen K, et al. Recombinant Modified Vaccinia Virus Ankara Expressing Antigen 85A Boosts BCG-Primed and Naturally Acquired Antimycobacterial Immunity in Humans. *Nat Med* (2004) 10(11):1240–4. doi: 10.1038/nm1128
50. Scriba TJ, Tameris M, Mansoor N, Smit E, van der Merwe L, Isaacs F, et al. Modified Vaccinia Ankara-Expressing Ag85A, a Novel Tuberculosis Vaccine, is Safe in Adolescents and Children, and Induces Polyfunctional CD4+ T Cells. *Eur J Immunol* (2010) 40(1):279–90. doi: 10.1002/eji.200939754
51. Pathan AA, Minassian AM, Sander CR, Rowland R, Porter DW, Poulton ID, et al. Effect of Vaccine Dose on the Safety and Immunogenicity of a Candidate TB Vaccine, MVA85A, in BCG Vaccinated UK Adults. *Vaccine* (2012) 30(38):5616–24. doi: 10.1016/j.vaccine.2012.06.084
52. Meyer J, Harris SA, Satti I, Poulton ID, Poyntz HC, Tanner R, et al. Comparing the Safety and Immunogenicity of a Candidate TB Vaccine MVA85A Administered by Intramuscular and Intradermal Delivery. *Vaccine* (2013) 31(7):1026–33. doi: 10.1016/j.vaccine.2012.12.042
53. Tchilian EZ, Desel C, Forbes EK, Bandermann S, Sander CR, Hill AV, et al. Immunogenicity and Protective Efficacy of Prime-Boost Regimens With Recombinant (Delta)ureC Hly+ Mycobacterium Bovis BCG and Modified Vaccinia Virus Ankara Expressing M. Tuberculosis Antigen 85A Against Murine Tuberculosis. *Infect Immun* (2009) 77(2):622–31. doi: 10.1128/IAI.00685-08
54. Ndiaye BP, Thienemann F, Ota M, Landry BS, Camara M, Dieye S, et al. Safety, Immunogenicity, and Efficacy of the Candidate Tuberculosis Vaccine MVA85A in Healthy Adults Infected With HIV-1: A Randomised, Placebo-Controlled, Phase 2 Trial. *Lancet Respir Med* (2015) 3(3):190–200. doi: 10.1016/S2213-2600(15)00037-5
55. Satti I, Meyer J, Harris SA, Manjaly Thomas ZR, Griffiths K, Antrobus RD, et al. Safety and Immunogenicity of a Candidate Tuberculosis Vaccine MVA85A Delivered by Aerosol in BCG-Vaccinated Healthy Adults: A Phase 1, Double-Blind, Randomised Controlled Trial. *Lancet Infect Dis* (2014) 14(10):939–46. doi: 10.1016/S1473-3099(14)70845-X
56. Manjaly Thomas ZR, Satti I, Marshall JL, Harris SA, Lopez Ramon R, Hamidi A, et al. Alternate Aerosol and Systemic Immunisation With a Recombinant Viral Vector for Tuberculosis, MVA85A: A Phase I Randomised Controlled Trial. *PloS Med* (2019) 16(4):e1002790. doi: 10.1371/journal.pmed.1002790
57. Riste M, Marshall JL, Satti I, Harris SA, Wilkie M, Lopez Ramon R, et al. Phase I Trial Evaluating the Safety and Immunogenicity of Candidate TB Vaccine MVA85A, Delivered by Aerosol to Healthy M.tb-Infected Adults. *Vaccines (Basel)* (2021) 9(4):396. doi: 10.3390/vaccines9040396
58. Nemes E, Hesseling AC, Tameris M, Mauff K, Downing K, Mulenga H, et al. Safety and Immunogenicity of Newborn MVA85A Vaccination and Selective, Delayed Bacille Calmette-Guerin for Infants of Human Immunodeficiency Virus-Infected Mothers: A Phase 2 Randomized, Controlled Trial. *Clin Infect Dis* (2018) 66(4):554–63. doi: 10.1093/cid/cix834
59. Sheehan S, Harris SA, Satti I, Hokey DA, Dheenadhayalan V, Stockdale L, et al. A Phase I, Open-Label Trial, Evaluating the Safety and Immunogenicity of Candidate Tuberculosis Vaccines AERAS-402 and MVA85A, Administered by Prime-Boost Regime in BCG-Vaccinated Healthy Adults. *PloS One* (2015) 10(11):e0141687. doi: 10.1371/journal.pone.0141687
60. Wilkie M, Satti I, Minhinnick A, Harris S, Riste M, Ramon RL, et al. A Phase I Trial Evaluating the Safety and Immunogenicity of a Candidate Tuberculosis Vaccination Regimen, ChAdOx1 85A Prime - MVA85A Boost in Healthy UK Adults. *Vaccine* (2020) 38(4):779–89. doi: 10.1016/j.vaccine.2019.10.102
61. Rowland R, Pathan AA, Satti I, Poulton ID, Matsumiya MM, Whittaker M, et al. Safety and Immunogenicity of an FP9-Vectored Candidate Tuberculosis Vaccine (FP85A), Alone and With Candidate Vaccine MVA85A in BCG-Vaccinated Healthy Adults: A Phase I Clinical Trial. *Hum Vaccin Immunother* (2013) 9(1):50–62. doi: 10.4161/hv.22464
62. Minhinnick A, Satti I, Harris S, Wilkie M, Sheehan S, Stockdale L, et al. A First-in-Human Phase 1 Trial to Evaluate the Safety and Immunogenicity of the Candidate Tuberculosis Vaccine MVA85A-IMX313, Administered to BCG-Vaccinated Adults. *Vaccine* (2016) 34(11):1412–21. doi: 10.1016/j.vaccine.2016.01.062
63. Leung-Theung-Long S, Gouanvic M, Coupet CA, Ray A, Tupin E, Silvestre N, et al. A Novel MVA-Based Multiphasic Vaccine for Prevention or Treatment of Tuberculosis Induces Broad and Multifunctional Cell-Mediated Immunity in Mice and Primates. *PloS One* (2015) 10(11):e0143552. doi: 10.1371/journal.pone.0143552
64. Nangpal P, Bahal RK, Tyagi AK. Boosting With Recombinant MVA Expressing M. Tuberculosis Alpha-Crystallin Antigen Augments the Protection Imparted by BCG Against Tuberculosis in Guinea Pigs. *Sci Rep* (2017) 7(1):17286. doi: 10.1038/s41598-017-17587-5
65. Smaill F, Jeyanathan M, Smieja M, Medina MF, Thanthrige-Don N, Zganiacz A, et al. A Human Type 5 Adenovirus-Based Tuberculosis Vaccine Induces Robust T Cell Responses in Humans Despite Preexisting Anti-Adenovirus Immunity. *Sci Transl Med* (2013) 5(205):205ra134. doi: 10.1126/scitranslmed.3006843
66. Jeyanathan M, Fritz DK, Afkhami S, Aguirre E, Howie KJ, Zganiacz A, et al. Aerosol Delivery, But Not Intramuscular Injection, of Adenovirus-Vectored Tuberculosis Vaccine Induces Respiratory-Mucosal Immunity in Humans. *JCI Insight* (2022) 7(3):e155655. doi: 10.1172/jci.insight.155655
67. Abel B, Tameris M, Mansoor N, Gelderbloem S, Hughes J, Abrahams D, et al. The Novel Tuberculosis Vaccine, AERAS-402, Induces Robust and Polyfunctional CD4+ and CD8+ T Cells in Adults. *Am J Respir Crit Care Med* (2010) 181(12):1407–17. doi: 10.1164/rccm.200910-1484OC
68. Kagina BM, Tameris MD, Geldenhuys H, Hatherill M, Abel B, Hussey GD, et al. The Novel Tuberculosis Vaccine, AERAS-402, is Safe in Healthy Infants Previously Vaccinated With BCG, and Induces Dose-Dependent CD4 and CD8T Cell Responses. *Vaccine* (2014) 32(45):5908–17. doi: 10.1016/j.vaccine.2014.09.001
69. Hoft DF, Blazevic A, Stanley J, Landry B, Sizemore D, Kpamegan E, et al. A Recombinant Adenovirus Expressing Immunodominant TB Antigens can Significantly Enhance BCG-Induced Human Immunity. *Vaccine* (2012) 30(12):2098–108. doi: 10.1016/j.vaccine.2012.01.048
70. van Zyl-Smit RN, Esmail A, Bateman ME, Dawson R, Goldin J, van Rikxoort E, et al. Safety and Immunogenicity of Adenovirus 35 Tuberculosis Vaccine Candidate in Adults With Active or Previous Tuberculosis. A Randomized Trial. *Am J Respir Crit Care Med* (2017) 195(9):1171–80. doi: 10.1164/rccm.201603-0654OC
71. Walsh DS, Owira V, Polhemus M, Otieno L, Andagalu B, Ogutu B, et al. Adenovirus Type 35-Vectored Tuberculosis Vaccine has an Acceptable Safety and Tolerability Profile in Healthy, BCG-Vaccinated, QuantiFERON((R))-TB Gold (+) Kenyan Adults Without Evidence of Tuberculosis. *Vaccine* (2016) 34(21):2430–6. doi: 10.1016/j.vaccine.2016.03.069
72. Churchyard GJ, Snowden MA, Hokey D, Dheenadhayalan V, McClain JB, Douoguih M, et al. The Safety and Immunogenicity of an Adenovirus Type 35-Vectored TB Vaccine in HIV-Infected, BCG-Vaccinated Adults With CD4(+) T Cell Counts >350 Cells/Mm(3). *Vaccine* (2015) 33(15):1890–6. doi: 10.1016/j.vaccine.2015.02.004
73. Sivakumaran D, Blatner G, Bakken R, Hokey D, Ritz C, Jenum S, et al. A 2-Dose AERAS-402 Regimen Boosts CD8(+) Polyfunctionality in HIV-Negative, BCG-Vaccinated Recipients. *Front Immunol* (2021) 12:673532. doi: 10.3389/fimmu.2021.673532
74. Wang J, Thorson L, Stokes RW, Santosuosso M, Huygen K, Zganiacz A, et al. Single Mucosal, But Not Parenteral, Immunization With Recombinant Adenoviral-Based Vaccine Provides Potent Protection From Pulmonary Tuberculosis. *J Immunol* (2004) 173(10):6357–65. doi: 10.4049/jimmunol.173.10.6357
75. Santosuosso M, Zhang X, McCormick S, Wang J, Hitt M, Xing Z. Mechanisms of Mucosal and Parenteral Tuberculosis Vaccinations:

Adenoviral-Based Mucosal Immunization Preferentially Elicits Sustained Accumulation of Immune Protective CD4 and CD8 T Cells Within the Airway Lumen. *J Immunol* (2005) 174(12):7986–94. doi: 10.4049/jimmunol.174.12.7986
76. Santosuosso M, McCormick S, Zhang X, Zganiacz A, Xing Z. Intranasal Boosting With an Adenovirus-Vectored Vaccine Markedly Enhances Protection by Parenteral Mycobacterium Bovis BCG Immunization Against Pulmonary Tuberculosis. *Infect Immun* (2006) 74(8):4634–43. doi: 10.1128/IAI.00517-06
77. Santosuosso M, McCormick S, Roediger E, Zhang X, Zganiacz A, Lichty BD, et al. Mucosal Luminal Manipulation of T Cell Geography Switches on Protective Efficacy by Otherwise Ineffective Parenteral Genetic Immunization. *J Immunol* (2007) 178(4):2387–95. doi: 10.4049/jimmunol.178.4.2387
78. Xing Z, McFarland CT, Sallenave JM, Izzo A, Wang J, McMurray DN. Intranasal Mucosal Boosting With an Adenovirus-Vectored Vaccine Markedly Enhances the Protection of BCG-Primed Guinea Pigs Against Pulmonary Tuberculosis. *PloS One* (2009) 4(6):e5856. doi: 10.1371/journal.pone.0005856
79. Vordermeier HM, Villarreal-Ramos B, Cockle PJ, McAulay M, Rhodes SG, Thacker T, et al. Viral Booster Vaccines Improve Mycobacterium Bovis BCG-Induced Protection Against Bovine Tuberculosis. *Infect Immun* (2009) 77(8):3364–73. doi: 10.1128/IAI.00287-09
80. Perez de Val B, Villarreal-Ramos B, Nofrarias M, Lopez-Soria S, Romera N, Singh M, et al. Goats Primed With Mycobacterium Bovis BCG and Boosted With a Recombinant Adenovirus Expressing Ag85A Show Enhanced Protection Against Tuberculosis. *Clin Vaccine Immunol* (2012) 19 (9):1339–47. doi: 10.1128/CVI.00275-12
81. Jeyanathan M, Shao Z, Yu X, Harkness R, Jiang R, Li J, et al. AdHu5Ag85A Respiratory Mucosal Boost Immunization Enhances Protection Against Pulmonary Tuberculosis in BCG-Primed Non-Human Primates. *PloS One* (2015) 10(8):e0135009. doi: 10.1371/journal.pone.0135009
82. Sekaly RP. The Failed HIV Merck Vaccine Study: A Step Back or a Launching Point for Future Vaccine Development? *J Exp Med* (2008) 205 (1):7–12. doi: 10.1084/jem.20072681
83. Quinn KM, Da Costa A, Yamamoto A, Berry D, Lindsay RW, Darrah PA, et al. Comparative Analysis of the Magnitude, Quality, Phenotype, and Protective Capacity of Simian Immunodeficiency Virus Gag-Specific CD8+ T Cells Following Human-, Simian-, and Chimpanzee-Derived Recombinant Adenoviral Vector Immunization. *J Immunol* (2013) 190 (6):2720–35. doi: 10.4049/jimmunol.1202861
84. Quinn KM, Zak DE, Costa A, Yamamoto A, Kastenmuller K, Hill BJ, et al. Antigen Expression Determines Adenoviral Vaccine Potency Independent of IFN and STING Signaling. *J Clin Invest* (2015) 125(3):1129–46. doi: 10.1172/JCI78280
85. Radosevic K, Wieland CW, Rodriguez A, Weverling GJ, Mintardjo R, Gillissen G, et al. Protective Immune Responses to a Recombinant Adenovirus Type 35 Tuberculosis Vaccine in Two Mouse Strains: CD4 and CD8 T-Cell Epitope Mapping and Role of Gamma Interferon. *Infect Immun* (2007) 75(8):4105–15. doi: 10.1128/IAI.00004-07
86. Darrah PA, Bolton DL, Lackner AA, Kaushal D, Aye PP, Mehra S, et al. Aerosol Vaccination With AERAS-402 Elicits Robust Cellular Immune Responses in the Lungs of Rhesus Macaques But Fails to Protect Against High-Dose Mycobacterium Tuberculosis Challenge. *J Immunol* (2014) 193 (4):1799–811. doi: 10.4049/jimmunol.1400676
87. Magalhaes I, Sizemore DR, Ahmed RK, Mueller S, Wehlin L, Scanga C, et al. rBCG Induces Strong Antigen-Specific T Cell Responses in Rhesus Macaques in a Prime-Boost Setting With an Adenovirus 35 Tuberculosis Vaccine Vector. *PloS One* (2008) 3(11):e3790. doi: 10.1371/journal.pone.0003790
88. Hokey DA, Wachholder R, Darrah PA, Bolton DL, Barouch DH, Hill K, et al. A Nonhuman Primate Toxicology and Immunogenicity Study Evaluating Aerosol Delivery of AERAS-402/Ad35 Vaccine: Evidence for Transient T Cell Responses in Peripheral Blood and Robust Sustained Responses in the Lungs. *Hum Vaccin Immunother* (2014) 10(8):2199–210. doi: 10.4161/hv.29108
89. Stylianou E, Griffiths KL, Poyntz HC, Harrington-Kandt R, Dicks MD, Stockdale L, et al. Improvement of BCG Protective Efficacy With a Novel Chimpanzee Adenovirus and a Modified Vaccinia Ankara Virus Both Expressing Ag85A. *Vaccine* (2015) 33(48):6800–8. doi: 10.1016/j.vaccine.2015.10.017
90. Pinpathomrat N, Bull N, Pasricha J, Harrington-Kandt R, McShane H, Stylianou E. Using an Effective TB Vaccination Regimen to Identify Immune Responses Associated With Protection in the Murine Model. *Vaccine* (2021) 39(9):1452–62. doi: 10.1016/j.vaccine.2021.01.034
91. Stylianou E, Harrington-Kandt R, Beglov J, Bull N, Pinpathomrat N, Swarbrick GM, et al. Identification and Evaluation of Novel Protective Antigens for the Development of a Candidate Tuberculosis Subunit Vaccine. *Infect Immun* (2018) 86(7):e00014-18. doi: 10.1128/IAI.00014-18
92. Jeyanathan M, Thanthrige-Don N, Afkhami S, Lai R, Damjanovic D, Zganiacz A, et al. Novel Chimpanzee Adenovirus-Vectored Respiratory Mucosal Tuberculosis Vaccine: Overcoming Local Anti-Human Adenovirus Immunity for Potent TB Protection. *Mucosal Immunol* (2015) 8(6):1373–87. doi: 10.1038/mi.2015.29
93. Afkhami S, Lai R, D'Agostino MR, Vaseghi-Shanjani M, Zganiacz A, Yao Y, et al. Single-Dose Mucosal Immunotherapy With Chimpanzee Adenovirus-Based Vaccine Accelerates Tuberculosis Disease Control and Limits Its Rebound After Antibiotic Cessation. *J Infect Dis* (2019) 220(8):1355–66. doi: 10.1093/infdis/jiz306
94. Stukova MA, Sereinig S, Zabolotnyh NV, Ferko B, Kittel C, Romanova J, et al. Vaccine Potential of Influenza Vectors Expressing Mycobacterium Tuberculosis ESAT-6 Protein. *Tuberculosis (Edinb)* (2006) 86(3-4):236–46. doi: 10.1016/j.tube.2006.01.010
95. Sereinig S, Stukova M, Zabolotnyh N, Ferko B, Kittel C, Romanova J, et al. Influenza Virus NS Vectors Expressing the Mycobacterium Tuberculosis ESAT-6 Protein Induce CD4+ Th1 Immune Response and Protect Animals Against Tuberculosis Challenge. *Clin Vaccine Immunol* (2006) 13(8):898–904. doi: 10.1128/CVI.00056-06
96. WHO. *WHO Global TB Report*. (2017). https://apps.who.int/iris/bitstream/handle/10665/259366/9789241565516-eng.pdf?sequence=1
97. Florido M, Muflihah H, Lin LCW, Xia Y, Sierro F, Palendira M, et al. Pulmonary Immunization With a Recombinant Influenza A Virus Vaccine Induces Lung-Resident CD4(+) Memory T Cells That are Associated With Protection Against Tuberculosis. *Mucosal Immunol* (2018) 11(6):1743–52. doi: 10.1038/s41385-018-0065-9
98. Beverley PC, Ruzsics Z, Hey A, Hutchings C, Boos S, Bolinger B, et al. A Novel Murine Cytomegalovirus Vaccine Vector Protects Against Mycobacterium Tuberculosis. *J Immunol* (2014) 193(5):2306–16. doi: 10.4049/jimmunol.1302523
99. Hansen SG, Zak DE, Xu G, Ford JC, Marshall EE, Malouli D, et al. Prevention of Tuberculosis in Rhesus Macaques by a Cytomegalovirus-Based Vaccine. *Nat Med* (2018) 24(2):130–43. doi: 10.1038/nm.4473
100. Abad-Fernandez M, Goonetilleke N. Human Cytomegalovirus-Vectored Vaccines Against HIV. *Curr Opin HIV AIDS* (2019) 14(2):137–42. doi: 10.1097/COH.0000000000000524
101. Gugliesi F, Coscia A, Griffante G, Galitska G, Pasquero S, Albano C, et al. Where do We Stand After Decades of Studying Human Cytomegalovirus? *Microorganisms* (2020) 8(5):685. doi: 10.3390/microorganisms8050685
102. Stockdale L, Nash S, Farmer R, Raynes J, Mallikaarjun S, Newton R, et al. Cytomegalovirus Antibody Responses Associated With Increased Risk of Tuberculosis Disease in Ugandan Adults. *J Infect Dis* (2020) 221(7):1127–34. doi: 10.1093/infdis/jiz581
103. van der Heijden YF, Zhang B, Chougnet CA, Huaman MA. Cytomegalovirus Infection Is Associated With Increased Prevalence of Latent Tuberculosis Infection. *Open Forum Infect Dis* (2021) 8(11):ofab539. doi: 10.1093/ofid/ofab539
104. Hu Z, Gu L, Li CL, Shu T, Lowrie DB, Fan XY. The Profile of T Cell Responses in Bacille Calmette-Guerin-Primed Mice Boosted by a Novel Sendai Virus Vectored Anti-Tuberculosis Vaccine. *Front Immunol* (2018) 9:1796. doi: 10.3389/fimmu.2018.01796
105. Hu Z, Jiang W, Gu L, Qiao D, Shu T, Lowrie DB, et al. Heterologous Prime-Boost Vaccination Against Tuberculosis With Recombinant Sendai Virus and DNA Vaccines. *J Mol Med (Berl)* (2019) 97(12):1685–94. doi: 10.1007/s00109-019-01844-3
106. Hashimoto D, Nagata T, Uchijima M, Seto S, Suda T, Chida K, et al. Intratracheal Administration of Third-Generation Lentivirus Vector Encoding MPT51 From Mycobacterium Tuberculosis Induces Specific

CD8+ T-Cell Responses in the Lung. *Vaccine* (2008) 26(40):5095–100. doi: 10.1016/j.vaccine.2008.03.101
107. Xu Y, Yang E, Wang J, Li R, Li G, Liu G, et al. Prime-Boost Bacillus Calmette-Guerin Vaccination With Lentivirus-Vectored and DNA-Based Vaccines Expressing Antigens Ag85B and Rv3425 Improves Protective Efficacy Against Mycobacterium Tuberculosis in Mice. *Immunology* (2014) 143 (2):277–86. doi: 10.1111/imm.12308
108. Britton G, MacDonald DC, Brown JS, Collins MK, Goodman AL. Using a Prime and Pull Approach, Lentivector Vaccines Expressing Ag85A Induce Immunogenicity But Fail to Induce Protection Against Mycobacterium Bovis Bacillus Calmette-Guerin Challenge in Mice. *Immunology* (2015) 146 (2):264–70. doi: 10.1111/imm.12498
109. Yang E, Wang F, Xu Y, Wang H, Hu Y, Shen H, et al. A Lentiviral Vector-Based Therapeutic Vaccine Encoding Ag85B-Rv3425 Potently Increases Resistance to Acute Tuberculosis Infection in Mice. *Acta Biochim Biophys Sin (Shanghai)* (2015) 47(8):588–96. doi: 10.1093/abbs/gmv059
110. Shakouri M, Moazzeni SM, Ghanei M, Arashkia A, Etemadzadeh MH, Azadmanesh K. A Novel Dendritic Cell-Targeted Lentiviral Vector, Encoding Ag85A-ESAT6 Fusion Gene of Mycobacterium Tuberculosis, Could Elicit Potent Cell-Mediated Immune Responses in Mice. *Mol Immunol* (2016) 75:101–11. doi: 10.1016/j.molimm.2016.04.014
111. Kalos M, Levine BL, Porter DL, Katz S, Grupp SA, Bagg A, et al. T Cells With Chimeric Antigen Receptors Have Potent Antitumor Effects and can Establish Memory in Patients With Advanced Leukemia. *Sci Transl Med* (2011) 3(95):95ra73. doi: 10.1126/scitranslmed.3002842
112. Gutierrez-Guerrero A, Cosset FL, Verhoeyen E. Lentiviral Vector Pseudotypes: Precious Tools to Improve Gene Modification of Hematopoietic Cells for Research and Gene Therapy. *Viruses* (2020) 12 (9):1016. doi: 10.3390/v12091016
113. Roediger EK, Kugathasan K, Zhang X, Lichty BD, Xing Z. Heterologous Boosting of Recombinant Adenoviral Prime Immunization With a Novel Vesicular Stomatitis Virus-Vectored Tuberculosis Vaccine. *Mol Ther* (2008) 16(6):1161–9. doi: 10.1038/mt.2008.59
114. Jeyanathan M, Damjanovic D, Shaler CR, Lai R, Wortzman M, Yin C, et al. Differentially Imprinted Innate Immunity by Mucosal Boost Vaccination Determines Antituberculosis Immune Protective Outcomes, Independent of T-Cell Immunity. *Mucosal Immunol* (2013) 6(3):612–25. doi: 10.1038/mi.2012.103
115. Zhang M, Dong C, Xiong S. Vesicular Stomatitis Virus-Vectored Multi-Antigen Tuberculosis Vaccine Limits Bacterial Proliferation in Mice Following a Single Intranasal Dose. *Front Cell Infect Microbiol* (2017) 7:34. doi: 10.3389/fcimb.2017.00034
116. Zhang M, Dong C, Xiong S. Heterologous Boosting With Recombinant VSV-846 in BCG-Primed Mice Confers Improved Protection Against Mycobacterium Infection. *Hum Vaccin Immunother* (2017) 13(4):816–22. doi: 10.1080/21645515.2016.1261229
117. Watanabe K, Matsubara A, Kawano M, Mizuno S, Okamura T, Tsujimura Y, et al. Recombinant Ag85B Vaccine by Taking Advantage of Characteristics of Human Parainfluenza Type 2 Virus Vector Showed Mycobacteria-Specific Immune Responses by Intranasal Immunization. *Vaccine* (2014) 32 (15):1727–35. doi: 10.1016/j.vaccine.2013.11.108
118. Nagatake T, Suzuki H, Hirata SI, Matsumoto N, Wada Y, Morimoto S, et al. Immunological Association of Inducible Bronchus-Associated Lymphoid Tissue Organogenesis in Ag85B-Rhpiv2 Vaccine-Induced Anti-Tuberculosis Mucosal Immune Responses in Mice. *Int Immunol* (2018) 30(10):471–81. doi: 10.1093/intimm/dxy046
119. Chen Z, Gupta T, Xu P, Phan S, Pickar A, Yau W, et al. Efficacy of Parainfluenza Virus 5 (PIV5)-Based Tuberculosis Vaccines in Mice. *Vaccine* (2015) 33(51):7217–24. doi: 10.1016/j.vaccine.2015.10.124
120. Vierboom MPM, Chenine AL, Darrah PA, Vervenne RAW, Boot C, Hofman SO, et al. Evaluation of Heterologous Prime-Boost Vaccination Strategies Using Chimpanzee Adenovirus and Modified Vaccinia Virus for TB Subunit Vaccination in Rhesus Macaques. *NPJ Vaccines* (2020) 5(1):39. doi: 10.1038/s41541-020-0189-2
121. Bettencourt P, Muller J, Nicastri A, Cantillon D, Madhavan M, Charles PD, et al. Identification of Antigens Presented by MHC for Vaccines Against Tuberculosis. *NPJ Vaccines* (2020) 5(1):2. doi: 10.1038/s41541-019-0148-y
122. Mosley JF2nd, Smith LL, Brantley P, Locke D, Como M. Vaxchora: The First FDA-Approved Cholera Vaccination in the United States. *P T* (2017) 42 (10):638–40.
123. Minassian AM, Satti I, Poulton ID, Meyer J, Hill AV, McShane H. A Human Challenge Model for Mycobacterium Tuberculosis Using Mycobacterium Bovis Bacille Calmette-Guerin. *J Infect Dis* (2012) 205(7):1035–42. doi: 10.1093/infdis/jis012
124. Harris SA, Meyer J, Satti I, Marsay L, Poulton ID, Tanner R, et al. Evaluation of a Human BCG Challenge Model to Assess Antimycobacterial Immunity Induced by BCG and a Candidate Tuberculosis Vaccine, MVA85A, Alone and in Combination. *J Infect Dis* (2014) 209(8):1259–68. doi: 10.1093/infdis/jit647
125. Kleinwaks G, Schmit V, Morrison J. Considering Human Challenge Trials for Tuberculosis Vaccine Development. *Vaccine* (2022) 40(2):173–4. doi: 10.1016/j.vaccine.2021.11.024
126. McShane H, Williams A. A Review of Preclinical Animal Models Utilised for TB Vaccine Evaluation in the Context of Recent Human Efficacy Data. *Tuberculosis (Edinb)* (2014) 94(2):105–10. doi: 10.1016/j.tube.2013.11.003
127. Dijkman K, Sombroek CC, Vervenne RAW, Hofman SO, Boot C, Remarque EJ, et al. Prevention of Tuberculosis Infection and Disease by Local BCG in Repeatedly Exposed Rhesus Macaques. *Nat Med* (2019) 25(2):255–62. doi: 10.1038/s41591-018-0319-9
128. Plumlee CR, Duffy FJ, Gern BH, Delahaye JL, Cohen SB, Stoltzfus CR, et al. Ultra-Low Dose Aerosol Infection of Mice With Mycobacterium Tuberculosis More Closely Models Human Tuberculosis. *Cell Host Microbe* (2021) 29(1):68–82.e5. doi: 10.1016/j.chom.2020.10.003
129. Park CO, Kupper TS. The Emerging Role of Resident Memory T Cells in Protective Immunity and Inflammatory Disease. *Nat Med* (2015) 21(7):688–97. doi: 10.1038/nm.3883
130. Parga-Vidal L, van Aalderen MC, Stark R, van Gisbergen K. Tissue-Resident Memory T Cells in the Urogenital Tract. *Nat Rev Nephrol* (2022) 18(4):209–23. doi: 10.1038/s41581-021-00525-0
131. Sollid LM. Gut Tissue-Resident Memory T Cells in Coeliac Disease. *Scand J Immunol* (2022) 95(1):e13120. doi: 10.1111/sji.13120
132. Lange J, Rivera-Ballesteros O, Buggert M. Human Mucosal Tissue-Resident Memory T Cells in Health and Disease. *Mucosal Immunol* (2021) 15(3):389–97. doi: 10.1038/s41385-021-00467-7
133. Ryan GE, Harris JE, Richmond JM. Resident Memory T Cells in Autoimmune Skin Diseases. *Front Immunol* (2021) 12:652191. doi: 10.3389/fimmu.2021.652191
134. Mueller SN, Mackay LK. Tissue-Resident Memory T Cells: Local Specialists in Immune Defence. *Nat Rev Immunol* (2016) 16(2):79–89. doi: 10.1038/nri.2015.3
135. Sakai S, Kauffman KD, Schenkel JM, McBerry CC, Mayer-Barber KD, Masopust D, et al. Cutting Edge: Control of Mycobacterium Tuberculosis Infection by a Subset of Lung Parenchyma-Homing CD4 T Cells. *J Immunol* (2014) 192(7):2965–9. doi: 10.4049/jimmunol.1400019
136. Torrado E, Fountain JJ, Liao M, Tighe M, Reiley WW, Lai RP, et al. Interleukin 27R Regulates CD4+ T Cell Phenotype and Impacts Protective Immunity During Mycobacterium Tuberculosis Infection. *J Exp Med* (2015) 212(9):1449–63. doi: 10.1084/jem.20141520
137. Sakai S, Kauffman KD, Sallin MA, Sharpe AH, Young HA, Ganusov VV, et al. CD4 T Cell-Derived IFN-Gamma Plays a Minimal Role in Control of Pulmonary Mycobacterium Tuberculosis Infection and Must Be Actively Repressed by PD-1 to Prevent Lethal Disease. *PloS Pathog* (2016) 12(5): e1005667. doi: 10.1371/journal.ppat.1005667
138. Hu Z, Zhao HM, Li CL, Liu XH, Barkan D, Lowrie DB, et al. The Role of KLRG1 in Human CD4+ T-Cell Immunity Against Tuberculosis. *J Infect Dis* (2018) 217(9):1491–503. doi: 10.1093/infdis/jiy046
139. Perdomo C, Zedler U, Kuhl AA, Lozza L, Saikali P, Sander LE, et al. Mucosal BCG Vaccination Induces Protective Lung-Resident Memory T Cell Populations Against Tuberculosis. *mBio* (2016) 7(6):e01686-16. doi: 10.1128/mBio.01686-16
140. Jeyanathan M, Afkhami S, Khera A, Mandur T, Damjanovic D, Yao Y, et al. CXCR3 Signaling Is Required for Restricted Homing of Parenteral Tuberculosis Vaccine-Induced T Cells to Both the Lung Parenchyma and Airway. *J Immunol* (2017) 199(7):2555–69. doi: 10.4049/jimmunol.1700382

141. Carpenter SM, Yang JD, Lee J, Barreira-Silva P, Behar SM. Vaccine-Elicited Memory CD4+ T Cell Expansion is Impaired in the Lungs During Tuberculosis. *PloS Pathog* (2017) 13(11):e1006704. doi: 10.1371/journal.ppat.1006704
142. Woodworth JS, Cohen SB, Moguche AO, Plumlee CR, Agger EM, Urdahl KB, et al. Subunit Vaccine H56/CAF01 Induces a Population of Circulating CD4 T Cells That Traffic Into the Mycobacterium Tuberculosis-Infected Lung. *Mucosal Immunol* (2017) 10(2):555–64. doi: 10.1038/mi.2016.70
143. Brinkmann V, Davis MD, Heise CE, Albert R, Cottens S, Hof R, et al. The Immune Modulator FTY720 Targets Sphingosine 1-Phosphate Receptors. *J Biol Chem* (2002) 277(24):21453–7. doi: 10.1074/jbc.C200176200
144. Connor LM, Harvie MC, Rich FJ, Quinn KM, Brinkmann V, Le Gros G, et al. A Key Role for Lung-Resident Memory Lymphocytes in Protective Immune Responses After BCG Vaccination. *Eur J Immunol* (2010) 40(9):2482–92. doi: 10.1002/eji.200940279
145. Netea MG, Quintin J, van der Meer JW. Trained Immunity: A Memory for Innate Host Defense. *Cell Host Microbe* (2011) 9(5):355–61. doi: 10.1016/j.chom.2011.04.006
146. Netea MG, van der Meer JW. Trained Immunity: An Ancient Way of Remembering. *Cell Host Microbe* (2017) 21(3):297–300. doi: 10.1016/j.chom.2017.02.003
147. Netea MG, Dominguez-Andres J, Barreiro LB, Chavakis T, Divangahi M, Fuchs E, et al. Defining Trained Immunity and its Role in Health and Disease. *Nat Rev Immunol* (2020) 20(6):375–88. doi: 10.1038/s41577-020-0285-6
148. Hu Z, Lu SH, Lowrie DB, Fan XY. Trained Immunity: A Yin-Yang Balance. *MedComm (2020)* (2022) 3(1):e121. doi: 10.1002/mco2.121
149. Giamarellos-Bourboulis EJ, Tsilika M, Moorlag S, Antonakos N, Kotsaki A, Dominguez-Andres J, et al. Activate: Randomized Clinical Trial of BCG Vaccination Against Infection in the Elderly. *Cell* (2020) 183(2):315–23.e9. doi: 10.1016/j.cell.2020.08.051
150. Prentice S, Nassanga B, Webb EL, Akello F, Kiwudhu F, Akurut H, et al. BCG-Induced non-Specific Effects on Heterologous Infectious Disease in Ugandan Neonates: An Investigator-Blind Randomised Controlled Trial. *Lancet Infect Dis* (2021) 21(7):993–1003. doi: 10.1016/S1473-3099(20)30653-8
151. Kleinnijenhuis J, Quintin J, Preijers F, Joosten LA, Ifrim DC, Saeed S, et al. Bacille Calmette-Guerin Induces NOD2-Dependent Nonspecific Protection From Reinfection *via* Epigenetic Reprogramming of Monocytes. *Proc Natl Acad Sci U S A* (2012) 109(43):17537–42. doi: 10.1073/pnas.1202870109
152. Verma D, Parasa VR, Raffetseder J, Martis M, Mehta RB, Netea M, et al. Anti-Mycobacterial Activity Correlates With Altered DNA Methylation Pattern in Immune Cells From BCG-Vaccinated Subjects. *Sci Rep* (2017) 7(1):12305. doi: 10.1038/s41598-017-12110-2
153. Vierboom MPM, Dijkman K, Sombroek CC, Hofman SO, Boot C, Vervenne RAW, et al. Stronger Induction of Trained Immunity by Mucosal BCG or MTBVAC Vaccination Compared to Standard Intradermal Vaccination. *Cell Rep Med* (2021) 2(1):100185. doi: 10.1016/j.xcrm.2020.100185
154. Moorlag S, Khan N, Novakovic B, Kaufmann E, Jansen T, van Crevel R, et al. Beta-Glucan Induces Protective Trained Immunity Against Mycobacterium Tuberculosis Infection: A Key Role for IL-1. *Cell Rep* (2020) 31(7):107634. doi: 10.1016/j.celrep.2020.107634
155. Khan N, Downey J, Sanz J, Kaufmann E, Blankenhaus B, Pacis A, et al. M. Tuberculosis Reprograms Hematopoietic Stem Cells to Limit Myelopoiesis and Impair Trained Immunity. *Cell* (2020) 183(3):752–70.e22. doi: 10.1016/j.cell.2020.09.062
156. Yao Y, Jeyanathan M, Haddadi S, Barra NG, Vaseghi-Shanjani M, Damjanovic D, et al. Induction of Autonomous Memory Alveolar Macrophages Requires T Cell Help and Is Critical to Trained Immunity. *Cell* (2018) 175(6):1634–50.e17. doi: 10.1016/j.cell.2018.09.042
157. D'Agostino MR, Lai R, Afkhami S, Khera A, Yao Y, Vaseghi-Shanjani M, et al. Airway Macrophages Mediate Mucosal Vaccine-Induced Trained Innate Immunity Against Mycobacterium Tuberculosis in Early Stages of Infection. *J Immunol* (2020) 205(10):2750–62. doi: 10.4049/jimmunol.2000532
158. Afkhami S, D'Agostino MR, Zhang A, Stacey HD, Marzok A, Kang A, et al. Respiratory Mucosal Delivery of Next-Generation COVID-19 Vaccine Provides Robust Protection Against Both Ancestral and Variant Strains of SARS-CoV-2. *Cell* (2022) 185(5):896–915.e19. doi: 10.1101/2021.07.16.452721
159. Goletti D, Lee MR, Wang JY, Walter N, Ottenhoff THM. Update on Tuberculosis Biomarkers: From Correlates of Risk, to Correlates of Active Disease and of Cure From Disease. *Respirology* (2018) 23(5):455–66. doi: 10.1111/resp.13272
160. Simmons JD, Stein CM, Seshadri C, Campo M, Alter G, Fortune S, et al. Immunological Mechanisms of Human Resistance to Persistent Mycobacterium Tuberculosis Infection. *Nat Rev Immunol* (2018) 18(9):575–89. doi: 10.1038/s41577-018-0025-3
161. Lu LL, Smith MT, Yu KKQ, Luedemann C, Suscovich TJ, Grace PS, et al. IFN-Gamma-Independent Immune Markers of Mycobacterium Tuberculosis Exposure. *Nat Med* (2019) 25(6):977–87. doi: 10.1038/s41591-019-0441-3
162. Chen ZY, Wang L, Gu L, Qu R, Lowrie DB, Hu Z, et al. Decreased Expression of CD69 on T Cells in Tuberculosis Infection Resisters. *Front Microbiol* (2020) 11:1901. doi: 10.3389/fmicb.2020.01901
163. Tait DR, Hatherill M, van der Meeren O, Ginsberg AM, Van Brakel E, Salaun B, et al. Final Analysis of a Trial of M72/AS01E Vaccine to Prevent Tuberculosis. *N Engl J Med* (2019) 381(25):2429–39. doi: 10.1056/NEJMoa1909953
164. *COVID-19 Vaccine Tracker and Landscape* (2022). Available at: https://www.who.int/publications/m/item/draft-landscape-of-covid-19-candidate-vaccines.

Conflict of Interest: The authors declare that the research was conducted in the absence of any commercial or financial relationships that could be construed as a potential conflict of interest.

frontiers | Frontiers in Immunology

OPINION
published: 08 July 2022
doi: 10.3389/fimmu.2022.953228

The Natural Effect of BCG Vaccination on COVID-19: The Debate Continues

Wenping Gong[1,2*†], *Huiru An*[1,2†], *Jie Wang*[1,2], *Peng Cheng*[1,2] *and Yong Qi*[3*]

[1] Tuberculosis Prevention and Control Key Laboratory, Senior Department of Tuberculosis, The 8th Medical Center of People's Liberation Army (PLA) General Hospital, Beijing, China, [2] Beijing Key Laboratory of New Techniques of Tuberculosis Diagnosis and Treatment, Senior Department of Tuberculosis, The 8th Medical Center of People's Liberation Army (PLA) General Hospital, Beijing, China, [3] Huadong Research Institute for Medicine and Biotechniques, Nanjing, China

OPEN ACCESS

Edited by:
Julia Y. Wang,
Curandis Inc., United States

Reviewed by:
Irina V. Kiseleva,
Institute of Experimental Medicine (RAS), Russia

***Correspondence:**
Wenping Gong
gwp891015@whu.edu.cn
Yong Qi
qslark@gmail.com

[†]These authors have contributed equally to this work

Specialty section:
This article was submitted to Vaccines and Molecular Therapeutics, a section of the journal Frontiers in Immunology

Received: 26 May 2022
Accepted: 20 June 2022
Published: 08 July 2022

Citation:
Gong W, An H, Wang J, Cheng P and Qi Y (2022) The Natural Effect of BCG Vaccination on COVID-19: The Debate Continues. Front. Immunol. 13:953228. doi: 10.3389/fimmu.2022.953228

Keywords: BCG (Bacille Calmette-Guérin), COVID-19, *Mycobacterium tuberculosis*, clinical trial, hospitalization, protective effect

INTRODUCTION

The coronavirus disease 2019 (COVID-19) pandemic caused by severe acute respiratory syndrome coronavirus 2 (SARS-CoV-2) infection has inflicted an unprecedented and significant toll on global public health and the economy. During the fight against the pandemic, the century-old tuberculosis (TB) vaccine Bacille Calmette Guérin (BCG), which has been reported to protect against infections of various respiratory pathogens other than *Mycobacterium tuberculosis* by inducing non-specific immune responses, was found to play an essential role against COVID-19 in various ecological, analytical, and animal studies (1, 2). However, its effectiveness remains controversial due to the limited number of published clinical trials (2). The effect of BCG vaccines appears to be quite non-specific or speculative. Currently there is no clear or strong evidence to support the notion that BCG vaccination confer protection to COVID-19. In the absence of evidence, the World Health Organization (WHO) issued a Scientific Brief on April 12, 2020, against BCG vaccination to prevent COVID-19, and this recommendation has remained unchanged to date (3).

NON-SPECIFIC IMMUNE RESPONSE INDUCED BY THE BCG

Our previous studies have reported that BCG vaccination could induce a non-specific immune response to fight against unrelated pathogens (2, 4–7). The non-specific immune response induced by BCG vaccination may be due to three potential mechanisms: trained immunity, heterologous immunity, and anti-inflammatory effect (2). Of the three possible mechanisms, trained immunity has received the most attention. Trained immunity is derived from immune memory in innate

immune cells such as monocytes and macrophages. The primary immunization of BCG can activate innate immune cells to produce IL-1β, TNF-α, and IL-6, generating trained monocytes/macrophages with an "infection memory." These trained monocytes/macrophages will respond rapidly by releasing higher levels of cytokines to combat the second unrelated pathogens' invasion (8). The trained immunity induced by BCG has been demonstrated in both animal experiments and human clinical trials, and it may be beneficial for the prevention and treatment of SARS-CoV-2 infection (2, 4–7, 9–11).

EARLY EVIDENCE ON BCG PREVENTION OF COVID-19

Early in the COVID-19 outbreak, the hypothesis that BCG could prevent COVID-19 infection was raised. Isabel N. Kantor was the first to publicly discuss whether BCG has preventive and protective effects against COVID-19 and how strong the association is between the "more BCG vaccination" and the " less COVID-19 infection" (12). Then, the lead investigator of the BRACE trial (NCT04327206) and the BCG-CORONA trial (NCT04328441) as well as the Director General of WHO discussed this hypothesis, and they suggested that BCG might reduce viremia following SARS-COV-2 exposure, thereby reducing the severity of COVID-19 and recovering faster (13). Furthermore, Luke A. J. O'Neill and Mihai G. Netea claimed that the BCG vaccine might well be a bridge to a specific COVID-19 vaccine due to the trained immunity induced by BCG.

Although this hypothesis offered a glimmer of hope to the panicked and helpless people in the early days of the COVID-19 pandemic, it still needed a lot of evidence to prove it. In the early months of the COVID-19 pandemic, findings from the ecological and analytical studies indicated that countries with low BCG coverage had significantly higher rates of COVID-19 morbidity and mortality than countries with high BCG coverage (14–40). On the contrary, other ecological and analytical studies found that BCG vaccination could not provide adequate protection against COVID-19 infection (41–50). The results of these ecological and analytical studies were contradictory, and the heterogeneity of these findings may originate from some confounding factors, such as population density, ethnicity, age structure, income, healthcare access and quality index, COVID-19 transmission progression, COVID-19 testing rate, non-pharmaceutical interventions, and geographical distribution (2, 5, 51–53). Therefore, these findings should be investigated by randomized clinical trials.

LATEST EVIDENCE ON BCG PREVENTION OF COVID-19

Recently, results of a double-blind, randomized, placebo-controlled clinical trial (NCT04379336), which aimed to evaluate the efficacy of BCG vaccination in delivering protection against COVID-19 in healthcare workers (HCWs) in South Africa, were published in the journal *eClinicalMedicine* and attracted wide attention (54). The study reported that BCG revaccination failed to protect HCWs from SARS-CoV-2 infection, severe COVID-19, hospitalization, and respiratory tract infections (RTIs), on the contrary, resulting in an unexpected trend toward more symptomatic and severe RTIs. Nevertheless, it is plausible that BCG offered protection from death. The results indicated that BCG had no statistically significant effect on COVID-19, which in our opinion, maybe still controversial.

A large number of COVID-19 immune-tolerant rather than sensitive participants recruited in the study may have influenced or masked the true protective effect of the BCG vaccine. However, the COVID-19-seropositive population, with a rate of 15.3% resistant to COVID-19-related severe disease, were not excluded. Considering that *M. tuberculosis*-infected mice were resistant to secondary SARS-CoV-2 infection (48), it's not inconceivable that the latent tuberculosis infection in the HCWs occupied 48.5% of all the participants might play resistant roles and influence the significant difference between groups. However, they were not excluded, either. More importantly, all the participants had previously received at least one dose of the BCG vaccine due to the vaccination policy of South Africa before the trial, which also could decrease the variation between the BCG revaccination and placebo groups. Interestingly, the only clinical trial to obtain results similar to this one also recruited volunteers who had received the BCG vaccine before in Poland (55), indicating the limitation should not be ignored.

Considering that many clinical trials began in the early days of the pandemic like this study, there must have been various drawbacks in their design due to the lack of understanding of the disease and its interaction with the BCG vaccine at that time. For instance, the BCG vaccination-caused scars would expose the participants' group and make the double-blind experimental design impossible. Furthermore, the young and middle-aged participants being relatively more resistant to COVID-19 than older people may mask the real efficacy of the BCG vaccine. Here we summarize the designs, results, and deficiencies of all published clinical studies (**Table 1**) (55–59) and hope to provide helpful information for more clinical studies involving the efficacy of BCG vaccination against COVID-19 or other virus infections in the future. After all, though more than 50 clinical trials have been registered, results of less than ten clinical trials have been published so far (2).

CONCLUSION

The hypothesis that BCG has a protective effect against COVID-19 has not been robustly verified. Therefore, the interpretation of any clinical trial results used to confirm this hypothesis should follow the principles of objectivity, science, and prudence.

TABLE 1 | Summary of the designs, results, and deficiencies of all published clinical studies.

	NCT04379336 (54)	NCT04414267 (56)	NCT03296423 (57)	NCT04648800 (55)	NCT04475302 (58)	NCT04537663 (59)
Sample size	1. 1000 healthcare workers were recruited from private and public healthcare facilities 2. 126 participants assigned to receive placebo; 139 participants assigned to receive BCG through the trail.	1. Elderly Greek individuals were randomized (1:1) to BCG revaccination or placebo group 2. Baseline characteristics are comparable between the two arms of vaccination 516 eligible participants 3. 6-month analysis was performed in 98 placebo-vaccinated individuals and 92 BCG-vaccinated individuals.	1. 202 elderly Greek individuals were enrolled; 4 participants withdrew consent. 2. Interim analysis included 78 participants in placebo group and 72 participants in BCG group	1. 717 HCWs were recruited, 363 (50.6%) individuals were excluded for Tuberculin test positive results. 2. 177 participants were randomly assigned to BCG group, and 177 to placebo group.	86 participants, Experimental group: 54 participants received 0.1 ml BCG intradermal injection. Control group: 32 participants were not vaccinated	6132 participants。 Participants will be randomized between intracutaneous administration of BCG vaccine (Danish strain 1331) or placebo (0.1ml 0.9% NaCl) in a 1:1 ratio.
Age (years)	39-40	>50	>65	>25	60-80	≥60
BCG strain	Danish strain 1331	Moscow strain 361- I	Danish strain 1331	Brazilian strain	NA	Danish strain 1331
Inclusion criteria	1. 15.3% of participants had a positive serology test indicating prior SARSCoV-2 exposure with no known history of COVID-19. 2. 485(48.5%) of participants had a positive QuantiFERON Gold Plus result, indicating have latent TB infection 3. adult healthcare workers, defined as any personnel working in a healthcare facility expected to be highly exposed to COVID-19,	Enrolled people should also have skin tuberculin test diameter less than 10mm and negative serum testing for immunoglobulin G and M against SARS-CoV-2.	The study enrolled elderly patients (age ≥ 65 years) of both genders who were discharged from hospital after hospitalization for a medical cause.	1. A health care professional (physician, nurse, midwife, paramedic, electroradiology technician, laboratory diagnostician, physiotherapist, nutritionist, orderly) aged > 25 years 2. No confirmed SARS-CoV-2 infection 3. Earlier vaccination against tuberculosis 4. Receive two doses of the COVID-19 vaccine as part of the National Immunization Program after December 27, 2020	"1. Elderly individuals between 60 - 80 years of age residing in hotspots for SARS-Cov2 infection were included in the study between July 2020 and September 2020 in Chennai, India. 2. No known history of HIV or on immunosuppressive drugs for malignancy or transplant"	"1. Age ≥60 years 2. Having a chronic disease or having undergone major surgery 3. Meeting at least one of the following criteria: (1).Planned to be discharged from the hospital or discharged from the hospital less than 6 weeks ago. Departments of interest are those that in the opinion of the principle investigator admit mostly vulnerable elderly and include but are not limited to: cardiology, pulmonology, internal medicine, neurology. (2).Visiting a medical outpatient clinic (3).Attending the thrombosis care service"
Exclusion criteria	1. Respiratory tract or other active infection, 2. COVID-19 treatment, 3. Contraindication to the BCG vaccine including known hypersensitivity to BCG, pregnancy or were breastfeeding, compromised immune system including HIV and cancer, 4. Receiving immunosuppressive therapy. 5. Previous COVID-19	1. Infection by HIV-1 2. Primary immunodeficiency. 3. Solid organ transplantation 4. Bone marrow transplantation 5. Intake of chemotherapy the last two months 6. Intake of radiotherapy the last two months 7. Active hemalogical or solid tumor malignancy 8. Intake of any anti-cytokine therapies 9. Intake of oral or intravenous steroids defined as daily doses of 10mg prednisone or equivalent for longer than the last 3 months.	1. Denial for written informed consent. 2. Solid organ malignancy or lymphoma diagnosed the last five years. 3. Treatment with oral or intravenous steroids. 4. Severe immunodeficiency, neutropenia, history of solid organ and bone marrow transplantation, intake of chemotherapy, primary immunodeficiency, severe lymphopenia and treatment with anti-cytokine	1. Hypersensitivity to any component of BCG 2. Hypersensitivity to previously administered tuberculin 3. HIV infection 4. Primary or secondary immunodeficiencies 5. Radiotherapy 6. Treatment with corticosteroids, ongoing immunosuppressive therapy 7. Neoplastic diseases 8. After stem cell transplantation and organ	1. Positive for SARS-Cov2 infection by either antibody (serology) or PCR test 2. HIV-infected or individuals with malignancy or on immunosuppressive drugs or transplant recipients and those on dialysis or anti-psychiatric medications or hypersensitivity to vaccinations	1. Fever (>38°C) within the past 24 hours 2. Suspicion of active viral or bacterial infection 3. Vaccination with live vaccine 4. Infection by HIV-1; neutropenic with less than 500 neutrophils/mm3; solid organ transplantation; bone marrow transplantation; hematological malignancy; chemo-, radio- or immunotherapy for solid organ malignancy; primary immunodeficiency; severe lymphopenia; treatment with any immunosuppressant drugs 5. Known history of a positive Mantoux or active TB 6. Born in a country with high incidence of TB 7. Active participation in another research study

(Continued)

TABLE 1 | Continued

	NCT04379336 (54)	NCT04414267 (56)	NCT03296423 (57)	NCT04648800 (55)	NCT04475302 (58)	NCT04537663 (59)
			therapies. 5. Positive IFN-γ Release Assay (IGRA)	transplantation 9. In the exacerbation stage of chronic diseases 10. Pregnancy 11. History of tuberculosis 12. Keloid at the vaccination site after previous BCG vaccination		8. History of COVID-19 9. Not able to perform the study procedures 10. Legally incapacitated or unwilling to provide informed consent
Intervention	BCG:0.1mL, placebo:0.1mL NaCl	Subdermal injection of 0.1ml of sodium chloride 0.9% or with 0.1ml of BCG vaccine	Intradermal vaccination with 0.1ml of sodium chloride 0.9% or with 0.1ml of BCG	Intradermal vaccination with 0.1ml of sodium chloride 0.9% or with 0.1ml of BCG	BCG: Single dose of 0.1ml of BCG vaccine. Placebo: No BCG vaccine	Intradermal injection in the left upper arm with BCG. Placebo: Intradermal injection of sterile 0.9% NaCl
Morbidity	A total of 99 COVID-19 event were record on BCG, and 93 COVID-19 events were record on placebo.	During these first 3 months after the vaccination, the overall incidence of COVID-19 was 10 patients in placebo *vs*. two patients in BCG group, p=0.086. In contrast, 6-months after vaccination, the total number of COVID-19 diagnoses (possible/probable/definitive) was significantly lower in the BCG-vaccinated group compared with the placebo group: OR 0.32 in multivariate analysis (95% CI 0.13-0.79, p=0.014)	The incidence of new infection was 42.3% (95% confidence intervals [CIs] 31.9%–53.4%) in the placebo group and 25.0% (95% CIs 16.4%–36.1%) in the BCG group.	COVID-19 events occurred in 161 participants among the BCG vaccinated people (23.16%) and was absent in 534 (76.84%) of the BCG non-vaccinated group.	NA	NA
Severe disease rate	A higher proportion of a total of 27 severe COVID-19 events were recorded on BCG (19, 70.4%) compared to placebo (8, 29.6%)	Definitive diagnosis of severe COVID-19 requiring hospitalization was present in 5 individuals in the placebo group and only one in the BCG group	NA	A serious adverse event (SAE) with hospitalization for COVID-19 occurred in one female participant	NA	
Hospitalization	1. The primary endpoint of hospitalization due to COVID-19 occurred in 15 (1.5%) participants: 10 (67%) on BCG compared to 5 (33%) on placebo, with an HR of 2.0 (95% CI 0.69 –5.9,p = 0.20) 2. The time-to-first hospitalization for all causes included 47 (4.7%) admissions; 27 (57.4%) on BCG and 20 (42.6%) on	NA	NA	NA	NA	

(Continued)

TABLE 1 | Continued

	NCT04379336 (54)	NCT04414267 (56)	NCT03296423 (57)	NCT04648800 (55)	NCT04475302 (58)	NCT04537663 (59)
	placebo with an HR of 1.36 (95% CI 0.72–2.49, p = 0.31).					
Mortality	Four participants (0.4%) died, two (50.0%) due to COVID-19 and one each (25.0%) due to bowel perforation and a cerebrovascular accident, all on placebo.	NA	NA	NA	NA	
Limitation	1. The lack of information on BCG vaccination at birth. 2. The lower-than-expected attack rate (19.2%) and hospitalisation rate (7.8%) 3. Participants with a positive serology test were included 4. Unblinded within a few days of enrollment 5. Participants with positive QuantiFERON results were included 6. The number of participants included in final analysis was not clear	1. Small sample size 2. Lack of microbiological testing in all patients with a clinical diagnosis of possible or probable COVID-19. 3. No conclusions can be drawn regarding the effect of BCG vaccination on the severe forms of COVID-19 4. Lack of information regarding the SARS-CoV-2 strains 5. Limited information regarding the impact of BCG on the specific immunological host defense pathways against SARS-CoV-2	1. Small sample size 2 The lack of repeat IGRA after vaccination 3. The absence of serological information on the incidence of various respiratory infections 4. The lack of information on BCG vaccination at birth. 5. The number of individuals participating in the trial is too low	1. The lack of a never-vaccinated control population. 2. Small sample size 3. The stimulation of non-specific effects after the BCG vaccine is associated 4. Lacking complete knowledge about all routes of influence of the BCG vaccine	1. Small sample size 2. This study did not examine the mechanical changes in the immune system.	1. Almost all individuals participating in this study received the BCG vaccine for the first time, as the Netherlands did not adopt a policy of vaccination with BCG in childhood. 2. There is no specific outcome data.

NA, not applicable.

Considering the ongoing pandemic and the possibility of novel variants or other pathogens emerging, the potential effect of BCG on COVID-19 needs to be further confirmed in rigorous randomized clinical trials.

AUTHOR CONTRIBUTIONS

Conceptualization: WG, YQ, and HA; Data curation: JW and PC; Formal analysis: YQ; Funding acquisition: WG; Methodology: HA, JW, and PC; Writing - original draft: WG and YQ; Writing - review and editing: HA, YQ, and WG. All authors contributed to the article and approved the submitted version.

FUNDING

This study was funded by the Beijing Municipal Science & Technology Commission (Grant No. 19L2065) and the Chinese PLA General Hospital (Grant No. QNC19047) to WG.

REFERENCES

1. Parmar K, Siddiqui A, Nugent K. Bacillus Calmette-Guerin Vaccine and Nonspecific Immunity. *Am J Med Sci* (2021) 361:683–9. doi: 10.1016/j.amjms.2021.03.003
2. Gong W, Mao Y, Li Y, Qi Y. BCG Vaccination: A Potential Tool Against COVID-19 and COVID-19-Like Black Swan Incidents. *Int Immunopharmacol* (2022) 108:108870. doi: 10.1016/j.intimp.2022.108870
3. WHO. *Bacille Calmette-Guérin (BCG) Vaccination and COVID-19*. Geneva: WHO (2020).

4. Gong W, Parkkila S, Wu X, Aspatwar A. SARS-CoV-2 Variants and COVID-19 Vaccines: Current Challenges and Future Strategies. *Int Rev Immunol* (2022) 41:1–22. doi: 10.1080/08830185.2022.2079642
5. Wang J, Zhang Q, Wang H, Gong W. The Potential Roles of BCG Vaccine in the Prevention or Treatment of COVID-19. *Front Biosci (Landmark Ed)* (2022) 27:157. doi: 10.31083/j.fbl2705157
6. Gong W, Aspatwar A, Wang S, Parkkila S, Wu X. COVID-19 Pandemic: SARS-CoV-2 Specific Vaccines and Challenges, Protection *via* BCG Trained Immunity, and Clinical Trials. *Expert Rev Vaccines* (2021) 20:857–80. doi: 10.1080/14760584.2021.1938550
7. Aspatwar A, Gong W, Wang S, Wu X, Parkkila S. Tuberculosis Vaccine BCG: The Magical Effect of the Old Vaccine in the Fight Against the COVID-19 Pandemic. *Int Rev Immunol* (2022) 41(2):283–96. doi: 10.1080/08830185.2021.1922685
8. Netea MG, Giamarellos-Bourboulis EJ, Domínguez-Andrés J, Curtis N, van Crevel R, van de Veerdonk FL, et al. Trained Immunity: A Tool for Reducing Susceptibility to and the Severity of SARS-CoV-2 Infection. *Cell* (2020) 181:969–77. doi: 10.1016/j.cell.2020.04.042
9. Brueggeman JM, Zhao J, Schank M, Yao ZQ, Moorman JP. Trained Immunity: An Overview and the Impact on COVID-19. *Front Immunol* (2022) 13:837524. doi: 10.3389/fimmu.2022.837524
10. Lee MH, Kim BJ. COVID-19 Vaccine Development Based on Recombinant Viral and Bacterial Vector Systems: Combinatorial Effect of Adaptive and Trained Immunity. *J Microbiol (Seoul Korea)* (2022) 60:321–34. doi: 10.1007/s12275-022-1621-2
11. You M, Chen L, Zhang D, Zhao P, Chen Z, Qin EQ, et al. Single-Cell Epigenomic Landscape of Peripheral Immune Cells Reveals Establishment of Trained Immunity in Individuals Convalescing From COVID-19. *Nat Cell Biol* (2021) 23:620–30. doi: 10.1038/s41556-021-00690-1
12. Kantor IN. BCG Versus COVID-19? *Medicina* (2020) 80:292–4.
13. Curtis N, Sparrow A, Ghebreyesus TA, Netea MG. Considering BCG Vaccination to Reduce the Impact of COVID-19. *Lancet* (2020) 395:1545–6. doi: 10.1016/S0140-6736(20)31025-4
14. Klinger D, Blass I, Rappoport N, Linial M. Significantly Improved COVID-19 Outcomes in Countries With Higher BCG Vaccination Coverage: A Multivariable Analysis. *Vaccines (Basel)* (2020) 8:378. doi: 10.3390/vaccines8030378
15. Miller A, Reandelar MJ, Fasciglione K, Roumenova V, Li Y, Otazu GH. Correlation Between Universal BCG Vaccination Policy and Reduced Morbidity and Mortality for COVID-19: An Epidemiological Study. *medRxiv* (2020). doi: 10.1101/2020.03.24.20042937
16. Gong W, Wu X. Is the Tuberculosis Vaccine BCG an Alternative Weapon for Developing Countries to Defeat COVID-19? *Indian J tuberculosis* (2021) 68:401–4. doi: 10.1016/j.ijtb.2020.10.012
17. Berg MK, Yu Q, Salvador CE, Melani I, Kitayama S. Mandated Bacillus Calmette-Guérin (BCG) Vaccination Predicts Flattened Curves for the Spread of COVID-19. *Sci Advances* (2020) 6:eabc1463. doi: 10.1126/sciadv.abc1463
18. Escobar LE, Molina-Cruz A, Barillas-Mury C. BCG Vaccine Protection From Severe Coronavirus Disease 2019 (COVID-19). *Proc Natl Acad Sci USA* (2020) 117:17720–6. doi: 10.1073/pnas.2008410117
19. Covián C, Retamal-Díaz A, Bueno SM, Kalergis AM. Could BCG Vaccination Induce Protective Trained Immunity for SARS-CoV-2? *Front Immunol* (2020) 11:970. doi: 10.3389/fimmu.2020.00970
20. Urashima M, Otani K, Hasegawa Y, Akutsu T. BCG Vaccination and Mortality of COVID-19 Across 173 Countries: An Ecological Study. *Int J Environ Res Public Health* (2020) 17(15):5589. doi: 10.3390/ijerph17155589
21. Joy M, Malavika B, Asirvatham ES, Sudarsanam TD, Jeyaseelan L. Is BCG Associated With Reduced Incidence of COVID-19? A Meta-Regression of Global Data From 160 Countries. *Clin Epidemiol Global Health* (2021) 9:202–3. doi: 10.1016/j.cegh.2020.08.015
22. Brooks NA, Puri A, Garg S, Nag S, Corbo J, Turabi AE, et al. The Association of Coronavirus Disease-19 Mortality and Prior Bacille Calmette-Guerin Vaccination: A Robust Ecological Analysis Using Unsupervised Machine Learning. *Sci Rep* (2021) 11:774. doi: 10.1038/s41598-020-80787-z
23. Li WX. Worldwide Inverse Correlation Between Bacille Calmette-Guérin (BCG) Immunization and COVID-19 Mortality. *Infection* (2021) 49:463–73. doi: 10.1007/s15010-020-01566-6
24. Jirjees FJ, Dallal Bashi YH, Al-Obaidi HJ. COVID-19 Death and BCG Vaccination Programs Worldwide. *Tuberc Respir Dis (Seoul)* (2021) 84:13–21. doi: 10.4046/trd.2020.0063
25. Islam MZ, Zahan MK, Al-Bari MAA. Convergence Between Global BCG Vaccination and COVID-19 Pandemic. *J Med virol* (2021) 93:1496–505. doi: 10.1002/jmv.26450
26. Senoo Y, Suzuki Y, Tsuda K, Tanimoto T, Takahashi K. Association Between COVID-19 Morbidity and Mortality Rates and BCG Vaccination Policies in OECD Countries. *J Infect Prev* (2021) 22:91–3. doi: 10.1177/1757177420976812
27. Kinoshita M, Tanaka M. Impact of Routine Infant BCG Vaccination on COVID-19. *J Infect* (2020) 81:625–33. doi: 10.1016/j.jinf.2020.08.013
28. Singh S, Maurya RP, Singh RK. "Trained Immunity" From Mycobacterium Spp. Exposure or BCG Vaccination and COVID-19 Outcomes. *PloS pathogens* (2020) 16:e1008969. doi: 10.1371/journal.ppat.1008969
29. Raham TF. Influence of Malaria Endemicity and Tuberculosis Prevalence on COVID-19 Mortality. *Public Health* (2021) 194:33–5. doi: 10.1016/j.puhe.2021.02.018
30. Inoue K, Kashima S. Association of the Past Epidemic of Mycobacterium Tuberculosis With Mortality and Incidence of COVID-19. *PloS One* (2021) 16:e0253169. doi: 10.1371/journal.pone.0253169
31. Chaudhari VL, Godbole CJ, Gandhe PP, Gogtay NJ, Thatte UM. Association of Bacillus Calmette Guerin Vaccine Strains With COVID-19 Morbidity and Mortality - Evaluation of Global Data. *Indian J Community Med* (2021) 46:727–30. doi: 10.4103/ijcm.IJCM_103_21
32. Kumar A, Misra S, Verma V, Vishwakarma RK, Kamal VK, Nath M, et al. Global Impact of Environmental Temperature and BCG Vaccination Coverage on the Transmissibility and Fatality Rate of COVID-19. *PloS One* (2020) 15:e0240710. doi: 10.1371/journal.pone.0240710
33. Abdulah DM, Hassan AB. Exploration of Association Between Respiratory Vaccinations With Infection and Mortality Rates of COVID-19. *Disaster Med Public Health Prep* (2021), 1–16. doi: 10.1017/dmp.2021.47
34. Pathak S, Jolly MK, Nandi D. Countries With High Deaths Due to Flu and Tuberculosis Demonstrate Lower COVID-19 Mortality: Roles of Vaccinations. *Hum Vaccin Immunother* (2021) 17:2851–62. doi: 10.1080/21645515.2021.1908058
35. Hidvégi M, Nichelatti M. Bacillus Calmette-Guerin Vaccination Policy and Consumption of Ammonium Chloride-Enriched Confectioneries May Be Factors Reducing COVID-19 Death Rates in Europe. *Israel Med Assoc J IMAJ* (2020) 8:435–8.
36. Ebina-Shibuya R, Horita N, Namkoong H, Kaneko T. Current National Policies for Infant Universal Bacille Calmette-Guérin Vaccination Were Associated With Lower Mortality From Coronavirus Disease 2019. *Clin Exp Vaccine Res* (2020) 9:179–82. doi: 10.7774/cevr.2020.9.2.179
37. Szigeti R, Kellermayer D, Trakimas G, Kellermayer R. BCG Epidemiology Supports its Protection Against COVID-19? A Word of Caution. *PloS One* (2020) 15:e0240203. doi: 10.1371/journal.pone.0240203
38. Lerm M. On the Relationship Between BCG Coverage and National COVID-19 Outcome: Could 'Heterologous' Herd Immunity Explain Why Some Countries Are Better Off? *J Intern Med* (2020) 288:682–8. doi: 10.1111/joim.13198
39. Hauer J, Fischer U, Auer F, Borkhardt A. Regional BCG Vaccination Policy in Former East- and West Germany May Impact on Both Severity of SARS-CoV-2 and Incidence of Childhood Leukemia. *Leukemia* (2020) 34:2217–9. doi: 10.1038/s41375-020-0871-4
40. Weng CH, Saal A, Butt WW, Bica N, Fisher JQ, Tao J, et al. Bacillus Calmette-Guérin Vaccination and Clinical Characteristics and Outcomes of COVID-19 in Rhode Island, United States: A Cohort Study. *Epidemiol infect* (2020) 148:e140. doi: 10.1017/S0950268820001569
41. Hamiel U, Kozer E, Youngster I. SARS-CoV-2 Rates in BCG-Vaccinated and Unvaccinated Young Adults. *Jama* (2020) 323:2340–1. doi: 10.1001/jama.2020.8189
42. Sayed A, Challa KT, Arja S. Epidemiological Differences of COVID-19 Over the World. *Cureus* (2020) 12:e10316. doi: 10.7759/cureus.10316
43. Hensel J, McAndrews KM, McGrail DJ, Dowlatshahi DP, LeBleu VS, Kalluri R. Protection Against SARS-CoV-2 by BCG Vaccination Is Not Supported by Epidemiological Analyses. *Sci Rep* (2020) 10:18377. doi: 10.1038/s41598-020-75491-x

44. Wassenaar TM, Buzard GS, Newman DJ. BCG Vaccination Early in Life Does Not Improve COVID-19 Outcome of Elderly Populations, Based on Nationally Reported Data. *Lett Appl Microbiol* (2020) 71:498–505. doi: 10.1111/lam.13365
45. Chimoyi L, Velen K, Churchyard GJ, Wallis R, Lewis JJ, Charalambous S. An Ecological Study to Evaluate the Association of Bacillus Calmette-Guerin (BCG) Vaccination on Cases of SARS-CoV2 Infection and Mortality From COVID-19. *PloS One* (2020) 15:e0243707. doi: 10.1371/journal.pone.0243707
46. de Chaisemartin C, de Chaisemartin L. Bacille Calmette-Guérin Vaccination in Infancy Does Not Protect Against Coronavirus Disease 2019 (COVID-19): Evidence From a Natural Experiment in Sweden. *Clin Infect Dis* (2021) 72: e501–e5. doi: 10.1093/cid/ciaa1223
47. Patella V, Sanduzzi A, Bruzzese D, Florio G, Brancaccio R, Fabbrocini G, et al. A Survey Among Italian Physicians During COVID-19 Outbreak. Could Bacillus Calmette-Guérin Vaccine Be Effective Against SARS-Cov2? *Front Pharmacol* (2021) 12:646570. doi: 10.3389/fphar.2021.646570
48. Chauhan A, Singh M, Agarwal A, Jaiswal N, M Lakshmi PV, Singh M. Exploring the Role of Bacillus Calmette-Guerin Vaccination in Protection Against COVID-19. *Int J mycobacteriol* (2021) 10:433–6. doi: 10.4103/ijmy.ijmy_179_21
49. Cerqueira S, Deps PD, Cunha DV, Bezerra NVF, Barroso DH, Pinheiro ABS, et al. The Influence of Leprosy-Related Clinical and Epidemiological Variables in the Occurrence and Severity of COVID-19: A Prospective Real-World Cohort Study. *PloS Negl Trop Dis* (2021) 15:e0009635. doi: 10.1371/journal.pntd.0009635
50. Bates MN, Herron TJ, Lwi SJ, Baldo JV. BCG Vaccination at Birth and COVID-19: A Case-Control Study Among U.S. Military Veterans. *Hum Vaccin Immunother* (2021) 18(1):1981084. doi: 10.1080/21645515.2021.1981084
51. Ogimi C, Qu P, Boeckh M, Bender Ignacio RA, Zangeneh SZ. Association Between Live Childhood Vaccines and COVID-19 Outcomes: A National-Level Analysis. *Epidemiol Infect* (2021) 149:e75. doi: 10.1017/S0950268821000571
52. Lindestam Arlehamn CS, Sette A, Peters B. Lack of Evidence for BCG Vaccine Protection From Severe COVID-19. *Proc Natl Acad Sci USA* (2020) 117:25203–4. doi: 10.1073/pnas.2016733117
53. Ritchie H, Mathieu E, Rodés-Guirao L, Appel C, Giattino C, Ortiz-Ospina E, et al. Responses to the Coronavirus Pandemic. In: *School OM*, editor. Oxford: Oxford Martin School (2022).
54. Upton CM, van Wijk RC, Mockeliunas L, Simonsson USH, McHarry K, van den Hoogen G, et al. Safety and Efficacy of BCG Re-Vaccination in Relation to COVID-19 Morbidity in Healthcare Workers: A Double-Blind, Randomised, Controlled, Phase 3 Trial. *EClinicalMedicine* (2022) 48:101414. doi: 10.1016/j.eclinm.2022.101414
55. Czajka H, Zapolnik P, Krzych Ł, Kmiecik W, Stopyra L, Nowakowska A, et al. A Multi-Center, Randomised, Double-Blind, Placebo-Controlled Phase III Clinical Trial Evaluating the Impact of BCG Re-Vaccination on the Incidence and Severity of SARS-CoV-2 Infections Among Symptomatic Healthcare Professionals During the COVID-19 Pandemic in Poland-First Results. *Vaccines (Basel)* (2022) 10(2):314. doi: 10.3390/vaccines10020314
56. Tsilika M, Taks E, Dolianitis K, Kotsaki A, Leventogiannis K, Damoulari C, et al. ACTIVATE-2: A Double-Blind Randomized Trial of BCG Vaccination Against COVID-19 in Individuals at Risk. *medRxiv* (2021). doi: 10.1101/2021.05.20.21257520
57. Giamarellos-Bourboulis EJ, Tsilika M, Moorlag S, Antonakos N, Kotsaki A, Domínguez-Andrés J, et al. Activate: Randomized Clinical Trial of BCG Vaccination Against Infection in the Elderly. *Cell* (2020) 183:315–23.e9. doi: 10.1016/j.cell.2020.08.051
58. Kumar NP, Padmapriyadarsini C, Rajamanickam A, Bhavani PK, Nancy A, Jeyadeepa B, et al. BCG Vaccination Induces Enhanced Frequencies of Dendritic Cells and Altered Plasma Levels of Type I and Type III Interferons in Elderly Individuals. *Int J Infect Dis IJID* (2021) 110:98–104. doi: 10.1016/j.ijid.2021.07.041
59. Dos Anjos LRB, da Costa AC, Cardoso A, Guimarães RA, Rodrigues RL, Ribeiro KM, et al. Efficacy and Safety of BCG Revaccination With M. Bovis BCG Moscow to Prevent COVID-19 Infection in Health Care Workers: A Randomized Phase II Clinical Trial. *Front Immunol* (2022) 13:841868. doi: 10.3389/fimmu.2022.841868

Conflict of Interest: The authors declare that the research was conducted in the absence of any commercial or financial relationships that could be construed as a potential conflict of interest.

Publisher's Note: All claims expressed in this article are solely those of the authors and do not necessarily represent those of their affiliated organizations, or those of the publisher, the editors and the reviewers. Any product that may be evaluated in this article, or claim that may be made by its manufacturer, is not guaranteed or endorsed by the publisher.

frontiers | Frontiers in Immunology

REVIEW
published: 28 July 2022
doi: 10.3389/fimmu.2022.944183

Progressive Host-Directed Strategies to Potentiate BCG Vaccination Against Tuberculosis

*Kriti Negi, Ashima Bhaskar and Ved Prakash Dwivedi**

Immunobiology Group, International Centre for Genetic Engineering and Biotechnology, New Delhi, India

The pursuit to improve the TB control program comprising one approved vaccine, *M. bovis* Bacille Calmette-Guerin (BCG) has directed researchers to explore progressive approaches to halt the eternal TB pandemic. *Mycobacterium tuberculosis* (*M.tb*) was first identified as the causative agent of TB in 1882 by Dr. Robert Koch. However, TB has plagued living beings since ancient times and continues to endure as an eternal scourge ravaging even with existing chemoprophylaxis and preventive therapy. We have scientifically come a long way since then, but despite accessibility to the standard antimycobacterial antibiotics and prophylactic vaccine, almost one-fourth of humankind is infected latently with *M.tb*. Existing therapeutics fail to control TB, due to the upsurge of drug-resistant strains and increasing incidents of co-infections in immune-compromised individuals. Unresponsiveness to established antibiotics leaves patients with no therapeutic possibilities. Hence the search for an efficacious TB immunization strategy is a global health priority. Researchers are paving the course for efficient vaccination strategies with the radically advanced operation of core principles of protective immune responses against *M.tb*. In this review; we have reassessed the progression of the TB vaccination program comprising BCG immunization in children and potential stratagems to reinforce BCG-induced protection in adults.

Keywords: adjunct vaccination strategies against tuberculosis, vaccine, BCG, host directed therapy, immunotherapy, memory T cells

OPEN ACCESS

Edited by:
Wenping Gong,
The 8th Medical Center of PLA General Hospital, China

Reviewed by:
Yu Pang,
Capital Medical University, China
Shen Chen,
Capital Medical University, China

***Correspondence:**
Ved Prakash Dwivedi
dwivedived235@gmail.com

Specialty section:
This article was submitted to Vaccines and Molecular Therapeutics, a section of the journal Frontiers in Immunology

Received: *14 May 2022*
Accepted: *21 June 2022*
Published: *28 July 2022*

Citation:
Negi K, Bhaskar A and Dwivedi VP (2022) Progressive Host-Directed Strategies to Potentiate BCG Vaccination Against Tuberculosis. Front. Immunol. 13:944183. doi: 10.3389/fimmu.2022.944183

INTRODUCTION

Tuberculosis (TB) is caused by the facultative intracellular pathogen *Mycobacterium tuberculosis* (*M.tb*). Since the 1800s, TB was the leading cause of health menace worldwide. Despite being declared a global health emergency in 1993 by World Health Organization (WHO), TB continues to be the leading cause of morbidity and mortality amongst bacterial infections (1). The majority of individuals remain asymptomatically and latently infected with *M.tb* owing to confiscation of the pathogen by immune cell populations and this does not lead to disease. Upon serious immunosuppression, around 10% of latently infected individuals develop active TB. Owing to the indefinability of the disease, explosive TB epidemics are hardly encountered which results in underestimated harm caused by *M.tb* worldwide (2). The host immune responses can restrict the pathogen but fail to accomplish complete bacterial sterility. The overwhelming progression of the

development of new therapeutics and the emergence of resistant pathogenic strains can be prevented by the enhancement of population-wide immunity against *M.tb* (3).

M.tb was originally identified in 1882 by Dr. Robert Koch as the causative agent of TB however, it has lurked among living beings since ancient times. 139 years post-discovery of this pathogen, it still endures as an eternal scourge ravaging globally. Current strategies fail to control TB, due to the upsurge of multidrug-resistant strains, increasing incidents of co-infections in immune-compromised individuals, and the emergence of TB-IRIS (Immune Responsive Inflammatory Syndrome). Globally in 2020, approximately 10 million people were disease-ridden with TB and an aggregate of 1.3 million lives were lost (together with 208000 people with HIV). Furthermore, almost one-fourth of humankind is infected asymptomatically (latently) with *M.tb*, with a 5-15% risk of progressing into clinical manifestations (1). An effective vaccine is indispensable to enhance population-wide immune protection and reduce disease burden. Vaccines operate by stimulating a cascade of immunological responses and ensuing the institution of immune memory against subsequent infections (4). Immune memory was originally described by the Greek historian Thucydides while observing survivors of the plague of Athens and comprehended that survivors have conferred life-long resistance to disease. Hence, he stated that "this disease never took any man the second time" (5). This feature of the immune system is a requisite evolutionary trait. Since historic eras for infectious diseases like smallpox, it is distinctly demonstrated that while initial infections had a fatality rate of 20% to 60% subsequently affected individuals were eternally immune to infection. Edward Jenner was the first to employ this hallmark feature of immunity to treat smallpox and provided a foundation for the development of vaccines (6). Secondary immune responses are refined protective responses mounted by sub-populations of memory cells on subsequent encounters which impart endurance to combat recurrent infections caused by pathogens in the environment. A series of events following primary exposure establishes a pool of long-lasting antigen-specific immune cells that mount quantitatively and/or qualitatively improved immune response upon reinfection. Documented from the times of ancient Greeks but still, many components of immune memory are still debatable (5). Immune memory is the cardinal property of the adaptive immune system and exclusively lymphocytes were known to mediate these responses. However, organisms that lack T and B lymphocytes similarly possess heightened proficiency to combat recurring infections caused by the same pathogen, demonstrating the existence of innate immune memory (7). Numerous studies in simpler living beings have reported that cells of the innate immune system can mount heightened secondary responses upon reinfection. Thus, the conventional characterization of immunological memory is continuously advancing (8). Better insights into the generation of immunological memory are fundamental to foster progressive vaccination strategies.

Despite pre-exposure vaccination with BCG, a large extent of latent TB infections urges the need for an efficacious complementary TB control strategy. It is evident that the most extensively used vaccine, Bacille Calmette-Guerin (BCG) which has existed for 100 years fails to impart long-term immunity and has limited efficacy against adult pulmonary TB (9). BCG immunization has a limited impact on *M.tb* transmission since it cannot inhibit primary infection or recrudescence of latent TB (10). Failure to develop a significantly effective vaccine has constrained the phasedown of the global TB burden (9). Furthermore, safety concerns regarding BCG immunization in immune-compromised individuals including HIV-TB coinfected individuals necessitate a vaccine that is safer and more efficient than BCG and can ameliorate infections (11). The efficacy of BCG against pulmonary TB is even more disappointing in tropical regions with a high TB burden (12). Escalating TB cases worldwide despite BCG administration further demands the advancement of the existing vaccination strategy. In the past decade, various research groups have utilized pioneering technologies to improve the current scenario. Progressive vaccine design strategies have been implemented and vaccine candidates have been evaluated in different clinical trials (13). It is challenging to discover more efficacious vaccine candidates for TB that can substitute BCG. It is highly critical to comprehend the shortcomings and prospects of novel vaccination strategies for better implementation and amendment of TB control measures. **Table 1** summarizes key desirable characteristics of improved vaccination strategy. In the current scenario, COVID-19 and TB are the top two causes of death from contagious diseases (1). The similarity in symptoms, risk factors, and primary organ affected further exacerbates the circumstances. TB-COVID-19 co-infection certainly intensifies the severity and threat of death. Even though both diseases primarily affect the lungs, due to disparities in modes of transmission and pathogenesis, distinct therapeutic measures are required (14). Nevertheless, with extraordinary scientific endeavour, information regarding the pathogenesis of SARS-CoV-2 was channelled to develop diagnostics, therapeutics, and vaccines

TABLE 1 | Desired characteristics for novel Tuberculosis immunization approaches.

S. No	Desired characteristics
1.	Safe to be administered in immunocompromised individuals at risk of developing active TB
2.	Expenses associated with regimen and dosage should be reasonable for high burdened developing countries.
3.	Immunization strategy must lower the risk of developing active pulmonary TB in adults previously vaccinated with BCG
4.	Must protect against *M.tb* infections for more than 10 years subsequent to immunization
5.	Minimum administrations requisite to elicit host protective responses
6.	Evaluation of protective immune correlates by employing established assays
7.	Must offer greater than 50% protective efficacy against established pulmonary TB

for COVID-19. Further, years of implementation of TB control programs were utilized to implement control strategies to constrain the pandemic (15). This prompts the necessity to retrospect and harnesses the paramount knowledge for progressive solutions to counteract the syndemic of COVID-19 and TB. Lessons learned from BCG vaccination for TB have been operative to control the COVID-19 pandemic owing to the broad-spectrum immunomodulatory potential of BCG (16). The emergence of Severe Acute Respiratory Syndrome Coronavirus 2 (SARS-CoV-2) and the consequent COVID-19 pandemic has negatively influenced the years of progress in tuberculosis (TB) control (17). Advancement in the direction to put an end to TB was hit hard by the ongoing COVID-19 pandemic. Reports of the World Health Organization (WHO) corroborate that advent of COVID-19 has caused a diminution in TB diagnosis and escan alation in mortality. To augment protective immune responses against TB in adults, massive scientific and economic attempts have been made globally. Aspiration to attain complete bacterial sterility to counteract active TB and restrict the transmission with next-generation vaccines has been actively trailed. Even with several vaccine candidates in different phases of clinical trials, we are yet to uncover vaccination strategies that can efficaciously restrict escalating TB burden worldwide (17). Hence, in this review, we have discussed strategies to augment the existing vaccination approach. Immune responses induced by BCG vaccination have been studied comprehensively in past and we are still uncovering new information regarding host responses stimulated by BCG that impede the establishment of effective memory responses (18). To improve the immunotherapeutic efficacy of BCG it is vital to completely understand the mechanism of BCG-induced immune responses. Modulation of host immunity *via* immunomodulators along with vaccination can be employed as a stratagem to incline immune responses to attain ever-lasting immunity against *M.tb* infections. We will reassess the radical approaches utilized by the researchers to limit the prevailing TB cases and how a better understanding of BCG is prime for progress in the TB vaccination program.

EXPEDITION FROM VIRULENT *M. BOVIS* TO THE BCG VACCINE:

Albert Calmette and Camille Guérin commenced the pursuit to develop a vaccine against TB in 1900 at the Pasteur Institute (19). They began by cultivating a virulent bovine strain of bacillus which was isolated from a tuberculous cow by Nocard. Initially, the bacilli were grown on glycerine, potato medium supplemented with ox bile to limit the clumping and attain homogenous bacterial suspension. This effort to minimize bacterial clumping additionally lowered the virulence of pathogen upon sub-culturing. This scientific observation provoked the scientists further to focus on using the attenuated strain of bacilli for the generation of TB vaccine (20). Till 1919, they successfully sub-cultured the bacilli more than 230 times. This strain failed to infect and cause TB in animals such as guinea pigs, cattle, and rabbits. Firstly named "Bacille Bilie Calmette-Guerin" this is now the most widely administered vaccine worldwide Bacille Calmette-Guerin (BCG) (20). BCG was first utilized in 1921 to immunize a new-born *via* oral route after which it was mass vaccinated to protect infants from disseminated forms of TB. To justify the escalating demand for vaccine strain worldwide, several laboratories around the world began sub-culturing BCG owing to which individuals around the world are vaccinated with characteristically distinct BCG strains (21). Based on existing knowledge, it is evident that diverse BCG strains have variable efficaciousness (22) and immunogenicity (23) but the most efficient BCG strain is yet to be established (23). As little as 1% augmented efficaciousness can rescue around 18,000 individuals and limit 83,000 TB cases in a year (24). Hence, to better understand the protective co-relates of BCG vaccination should be the top priority to upgrade the vaccination strategy.

BCG INDUCED PROTECTION AGAINST TB

Since the launch of BCG in TB immunization programs, numerous lives have been saved owing to the only existent TB vaccine (19). The percentage decline in disease that can be attributed to vaccination outlines the clinical effectiveness of a vaccine. Mainly, the BCG vaccine is administered to protect against TB. However, the protective efficacy of BCG is assessed distinctively in the case of disseminated TB in children and adult pulmonary TB on the account of colossal discrepancy (25). One of the multifaceted explanations can be the intricate biology of TB establishment and progression in humans (26). In the majority of *M.tb* infections, the immune system can proficiently restrict the progression of the pathogen to cause active TB. However, the endeavour to eliminate the bacilli completely is rarely achieved and can culminate into escalated inflammatory responses that direct distinct phases of disease such as latent TB and associated immunopathogenesis (27). The aim is to strike a balance for the resolution of *M.tb* infection exclusive of detrimental inflammation. For more than a century, researchers have attempted to ascertain correlates of BCG-induced defenses in humans through various animal models (10) and clinical trials (28). Additional to *M.tb* infections, broad-spectrum immunomodulatory characteristics of BCG are utilized to treat bladder cancer (29), asthma (30), leishmaniasis (31) and warts (32). While our understanding of key immunological aspects is continuously expanding (33), we have attained substantial knowledge regarding innate and adaptive immune responses to *M.tb* infection and BCG immunization which is briefly depicted in **Figure 1** and will be reviewed thoroughly in this section.

Innate immune system function as the first line of defense in confronting *M.tb* infections (34). The innate immune responses are the key component of the host immune responses engaged promptly at the site of infection (35). Even in the course of intradermal BCG immunization, early immune responses are elicited by resident epidermal macrophages (36), neutrophils

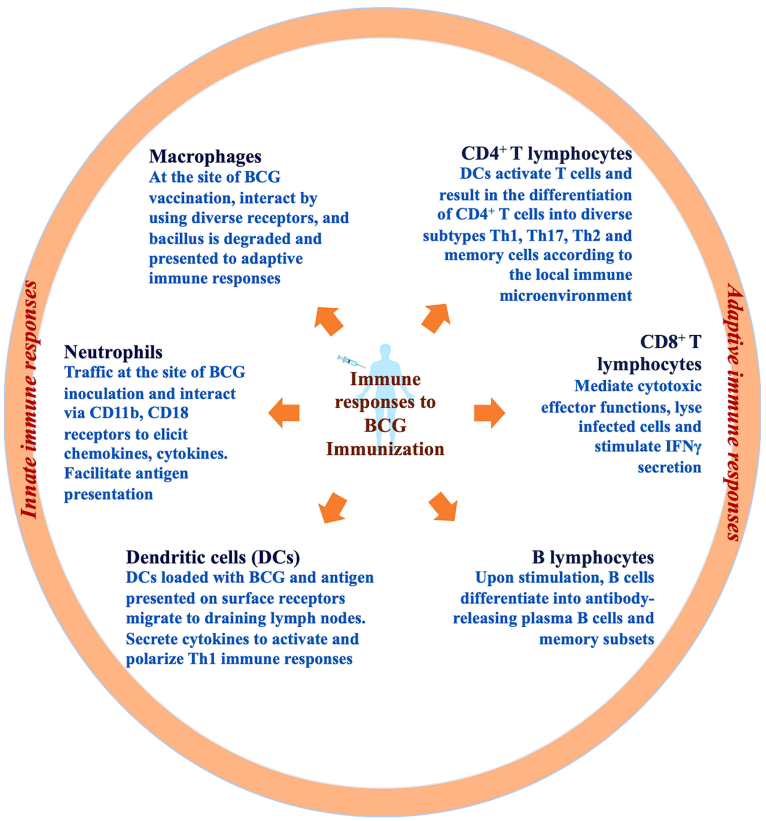

FIGURE 1 | Immune responses to BCG immunization. Immune responses to the BCG vaccine initiate at the site of inoculation by induction of innate immune cells such as resident macrophages, neutrophils, and dendritic cells. Innate immune cells internalize, degrade and present antigen of bacilli *via* surface receptors to further activate adaptive immune cells. Chiefly, DCs loaded with bacilli drain to the lymph nodes and result in lymphocyte stimulation and activation. T and B lymphocytes further differentiate into diverse subtypes including effector and memory cells.

(37), and dendritic cells (DCs) (38). BCG comprises pathogen-associated molecular patterns (PAMPs) such as cellular components (mycolic acids, peptidoglycans, and arabinogalactans) which are recognized by diverse PAMP recognizing receptors (PRRs) present on the surface of innate immune cells. Diverse PRRs abundantly expressed on innate subsets such as complement receptor 3 (CR3) (39), TLR2/4/9 (40), mannose receptor (41), Ca^{2+}-dependent lectin (MINCLE) receptors on macrophages (42), nucleotide-binding oligomerization domain (NOD)-like receptors NOD2 on monocytes, CD18, FcγRII, and FcγRIII on neutrophils and DC-SIGN, CD11c, and CD205 on dendritic cells initiate the prompt innate immune responses upon BCG immunization (43). Disparities in the cellular composition of BCG and *M.tb* has been linked with recognition by different PRRs which further influences the uptake, processing and representation of antigens to other immune cells. Since the receptor involved determines the fate of downstream signaling, the variation in receptor utilization can be further associated with relatively inefficient immune responses in the case of BCG (44). Examination of skin biopsies demonstrated that BCG blister point majorly comprises $CD15^+$ neutrophils, a small proportion of $CD14^+$ monocytes, and an infinitesimal population of $CD3^+$ T lymphocytes (45). However, in whole blood culture experiments, $CD56^+$ NK cells, γδ T cells, NKT cells, and cells from MAIT were found to be associated with BCG-induced immunity (46). In response to BCG vaccination, innate immune responses such as ROS/RNI generation by neutrophils, the release of monocytic chemokines like IL-6, TNF-α, MIP-1α, MIP-1β, IL-8, and IL-1α within 1-3 hours is initiated to direct systemic immune responses (45). BCG is known to effectively activate monocytic populations (47). In animal models, subsequent to BCG immunization mycobacterial extermination by macrophages was demonstrated independent of adaptive immune responses (48). Deficit immune responses induced by macrophages subsequent to BCG vaccination downgrade bacterial clearance. Furthermore, guinea pigs immunized with BCG upon H37Rv infection demonstrated enhancement of phagosome-lysosomal fusion with a considerable reduction in mycobacterial burden (47).

Dendritic cells (DCs) function as a nexus between innate and adaptive immune responses by presenting processed antigens to T lymphocytes post BCG immunization *via* IL-1R, MyD88 pathway (49). BCG immunization is known to enhance DC maturation and activation by upregulating the expression of markers implicated in antigen presentation such as MHC-II, CD40, CD80, and CD86 (35). Nonetheless, BCG immunization is also linked with the stimulation

of IL-10 and IL-4 cytokines by DCs which can bias the differentiation of T lymphocytes toward the T_H2 subtype and can be the cause of weakened BCG effectiveness (49). Nonetheless, the majority of information concerning the role of DCs in the case of BCG inoculation is from *in vitro* studies. The observation that *in vitro* BCG stimulation, initiates aggregation of DCs, upregulates antigen presentation with reduced endocytosis, and stimulation of TNF-α infers that DCs contribute to the initiation of immune responses. However, it is concerning that compared to *M.tb* infection these responses are inadequate to impart requisite protection (50). Apart from the major innate immune cell populations, innate lymphoid cells (ILCs) and mucosal-associated invariant T cells (MAIT) have been connected with BCG-induced innate protection (36). However, fragmentary information is accessible regarding these subsets and further exploration is necessitated.

It is now well-known that analogous to antigen-specific responses elicited by adaptive immunity, subsequent to pathogenic insults cells of innate immunity elicit heterologous memory responses (7). Distinct reports have demonstrated that natural killer (NK) cells and macrophages which have formerly encountered pathogens through epigenetic remodeling are trained to respond to distinct pathogens (51). It has been observed that epigenetic modifications such as H3K4me1, H3K4me3, and H3K27ac have been associated with the reprogramming of monocytic populations owing to unfastening of chromatin positions at the promoters of pro-inflammatory cytokines (52). BCG immunization leads to the expansion of Hematopoietic stem cells (HSCs), drives myelopoiesis and *via* epigenetic reprograming enhances host protective immune responses (53). Furthermore, it is established that macrophages interact with NK cells and bring about the refinement of innate immune responses against pathogenic insults (54). With a deeper insight into trained immunity, it was observed that BCG vaccination in healthy individuals stimulates NK cells and macrophages to uphold cytokine generation in response to *ex vivo* stimulation (55). The broad-spectrum immunomodulatory potential of BCG has been employed for the treatment of diverse ailments including the COVID-19 disease caused by SARS-CoV-2 (56). It has been experimentally proved that BCG *via* epigenetic reprogramming of immune cells exhibits cross-protection against diverse pathogens (57). The research demonstrates the impact of BCG vaccination on the induction of genome-wide histone modifications in trained monocytes which participate in IL-1β generation and the reduction of the yellow fever virus (YFV) burden (58). BCG-induced protection against YFV infection substantiates the broad-spectrum effectiveness of the vaccine against diverse viral infections such as influenza A (H1N1) virus, herpes simplex virus (HSV), and human papillomavirus (HPV) (59). Based on this information, BCG vaccination was evaluated initially during the COVID-19 pandemic. Preliminary ecological studies demonstrated that COVID-19 cases and deaths per population were fewer in countries with BCG vaccination schedules (60). The notion of inducing anti-viral immunity by employing BCG was based on the generation of heterologous immune responses (61). Since it was found that the envelope protein of the SARS-CoV-2 virus shared certain homology with strains of *Mycobacterium* species (62). It was inferred that the homology was associated with the induction of host-protective T_h1/T_h17 responses. The concept of trained immunity and heterologous responses were utilized to exploit BCG vaccination in the era of COVID-19. Since the majority of individuals are already vaccinated with BCG, it is judicious to keep BCG in reflection while developing new vaccination strategies. The fight to halt TB must continue progressively while dealing with the ongoing COVID-19 pandemic (17).

Till now adequate information is established regarding protective correlates against TB. Adaptive immune responses play a vital role in eliciting pathogen-specific immune responses with superior efficacy (26). The protective role of T lymphocytes was primarily demonstrated by the adoptive transfer of $CD4^+$ and $CD8^+$ T cells from BCG immunized mice to T and B cell-deficient (Rag1-/-) knockout mice (63). T lymphocytes contribute significantly against *M.tb* infections upon activation by components of innate immunity. The induction of T_h1/T_h17 immune responses and IFN-γ secretion is positively linked with augmented clinical outcomes in TB patients (26). Several studies have demonstrated mechanistic insights of BCG-induced defenses as a consequence of T_h1 cells through IFN-γ secretion (64). The paramount contribution of T_h1 responses was also demonstrated in infants vaccinated with BCG wherein T_h1 responses prevailed for more than a year contrary to pronounced T_h2 responses in unvaccinated infants (65). Furthermore, for the next few years, BCG-induced protection was attributable to IFN-γ releasing T lymphocytes (65). However, the outcomes of BCG immunization are still disputable and not strongly concurrent with specific immune responses. In IFN-γ deficient mice, BCG immunization demonstrated considerable protection against *M.tb* infection that vanished after depletion of $CD4^+$ T lymphocytes (66). Comparable outcomes were achieved in a study involving humans vaccinated with BCG wherein restricted *M.tb* progression and protection were linked with IFN-γ independent $CD8^+$ immunological responses (67). It is established now that polyfunctional $CD4^+$ T lymphocytes play a vital role in enhancing defenses against *M.tb* by secreting cytokines in different combinations to amend the microenvironment at the site of infection (68). It was confirmed that BCG immunization in infants does not elicit polyfunctional immune responses linked with effective protection against *M.tb* (12). However, immunization with a booster dose of MVA85A (modified vaccinia virus Ankara expressing antigen 85A) in BCG vaccinated adults confirmed induction of polyfunctional T cell responses (69). This gave rise to the hypothesis of heterologous boosting of BCG immunization for robust protective immunity against *M.tb*. Thereafter, failure of MVA85A heterologous boosting in infants to induce efficacious immune responses even with induction of polyfunctional T responses blurred the resolution of protective efficacy (70). Similarly, $CD8^+$ T cells exhibit antimycobacterial activity and are directly involved in *M.tb* killing, cytotoxic extermination of infected cell populations, and IFN-γ secretion (71). In human samples, $CD8^+$ T cells have been shown to distinctively identify and kill infected macrophages along with internalized *M.tb* with granular discharge comprising perforin and

granulysin (63). Therefore, subsiding the bacterial burden and effectively enhancing defenses against *M.tb*. The vitality of MHC class I-restricted $CD8^+$ T cells was demonstrated in β2-microglobulin (β2m) deficient mice incapable of restricting *M.tb* infection (72). It is not feasible to achieve sterilizing immunity against reinfections with mycobacteria subsequent to pathogen clearance with antimycobacterial drugs. Several studies have emphasized the significance of IL-17 generating $CD4^+$ T lymphocytes in mediating protection from reinfections and improving clinical outcomes upon vaccination (73). Consistent with these reports, in BCG immunized mice, T_h1 responses in the lungs were shown to be reliant on IL-17A and IL-23 secreted by antigen-specific T_h17 cells (73). In non-human primates (NHPs) administering a high dose of intradermal or intravenous BCG was linked with augmented protection from *M.tb* as a consequence of $CD4^+$ T lymphocytes with T_h1/T_h17 phenotypic characteristics (74). Thus, augmenting T_h1/T_h17 responses induced by BCG offer prospective solutions against TB (74). BCG immunization has been linked with the enhancement of regulatory T cells (T_{regs}) *via* alteration of immune metabolic pathways which consequently reduces the protective efficacy against TB. Depletion of T_{regs} can result in enrichment of T_h1, cytotoxic T cell responses with enhanced bacterial extermination upon infection (75). Boosting BCG with a novel vaccine candidate comprising Ag85B-Mpt64 (76–84)-Mtb8.4 (AMM) along with composite adjuvant lowers the T_{reg} population which was associated with enhanced protection in the mice model (85). Nonetheless, few studies have also demonstrated unaltered outcomes in BCG immunization upon prior T_{regs} depletion (86). Hence, further analysis is necessitated to validate the prospects for utilization in clinical operation. Regardless, the potential of the BCG vaccine to enrich T_{regs} and inhibit detrimental inflammation has been employed to treat diverse disorders including SARS-CoV-2 infection-induced cytokine storm in the COVID-19 pandemic (87). Additionally, BCG administration has been linked with increased IL-10 secretion in animal models which consequently restricts anti-mycobacterial pro-inflammatory responses induced by vaccination (88). Furthermore, obstruction of IL-10 signal transduction in the course of BCG immunization improved protective immune responses by mounting T_h1, and T_h17 responses (89). Hence, striking the immunological balance to achieve affirmative outcomes is requisite to alleviate BCG-induced protection.

APPROACHES TO AMEND INADEQUACIES OF BCG VACCINE

Despite numerous limitations of the BCG vaccine, it is still challenging to stumble upon more effective vaccine candidates for TB (90). BCG is unquestionably the most reliant vaccine for the prevention of disseminated forms of TB in children (91). Hence, it is critical to comprehend the shortcomings of BCG to extemporize protection by progressive approaches. It is widely proclaimed that wearying BCG immunity is a consequence of the non-existent T cell epitopes of *M.tb* in BCG vaccine strains (92). It is also established that expansion and differentiation of effector T cells declines in age-dependent manner upon BCG inoculation inferring toward weakened central memory responses (93). The contracted pool of antigen-specific memory populations is the basis for short-term protection against *M.tb* infections (93). Furthermore, the variable efficaciousness of BCG-induced defenses is associated with multifold factors such as ecological aspects, genetics, and differences in nutritional profiles amongst populations, listed in **Figure 2**. A major rationale for highly variable BCG efficacy in adults is exposure to environmental non-tuberculous mycobacteria (NTM). Prevalence of NTMs in tropical regions has been linked with low efficacy of BCG and consequent high TB burden due to pre-immunization exposure induced variation in protective efficacy (94). In the regions nearby the equator, UV exposure has been connected with a reduction in BCG efficacy which was further demonstrated in animal models with alterations in cytokine profiles when exposed to UV at the time of BCG immunization (60). Furthermore, variations in handling protocols and numerous passages of BCG vaccine strains have given rise to alterability in immunogenicity of BCG vaccine strains worldwide (95). Despite the wavering protective efficacy of BCG vaccine is deemed to be safe and is administered worldwide is numerous vaccination programs. However, with the raising concerns in immune-compromised HIV-TB co-infected individuals, WHO has addressed disputes regarding the utility of live vaccine in diverse risk groups. In immune-deficient children seldomly BCG vaccination can lead to systemic BCGosis. Atypical adverse reactions were detected in children with chronic granulomatous disease, Di George syndrome and severe combined immune deficiency (SCID) which can result in deadly consequences if unmanaged (96). In immunocompromised individuals especially neonates vaccination can also result in BCG lymphadenitis and disseminated BCG infection which is one of the most detrimental consequence of BCG vaccination (97). Hence, due to the overabundance of factors contributing to undermining protection elicited by BCG progressive approaches have been employed to improvise BCG against *M.tb*.

REPLACING OR RECLAIMING BCG

The major TB burden worldwide accountable for morbidity and mortality is due to adult pulmonary TB cases (1). The interval of weakening of BCG-induced defenses overlaps with an escalated incidence of *M.tb* infections in adults. On the surface foremost justification for the incompetence of the BCG vaccine appears to be immunization in the early years of life which imparts limited protection (90). The prospects of the End TB Strategy hence seem bleak without an improvised vaccination stratagem. Since BCG is the most widely utilized vaccine in the world and imparts protection in infants against disseminated forms of TB, it is judicious to reclaim BCG-induced protection rather than displacing it with a replacement. Fundamental strategy to amend BCG efficacy is by utilizing prime boost vaccination approach (98). Since one of the many desired characteristics for upcoming vaccine candidates is to efficaciously improvise the existing TB control approach i.e. prophylactic BCG immunization (99). Alternatives to strengthen the existing TB control program comprises developing a booster vaccine to augment the protective efficacy of BCG or supplementing immunotherapeutic as

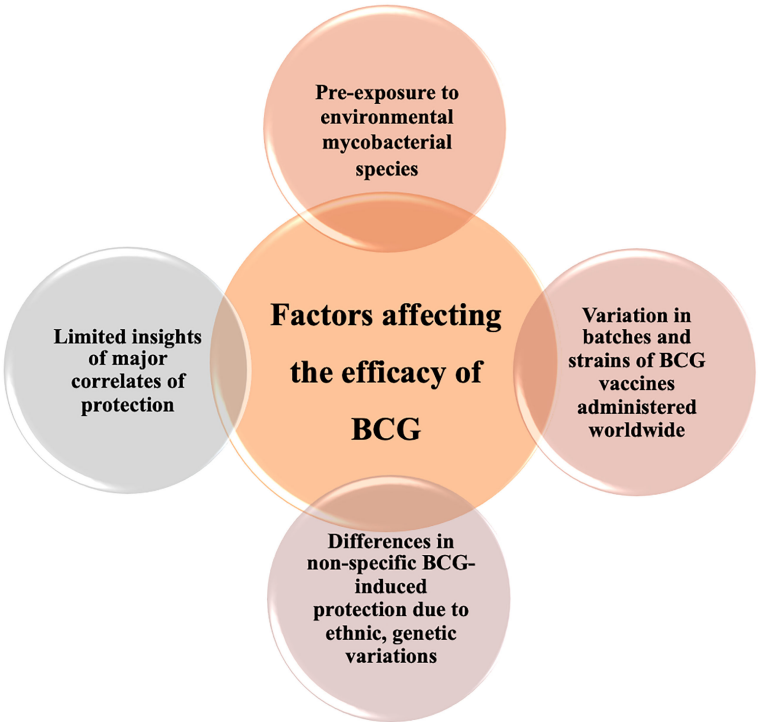

FIGURE 2 | Diverse factors associated with variable efficacy of BCG. Inconsistent efficacy of BCG vaccination can be linked to numerous host factors including genetics, geographical representation, ethnicity, and fragmentary immunological insight addition to variation in BCG vaccine strains with distinct characteristics.

an adjunct to strengthen BCG-induced immunity. Our research group has endeavored and designed a novel vaccine comprising TLR2 and TLR9 agonist along with collective of 7 overlapping immunogenic *M.tb* peptides, packed together in a liposome (PTL). We have demonstrated that intranasal immunization with PTL along with BCG drastically condensed the bacterial burden, enhanced host protective T cell responses with expansion of polyfunctional T cells as well as memory T cell subsets. Furthermore, host protective immune responses were *M.tb* specific owing to which spectrum of host protective signaling pathways critical to control TB were activated in response to PTL BCG co-immunization (100). Further assessment in higher animal models like Non-human primates (NHPs) is coveted to further validate our findings and progress the research to higher phases. We and various groups worldwide have actively devised and pursued strategies to develop new vaccine candidates, booster vaccines and immunotherapeutic to augment BCG efficacy against *M.tb* infection. However, in this review we have discussed about new TB vaccines in brief and have focused on host immunotherapeutic approaches comprehensively.

NEW VACCINES AGAINST TB

The necessity of an alternate vaccination strategy for TB control has not been overlooked and researchers around the world are actively pursuing diverse vaccine candidates to improve existing circumstances (99). On the account of immense attempts, several groups have developed vaccines by employing diverse approaches to control TB. Some classic examples include the attenuated *M.tb* bacilli strains (101) with high immunogenicity (102), the generation of genetically modified BCG strains for better immune responses (70), sub-unit vaccines incorporating immunogens absent in BCG (103), and adjuvants with enhanced potency. Major TB vaccine candidates in advanced clinial trials are tabulated in **Table 2**. A myriad of challenges is liable for slow progress in vaccine development against TB. One of which is the necessity for a vaccine that protects against adult pulmonary TB, in individuals who are presently vaccinated with BCG. Ideally, the development of vaccine candidates that can efficaciously impart protection to individuals previously exposed to mycobacteria including BCG, *M.tb* and environmental mycobacterial species would be enviable. So as to boost the immune responses thereby limiting adult pulmonary TB infections (19). Diverse studies incorporating booster vaccinations are under evaluation in animal models (104). With the advancement in technology and knowledge regarding host protective defense mechanisms, especially antigen-specific immune responses accountable for effective responses against *M.tb* we are surpassing conventional vaccination approaches. With improved understanding regarding known correlates of protection, research groups are assessing strategies to enhance long-lasting protective immune responses by employing progressive targets. What we have learned in the past decade from BCG trials as well as recent COVID-19 trials can be employed in the future to better interpret

TABLE 2 | Major TB vaccine candidates in clinical trials:.

Vaccine candidate	Composition	Clinical Trial	Clinical trial Identifier	Ref.
		Inactivated whole-cell vaccines		
DAR-901	Inactivated *Mycobacterium obusense*	Phase 2, randomized, placebo-controlled, double-blind study to evaluate the efficacy of DAR-901 TB booster to prevent TB in adolescents.	NCT02712424	(1)
MIP	Inactivated *Mycobacterium indicus pranii*	Phase 3, randomized, double-blind, interventional study to determine the efficacy and safety of MIP as an adjunct in Category I pulmonary TB patients	NCT00341328	(2)
RUTI®	Detoxified, fragmented *M.tb* contained in liposomes	Phase 2, randomized, double-blind, placebo-controlled interventional trial to assess the therapeutic vaccine, RUTI against TB	NCT01136161, NCT04919239	(3, 4)
Vaccae™	Heat-inactivated *Mycobacterium vaccae*	Phase 3, randomized, double-blind, interventional trial to assess the safety and efficacy to prevent TB in high-risk groups of TB infection	NCT01979900	(5)
		Live attenuated vaccines		
MTBVAC	Live attenuated *M.tb* vaccine with PhoP and FadD26 deletions	Phase 3, randomized, quadruple masking intervention to determine safety, efficacy and immunogenicity in newborns	NCT04975178	(6)
VPM1002	Live recombinant BCG vaccine strain with urease C deletion engineered to express listeriolysin rather than urease C	Phase 3, multicenter, double-blind, randomized, active-controlled trial to examine the safety, efficacy and immunogenicity to prevent *M.tb* infection	NCT04351685	(7)
		Subunit vaccines		
M72/ ASO1E	Fusion protein subunit vaccine based on 32A and 39A prepared in $AS01_E$ adjuvant	Phase 2, randomized, interventional clinical trial to determine the efficacy of TB vaccine candidate in Adults	NCT01755598	(8)
H56:IC31	Recombinant vaccine comprising proteins of *M.tb* (85B, ESAT6, Rv2660c) and IC31 adjuvant	Phase 2, randomized (1:1), double-blind, placebo-controlled trial to determine efficacy of H56:IC31 in preventing rate of TB recurrence	NCT03512249	(9)
GamTBvac	Recombinant subunit vaccine formulation comprising modified Ag85a and ESAT6-CFP10 *M.tb* antigens and CpG ODN adjuvant	Phase 3, randomized, multicentered, double-blind, placebo-controlled intervention to determine safety and efficaciousness of GamTBvac against pulmonary TB	NCT04975737	(10)
ID93/GLA-SE	ID93 is a recombinant fusion protein comprising 4 antigens from virulence-associated proteins in GLA-SE i.e., oil-in-water emulsion	Phase 2a, randomized, placebo-controlled, double-blind intervention to evaluate safety and effectiveness of ID93/GLA-SE in TB patients	NCT02465216	(11)

the lacunae which can be resolved for an improved TB vaccination program (16).

HOST-DIRECTED STRATEGIES TO IMPROVE BCG EFFICIENCY

The outcome of *M.tb* infection is determined not just by the action of the pathogen but also by the host response. So as to achieve the goal of the End TB strategy, progressive efforts are being made to establish efficacious therapeutics (17). In an attempt to achieve this goal, host-directed therapeutics with the potential to reprogram host defenses for better clinical outcomes are under consideration. Since it is known that in the majority of individuals, the immune system can self-reliantly eradicate the pathogen. Augmenting this phenomenon so as to achieve complete sterility can offer benefits to the existing global TB burden. TB is a chronic disease with a spectrum of pathologies (26). Hence, we need to move ahead from conventional antibiotics toward host-directed therapies for improved clinical outcomes. HDT has found a niche in the treatment of various diseases (105). However, we need more efforts to establish a standard HDT as an adjunct to conventional ATT for the augmentation of disease burden. So as to achieve this target it is a prerequisite to determine key host immune targets for better outcomes. HDTs aim at diverse pathways critical for determining the fate of the infection. HDTs work by restricting pathways exploited by pathogens or by ameliorating host protective immune responses (105). With the advancement in understanding, diverse factors contributing to the establishment of infection have been identified. The primary goal of TB drug discovery is to exterminate both active and persistent bacteria so as to attain complete sterility. Challenge is to aim at heterogenous *M.tb* populations that respond distinctly to therapeutics. It is essential to be reminiscent of the fact that *M.tb* infection can instigate a continuum of host responses owing to distinctive physiologies of heterogeneous bacterial populations. Furthermore, a profound assessment of stochastically and phenotypically drug-resistant persisting populations of *M.tb* subsequent to drug therapy is requisite to cope with TB relapse and reactivation (106). Better insight into mechanisms targeted to exterminate persistent populations is necessitated since it is not conclusive whether targeting bacterial membrane or prime respiratory components will eradicate latent bacteria. It is the need of the hour to get hold of innovative drugs to establish efficacious therapy to attain the goals of the End TB strategy. To accelerate the search for the right drugs, United States Food and Drug Administration (FDA) approved compounds are also under evaluation and operation (107).

Futuristic therapeutics should aim to shorten the duration of conventional ATT by proficient elimination of persistent bacterial populations, which also result in drug-resistant strains. With the constant expansion of drug resistance, options for treatment are continuously depleting. Chiefly, in terms of drug-resistant TB, HDTs can be employed to augment antimicrobial host defences

or to restrain detrimental inflammation instigated by infection. Some of the prospective HDTs against *M.tb* are listed in **Table 3, summarised in Figure 3** and further mechanism of protection is elaborated in different sections. Furthermore, HDTs that can limit the hepatotoxicity associated with conventional antibiotics are desired to subside unfavourable outcomes of extensive therapies. Theoretically HDTs surpass diverse issues associated with pathogen-directed therapeutics. HDTs augment host immune responses with sufficient proficiency to restrict the progression of the disease. Furthermore, targeting host components provide the advantage of reducing the generation of antibiotic resistance (129). Therapeutics targeting host components avoid the chances of drug resistance which is a global health concern. However, if not chosen wisely targeting host components can lead to off-target binding and might accelerate the chances of detrimental side effects. Thus, our knowledge regarding targeted mechanisms is vital to developing therapies to reprogram host defences for efficacious TB treatment.

ESTABLISHED HOST-DIRECTED STRATEGIES TO POTENTIATE BCG VACCINATION

In an attempt to achieve the targets of End TB strategy, diverse host-directed therapeutics with the potential to reprogram host defences for better clinical outcomes are under consideration. Since it is known that in the majority of individuals, the immune system can self-reliantly eradicate the pathogen. Augmenting host defences so as to achieve complete sterility can offer benefits in reducing existing global TB burden. To achieve superior effectiveness against *M.tb* infections, researchers have evaluated the administration of immunomodulators along with antibiotics and vaccines. This was widely employed in cancer therapies wherein inhibition of anti-inflammatory cytokines, and inhibitory signaling receptors such as PD-1 and CTLA-4 were found effective in augmenting tumor recession (130). Likewise, therapeutics known for inhibition of detrimental immune responses were found effective in improving tumor vaccine efficacies. Constructive outcomes were detected against breast cancer and pancreatic adenocarcinoma by the utilization of COX-2 inhibitors (131). In HIV-infected individuals, therapy with COX-2 inhibitor augmented effector and memory responses induced by T cell targeting vaccine; tetanus toxoid (132). Selected clinical trials that have evaluated immunomodulatory strategies adjunct to BCG immunization for improved clinical results have been listed in **Table 4** (133). Furthermore, modulation of monocytic cell populations has been exploited as a prospective strategy for augmenting efficacy of BCG vaccination. Abundance of uric acid crystals namely monosodium urate (MSU) have been linked with bone inflammation and associated immune responses (110). Presence of MSU crystals was further linked with coexisting *M.tb* joint infection in patients suffering from gout (134). MSU treatment in the THP-1 cell line brings about a generation of ROS, stimulation of phagosome-lysosome fusion, and *via* NOD-like receptor signaling enhanced BCG clearance (135). MSU alone has no anti-bacterial activity inferring potential to promote bacterial clearance by immunomodulation. MSU therapy in adjunct to BCG vaccination *in vivo* led to a reduction in bacterial burden in draining lymph nodes. However, MSU treatment did not affect the viability of BCG. As compared to BCG alone, MSU therapy significantly reduced the bacterial burden in the lungs and spleens of *M.tb* infected mice (110). Based on affirmative evidences of Vitamin D supplementation in restraint of *M.tb* infections (136), several research groups have correlated protective efficacy of BCG immunization in infants with Vitamin D levels (137). One of the research group has observed increase in Vitamin D levels in infants vaccinated with BCG and have linked the upsurge with non-specific immune responses detected subsequent to vaccination (138). In another study, infants supplemented with Vitamin D were expected to elicit protective IFN-γ responses against *M.tb* infection (137).

TABLE 3 | Potential host directed immunotherapeutic approaches against *M.tb* infection.

S. No.	Therapeutic candidates	Host protective immunological characteristics	References
1.	Ibuprofen	Inhibits neutrophil infiltration and detrimental inflammation at the site of infection	(108, 109)
2.	Acetylsalicylic acid (Aspirin)	Anti-inflammatory responses reduce detrimental pathology	(108)
3.	Monosodium Urate (MSU)	Activation of immune responses to augment antimycobacterial efficacy of BCG	(110)
4.	Calcimycin	Induction of autophagy by binding to P2X7 receptors	(111)
5.	Verapamil	Inhibits LTCC channels thereby induces autophagy by increasing Ca^{2+} levels.	(112)
6.	Clofazimine	Enrichment of stem cell memory T memory responses upon BCG revaccination	(113)
7.	Luteolin	Inhibition of $Kv_{1.3}$ K^+ channels, enhancement of antimycobacterial and T cell memory immune response	(114, 115)
8.	Rapamycin (Sirolimus)	Enhances antigen processing and presentation and directs T_h1 immunity	(116)
9.	Tat-beclin-1 fusion peptide	Autophagy induction and reduction in progression of pathogens	(117)
10.	Gefitinib	Enhances lysosomal biogenesis, action and bacterial degradation	(118)
11.	2-deoxyglucose (2-DG)	Metabolic reprograming induced reduction in pathological damage	(119)
12.	Ritonavir (Norvir)	Glucose transporter agonist induces protection against HIV as well as *M.tb*	(120)
13.	FX11	Lactate dehydrogenase inhibitor reduces oxidative stress and downgrade iNOS	(121)
14.	TEPP46	Limits inflammation by reducing PKM2 activation	(122)
15.	Metformin	Induces AMPK mediated signaling, induction of ROS and intracellular bacterial killing	(123)
16.	AICAR	Stimulate anti-microbial immune responses by *via* (PPARGC1) linked pathways	(124)
17.	C75	Inhibits lipid derived droplets biogenesis, enhances ROS, NO production and polarizes macrophages from M1 to M2	(125)
18.	Cerulenin	Inhibition of fatty acid synthase, uncouples UCP2 and promotes NLRP3 activation	(126)
19.	GW9662	PPARγ antagonist can regulate inflammation and disease progression by altering metabolism in macrophages.	(127)
20.	AGK2	Inhibits host sirtuin2 (SIRT2) and enhances bacterial clearance, host protective immune responses	(128)

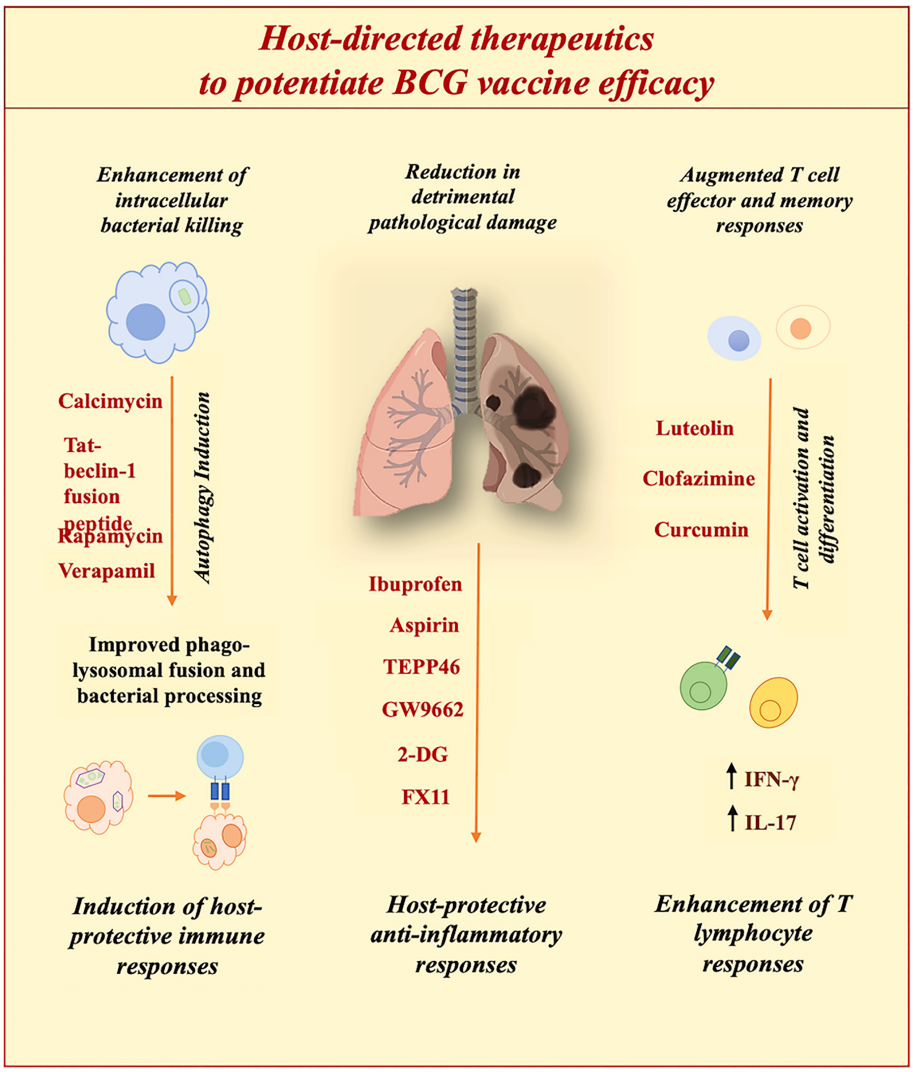

FIGURE 3 | Potential of host-directed therapies (HDTs) to improve BCG efficacy. Diverse HDTs aiming at distinct pathways are under evaluation to improve clinical outcomes. HDTs restrict pathogen-induced subversion strategies to ameliorate host defenses against *M.tb*.

TABLE 4 | List of clinical trials evaluating BCG immunization along with diverse immunotherapeutic for efficient medical utility against diverse disease conditions.

BCG vaccine and immunotherapeutic regimen	Clinical trial	Trial identifier	Diseased condition	Ref.
Intravesical hyaluronic acid (HA) with BCG	Phase 2, randomized, pilot study to examine effect of HA in reducing BCG induced local cytotoxicity	NCT02207608	Bladder urothelial cell carcinoma	(12)
Tislelizumab in Combination with BCG	Phase 2, open-label, single-arm, single center trial to evaluate safety and effectiveness of Tislelizumab along with BCG (TACBIN-01)	NCT04922047	High risk urinary bladder cancers	(13)
Vitamin D supplementation in adjunct to BCG immunization in infants	Randomized, double masked, interventional study to evaluate impact of vitamin D supplement in infants prior to BCG vaccination	NCT01288950	Tuberculosis	(14)
Vitamin A with BCG Vaccine	Phase 4, randomized, double-masked intervention to evaluate the utility of high-dose vitamin A supplementation in infants along with BCG vaccine at birth	NCT00168597	Mortality and morbidity in infants	(15)
Monoclonal Antibody A1G4 and BCG	Phase 1 intervention to evaluate the efficacy of monoclonal antibody A1G4 along with BCG in cancer patients	NCT00003023	* Neuroblastoma, Sarcoma	(16)

However, this clinical trial waned to provide evidences of Vitamin D induced protection in augmenting BCG efficacy. Further assessment is requisite to explore prospects of Vitamin D supplementation along with BCG immunization. Potential of established immunomodulators with BCG have been improvised for better clinical outcomes. One such study demonstrated induction of superior host protective T cell responses upon co-administering curcumin nanoparticles along with BCG immunization in murine model (139). Clofazimine (CLOF), an authorised therapeutic for leprosy treatment and second-line drug used in combinations against drug-resistant *M.tb* strains has also demonstrated affirmative outcomes in mice model. BCG revaccination along with CLOF administration significantly augmented T cell memory responses comprising enhancement of stem cell-like memory T cell responses (T_{SCM}) along with successive effector and memory T cell populations (113). So as to further resolve the prospects of above-mentioned strategies in enhancement of BCG efficacy, further studies in higher animal models such as non-human primates (NHPs) and clinical trials is necessitated without delay.

MODULATION OF IMMUNE RESPONSES TO IMPROVE PROTECTIVE EFFICACY

With the rise of genomics, researchers have utilized the genomic information of *M.tb* and *M. bovis* BCG vaccine strains for assessing variations that can be benefitted to develop better vaccination strategies (95). The revelation of the entire *M.tb* genome revolutionized TB research by expanding the knowledge of central immunomodulatory components (140). To achieve superior effectiveness against *M.tb* infections, researchers have evaluated the administration of immunomodulators along with vaccines. This was widely employed in cancer therapies wherein inhibition of anti-inflammatory cytokines, and inhibitory signaling receptors such as PD-1 and CTLA-4 were found effective in augmenting tumor recession (130). Likewise, therapeutics known for inhibition of detrimental immune responses were found effective in improving tumor vaccine efficacies. Constructive outcomes were detected against breast cancer and pancreatic adenocarcinoma by the utilization of COX-2 inhibitors (131). In HIV-infected individuals, therapy with COX-2 inhibitor augmented effector and memory responses induced by T cell targeting vaccine; tetanus toxoid (132). Inhibition of neutrophil infiltration at the site of *M.tb* infection by **Ibuprofen** (IBP) resulted in improved clinical outcomes and a reduction in bacterial burden in C3HeB/FeB mice (109). IBP is also known to possess specific antitubercular characteristics (141). Furthermore, IBP along with another drug; **acetylsalicylic acid** was evaluated to be repurposed as an adjunct therapy in TB patients (108). In murine model of TB, drugs were associated with enhancement of pyrazinamide (PYZ) antimycobacterial efficacy (142). This approach can be further exploited to amend BCG-induced responses. These studies indicate that treatment with immunomodulatory compounds or enriching host protective responses along with BCG might can effectively enhance protection induced by BCG vaccination.

TARGETING HOST ION CHANNELS

Another strategy is to aim at host ion channels, that orchestrate physiological features of various cell populations by operating ions facilitated currents throughout cellular and subcellular membranes (143). Intracellular calcium levels are known to regulate key immune responses in the host, directly or by directional alteration of other vital ions such as potassium (K^+), sodium (Na^+), and chloride (Cl^-) ions within immune cell populations (144). Obstruction of ion channels by employing diverse blockers has been assessed as a therapeutic target for diseases like hypertension (145). Research groups have also examined ion channel blockers for boosting anti-microbial immune responses. Intracellular calcium (Ca^{2+}) levels play a vital role in the regulation of antimycobacterial mechanisms such as autophagy, maturation of phagosome, and induction of apoptosis (146). However, the impact of Ca^{2+} levels on processes like autophagy additionally depends on the involvement of diverse ion channels contributing to the maintenance of current (147). For instance, it has been observed that Ca^{2+} currents *via* Voltage-gated calcium channels (VGCCs) impede induction of autophagy (147) while Ca^{2+} currents through P2X purinoceptor 7 (P2X7) receptor heighten autophagy induction and intracellular extermination of *M. bovis* BCG in macrophages. **Calcimycin,** an ionophore binds to P2X7 receptor which leads to rise in intracellular $Ca2^+$ levels and exerts antimycobacterial activity against *M. bovis* BCG (111) by stimulation of autophagy (148). Administering $Ca2^+$ ion channel blockers was linked with a 32% reduction in risk of progression into a diseased state, in a clinical study in TB patients with heart and cerebrovascular diseases (149). Diverse Ca^{2+} ion channel blockers evaluated in the investigation exhibited variable consequences. L-type calcium channel (LTCC) blocker – **verapamil,** an FDA approved drug is utilized to treat abnormalities in heart rhythms, angina (150), and hypertension (151). In macrophages, LTCCs attenuate Ca^{2+} discharge from the endoplasmic reticulum (ER) leading to inhibition of macrophage activation. So as to bypass host immune responses *M.tb* upregulates the expression of VGCCs in APCs. Verapamil administration inhibits LTCC currents thereby escalating Ca^{2+} concentration in the cytosol which upregulates autophagy and bacterial clearance in *M.tb* (143). Additionally, LTCC ion channel blockers can alter iron-associated metabolic pathways thereby impeding iron accessibility which lowers intracellular bacterial survival (143). Furthermore, verapamil acts synergistically with first-line anti-TB drugs- INH (152), and RIF (153) in lowering the bacterial burden in cultures, macrophages, and murine models of TB. In another study, antimycobacterial activity of verapamil was confirmed with several TB drugs including bedaquiline (BDQ) and clofazimine (CFZ) and decreased bacterial load was linked

with induction of membrane stress responses as a consequence of verapamil induced membrane function disruption (154). In the murine model, adjunctive verapamil administration augmented efficacy of recently approved MDR-TB drug; bedaquiline at lower doses and diminished the emergent resistant strains (155). Furthermore, progressive approaches such as assessment of inhalable verapamil-rifapentine particles has been assessed by researchers for utility as ATT (156). Even with significant pieces of evidence regarding anti-TB activity and negligible toxicity, verapamil has not transitioned into clinical setup. Further assessment of the anti-TB potential of verapamil along with BCG immunization is necessitated to evaluate the impact on modulating immunological responses. Similarly, Numerous K^+ ion channel blockers have been assessed as prospective anti-TB therapeutics owing to their physiochemical ability to activate macrophages. **Clofazimine** (CFZ) is a conventional first-line drug used for leprosy treatment along with RIF and dapsone (157). It was initially developed against *M.tb* but was found not as efficacious as INH and RIF. However, with emergent drug-resistant strains, it has been recently employed as a second-line anti-TB drug (158). Numerous clinical trials (BEAT-TB (159), endTB-Q (160), and TB-PRACTECAL (161)) are investigating the efficaciousness of regimens comprising clofazimine. Furthermore, phase-2 clinical trial CLO-FAST is examining 3-month ATT comprising clofazimine and rifapentine against drug-sensitive *M.tb* (162). In addition to antimycobacterial activity, clofazimine is a potent immunomodulator. It inhibits $Kv_{1.3}$ K^+ channels which are expressed in various immune cells (163). Clofazimine-induced inhibition of $Kv_{1.3}$ K^+ channels abundantly present on T effector memory cells (T_{EM}) enhances the efficacy of BCG vaccination in a murine model of TB by specifically promoting the expansion of the T central memory cell population (T_{CM}). Furthermore, CFZ enriches stem cell memory T cell responses upon BCG revaccination (113). In a similar manner, we have demonstrated the efficacy of less toxic, phytochemical namely Luteolin an established $Kv_{1.3}$ K^+ channel blocker in augmenting BCG-induced immune responses by enriching T_{CM} memory responses, improving T_{CM} : T_{EM} ratio and enhances host protective T_h1 and T_h17 immune responses against *M.tb* infection in the murine model of TB (115). Furthermore, immune-protective properties of luteolin condensed the time period of bacterial clearance with INH owing to augmented T_h1 and T_h17 immune responses and eased pathological damage and TB associated hepatotoxity *in vivo* (114).

IMPROVING ANTI-MICROBIAL IMMUNE RESPONSES

Therapeutic modulation of host immune responses to achieve complete sterility is another approach that has been pursued by several research groups (129). *M.tb* utilizes complex artillery to evade immune cell populations and associated defense mechanisms. *M.tb* owing to mycobacterial virulence factors such as cell wall component- mannose-capped lipoarabinomannan is known to inhibit phagolysosome fusion in macrophages. It is a vital phenomenon critical for curbing infection at an early stage (26). However, this can be enforced by autophagy induction, which is another cellular mechanism by which detrimental cytosolic molecules and organelles are targeted to lysosomes for degradation. Early secreted antigen 6 secretion system-1 (ESX-1) of *M.tb* is known to permeabilize the phagosome to escape degradation (164). However, this facilitates processing by components of ubiquitin-mediated autophagy mechanism and results in a reduction in *M.tb* persistence (165). Furthermore, stimulation of autophagy sequesters and degrades bacterial components and can also contribute to fostering antigen presentation and moderating pathology (166). The most widely studied autophagy inducer – **rapamycin (Sirolimus)** is known to inhibit the mammalian target of rapamycin (mTOR) which negatively regulates autophagy. It is majorly employed in organ transplantation owing to the immunosuppressive nature of the drug (167). Researchers have attempted re-purposing of Rapamycin, an autophagy inducer to heighten antigen processing and presentation in murine antigen-presenting cells (APCs) (168). It is well established that confiscation of BCG within phagosome and inability to fuse with lysosome reduces the efficacy of antigenic peptide presentation on DCs. Dendritic cells (DCs) treated with autophagy inducer, rapamycin enhanced T_h1 responses against *M.tb* (116). Improvement in DC activation and T_h1 responses against *M.* with concurrent rapamycin and BCG administration offers prospective approach to autophagy mediated enhancement of bacterial clearance (116). Similarly, the efficacy of BCG can be augmented by simultaneous treatment to direct host responses toward bacterial extermination to achieve complete sterility (116). Few piecemeal studies have questioned the immunotherapeutic strategies to enhance vaccine efficiency against TB, however a great deal is yet to be explored (169). However, side effects associated with rapamycin administration such as interstitial pneumonitis can be alarming in TB patients with substantial pathology (170). Furthermore, metabolization of rapamycin by hepatic enzyme CYP3A4 limits its utility in TB patients since CYP3A4 is intensely stimulated by standard ATT antibiotic – INH (171). Due to the mentioned limitations rapamycin has not been further evaluated as HDT against *M.tb*. **Vadimezan (also known as DMXAA)** is another prospective autophagy inducer. It is an established antitumor agent as well as in mice it triggers, a stimulator of IFN genes (STING) dependent autophagy mechanism (172). However, it was found inefficacious in humans (173). Research groups have further examined the utility of fusion peptides for the induction of autophagy. **Tat-beclin-1 fusion peptide** an autophagy inducer (174) was found to restrict the proliferation of diverse pathogenic strains and heightened survival rates in infected mice (117). Though, restrictions like regular administration by injection constrain the clinical utility of HDT. Alternatively, an inhibitor of epidermal growth factor receptor (EGFR) was found to limit *M.tb* proliferation in macrophages and reduces bacterial burden in the lungs of infected mice *via* autophagy induction (175). In *M.tb* infected macrophages treated with **Gefitinib**; tyrosine kinase inhibitor, lysosomal biogenesis, function and targeting of bacteria

to lysosome for degradation is increased thereby decreasing bacterial burden *via* EGFR signaling in macrophages (118). However, there is a need to further analyse pieces of evidence and peripheral markers of autophagy for certainty. With the advancement in technologies, sophisticated approaches to evaluate the induction of autophagy can evolve the quest for superior autophagy inducers that can be employed to enhance bacterial killing by limiting dissemination.

TARGETING HOST METABOLISM

Research focus has shifted radically in the past decade towards metabolic shifts in response to infections. Immunometabolism is an emerging field that focuses on the impact of the metabolic state of immune cell populations to provide better insight into disease progression and pathogenesis (176). In the initial course of *M.tb* infection, metabolic shift is observed to defend the host. Immune protective responses such as stimulation of pro-inflammatory cytokines, and nitric oxide (NO) release is directed *via* HIF-1-dependent glycolytic pathways (177). However, *M.tb* is known to stimulate the Warburg effect so as to inhibit anti-microbial host immune responses (178). Host metabolism is utilized by *M.tb* to survive and proliferate by escaping host protective immune mechanisms (179). This infers that metabolic reprogramming is vital for defense against *M.tb* so as to augment efficacious sterilization mechanisms. **2-deoxyglucose (2-DG)** an inhibitor of hexokinase enzyme, can limit the IL1-β generation in LPS-activated macrophages and result in succinate accumulation (180). 2-DG stimulated glycolysis inhibition can additionally result in a reduction in lung damage induced by LPS (181) *via* moderating nuclear PKM2-STAT3 signaling. Further, prospects of 2-DG to restrict pathological damage in TB cases can be assessed for augmented clinical outcomes. Similarly, **ritonavir** (Norvir), a protease inhibitor widely used as antiretroviral medication to treat HIV infections (120), is additionally known for capability to act as an glucose transporter agonist (182). Researchers have evaluated combinations of HIV drugs including ritonavir along with ATT so as to effectively counter HIV-TB coinfections (183). Strategic arrangement by utilizing characteristics of ritonavir to inhibit host glucose transporters can be assessed further in case of HIV-TB patients to better understand mechanism of protection. Inhibitor of pyruvate dehydrogenase kinase- **dichloroacetate**, is a small molecule that increases pyruvate flux into mitochondria and skews metabolism toward glucose oxidation rather than glycolysis (184). Inhibition of pyruvate dehydrogenase kinase was established as a host target to counter infection of *Salmonella enterica serovar typhimurium via* metabolic reprogramming of M1 macrophages. However, intracellular burden for *M.tb* was not reduced upon dichloroacetate treatment, alternate inhibitors can be explored with similar objective (185). Another small molecule and lactate dehydrogenase inhibitor – **FX11 (**3-dihydroxy-6-methyl-7-(phenylmethyl)-4-propylnaphthalene-1-carboxylic acid]) is known for induction of oxidative stress and reduction in tumour advancement (121). Downregulation of iNOS and cytokine generation was achieved in LPS-activated RAW 264.7 macrophages upon FX11 induced lactate dehydrogenase inhibition (186). Similarly, the inhibitor of pyruvate kinase– **TEPP46** significantly reduced PKM2 activation in LPS-induced macrophages which led to a lowering of IL-1β generation (122). Hence, small molecule inhibitors can be employed to direct metabolic flux for desired clinical outcomes to resolve immunopathology of TB by regulating host metabolism.

M.tb manipulates lipid and fatty acid metabolic pathways of the host for its persistence and proliferation (187). Foamy macrophages recruited around *M.tb* infected phagocytes, supply nutrition and support in the course of infection. *M.tb* manipulates host cells to synthesize lipids and fatty acids. Hence, components of lipid synthesis pathways manipulated by *M.tb* for survival can be targeted as HDT (188). Metabolic energy sensors such as AMP-activated protein kinase (AMPK) play a vital role in the regulation of key host protective mechanisms against infections (189). An approved type 2 diabetes drug, **Metformin** which activates the AMPK-mediated signaling mechanism has been evaluated for TB (190). Metformin induces the generation of mitochondrial reactive oxygen species (ROS) resulting in restriction in intracellular growth of *M.tb* and limiting the activation of the inflammatory gene (191). In *M.tb* infected guinea pigs, metformin acts synergistically with conventional ATT drugs – INH and ETH (192). Metformin administration causes a significant reduction in latent TB incidences in prone diabetic individuals (193). This HDT can be evaluated proficiently at advanced clinical stages. Another AMPK activator, 5-aminoimidazole-4-carboxamide-1-1-β-D-ribofuranoside **(AICAR)** stimulates anti-microbial responses by activating autophagic pathways in macrophages. AMPK activation by AICAR further controls the biogenesis of mitochondria and metabolic state in macrophages by inducing peroxisome proliferator-activated receptor gamma coactivator-1 (PPARGC1) associated pathways (124). Components of host machinery that curb the metabolism of lipids can reduce detrimental inflammation thereby establishing a balanced immune state. Fatty acid synthase inhibitors such as **C75** and **cerulenin** are prospective targets for the augmentation of efficacious immune responses. Inhibition of lipid-derived droplets by C75 can lead to polarization of macrophages from the M1 to M2 subset causing enhancement of ROS and NO production (125). C75 and cerulenin-mediated inhibition of fatty acid synthase lead to uncoupling protein-2 (UCP2) mediated NLRP3 inflammasome activation (126). PPARγ antagonist, **GW9662** is known to regulate vital processes such as metabolism, inflammation, and disease progression (127) in macrophages infected with *M. bovis* BCG (76). Link between inflammation and lipid metabolism associated PPARγ signaling can be exploited to potentiate BCG-induced protection (76). This infers that reprogramming key components of lipid metabolism can be a prospective target for progressive TB therapeutics. Sirtuins (SIRTs) are another prospective target with the potential to be targeted for the augmentation of host defences (77). SIRTs are deacetylases that regulate cellular mechanisms like inflammatory responses, regulation of lipid metabolism by modulating components of NF-κB immune signaling, and anti-inflammatory

responses by regulation of Peroxisome proliferator-activated receptor gamma coactivator 1-alpha (PGC-1α) (78). It has been observed that SIRT-1 expression is diminished drastically in *M.tb* infected THP-1 cells. SIRT-1 downregulates RelA/p65 unit of NF-κB so as to modulate inflammation (79). SIRT-6 is also known to diminish pro-inflammatory and anti-microbial responses in the early course of *M.tb* infection (80). Furthermore, SIRT2 has been established as an immunotherapeutic target against *M.tb* infection in mice model of TB (128). It was observed that subsequent to *M.tb* infection, SIRT2 expression increases along with translocation to nucleus to induce immune dampening epigenetic modifications. However, chemical inhibition of SIRT2 using established inhibitor, **AGK2** dramatically augmented bacterial clearance and host protective immune responses. Since, existing literature is available regarding SIRT2 induced metabolic programming (81) and signal transduction (82). Further progressive approaches can be shaped by targeting key physiological factors of host.

TARGETING MICRORNAS

miRNAs are non-coding RNAs that are involved at post-transcriptional levels to regulate array of genes decisive of immune responses (83). Over 2000 functional miRNAs are encoded by human genome (84) which regulate diverse protein-coding transcripts (194). It is now well-established that miRNAs distinctly regulate host immune responses against *M.tb* infection (195). Differential expression of miRNAs can signify the advancement of disease from latent to an active infection (196). Furthermore, miRNAs play a significant role in the moderation of apoptotic and autophagic responses during *M.tb* infection (196). Owing to advancements in technology, miRNA delivery is being employed to treat diverse diseases. This further pave way for the application of miRNAs as HDT against TB (197). Several studies have assessed mechanisms by which *M.tb* temper host immune responses for survival in an antimicrobial milieu. Diverse immune mechanisms such as phagolysosome maturation in APCs, cytokine stimulation by immune cell populations, and antigen processing and presentation are dynamically manipulated by *M.tb*. These cellular processes are strictly regulated by an assortment of miRNAs in the host (198). *M.tb* is additionally known to alter miRNA expression associated with key biological responses to escape host immune responses (199). Additionally, expectations of combined regulation of transcriptional network by miRNAs and transcription factors represent miRNAs linked with diseases as a novel category of therapeutics.

miRNAs involved in immune pathways are extensively studied for mycobacterial infections (200). It is well-known that during *M.tb* infection miR-125b inhibits TNF biosynthesis in human alveolar macrophages (201). Several research groups have observed that *M.tb* infection results in differential expression of miRNAs which determines the fate of immune responses (202). However, comprehensive knowledge is requisite for progressive considerations. Participation of miRNAs in *M.tb* induced autophagy (203) and apoptosis has provoked further interest to maneuver miRNAs for HDTs. Upon *M.tb* infection, diverse cell populations respond varyingly in conjunction with variations in miRNA expression. Upregulation of miR-155 has been observed in bone marrow-derived macrophages of mice infected with *M.tb* (204). In contrast, downregulation of miR-155 has been observed in peripheral blood mononuclear cells (PBMCs) derived macrophages upon *M.tb* infection (201). Mycobacterial infection in human monocyte-derived macrophages results in overexpression of miR-29a, miR-886-5p, and let-7e, which further target caspase 3 and caspase 7 as predicted by the integrated analysis. Differential expression of miR155, miR-146a, miR145, miR222, miR-27a, and miR-27b was observed in human macrophages infected with virulent *M.tb* H37Rv and avirulent strain *M. bovis* BCG. Downregulation of miRNA involved in the regulation of inflammation and lipid metabolism was observed. Furthermore, miR-145 known for induction of apoptosis has been reported to be downregulated upon infection with a virulent *M.tb* strain, which results in overexpression of targets which inhibit apoptosis (205). Based on microarray analysis, global changes in miRNA expression screened nine miRNA genes which were differentially expressed in *M.tb* H37Rv and *M.tb* H37Ra infected THP-1 cells. These differentially expressed miRNAs such as miR-30a, miR-30e, miR-155, miR-1275, miR-3665, miR3178, miR-4484, miR-4668-5p, and miR-4497 contribute in diverse physiological aspects. miR-155 interacts with negative regulators involved in TNF- α generation (201). Evaluation of PBMCs and pleural fluid mononuclear cells (PFMCs) linked miRNA expression with levels of IL-6 cytokine. Additionally, it has been observed that the highly-virulent Beijing/W TB strain represses plenty of miRNA in human macrophages as compared to non-Beijing/W TB strains. Alterations in miRNAs have been observed in patients with active TB. The functional assessment demonstrated that miR-144 restrains T-cell expansion and generation of key cytokines, INF-γ and TNF-α. In RAW264.7 cells, upon BCG inoculation, miRNA-144-3p overexpression is linked with inhibition of autophagy and antimycobacterial activity (206). Elevation in miR-424 and miR-365 levels has been detected in active TB patients. Diverse miRNA contributes to determining the fate of infection. Regulation of immune cell activation by miR-155, miR-146a, miR-21, and miR-9 (207), TLR signaling is positively regulated by miR155 (208). Subsequent to *M. bovis* BCG infection significant increase in miR-155 expression is observed in macrophages, which modulates diverse innate immune responses including ROS generation (209). It additionally plays role in apoptosis induction in macrophages upon *M. bovis* BCG inoculation which modulates cellular physiology and immune responses (210). In *M.tb* infected human alveolar macrophages, miR-125b inhibits TNF generation (201). miR-29 targets IFN-γ and regulate immune responses linked to *M.tb* infection (211). miR-223 targets several chemo-attractants such as CXCL2, CCL3 and contributes to directing immune response (212). It has been evaluated that endogenous block of miR-29 in transgenic mice, augmented resistance to *M.tb* infection (211). miR-27a targets IRAK4 and restrict immune response in TB (213). Another study demonstrated that BCG infection in RAW264.7 cells

upregulates miR-17-5p which was linked with augmented BCG dissemination and enhanced autophagosome related protein expression (214). As revealed diverse miRNAs are under evaluation owing to gene modulatory potentials. However, our knowledge regarding role of specific miRNA overexpression upon BCG inoculation is still fragmentary. Utilization of miRNAs to augment host immune responses, paves way for advancement in therapeutics for various diseased conditions. Differential expression of miRNAs can be moulded in such a way to achieve better clinical outcomes in TB patients. Progressive therapeutics are employing miRNA-mimics (215), antisense oligonucleotides (216) to manipulate immune responses. Although several research groups have evaluated the utility of miRNA manipulation as HDT against *M.tb*, further assessment is necessitated to establish the prominence of miRNA as therapeutic. We required more studies to comprehend the contribution of miRNA in host-pathogen interactions and a progressive strategy for augmenting conventional therapies.

CONCLUSIONS AND FUTURE PERSPECTIVE

Despite incessant debates on the variable protective efficiency of BCG, it prevails as the only vaccine for TB prevention. Owing to considerable protection in children against disseminated forms of TB, it remains a key component of TB control programs in various countries (90). Throughout our review, we have mentioned several shortcomings and lacunae linked with the failure of the TB vaccination strategy. One of which is the complexity of the disease itself, as we are envisaging resolutions that can impart complete sterility, which is seldomly accomplished in the natural course of infection (26). In this aspect, TB diverges from the diseases that are preventable *via* vaccination. Hence, progressive approaches were pursued with the utilization of known immune correlates of protection. To surpass the previously failed attempts, it is vital to redirect focus on immunological pathways that can be augmented for better clinical implications (217). Since adult pulmonary TB mainly accounts for *M.tb* transmission, advances to tackle the inadequacies of BCG to impart long-lasting immunological memory should be highlighted as a better immunization stratagem. With extraordinary scientific efforts to counteract the most fatal pathogens known to humankind, we have progressed to a situation wherein we can harness establish knowledge and immunological concepts to deal with the shortcomings of existing approaches and improvise for robust clinical trajectories. Since the most of individuals worldwide are already vaccinated with BCG, it is judicious to keep BCG in reflection while developing new vaccination strategies. Scientific communities are attempting stratagems to prevent millions of deaths from escalating infectious diseases by investing on immunotherapeutic approaches to augment immunological responses.

AUTHOR CONTRIBUTIONS

KN, VD wrote the manuscript. AB edited the manuscript. VD conceived the hypothesis. All authors contributed to the article and approved the submitted version.

REFERENCES

1. World Health Organization. *Global Tuberculosis Report 2021*. Geneva: World Health Organization (2021). Available at: https://apps.who.int/iris/handle/10665/346387.
2. Sutherland I, Svandová E, Radhakrishna S. The Development of Clinical Tuberculosis Following Infection With Tubercle Bacilli. 1. A Theoretical Model for the Development of Clinical Tuberculosis Following Infection, Linking From Data on the Risk of Tuberculous Infection and the Incidence of Clinical Tuberculosis in the Netherlands. *Tubercle* (1982) 63(4):255–68. doi: 10.1016/S0041-3879(82)80013-5
3. Onozaki I, Raviglione M. Stopping Tuberculosis in the 21st Century: Goals and Strategies. *Respirology* (2010) 15(1):32–43. doi: 10.1111/j.1440-1843.2009.01673.x
4. *Elsevier_Vaccine_Immunology*. Available at: https://www.vacunashnrg.com.ar/archivosInteres/Elsevier_Vaccine_immunology.pdf.
5. Holladay AJ, Poole JCF. Thucydides and the Plague of Athens. *Classical Quarterly* (1979) 29(2):282–300. doi: 10.1017/S0009838800035928
6. Riedel S. Edward Jenner and the History of Smallpox and Vaccination. *Proc (Bayl Univ Med Cent)* (2005) 18(1):21–5. doi: 10.1080/08998280.2005.11928028
7. Netea MG, Quintin J, van der Meer JWM. Trained Immunity: A Memory for Innate Host Defense. *Cell Host Microbe* (2011) 9(5):355–61. doi: 10.1016/j.chom.2011.04.006
8. Netea MG, Schlitzer A, Placek K, Joosten LAB, Schultze JL. Innate and Adaptive Immune Memory: An Evolutionary Continuum in the Host's Response to Pathogens. *Cell Host Microbe* (2019) 25(1):13–26. doi: 10.1016/j.chom.2018.12.006
9. BCG. Available at: https://www.who.int/teams/health-product-policy-and-standards/standards-and-specifications/vaccines-quality/bcg.
10. Mack U, Migliori GB, Sester M, Rieder HL, Ehlers S, Goletti D, et al. LTBI: Latent Tuberculosis Infection or Lasting Immune Responses to M. tuberculosis? A TBNET Consensus Statement. *Eur Respir J* (2009) 33 (5):956–73. doi: 10.1183/09031936.00120908
11. Ottenhoff THM, Kaufmann SHE. Vaccines Against Tuberculosis: Where Are We and Where Do We Need to Go? *PloS Pathog* (2012) 8(5):e1002607. doi: 10.1371/journal.ppat.1002607
12. Moliva JI, Turner J, Torrelles JB. Immune Responses to Bacillus Calmette–Guérin Vaccination: Why Do They Fail to Protect Against Mycobacterium Tuberculosis? *Front Immunol* 8:407. doi: 10.3389/fimmu.2017.00407
13. Hatherill M, White RG, Hawn TR. Clinical Development of New TB Vaccines: Recent Advances and Next Steps. *Front Microbiol* (2020) 10:3154. doi: 10.3389/fmicb.2019.03154
14. Song WM, Zhao J, Zhang QY, Liu S, Zhu XH, An Q, et al. COVID-19 and Tuberculosis Coinfection: An Overview of Case Reports/Case Series and Meta-Analysis. *Front Med* (2021) 8:657006. doi: 10.3389/fmed.2021.657006
15. WHO Information Note. *COVID-19 Considerations for Tuberculosis (TB) Care* . Available at: https://www.who.int/publications-detail-redirect/WHO-2019-nCoV-TB-care-2021.1.
16. Gonzalez-Perez M, Sanchez-Tarjuelo R, Shor B, Nistal-Villan E, Ochando J. The BCG Vaccine for COVID-19: First Verdict and Future Directions. *Front Immunol* (2021) 12:632478. doi: 10.3389/fimmu.2021.632478
17. *Global Tuberculosis Programme*. Available at: https://www.who.int/teams/global-tuberculosis-programme/covid-19.
18. *Does the Efficacy of BCG Decline With Time Since Vaccination?* Available at: https://www.ingentaconnect.com/content/iuatld/ijtld/1998/00000002/00000003/art00005.
19. *BCG: To Face an Ancient Enemy*. Available at: https://www.nature.com/articles/d42859-020-00010-x.

20. *History-Of-BCG-Vaccine*. Available at: https://association-camille-guerin.com/chabonnes/wp-content/uploads/History-of-BCG-Vaccine.pdf.
21. Kaufmann SH. Vaccine Development Against Tuberculosis Over the Last 140 Years: Failure as Part of Success. *Front Microbiol* 12:750124. doi: 10.3389/fmicb.2021.750124
22. Genome Plasticity of BCG and Impact on Vaccine Efficacy. *PNAS*. doi: 10.1073/pnas.0700869104
23. Ritz N, Hanekom WA, Robins-Browne R, Britton WJ, Curtis N. Influence of BCG Vaccine Strain on the Immune Response and Protection Against Tuberculosis. *FEMS Microbiol Rev* (2008) 32(5):821–41. doi: 10.1111/j.1574-6976.2008.00118.x
24. Kaufmann SH. Vaccination Against Tuberculosis: Revamping BCG by Molecular Genetics Guided by Immunology. *Immunology*. doi: 10.3389/fimmu.2020.00316
25. *Issues Relating to the Use of BCG in Immunization Programmes: A Discussion Document*. Available at: https://apps.who.int/iris/handle/10665/66120.
26. Flynn JL, Chan J. Immunology of Tuberculosis. *Annu Rev Immunol* (2001) 19:93–129. doi: 10.1146/annurev.immunol.19.1.93
27. De Martino M, Lodi L, Galli L, Chiappini E. Immune Response to Mycobacterium Tuberculosis: A Narrative Review. *Front Pediatr* 7:350. doi: 10.3389/fped.2019.00350
28. Tuberculosis Vaccine Development: Progress in Clinical Evaluation. *Clin Microbiol Rev*. doi: 10.1128/CMR.00100-19
29. Lamm DL, Morales A. A BCG Success Story: From Prevention of Tuberculosis to Optimal Bladder Cancer Treatment. *Vaccine* (2021) 39 (50):7308–18. doi: 10.1016/j.vaccine.2021.08.026
30. El-Zein M, Parent ME, Benedetti A, Rousseau MC. Does BCG Vaccination Protect Against the Development of Childhood Asthma? A Systematic Review and Meta-Analysis of Epidemiological Studies. *Int J Epidemiol* (2010) 39(2):469–86. doi: 10.1093/ije/dyp307
31. Pereira LIA, Dorta ML, Pereira AJCS, Bastos RP, Oliveira MAP, Pinto SA, et al. Increase of NK Cells and Proinflammatory Monocytes are Associated With the Clinical Improvement of Diffuse Cutaneous Leishmaniasis After Immunochemotherapy With BCG/Leishmania Antigens. *Am J Trop Med Hyg* (2009) 81(3):378–83. doi: 10.4269/ajtmh.2009.81.378
32. Rao AG, Haqqani R. Study of BCG Immunotherapy in the Management of Multiple, Extensive Non-Genital Cutaneous Common Warts. *Indian Dermatol Online J* (2020) 11(5):784–8. doi: 10.4103/idoj.IDOJ_461_19
33. ON IMMUNOLOGICAL MEMORY. *Annu Rev Immunol*. doi: 10.1146/annurev.immunol.14.1.333
34. Chai Q, Wang L, Liu CH, Ge B. New Insights Into the Evasion of Host Innate Immunity by Mycobacterium Tuberculosis. *Cell Mol Immunol* (2020) 17 (9):901–13. doi: 10.1038/s41423-020-0502-z
35. Liu CH, Liu H, Ge B. Innate Immunity in Tuberculosis: Host Defense vs Pathogen Evasion. *Cell Mol Immunol* (2017) 14(12):963–75. doi: 10.1038/cmi.2017.88
36. Bickett TE, McLean J, Creissen E, Izzo L, Hagan C, Izzo AJ, et al. Characterizing the BCG Induced Macrophage and Neutrophil Mechanisms for Defense Against Mycobacterium Tuberculosis. *Front Immunol* (2020) 11:1202. doi: 10.3389/fimmu.2020.01202
37. Abadie V, Badell E, Douillard P, Ensergueix D, Leenen PJM, Tanguy M, et al. Neutrophils Rapidly Migrate *via* Lymphatics After Mycobacterium Bovis BCG Intradermal Vaccination and Shuttle Live Bacilli to the Draining Lymph Nodes. *Blood* (2005) 106(5):1843–50. doi: 10.1182/blood-2005-03-1281
38. Khader SA, Divangahi M, Hanekom W, Hill PC, Maeurer M, Makar KW, et al. Targeting Innate Immunity for Tuberculosis Vaccination. *J Clin Invest* (2019) 129(9):3482–91. doi: 10.1172/JCI128877
39. Sendide K, Reiner NE, Lee JSI, Bourgoin S, Talal A, Hmama Z. Cross-Talk Between CD14 and Complement Receptor 3 Promotes Phagocytosis of Mycobacteria: Regulation by Phosphatidylinositol 3-Kinase and Cytohesin-1. *J Immunol* (2005) 174(7):4210–9. doi: 10.4049/jimmunol.174.7.4210
40. Heldwein KA, Liang MD, Andresen TK, Thomas KE, Marty AM, Cuesta N, et al. TLR2 and TLR4 Serve Distinct Roles in the Host Immune Response Against Mycobacterium Bovis BCG. *J Leukoc Biol* (2003) 74(2):277–86. doi: 10.1189/jlb.0103026
41. The Mannose Receptor is Expressed by Subsets of APC in non-Lymphoid Organs. *BMC Immunol*. doi: 10.1186/1471-2172-6-4
42. *Human and Mouse Macrophage-Inducible C-Type Lectin (Mincle) Bind Candida Albicans*.
43. Moliva JI, Turner J, Torrelles JB. Immune Responses to Bacillus Calmette–Guérin Vaccination: Why Do They Fail to Protect Against Mycobacterium Tuberculosis? *Front Immunol* (2017) 8:407. doi: 10.3389/fimmu.2017.00407
44. *Mycobacteria Use Their Surface-Exposed Glycolipids to Infect Human Macrophages Through a Receptor-Dependent Process*.
45. Sugisaki K, Dannenberg AM, Abe Y, Tsuruta J, Su WJ, Said W, et al. Nonspecific and Immune-Specific Up-Regulation of Cytokines in Rabbit Dermal Tuberculous (BCG) Lesions. *J Leukoc Biol* (1998) 63(4):440–50. doi: 10.1002/jlb.63.4.440
46. Morel C, Badell E, Abadie V, Robledo M, Setterblad N, Gluckman JC, et al. Mycobacterium Bovis BCG-Infected Neutrophils and Dendritic Cells Cooperate to Induce Specific T Cell Responses in Humans and Mice. *Eur J Immunol* (2008) 38(2):437–47. doi: 10.1002/eji.200737905
47. Jeevan A, Majorov K, Sawant K, Cho H, McMurray DN. Lung Macrophages From Bacille Calmette-Guérin-Vaccinated Guinea Pigs Suppress T Cell Proliferation But Restrict Intracellular Growth of M. Tuberculosis After Recombinant Guinea Pig Interferon-Gamma Activation. *Clin Exp Immunol* (2007) 149(2):387–98.
48. Ly LH, Barhoumi R, Cho SH, Franzblau SG, McMurray DN. Vaccination With Bacille-Calmette Guérin Promotes Mycobacterial Control in Guinea Pig Macrophages Infected *In Vivo*. *J Infect Dis* (2008) 198(5):768–71. doi: 10.1086/590436
49. Kapsenberg ML. Dendritic-Cell Control of Pathogen-Driven T-Cell Polarization. *Nat Rev Immunol* (2003) 3(12):984–93. doi: 10.1038/nri1246
50. Thurnher M, Ramoner R, Gastl G, Radmayr C, Böck G, Herold M, et al. Bacillus Calmette-Guérin Mycobacteria Stimulate Human Blood Dendritic Cells. *Int J Cancer* (1997) 70(1):128–34. doi: 10.1002/(SICI)1097-0215(19970106)70:1<128::AID-IJC19>3.0.CO;2-H
51. Ferreira AV, Domiguéz-Andrés J, Netea MG. The Role of Cell Metabolism in Innate Immune Memory. *J Innate Immun* (2022) 14(1):42–50. doi: 10.1159/000512280
52. van der Heijden CDCC, Noz MP, Joosten LAB, Netea MG, Riksen NP, Keating ST. Epigenetics and Trained Immunity. *Antioxid Redox Signal* (2018) 29(11):1023–40. doi: 10.1089/ars.2017.7310
53. Kaufmann E, Sanz J, Dunn JL, Khan N, Mendonça LE, Pacis A, et al. BCG Educates Hematopoietic Stem Cells to Generate Protective Innate Immunity Against Tuberculosis. *Cell* (2018) 172(1–2):176–190.e19. doi: 10.1016/j.cell.2017.12.031
54. Michel T, Hentges F, Zimmer J. Consequences of the Crosstalk Between Monocytes/Macrophages and Natural Killer Cells. *Front Immunol* (2012) 3:403.
55. Moorlag SJCFM, Rodriguez-Rosales YA, Gillard J, Fanucchi S, Theunissen K, Novakovic B, et al. BCG Vaccination Induces Long-Term Functional Reprogramming of Human Neutrophils. *Cell Rep* (2020) 33(7):108387. doi: 10.1016/j.celrep.2020.108387
56. Escobar LE, Molina-Cruz A, Barillas-Mury C. BCG Vaccine Protection From Severe Coronavirus Disease 2019 (COVID-19). *PNAS* (2020) 117 (30):17720–6. doi: 10.1073/pnas.2008410117
57. Trained Immunity Confers Broad-Spectrum Protection Against Bacterial Infections. *The Journal of Infectious Diseases*. Oxford Academic [Internet]. Available from: https://academic.oup.com/jid/article/222/11/1869/5691195.
58. Arts RJW, Moorlag SJCFM, Novakovic B, Li Y, Wang SY, Oosting M, et al. BCG Vaccination Protects Against Experimental Viral Infection in Humans Through the Induction of Cytokines Associated With Trained Immunity. *Cell Host Microbe* (2018) 23(1):89–100. doi: 10.1016/j.chom.2017.12.010
59. Adesanya OA, Uche-Orji CI, Adedeji YA, Joshua JI, Adesola AA, Chukwudike CJ. Bacillus Calmette-Guerin (BCG): The Adroit Vaccine. *AIMS Microbiol* (2021) 7(1):96–113. doi: 10.3934/microbiol.2021007
60. Chimoyi L, Velen K, Churchyard GJ, Wallis R, Lewis JJ, Charalambous S. An Ecological Study to Evaluate the Association of Bacillus Calmette-Guerin (BCG) Vaccination on Cases of SARS-CoV2 Infection and Mortality From COVID-19. *PloS One* (2020) 15(12):e0243707. doi: 10.1371/journal.pone.0243707
61. O'Neill LAJ, Netea MG. BCG-Induced Trained Immunity: Can it Offer Protection Against COVID-19? *Nat Rev Immunol* (2020) 20(6):335–7. doi: 10.1038/s41577-020-0337-y

62. Nuovo G, Tili E, Suster D, Matys E, Hupp L, Magro C. Strong Homology Between SARS-CoV-2 Envelope Protein and a Mycobacterium Sp. Antigen Allows Rapid Diagnosis of Mycobacterial Infections and may Provide Specific Anti-SARS-CoV-2 Immunity *via* the BCG Vaccine. *Ann Diagn Pathol* (2020) 48:151600. doi: 10.1016/j.anndiagpath.2020.151600
63. Prezzemolo T, Guggino G, La Manna MP, Di Liberto D, Dieli F, Caccamo N. Functional Signatures of Human CD4 and CD8 T Cell Responses to Mycobacterium Tuberculosis. *Front Immunol* (2014). doi: 10.3389/fimmu.2014.00180
64. Covián C, Fernández-Fierro A, Retamal-Díaz A, Díaz FE, Vasquez AE, Lay MK, et al. BCG-Induced Cross-Protection and Development of Trained Immunity: Implication for Vaccine Design. *Front Immunol* (2019) 10:2806. doi: 10.3389/fimmu.2019.02806
65. Marchant A, Goetghebuer T, Ota MO, Wolfe I, Ceesay SJ, De Groote D, et al. Newborns Develop a Th1-Type Immune Response to Mycobacterium Bovis Bacillus Calmette-Guérin Vaccination. *J Immunol* (1999) 163(4):2249–55.
66. Moliva JI, Turner J, Torrelles JB. Immune Responses to Bacillus Calmette-Guérin Vaccination: Why Do They Fail to Protect Against Mycobacterium Tuberculosis? *Front Immunol* (2017) 8:407. doi: 10.3389/fimmu.2017.00407
67. Murray RA, Mansoor N, Harbacheuski R, Soler J, Davids V, Soares A, et al. Bacillus Calmette Guerin Vaccination of Human Newborns Induces a Specific, Functional CD8+ T Cell Response. *J Immunol* (2006) 177 (8):5647–51. doi: 10.4049/jimmunol.177.8.5647
68. Lewinsohn DA, Lewinsohn DM, Scriba TJ. Polyfunctional CD4+ T Cells As Targets for Tuberculosis Vaccination. *Front Immunol* (2017) 8:1262. doi: 10.3389/fimmu.2017.01262
69. Beveridge NER, Price DA, Casazza JP, Pathan AA, Sander CR, Asher TE, et al. Immunisation With BCG and Recombinant MVA85A Induces Long-Lasting, Polyfunctional Mycobacterium Tuberculosis-Specific CD4+ Memory T Lymphocyte Populations. *Eur J Immunol* (2007) 37(11):3089–100. doi: 10.1002/eji.200737504
70. Tameris MD, Hatherill M, Landry BS, Scriba TJ, Snowden MA, Lockhart S, et al. Safety and Efficacy of MVA85A, a New Tuberculosis Vaccine, in Infants Previously Vaccinated With BCG: A Randomised, Placebo-Controlled Phase 2b Trial. *Lancet* (2013) 381(9871):1021–8. doi: 10.1016/S0140-6736(13)60177-4
71. Lin PL, Flynn JL. CD8 T Cells and Mycobacterium Tuberculosis Infection. *Semin Immunopathol* (2015) 37(3):239–49. doi: 10.1007/s00281-015-0490-8
72. Flynn JL, Goldstein MM, Triebold KJ, Koller B, Bloom BR. Major Histocompatibility Complex Class I-Restricted T Cells are Required for Resistance to Mycobacterium Tuberculosis Infection. *Proc Natl Acad Sci USA* (1992) 89(24):12013–7. doi: 10.1073/pnas.89.24.12013
73. Khader SA, Bell GK, Pearl JE, Fountain JJ, Rangel-Moreno J, Cilley GE, et al. IL-23 and IL-17 in the Establishment of Protective Pulmonary CD4+ T Cell Responses After Vaccination and During Mycobacterium Tuberculosis Challenge. *Nat Immunol* (2007) 8(4):369–77. doi: 10.1038/ni1449
74. Darrah PA, Zeppa JJ, Maiello P, Hackney JA, Wadsworth MH, Hughes TK, et al. Prevention of Tuberculosis in Macaques After Intravenous BCG Immunization. *Nature* (2020) 577(7788):95–102. doi: 10.1038/s41586-019-1817-8
75. Jaron B, Maranghi E, Leclerc C, Majlessi L. Effect of Attenuation of Treg During BCG Immunization on Anti-Mycobacterial Th1 Responses and Protection Against Mycobacterium Tuberculosis. *PloS One* (2008) 3 (7):e2833. doi: 10.1371/journal.pone.0002833
76. Almeida P, Silva A, maya-monteiro C, Törőcsik D, D'Avila H, Dezso B, et al. Mycobacterium Bovis Bacillus Calmette-Guerin Infection Induces TLR2-Dependent Peroxisome Proliferator-Activated Receptor Expression and Activation: Functions in Inflammation, Lipid Metabolism, and Pathogenesis. *J Immunol (Baltimore Md : 1950)* (2009) 183:1337–45. doi: 10.4049/jimmunol.0900365
77. Jayashankar L, Hafner R. Adjunct Strategies for Tuberculosis Vaccines: Modulating Key Immune Cell Regulatory Mechanisms to Potentiate Vaccination. *Cell Mol Immunol* (2020) 17(9):901–13 doi: 10.3389/fimmu.2016.00577
78. Transcriptional Targets of Sirtuins in the Coordination of Mammalian Physiology - ScienceDirect.
79. Cheng CY, Gutierrez NM, Marzuki MB, Lu X, Foreman TW, Paleja B, et al. Host Sirtuin 1 Regulates Mycobacterial Immunopathogenesis and Represents a Therapeutic Target Against Tuberculosis. *Sci Immunol* (2017) 2(9):eaaj1789. doi: 10.1126/sciimmunol.aaj1789
80. Emerging Therapeutic Potential of SIRT6 Modulators. *J Medicinal Chem*. doi: 10.1021/acs.jmedchem.1c00601
81. Hamaidi I, Zhang L, Kim N, Wang MH, Iclozan C, Fang B, et al. Sirt2 Inhibition Enhances Metabolic Fitness and Effector Functions of Tumor-Reactive T Cells. *Cell Metab* (2020) 32(3):420–36. doi: 10.1016/j.cmet.2020.07.008
82. Nguyen P, Lee S, Lorang-Leins D, Trepel J, Smart DK. SIRT2 Interacts With β-Catenin to Inhibit Wnt Signaling Output in Response to Radiation-Induced Stress. *Mol Cancer Res* (2014) 12(9):1244–53. doi: 10.1158/1541-7786.MCR-14-0223-T
83. O'Connell RM, Rao DS, Chaudhuri AA, Baltimore D. Physiological and Pathological Roles for microRNAs in the Immune System. *Nat Rev Immunol* (2010) 10(2):111–22. doi: 10.1038/nri2708
84. Kozomara A, Birgaoanu M, Griffiths-Jones S. Mirbase: From microRNA Sequences to Function. *Nucleic Acids Res* (2019) 47(D1):D155–62. doi: 10.1093/nar/gky1141
85. Luo Y, Jiang W, Da Z, Wang B, Hu L, Zhang Y, et al. Subunit Vaccine Candidate AMM Down-Regulated the Regulatory T Cells and Enhanced the Protective Immunity of BCG on a Suitable Schedule. *Scand J Immunol* (2012) 75(3):293–300. doi: 10.1111/j.1365-3083.2011.02666.x
86. Quinn KM, Rich FJ, Goldsack LM, de Lisle GW, Buddle BM, Delahunt B, et al. Accelerating the Secondary Immune Response by Inactivating CD4+CD25+ T Regulatory Cells Prior to BCG Vaccination Does Not Enhance Protection Against Tuberculosis. *Eur J Immunol* (2008) 38(3):695–705. doi: 10.1002/eji.200737888
87. Kamat S, Kumari M. BCG Against SARS-CoV-2: Second Youth of an Old Age Vaccine? *Front Pharmacol* (2020) 11:1050. doi: 10.3389/fphar.2020.01050
88. Madura Larsen J, Stabell Benn C, Fillie Y, van der Kleij D, Aaby P, Yazdanbakhsh M. BCG Stimulated Dendritic Cells Induce an Interleukin-10 Producing T-Cell Population With No T Helper 1 or T Helper 2 Bias *In Vitro*. *Immunology* (2007) 121(2):276–82. doi: 10.1111/j.1365-2567.2007.02575.x
89. Pitt JM, Stavropoulos E, Redford PS, Beebe AM, Bancroft GJ, Young DB, et al. Blockade of IL-10 Signaling During Bacillus Calmette-Guérin Vaccination Enhances and Sustains Th1, Th17, and Innate Lymphoid IFN-γ and IL-17 Responses and Increases Protection to Mycobacterium Tuberculosis Infection. *J Immunol* (2012) 189(8):4079–87. doi: 10.4049/jimmunol.1201061
90. Andersen P, Doherty TM. The Success and Failure of BCG - Implications for a Novel Tuberculosis Vaccine. *Nat Rev Microbiol* (2005) 3(8):656–62. doi: 10.1038/nrmicro1211
91. Pang Y, Zhao A, Cohen C, Kang W, Lu J, Wang G, et al. Current Status of New Tuberculosis Vaccine in Children. *Hum Vaccin Immunother* (2016) 12 (4):960–70. doi: 10.1080/21645515.2015.1120393
92. Zhang W, Zhang Y, Zheng H, Pan Y, Liu H, Du P, et al. Genome Sequencing and Analysis of BCG Vaccine Strains. *PloS One* (2013) 8(8):e71243. doi: 10.1371/journal.pone.0071243
93. Whittaker E, Nicol MP, Zar HJ, Tena-Coki NG, Kampmann B. Age-Related Waning of Immune Responses to BCG in Healthy Children Supports the Need for a Booster Dose of BCG in TB Endemic Countries. *Sci Rep* (2018) 8 (1):15309. doi: 10.1038/s41598-018-33499-4
94. Poyntz HC, Stylianou E, Griffiths KL, Marsay L, Checkley AM, McShane H. Non-Tuberculous Mycobacteria Have Diverse Effects on BCG Efficacy Against Mycobacterium Tuberculosis. *Tuberc (Edinb)* (2014) 94(3):226–37. doi: 10.1016/j.tube.2013.12.006
95. Behr MA. BCG–different Strains, Different Vaccines? *Lancet Infect Dis* (2002) 2(2):86–92. doi: 10.1016/S1473-3099(02)00182-2
96. *WHO-IVB-18.06-Eng.Pdf* (2022). Available at: http://apps.who.int/iris/bitstream/handle/10665/273089/WHO-IVB-18.06-eng.pdf?ua=1.
97. Elsidig N, Alshahrani D, Alshehri M, Alzahrani M, Alhajjar S, Aljummah S, et al. Bacillus Calmette–Guérin Vaccine Related Lymphadenitis in Children: Management Guidelines Endorsed by the Saudi Pediatric Infectious Diseases Society (SPIDS). *Int J Pediatr Adolesc Med* (2015) 2(2):89–95. doi: 10.1016/j.ijpam.2015.05.003

98. Andersen P, Kaufmann SHE. Novel Vaccination Strategies Against Tuberculosis. *Cold Spring Harb Perspect Med* (2014) 4(6):a018523. doi: 10.1101/cshperspect.a018523
99. *New TB Vaccine Research* (2022). Available at: https://www.who.int/teams/global-tuberculosis-programme/research-innovation/vaccines.
100. Kumar S, Bhaskar A, Patnaik G, Sharma C, Singh DK, Kaushik SR, et al. Intranasal Immunization With Peptide-Based Immunogenic Complex Enhances BCG Vaccine Efficacy in a Murine Model of Tuberculosis. *JCI Insight* (2021) 6(4):145228. doi: 10.1172/jci.insight.145228
101. MTBVAC: Attenuating the Human Pathogen of Tuberculosis (TB) Toward a Promising Vaccine Against the TB Epidemic. *Immunology*. doi: 10.3389/fimmu.2017.01803
102. Jensen K, Ranganathan UDK, Van Rompay KKA, Canfield DR, Khan I, Ravindran R, et al. A Recombinant Attenuated Mycobacterium Tuberculosis Vaccine Strain Is Safe in Immunosuppressed Simian Immunodeficiency Virus-Infected Infant Macaques. *Clin Vaccine Immunol* (2012) 19(8):1170–81. doi: 10.1128/CVI.00184-12
103. Woodworth JS, Clemmensen HS, Battey H, Dijkman K, Lindenstrøm T, Laureano RS, et al. A Mycobacterium Tuberculosis-Specific Subunit Vaccine That Provides Synergistic Immunity Upon Co-Administration With Bacillus Calmette-Guérin. *Nat Commun* (2021) 12(1):6658.
104. Dalmia N, Ramsay AJ. Prime-Boost Approaches to Tuberculosis Vaccine Development. *Expert Rev Vaccines* (2012) 11(10):1221–33. doi: 10.1586/erv.12.94
105. Kaufmann SHE, Dorhoi A, Hotchkiss RS, Bartenschlager R. Host-Directed Therapies for Bacterial and Viral Infections. *Nat Rev Drug Discov* (2018) 17 (1):35–56. doi: 10.1038/nrd.2017.162
106. Koul A, Arnoult E, Lounis N, Guillemont J, Andries K. The Challenge of New Drug Discovery for Tuberculosis. *Nature* (2011) 469(7331):483–90. doi: 10.1038/nature09657
107. *Commissioner O of the. FDA Approves New Drug for Treatment-Resistant Forms of Tuberculosis That Affects the Lungs* (2022). Available at: https://www.fda.gov/news-events/press-announcements/fda-approves-new-drug-treatment-resistant-forms-tuberculosis-affects-lungs.
108. *Fundació Institut Germans Trias I Pujol. Phase 2b Randomized Double-Blind, Placebo-Controlled Trial to Estimate the Potential Efficacy and Safety of Two Repurposed Drugs, Acetylsalicylic Acid and Ibuprofen, for Use as Adjunct Therapy Added to, and Compared With, the Standard WHO-Recommended TB Regimen (SMA-Tb)*. Available at: https://clinicaltrials.gov/ct2/show/NCT04575519.
109. Muefong CN, Sutherland JS. Neutrophils in Tuberculosis-Associated Inflammation and Lung Pathology. *Front Immunol* 11:962. doi: 10.3389/fimmu.2020.00962
110. *Monosodium Urate Crystals Promote Innate Anti-Mycobacterial Immunity and Improve BCG Efficacy as a Vaccine Against Tuberculosis* (2022). Available at: https://www.ncbi.nlm.nih.gov/pmc/articles/PMC4449037/.
111. *Calcimycin Mediates Mycobacterial Killing by Inducing Intracellular Calcium-Regulated Autophagy in a P2RX7 Dependent Manner* (2022).
112. *Role of Calcium Channels in Cellular Antituberculosis Effects: Potential of Voltage-Gated Calcium-Channel Blockers in Tuberculosis Therapy - ScienceDirect*. Available at: https://www.sciencedirect.com/science/article/pii/S1684118214002102.
113. Ahmad S, Bhattacharya D, Gupta N, Rawat V, Tousif S, Van Kaer L, et al. Clofazimine Enhances the Efficacy of BCG Revaccination *via* Stem Cell-Like Memory T Cells. *PloS Pathog* (2020) 16(5):e1008356. doi: 10.1371/journal.ppat.1008356
114. Singh DK, Tousif S, Bhaskar A, Devi A, Negi K, Moitra B, et al. Luteolin as a Potential Host-Directed Immunotherapy Adjunct to Isoniazid Treatment of Tuberculosis. *PloS Pathogens* (2021) 17(8):e1009805. doi: 10.1371/journal.ppat.1009805
115. Singh DK, Dwivedi VP, Singh SP, Kumari A, Sharma SK, Ranganathan A, et al. Luteolin-Mediated Kv1.3 K+ Channel Inhibition Augments BCG Vaccine Efficacy Against Tuberculosis by Promoting Central Memory T Cell Responses in Mice. *PloS Pathogens* (2020) 16(9):e1008887.
116. Jagannath C, Bakhru P. Rapamycin-Induced Enhancement of Vaccine Efficacy in Mice. *Methods Mol Biol* (2012) 821:295–303. doi: 10.1007/978-1-61779-430-8_18
117. Nikouee A, Kim M, Ding X, Sun Y, Zang QS. Beclin-1–Dependent Autophagy Improves Outcomes of Pneumonia-Induced Sepsis. *Front Cell Infect Microbiol* (2021). doi: 10.3389/fcimb.2021.706637
118. Sogi KM, Lien KA, Johnson JR, Krogan NJ, Stanley SA. The Tyrosine Kinase Inhibitor Gefitinib Restricts Mycobacterium Tuberculosis Growth Through Increased Lysosomal Biogenesis and Modulation of Cytokine Signaling. *ACS Infect Dis* (2017) 3(8):564–74. doi: 10.1021/acsinfecdis.7b00046
119. Tan SY, Kelkar Y, Hadjipanayis A, Shipstone A, Wynn TA, Hall JP. Metformin and 2-Deoxyglucose Collaboratively Suppress Human CD4+ T Cell Effector Functions and Activation-Induced Metabolic Reprogramming. *J Immunol* (2020) 205(4):957–67. doi: 10.4049/jimmunol.2000137
120. *Ritonavir - an Overview | ScienceDirect Topics* (2022). Available at: https://www.sciencedirect.com/topics/medicine-and-dentistry/ritonavir.
121. Le A, Cooper CR, Gouw AM, Dinavahi R, Maitra A, Deck LM, et al. Inhibition of Lactate Dehydrogenase A Induces Oxidative Stress and Inhibits Tumor Progression. *Proc Natl Acad Sci U S A* (2010) 107(5):2037–42. doi: 10.1073/pnas.0914433107
122. Palsson-McDermott EM, Curtis AM, Goel G, Lauterbach MA, Sheedy FJ, Gleeson LE, et al. Pyruvate Kinase M2 Regulates Hif-1α Activity and IL-1β Induction, and is a Critical Determinant of the Warburg Effect in LPS-Activated Macrophages. *Cell Metab* (2015) 21(1):65–80. doi: 10.1016/j.cmet.2014.12.005
123. Yu X, Li L, Xia L, Feng X, Chen F, Cao S, et al. Impact of Metformin on the Risk and Treatment Outcomes of Tuberculosis in Diabetics: A Systematic Review. *BMC Infect Dis* (2019) 19:859. doi: 10.1186/s12879-019-4548-4
124. AICAR Inhibits Nfκb DNA Binding Independently of AMPK to Attenuate LPS-Triggered Inflammatory Responses in Human Macrophages. *Sci Rep*.
125. Classical Activation of Macrophages Leads to Lipid Droplet Formation Without *De Novo* Fatty Acid Synthesis. *Immunology*. doi: 10.3389/fimmu.2020.00131
126. Moon JS, Lee S, Park MA, Siempos II, Haslip M, Lee PJ, et al. UCP2-Induced Fatty Acid Synthase Promotes NLRP3 Inflammasome Activation During Sepsis. *J Clin Invest* (2015) 125(2):665–80. doi: 10.1172/JCI78253
127. Seargent JM, Yates EA, Gill JH. GW9662, a Potent Antagonist of Pparγ, Inhibits Growth of Breast Tumour Cells and Promotes the Anticancer Effects of the Pparγ Agonist Rosiglitazone, Independently of Pparγ Activation. *Br J Pharmacol* (2004) 143(8):933–7. doi: 10.1038/sj.bjp.0705973
128. Bhaskar A, Kumar S, Khan MZ, Singh A, Dwivedi VP, Nandicoori VK. Host Sirtuin 2 as an Immunotherapeutic Target Against Tuberculosis. *eLife* (2020) 9:e55415. doi: 10.7554/eLife.55415
129. Young C, Walzl G, Du Plessis N. Therapeutic Host-Directed Strategies to Improve Outcome in Tuberculosis. *Mucosal Immunol* (2020) 13(2):190–204.
130. Duraiswamy J, Kaluza KM, Freeman GJ, Coukos G. Dual Blockade of PD-1 and CTLA-4 Combined With Tumor Vaccine Effectively Restores T Cell Rejection Function in Tumors. *Cancer Res* (2013) 73(12):3591–603. doi: 10.1158/0008-5472.CAN-12-4100
131. Menter DG, Schilsky RL, DuBois RN. Cyclooxygenase-2 and Cancer Treatment: Understanding the Risk Should Be Worth the Reward. *Clin Cancer Res* (2010) 16(5):1384–90. doi: 10.1158/1078-0432.CCR-09-0788
132. Pettersen FO, Torheim EA, Dahm AEA, Aaberge IS, Lind A, Holm M, et al. An Exploratory Trial of Cyclooxygenase Type 2 Inhibitor in HIV-1 Infection: Downregulated Immune Activation and Improved T Cell-Dependent Vaccine Responses▽. *J Virol* (2011) 85(13):6557–66. doi: 10.1128/JVI.00073-11
133. *Home - ClinicalTrials.Gov* (2022). Available at: https://www.clinicaltrials.gov/.
134. Lorenzo JP, Csuka ME, Derfus BA, Gotoff RA, McCarthy GM. Concurrent Gout and Mycobacterium Tuberculosis Arthritis. *J Rheumatol* (1997) 24 (1):184–6.
135. Jhang JJ, Cheng YT, Ho CY, Yen GC. Monosodium Urate Crystals Trigger Nrf2- and Heme Oxygenase-1-Dependent Inflammation in THP-1 Cells. *Cell Mol Immunol* (2015) 12(4):424–34. doi: 10.1038/cmi.2014.65
136. Ganmaa D, Uyanga B, Zhou X, Gantsetseg G, Delgerekh B, Enkhmaa D, et al. Vitamin D Supplements for Prevention of Tuberculosis Infection and Disease. *New Engl J Med* (2020) 383(4):359–68. doi: 10.1056/NEJMoa1915176
137. Abdelgawad AA, Saoud HAEA, Mohamed AG, Fathi MA, Mokhtar ER. Evaluation of BCG Vaccine Immunogenicity in Relation to Vitamin D Status

in a Group of Egyptian Children. *Open J Pediatr* (2020) 10(2):320–31. doi: 10.4236/ojped.2020.102033
138. Lalor MK, Floyd S, Gorak-Stolinska P, Weir RE, Blitz R, Branson K, et al. BCG Vaccination: A Role for Vitamin D? *PloS One* (2011) 6(1):e16709. doi: 10.1371/journal.pone.0016709
139. Ahmad S, Bhattacharya D, Kar S, Ranganathan A, Van Kaer L, Das G. Curcumin Nanoparticles Enhance Mycobacterium Bovis BCG Vaccine Efficacy by Modulating Host Immune Responses. *Infect Immun* (2019) 87 (11):e00291–19. doi: 10.1128/IAI.00291-19
140. Cole ST, Brosch R, Parkhill J, Garnier T, Churcher C, Harris D, et al. Deciphering the Biology of Mycobacterium Tuberculosis From the Complete Genome Sequence. *Nature* (1998) 393(6685):537–44. doi: 10.1038/31159
141. Guzman JD, Evangelopoulos D, Gupta A, Birchall K, Mwaigwisya S, Saxty B, et al. Antitubercular Specific Activity of Ibuprofen and the Other 2-Arylpropanoic Acids Using the HT-SPOTi Whole-Cell Phenotypic Assay. *BMJ Open* (2013) 3(6):e002672. doi: 10.1136/bmjopen-2013-002672
142. Byrne ST, Denkin SM, Zhang Y. Aspirin and Ibuprofen Enhance Pyrazinamide Treatment of Murine Tuberculosis. *J Antimicrob Chemother* (2007) 59(2):313–6.
143. Mitini-Nkhoma SC, Chimbayo ET, Mzinza DT, Mhango DV, Chirambo AP, Mandalasi C, et al. Something Old, Something New: Ion Channel Blockers as Potential Anti-Tuberculosis Agents. *Front Immunol* (2021). doi: 10.3389/fimmu.2021.665785
144. *Ion Channels in Innate and Adaptive Immunity*.
145. Baker EH. Ion Channels and the Control of Blood Pressure. *Br J Clin Pharmacol* (2000) 49(3):185–98. doi: 10.1046/j.1365-2125.2000.00159.x
146. Inhibition of Ca2+ Signaling by Mycobacterium tuberculosisIs Associated With Reduced Phagosome–Lysosome Fusion and Increased Survival Within Human Macrophages(2022). Available at: https://www.ncbi.nlm.nih.gov/pmc/articles/PMC2195750/.
147. Kondratskyi A, Kondratska K, Skryma R, Klionsky DJ, Prevarskaya N. Ion Channels in the Regulation of Autophagy. *Autophagy* (2017) 14(1):3–21.
148. Mawatwal S, Behura A, Ghosh A, Kidwai S, Mishra A, Deep A, et al. Calcimycin Mediates Mycobacterial Killing by Inducing Intracellular Calcium-Regulated Autophagy in a P2RX7 Dependent Manner. *Biochim Biophys Acta Gen Subj* (2017) 1861(12):3190–200. doi: 10.1016/j.bbagen.2017.09.010
149. Lee CC, Lee MTG, Hsu WT, Park JY, Porta L, Liu MA, et al. Use of Calcium Channel Blockers and Risk of Active Tuberculosis Disease: A Population-Based Analysis. *Hypertension* (2021) 77(2):328–37. doi: 10.1161/HYPERTENSIONAHA.120.15534
150. Vohra J. Verapamil in Cardiac Arrhythmias: An Overview. *Clin Exp Pharmacol Physiol Suppl* (1982) 6:129–34.
151. Fahie S, Cassagnol M. Verapamil. In: *StatPearls*. Treasure Island (FL: StatPearls Publishing (2022). Available at: http://www.ncbi.nlm.nih.gov/books/NBK538495/.
152. de Souza JVP, Murase LS, Caleffi-Ferracioli KR, Palomo CT, de Lima Scodro RB, Siqueira VLD, et al. Isoniazid and Verapamil Modulatory Activity and Efflux Pump Gene Expression in Mycobacterium Tuberculosis. *Int J Tuberc Lung Dis* (2020) 24(6):591–6. doi: 10.5588/ijtld.19.0458
153. Demitto F de O, Amaral RCR do, Maltempe FG, Siqueira VLD, Scodro RB de L, Lopes MA, et al. *In Vitro* Activity of Rifampicin and Verapamil Combination in Multidrug-Resistant Mycobacterium Tuberculosis. *PloS One* (2015) 10(2):e0116545.
154. Chen C, Gardete S, Jansen RS, Shetty A, Dick T, Rhee KY, et al. Verapamil Targets Membrane Energetics in Mycobacterium Tuberculosis. *Antimicrob Agents Chemother* (2018) 62(5):e02107–17. doi: 10.1128/AAC.02107-17
155. Gupta S, Tyagi S, Bishai WR. Verapamil Increases the Bactericidal Activity of Bedaquiline Against Mycobacterium Tuberculosis in a Mouse Model. *Antimicrob Agents Chemother* (2015) 59(1):673–6. doi: 10.1128/AAC.04019-14
156. Parumasivam T, Chan JGY, Pang A, Quan DH, Triccas JA, Britton WJ, et al. *In Vitro* Evaluation of Inhalable Verapamil-Rifapentine Particles for Tuberculosis Therapy. *Mol Pharmaceutics* (2016) 13(3):979–89. doi: 10.1021/acs.molpharmaceut.5b00833
157. *9789290226383-Eng.Pdf*. Available at: https://apps.who.int/iris/bitstream/handle/10665/274127/9789290226383-eng.pdf.
158. Gopal M, Padayatchi N, Metcalfe JZ, O'Donnell MR. Systematic Review of Clofazimine for the Treatment of Drug-Resistant Tuberculosis. *Int J Tuberc Lung Dis* (2013) 17(8):1001–7. doi: 10.5588/ijtld.12.0144
159. Conradie F. *An Open Label, Randomized Controlled Trial to Establish the Efficacy and Safety of a Study Strategy Consisting of 6 Months of Bedaquiline (BDQ), Delamanid (DLM), and Linezolid (LNZ), With Levofloxacin (LVX) and Clofazimine (CFZ) Compared to the Current South African Standard of Care (Control Strategy) for 9 Months for the Treatment of Rifampicin Resistant Tuberculosis (RR-Tb)* (2022). Available at: https://clinicaltrials.gov/ct2/show/NCT04062201.
160. *endTB Clinical Trials* . Available at: http://www.endtb.org/clinical-trial.
161. Medecins Sans Frontieres, Netherlands. *A Randomised, Controlled, Open-Label, Phase II-III Trial to Evaluate the Safety and Efficacy of Regimens Containing Bedaquiline and Pretomanid for the Treatment of Adult Patients With Pulmonary Multidrug Resistant Tuberculosis* (2021). Available at: https://clinicaltrials.gov/ct2/show/NCT02589782.
162. National Institute of Allergy and Infectious Diseases (NIAID). *A Phase IIc Trial of Clofazimine- and Rifapentine-Containing Treatment Shortening Regimens in Drug-Susceptible Tuberculosis: The CLO-FAST Study*. Available at: https://clinicaltrials.gov/ct2/show/NCT04311502.
163. Ren YR, Pan F, Parvez S, Fleig A, Chong CR, Xu J, et al. Clofazimine Inhibits Human Kv1.3 Potassium Channel by Perturbing Calcium Oscillation in T Lymphocytes. *PloS One* (2008) 3(12):e4009.
164. Mycobacterial ESX-1 Secretion System Mediates Host Cell Lysis Through Bacterium Contact-Dependent Gross Membrane Disruptions. *PNAS*. doi: 10.1073/pnas.1620133114
165. ESX-1 Dependent Impairment of Autophagic Flux by Mycobacterium Tuberculosis in Human Dendritic Cells.
166. Levine B, Mizushima N, Virgin HW. Autophagy in Immunity and Inflammation. *Nature* (2011) 469(7330):323–35. doi: 10.1038/nature09782
167. Li J, Kim SG, Blenis J. Rapamycin: One Drug, Many Effects. *Cell Metab* (2014) 19(3):373–9. doi: 10.1016/j.cmet.2014.01.001
168. Jagannath C, Lindsey DR, Dhandayuthapani S, Xu Y, Hunter RL, Eissa NT. Autophagy Enhances the Efficacy of BCG Vaccine by Increasing Peptide Presentation in Mouse Dendritic Cells. *Nat Med* (2009) 15(3):267–76. doi: 10.1038/nm.1928
169. Schaible UE, Linnemann L, Redinger N, Patin EC, Dallenga T. Strategies to Improve Vaccine Efficacy Against Tuberculosis by Targeting Innate Immunity. *Front Immunol* (2017). doi: 10.3389/fimmu.2017.01755
170. Alkhunaizi AM, Al-Khouzaie TH, Alsagheir AI. Sirolimus-Induced Interstitial Lung Disease and Resolution After Conversion to Everolimus. *Respir Med Case Rep* (2020) 30:101109. doi: 10.1016/j.rmcr.2020.101109
171. Sattler M, Guengerich FP, Yun CH, Christians U, Sewing KF. Cytochrome P-450 3A Enzymes are Responsible for Biotransformation of FK506 and Rapamycin in Man and Rat. *Drug Metab Dispos* (1992) 20(5):753–61.
172. Baguley BC, Siemann DW. Temporal Aspects of the Action of ASA404 (Vadimezan; DMXAA). *Expert Opin Investig Drugs* (2010) 19(11):1413–25. doi: 10.1517/13543784.2010.529128
173. Daei Farshchi Adli A, Jahanban-Esfahlan R, Seidi K, Samandari-Rad S, Zarghami N. An Overview on Vadimezan (DMXAA): The Vascular Disrupting Agent. *Chem Biol Drug Des* (2018) 91(5):996–1006. doi: 10.1111/cbdd.13166
174. Levine BC, SHOJI-KAWATA S. *Autophagy-Inducing Peptide* (2013). Available at: https://patents.google.com/patent/WO2013119377A1/en.
175. Kim YS, Silwal P, Kim SY, Yoshimori T, Jo EK. Autophagy-Activating Strategies to Promote Innate Defense Against Mycobacteria. *Exp Mol Med* (2019) 51(12):151. doi: 10.1038/s12276-019-0290-7
176. Kominsky DJ, Campbell EL, Colgan SP. Metabolic Shifts in Immunity and Inflammation. *J Immunol* (2010) 184(8):4062–8. doi: 10.4049/jimmunol.0903002
177. Nitric Oxide Orchestrates Metabolic Rewiring in M1 Macrophages by Targeting Aconitase 2 and Pyruvate Dehydrogenase. *Nat Commun*.
178. Infection With Mycobacterium Tuberculosis Induces the Warburg Effect in Mouse Lungs. *Sci Rep*.
179. Chai Q, Wang L, Liu CH, Ge B. New Insights Into the Evasion of Host Innate Immunity by Mycobacterium Tuberculosis. *Cell Mol Immunol* 17(9):901–13. doi: 10.1038/s41423-020-0502-z192

180. Torretta S, Scagliola A, Ricci L, Mainini F, Di Marco S, Cuccovillo I, et al . D-Mannose Suppresses Macrophage IL-1β Production. *Nat Commun* 11(1):1–2. doi: 10.1038/s41467-1409 020-20164-6193
181. Zhong WJ, Yang HH, Guan XX, Xiong JB, Sun CC, Zhang CY, et al. Inhibition of Glycolysis Alleviates Lipopolysaccharide-Induced Acute Lung Injury in a Mouse Model. *J Cell Physiol* (2019) 234(4):4641–54. doi: 10.1002/jcp.27261
182. Vyas AK, Koster JC, Tzekov A, Hruz PW. Effects of the HIV Protease Inhibitor Ritonavir on GLUT4 Knock-Out Mice. *J Biol Chem* (2010) 285 (47):36395–400. doi: 10.1074/jbc.M110.176321
183. Pharmacokinetic Evaluation of Rifabutin in Combination With Lopinavir-Ritonavir in Patients With HIV Infection and Active Tuberculosis. *Clin Infect Dis*. https://academic.oup.com/cid/article/49/9/1305/299191?login=false. doi: 10.1086/606056
184. Michelakis ED, Webster L, Mackey JR. Dichloroacetate (DCA) as a Potential Metabolic-Targeting Therapy for Cancer. *Br J Cancer* (2008) 99(7):989–94. doi: 10.1038/sj.bjc.6604554
185. van Doorn CLR, Schouten GK, van Veen S, Walburg KV, Esselink JJ, Heemskerk MT, et al. Pyruvate Dehydrogenase Kinase Inhibitor Dichloroacetate Improves Host Control of Salmonella Enterica Serovar Typhimurium Infection in Human Macrophages. *Front Immunol* (2021) 12:739938. doi: 10.3389/fimmu.2021.739938
186. Song YJ, Kim A, Kim GT, Yu HY, Lee ES, Park MJ, et al. Inhibition of Lactate Dehydrogenase A Suppresses Inflammatory Response in RAW 264.7 Macrophages. *Mol Med Rep* (2019) 19(1):629–37.
187. Intracellular Mycobacterium Tuberculosis Exploits Host-Derived Fatty Acids to Limit Metabolic Stress.
188. Foamy Macrophages and the Progression of the Human TB Granuloma.
189. Hardie DG. AMP-Activated Protein Kinase—An Energy Sensor That Regulates All Aspects of Cell Function. *Genes Dev* (2011) 25(18):1895–908. doi: 10.1101/gad.17420111
190. Zhang M, He JQ. Impacts of Metformin on Tuberculosis Incidence and Clinical Outcomes in Patients With Diabetes: A Systematic Review and Meta-Analysis. *Eur J Clin Pharmacol* (2020) 76(2):149–59. doi: 10.1007/s00228-019-02786-y
191. Mitochondrial Reactive Oxygen Species: Double-Edged Weapon in Host Defense and Pathological Inflammation During Infection.
192. Metformin Enhances Protection in Guinea Pigs Chronically Infected With Mycobacterium Tuberculosis. *Sci Rep*.
193. Magee MJ, Salindri AD, Kornfeld H, Singhal A. Reduced Prevalence of Latent Tuberculosis Infection in Diabetes Patients Using Metformin and Statins. *Eur Respir J* (2019) 53(3). doi: 10.1183/13993003.01695-2018
194. Bartel DP. Metazoan MicroRNAs. *Cell* (2018) 173(1):20–51. doi: 10.1016/j.cell.2018.03.006
195. Agarwal RG, Sharma P, Nyati KK. microRNAs in Mycobacterial Infection: Modulation of Host Immune Response and Apoptotic Pathways. *Immune Netw* (2019) 19(5):e30. doi: 10.4110/in.2019.19.e30
196. Sabir N, Hussain T, Shah SZ, Peramo A, Zhao D, Zhou X. miRNAs in tuberculosis: new avenues for diagnosis and host-directed therapy. *Front Microbiol* (2018) 9:602. doi: 10.3389/fmicb.2018.00602
197. Sampath P, Periyasamy KM, Ranganathan UD, Bethunaickan R. Monocyte and Macrophage miRNA: Potent Biomarker and Target for Host-Directed Therapy for Tuberculosis. *Front Immunol* (2021). doi: 10.3389/fimmu.2021.667206
198. Yang T, Ge B. miRNAs in Immune Responses to Mycobacterium Tuberculosis Infection. *Cancer Lett* (2018), 431:22–30. doi: 10.1016/j.canlet.2018.05.028
199. Das K, Garnica O, Dhandayuthapani S. Modulation of Host miRNAs by Intracellular Bacterial Pathogens. *Front Cell Infect Microbiol* (2016) 6:79. doi: 10.3389/fcimb.2016.00079
200. Mehta MD, Liu PT. microRNAs in Mycobacterial Disease: Friend or Foe? *Front Genet* (2014) 5:231. doi: 10.3389/fgene.2014.00231
201. Mycobacterium Tuberculosis Lipomannan Blocks TNF Biosynthesis by Regulating Macrophage MAPK-Activated Protein Kinase 2 (MK2) and microRNA miR-125b.
202. Harapan H, Fitra F, Ichsan I, Mulyadi M, Miotto P, Hasan NA, et al. The Roles of microRNAs on Tuberculosis Infection: Meaning or Myth? *Tuberc (Edinb)* (2013) 93(6):596–605. doi: 10.1016/j.tube.2013.08.004
203. Ouimet M, Koster S, Sakowski E, Ramkhelawon B, van Solingen C, Oldebeken S, et al. Mycobacterium Tuberculosis Induces the miR-33 Locus to Reprogram Autophagy and Host Lipid Metabolism. *Nat Immunol* (2016) 17(6):677–86. doi: 10.1038/ni.3434
204. Kumar M, Sahu SK, Kumar R, Subuddhi A, Maji RK, Jana K, et al. MicroRNA Let-7 Modulates the Immune Response to Mycobacterium Tuberculosis Infection *via* Control of A20, an Inhibitor of the NF-κb Pathway. *Cell Host Microbe* (2015) 17(3):345–56. doi: 10.1016/j.chom.2015.01.007
205. Starczynowski DT, Kuchenbauer F, Argiropoulos B, Sung S, Morin R, Muranyi A, et al. Identification of miR-145 and miR-146a as Mediators of the 5q– Syndrome Phenotype. *Nat Med* 16(1):49–58. doi: 10.1038/nm.2054
206. Guo L, Zhou L, Gao Q, Zhang A, Wei J, Hong D, et al. MicroRNA-144-3p Inhibits Autophagy Activation and Enhances Bacillus Calmette-Guérin Infection by Targeting ATG4a in RAW264.7 Macrophage Cells. *PloS One* (2017) 12(6):e0179772.
207. Belver L, Papavasiliou NF, Ramiro AR. MicroRNA Control of Lymphocyte Differentiation and Function. *Curr Opin Immunol* (2011) 23(3):368–73. doi: 10.1016/j.coi.2011.02.001
208. He X, Jing Z, Cheng G. MicroRNAs: New Regulators of Toll-Like Receptor Signalling Pathways. *BioMed Res Int* (2014) 2014:945169. doi: 10.1155/2014/945169
209. Wang J, Wu M, Wen J, Yang K, Li M, Zhan X, et al. MicroRNA-155 Induction by Mycobacterium Bovis BCG Enhances ROS Production Through Targeting SHIP1. *Mol Immunol* (2014) 62(1):29–36. doi: 10.1016/j.molimm.2014.05.012
210. Ghorpade DS, Leyland R, Kurowska-Stolarska M, Patil SA, Balaji KN. MicroRNA-155 Is Required for Mycobacterium Bovis BCG-Mediated Apoptosis of Macrophages. *Mol Cell Biol* (2012) 32(12):2239–53. doi: 10.1128/MCB.06597-11
211. Ma F, Xu S, Liu X, Zhang Q, Xu X, Liu M, et al. The microRNA miR-29 Controls Innate and Adaptive Immune Responses to Intracellular Bacterial Infection by Targeting Interferon-γ. *Nat Immunol* (2011) 12(9):861–9. doi: 10.1038/ni.2073
212. MicroRNA-223 Controls Susceptibility to Tuberculosis by Regulating Lung Neutrophil Recruitment.
213. Wang J, Jia Z, Wei B, Zhou Y, Niu C, Bai S, et al. MicroRNA-27a Restrains the Immune Response to Mycobacterium Tuberculosis Infection by Targeting IRAK4, a Promoter of the NF-κb Pathway. *Int J Clin Exp Pathol* (2017) 10(9):9894–901.
214. Duan X, Zhang T, Ding S, Wei J, Su C, Liu H, et al. microRNA-17-5p Modulates Bacille Calmette-Guerin Growth in RAW264.7 Cells by Targeting Ulk1. *PloS One* (2015) 10(9):e0138011. doi: 1468 10.1371/journal.pone.0138011
215. Inhibition of microRNA Function by antimiR Oligonucleotides.
216. Di Fusco D, Dinallo V, Marafini I, Figliuzzi MM, Romano B, Monteleone G. Antisense Oligonucleotide: Basic Concepts and Therapeutic Application in Inflammatory Bowel Disease. *Front Pharmacol* (2019). doi: 10.3389/fphar.2019.00305
217. Young C, Walzl G, Du Plessis N. Therapeutic Host-Directed Strategies to Improve Outcome in Tuberculosis. *Mucosal Immunol* (2020) 13(2):190–204. doi: 10.1038/s41385-019-0226-5

Conflict of Interest: The authors declare that the research was conducted in the absence of any commercial or financial relationships that could be construed as a potential conflict of interest.

frontiers | Frontiers in Immunology

TYPE Original Research
PUBLISHED 08 August 2022
DOI 10.3389/fimmu.2022.943174

OPEN ACCESS

EDITED BY
Wenping Gong,
The 8th Medical Center of PLA General Hospital, China

REVIEWED BY
Mohd Saqib,
Albany Medical College, United States
Lucero Ramón-Luing,
Instituto Nacional de Enfermedades Respiratorias-México (INER), Mexico

*CORRESPONDENCE
Xiao-Lian Zhang
zhangxiaolian@whu.edu.cn

SPECIALTY SECTION
This article was submitted to Vaccines and Molecular Therapeutics, a section of the journal Frontiers in Immunology

RECEIVED 13 May 2022
ACCEPTED 20 July 2022
PUBLISHED 08 August 2022

CITATION
Wu J, Luo F-L, Xie Y, Xiong H, Gao Y, Liu G and Zhang X-L (2022) EST12 regulates Myc expression and enhances anti-mycobacterial inflammatory response *via* RACK1-JNK-AP1-Myc immune pathway. *Front. Immunol.* 13:943174. doi: 10.3389/fimmu.2022.943174

EST12 regulates Myc expression and enhances anti-mycobacterial inflammatory response *via* RACK1-JNK-AP1-Myc immune pathway

Jian Wu[1], Feng-Ling Luo[1], Yan Xie[1], Huan Xiong[1], Yadong Gao[2], Guanghui Liu[2] and Xiao-Lian Zhang[1,2,3,4]*

[1]Hubei Province Key Laboratory of Allergy and Immunology and Department of Immunology, Wuhan University School of Basic Medical Sciences, Wuhan, China, [2]Department of Allergy, Zhongnan Hospital of Wuhan University, Wuhan, China, [3]State Key Laboratory of Virology, Frontier Science Center for Immunology and Metabolism and Medical Research Institute, Wuhan University, Wuhan, China, [4]Wuhan Research Center for Infectious Diseases and Cancer, Chinese Academy of Medical Sciences, Wuhan, China

c-Myc (Myc) is a well-known transcription factor that regulates many essential cellular processes. Myc has been implicated in regulating anti-mycobacterial responses. However, its precise mechanism in modulating mycobacterial immunity remains elusive. Here, we found that a secreted Rv1579c (early secreted target with molecular weight 12 kDa, named EST12) protein, encoded by virulent *Mycobacterium tuberculosis* (*M.tb*) H37Rv region of deletion (RD)3, induces early expression and late degradation of Myc protein. Interestingly, EST12-induced Myc was further processed by K48 ubiquitin proteasome degradation in E3 ubiquitin ligase FBW7 dependent manner. EST12 protein activates JNK-AP1-Myc signaling pathway, promotes Myc binding to the promoters of IL-6, TNF-α and iNOS, then induces the expression of pro-inflammatory cytokines (IL-6 and TNF-α)/inducible nitric oxide synthase (iNOS)/nitric oxide (NO) to increase mycobacterial clearance in a RACK1 dependent manner, and these effects are impaired by both Myc and JNK inhibitors. Macrophages infected with EST12-deficiency strain (H37RvΔEST12) displayed less production of iNOS, IL-6 and TNF-α. In conclusion, EST12 regulates Myc expression and enhances anti-mycobacterial inflammatory response *via* RACK1-JNK-AP1-Myc immune pathway. Our finding provides new insights into *M.tb*-induced immunity through Myc.

KEYWORDS

***Mycobacterium tuberculosis* (*M.tb*), Myc, Rv1579c/EST12, classical macrophage activation, IL-6, TNF-α**

Introduction

Tuberculosis (TB) seriously threatens human health and causes a huge medical burden. According to the Global tuberculosis report 2021, it's estimated that 9.87 million people suffered from TB, and 1.28 million TB associated deaths occurred in 2020 worldwide (1). As the only available TB vaccine, Bacille Calmette-Guérin (BCG) has limited protective efficacy in adults. Lack of effective vaccine, emergence of extensively drug-resistant tuberculosis (XDR-TB) and the side effects of toxic chemotherapeutic agents make it urgently needed to unveil the precise mechanisms that regulate mycobacterial immune response.

Sixteen regions of deletion (RDs), which are present in *M.tb* H37Rv and part of *Mycobacterium bovis*, but absent in BCG, have been identified by comparative genomic analysis (2). Recently, more and more functions of the RD proteins have been reported, suggesting that RD region-encoded proteins play important roles in the pathogenicity and immunogenicity of *M.tb*. For example, 6-kDa early secreted antigenic target (ESAT6), 10-kDa culture filtrate protein (CFP10) and MPT64, encoded by RD1-2, contribute to the survival or persistent growth of *M.tb* in macrophages (3, 4). Rv1768 of RD14 was recently identified to promote *M.tb* survival in macrophages by regulating NF-κB-TNF-α signaling and arachidonic acid metabolism through interacting with S100A9 (5). However, functions of most other RD-encoding proteins are unknown yet.

As the primary host cell for *M.tb*, macrophages eliminate intracellular *M.tb* mainly by secreting pro-inflammatory cytokines such as IL-6 and TNF-α. Macrophages also act as antigen presenting cells and present *M.tb* antigens to specific T cells through major histocompatibility complex (MHC) and activate specific $CD4^+$ T and $CD8^+$ T response (6). It's well-known that pro-inflammatory M1 macrophages play a critical role in eliminating *M.tb*, while M2 macrophages are beneficial for the survival of *M.tb* and the formation of granulomas (7).

Myc is a versatile oncoprotein which regulates cell growth, differentiation, genome instability, apoptosis, etc. (8). As a prominent oncogene, the Myc target gene network is estimated to comprise about 15% of all genes from flies to humans (9) and is involved in various physiological functions and clinical diseases including TB. Mycobacteria including BCG, *M. avium*, *M. chelonae*, or *M. kansasii* have been reported to induce Myc expression (10). It is interesting that multifunctional proto-oncogene myc could be up-regulated by different species of mycobacteria, and plays a critical role in anti-mycobacterial responses (10). It was also reported that ESAT6 could downregulate lipopolysaccharide induced Myc expression *via* ERK1/2 signal pathway (11). However, the role and mechanism of Myc in modulating mycobacterial immunity during virulent *M.tb* H37Rv infection remain elusive.

Recently we have reported a secreted *M.tb* Rv1579c (early secreted target with molecular weight 12 kDa, named EST12) protein, encoded by virulent *M.tb* H37Rv RD3, binds to the receptor for activated C kinase 1 (RACK1) of macrophage and activates a RACK1–NLRP3–gasdermin D pyroptosis–IL-1β immune pathway (12). In the present study, we further found that EST12 protein induced the early expression and late K48 ubiquitination and degradation of Myc protein. EST12 activated RACK1-JNK-AP1-Myc signaling pathway which contributes to anti-mycobacterial inflammatory response of macrophages. Our study provides the first proof that Myc acts as a critical host transcriptional factor for mycobacterial EST12-induced anti-mycobacterial response and plays a pivotal role in *M.tb*-induced innate immunity.

Materials and methods

BMDM preparation and cell culture

Bone marrow-derived macrophages (BMDMs) were isolated from the tibia and fibula of C57BL/6 mice and induced to M0 with 50 ng/mL M-CSF (416-ML, R&D Systems, USA) for 6 days. For M1 polarized macrophages, M0 BMDMs were stimulated with 100 ng/ml LPS (L4391,Sigma, USA) and 20 ng/ml IFN-γ (485-MI, R&D Systems, USA) for 48 h. For M2 polarized macrophages, M0 BMDMs were stimulated with 20 ng/ml IL-4 (404-ML, R&D Systems, USA) and 20 ng/ml IL-13 (413-ML, R&D Systems, USA) for 48 h. Mouse RAW264.7 cells (C7505) and human THP1 cells (GDC0100) were originally obtained from China Center for Type Culture Collection (CCTCC, Wuhan, China). Both RAW264.7 and THP1 cells used were in less than 10 passage numbers (13). All above cells were cultured in Dulbecco's Modified Eagle Medium (DMEM, Gibco) supplemented with 10% fetal bovine serum (FBS, Gibco).

Bacterial strains

M.tb H37Rv [strain American Type Culture Collection (ATCC) 27294], *M.tb H37Rv*ΔEST12 (ΔEST12), *H37Rv*ΔEST12::EST12 (ΔEST12::EST12) and *M. bovis* BCG (Pasteur strain ATCC 35734) were maintained in our lab according to previous publications (12, 14, 15). Briefly, the mycobacterial strains were cultured in Middlebrook 7H9 broth (7H9) supplemented with 10% oleic acid–albumin–dextrose–catalase (OADC) and 0.05% Tween 80 (Sigma-Aldrich) or on Middlebrook 7H10 agar (BD Biosciences). *Escherichia coli* (*E. coli*) DH5α (strain ATCC 25922) and *E. coli* BL-21 (stain ATCC BAA-1025) were propagated from laboratory stocks (School of Medicine, Wuhan University, Wuhan, China), and cultured in LB medium.

Animals

WT C57BL/6 mice (6–8-week-old) were purchased from the Centre of Animal Experiments of Wuhan University. RACK1

knock out (KO) (12), IL-6 KO, TLR2 KO and TLR4 KO (5) C57BL/6 mice were maintained in Animal Laboratory Center of Wuhan University. All animals received humane care according to the criteria outlined in the Guide for the Care and Use of Laboratory Animals prepared by the National Academy of Sciences and published by the National Institutes of Health (NIH publication no. 86-23, revised 1985). All animal protocols were approved by the Institutional Animal Care and Use Committee of the Institute of Model Animals of Wuhan University (nos. S01319070R and S01317012S).

Recombinant EST12 protein preparation

E. coli BL21 (DE3) were transformed with expression plasmid pET-28a-EST12 with 6×His-tag. Expression of recombinant EST12 protein was induced by isopropyl-β-D-thiogalactopyranoside (IPTG) at 25°C for 16 h. The bacteria were resuspended in phosphate-buffered saline (PBS) and disrupted by dynamic high-pressure homogenization, then the cell debris was removed by centrifugation at 14,000 g at 4°C for 15 min. The supernatants were incubated with Ni-agarose pre-equilibrated with 10 mM imidazole solution [25 mM Tris-HCl, 200 mM NaCl, and 10 mM imidazole (pH 7.4)]. The recombinant proteins were eluted with 20, 40, 60-, 80-, 100- and 200-mM imidazole buffer (with 25 mM Tris-HCl and 200 mM NaCl, pH 7.4). The purified recombinant proteins were further purified using endotoxin-free purification polymyxin B columns and analyzed by sodium dodecyl sulfate-polyacrylamide gel electrophoresis (SDS-PAGE) and Western blot with antibody against His-tag. EST12 protein concentration was determined by bicinchoninic acid (BCA) method.

Transcriptional sequencing

RAW264.7 cells (1×10^7) were stimulated with 2 μM EST12 protein for 3 h. The total RNA of treated cells was extracted with Trizol and mRNA sequencing was performed by Allwegene (Allwegene Biotech, www.allwegene.com).

Reverse transcription-quantitative real time PCR

The total RNA from cells was extracted with Trizol reagent (Invitrogen Corp, Carlsbad, CA, USA) and reverse-transcribed using a cDNA reverse transcription kit (Toyobo, Osaka, Japan) with Oligo dT primers. The reverse transcribed cDNA was used as a template for qPCR reactions along with SYBR Green Real time PCR Master Mix (Toyobo, Osaka, Japan) and 0.4 μM primers (primer sequences shown in Supplementary Table 1, primers were synthesized by TSINGKE, Wuhan). The qPCR reactions were run on an ABI Step One Plus (Applied Biosystems) using standard cycling conditions. Relative RNA levels were calculated by the comparative cycle threshold (CT) method ($2^{-\Delta\Delta CT}$ method) (16), where CT represents the amplification cycle number at which the fluorescence generated within a reaction rises above a defined threshold fluorescence and ΔΔCT = experimental groups ($Ct_{Target\ gene} - Ct_{GAPDH}$) − control groups ($Ct_{Target\ gene} - Ct_{GAPDH}$). The mRNA levels of each gene in the experimental groups were then presented as the fold levels relative to the blank control groups calculated by the following formula: $2^{-\Delta\Delta CT}$.

Cell transfection

RAW264.7 cells were cultured in DMEM supplemented with 10% (v/v) heat-inactivated FBS. After reaching 70%-90% confluence, transient transfection was performed with jetPEI-Macrophage (Polyplus) following the manufacturer's instructions. For siRNA transfection, the silencing RNA (siRNA) of E3 ubiquitin ligase FBW7 and control siRNA were synthesized from TSINGKE company (Wuhan, China). RAW264.7 cells were transfected with 100 nM siRNA. Transfection efficiency was measured by Western blot after 48 h post transfection. The sequences of siRNAs were listed in Supplementary Table 2.

Nuclear/cytoplasmic fractionation and Western blot analysis

Cells were harvested and lysed in RIPA buffer supplemented with protease inhibitors (P-8340, Sigma-Aldrich, US). For cell localization analysis of target proteins, nuclear and cytoplasmic proteins of EST12-stimulated RAW264.7 cells were extracted with Nuclear and Cytoplasmic Protein Extraction Kit (P0027, Beyotime, China) according to the manufacturer's recommended protocol. Protein concentrations in cell lysates or extracted nuclear and cytoplasmic proteins were determined with the Pierce™ BCA Protein Assay Kit (23225, Thermo Fischer Scientific, US), and 60 μg of each protein sample was loaded and separated on SDS-PAGE (5% for concentration gel, 12% for separation gel) after being denatured at 98°C for 8 min with SDS loading buffer. Proteins were transferred onto a nitrocellulose membrane which was subsequently blocked for 2 h with a 5% BSA solution (prepared in TBS with 0.05% Tween-20) and incubated overnight with primary antibodies (diluted at 1:1000). Myc (10828-1-AP, Proteintech, China), GAPDH (60004-1-Ig, Proteintech, China), β-Tubulin (A12289, ABclonal, China), p-JNK (AP0276, ABclonal, China), p-cJun (AP0105, ABclonal, China), p-cFos (AP0038, ABclonal, China), p-Myc S62 (AP0989, ABclonal, China), p-Myc T58 (AP0990, ABclonal, China), H3 (17168-1-AP, Proteintech, China), RACK1

(ab129084, abcam, UK), inducible nitric oxide synthase (iNOS) (A3774, ABclonal, China), Arg1 (A4923, ABclonal, China), HA-Tag (66006-2-Ig, Proteintech, China), His Tag (AE003, ABclonal, China), FBW7 (28424-1-AP, Proteintech, China), TLR2 (A19125, ABclonal, China), TLR4 (A5258, ABclonal, China). Membranes were then incubated with horse radish peroxidase (HRP)-conjugated secondary antibodies (1:5000 dilution, goat anti mouse IgG KR0026, goat anti Rabbit IgG KR0023, KeRui, Wuhan) and detected by LumiGlo Reserve™ Chemiluminescent Substrate Kit (54-61-01, Sera care, Life Sciences, MA, US). Protein bands were visualized using the UVP BioSpectrum™ 500 Imaging System with the VisionWorks® images acquisition and analysis software (Analytik Jena, CA, US).

Dual Luciferase Reporter Assay

The Dual-Luciferase® Reporter Assay System (Promega, Madison, United States) was used to detect EST12-induced IL-6 and TNF-α activation on a GloMax® 20/20 tube luminometer (Promega, Madison, United States). Briefly, RAW264.7 cells were co-transfected with pGL3- IL-6-luc and internal control Renilla plasmid or pGL3- TNF-α-luc and internal control Renilla plasmid. Then, 24 h post-transfection, cells were treated with 2 μM EST12 in the presence of 20 μM Myc inhibitor (10058-F4, Selleck) or not. After 1 h, the cells were harvested. Luciferase activity was measured using the Dual-Luciferase Reporter Assay System according to the manufacturer's instructions (Promega, Madison, United States). Data were normalized for transfection efficiency by dividing firefly luciferase activity with that of Renilla luciferase.

Cleavage under targets and tagmentation sequencing

RAW264.7 cells (1×10^7) were stimulated with 2 μM EST12 for 1 h, then treated or untreated RAW264.7 cells were collected and sent to DIATRE Biotechnology (Shanghai, China) in dry ice for CUT&Tag sequencing. Briefly, in this method, a highly active Tn5 transposase is fused to Protein A, and a library-building linker primer is loaded to form a pA-Tn5 transposition complex. Under the guidance of Myc antibody (10828-1-AP, Proteintech, China), the pA-Tn5 transposition complex can target and cut the DNA sequence near Myc-bound region.

Chromatin immunoprecipitation and quantitative polymerase chain reaction

2 μM EST12-stimulated RAW264.7 cells were lysed and sonicated with Bioruptor Non-Contact Automatic Ultrasonic Disruptor (Diagenode, Belgium), ultrasonic condition is 30 s on, 30 s off, 20 cycles. Then samples were incubated with beads conjugated with anti-Myc (10828-1-AP, Proteintech, China) or H3-K4 (A2357, ABclonal, China) antibody. Captured DNA was purified with DNA Purification Kit (DP214, TIANGEN, Beijing) and used for quantitative PCR analysis. The primers were synthesized from TSINGKE (Wuhan, China) and listed in Supplementary Table 3.

Electrophoretic mobility shift assay

RAW264.7 cells (1×10^7) were seeded into 10 cm dishes and stimulated with 2 μM EST12 for 1 h, the nuclear extracts were prepared by Nuclear and Cytoplasmic Protein Extraction Kit (P0027, Beyotime, China). EMSA assays were done with Chemiluminescent EMSA kits (GS009, Beyotime, China). 5 μg nuclear extracts were incubated with 1× binding buffer and biotin-labeled probe or unlabeled probes for 30 min at room temperature (RT). The samples were electrophoresed on a 6% polyacrylamide gel in 0.5 × TBE at 100 V for 1 h and transferred onto a nylon membrane in 0.5 × TBE at 300 mA for 1 h. After transfer and 254 nm UV cross-linking, the membrane was detected with Streptavidin-HRP. Biotin-labeled and unlabeled probes were synthesized from TSINGKE (Wuhan, China) and listed in Supplementary Table 4.

Plasmid DNA construction

cDNA of Myc was cloned into pcDNA3.1 vector (Invitrogen, Carlsbad, CA) using the templates kindly provided by Professor Jiahuai Han of Xiamen University, and the restriction enzyme cutting sites are *Eco*RI and *Bam*HI. The promoter region of IL-6 (1201 bp) and TNF-α (1238 bp) were cloned into pGL3-basic by method of homologous recombination, the genome of RAW264.7 cells was extracted with TIANTGEN Cell Genomic DNA Extraction Kit (TIANGEN, DP304, China) and used as template. Restriction enzymes *Xho*I and *Hin*dIII were used to digest the pGL3-basic. Primers were synthesized from TSINGKE (Wuhan, China) and listed in Supplementary Table 5.

Enzyme-linked immunosorbent assay and NO measurement

Cytokine production of treated cells was measured by ELISA using the corresponding ELISA kits according to the manufacturers' protocols. IL-6 (DKW1210602, Dakewe Biotech, China); TNF-α (DKW1217202 Dakewe Biotech, China); IL-10 (CME0016, 4A Biotech, China); TGF-β (DKW1217102 Dakewe Biotech, China). For NO measurement, culture supernatants were harvested after stimulation of macrophages with EST12 protein for indicated time. The release NO level was determined using the

NO assay kit (Beyotime, Shanghai, China). Supernatants were added to an equal volume of Griess reagent in duplicate on a 96-well plate and incubated at room temperature for 15 min. Absorbance (540 nm) was measured and NO concentrations were estimated using a standard NO curve. The experiments were performed in triplicate.

Immunoprecipitation

MG-132 (5 μM) pretreated RAW264.7 cells (1×10^7) were stimulated with 2 μM EST12 protein for 0, 1 or 12 h, and then cells were collected and lysed with 700 μL RIPA buffer on ice for 20 min. After centrifuge at 14,000 g for 20 min at 4°C, 3 μg anti-Myc antibody (10828-1-AP, Proteintech, China) and 20 μL 50% protein A/G beads buffer were added and incubated at 4°C overnight, then protein A/G captured complex was eluted. Myc and FBW7 protein levels were detected by Western blot using anti-Myc antibody and anti-FBW7 antibody (28424-1-AP, Proteintech, China).

Colony forming unit assay

For intracellular mycobacterial survival assay, RAW264.7 cells (5×10^5) were infected with WT (H37Rv), EST12 deficiency H37Rv (H37RvΔEST12) or complement strain (H37RvΔEST12::EST12) at MOI=10 for 4 h. RAW264.7 cells were then washed with PBS for three times to remove extracellular bacteria, and DMEM medium supplemented with gentamicin (10 μg/ml) was added and further incubated in the presence or absence of Myc inhibitor (20 μM) (10058-F4, MCE, shanghai) or JNK inhibitor (10 μM) (JNK-IN-7, Topscience, shanghai) for 4 h, 8 h, 24 h and 48 h, respectively. Cells were lysed and intracellular bacteria were plated and counted on 7H10 medium.

For BCG infection assay, WT BMDMs (5×10^5) or IL-6 KO BMDMs were infected with BCG at MOI=10 for 4 h, then cells were washed with PBS for three times to remove extracellular bacteria, and then purified EST12 (2 μM) was added with or without the presence of TNF-α neutralizing antibody (MAB4101, R&D Systems, USA) (10 μg/ml) and further incubated for 8 h. Cells were lysed and intracellular bacteria were plated and counted on 7H10 medium.

Immunofluorescence microscopy

RAW264.7 cells were pretreated with MG-132 (5 μM) for 1 h and treated with 2 μM purified EST12 protein for indicated time. Media was removed from stimulated macrophages and the dishes were submerged in 4% paraformaldehyde (PFA). The fixed dishes were submerged in PBS to remove residual PFA and then cells were permeabilized with 0.1% Triton X-100 in PBS for 5 minutes at room temperature (RT), washed in PBS and blocked in PBS containing 10% donkey serum. Primary antibodies against FBW7 (28424-1-AP, Proteintech, China) and Myc (M4439, Sigma-Aldrich, USA) were used at a 1:50 dilution in PBS with 3% serum and incubated at 4°C overnight. Then Alexa Fluor 594-conjugated goat anti-rabbit IgG (A-11037, ThermoFisher, USA) or Alexa Fluor 488-conjugated goat anti-mouse IgG (A28175, ThermoFisher, USA) was used at 1:500 dilution in PBS with 3% FBS and incubated at RT for 1 h. Dishes were washed to remove the unbound secondary antibody and the cellular nuclei DNA was stained with DAPI. Fluormount-G Anti-Fade Mounting Medium (Southern Biotech) was added to each well to protect the fluorescent signal. Confocal fluorescence microscopy was performed using ZEISS LSM880 microscope and representative images were captured.

Flow cytometry

BMDMs (1×10^6) were stimulated with 2 μM EST12 protein for 12 h or 24 h, then cells were collected and incubated with APC-F4/80 (QA17A29, BioLegend, USA), FITC-CD80 (16-10A1, BioLegend, USA) and PE-CD86 (A17199A, BioLegend, USA) at 4°C for 30 min. Then cells were washed three times with PBS and subsequently used for flow cytometry using FACSCalibur (BD Biosciences) flow cytometer and analyzed by FlowJo 10.7.

Statistical analysis

Results were plotted by GraphPad Prism v9 (GraphPad Software, San Diego, CA, USA). For analysis of the statistical significance of differences between two groups, two-tailed unpaired Student's t-tests was used. For analysis of the statistical significance of differences among more than two groups, one-way ANOVA with Tukey's multiple comparisons test was used. To assess the statistical significance of differences among multiple groups when the experimental design involved multiple conditions, such as time points or bacterial types in addition to differences in inhibitor treatment, two-way ANOVA with Tukey's multiple comparisons test was used. Data are presented as mean ± SEM, n=3. P values < 0.05 were considered statistically significant. *, $p < 0.05$; **, $p < 0.01$; ***, $p < 0.001$.

Results

Mycobacterial EST12 induces early Myc expression in macrophages during *M.tb* infection

M.tb-infected lungs are often accompanied by chronic inflammation and it has been reported that chronic TB

infection can induce lung squamous cell carcinoma in a mouse model (17), therefore, we examined the inflammation- and cancer-related differentially expressed genes in EST12-stimulated mouse RAW264.7 cells through transcriptome sequencing. Recombinant EST12 protein was purified and used to treat RAW264.7 cells for 3 h (Figure S1A; Figure 1A). As shown in Figure 1A, EST12 not only significantly increased the expression of pro-inflammatory cytokine genes (such as IL-6 and TNF-α) (Figure 1A), but also induced the expression of four oncogenes (RB1, Myc, KRAS and PTEN). We confirmed that EST12 significantly upregulated the expression of IL-6 and TNF-α by RT-qPCR (Figures 1B, C). Furthermore, we found that Myc was the most significantly upregulated by EST12 protein treatment (Figure 1D), although EST12 also induced early expression of RB1, KRAS and PTEN oncogenes at mRNA level (Figures S1B–D). Next, the Myc protein level in EST12-stimulated RAW264.7 cells was analyzed by Western blot (Figure 1E). As shown in Figures 1D, E, EST12 upregulated the early transcription of Myc in RAW264.7 cells (within 6 h stimulation, Figure 1D) and transitorily activated Myc protein expression with decreased Myc protein levels at later stage (1 h post-stimulation of EST12) (Figure 1E). Furthermore, EST12 KO strain (H37RvΔEST12) infection decreased the expression of Myc protein in RAW264.7 cells compared with WT H37Rv and the complementary strain H37RvΔEST12::EST12 (H37RvΔEST12 strain rescued with EST12) infection (Figures 1F; S1E, F). We also found that BCG infection also induced Myc expression in RAW264.7 cells (Figure 1G), suggesting that other factors of mycobacterium, except EST12, might also be involved in induction of Myc expression. Consistently, exogenous EST12 protein could also upregulate Myc expression during BCG infection in RAW264.7 cells (Figure 1G). Similarly, we found that EST12 significantly induced the expression of Myc in human-derived macrophage THP1 cells (Figure 1H). Altogether, we found that mycobacterial EST12 could induce early expression of Myc protein in macrophages.

EST12 induces the expression and phosphorylation of Myc through JNK-AP1-Myc signaling pathway

To further unveil the molecular pathways involved in EST12-induced Myc activation, we extracted the nuclear and cytoplasmic proteins from EST12-treated RAW264.7 cells. Time-course and Western blot analysis showed that EST12 induced and activated cytoplasmic JNK phosphorylation (p-JNK) (reached peak at 15-30 min), nuclear p-cJun and p-cFos (p-AP1) (AP1 consists of c-Jun and c-Fos) (reached peak at 30 min) and both cytoplasmic and nuclear p-Myc at Ser62 (reached peak at 30 min~60 min) (Figure 2A), while p-Myc (Thr58) expression was not activated, but displayed a decrease within 1 h stimulation of EST12 (Figure 2A). These results suggest that EST12 activates early phosphorylation of Myc at Ser62 and p-JNK-p-AP1-p-Myc (S62) signaling. Further, JNK inhibitor significantly blocked EST12-induced p-JNK, p-p-cJun, p-cFos and p-Myc (S62) expression (Figure 2B).

Our previous study has demonstrated that *M.tb* EST12 protein binds RACK1 and activates a RACK1–NLRP3–gasdermin D pyroptosis–IL-1β immune pathway (12). Here we further demonstrated that EST12 induced p-JNK (Figure 2C) and Myc (Figure 2D) expression in WT macrophages but not in RACK1 KO macrophages, suggesting that EST12 induced p-JNK and Myc expression dependent on RACK1. Therefore, these data suggest that EST12-RACK1 interaction induces the expression and phosphorylation of Myc through JNK-AP1-Myc signal pathway.

M.tb-EST12 induces the production of proinflammatory cytokines and iNOS/NO at later stage to increase mycobacterial clearance

Proinflammatory cytokines IL-6 and TNF-α could increase the elimination of intracellular *M.tb* (10). As EST12 increased the expression of macrophage IL-6 and TNF-α (Figure 1A), we wonder whether EST12 could alter the characteristics of macrophage activation and polarization through activating Myc. Furthermore, we pretreated RAW264.7 cells with DMSO or Myc inhibitor 10058-F4, followed by stimulation with EST12 protein. Western blot analysis showed that EST12 significantly induced early Myc expression (1 h post-stimulation of *M.tb*-EST12) (lane 2 vs. lane 1, Figure 3A). At later stage, 12-24 h post-stimulation of EST12 increased classical M1 polarization-related factor iNOS expression (lane 3 and 4, Figure 3A) but inhibited M2 polarization factor Arg1 or Myc expression (Line 3 and 4, Figure 3A). EST12 regulated Myc expression, in a trend consistent with that of Arg-1 expression which also showed decreased expression after 12 h stimulation of EST12 and early expression at 0-1 h post-stimulation of EST12 (Figure 3A). Myc inhibitor treatment blocked EST12-induced iNOS expression (Figure 3A).

Consistently, ELISA analysis showed that EST12 significantly induced the expression of IL-6 (Figure 3B), TNF-α (Figure 3C) and NO (Figure 3D), but Myc inhibitor treatment blocked these effects (Figures 3B–D). Furthermore, Myc inhibitor blocked H37Rv infection-induced expression of iNOS and Arg-1 (Figure 3E), IL-6 (Figure 3F) and TNF-α (Figure 3G). However, EST12 stimulation had no effects on the production of the secreted IL-10 (Figure S2A) and TGF-β (Figure S2B) in RAW264.7 cells. We also determined that EST12 significantly upregulated the expression of CD80, CD86 of macrophages by FCM analysis (Figures S2C, D), and increased the production of

10.3389/fimmu.2022.943174

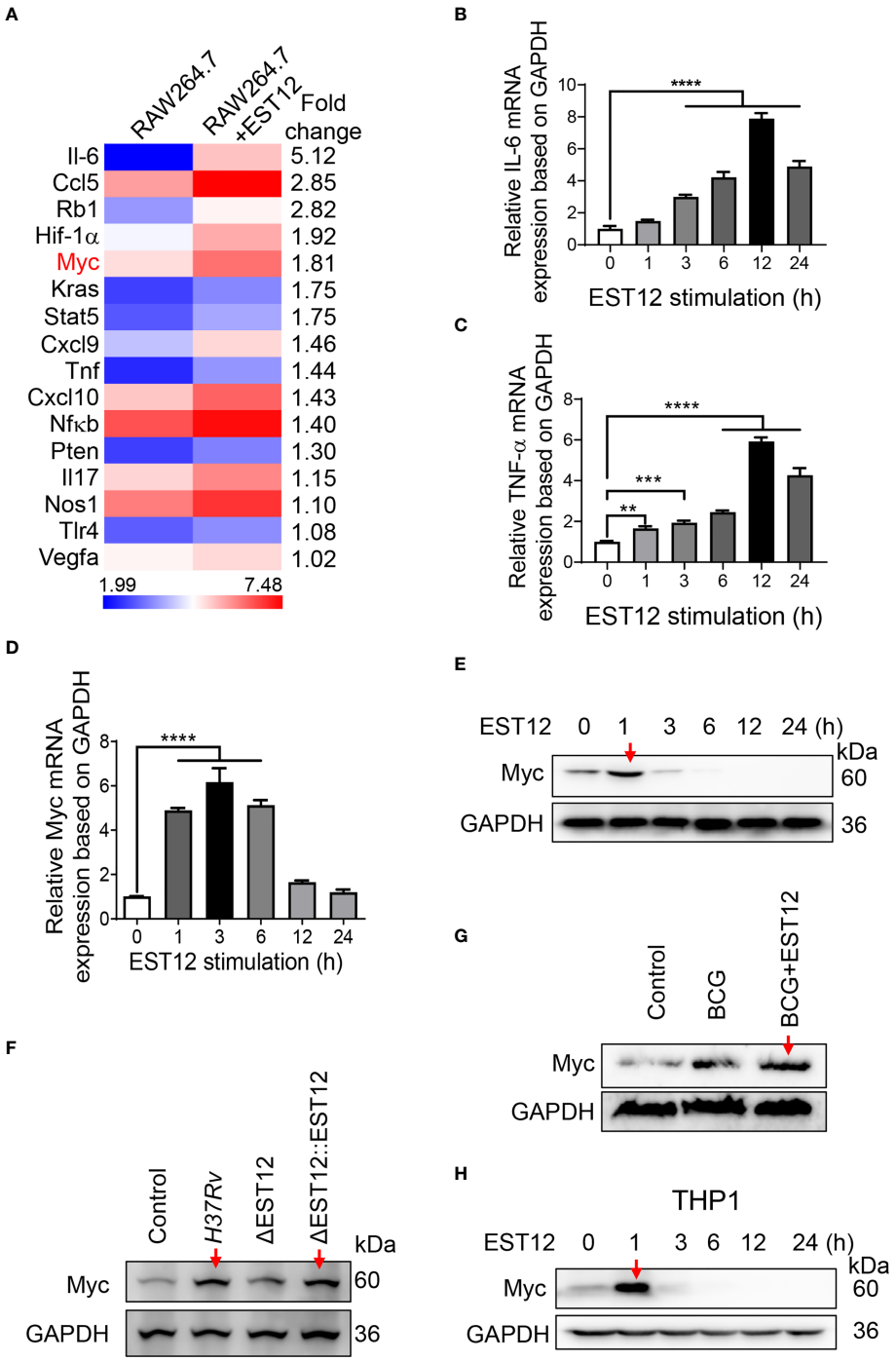

FIGURE 1
Mycobacterial EST12 induces early Myc expression in macrophages during *M.tb* infection. **(A)** RAW264.7 cells were stimulated with EST12 protein (2 μM) for 3 h, then the differentially expressed genes were detected by transcriptional sequencing. The inflammation and cancer-related genes were displayed in heatmap.**(B-E)** RAW264.7 cells were stimulated with EST12 protein (2 μM) for the indicated time. The mRNA levels of IL-6 **(B)**, TNF-α **(C)** and Myc **(D)** were determined by RT-qPCR, and the protein level of Myc was determined by Western blot **(E)**. **(F)** RAW264.7 cells infected with WT *M.tb* H37Rv, H37RvΔEST12 or H37RvΔEST12::EST12 for 24 h, and Myc expression in each cell lysates were detected by Western blot. **(G)** RAW264.7 cells were infected with BCG (MOI=10) for 24 h, and then stimulated with or without EST12 protein (2 μM) for 1 h, the expression of Myc was detected by Western blot. **(H)** THP1 cells were induced with PMA (100 ng/ml) for 24 h and then stimulated with EST12 protein (2 μM) for the indicated time, the protein levels of Myc expression were determined by Western blot. One-way ANOVA with Tukey's multiple comparisons test was used to assess the statistical significance in **(B–D)** (vs. 0 h). The data are expressed as the mean ± SEM of three independent experiments, $p > 0.05$, not significant (ns), $^{**}p < 0.01$, $^{***}p < 0.001$, or $^{****}p < 0.0001$.

10.3389/fimmu.2022.943174

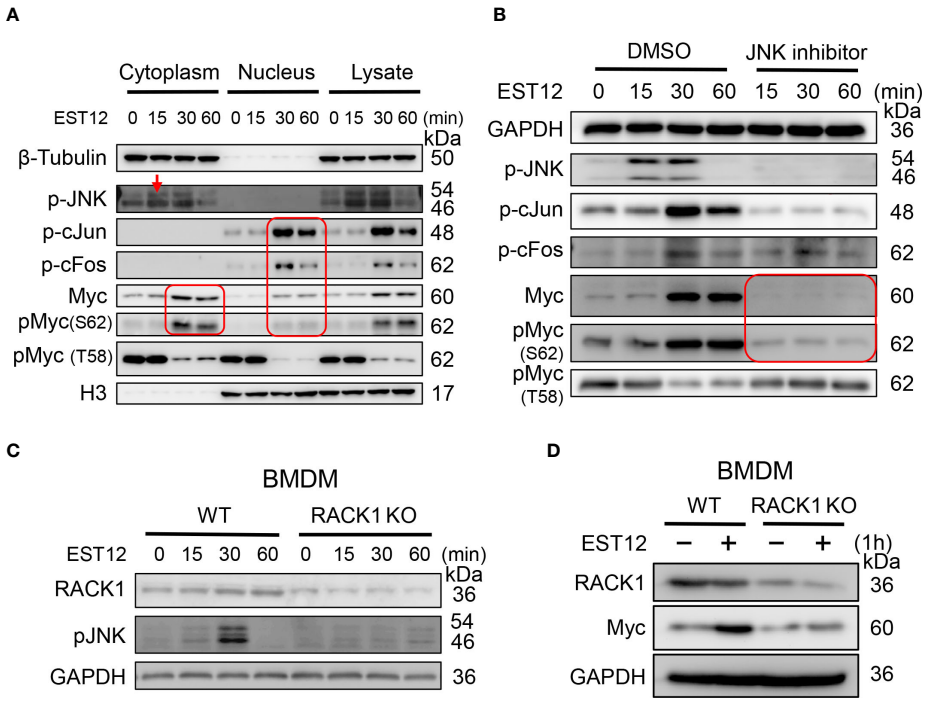

FIGURE 2
EST12 induces the expression and phosphorylation of Myc through JNK-AP1-Myc signaling pathway. **(A)** RAW264.7 cells were treated with EST12 protein (2 μM) for the indicated time, then the nucleus and cytoplasm were separated. The expression of p-JNK, p-c-Jun, p-cFos, Myc and p-Myc (S62/T58) in the cytoplasm, nucleus and total cell lysate were detected by Western blot. **(B)** RAW264.7 cells were pretreated with JNK inhibitor (10 μM) for 1 h and then stimulated with EST12 for the indicated time, the expression of p-JNK, p-AP1, Myc and p-Myc (S62/T58) was analyzed by Western blot. **(C, D)** WT or RACK1 KO BMDMS were stimulated with EST12 protein (2 μM) for the indicated time, the expression of p-JNK **(C)** and Myc **(D)** was detected by Western blot.

the secreted IL-1β (Figure S2E) and IL-12 (Figure S2F), but not IFN-γ (Figure S2G) by ELISA.

As predicted, *M.tb* H37Rv and H37RvΔEST12::EST12 infection of RAW264.7 led to less CFUs compared to H37RvΔEST12 at 4 h, 8 h, 24 h and 48 h post-infection (Figure 3H). While Myc inhibitor pretreatment increased the survival of intracellular *M.tb* H37Rv and H37RvΔEST12::EST12 strains in RAW264.7 cells, and H37RvΔEST12 as well (Figures 3I, J), suggesting that other factors, except EST12, might also induce Myc expression. Consistently, we observed similar results in JNK inhibitor pretreated RAW264.7 cells (Figures 3K, L). Furthermore, exogenous EST12 protein treatment after BCG infection of macrophages could also repress intracellular BCG survival (Figures 3M, N). However, intracellular BCG survival was increased in IL-6 KO BMDMs (Figures 3M, S3A) or in the presence of TNF-α neutralization antibody (Figures 3N, S3B). We also observed that exogenous EST12 protein treatment could repress intracellular BCG survival in IL-6 KO BMDMs (Figure 3M) or in the presence of TNF-α neutralization antibody (Figure 3N), as well.

All these results suggest that EST12 induces early Myc expression. At later stage (12-24 h post-stimulation of *M.tb*-EST12), EST12 increased iNOS/NO expression, but decreased Arg1 or Myc expression with associated induction of IL-6, TNF-α and IL-1β to increase mycobacterial clearance. EST12 stimulation also induced the expression of CD80 and CD86, but not IL-10 and TGF-β.

EST12 promotes Myc to bind to the promoters of IL-6 and TNF-α, and then induces IL-6 and TNF-α expression

In order to further determine whether Myc acts as a critical transcription factor for *M.tb*-EST12-induced production of IL-6 and TNF-α. We cloned the full length and different truncated sequences of IL-6 and TNF-α promoters into the pGL3 vector as shown in Figures 4A, B respectively. Then we performed dual luciferase assays to confirm the induction of IL-6 and TNF-α expression by EST12 protein. Our results showed that EST12 significantly upregulated the transcription of IL-6 (Figure 4A) and TNF-α (Figure 4B), and the critical regulatory sites are -808 bp to -381 bp and -329 bp to +33 bp of IL-6 and TNF-α promoter regions, respectively (Figures 4A, B). Furthermore, we

10.3389/fimmu.2022.943174

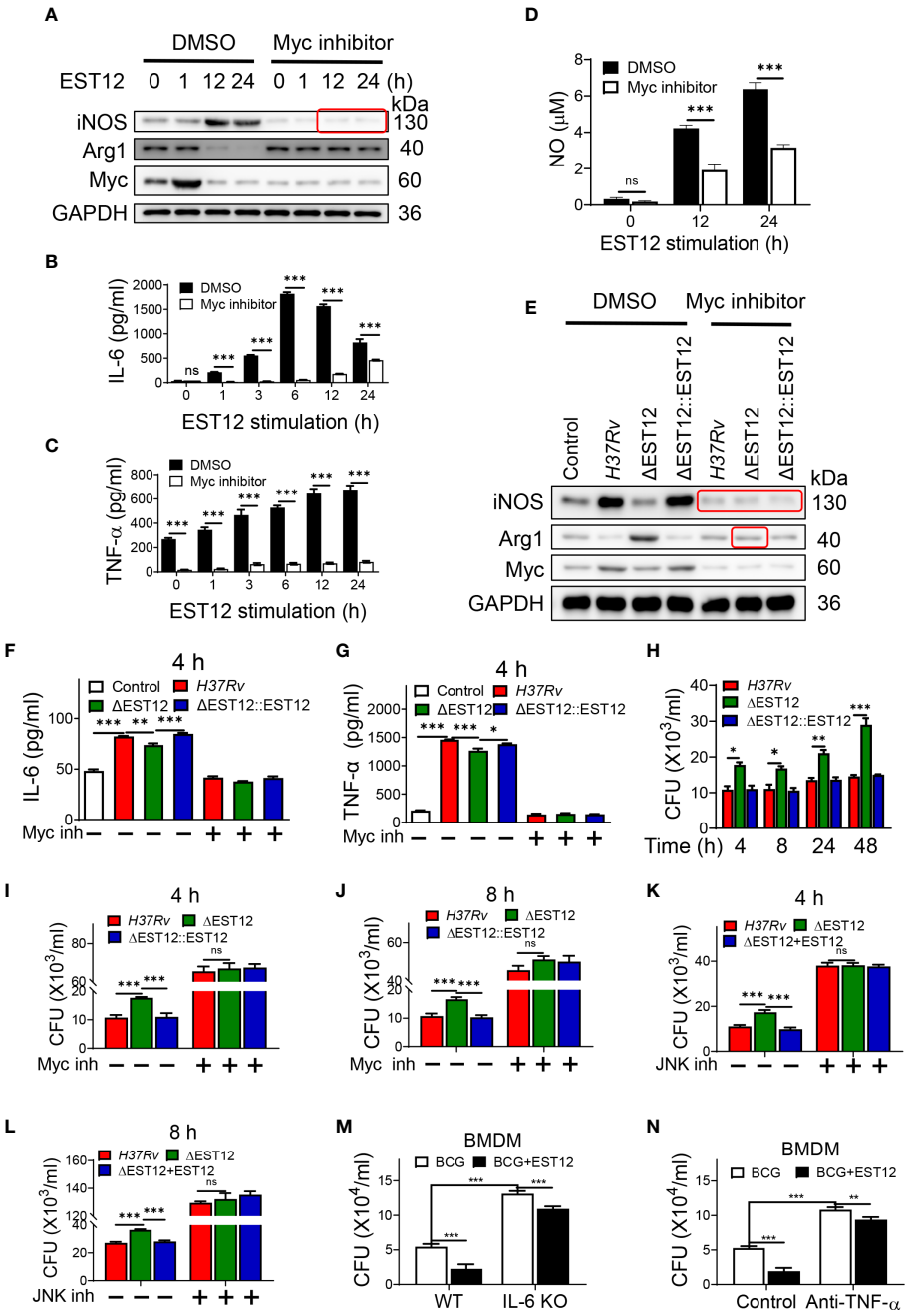

FIGURE 3
EST12-induced Myc-mediated classical M1 cytokines expression and activation eliminates intracellular *M.tb*. **(A–D)** RAW264.7 cells were pretreated with Myc inhibitor (10058-F4, 20 μM) (Myc inh) for 1h, and then stimulated with EST12 protein for the indicated time, the expression of iNOS and Arg1 was determined by Western blot **(A)**; the levels of the secreted IL-6 **(B)** and TNF-α **(C)** were determined by ELISA; NO levels in the supernatant were determined as described in Materials and Methods **(D)**. **(E–G)** RAW264.7 cells were infected with each indicated *M.tb* strains at MOI=10 and cultured with or without Myc inhibitor for 24 h, the expression of iNOS and Arg1 was determined by Western blot **(E)**; the levels of the secreted IL-6 **(F)** and TNF-α **(G)** were determined by ELISA. **(H–L)** RAW264.7 cells were infected with indicated *M.tb* strains and cultured with or without Myc inhibitor or JNK inhibitor. The cells were lysed and the CFUs of the intracellular *M.tb* were enumerated at 4 h, 8 h, 24 h or 48 h post infection. **(M)** BMDMs isolated from WT or IL-6 KO C57BL/6 mice were infected with BCG at MOI=10. Then BMDMs were stimulated with EST12 protein (2 μM) for 8 h. The cells were lysed and the CFUs of intracellular *M.tb* were enumerated. **(N)** BMDMs from WT C57BL/6 mice were infected with BCG at MOI=10. Then, BMDMs were stimulated with EST12 (2 μM) with or without TNF-α neutralizing antibody (10 μg/ml) for 8 h. The cells were lysed and the CFUs of the intracellular *M.tb* were enumerated. One-way ANOVA with Tukey's multiple comparisons test was used to assess the statistical difference in **(F, G)**. Two-way ANOVA with Tukey's multiple comparisons test was used to assess the statistical significance in **(B–D)** and **(H–N)**. The data are expressed as the mean ± SEM of three independent experiments. $p > 0.05$, not significant (ns), $^{*}p < 0.05$, $^{**}p < 0.01$, or $^{***}p < 0.001$.

transfected pGL3-IL-6-2 (IL-6 promoter region from -808 bp to +21 bp) and pGL3-TNF-α-3 (TNF-α promoter region from -329 bp to +33bp) into RAW264.7 cells and confirmed that EST12 stimulation significantly induced IL-6 and TNF-α activation, however, Myc inhibitor significantly blocked EST12's inductive effects (Figures 4C, D). To confirm Myc binding to the promoter sequences of IL-6 and TNF-α, we analyzed the results of CUT&Tag sequencing which captured differential sequences between EST12-treated RAW264.7 group and control group with anti-Myc antibody. Our CUT&Tag results showed that EST12 induced specific differential peaks at the promoter regions of IL-6, TNF-α (Figure 4E) and iNOS (Figure S3C). We focused the further research on exploring how EST12 induces the expression of IL-6 and TNF-α through Myc. Then ChIP-qPCR assays confirmed that the critical binding site of Myc is located at the -516 bp to -367 bp, but not at -385 bp to -277 bp of IL-6 promoter region during EST12 stimulation (Figures 4E, left, 4F, G). Similarly, we also found that the Myc critical binding site is located at the -106 bp to +33 bp, but not at -223 bp to -88 bp of TNF-α promoter region during EST12 stimulation (Figures 4E, right 4H, I). H3-K4 was used as a positive transcriptional factor control (Figures 4F–I).

Next, we further performed EMSA to determine whether EST12 induced-Myc bound the IL-6 and TNF-α promoters using the corresponding 31-nucleotide DNA probe (Supplementary Table 4) containing the potential Myc transcription factor binding region. Nuclear protein extracts from EST12-pretreated RAW264.7 cells displayed stronger binding to the probe (Figures 4J, K Lane 3 vs. Lane 2) than those from untreated RAW264.7 cells. The binding was abrogated when the extract was incubated with a 10-fold excess of the unlabeled 'competitor' probe (Figures 4J, K Lane4), but when we mutated the E-box (the classical Myc binding motif) (Figure 4L) like sequence "CATGTG" of IL-6 promoter or "CAGACG" of TNF-α promoter (Figure 4M, Supplementary Table 4, underlined), the mutant (Mut) 'competitor' probe did not abolish binding, providing additional evidence for its specificity (Figures 4J, K Lane5). These results suggested that EST12 induced Myc binding to the promoters of IL-6 and TNF-α at E-box like sequence, and thus increased the expression of these cytokines.

EST12 decreased Arg1 or Myc expression and increased classical M1 activation and pro-inflammatory response relying on RACK1 and JNK at later stage

As the above results showed that EST12 induced early Myc expression (1 h post-stimulation of *M.tb*-EST12), but decreased M2 polarization-related factor Arg1 or Myc expression and increased classical M1 polarization-related factor iNOS and pro-inflammatory cytokines (IL-6 and TNF-α) expression at later stage (12-24 h post-stimulation of *M.tb*-EST12, Figure 3A). We next examined whether these effects of EST12 relying on RACK1 and JNK. Compared with WT BMDMs, RACK1 deficiency (RACK1 KO) significantly decreased EST12-induced iNOS (Figure 5A), NO (Figure 5B), IL-6 (Figure 5C) and TNF-α (Figure 5D) at later stage (12-24 h post-stimulation of *M.tb*-EST12). Similarly, we found that EST12 induced iNOS (Figure 5E), NO (Figure 5F), IL-6 (Figure 5G) and TNF-α (Figure 5H) expression dependent on JNK, and JNK inhibitor significantly arrested EST12-induced effects (Figures 5E–H). Altogether, above results demonstrated that *M.tb*-EST12 decreased M2 polarization-related factor Arg1 or Myc expression and increased pro-inflammatory response and classical M1 activation dependent on RACK1 and JNK at later stage.

Host E3 ubiquitin ligase FBW7 mediates the K48 ubiquitination and degradation of Myc at late stage

As shown in Figure 1E, we found that EST12 stimulation induced Myc protein expression in macrophages at early stage (within 1h stimulation of EST12) and then decreased after 1 h. In order to detect whether late degradation of Myc protein is specific to EST12, we removed EST12 protein by replacing fresh media after 1 h stimulation of RAW264.7 cells with EST12 as indicated in Figure 6A, and found that Myc protein late degradation was significantly alleviated (Figure 6A). This result suggests that EST12 specifically induces early expression and late degradation of Myc protein. We further found that ubiquitin proteasome inhibitor MG-132 blocked EST12-induced Myc degradation (Figure 6B). Cycloheximide (CHX, a protein synthesis inhibitor) chase assay further demonstrated that Myc displayed significantly shortened half-life in EST12-treated RAW264.7 cells compared to the control group (Figure 6C). Furthermore, co-transfection experiment demonstrated that EST12 specifically upregulated K48 ubiquitination of Myc but not K63 ubiquitination (Figure 6D). Further, we found that after EST12 stimulation, dephosphorylation at Ser62-Myc and phosphorylation at Thr58-Myc at later stage (after 6 h stimulation of EST12, Figure 6E) was observed, suggesting that EST12 mainly triggers Myc Thr58 phosphorylation, but not Ser62, during the K48 ubiquitination degradation process of Myc at later stage (Figure 6E). Previous reports have shown that pS62-Myc is efficiently dephosphorylated by protein phosphatase 2A (PP2A) and T58-Myc is ubiquitinated by the E3 ubiquitin ligase SCF-FBW7, thus ultimately leading to proteosome-mediated degradation of Myc (18). Therefore, what we observed (in Figure 6E) might be the results of dephosphorylation at Ser62-Myc and phosphorylation at Thr58-Myc at later stage, which facilitates the ubiquitination degradation process of Myc.

10.3389/fimmu.2022.943174

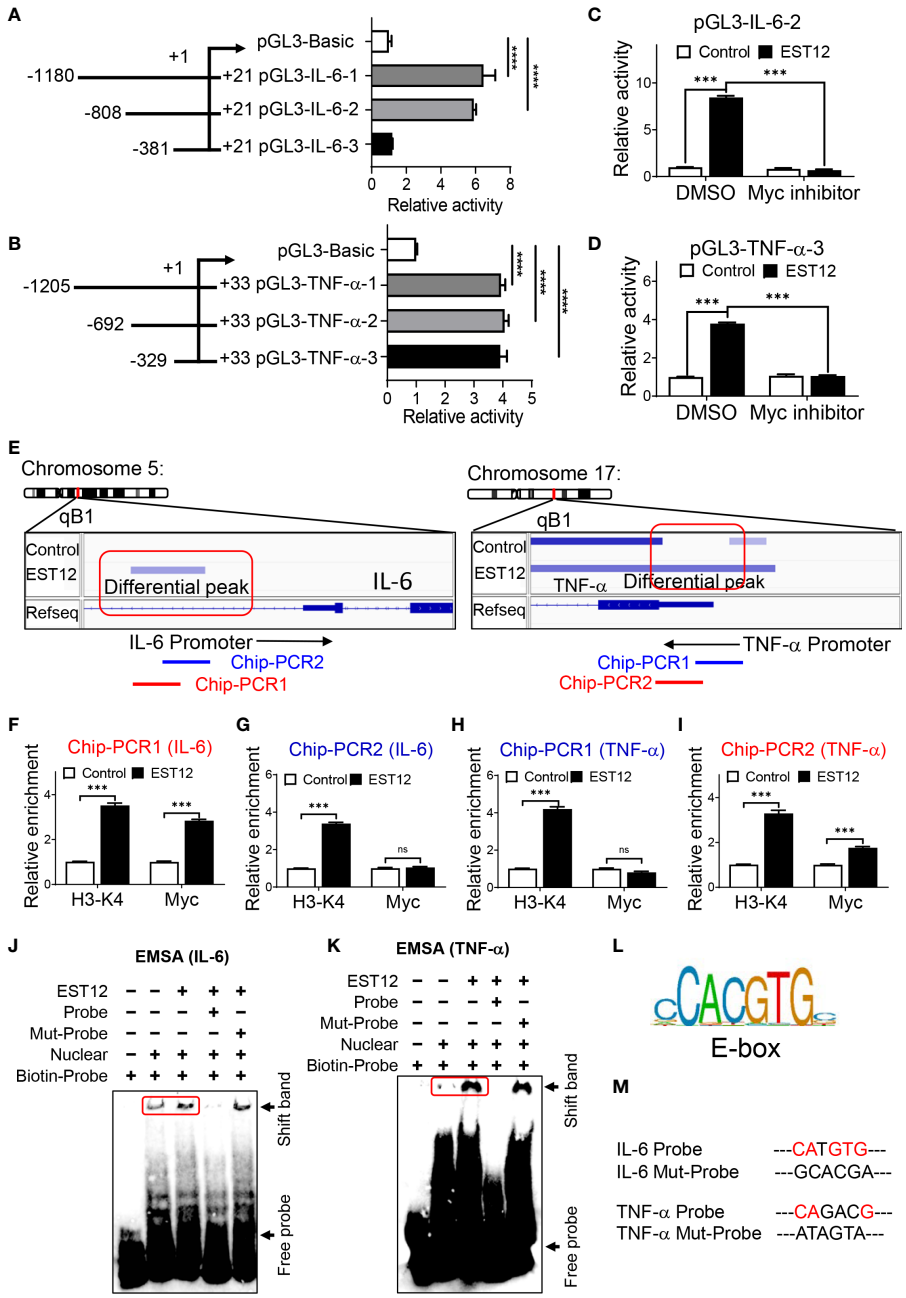

FIGURE 4
EST12 promotes Myc to bind to the promoters of IL-6 and TNF-α, and then induces IL-6 and TNF-α expression. **(A, B)** The different truncation regions of IL-6 and TNF-α promoters were cloned into pGL3-basic plasmid. Each plasmid was co-transfected with control fluorescent plasmid Renilla into RAW264.7 cells for 24 h. Then cells were stimulated with EST12 protein (2 μM) for 1 h. The cells were lysed and luciferase activities of each group were measured as described in Materials and Methods. **(C, D)** RAW264.7 cells were transfected with pGL3-IL-6-2 **(C)** or pGL3-TNF-α-3 **(D)**. Then cells were treated with Myc inhibitor (10058-F4, 20 μM) for 1 h, then stimulated with EST12 protein (2 μM) for 1 h. Then cells were lysed and the luciferase activities were measured. **(E)** RAW264.7 cells were stimulated with EST12 protein (2 μM) for 1 h, and then proceeded CUT&Tag sequencing analysis as described in Materials and Methods. **(F–K)** The effects of EST12-induced Myc binding to the promoters of IL-6 and TNF-α were analyzed by ChIP-qPCR **(F–I)** and EMSA **(J, K)**, respectively. IL-6: PCR1 (-516, -367), PCR2 (-385, -277); TNF-α: PCR1 (-223, -88), PCR2 (-106, +33). **(L)** The classical E-box motif. **(M)** Mutation sites used in **(J, K)** One-way ANOVA with Tukey's multiple comparisons test was used to assess the statistical difference in **(A, B)**. Two-way ANOVA with Tukey's multiple comparisons test was used to assess the statistical difference in **(C, D)** and **(F–I)** (vs. Control). The data are expressed as the mean ± SEM of three independent experiments. $p > 0.05$, not significant (ns), ***$p < 0.001$, or ****$p < 0.0001$.

10.3389/fimmu.2022.943174

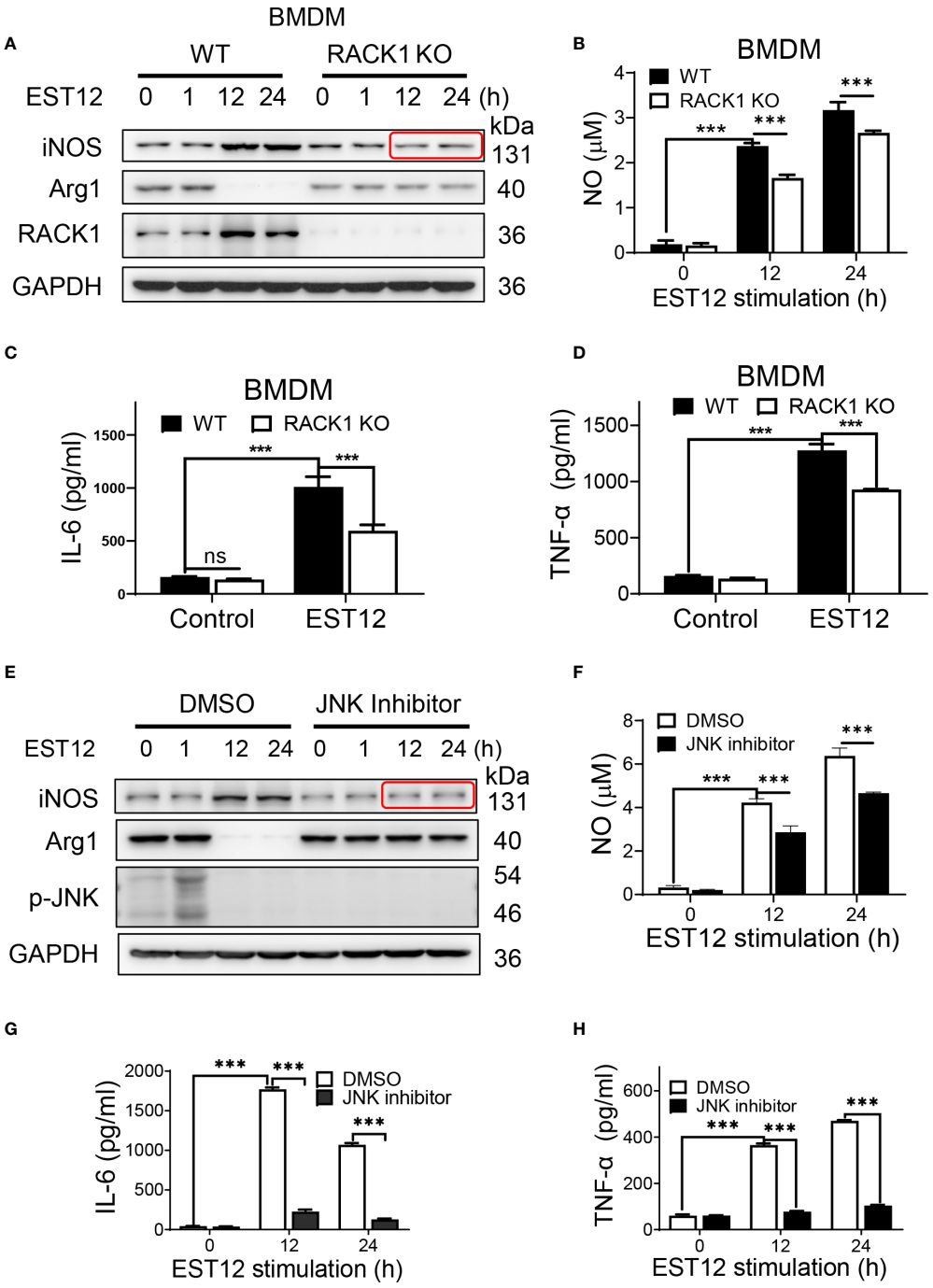

FIGURE 5
EST12 induces classical M1 activation relying on RACK1-JNK signaling pathway. **(A-D)** BMDMS isolated from WT, RACK1 KO C57BL/6 mice, respectively, were stimulated with EST12 protein (2 μM) for the indicated time, the expression of iNOS and Arg1 was determined by Western blot **(A)**; NO in the supernatant was determined as described above **(B)**; the secreted IL-6 **(C)** and TNF-α **(D)** levels were determined by ELISA. **(E-H)** RAW264.7 cells were pretreated with JNK inhibitor (10 μM), and then stimulated with EST12 protein (2 μM) for the indicated time, the expression of iNOS and Arg1 was determined by Western blot **(E)**; NO in the supernatant was determined as described above **(F)**; the expression of IL-6 **(G)** and TNF-α **(H)** were determined by ELISA. Two-way ANOVA with Tukey's multiple comparison test was used for **(B-D)** and **(F-H)**. The data are expressed as the mean ± SEM of three independent experiments. $p > 0.05$, not significant (ns), ***$p < 0.001$.

10.3389/fimmu.2022.943174

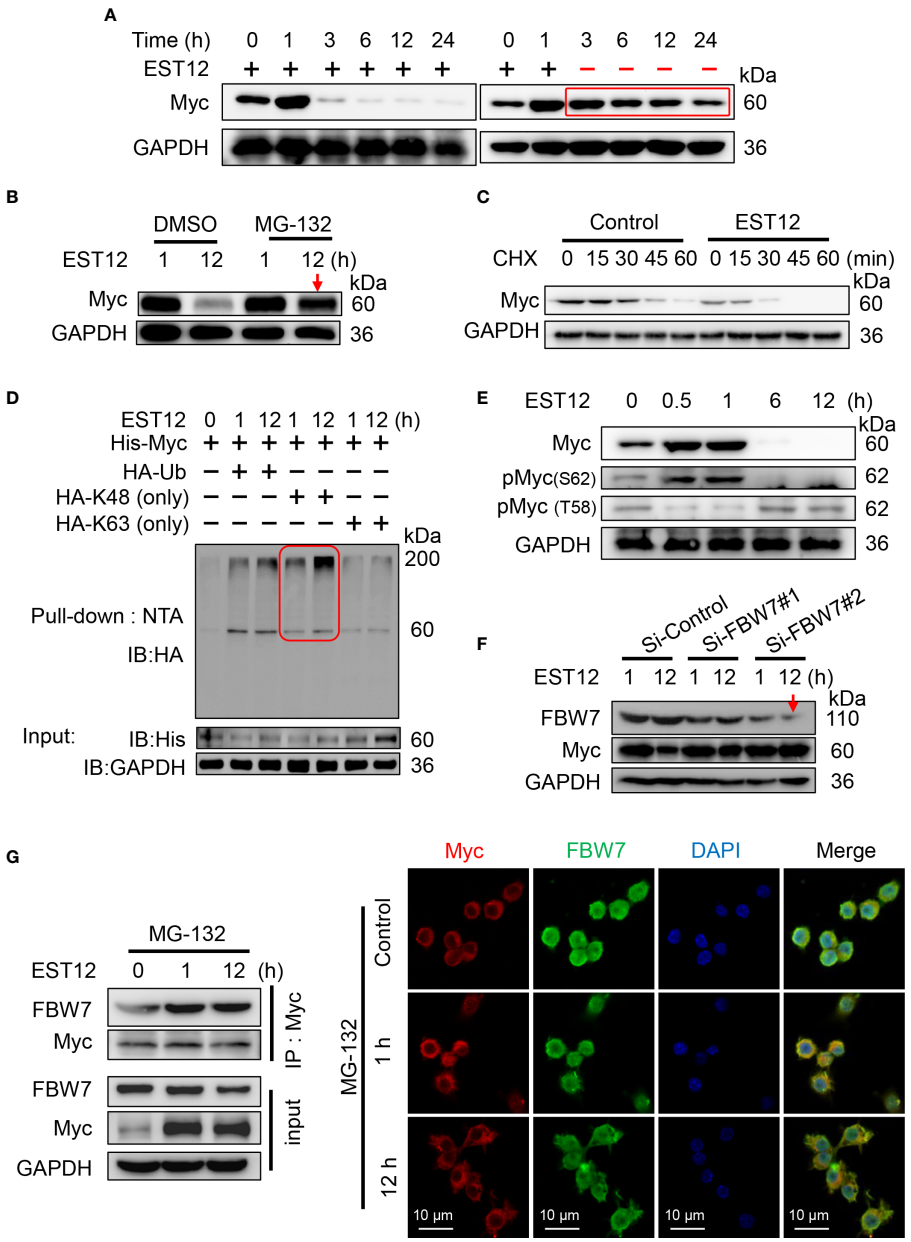

FIGURE 6
E3 ubiquitin ligase FBW7 mediates Myc K48 ubiquitination and degradation. **(A)** EST12 protein (2 μM) was added to stimulate RAW264.7 cells for 1 h. Then supernatants were replaced with fresh media to remove EST12, and cells were further incubated for the indicated time. The cell lysates were collected and Myc expression was analyzed by Western blot. **(B)** RAW264.7 cells were pretreated with MG-132 (5 μM), and then stimulated with EST12 protein (2 μM) for 1 or 12 h. Then the expression of Myc was analyzed by Western blot. **(C)** RAW264.7 cells were stimulated with EST12 protein (2 μM) for 1 h, then treated with CHX (20 μg/ml) for the indicated time, the expression of Myc was detected by Western blot. **(D)** RAW264.7 cells were transfected with the indicated plasmids, and then cell lysates were pulled down using Ni-NTA agarose. The ubiquitylation level of Myc was determined by Western blot with antibody against HA tag. **(E)** RAW264.7 cells were stimulated with EST12 protein (2 μM) for indicated time, the expression of Myc, pMyc (S62) and pMyc (T58) were detected by Western blot. **(F)** After RAW 264.7 cells were transfected with indicated siRNA for 36 h, cells were treated with EST12 protein (2 μM) for 1 or 12 h, then the expression of Myc and FBW7 were analyzed by Western blot. **(G)** MG-132-pretreated RAW264.7 cells were stimulated with EST12 protein (2 μM) for the indicated time, co-immunoprecipitation was performed with antibody against Myc. The expression of Myc and FBW7 was detected by Western blot (left), and the expression and co-localization between Myc (red) and FBW7 (green) were determined by confocal fluorescence microscopy (right). Scale bar: 10 μm.

To further identify which E3 ubiquitin ligase mediated EST12-induced Myc degradation, we silenced the best-studied Myc specific E3 ubiquitin ligase FBW7 with siRNAs. As shown in Figure 6F, Si-FBW7#2 siRNA-mediated FBW7 knockdown significantly hindered EST12-induced Myc degradation. Furthermore, MG-132-pretreated RAW264.7 cells were stimulated with EST12 for 1 or 12 h, co-immunoprecipitation (Figure 6G, left) and immunofluorescence (Figure 6G, right) experiments were performed to explore the interaction between Myc and E3 ubiquitin ligase FBW7. As shown in Figure 6G, although EST12 does not induce the expression of FBW7, it significantly increased the binding of FBW7 to Myc (Figure 6G, left), and EST12 treatment for 1h and 12 h promoted the colocalization of FBW7 and Myc as indicated by immunofluorescence assay (Figure 6G, red and green merged as yellow part). A recent work reported that eleven–nineteen lysine-rich leukemia (ELL) could also function as an E3 ubiquitin ligase, target Myc proteasomal degradation and suppress tumor growth (19). However, we did not found ELL was involved in EST12-induced K48 ubiquitination and degradation of Myc, since knockdown of ELL expression did not increase Myc expression (Figure S3D).

Taken together, these results demonstrated that host E3 ubiquitin ligase FBW7 bound with Myc and mediated EST12-induced Myc ubiquitination and degradation.

EST12 induces Myc expression and activation through endocytosis of macrophage not through binding to TLR2/4 of macrophage

To explore whether EST12 upregulates Myc expression of macrophage through binding to TLR2/4 receptors of macrophages, BMDMs were used. Consistently with the previous report that Myc is expressed in BMDMs M0 (20), we found that Myc could be expressed in M2 and weakly expressed in M0 BMDMs, but not in M1 BMDMs (Figure 7A). Both WT M0 BMDMs and TLR2/4 KO M0 BMDMs were stimulated with EST12 protein (Figures 7B, C) or infected with *M.tb* H37Rv (Figure 7D). As evidenced in Figures 7B–D, TLR2 or TLR4 deficiencies did not decrease EST12 or *M.tb* H37Rv-induced Myc expression. However, when we pretreated RAW264.7 cells with 2.5 μM phagocytosis inhibitor cytochalasin D, we found that EST12-induced Myc expression was significantly blocked (Figure 7E). Consistently, as shown in immunofluorescence assay, cytochalasin D significantly blocked macrophage uptake of EST12 protein and macrophage Myc expression (Figure 7F), suggesting mycobacterial secreted EST12 protein enters cells through endocytosis not through binding to TLR2/4 of macrophages.

Discussion

In this study, we found that *M.tb*-EST12 protein and *M.tb* H37Rv infection induced the expression of Myc in both human THP1 cells and mouse macrophages (RAW264.7 and BMDMs). Importantly, we demonstrated that EST12 protein induced early expression and late K48 ubiquitination and degradation of Myc protein. EST12 activates JNK-AP1-Myc signaling pathway, promotes Myc to bind to the promoters of IL-6, TNF-α and iNOS, and then induces the expression of IL-6, TNF-α and iNOS, which further contributes to anti-mycobacterial effects. Our data suggest that Myc acts as a critical transcriptional factor and plays a pivotal role in *M.tb*-induced innate immunity (Figure 8).

Macrophages are the main effective immune cells in anti-TB immune response through mediating the pro-inflammatory response and immune clearance of *M.tb*. It is well known that classically activated M1 macrophages are the most effective immune cells for killing *M.tb* (21). JNK pathway has been reported to contribute to the expression of various pro-inflammatory cytokines such as IL-6 for *M.tb* clearance (22). The expression levels of various cytokines and chemokines play important roles in *M.tb* infection (23). Among them, *M.tb* infection promotes the expression of iNOS, or secretion of NO, IL-1β, TNF-α and IL-6 (24, 25). IL-1β directly kills *M.tb* or upregulates TNF-α expression and promotes macrophages apoptosis to eliminate *M.tb* (26, 27). Both IL-6 and TNF-α could increase the elimination of intracellular *M.tb* (10). IL-6 is a pleotropic cytokine that regulates both pro- and anti-inflammatory cytokine production (28). IL-6 knockdown resulted in increased bacterial burden in *M.tb* infected mouse macrophages and IL-6-deficient mice are susceptible to *M.tb* infection, indicating that IL-6 has an effect on the protective immune response against *M.tb* (29, 30). Other report also showed that mycobacteria- induced Myc expression is associated with the induction of inflammatory cytokines IL-6 and TNF-α and with the suppression of intracellular mycobacterial growth (10). Consistently, here we found that mycobacterial EST12 protein induced IL-6 and TNF-α expression of macrophages associated with anti-*M.tb* function (Figures 3M, N). Both IL-6 and TNF-α acted as pro-inflammatory cytokines and exerted the anti-*M.tb* function, since IL-6/TNF-α deficiency increased the survival of intracellular mycobacteria (Figures 3M, N). Recently, we have demonstrated that *M.tb*-EST12 could induce ROS expression (12), and ROS contributed to iNOS expression (18). Here, we demonstrated *M.tb* EST12 increased iNOS, NO, IL-6 and TNF-α expression and increased *M.tb* clearance depend on RACK1, Myc and JNK in macrophages (Figures 3I–L), and IL-6 KO or anti-TNF-α antibody treatment abrogated these effects. Since Myc is essential for cell survival and knockout of Myc is lethal to mice (data not shown). Unfortunately, we were unable to obtain

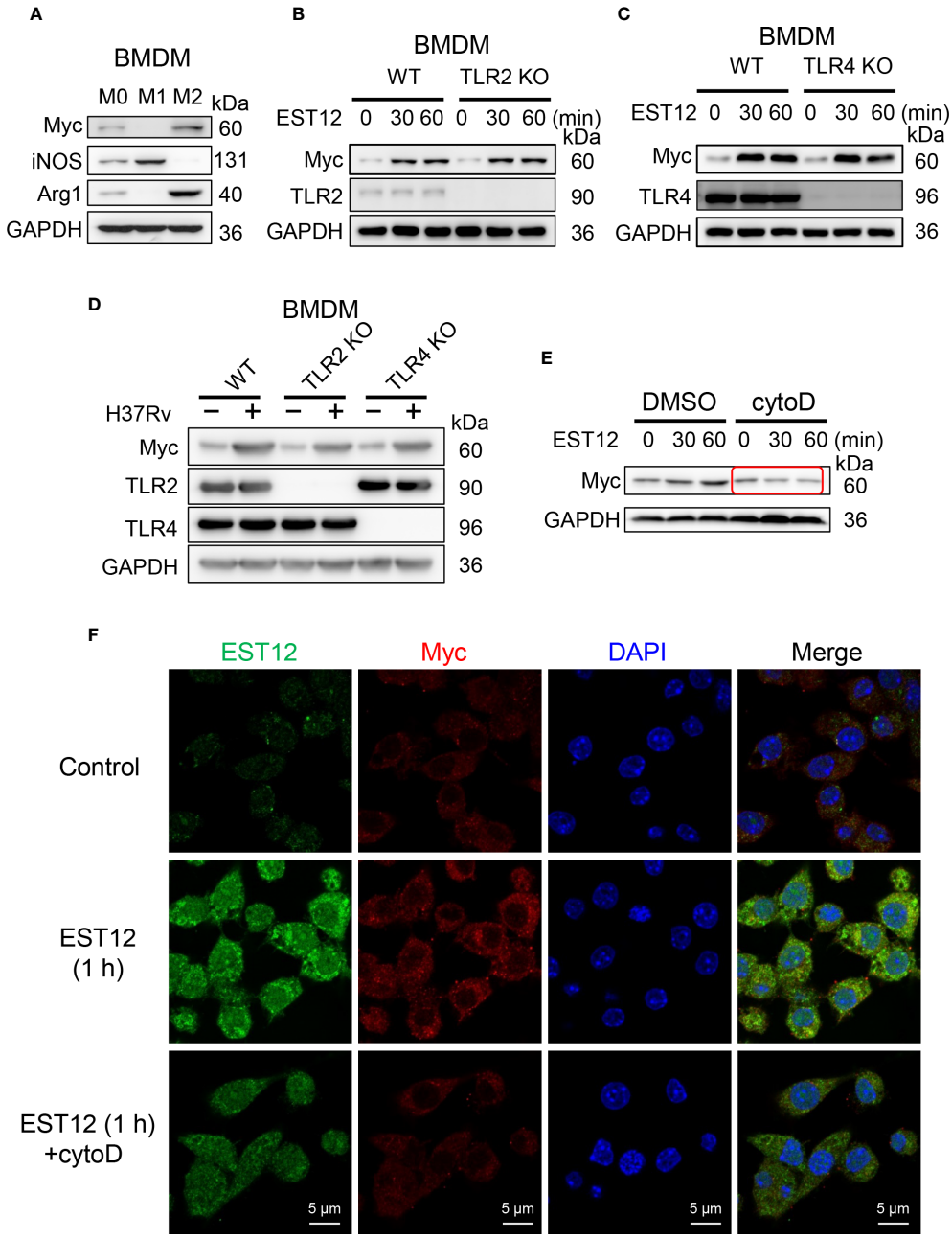

FIGURE 7
EST12 induces Myc expression and activation through endocytosis but not through binding of TLR2/4 of macrophage. **(A)** Myc expression was analyzed in M0-, M1- and M2-BMDMs by Western blot. **(B, C)** BMDMs isolated from WT, TLR2 KO **(B)** or TLR4 KO **(C)** mice were stimulated with EST12 protein (2 μM) for the indicated time, the expression of Myc was analyzed by Western blot. **(D)** BMDMs isolated from WT, TLR2 KO and TLR4 KO C57BL/6 mice, respectively, were infected with H37Rv at MOI = 10 for 24 h, the expression of Myc was detected by Western blot. **(E, F)** RAW264.7cells were stimulated with EST12 protein (2 μM) for 1 h in the presence or absence of Cytochalasin D (2.5 μM), the expression of Myc was detected by Western blot **(E)** and immunofluorescence **(F)**.

macrophage conditional Myc KO homozygous mice to perform *in vivo* experiment.

Myc has been reported to be critical for the induction and maintenance of the M2-like macrophage state (31). Our results in Figure 3A suggest that EST12-induced Myc expression in a trend consistent with that of Arg-1 expression with M2-like macrophage phenotype. It was also reported that silencing of Myc attenuated BCG-induced IL-6 and TNF-α expression (10).

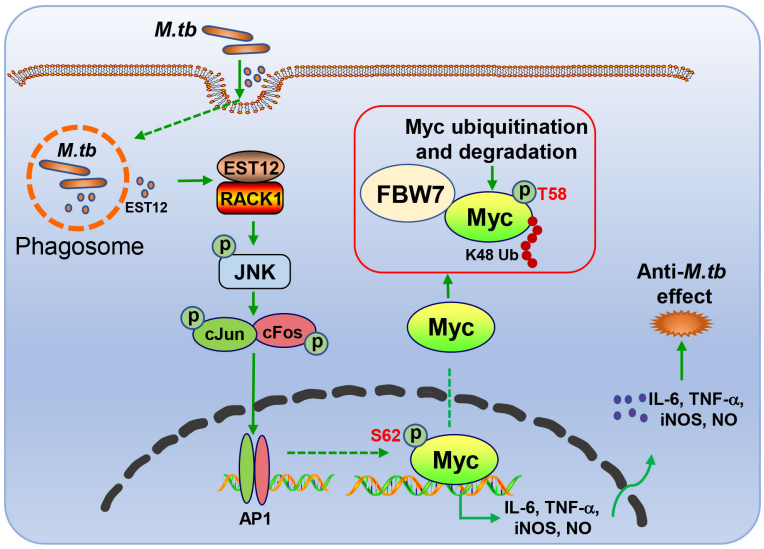

FIGURE 8
Schematic diagram of EST12-induced anti-*M.tb* immune effect through RACK1-JNK-AP1-Myc signaling axis.

However, the mechanism of Myc-induced IL-6 and TNF-α has not been reported yet. In this report, we firstly clarify how Myc induces the expression of IL-6 and TNF-α, and determine that Myc acts as a critical transcription factor to bind the promoters of these genes and induce their expression. We demonstrated Myc inhibitor decreased EST12 or H37Rv-induced IL-6 and TNF-α expression.

As a transcription factor, Myc could rapidly degrade following synthesis, and its half-life was about 20 min (32). Ubiquitin–proteasome system (UPS) is the most important mechanism for regulating Myc protein level (33). And FBW7 is the best-studied E3 ubiquitin ligase for Myc (8). Consistently, we found that FBW7 interacted with Myc and mediated EST12-induced K48 ubiquitination and degradation of Myc at late stage (Figures 6D, F, G).

Previous reports showed that the increased phosphorylation of Myc S62 promoted the stability of Myc protein, and phosphorylated S62 would also help Myc bind to GSK3β, which mediated phosphorylation of T58 and Myc ubiquitination degradation by FBW7 (32). In the present study, we found that EST12 could activate Myc by promoting S62 phosphorylation, decreasing T58 phosphorylation at the early stage (within 1 h stimulation of EST12) (Figure 2A). EST12 stimulation induced T58 phosphorylation of Myc at later stage (6 h post-stimulation of EST12) (Figure 6E), which might ultimately lead Myc to bind and recruit FBW7 for K48 poly-ubiquitination and degradation of Myc. A latest research report proposed a new mechanism for Myc S67 phosphorylation to antagonize GSK3β binding and thereby enhance the stability of Myc protein (34). Since antibody against Myc S67 phosphorylation is not commercially available, whether EST12 could induce Myc S67 phosphorylation requires further investigation in future.

Our results suggest that EST12-induced early Myc expression is beneficial for the induction of pro-inflammatory cytokines (such as IL-6 and TNF-α), which may contribute to host defense against mycobacteria. On the other hand, EST12 induces late K48 ubiquitination and degradation of Myc protein and decreases M2 polarization related factor Arg1 or Myc expression and increases classical M1 activation (iNOS/NO expression) at later stage (after 12 hour stimulation of EST12), which may also contribute to enhancement of anti-mycobacterial immunity. Previous reports have shown that c-Myc plays a positive role in phagocytosis, contributing to host defense against mycobacteria (35). Because of Myc-targeted gene network (9), it is highly possible for Myc to directly or indirectly affect phagocytosis or other processes, which need to be further investigated. As other signaling pathways (such as NF-κB mediated pathway) were also reported to mediate *M.tb*-induced inflammatory response (36), Myc might not be the only trigger of this process.

In addition, it has recently been reported that TB aggravates the progress of COVID-19 infection which accompanied cytokine storm with elevated IL-6 and TNF-α (37). Here both *M.tb* and *M.tb*-EST12 significantly induced pro-inflammatory cytokines IL-6 and TNF-α expression, suggesting that *M.tb*-induced pro-inflammatory cytokines might possibly have implication on inflammation of severity COVID-19.

Taken together, our findings suggest that *M.tb* secreted effector protein EST12 regulates early expression and late K48

ubiquitination and degradation of Myc protein, EST12 regulates Myc expression and enhances anti-mycobacterial inflammatory response *via* RACK1-JNK-AP1-Myc immune pathway. Our finding provides new insights into *M.tb*-induced immunity through Myc.

Data availability statement

The raw data of sequencing has been deposited at GEO database. Accession numbers: RNA-seq (GSE210088), Cut&Tag-seq (GSE210089).

Ethics statement

The animal study was reviewed and approved by committee on ethics in the Care and Use of Laboratory Animals of Wuhan University.

Author contributions

X-LZ designed and supervised the research. JW conducted the experiments. HX, GL, and YG gave helps to the experiments. JW, X-LZ, F-LL, and YX analyzed the data and wrote the manuscript. All authors contributed to the article and approved the submitted version.

Funding

This study was supported by grants from the National Grand Program on Key Infectious Disease of China (2017ZX10201301-006 and 2012ZX10003002-015), the National Key R&D Program of China (2018YFA0507603), the National Natural Science Foundation of China (91740120 and 22077097), the National Outstanding Youth Foundation of China (81025008), Hubei Province's Outstanding Medical Academic Leader Program (523-276003), Hubei Province Key R&D Program (2020BCB020), Research and Innovation Team Project of Hubei Provincial Health Commission (WJ2021C002), the Medical Science Advancement Program (Basic Medical Sciences) of Wuhan University (TFJC 2018002), the Fundamental Research Funds for the Central Universities and Foundation Committee Innovation Group Project (21721005).

Acknowledgments

The author would like to thank professor Jiahuai Han of Xiamen University for kindly providing the template of Myc DNA.

Conflict of interest

The authors declare that the research was conducted in the absence of any commercial or financial relationships that could be construed as a potential conflict of interest.

Publisher's note

Supplementary material

The Supplementary Material for this article can be found online at: https://www.frontiersin.org/articles/10.3389/fimmu.2022.943174/full#supplementary-material

References

1. Global tuberculosis report 2021. Geneva: World Health Organization (2021).

2. Behr MA, Wilson MA, Gill WP, Salamon H, Schoolnik GK, Rane S, et al. Comparative genomics of bcg vaccines by whole-genome DNA microarray. *Science* (1999) 284(5419):1520–3. doi: 10.1126/science.284.5419.1520

3. Zonghai C, Tao L, Pengjiao M, Liang G, Rongchuan Z, Xinyan W, et al. Mycobacterium tuberculosis Esat6 modulates host innate immunity by downregulating mir-222-3p target pten. *Biochim Biophys Acta Mol Basis Dis* (2022) 1868(1):166292. doi: 10.1016/j.bbadis.2021.166292

4. Samuchiwal SK, Tousif S, Singh DK, Kumar A, Ghosh A, Bhalla K, et al. A peptide fragment from the human Cox3 protein disrupts association of mycobacterium tuberculosis virulence proteins esat-6 and Cfp10, inhibits mycobacterial growth and mounts protective immune response. *BMC Infect Dis* (2014) 14:355. doi: 10.1186/1471-2334-14-355

5. Liu S, Xie Y, Luo W, Dou Y, Xiong H, Xiao Z, et al. Pe_Pgrs31-S100a9 interaction promotes mycobacterial survival in macrophages through the regulation of nf-Kappab-Tnf-Alpha signaling and arachidonic acid metabolism. *Front Microbiol* (2020) 11:845. doi: 10.3389/fmicb.2020.00845

6. Wu Y, Tian M, Zhang Y, Peng H, Lei Q, Yuan X, et al. Deletion of Bcg_2432c from the bacillus calmette-guerin vaccine enhances autophagy-mediated immunity against tuberculosis. *Allergy* (2022) 77(2):619–32. doi: 10.1111/all.15158

7. Chatterjee S, Yabaji SM, Rukhlenko OS, Bhattacharya B, Waligurski E, Vallavoju N, et al. Channeling macrophage polarization by rocaglates increases

macrophage resistance to mycobacterium tuberculosis. *iScience* (2021) 24 (8):102845. doi: 10.1016/j.isci.2021.102845

8. Li S, Zhang L, Zhang G, Shangguan G, Hou X, Duan W, et al. A nonautophagic role of Atg5 in regulating cell growth by targeting c-myc for proteasome-mediated degradation. *iScience* (2021) 24(11):103296. doi: 10.1016/j.isci.2021.103296

9. Dang CV, O'Donnell KA, Zeller KI, Nguyen T, Osthus RC, Li F. The c-myc target gene network. *Semin Cancer Biol* (2006) 16(4):253–64. doi: 10.1016/j.semcancer.2006.07.014

10. Yim HC, Li JC, Pong JC, Lau AS. A role for c-myc in regulating anti-mycobacterial responses. *Proc Natl Acad Sci U.S.A.* (2011) 108(43):17749–54. doi: 10.1073/pnas.1104892108

11. Ganguly N, Giang PH, Basu SK, Mir FA, Siddiqui I, Sharma P. Mycobacterium tuberculosis 6-kda early secreted antigenic target (Esat-6) protein downregulates lipopolysaccharide induced c-myc expression by modulating the extracellular signal regulated kinases 1/2. *BMC Immunol* (2007) 8:24. doi: 10.1186/1471-2172-8-24

12. Qu Z, Zhou J, Zhou Y, Xie Y, Jiang Y, Wu J, et al. Mycobacterial Est12 activates a Rack1-Nlrp3-Gasdermin d pyroptosis-Il-1beta immune pathway. *Sci Adv* (2020) 6(43):eaba4733. doi: 10.1126/sciadv.aba4733

13. Abdul-Hamid NA, Abas F, Maulidiani M, Ismail IS, Tham CL, Swarup S, et al. Nmr metabolomics for evaluating passage number and harvesting effects on mammalian cell metabolome. *Anal Biochem* (2019) 576:20–32. doi: 10.1016/j.ab.2019.04.001

14. Jain P, Hsu T, Arai M, Biermann K, Thaler DS, Nguyen A, et al. Specialized transduction designed for precise high-throughput unmarked deletions in mycobacterium tuberculosis. *mBio* (2014) 5(3):e01245–14. doi: 10.1128/mBio.01245-14

15. Bardarov S, Bardarov S, Pavelka MS, Sambandamurthy V, Larsen M, Tufariello J, et al. Specialized transduction: An efficient method for generating marked and unmarked targeted gene disruptions in mycobacterium tuberculosis, m. bovis bcg and m. smegmatis. *Microbiol (Reading)* (2002) 148(Pt 10):3007–17. doi: 10.1099/00221287-148-10-3007

16. Schmittgen TD, Livak KJ. Analyzing real-time pcr data by the comparative C(T) method. *Nat Protoc* (2008) 3(6):1101–8. doi: 10.1038/nprot.2008.73

17. Nalbandian A, Yan BS, Pichugin A, Bronson RT, Kramnik I. Lung carcinogenesis induced by chronic tuberculosis infection: The experimental model and genetic control. *Oncogene* (2009) 28(17):1928–38. doi: 10.1038/onc.2009.32

18. Yeh E, Cunningham M, Arnold H, Chasse D, Monteith T, Ivaldi G, et al. A signalling pathway controlling c-myc degradation that impacts oncogenic transformation of human cells. *Nat Cell Biol* (2004) 6(4):308–18. doi: 10.1038/ncb1110

19. Chen Y, Zhou C, Ji W, Mei Z, Hu B, Zhang W, et al. Ell targets c-myc for proteasomal degradation and suppresses tumour growth. *Nat Commun* (2016) 7:11057. doi: 10.1038/ncomms11057

20. Liu L, Lu Y, Martinez J, Bi Y, Lian G, Wang T, et al. Proinflammatory signal suppresses proliferation and shifts macrophage metabolism from myc-dependent to Hif1alpha-dependent. *Proc Natl Acad Sci U.S.A.* (2016) 113(6):1564–9. doi: 10.1073/pnas.1518000113

21. Huang Z, Luo Q, Guo Y, Chen J, Xiong G, Peng Y, et al. Mycobacterium tuberculosis-induced polarization of human macrophage orchestrates the formation and development of tuberculous granulomas *in vitro*. *PloS One* (2015) 10(6):e0129744. doi: 10.1371/journal.pone.0129744

22. Zhong J, Wang H, Chen W, Sun Z, Chen J, Xu Y, et al. Ubiquitylation of Mfhas1 by the ubiquitin ligase Praja2 promotes M1 macrophage polarization by activating jnk and P38 pathways. *Cell Death Dis* (2017) 8(5):e2763. doi: 10.1038/cddis.2017.102

23. Cooper AM, Mayer-Barber KD, Sher A. Role of innate cytokines in mycobacterial infection. *Mucosal Immunol* (2011) 4(3):252–60. doi: 10.1038/mi.2011.13

24. Basu S, Fowler BJ, Kerur N, Arnvig KB, Rao NA. Nlrp3 inflammasome activation by mycobacterial esat-6 and dsrna in intraocular tuberculosis. *Microb Pathog* (2018) 114:219–24. doi: 10.1016/j.micpath.2017.11.044

25. Dorhoi A, Nouailles G, Jorg S, Hagens K, Heinemann E, Pradl L, et al. Activation of the Nlrp3 inflammasome by mycobacterium tuberculosis is uncoupled from susceptibility to active tuberculosis. *Eur J Immunol* (2012) 42 (2):374–84. doi: 10.1002/eji.201141548

26. Jayaraman P, Sada-Ovalle I, Nishimura T, Anderson AC, Kuchroo VK, Remold HG, et al. Il-1beta promotes antimicrobial immunity in macrophages by regulating tnfr signaling and caspase-3 activation. *J Immunol* (2013) 190(8):4196–204. doi: 10.4049/jimmunol.1202688

27. Verway M, Bouttier M, Wang TT, Carrier M, Calderon M, An BS, et al. Vitamin d induces interleukin-1beta expression: Paracrine macrophage epithelial signaling controls m. *Tuberc Infect PloS Pathog* (2013) 9(6):e1003407. doi: 10.1371/journal.ppat.1003407

28. Kamimura D, Ishihara K, Hirano T. Il-6 signal transduction and its physiological roles: The signal orchestration model. *Rev Physiol Biochem Pharmacol* (2003) 149:1–38. doi: 10.1007/s10254-003-0012-2

29. Ladel CH, Blum C, Dreher A, Reifenberg K, Kopf M, Kaufmann SH. Lethal tuberculosis in interleukin-6-Deficient mutant mice. *Infect Immun* (1997) 65 (11):4843–9. doi: 10.1128/iai.65.11.4843-4849.1997

30. Martinez AN, Mehra S, Kaushal D. Role of interleukin 6 in innate immunity to mycobacterium tuberculosis infection. *J Infect Dis* (2013) 207(8):1253–61. doi: 10.1093/infdis/jit037

31. Pello OM. Macrophages and c-myc cross paths. *Oncoimmunology* (2016) 5 (6):e1151991. doi: 10.1080/2162402X.2016.1151991

32. Farrell AS, Sears RC. Myc degradation. *Cold Spring Harb Perspect Med* (2014) 4(3):a014365. doi: 10.1101/cshperspect.a014365

33. Thomas LR, Tansey WP. Proteolytic control of the oncoprotein transcription factor myc. *Adv Cancer Res* (2011) 110:77–106. doi: 10.1016/B978-0-12-386469-7.00004-9

34. Jiang J, Wang J, Yue M, Cai X, Wang T, Wu C, et al. Direct phosphorylation and stabilization of myc by aurora b kinase promote T-cell leukemogenesis. *Cancer Cell* (2020) 37(2):200–15.e5. doi: 10.1016/j.ccell.2020.01.001

35. Wang LJ, Li JCB, Lau ASY. The role of c-myc in phagocytosis of mycobacteria in human macrophages. *J Immunol* (2013) 190:130.6.

36. Sharma N, Shariq M, Quadir N, Singh J, Sheikh JA, Hasnain SE, et al. Mycobacterium tuberculosis protein Pe6 (Rv0335c), a novel Tlr4 agonist, evokes an inflammatory response and modulates the cell death pathways in macrophages to enhance intracellular survival. *Front Immunol* (2021) 12:696491. doi: 10.3389/fimmu.2021.696491

37. Kovalchuk A, Wang B, Li D, Rodriguez-Juarez R, Ilnytskyy S, Kovalchuk I, et al. Fighting the storm: Could novel anti-tnfalpha and anti-Il-6 c. sativa cultivars tame cytokine storm in covid-19? *Aging (Albany NY)* (2021) 13(2):1571–90. doi: 10.18632/aging.202500

frontiers | Frontiers in Immunology

TYPE Original Research
PUBLISHED 23 August 2022
DOI 10.3389/fimmu.2022.943667

OPEN ACCESS

EDITED BY
Wenping Gong,
The 8th Medical Center of PLA General Hospital, China

REVIEWED BY
Anuradha Rajamanickam,
International Centers for Excellence in Research (ICER), India
Guangcun Deng,
Ningxia University, China
Erwan Pernet,
McGill University Health Center, Canada
Oscar Taboga,
Instituto Nacional de Tecnología Agropecuaria, Argentina

*CORRESPONDENCE
Yinlan Bai
yinlanbai@fmmu.edu.cn
Fanglin Zhang
flzhang@fmmu.edu.cn

†These authors have contributed equally to this work

SPECIALTY SECTION
This article was submitted to Vaccines and Molecular Therapeutics, a section of the journal Frontiers in Immunology

RECEIVED 14 May 2022
ACCEPTED 13 July 2022
PUBLISHED 23 August 2022

CITATION
Ning H, Kang J, Lu Y, Liang X, Zhou J, Ren R, Zhou S, Zhao Y, Xie Y, Bai L, Zhang L, Kang Y, Gao X, Xu M, Ma Y, Zhang F and Bai Y (2022) Cyclic di-AMP as endogenous adjuvant enhanced BCG-induced trained immunity and protection against *Mycobacterium tuberculosis* in mice. *Front. Immunol.* 13:943667. doi: 10.3389/fimmu.2022.943667

Cyclic di-AMP as endogenous adjuvant enhanced BCG-induced trained immunity and protection against *Mycobacterium tuberculosis* in mice

Huanhuan Ning[1†], Jian Kang[1†], Yanzhi Lu[1†], Xuan Liang[1,2], Jie Zhou[3], Rui Ren[1], Shan Zhou[4], Yong Zhao[5], Yanling Xie[1,6], Lu Bai[1,6], Linna Zhang[7], Yali Kang[1,7], Xiaojing Gao[1,7], Mingze Xu[1], Yanling Ma[2], Fanglin Zhang[1*] and Yinlan Bai[1*]

[1]Department of Microbiology and Pathogen Biology, School of Preclinical Medicine, Air Force Medical University, Xi'an, China, [2]College of Life Sciences, Northwest University, Xi'an, China, [3]Department of Endocrinology, Xijing Hospital, Air Force Medical University, Xi'an, China, [4]Department of Clinical Laboratory, Xijing Hospital, Air Force Medical University, Xi'an, China, [5]Laboratory Animal Center, Air Force Medical University, Xi'an, China, [6]School of Life Sciences, Yan'an University, Yan'an, China, [7]Department of Physiology, Basic Medical School, Ningxia Medical University, Yinchuan, China

Bacillus Calmette-Guérin (BCG) is a licensed prophylactic vaccine against tuberculosis (TB). Current TB vaccine efforts focus on improving BCG effects through recombination or genetic attenuation and/or boost with different vaccines. Recent years, it was revealed that BCG could elicit non-specific heterogeneous protection against other pathogens such as viruses through a process termed trained immunity. Previously, we constructed a recombinant BCG (rBCG-DisA) with elevated c-di-AMP as endogenous adjuvant by overexpressing di-adenylate cyclase of *Mycobacterium tuberculosis* DisA, and found that rBCG-DisA induced enhanced immune responses by subcutaneous route in mice after *M. tuberculosis* infection. In this study, splenocytes from rBCG-DisA immunized mice by intravenous route (i.v) elicited greater proinflammatory cytokine responses to homologous and heterologous re-stimulations than BCG. After *M. tuberculosis* infection, rBCG-DisA immunized mice showed hallmark responses of trained immunity including potent proinflammatory cytokine responses, enhanced epigenetic changes, altered lncRNA expressions and metabolic rewiring in bone marrow cells and other tissues. Moreover, rBCG-DisA immunization induced higher levels of antibodies and T cells responses in the lung and spleen of mice after *M. tuberculosis* infection. It was found that rBCG-DisA resided longer than BCG in the lung of *M. tuberculosis* infected mice implying prolonged duration of

vaccine efficacy. Then, we found that rBCG-DisA boosting could prolong survival of BCG-primed mice over 90 weeks against *M. tuberculosis* infection. Our findings provided *in vivo* experimental evidence that rBCG-DisA with c-di-AMP as endogenous adjuvant induced enhanced trained immunity and adaptive immunity. What's more, rBCG-DisA showed promising potential in prime-boost strategy against *M. tuberculosis* infection in adults.

KEYWORDS

Bacillus Calmette-Guérin, cyclic di-AMP, trained immunity, adjuvant, *Mycobacterium tuberculosis*

Introduction

Bacillus Calmette-Guérin (BCG) is a live attenuated vaccine for the prevention of tuberculosis (TB), which is caused by *Mycobacterium tuberculosis* infection. Usually, BCG is inoculated to newborns after birth, of which protection efficiency against meningitis and miliary TB is over 70% (1). Whereas its protection efficacy varies from 0% to 80% against pulmonary TB in adults (2). Vaccinology to improve the efficacy of canonical BCG shows good application prospects, which is necessary to control TB epidemic.

BCG was obtained from virulent *Mycobacterium bovis*, which could elicit heterologous protective immune response against *M. tuberculosis* infection. Additionally, BCG has been found to elicit non-specific protection against non-mycobacterial bacteria infections (3), viral infections (4), tumors (5), and autoimmune diseases (3). This phenomenon of BCG-induced heterologous protection has been referred to as trained immunity (6). The hallmarks of trained immunity include elevated levels of proinflammatory cytokine responses, myeloid cells and macrophage reprogramming towards inflammatory, activated phenotypes, epigenetic modifications, and metabolomic changes towards glycolysis (7–9). BCG vaccination shows long-term effects on innate immunity, which lasts for at least one year and then wanes in mice model (10). It is speculated that increasing morbidity of TB adults in BCG vaccinated population may be related to the waning efficiency of BCG (11, 12). Furthermore, BCG vaccination could promote protective monocyte responses against severe acute respiratory syndrome coronavirus 2 (SARS-CoV-2) (13, 14), though its protective effect on SARS-CoV-2 remains controversial (15, 16). Therefore, it is reasonable to increase the protection of BCG by exploring new BCG strains or booster vaccines to enhance BCG-induced trained immunity.

Cyclic di-AMP (c-di-AMP) is a ubiquitous bacterial second messenger (17, 18), which regulates various bacterial physiological processes including bacterial virulence. What's more, there is growing evidence that c-di-AMP as a pathogen associated molecular pattern (PAMP) is engaged in host innate immune response including type I IFN response, autophagy, as well as inflammasome activation (19–21). Our previous work initially confirmed that Rv3586 is the only diadenylate cyclase (DacA, or DisA) (22), and Rv2837c is a cyclic nucleotide phosphodiesterase (CnpB) as a c-di-AMP hydrolyzing enzyme in *M. tuberculosis* (23). Either overexpression of DisA or deletion of CnpB could promote the accumulation of c-di-AMP in *M. tuberculosis* (23–25), BCG (24, 26, 27), as well as *M. smegmatis* (28–30). Further, we constructed a c-di-AMP elevated BCG with *disA* overexpressing (rBCG-DisA) and found that it induced stronger immune responses compared with BCG after *M. tuberculosis* infection in mice, with elevated cytokine responses of IL-6, TNF-α and enrichment of tri-methylation of lysine 4 on histone H3 (H3K4me3), which showed an enhanced trained immunity induced by rBCG-DisA (27).

However, we found that rBCG-DisA immunization by subcutaneous (s.c) route did not provide extra protection against *M. tuberculosis* in the mice model of i.v infection (27). While a similar rBCG-DisA with MT3692 (*M. tuberculosis* CDC1551 DisA, 100% similarity with Rv3586) overexpression has been shown to provide enhanced protection against aerosol *M. tuberculosis* infection compared to BCG in the guinea pig model (31). Moreover, rBCG-DisA induced improved antitumor efficacy by intravesical instillation in a rat model of bladder cancer, which was identified as an improved trained immunity compared with BCG in primary human and murine macrophages *in vitro* (32). It has been proved that BCG vaccination by i.v route is superior to induce trained immunity than that of s.c route (33). In addition, administration of BCG by i.v route conferred protection against *M. tuberculosis* challenge in non-human primate (34). In this study, we further explored immune responses induced by i.v rBCG-DisA especially trained immunity *in vivo*, and evaluated its protection efficiency and as a boosting vaccine for BCG-primed mice against *M. tuberculosis* intranasal (i.n) infection in mice model.

Materials and methods

Mice, bacterial strains, and cell lines

Six- to eight-week C57BL/6J male mice were purchased from Animal Center of Air Force Medical University. Recombinant BCG overexpressing DisA (termed as rBCG-DisA) was constructed in our previous work (27). *M. tuberculosis* H37Ra, BCG were grown in Middlebrook 7H9 broth (BD) supplemented with 0.5% (v/v) glycerol, 0.05% Tween 80 and 10% oleic acid albumin-dextrose-catalase (OADC) (BD) at 37°C. rBCG-DisA was grown in complete 7H9 medium with 25μg/mL kanamycin. All mycobacteria were plated on 7H10 agar (BD) supplemented with 10% OADC for colony forming units (CFUs) enumeration. *Staphylococcus aureus* was grown in LB medium at 37°C. Murine macrophage cell line RAW264.7 was used for *in vitro* experiments.

Vaccination and infection of mice

Mice were anesthetized with an intraperitoneal injection of 50mg/kg pentobarbital sodium. Then, mice were vaccinated with 1×10^6 CFU single bacterial suspension of BCG or rBCG-DisA in 200μL PBS at the base of the tail by i.v route, respectively (33). After 12 weeks, all vaccinated mice were challenged with 2×10^5 CFU *M. tuberculosis* H37Ra in 50μL PBS by i.n route. Normal mice (Naïve) and *M. tuberculosis* H37Ra infected mice without vaccination (UN) were used as control. At 12 weeks post vaccination and 6 weeks post infection, mice were euthanatized for immunological assays, histopathological analysis and CFUs measurements.

Antigen-specific antibody detection by ELISA

Sera from all mice were collected at indicated time points after vaccination or infection respectively. Enzyme linked immunosorbent assay (ELISA) microplates were coated with BCG or DisA antigen at 10μg/mL. Sera were diluted with PBS at indicated dilutions. Antigen-specific IgG level was measured by ELISA. The absorbance was detected at 450 nm by microplate reader (BioTek).

Splenocytes preparation, stimulation, and detection of proliferation *in vitro*

Spleen single cell suspensions were prepared and 1×10^6 splenocytes were seeded and stimulated by BCG proteins (25μg/mL) for 72h. Cell proliferation was determined by CFSE (Sigma) reagent according to previous study (27, 35). For cytokines measurement, 1×10^6 cells were seeded in 96-well microplates stimulated with BCG proteins (25μg/mL), *M. tuberculosis* proteins (25μg/mL), *S. aureus* proteins (25μg/mL), *E. coli* O111: B4 lipopolysaccharide (LPS) (100ng/mL) (InvivoGen) for 72h, respectively. Cells were incubated at 37°C with 5% CO_2 and supernatants were collected for cytokines assays.

Determination of cytokines production by ELISA

Cytokines measurement in the cell supernatants was performed using commercial ELISA kits. Cytokines detection of IFN-γ, IL-2, IL-10, IL-17, TNF-α, IL-1β, IL-6 (from Thermo Fisher), CXCL9, CXCL10 and CXCL11 (CLOUD-CLONE CORP, China) were performed according to the instructions. Cell supernatants and diluted standards were added 100μL/well, then incubated at room temperature for 2h. Finally, ELISA plates were monitored at 450 nm using a microplate reader (BioTek).

Flow cytometry

Splenocytes were washed with PBS containing 2.5% FBS. Cells were resuspended in 100μL Staining Buffer (BioLegend) containing TruStain Fc PLUS (anti-mouse CD16/32) (BioLegend) and incubated for 10min on ice. Cells were stained with fluorochrome-labeled antibodies of CD3 (17A2), CD4 (RM4-5), CD8 (53-6.7), CD19 (6D5), CD49 (DX5), CD11b (M1/70), Ly-6G (1A8) (BioLegend) for 30min at 4°C, then washed with PBS containing 2.5% FBS twice. Finally, cells were resuspended in 500μL Staining Buffer for flow cytometry analysis (BD FACSCanto). The frequency of specific cell subpopulation was analyzed using FlowJo V10 (Tree Star Inc.).

Generation of BMDMs

After 4 weeks of vaccination, bone marrow from both femurs and tibiae was harvested in RPMI 1640. Cells were subsequently resuspended in RPMI 1640 supplemented with 10% FBS, 100U/mL penicillin, 100mg/mL streptomycin and 100ng/mL M-CSF (PeproTech). Cells were seeded in Petri dishes (100 mm). After 3 days of incubation at 37°C with 5% CO_2, the medium was removed and replaced with fresh medium. Cells were cultured for another 2 days allowing to differentiate into macrophages. On day 5, cells were harvested and resuspended in complete RPMI 1640 medium for *in vitro* assay.

Macrophage infection

RAW264.7 macrophages and BMDMs of 2×10^5 were seeded in 24-well plates supplemented with complete RPMI 1640

without penicillin/streptomycin, and incubated at 37°C with 5% CO_2 overnight. Cells were infected with *M. tuberculosis* attenuated strain H37Ra (MOI = 1), BCG and rBCG-DisA (MOI = 10). Cells were incubated for 4h at 37°C with 5% CO_2. Subsequently, cells were washed with cold sterile PBS for 3 times, and then incubated in complete RPMI 1640 without penicillin/streptomycin. This time point was termed as 0 d post infection (dpi). Intracellular bacteria CFUs from lysed cells by 0.025% SDS were enumerated on plates at day 1, 3 and 5 post infection.

Quantitative RT-PCR

Total RNA of mice tissues and bone marrow (BM) cells was extracted using the RNeasy kit (Omega Bio-Tek) following the manufacturer's instruction, and quantified by microplate reader (BioTek). Next, elimination of genomic DNA and cDNA synthesis of 500 ng RNA were performed by HiScript Reverse Transcriptase Kit (Vazyme). Quantitative RT-PCR assay was performed using SYBR qPCR Master Mix (Vazyme). Fold changes of mRNA expression of indicated genes was calculated according to $2^{-\Delta\Delta Ct}$, gene of *gapdh* was used as expression normalization. Primers used in this study were synthesized by Tsingke Biological Technology and listed in Table S1.

Histopathology and immunohistochemistry

For histopathology, upper lobes of left lungs and 1/3 of spleen tissue in infected mice was fixed in 10% buffered formalin. The tissue was dehydrated and embedded in paraffin wax. Sections (5μm) were cut and transferred onto glass slides. Hematoxylin/eosin (H&E) staining for pathohistological analysis was performed by the Department of Histopathology (Air Force Medical University, China), and results were quantified by Image J software.

The counts of CD4 and CD8 T cells and expression levels of H3 mono-, or tri-methylated at lysine 4 (H3K4me1, or H3K4me3) and H3K27 acetylation (H3K27ac) in the lung were determined by immunohistochemistry (IHC). Antibodies used in IHC assays were rabbit mAb anti-CD4 (D7D2Z) (CST), rabbit mAb CD8α (D4W2Z) (CST), rabbit mAb anti-Histone H3 (mono methyl K4) (Abcam), rabbit mAb anti-Histone H3 (acetyl K27) (Abcam), rabbit mAb anti-Histone H3 (tri methyl K4) (Abcam). Secondary antibody used was HRP-conjugated anti-rabbit antibody (Jackson Immunoresearch Laboratories). IHC assay was performed by Chengdu Lilai Biotechnology Company (Chengdu, China). IHC images were quantitatively analyzed with Image J software.

Sera collection and extraction for metabolomics analysis

Whole blood samples from C57BL/6J mice were drawn at 6 weeks post *M. tuberculosis* infection. Sera were separated by centrifugation at 3 000 rpm for 5min after blood samples were incubated at 37°C for 30min. For LC-MS/MS analysis, 100μL serum was thoroughly mixed with 100μL pre-cooled water and 400μL cold methanol acetonitrile (v/v, 1:1) through vortex. Then, the mixture was processed with sonication for 1h on ice, and incubated at -20°C for 1h. The mixture was centrifuged at 4°C for 20min with 14 000g. The supernatants were harvested and dried under vacuum. 100 μL acetonitrile water solution (v/v, 1:1) was added to redissolve the samples, then centrifuged at 16 000g at 4°C for 20min. The supernatant was harvested for further analysis. Extraction of samples was performed by Bioprofile (Shanghai, China).

Liquid chromatography tandem mass spectrometry (LC-MS/MS) based untargeted metabolomics analysis

For hydrophilic interaction liquid chromatography (HILIC) separation, samples were analyzed using a 2.1mm×100mm ACQUIY UPLC BEH Amide 1.7μm column (Waters, Ireland) by SHIMADZU-LC30 ultra-high performance liquid chromatography system (UHPLC, Shimadzu). Both electro-spray ionization (ESI) positive mode and negative mode were applied for MS data acquisition by QE Plus mass spectrometer (Thermo Fisher). The raw MS data were processed using MS-DIAL for peak alignment, retention time correction and peak area extraction. The metabolites were identified by accuracy mass (mass tolerance <0.01Da) and MS/MS data (mass tolerance <0.02Da) which were matched with Human Metabolome Database (HMDB) and Massbank databases. For the extracted data, ion peaks with the missing values >50% were deleted from the group. The total peak areas of positive and negative ion data were normalized, positive and negative ion peaks were integrated, and R software was used for pattern recognition. After the data were pretreated by Unit variance Scaling, subsequent data analysis was performed. LC-MS/MS based untargeted metabolomics analysis and data analysis were performed by Bioprofile (Shanghai, China).

CFU enumeration and genotypic identification of bacilli by PCR

Lungs and spleens of mice were aseptically removed and homogenized through a 40μm cell strainer in 4mL RPIM 1640 medium. Then the tissue homogenates were serially diluted and plated on 10% OADC supplemented 7H10 agar plates

containing polymyxin B sulfate (80μg/mL) and azlocillin sodium (5μg/mL) to avoid other bacterial contamination. Bacterial colonies were counted following 3-4 weeks of incubation at 37°C. The number of single colony of bacilli was recorded, and CFUs data are represented as Log_{10}CFU. In order to distinguish *M. tuberculosis* H37Ra and BCG/rBCG-DisA, colonies on the plate were amplified by PCR with *ag85b* (present in both BCG and H37Ra) and *cfp10-esat-6* operon (only present in H37Ra) fragments (Table S1).

Strategy of prime-boost and *M. tuberculosis* challenge

Female BALB/c mice were vaccinated with 1×10^7 CFU of BCG by s.c route. At 58-week after vaccination, mice received a second boosting vaccination with the same dose and route of rBCG-DisA. Six weeks post boost, mice were challenged with 1×10^5 CFU of *M. tuberculosis* H37Ra by i.n route. After infection, mice body weights were monitored weekly and survivals were recorded.

Statistical analysis

Results were represented as mean values ± SEM. Statistical analysis of data performed by Graphpad Prism 9.0 Software (Graphpad Software, USA). Statistical significances were determined by two-tailed Student's *t* test or for multiple comparisons by one-way ANOVA. For analysis of survival curves, we used log-rank test. The results were significant when $^*P < 0.05$, $^{**}P < 0.01$, $^{***}P < 0.001$, $^{****}P < 0.0001$ as given in the figure legends unless otherwise specified.

Results

rBCG-DisA elicited greater proinflammatory cytokine responses to homologous and heterologous re-stimulations than BCG

Following exposure to infectious agents or vaccines, trained immunity can mount a faster and greater response against secondary challenge with homologous or even heterologous pathogens (8). Proinflammatory cytokines and chemokines have been reported as primary indicators of trained immunity, mainly including TNF-α, IL-1β, IL-6, CXCL9, CXCL10 and CXCL11 (36, 37). Both *in vitro* and *in vivo* experiments have shown that BCG immunization could induce increased extensive cytokine responses of IL-1β, TNF-α and IL-6 after training with BCG (33, 36, 38). It has been demonstrated that rBCG-DisA could elicit greater proinflammatory cytokines including IFN-β, IL-1β, IL-6 and TNF-α than that of BCG in primary human and murine macrophages (31, 32). In this study, splenocytes of immunized mice were re-stimulated with BCG, *M. tuberculosis*, *S. aureus* and *E. coli* LPS respectively (Figure 1A). BCG immunization by i.v route induced more IL-1β, IL-6, TNF-α, CXCL9 and CXCL11 releases to homologous stimulus re-stimulation in splenocytes of mice (Figure 1B). Our previous study found that rBCG-DisA immunization by s.c route only induced elevated IL-6 production in splenocytes of mice (27). Here, rBCG-DisA immunization induced elevated proinflammatory cytokines and chemokines of IL-1β, IL-6, TNF-α, CXCL9 and CXCL11 releases than that of BCG in splenocytes of mice responding to homologous antigens, and CXCL10 was under the limit of detection (Figure 1B).

Besides, BCG immunization increased the heterologous IFN-γ production and induced long lasting heterologous IL-17 responses in mice (39). Previously, we showed that splenocytes of rBCG-DisA s.c immunized mice produced Th1/Th2 cytokines of IFN-γ, IL-2 and IL-10 as that of BCG to homologous proteins (27). In this study, BCG immunization by i.v route induced slightly elevated IFN-γ and IL-10 production, while rBCG-DisA i.v immunization induced elevated IL-2 and IL-10 production to homologous proteins in splenocytes of mice (Figure 1B). It was found that BCG and rBCG-DisA did not induce IL-17 production to homologous proteins in splenocytes of mice after 4 weeks of immunization by i.v route (Figure 1B). rBCG-DisA immunization induced comparable levels of IFN-γ and IL-17 secretion after re-stimulated by homologous stimulus as that of BCG, but higher levels of IL-2 and IL-10 than that of BCG (Figure 1B).

It was proved that BCG trained innate immune cells showed specific responses according to different stimuli (37). Then splenocytes of immunized mice were re-stimulated with *M. tuberculosis*, *S. aureus*, and *E.coli* LPS respectively (Figure 1A). BCG immunization induced an enhanced IL-1β release to LPS, but not to *M. tuberculosis* and *S. aureus* (Figure 1C). rBCG-DisA immunization caused elevated releases of TNF-α to three bacterial components than that of BCG immunized mice, and IL-6 to *M. tuberculosis* and *S. aureus* (Figure 1C). Splenocytes from BCG and rBCG-DisA immunized mice produced significant chemokines of CXCL9 and CXCL11 responded to *M. tuberculosis* re-stimulation (Figure 1C). These data suggested that rBCG-DisA with c-di-AMP as endogenous adjuvant elicited enhanced proinflammatory cytokine responses in mice to homologous and heterologous stimuli.

Further, intracellular survival of BCG and rBCG-DisA in RAW264.7 macrophages were counted on plates. rBCG-DisA showed a slight decline on survival within 3 days, and increased at 5 days after infection, but no differences were found between two strains (Figure 1D). It was reported that a similar rBCG-DisA increased the levels of phagocytosis and autophagic processing within macrophages than BCG (32). After 4 weeks of immunization by i.v route, rBCG-DisA loads decreased in

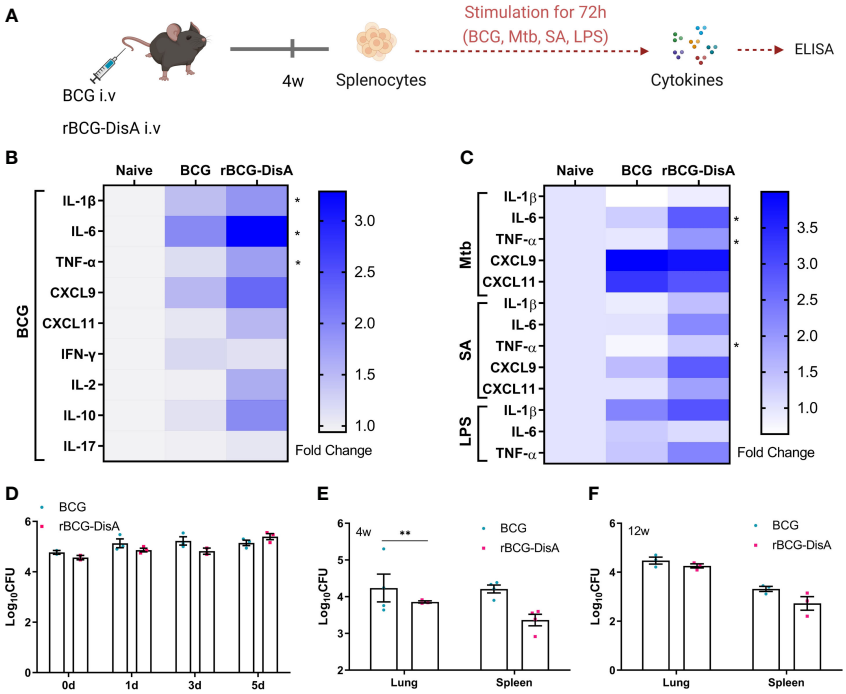

FIGURE 1
Inflammatory cytokine levels of rBCG-DisA i.v vaccinated mice and intracellular survival of rBCG-DisA in macrophages and mice. **(A)** Schematic diagram of homologous or heterologous stimulation of splenocytes *in vitro* (created with BioRender.com). After 4 weeks of BCG and rBCG-DisA i.v vaccination, splenocytes were isolated and re-stimulated with BCG protein extracts (BCG) (25μg/mL), *M. tuberculosis* (Mtb) (25μg/mL), *S. aureus* (SA) (25μg/mL), and *E. coli* O111:B4 LPS (LPS) (100ng/mL) for 72h *in vitro*. Normal mice (Naïve) were used as control. Supernatants were collected to measure cytokine secretion level by ELISA. **(B, C)** Cytokines and chemokines production of IL-1β, IL-6, TNF-α, CXCL9, CXCL11, IFN-γ, IL-2, IL-10 and IL-17 in supernatants were determined after re-stimulations by ELISA. The results are expressed as relative folds of each cytokine concentration (ng/mL) compared to the Naïve group (n=3). **(D)** Intracellular survival of BCG and rBCG-DisA in RAW264.7 macrophages at 0, 1, 3, and 5 days post infection (MOI=10). **(E, F)** The number of bacilli in the lung and spleen of mice was measured after 4 **(E)** and 12 **(F)** weeks of i.v immunization, respectively (n=3). (Panels **B, C**, $^{*}P < 0.05$ stands for rBCG-DisA v.s BCG group. Panel **E**, $^{**}P < 0.01$.).

organs, especially in the lung of mice, but showed no difference compared with that of BCG in the lung and a slight decrease in the spleen after 12 weeks (Figures 1E, F). A latest study demonstrated that the similar rBCG-DisA based on another strain of Tice BCG proliferated to a lower degree in the lung of mice through aerosol inhalation (32). These results implied that enhanced cytokine responses of rBCG-DisA were not caused by different persistence of bacteria in host.

rBCG-DisA immunization triggered similar cytokine responses in the spleen of mice with BCG did after *M. tuberculosis* challenge

After 12 weeks of i.v immunization, mice were re-stimulated with *M. tuberculosis* H37Ra infection by i.n route (Figure S1A). At 6 weeks post *M. tuberculosis* challenge, spleen tissues were separated for detecting the transcription levels of cytokines and chemokines. As showed in Figure 2A, rBCG-DisA immunization induced similar transcription levels of almost all of proinflammatory cytokines and chemokines than un-immunized and BCG in the spleen after *M. tuberculosis* infection. Significant CXCL15 (IL-8) was reported before (36, 37, 40), which was not obvious in splenocytes of rBCG-DisA group. rBCG-DisA immunized mice showed an increasing trend on the transcription levels of IFN-γ, IL-2 and IL-10 in the spleen after *M. tuberculosis* infection, though no significant differences compared with that of UN and BCG immunized mice (Figure 2A). We speculated that splenocytes may not fully stimulated by i.n *M. tuberculosis in vivo* compared with proteins doses used *in vitro*. Further, we stimulated splenocytes from *M. tuberculosis* infected mice with homologous and heterologous stimuli. We found that rBCG-DisA immunization induced higher IL-6, IFN-γ and IL-10 secretions than BCG to homologous but not heterologous stimuli after *M. tuberculosis* infection (Figures 2B–E; S1B–E). We also showed that splenocytes from rBCG-DisA immunized mice and *M. tuberculosis* infected mice did not induce IL-1β to LPS stimulation, as UN and BCG groups did (Figure 2D).

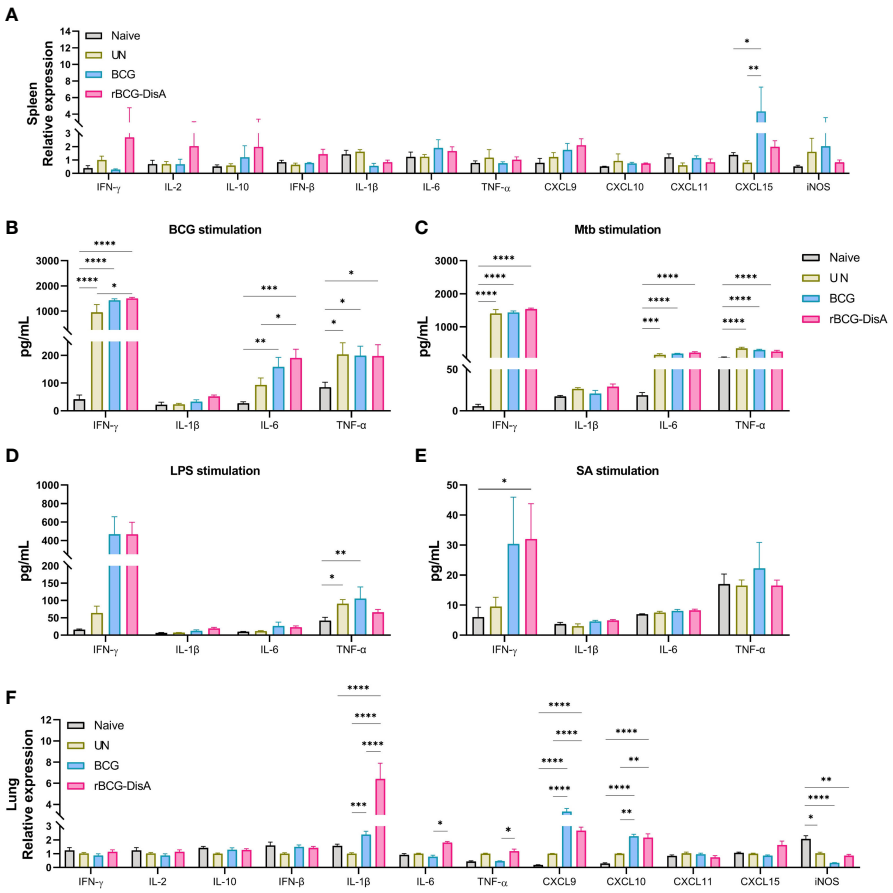

FIGURE 2
Inflammatory cytokines expression in the spleen and lung of vaccinated mice after *M. tuberculosis* infection. Mice were vaccinated by i.v BCG and rBCG-DisA for 12 weeks. Then, mice were infected with *M. tuberculosis* by i.n route, normal mice (Naïve) and *M. tuberculosis* infected mice without immunization (UN) were used as control. **(A)** At 6 weeks post infection, transcription level of indicated genes in the spleen of mice was assayed by quantitative RT-PCR (n=3). **(B–E)** At 6 weeks post infection, splenocytes were isolated and re-stimulated with BCG protein extracts (BCG) (25μg/mL) **(B)**, *M. tuberculosis* (Mtb) (25μg/mL) **(C)**, *E. coli* O111:B4 LPS (LPS) (100ng/mL) **(D)**, and *S. aureus* (SA) (25μg/mL) **(E)** for 72h *in vitro*. Cytokines production of IFN-γ, IL-1β, IL-6 and TNF-α in supernatants were determined by ELISA (n=4). **(F)** At 6 weeks post infection, transcription level of indicated genes in the lung of mice was assayed by quantitative RT-PCR (n=3). (*P < 0.05, **P < 0.01, ***P < 0.001,****P < 0.0001.).

rBCG-DisA elicited greater inflammatory cytokines in the lung of mice after *M. tuberculosis* intranasal challenge

In this study, mice were immunized and then re-stimulated with *M. tuberculosis* infection by i.n route (Figure S1A). Lung tissues were also separated for detecting the transcription levels of cytokines and chemokines. rBCG-DisA i.v immunization significantly up-regulated proinflammatory cytokines of IL-1β, IL-6, and TNF-α in the lung than BCG i.v immunization after 6 weeks of *M. tuberculosis* challenge (Figure 2F). For chemokines, BCG and rBCG-DisA immunization promoted a similar increasing of CXCL9 and CXCL10, and rBCG-DisA immunization induced a slight increasing trend of CXCL15 expression in the lung after *M. tuberculosis* infection (Figure 2F). However, the results showed that the transcription levels of IFN-γ, IL-2 and IL-10 in the lung were no changes after *M. tuberculosis* infection in the lung of all groups (Figure 2F). These data suggested that rBCG-DisA immunization induced higher level of trained immunity in the lung, and were in line with such recombinant BCG that could trigger proinflammatory cytokine responses *in vitro* of BMDMs and macrophage cell line (31, 32).

rBCG-DisA enhanced epigenetic changes than BCG in mice after *M. tuberculosis* challenge

More data showed BCG is an inducer of trained immunity through increased transcription of proinflammatory cytokine and chemokine genes by epigenetic modifications (33, 41). It has

been proved that epigenetic signatures of H3K4me3 and H3K27ac would decrease gradually with BCG inoculation time, and H3K4me1 persisted for long time to form immune memory (42, 43). Previously, we had identified that rBCG-DisA immunization by s.c route induced an enhanced H3K4me3 in the lung of mice after 4 weeks of *M. tuberculosis* infection (27). In this study, mice were immunized by i.v route for 12 weeks and challenged with *M. tuberculosis* (Figure S1A). Above, we had already established that rBCG-DisA acted as a more potent inducer of TNF-α and IL-6 production than BCG after re-stimulations *in vitro* (Figures 1B, C) and in the lung of mice (Figure 2F). Further, we detected epigenetic signatures of BCG-induced trained immunity including H3K4me3, H3K4me1 and H3K27ac by IHC in the lung of *M. tuberculosis* infected mice. It was shown that rBCG-DisA immunization by i.v route could obviously elicit enhanced epigenetic changes of H3K4me1 and H3K4me3, and a mild increasing in H3K27ac (Figure 3A), which suggested that rBCG-DisA elicited extended epigenetic changes compared with BCG, especially H3K4me1 for long time of immune memory.

rBCG-DisA caused lncRNA expression changes in BM cells as well as in the lung of mice after *M. tuberculosis* challenge as BCG

It has been reported that i.v BCG could access bone marrow to expand hematopoietic stem cells (HSCs) and promotes myelopoiesis, and educated HSCs to generate trained monocytes/macrophages (33). To further characterize the trained immunity-inducing potential of rBCG-DisA versus BCG, we investigated the cytokine and chemokine expressions of BM cells from mice after 8 weeks i.v immunization. It was found that enhanced IL-6 expression was induced in BM cells of rBCG-DisA immunized mice compared with Naïve and BCG (Figure 3B). Whereas, rBCG-DisA immunization did not trained BM cells to express more IL-1β and CXCL9 as BCG did (Figure 3B). There were no significant differences in expressions of other cytokines and chemokines including IFN-γ, IFN-β, CXCL10, CXCL11, CXCL15 and iNOS (Figure S2). These results suggested BCG and rBCG-DisA immunization elicited different trained immune responses in central immune organ in mice.

Long noncoding RNAs (lncRNAs) are increasingly appreciated as regulators of cell-specific gene expression, which may involve in regulation of trained immunity. It has been identified that a lncRNA, named as stream master lncRNA of the inflammatory chemokine locus (UMLILO), could be brought proximal to immune genes (CXCL1, CXCL2, CXCL3, and CXCL15) prior to their activation and involve in innate immune defense (44). Since UMLILO is absent in mice, we detected some candidates lncRNAs that mediates expressions of immune response genes. It was found that lncRNA cyclooxygenase-2 (cox-2) (lincRNA-Cox2) was significantly increased in patients and macrophages with *M. tuberculosis* H37Ra infection (45). Both BCG and rBCG-DisA just induced a slight increase of lincRNA-Cox2 expression in BM cells from immunized mice (Figure 3C). After *M. tuberculosis* challenge, lincRNA-Cox2 expression level in the lung decreased, while the expression level in the spleen remained unchanged (Figures 3D, E).

It was reported that lncRNA NEAT1 (nuclear paraspeckle assembly transcript 1) was highly expressed in PBMCs and granulomatous tissue from TB patients, as well as in *M. tuberculosis* infected macrophages, and declined gradually with treatment (46). LncRNA NEAT1 appears in two isoforms of NEAT1-1 (short isoform) and NEAT1-2 (long isoform). We found that both BCG and rBCG-DisA seemed to inhibit NEAT1 expression in BM cells of immunized mice (Figure 3C). NEAT1 expression levels were elevated in the lung of BCG and rBCG-DisA immunized mice after *M. tuberculosis* infection (Figure 3D). Noticeably, rBCG-DisA immunization induced significant NEAT1 expression in the lung and spleen compared with that of BCG (Figures 3D, E). And there were no differences of NEAT1-2 expression levels between mice with BCG and rBCG-DisA immunizations (Figures 3D, E).

LncRNA NeST (Tmevpg1, abbreviates Nettoie Salmonella pas Theiler's) is located in the nucleus, which is an enhancer lncRNA. In activated $CD8^+$ T cells, NeST could recruit mixed lineage leukemia protein (MLL) and transactivate IFN-γ by binding to the adaptor protein WD repeat-containing protein 5 (WDR5) (47). It was observed that rBCG-DisA immunization elicited significant NeST transcription in BM cells of mice than that of BCG (Figure 3C). Similar increases were observed in the lung and spleen of rBCG-DisA i.v mice post *M. tuberculosis* infection (Figures 3D, E).

LncRNA NRON (noncoding repressor of nuclear factor of activates T cells $^{[NFAT]}$) is highly expressed in resting $CD4^+$ T lymphocytes, which potently suppresses the latent HIV-1 transcription (48). Our data revealed that both BCG and rBCG-DisA i.v vaccination repressed the expression of NRON in BM cells (Figure 3C). After *M. tuberculosis* infection, rBCG-DisA increased the level of NRON than BCG in the spleen but not in the lung (Figures 3D, E).

rBCG-DisA vaccination leads to an altered metabolic profile after *M. tuberculosis* challenge

Metabolic rewiring is the major signature of BCG-induced trained immunity. We collected sera at 8 weeks post infection for untargeted metabolomics analysis based on LC-MS (Figure 4A). To reveal the changes of metabolites in BCG or rBCG-DisA immunized mice, supervised multivariate orthogonal partial

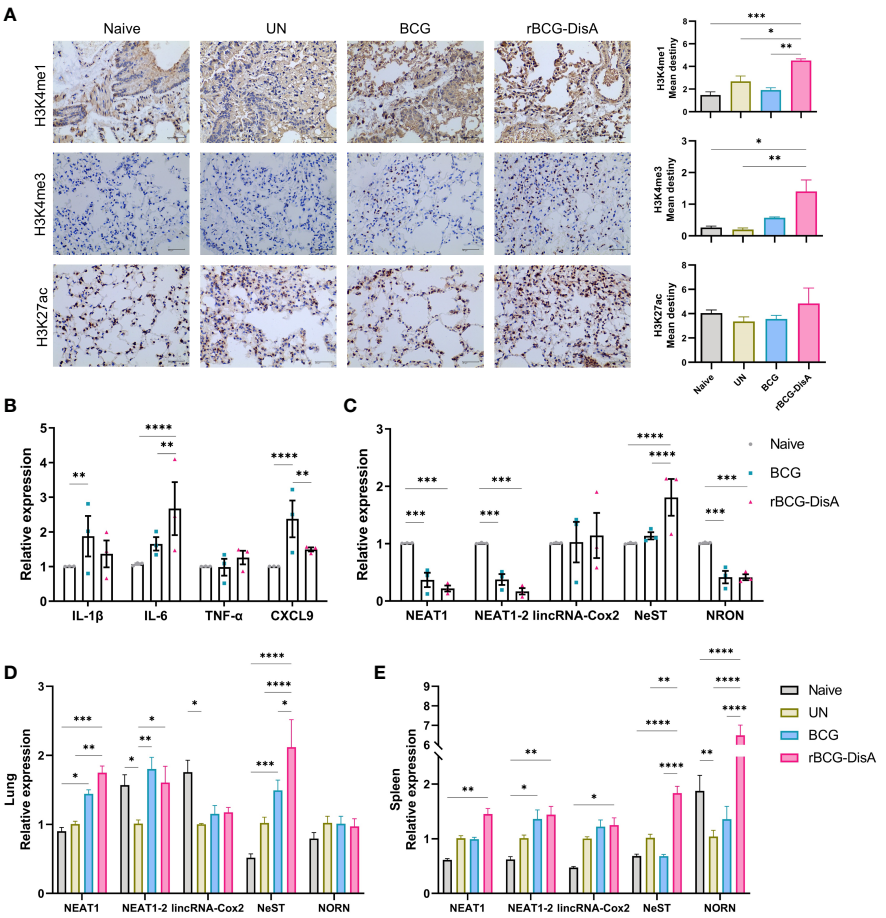

FIGURE 3
Expression of lncRNA and histone modifications in BM cells, lung and spleen of mice. Mice were vaccinated by i.v BCG and rBCG-DisA for 8 weeks (for BM cells isolation) and 12 weeks (for infection). Then, mice were infected with *M. tuberculosis* by i.n route, normal mice (Naïve) and *M. tuberculosis* infected mice without immunization (UN) were used as control. **(A)** At 6 weeks post infection, immunohistochemical analysis of H3K4me1, H3K4me3, and H3K27ac expression in the lung tissue (left). Quantitative analysis of H3K4me1, H3K4me3, and H3K27ac expression by Image J (right) (n=3). **(B, C)** At 8 weeks after BCG and rBCG-DisA i.v immunization, the expression of indicated cytokines **(B)** and non-coding RNA **(C)** in BM cells was detected by quantitative RT-PCR (n=3). **(D, E)** At 6 weeks post infection, immune responses were detected. Levels of indicated noncoding RNA in the lung **(D)** and spleen **(E)** were assayed by quantitative RT-PCR (n=3). (*P < 0.05, **P < 0.01, ***P < 0.001, ****P < 0.0001.).

least squares discriminate analysis (OPLS-DA) models were constructed to discriminate the differentiating variables. The results showed that rBCG-DisA group was obviously separated from the BCG group (Figure 4B), indicating that these two groups had different metabolic profiles in sera. Among these differentially expressed metabolites of rBCG-DisA v.s BCG, first proportion (26.67%) belonged to lipids or lipid-like molecules, and the subsequent proportions were organic acids or organic nitrogen molecules, respectively (Figures 4C, D). Through KEGG analysis, it was found that metabolites were mainly enriched in metabolic pathways such as lipolysis, aldosterone synthesis, protein digestion and absorption, etc. (Figure 4E). As shown in Figure 4F, the level of acetylcarnitine was up-regulated in rBCG-DisA immunized mice after *M. tuberculosis* infection, which helps long-chain fatty acyl-CoA to enter mitochondria, indicating that fatty acid oxidation and energy metabolism were promoted (49). Arachidonic acid, which inhibits fat mobilization, was also down-regulated in rBCG-DisA-immunized mice (Figure 4F). Thus, rBCG-DisA immunization promoted fat mobilization and lipolysis in mice.

rBCG-DisA repressed specific IgG and CD4$^+$ T cells by intravenous immunization

It is concluded that the heterologous protection conferred by BCG is likely the result of two mechanisms that synergize to

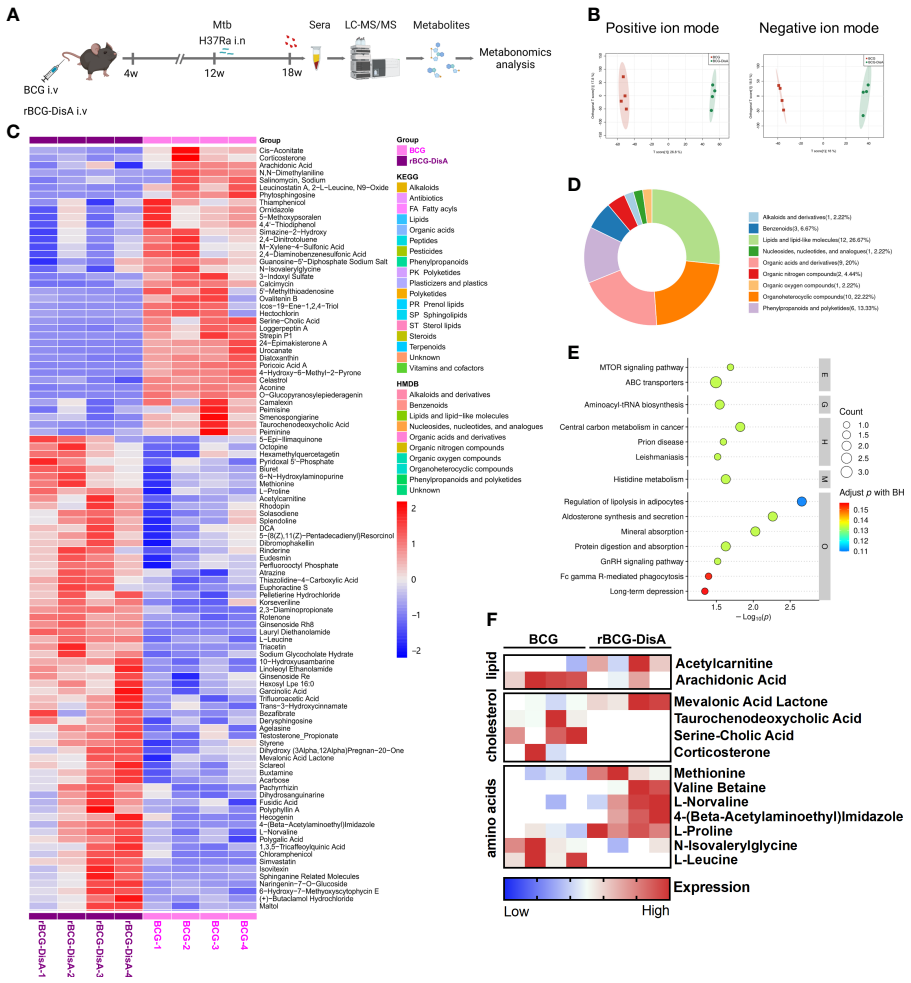

FIGURE 4
Metabonomics analysis of mice vaccinated with BCG or rBCG-DisA after *M. tuberculosis* infection. Mice were vaccinated by BCG and rBCG-DisA for 6 weeks. Then, mice were infected with *M. tuberculosis* by i.n route, normal mice (Naïve) and *M. tuberculosis* infected mice without immunization (UN) were used as control. At 8 weeks post infection, sera were harvested for metabonomics analysis (n=4). **(A)** A scheme diagram of detection on sera of mice vaccine with BCG or rBCG-DisA (created with BioRender.com). **(B)** OPLS-DA score plots of positive and negative ion modes of BCG and rBCG-DisA groups (n=4). **(C)** Heatmap of differential expressed metabolites of rBCG-DisA v.s BCG (n=4). **(D)** Circle diagram of metabolites classification of rBCG-DisA v.s BCG (n=4). **(E)** KEGG pathway enrichment of metabolites of rBCG-DisA v.s BCG (n=4). **(F)** Heatmap of differential expressed metabolites regarding lipid, cholesterol and amino acids metabolism of rBCG-DisA v.s BCG (n=4).

induce protection: heterologous T cell immunity and trained immunity (3, 39). Previously, we found that rBCG-DisA s.c administration induces comparable humoral and cellular immune responses as BCG did in mice (27). We further analyzed the level of adaptive immune response in mice vaccinated with i.v BCG and rBCG-DisA strains. During the whole experiment, mice showed similar general behaviors such as spontaneous behavior, arousal behavior, grooming behavior, fecal traits among Naïve, BCG and rBCG-DisA groups. The body weights of BCG group mice increased steadily comparable to Naïve mice within 12 weeks after vaccination (Figure 5A). rBCG-DisA vaccinated mice showed lower weight gain than control and BCG mice (Figure 5A).

BCG administrated by i.v route induced higher mycobacteria-specific humoral immune response (Figures 5B, C; S3A). Whereas, rBCG-DisA i.v vaccination may repress the increasing of IgG than BCG 4-week and 12-week post vaccination (Figures 5B, C, S3A). BCG vaccination induced long-lasting effects of Th1/Th17 responses, and T-cell subpopulations did not show major shifts in CD4 and CD8 lymphocytes for at least one year in healthy volunteers (39). The proliferation of mice splenocytes were comparable in both two vaccinated groups compared to that of Naïve mice after re-stimulated by mycobacteria antigens by CFSE staining (Figure S3B). We found that rBCG-DisA immunization by s.c route increased the proportion of $CD4^+$ but not $CD8^+$ T cells (27).

Whereas, rBCG-DisA vaccination by i.v route reduced the number and proportion of $CD4^+$ T cells compared to both control and BCG groups (Figure 5D, S3D), and no significant changes on $CD8^+$ T cells (Figure 5D, S3C).

rBCG-DisA vaccination increased the $CD4^+$ and $CD8^+$ T cells after *M. tuberculosis* infection

After 12 weeks of i.v immunization, mice were infected with *M. tuberculosis* H37Ra by i.n route (Figure S1A). Six weeks post *M. tuberculosis* challenge, BCG i.v immunized mice exhibited low mycobacteria-specific IgG as Naïve and *M. tuberculosis* H37Ra i.n infection (UN) mice (Figure 6A). rBCG-DisA vaccination elicited stronger BCG- and DisA-specific IgG than that of BCG (Figures 6A, B). To our surprise, all infected mice showed similar percentages of T cell, B cell, NK cell, macrophage and neutrophil with Naïve mice (Figure S4). Further analysis of T cell subsets found that *M. tuberculosis* H37Ra i.n infection (UN) had negligible effect on proportions of $CD4^+$ T cells, but caused a significant decline of $CD8^+$ T cells in splenocytes (Figure 6C). BCG i.v immunized mice showed a decline of $CD4^+$ T cells compared with UN group, but rBCG-DisA didn't (Figure 6C). Both BCG and rBCG-DisA immunization resisted the reduce of $CD8^+$ T cells caused by *M. tuberculosis* infection, and BCG showed a significant increase compared with UN group (Figure 6C). rBCG-DisA immunization kept the percentage of $CD8^+$ T cells in splenocytes after *M. tuberculosis* infection closed to that of Naïve mice (Figure 6C).

Above results showed that rBCG-DisA i.v vaccinated mice exhibited greater innate immune inflammatory responses in the lung after *M. tuberculosis* infection (Figure 2F). Further, adaptive immune response in the lung was observed through the distribution of $CD4^+$ and $CD8^+$ T cells in the lung by IHC after *M. tuberculosis* infection by i.n route. As illustrated in Figure 6D, BCG i.v immunization caused similar T cells distribution after *M. tuberculosis* infection with UN group. More importantly, it was clearly showed that increased of $CD4^+$ and $CD8^+$ T cells in the lung of rBCG-DisA immunized mice after *M. tuberculosis* i.n infection (Figure 6D) implying significant T cell infiltration against infection.

rBCG-DisA caused similar pathological changes as BCG after *M. tuberculosis* intranasal challenge

Since trained immunity confers broad immunological protection, it was worried that enhanced immune response of reprogrammed innate immune cells might result in the development or persistence of chronic metabolic, autoimmune or neuro-inflammatory disorders (50). rBCG-DisA induced stronger innate and adaptive immune responses, and did not cause excessive immunopathological damages by s.c inoculating

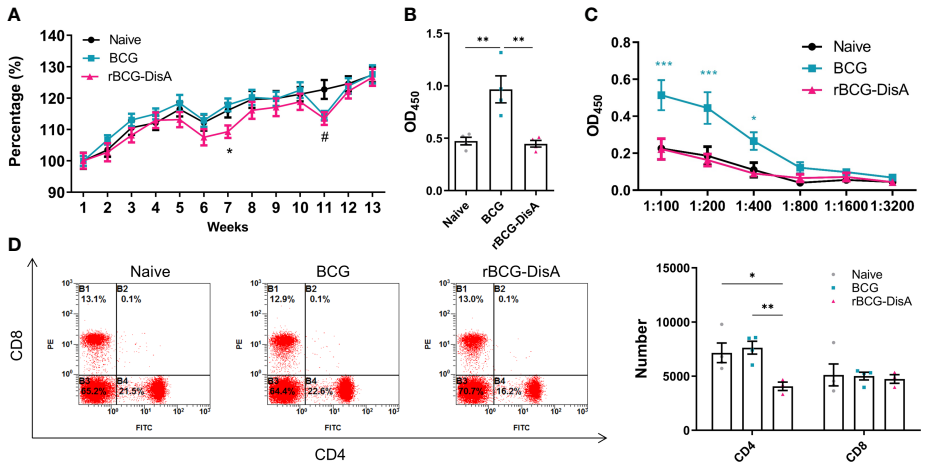

FIGURE 5
Adaptive immune response induced by rBCG-DisA vaccination. Male C57BL/6J mice were vaccinated with $1x10^6$ CFU BCG and rBCG-DisA by i.v route. At 4- and 12-week post vaccination, immune responses were determined. Normal mice (Naïve) were used as control. **(A)** Dynamic monitoring of mice body weights at each week after immunization. Data were presented as a percentage of body weight to initial body weight (n=3). **(B)** After 4 weeks of i.v immunization, BCG-specific IgG levels in mice sera (1:200) were assayed by ELISA (n=4). **(C)** After 12 weeks of i.v immunization, BCG-specific IgG titers in sera of mice at indicated dilutions were assayed by ELISA (n=4). **(D)** After 4 weeks of i.v immunization, CD4 and CD8 T cells in splenocytes were analyzed by flow cytometry of immunized mice (left). Numbers of CD4 and CD8 T cells in splenocytes were measured by flow cytometry (n=4) (right). (Panel **A**, $^*P < 0.05$ stands for rBCG-DisA v.s BCG, $^{\#}P < 0.05$ stands for rBCG-DisA v.s Naïve. Panel **C**, $^*P < 0.05$ and $^{***}P < 0.001$ stand for rBCG-DisA v.s BCG/Naïve. Panel **D**, $^*P < 0.05$, $^{**}P < 0.01$.).

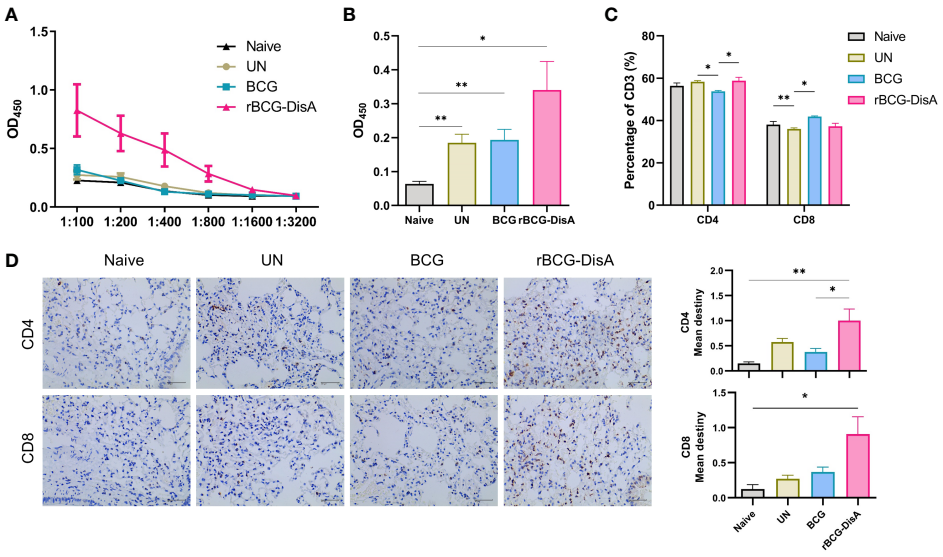

FIGURE 6
Analysis of specific antibodies and T cells in the spleen and lung of vaccinated mice after *M. tuberculosis* infection. Mice were vaccinated by i.v BCG and rBCG-DisA for 12 weeks. Then, mice were infected with *M. tuberculosis* by i.n route, normal mice (Naive) and *M. tuberculosis* infected mice without immunization (UN) were used as control. **(A)** At 6 weeks post infection, BCG-specific IgG titers in sera were determined by ELISA at indicated dilutions (n=4). **(B)** At 6 weeks post infection, DisA-specific IgG levels in sera was determined by ELISA at dilution of 1:200 (n=4). **(C)** At 6 weeks post infection, proportions of CD4 and CD8 T cells in splenocytes were assayed by flow cytometry (n=4). **(D)** At 6 weeks post infection, immunohistochemical analysis of CD4 and CD8 T cells in the lung of mice (left). Quantitative analysis of CD4 and CD8 T cells by Image J (right) (n=3). (*P < 0.05, **P < 0.01.).

in mice or intradermally route in guinea pig model (27, 31). Recently, the latest research demonstrates that a similar rBCG-DisA with different BCG strain was less pathogenic in immunocompromised SCID mice (32). As shown in Figure 7A, we did not observe the characteristics of tuberculosis such as tubercle and caseous necrosis in both lung and spleen tissues of infected mice. In the lung, *M. tuberculosis* infected mice exhibited obviously inflammatory cells infiltration (Figure 7A). In the lung of BCG and rBCG-DisA immunized mice, the alveolar structures were intact basically, accompanied with occasional thickening of alveolar mesenchyme, inflammatory cell infiltration, erythrocyte and histological fluid exudation (Figure 7A). Additionally, spleen of two immunized groups showed inflammatory cell infiltration as un-immunized mice after *M. tuberculosis* infection (Figure 7A). Overall, the inflammatory manifestations in the lung were comparable between rBCG-DisA and BCG vaccinated mice after *M. tuberculosis* challenge.

rBCG-DisA provided similar protection against *M. tuberculosis* intranasal infection and persisted longer in the lung than BCG

After 12 weeks of immunization by i.v route, mice were infected with *M. tuberculosis* H37Ra infection by i.n route (Figure S1A). Six weeks post *M. tuberculosis* H37Ra i.n infection, the number of bacilli in the spleen and lung of mice was enumerated on plates. Considering that bacilli colonies could be *M. tuberculosis*, BCG or rBCG-DisA, we randomly selected numbers of bacterial clones for identification with specific primers (Table S1). The results showed that *M. tuberculosis* H37Ra were not identified under our detection method in the spleen and lung of BCG and rBCG-DisA immunized mice (Figure 7B). While, genotype identification of bacillus showed that the clones in two immunized groups were BCG or rBCG-DisA strains (Figure 7C). Further, we found BCG below the limit of detection in the lung after *M. tuberculosis* infection, but only two of eight mice showed non-sterilized of rBCG-DisA (Figure 7C). While the distribution of BCG and rBCG-DisA were similar in the spleen after H37Ra challenge (Figure 7C). These results suggested that rBCG-DisA immunization by i.v route could provide long-term protection than BCG after *M. tuberculosis* infection, which may be resulted from longtime survival of rBCG-DisA in the lung.

rBCG-DisA boosting prolonged the lifespan of BCG-primed mice against *M. tuberculosis* intranasal infection

BCG-induced trained immunity gradually declines over time and vaccination protection declines with time, so a booster vaccine may be given in adolescence or adults when the effects

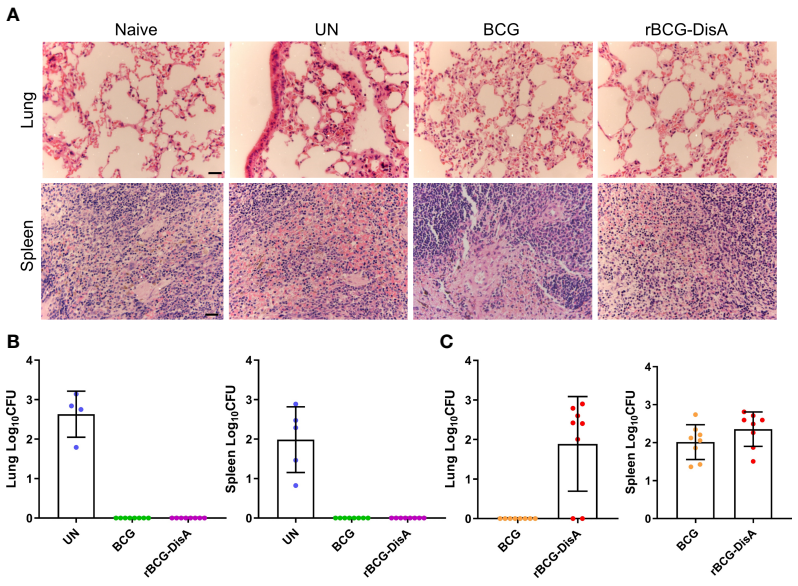

FIGURE 7
Histopathological changes and bacilli number of mice after *M. tuberculosis* infection. Mice were vaccinated by i.v BCG and rBCG-DisA for 12 weeks. Then, mice were infected with *M. tuberculosis* by i.n route, normal mice (Naïve) and *M. tuberculosis* infected mice without immunization (UN) were used as control. **(A)** At 6 weeks post infection, representative images of H&E-stained lung tissue sections at ×40 magnification (scale bar=100 μm). **(B, C)** At 6 weeks post infection, bacilli burdens in the lung and spleen were incubated at 37°C for 3-4 weeks (*n*=4~8). The colonies on the plates were determined according to the time of colony formation, morphology and genotype verification to determine whether the clone was *M. tuberculosis* [*ag85B* (+), *cfp10-esat-6* (+)] **(B)** or BCG/rBCG-DisA [*ag85B* (+), *cfp10-esat-6* (-)] **(C)**.

of BCG may start to wane (11, 12). In this study, BALB/c mice were primed by s.c BCG for 58 weeks, then mice were boosted with rBCG-DisA at the same route (Figure 8A). After 6 weeks, mice were challenged by *M. tuberculosis* H37Ra i.n infection (Figure 8A). rBCG-DisA boosted mice showed a weight maintenance within 9 weeks infection, compared with weight loss in BCG-primed with or without *M. tuberculosis* infected mice (Figure 8B). We observed a significant longevity in rBCG-DisA boosted mice compared to only BCG primed mice after *M. tuberculosis* i.n challenge (Figure 8B). BCG primed mice all died within 14 weeks after *M. tuberculosis* infection, and all non-infected mice died within 87 weeks (Figure 8C). Surprisingly, until now 66% of rBCG-DisA boosted mice were alive over 90 weeks (Figure 8C). Thus, rBCG-DisA may be used as a candidate vaccine for BCG prime-boost regimens against *M. tuberculosis* infection in adults.

Discussion

In the previous study, we found that rBCG-DisA by s.c route induced stronger immune responses compared with BCG in mice, which suggested an enhanced trained immunity was induced in mice (27). It has been proved that BCG accesses to BM and educate HSCs to generate epigenetically modified macrophages, and provide protective innate immunity against *M. tuberculosis* through trained immunity (33). In this study, we provided *in vivo* experimental evidence that rBCG-DisA with c-di-AMP as endogenous adjuvant could induce enhanced trained immunity and concomitant activated adaptive immune response, which showed a significant protection against *M. tuberculosis* infection in prime-boost strategy in adult mice.

Trained monocytes and macrophages display functional and epigenetic reprogramming, leading to increased production of cytokines and chemokines, which are viewed as primary indicators of trained immunity (37), and improved phagocytosis and killing capacity (51, 52). c-di-AMP has been identified to be a potent inducer of several proinflammatory cytokines and chemokines such as IL-1β, IL-6, and TNF-α in macrophages (27, 31, 32, 53). These proinflammatory cytokines are also considered as mediators of trained immunity (8, 9, 54, 55). It has been reported that rBCG-DisA could elicit greater proinflammatory cytokines than that of BCG in primary human and murine macrophages (27, 31, 32). Our data showed that BCG and rBCG-DisA elicited proinflammatory cytokines and chemokines transcriptions with different models in splenocytes of immunized mice, according to homologous or heterologous stimuli (Figures 1B, C). Remarkably, rBCG-DisA immunization induced enhanced proinflammatory cytokines, chemokines and Th1/Th2 cytokines transcriptions to re-stimulations *in vitro* than BCG in splenocytes of immunized mice (Figure 1B), and significant proinflammatory cytokines transcriptions in the lung to re-stimulation of *M. tuberculosis* i.n

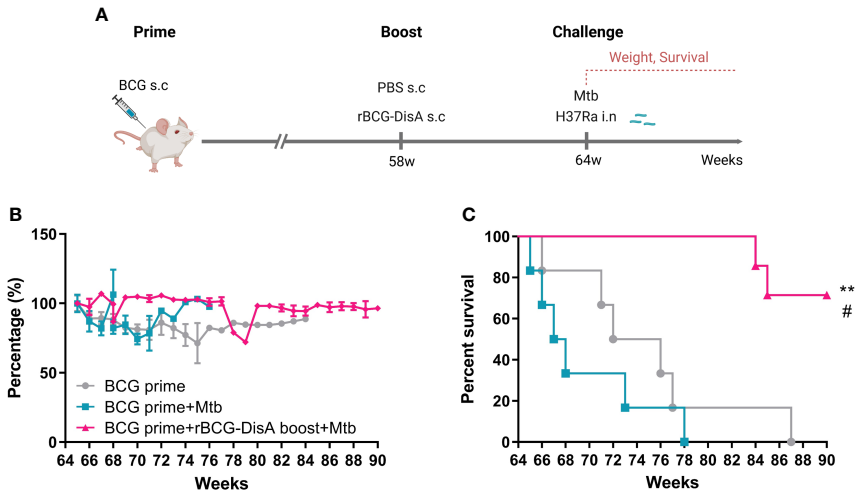

FIGURE 8
Body weight and survival in BCG prime following rBCG-DisA boost mice after *M. tuberculosis* infection. **(A)** BALB/c mice were primed by s.c BCG for 58-week following s.c rBCG-DisA boosting for 6-week. Subsequently, mice infected with *M. tuberculosis* by i.n route. Body weight and survival of mice were continuously monitored post *M. tuberculosis* infection. The schematic diagram of prime-boost strategy was created with BioRender.com. **(B)** Dynamic monitoring of mouse body weight at each week after *M. tuberculosis* infection. Results are presented as a percentage of body weight to initial body weight. **(C)** Survival of mice after *M. tuberculosis* infection (n=5~6). (Panel **C**, $^{**}P < 0.01$ stands for rBCG-DisA boosting group v.s BCG primed group. $^{\#}P < 0.05$ stands for rBCG-DisA boosting group v.s and BCG primed+Mtb group.).

infection (Figure 3F). However, rBCG-DisA did not improve phagocytosis and killing capacity of macrophages than that of BCG as other inducer of trained immunity (Figure 1D) (51).

Generally, the induction of trained immunity is accompanied with the epigenetic modification at the promoters of cytokines such as IL-1β, IL-6, and TNF-α (56). Accumulations of H3K4me1 and H3K4me3 caused by rBCG-DisA may contribute to higher IL-6 than BCG in BM cells (Figures 2F, 3A). However, the molecular mechanism of histones regulating the expression of inflammation-related genes have not yet been elucidated. H3K4me3 is directed to specific promoters in the genome by the presence of a class of lncRNAs, called immune gene-proximal lncRNAs (IPLs), which to be brought proximal to immune genes prior to their activation (44). UMLILO is the first reported IPL, which acts in *cis* to direct the WDR5MLL1 complex across the chemokine promoters (44). Surprisingly, an enhancer lncRNA of NeST, which binding to the adaptor protein WDR5 (47), was greater up-regulated in BM cells of rBCG-DisA i.v immunized mice than that of BCG, as well as in the lung and spleen after *M. tuberculosis* i.n infection (Figures 3C–E). IPLs are transcribed in a NFAT. Silencing of IPLs or abrogation of NFAT signaling results in loss of H3K4me3 accumulation at trained immune genes (44). We found that lncRNA NRON was repressed in BM cells of both BCG and rBCG-DisA i.v immunized mice, and showed no change in the lung but up-regulated in the spleen of rBCG-DisA i.v immunized mice to re-stimulation of *M. tuberculosis* infection (Figures 3C–E). Then we found that the expression of NEAT1 was down-regulated in BM cells of both BCG and rBCG-DisA immunized mice, but up-regulated significantly in the organs of rBCG-DisA immunized mice after *M. tuberculosis* challenge (Figures 3C–E). A growing body of research has revealed abnormally expressed lncRNAs in macrophages of TB patients (57). Thus, these lncRNAs that screened in this study may play roles in the regulation of the trained immunity, which should be investigated further.

Studies have demonstrated that immunological signals, metabolic rewiring of cell metabolism, and epigenetic reprogramming are integrated, representing the molecular substrates for induction of trained immunity (52). A recently research reported that another DisA overexpressing BCG (BCG Tice strain) elicited increased glycolytic metabolites, reduced kynurenine accumulation and itaconate production than wild type BCG in human or murine macrophages (32). However, these observations usually were generated *in vitro* model with different types of macrophages, which are known to arise from distinct cell lineages emerging at different stages in embryonic development. Thus, *in vivo* reality is of much greater nuance and complexity than can be accommodated by a macrophages model. In this study, we checked the metabolic profiles of mice immunized by BCG and rBCG-DisA after *M. tuberculosis* infection by metabolomic analysis, and found that increased fatty acid oxidation, fat mobilization, lipolysis and energy metabolism, as well as mTOR activation (Figure 4). It has been confirmed that induction of trained immunity accompanied by activated STING with enhanced mTOR-HIF-

1α pathway activation and concomitant elevation in glucose transporter levels (58–60), which implied that rBCG-DisA promoted glycolysis in mice post *M. tuberculosis* infection. Besides, mTOR has been implicated in both the breakdown and synthesis of fatty acids, and rBCG-DisA immunized mice presented fatty acid oxidation trend. Thus, rBCG-DisA vaccination increased the catabolic signatures of fat mobilization and lipolysis than BCG in mice after *M. tuberculosis* infection. Cholesterol metabolism is a part of lipid metabolism. BCG-induced activation of TCA cycle promotes acetyl-CoA production, causes mevalonate accumulation, which promotes cholesterol synthesis (61). rBCG-DisA induced down-regulation of taurochenodeoxycholic acid, serine-cholic acid, and corticosterone, while the expression of mevalonic acid lactone inhibiting mevalonic acid synthesis was up-regulated (Figures 4C, F), suggesting that cholesterol synthesis in rBCG-DisA immunized mice was inhibited compared with BCG. Besides, rBCG-DisA induced up-regulation of essential amino acids and their metabolites such as methionine, valine betaine, L-norvaline valine, etc. Meanwhile, the expression of non-essential amino acid and its metabolites like L-proline, 4-(beta-acetylaminoethyl) imidazole (also called N-acetylhistamine) increased. The level of essential amino acids is positively correlated with activation of immune system induced by *M. tuberculosis* (62). And N-acetylhistamine may be related to anaphylaxis (63). Thus, shifts in metabolite levels may be a plausible mechanism behind the integration of immuno-metabolic and epigenetic programs for the enhanced trained immunity induced by rBCG-DisA immunization in mice.

Trained immunity is mediated by innate immune cells such as monocytes, macrophages, or NK cells (64), which produce heterologous lymphocyte activation, resulting in enhanced proinflammatory cytokines production, macrophage activity, T cell responses, and antibody titers (52). Activation of surface molecules such as pattern recognition receptor (PRR) and signaling pathways leading to the induction of Th1/Th2/Th17 response during trained immunity (39, 64). BCG could drive a robust mycobacteria specific antibody response in plasma and lungs, including IgG1, IgA, and IgM by i.v route, which could provide protection to an attenuated strain of *M. tuberculosis* (Δ*sigH* in the *M. tuberculosis* CDC1551) in macaques (65). Present study revealed that rBCG-DisA i.v immunization led to lower specific IgG than BCG (Figures 5B, C, S3A), which was inconsistent with our previous research by s.c route (27). While, anti-DisA antibody levels raised than that of BCG after *M. tuberculosis* infection (Figure 6B), which further confirmed strong immunogenicity of DisA as our previous work (27). Here, i.v rBCG-DisA led to the increasing of CD4 T cells in the spleen of C57BL/6J mice compared with BCG after *M. tuberculosis* infection (Figure 6C), as that of by s.c route in BALB/c mice (27). Unexpectedly, rBCG-DisA immunized mice showed a significant increase CD4 T cells in the lung after *M. tuberculosis* infection, which suggested that enhanced cellular immune response induced in the lung of mice. Besides, our recent work showed that elevated c-di-AMP regulated expressions of several immune-associated proteins, and increased immunogenicity of *Mycobacterium smegmatis* by s.c route in mice (30). Hence, immune responses was induced by rBCG-DisA i.v immunization may be the results of the dual functions of overexpressed DisA and c-di-AMP regulated proteins.

Above, we had showed that rBCG-DisA i.v immunization could induce enhanced trained immunity as well as adaptive immunity in mice, especially accumulated T cells in the lung (Figure 6D). We found that rBCG-DisA i.v immunization could retain the body weight compared with BCG in mice (Figure 5A), but did not observe adverse reactions during the experiment, and pathological damage by H&E staining (Figure 7A). As well, H37Ra can be used as a surrogate for studying *M. tuberculosis* virulence in biosafety level 2 (BSL2) facilities (66). Previous, we showed that *M. tuberculosis* H37Ra and H37Rv were capable to induce comparable levels of humoral and cellular immunity by i.v route (67). The protection efficiency data showed that rBCG-DisA i.v vaccination promoted the clearance of *M. tuberculosis* H37Ra to undetectable in the lung and spleen of mice as BCG (Figure 7B). It was noted that rBCG-DisA rather than BCG was capable of long-term persistence in the lung after *M. tuberculosis* infection (Figure 7C). The longer resident of rBCG-DisA in the lung of mice may explain elevated T cell responses (Figure 6D, 7D) and enhanced epigenetic modification, especially immune memory related H3K4me1 (Figure 3A). While, BMDMs from both rBCG-DisA and BCG immunized mice showed similar proinflammatory cytokine responses and protection against *M. tuberculosis* H37Ra infection (Figures S5A–D). It has been elucidated that BMDMs from BCG vaccinated mice could inhibit intracellular survival of virulent H37Rv (33). We speculate that the virulence and MOI of *M. tuberculosis* strain caused differences in results. Together, these results showed that rBCG-DisA may provide longer protective after *M. tuberculosis* infection, which was attributed to enhanced T cell immunity as well as trained immunity (3, 39).

It was reported that the protection efficacy of BCG vaccination at birth rarely persists beyond 15-20 years in TB epidemic regions, but highly variable in adults (68, 69). Currently, several new mycobacterial vaccine designs that aimed to improve the efficacy over BCG have been evaluated in animal models and some in humans, such as boosting BCG with homologous BCG or heterogeneous vaccines such as subunit vaccine of H4:IC31 (70). In view of the waned protective efficiency after one year of BCG vaccination (10, 71), we had a try to boost BCG-primed mice of 58 weeks with rBCG-DisA by s.c route (Figure 8A). Surprisingly, we found that rBCG-DisA boosting could help mice resist weight loss and significantly prolonged survival of mice after *M. tuberculosis* i.n challenge (Figures 8B, C). Regrettably, our prime-boost experiment was lack of a control group of un-primed mice. Epidemiological data suggest that BCG vaccination is safe and decreases the infections of all causes in the elderly, especially

respiratory tract infections (7, 72). Hence, our results suggested a promising potential of rBCG-DisA in prime-boost strategy, especially in adults.

In present study, enhanced immune responses including trained immunity and adaptive immune response induced by rBCG-DisA i.v immunization were investigated. rBCG-DisA induced innate immunity including potent proinflammatory cytokine responses, epigenetic modification, altered lncRNA and metabolic profile. These results suggested that rBCG-DisA induced enhanced trained immunity, which may be stored within BM progenitor cells against infection over long periods. Additionally, vaccination to enhance trained immunity is a promising strategy which will be applied to adults or immunocompromised individuals due to defective adaptive immunity (52, 52, 54).

Data availability statement

The raw data supporting the conclusions of this article will be made available by the authors, without undue reservation. The metabolome sequencing data presented in the study are deposited in the MetaboLights repository (URL https://www.ebi.ac.uk/metabolights/MTBLS5496), accession number MTBLS5496.

Ethics statement

The animal study was reviewed and approved by The Institutional Ethics Committee of Second Affiliated Hospital of Air Force Medical University, using the recommendations from the Guide for the Care and Use of Laboratory Animals of the Institute (approval no. TDLL-20190213).

Author contributions

HN, JK, YL, XL, RR, YZ, YX, LB, YK, XG, and MX performed experiments and analyzed data. JZ, SZ, LZ, and YM contributed cells, reagents and expertise. HN, YL, and YB wrote the manuscript. YB and FZ conceived and designed experiments. YB supervised this work. All authors have read and agreed with the data.

Funding

This study was funded by National Natural Science Foundation (No. 81971560, 81371774, 81671638), National Major Special Projects of 13th Five-year Plan (No. 2018ZX10302302002004), Provincial Natural Science Foundation of Shaanxi Province (No. 2022ZDLSF01-07, 2019ZDLSF02-04), and Ningxia Natural Science Foundation (No. 2021AAC03124).

Conflict of interest

The authors declare that the research was conducted in the absence of any commercial or financial relationships that could be construed as a potential conflict of interest.

The reviewer GD declared a shared affiliation, with no collaboration, with some of the authors, LZ, YK, XG, to the handling editor at the time of the review.

Publisher's note

Supplementary material

The Supplementary Material for this article can be found online at: https://www.frontiersin.org/articles/10.3389/fimmu.2022.943667/full#supplementary-material

References

1. Ahmed A, Rakshit S, Adiga V, Dias M, Dwarkanath P, D'Souza G, et al. A century of BCG: Impact on tuberculosis control and beyond. *Immunol Rev* (2021) 301(1):98–121. doi: 10.1111/imr.12968

2. Brewer TF. Preventing tuberculosis with bacillus calmette-guerin vaccine: a meta-analysis of the literature. *Clin Infect Dis* (2000) 31 (Suppl 3):S64–67. doi: 10.1086/314072

3. Singh AK, Netea MG, Bishai WR. BCG Turns 100: its nontraditional uses against viruses, cancer, and immunologic diseases. *J Clin Invest* (2021) 131(11): e148291. doi: 10.1172/JCI148291

4. Moorlag S, Arts RJW, van Crevel R, Netea MG. Non-specific effects of BCG vaccine on viral infections. *Clin Microbiol Infect* (2019) 25(12):1473–8. doi: 10.1016/j.cmi.2019.04.020

5. Jordan B, Meeks JJ. T1 bladder cancer: current considerations for diagnosis and management. *Nat Rev Urol* (2019) 16(1):23–34. doi: 10.1038/s41585-018-0105-y

6. Netea MG, Quintin J, van der Meer JW. Trained immunity: a memory for innate host defense. *Cell Host Microbe* (2011) 9(5):355–61. doi: 10.1016/j.chom.2011.04.006

7. Giamarellos-Bourboulis EJ, Tsilika M, Moorlag S, Antonakos N, Kotsaki A, Domínguez-Andrés J, et al. Activate: Randomized clinical trial of bcg vaccination against infection in the elderly. *Cell* (2020) 183(2):315–323.e9. doi: 10.1016/j.cell.2020.08.051

8. Netea MG, Dominguez-Andres J, Barreiro LB, Chavakis T, Divangahi M, Fuchs E, et al. Defining trained immunity and its role in health and disease. *Nat Rev Immunol* (2020) 20(6):375–88. doi: 10.1038/s41577-020-0285-6

9. Soto JA, Galvez NMS, Andrade CA, Ramirez MA, Riedel CA, Kalergis AM, et al. BCG Vaccination induces cross-protective immunity against pathogenic microorganisms. *Trends Immunol* (2022) 43(4):322–35. doi: 10.1016/j.it.2021.12.006

10. McShane H. Tuberculosis vaccines: beyond bacille calmette-guerin. *Philos Trans R Soc Lond B Biol Sci* (2011) 366(1579):2782–9. doi: 10.1098/rstb.2011.0097

11. Dalmia N, Ramsay AJ. Prime-boost approaches to tuberculosis vaccine development. *Expert Rev Vaccines* (2012) 11(10):1221–33. doi: 10.1586/erv.12.94

12. Nguipdop-Djomo P, Heldal E, Rodrigues LC, Abubakar I, Mangtani P. Duration of BCG protection against tuberculosis and change in effectiveness with time since vaccination in Norway: a retrospective population-based cohort study. *Lancet Infect Dis* (2016) 16(2):219–26. doi: 10.1016/S1473-3099(15)00400-4

13. White AD, Sibley L, Sarfas C, Morrison AL, Bewley K, Churchward C, et al. Influence of aerosol delivered BCG vaccination on immunological and disease parameters following SARS-CoV-2 challenge in rhesus macaques. *Front Immunol* (2021) 12:801799. doi: 10.3389/fimmu.2021.801799

14. Ahmed SM, Nasr MA, Elshenawy SE, Hussein AE, El-Betar AH, Mohamed RH, et al. BCG Vaccination and the risk of COVID 19: A possible correlation. *Virology* (2022) 565:73–81. doi: 10.1016/j.virol.2021.10.003

15. Hilligan KL, Namasivayam S, Clancy CS, O'Mard D, Oland SD, Robertson SJ, et al. Intravenous administration of BCG protects mice against lethal SARS-CoV-2 challenge. *J Exp Med* (2022) 219(2):e20211862. doi: 10.1084/jem.20211862

16. Kaufmann E, Khan N, Tran KA, Ulndreaj A, Pernet E, Fontes G, et al. BCG Vaccination provides protection against IAV but not SARS-CoV-2. *Cell Rep* (2022) 38(10):110502. doi: 10.1016/j.celrep.2022.110502

17. Witte G, Hartung S, Buttner K, Hopfner KP. Structural biochemistry of a bacterial checkpoint protein reveals diadenylate cyclase activity regulated by DNA recombination intermediates. *Mol Cell* (2008) 30(2):167–78. doi: 10.1016/j.molcel.2008.02.020

18. Kalia D, Merey G, Nakayama S, Zheng Y, Zhou J, Luo Y, et al. Nucleotide, c-di-GMP, c-di-AMP, cGMP, cAMP, (p)ppGpp signaling in bacteria and implications in pathogenesis. *Chem Soc Rev* (2013) 42(1):305–41. doi: 10.1039/c2cs35206k

19. Fu T, Zhao Y, Xi J. A new second messenger: Bacterial c-di-AMP. *Crit Rev Eukaryot Gene Expr* (2016) 26(4):309–16. doi: 10.1615/CritRevEukaryotGeneExpr.2016016642

20. Fahmi T, Port GC, Cho KH. C-di-AMP: An essential molecule in the signaling pathways that regulate the viability and virulence of gram-positive bacteria. *Genes (Basel)* (2017) 8(8):197. doi: 10.3390/genes8080197

21. Devaux L, Kaminski P-A, Trieu-Cuot P, Firon A. Cyclic di-AMP in host–pathogen interactions. *Curr Opin Microbiol* (2018) 41:21–8. doi: 10.1016/j.mib.2017.11.007

22. Bai Y, Yang J, Eisele LE, Underwood AJ, Koestler BJ, Waters CM, et al. Two DHH subfamily 1 proteins in streptococcus pneumoniae possess cyclic di-AMP phosphodiesterase activity and affect bacterial growth and virulence. *J Bacteriol* (2013) 195(22):5123–32. doi: 10.1128/JB.00769-13

23. Yang J, Bai Y, Zhang Y, Gabrielle VD, Jin L, Bai G. Deletion of the cyclic di-AMP phosphodiesterase gene (cnpB) in mycobacterium tuberculosis leads to reduced virulence in a mouse model of infection. *Mol Microbiol* (2014) 93(1):65–79. doi: 10.1111/mmi.12641

24. Dey B, Dey RJ, Cheung LS, Pokkali S, Guo H, Lee JH, et al. A bacterial cyclic dinucleotide activates the cytosolic surveillance pathway and mediates innate resistance to tuberculosis. *Nat Med* (2015) 21(4):401–6. doi: 10.1038/nm.3813

25. Dey RJ, Dey B, Zheng Y, Cheung LS, Zhou J, Sayre D, et al. Inhibition of innate immune cytosolic surveillance by an m. tuberculosis phosphodiesterase. *Nat Chem Biol* (2017) 13(2):210–7. doi: 10.1038/nchembio.2254

26. Zhang Y, Yang J, Bai G. Cyclic di-AMP-mediated interaction between mycobacterium tuberculosis DeltacnpB and macrophages implicates a novel strategy for improving BCG vaccination. *Pathog Dis* (2018) 76(2):fty008. doi: 10.1093/femspd/fty008

27. Ning H, Wang L, Zhou J, Lu Y, Kang J, Ding T, et al. Recombinant BCG with bacterial signaling molecule cyclic di-AMP as endogenous adjuvant induces elevated immune responses after mycobacterium tuberculosis infection. *Front Immunol* (2019) 10:1519. doi: 10.3389/fimmu.2019.01519

28. Zhang L, Li W, He ZG. DarR, a TetR-like transcriptional factor, is a cyclic di-AMP-responsive repressor in mycobacterium smegmatis. *J Biol Chem* (2013) 288(5):3085–96. doi: 10.1074/jbc.M112.428110

29. Tang Q, Luo Y, Zheng C, Yin K, Ali MK, Li X, et al. Functional analysis of a c-di-AMP-specific phosphodiesterase MsPDE from mycobacterium smegmatis. *Int J Biol Sci* (2015) 11(7):813–24. doi: 10.7150/ijbs.11797

30. Ning H, Liang X, Xie Y, Bai L, Zhang W, Wang L, et al. C-di-AMP accumulation regulates growth, metabolism, and immunogenicity of mycobacterium smegmatis. *Front Microbiol* (2022) 13:865045. doi: 10.3389/fmicb.2022.865045

31. Dey RJ, Dey B, Singh AK, Praharaj M, Bishai W. Bacillus calmette-guerin overexpressing an endogenous stimulator of interferon genes agonist provides enhanced protection against pulmonary tuberculosis. *J Infect Dis* (2020) 221(7):1048–56. doi: 10.1093/infdis/jiz116

32. Singh AK, Praharaj M, Lombardo KA, Yoshida T, Matoso A, Baras AS, et al. Re-engineered BCG overexpressing cyclic di-AMP augments trained immunity and exhibits improved efficacy against bladder cancer. *Nat Commun* (2022) 13(1):878. doi: 10.1038/s41467-022-28509-z

33. Kaufmann E, Sanz J, Dunn JL, Khan N, Mendonca LE, Pacis A, et al. BCG Educates hematopoietic stem cells to generate protective innate immunity against tuberculosis. *Cell* (2018) 172(1-2):176–90.e119. doi: 10.1016/j.cell.2017.12.031

34. Darrah PA, Zeppa JJ, Maiello P, Hackney JA, Wadsworth M, Hughes TK, et al. Prevention of tuberculosis in macaques after intravenous BCG immunization. *Nature* (2020) 577(7788):95–102. doi: 10.1038/s41586-019-1817-8

35. Lu Y, Kang J, Ning H, Wang L, Xu Y, Xue Y, et al. Immunological characteristics of mycobacterium tuberculosis subunit vaccines immunized through different routes. *Microb Pathog* (2018) 125:84–92. doi: 10.1016/j.micpath.2018.09.009

36. Arts RJW, Moorlag S, Novakovic B, Li Y, Wang SY, Oosting M, et al. BCG Vaccination protects against experimental viral infection in humans through the induction of cytokines associated with trained immunity. *Cell Host Microbe* (2018) 23(1):89–100 e105. doi: 10.1016/j.chom.2017.12.010

37. Joosten SA, van Meijgaarden KE, Arend SM, Prins C, Oftung F, Korsvold GE, et al. Mycobacterial growth inhibition is associated with trained innate immunity. *J Clin Invest* (2018) 128(5):1837–51. doi: 10.1172/JCI97508

38. Arts RJ, Blok BA, Aaby P, Joosten LA, de Jong D, van der Meer JW, et al. Long-term *in vitro* and *in vivo* effects of gamma-irradiated BCG on innate and adaptive immunity. *J Leukoc Biol* (2015) 98(6):995–1001. doi: 10.1189/jlb.4MA0215-059R

39. Kleinnijenhuis J, Quintin J, Preijers F, Benn CS, Joosten LA, Jacobs C, et al. Long-lasting effects of BCG vaccination on both heterologous Th1/Th17 responses and innate trained immunity. *J Innate Immun* (2014) 6(2):152–8. doi: 10.1159/000355628

40. Smith SG, Kleinnijenhuis J, Netea MG, Dockrell HM. Whole blood profiling of bacillus calmette-Guérin-Induced trained innate immunity in infants identifies epidermal growth factor, IL-6, platelet-derived growth factor-AB/BB, and natural killer cell activation. *Front Immunol* (2017) 8:644. doi: 10.3389/fimmu.2017.00644

41. van Puffelen JH, Keating ST, Oosterwijk E, van der Heijden AG, Netea MG, Joosten LA, et al. Trained immunity as a molecular mechanism for BCG immunotherapy in bladder cancer. *Nat Rev Urol* (2020) 17(9):513–25. doi: 10.1038/s41585-020-0346-4

42. Arts RJW, Netea MG. Adaptive characteristics of innate immune responses in macrophages. *Microbiol Spectr* (2016) 4(4):MCHD-0023-2015. doi: 10.1128/microbiolspec.MCHD-0023-2015

43. Netea MG, Schlitzer A, Placek K, Joosten LAB, Schultze JL. Innate and adaptive immune memory: an evolutionary continuum in the host's response to pathogens. *Cell Host Microbe* (2019) 25(1):13–26. doi: 10.1016/j.chom.2018.12.006

44. Fanucchi S, Fok ET, Dalla E, Shibayama Y, Borner K, Chang EY, et al. Immune genes are primed for robust transcription by proximal long noncoding RNAs located in nuclear compartments. *Nat Genet* (2019) 51(1):138–50. doi: 10.1038/s41588-018-0298-2

45. Li D, Gao C, Zhao L, Zhang Y. Inflammatory response is modulated by lincRNACox2 *via* the NFkappaB pathway in macrophages infected by mycobacterium tuberculosis. *Mol Med Rep* (2020) 21(6):2513–21. doi: 10.3892/mmr.2020.11053

46. Huang S, Huang Z, Luo Q, Qing C. The expression of lncRNA NEAT1 in human tuberculosis and its antituberculosis effect. *BioMed Res Int* (2018) 2018:9529072. doi: 10.1155/2018/9529072

47. Gomez JA, Wapinski OL, Yang YW, Bureau JF, Gopinath S, Monack DM, et al. The NeST long ncRNA controls microbial susceptibility and epigenetic activation of the interferon-γ locus. *Cell* (2013) 152(4):743–54. doi: 10.1016/j.cell.2013.01.015

48. Li J, Chen C, Ma X, Geng G, Liu B, Zhang Y, et al. Long noncoding RNA NRON contributes to HIV-1 latency by specifically inducing tat protein degradation. *Nat Commun* (2016) 7:11730. doi: 10.1038/ncomms11730

49. Adeva-Andany MM, Carneiro-Freire N, Seco-Filgueira M, Fernández-Fernández C, Mouriño-Bayolo DJM. Mitochondrial β-oxidation of saturated fatty acids in humans. *Mitochondrion* (2019) 46:73–90. doi: 10.1016/j.mito.2018.02.009

50. Włodarczyk M, Druszczyńska M, Fol M. Trained innate immunity not always amicable. *Int J Mol Sci* (2019) 20(10):2565. doi: 10.3390/ijms20102565

51. Quintin J, Saeed S, Martens JHA, Giamarellos-Bourboulis EJ, Ifrim DC, Logie C, et al. Candida albicans infection affords protection against reinfection *via* functional reprogramming of monocytes. *Cell Host Microbe* (2012) 12(2):223–32. doi: 10.1016/j.chom.2012.06.006

52. Khader SA, Divangahi M, Hanekom W, Hill PC, Maeurer M, Makar KW, et al. Targeting innate immunity for tuberculosis vaccination. *J Clin Invest* (2019) 129(9):3482–91. doi: 10.1172/jci128877

53. Mahmoud L, Abdulkarim AS, Kutbi S, Moghrabi W, Altwijri S, Khabar KSA, et al. Post-transcriptional inflammatory response to intracellular bacterial c-di-AMP. *Front Immunol* (2019) 10:3050. doi: 10.3389/fimmu.2019.03050

54. Covian C, Fernandez-Fierro A, Retamal-Diaz A, Diaz FE, Vasquez AE, Lay MK, et al. BCG-Induced cross-protection and development of trained immunity: Implication for vaccine design. *Front Immunol* (2019) 10:2806. doi: 10.3389/fimmu.2019.02806

55. O'Neill LAJ, Netea MG. BCG-Induced trained immunity: can it offer protection against COVID-19? *Nat Rev Immunol* (2020) 20(6):335–7. doi: 10.1038/s41577-020-0337-y

56. Koeken V, Verrall AJ, Netea MG, Hill PC, van Crevel R. Trained innate immunity and resistance to mycobacterium tuberculosis infection. *Clin Microbiol Infect* (2019) 25(12):1468–72. doi: 10.1016/j.cmi.2019.02.015

57. Wei L, Liu K, Jia Q, Zhang H, Bie Q, Zhang B. The roles of host noncoding RNAs in mycobacterium tuberculosis infection. *Front Immunol* (2021) 12:664787. doi: 10.3389/fimmu.2021.664787

58. Cheng SC, Quintin J, Cramer RA, Shepardson KM, Saeed S, Kumar V, et al. mTOR- and HIF-1α-mediated aerobic glycolysis as metabolic basis for trained immunity. *Science* (2014) 345(6204):1250684. doi: 10.1126/science.1250684

59. Arts RJW, Carvalho A, La Rocca C, Palma C, Rodrigues F, Silvestre R, et al. Immunometabolic pathways in BCG-induced trained immunity. *Cell Rep* (2016) 17(10):2562–71. doi: 10.1016/j.celrep.2016.11.011

60. Gomes MTR, Guimarães ES, Marinho FV, Macedo I, Aguiar E, Barber GN, et al. STING regulates metabolic reprogramming in macrophages *via* HIF-1α during brucella infection. *PloS Pathog* (2021) 17(5):e1009597. doi: 10.1371/journal.ppat.1009597

61. Bekkering S, Arts RJW, Novakovic B, Kourtzelis I, van der Heijden C, Li Y, et al. Metabolic induction of trained immunity through the mevalonate pathway. *Cell* (2018) 172(1-2):135–146 e139. doi: 10.1016/j.cell.2017.11.025

62. Crowther RR, Qualls JE. Metabolic regulation of immune responses to mycobacterium tuberculosis: A spotlight on l-arginine and l-tryptophan metabolism. *Front Immunol* (2020) 11:628432. doi: 10.3389/fimmu.2020.628432

63. Xu Y, Guo N, Dou D, Ran X, Liu C. Metabolomics analysis of anaphylactoid reaction reveals its mechanism in a rat model. *Asian Pac J Allergy Immunol* (2017) 35(4):224–32. doi: 10.12932/AP0845

64. Kleinnijenhuis J, Quintin J, Preijers F, Joosten LA, Jacobs C, Xavier RJ, et al. BCG-Induced trained immunity in NK cells: Role for non-specific protection to infection. *Clin Immunol* (2014) 155(2):213–9. doi: 10.1016/j.clim.2014.10.005

65. Irvine EB, O'Neil A, Darrah PA, Shin S, Choudhary A, Li W, et al. Robust IgM responses following intravenous vaccination with bacille calmette-guerin associate with prevention of mycobacterium tuberculosis infection in macaques. *Nat Immunol* (2021) 22(12):1515–23. doi: 10.1038/s41590-021-01066-1

66. Yang SJ, Chen YY, Hsu CH, Hsu CW, Chang CY, Chang JR, et al. Activation of M1 macrophages in response to recombinant TB vaccines with enhanced antimycobacterial activity. *Front Immunol* (2020) 11:1298. doi: 10.3389/fimmu.2020.01298

67. Ning H, Lu Y, Kang J, Xu Y, Wang L, Wang Y, et al. Establishment of mouse models of persistent tuberculosis and characteristics of that infection. *J Pathogen Biol* (2017) 12(03):219–23. doi: 10.13350/j.cjpb.170306

68. Mangtani P, Abubakar I, Ariti C, Beynon R, Pimpin L, Fine PE, et al. Protection by BCG vaccine against tuberculosis: a systematic review of randomized controlled trials. *Clin Infect Dis* (2014) 58(4):470–80. doi: 10.1093/cid/cit790

69. Dockrell HM, Smith SG. What have we learnt about BCG vaccination in the last 20 Years? *Front Immunol* (2017) 8:1134. doi: 10.3389/fimmu.2017.01134

70. Nemes E, Geldenhuys H, Rozot V, Rutkowski KT, Ratangee F, Bilek N, et al. Prevention of m. tuberculosis infection with H4:IC31 vaccine or BCG revaccination. *N Engl J Med* (2018) 379(2):138–49. doi: 10.1056/NEJMoa1714021

71. Keyser A, Troudt JM, Taylor JL, Izzo AA. BCG Sub-strains induce variable protection against virulent pulmonary mycobacterium tuberculosis infection, with the capacity to drive Th2 immunity. *Vaccine* (2011) 29(50):9308–15. doi: 10.1016/j.vaccine.2011.10.019

72. Pavan Kumar N, Padmapriyadarsini C, Rajamanickam A, Marinaik SB, Nancy A, Padmanaban S, et al. Effect of BCG vaccination on proinflammatory responses in elderly individuals. *Sci Adv* (2021) 7(32):eabg7181. doi: 10.1126/sciadv.abg7181

frontiers | Frontiers in Immunology

TYPE Original Research
PUBLISHED 31 August 2022
DOI 10.3389/fimmu.2022.943558

OPEN ACCESS

EDITED BY
Wenping Gong,
The 8th Medical Center of PLA General Hospital, China

REVIEWED BY
Suraj Sable,
Centers for Disease Control and Prevention (CDC), United States
Mario Alberto Flores-Valdez,
CONACYT Centro de Investigación y Asistencia en Tecnología y Diseño del Estado de Jalisco (CIATEJ), Mexico

*CORRESPONDENCE
Luciana Cezar de Cerqueira Leite
luciana.leite@butantan.gov.br

SPECIALTY SECTION
This article was submitted to Vaccines and Molecular Therapeutics, a section of the journal Frontiers in Immunology

RECEIVED 13 May 2022
ACCEPTED 26 July 2022
PUBLISHED 31 August 2022

CITATION
Trentini MM, Kanno AI, Rodriguez D, Marques-Neto LM, Eto SF, Chudzinki-Tavassi AM and Leite LCC (2022) Recombinant BCG expressing the LTAK63 adjuvant improves a short-term chemotherapy schedule in the control of tuberculosis in mice. *Front. Immunol.* 13:943558. doi: 10.3389/fimmu.2022.943558

Recombinant BCG expressing the LTAK63 adjuvant improves a short-term chemotherapy schedule in the control of tuberculosis in mice

Monalisa Martins Trentini[1], Alex Issamu Kanno[1], Dunia Rodriguez[1], Lazaro Moreira Marques-Neto[1], Silas Fernandes Eto[2,3], Ana Marisa Chudzinki-Tavassi[2,3] and Luciana Cezar de Cerqueira Leite[1]*

[1]Laboratório de Desenvolvimento de Vacinas, Instituto Butantan, São Paulo, Brazil, [2]Laboratory Center of Excellence in New Target Discovery (CENTD) Special Laboratory, Instituto Butantan, São Paulo, Brazil, [3]Center of Innovation and Development, Laboratory of Development and Innovation, Instituto Butantan, São Paulo, Brazil

Tuberculosis (TB) is one of the deadliest infectious diseases around the world. Prevention is based on the prophylactic use of BCG vaccine, effective in infants but as protection wanes with time, adults are less protected. Additionally, chemotherapy requires the use of many antibiotics for several months to be effective. Immunotherapeutic approaches can activate the immune system, intending to assist chemotherapy of TB patients, improving its effectiveness, and reducing treatment time. In this work, the recombinant BCG expressing LTAK63 (rBCG-LTAK63) was evaluated for its immunotherapeutic potential against TB. Bacillary load, immune response, and lung inflammation were evaluated in mice infected with *Mycobacterium tuberculosis* (*Mtb*) and treated either with BCG or rBCG-LTAK63 using different routes of administration. Mice infected with *Mtb* and treated intranasally or intravenously with rBCG-LTAK63 showed a reduced bacillary load and lung inflammatory area when compared to the group treated with BCG. In the spleen, rBCG-LTAK63 administered intravenously induced a higher inflammatory response of $CD4^+$ T cells. On the other hand, in the lungs there was an increased presence of $CD4^+IL\text{-}10^+$ and regulatory T cells. When combined with a short-term chemotherapy regimen, rBCG-LTAK63 administered subcutaneously or intravenously decreases the *Mtb* bacillary load, increases the anti-inflammatory response, and reduces tissue inflammation. These findings highlight the potential of rBCG-LTAK63 in assisting chemotherapy against *Mtb*.

KEYWORDS

BCG, tuberculosis, recombinant BCG, rBCG-LTAK63, immunotherapy, immunotherapeutic vaccine

Introduction

TB is a global infectious disease that affects millions of people each year. While most patients will be clinically asymptomatic and classified as latent TB, it can change to an active form under several conditions. Even with the availability of prophylactic and therapeutic treatments, TB mortality was approximately 1.5 million in 2020 (1). The chemotherapy for TB demands the administration of several antibiotics for at least 6 months, which leads several patients to abandon the treatment after a transitory recovery (1, 2). Incomplete treatment contributes to the emergence of multidrug-resistant TB strains which requires an even more prolonged and complex antibiotic therapy. Although current efforts in prevention and treatment have decreased its prevalence, the situation remains far from being resolved. As a result, new strategies to treat TB patients are constantly under investigation.

The use of vaccines as immunotherapy in the treatment of TB patients is an attractive idea as it can reduce the *Mtb* bacillary load and result in a better clinical outcome. Immunotherapy using vaccines may be especially helpful if combined with chemotherapy (3, 4). While most vaccines in clinical trials were devised as prophylactic, a limited number are also under evaluation in a post-infection immunotherapy regimen. Whole-cell vaccines are among the most advanced ones in clinical trials to which antituberculosis effect are usually associated with an increased Th1 immune response (5–11). rBCG-LTAK63 is a recombinant BCG expressing the LTAK63 adjuvant, the genetically detoxified subunit A of the LT toxin from *Escherichia coli* (12). Immunization of mice with rBCG-LTAK63 induces improved protection against *Mtb* challenge. Protection was associated with an increased production of Th1-related cytokines in immunized mice as well as an increase in innate and long-term immune responses (13). Interestingly, after the *Mtb* challenge, mice immunized with rBCG-LTAK63 showed an increased production of regulatory-related cytokines (TGF-beta and IL-10) in the lungs, resulting in considerable reduction of the inflammation associated with infection (12). We hypothesize that the therapeutic use of rBCG-LTAK63 could induce an improved control over the bacillary load and inflammation caused by *Mtb* infection.

In this context, we have evaluated the effect of rBCG-LTAK63 in the treatment of Mtb-infected mouse models and provide compelling evidence that it can be effective as immunotherapy for TB. Our findings also demonstrate that in a scenario where the antibiotic therapy is shorter – mimicking a discontinued chemotherapy – the immunotherapy with rBCG-LTAK63 can activate the immune system, reduce the Mtb bacillary load and the inflammation associated with the disease.

Material and methods

Animals

Six-week-old BALB/c female mice from the Biotério Central of Instituto Butantan were housed and bred in micro isolators adapted to HEPA filtered racks with 12 h light/dark cycles, temperature ranging from 20 to 22°C, and 60% humidity at the animal housing facilities of the Laboratório de Desenvolvimento de Vacinas, Instituto Butantan. This study and protocols were approved by the Ethical Committee on Animal Use of Instituto Butantan (Protocol number: 5135010819).

Mtb intranasal infection

Aliquots of *Mtb* (H37Rv) maintained at –80° C were thawed, and the concentration adjusted to 1.25 x 10^4 CFU/mL. Groups of 5 mice under mild anesthesia were instilled with 40 µL (500 CFU) into the nostrils with aid of a micropipette. CFU recovered from the lungs of an extra control group (with 5 animals) thirty days after infection was evaluated prior to the beginning of treatment. At this point, the CFU was 1.59 ± 0.52 x 10^6 CFU/lung (SD).

Tuberculosis immunotherapy protocols

Frozen aliquots of rBCG-LTAK63 were diluted in PBS 0.05% Tween 80 and 10^6 CFU/mouse administered through different routes. The native BCG Moreau vaccine (10^6 CFU/mouse) was administered as control. The immunotherapeutic protocol of infected animals was performed as previously described (14, 15). Briefly, after four weeks of infection, the groups of BALB/c mice were treated either with one or two doses (30 days interval) of BCG or rBCG-LTAK63 administered *via* subcutaneous (SC, 100 µl), intranasal (IN, 40 µl), or intravenous (IV, 100 µl) routes. As control, chemotherapy with antibiotics consisting of rifampicin (RIF, 20 mg/kg) and isoniazid (INH, 50 mg/kg) (Sigma-Aldrich®, Merck KGa, St Louis, MO, USA) was given daily by gavage for four weeks. Mice were euthanized four and eight weeks after the immunotherapy, the spleen and/or lung (cranial and median lobes) collected, homogenized, diluted and plated on Middlebrook 7H10 agar (BD Difco™, Detroit, MI, USA), supplemented with 0.5% glycerol (Sigma-Aldrich®), 10% OADC (oleic acid-albumin-dextrose-catalase; BBL, Cockeysville, MD, USA), 5 µg/ml of TCH (2-thiophenecarboxylic acid hydrazide, Sigma-Aldrich®, a BCG growth inhibitor) and incubated at 37°C and 5% CO_2 for 2-3 weeks to verify the bacterial load as determined by the number of CFU recovered. To evaluate the combination of chemotherapy plus immunotherapy, 4 weeks after infection, RIF (20 mg/kg) and INH (50 mg/kg) were

administered by daily gavage for only 2 weeks (short-term chemotherapy). After 2 weeks interval, one dose of rBCG-LTAK63 (10^6 CFU/mouse) was administered *via* SC, IN or IV routes. The immune response and bacterial burden were evaluated 8 weeks after the immunotherapy.

Inflammatory immune response

Cell preparations were done as previously described (16). Briefly, mice were euthanized, and the lungs and spleens collected in ice-cold RPMI-1640 (Sigma-Aldrich®). The lungs were digested with DNAse IV (30 µg/mL; Sigma-Aldrich®) and collagenase III (0.7 mg/mL; Sigma-Aldrich®) for 30-40 min at 37°C. The digested tissue was prepared as single-cell suspensions using 70 µm cell strainers (BD Pharmingen™, San Diego, CA), erythrocytes were lysed with an RBC lysis solution (150 mM NH_4Cl, 10 mM $KHCO_3$ pH 7.4), the cells were washed once and resuspended in RPMI-1640. Cells were counted in a Neubauer chamber using Trypan Blue and adjusted to 1×10^6 cells/mL and distributed in 96-well plates (Corning®, NY, USA). The cells were stimulated with anti-CD3 (1 µg/mL, clone: OKT3, BD Pharmingen™) plus anti-CD28 (1 µg/mL, clone: CD82.2, BD Pharmingen™) for 48 h at 37 °C and 5% CO_2. The supernatant was collected, and the concentration of cytokines determined by Cytometric Bead Array (BD Pharmingen™) using the Mouse Th1/Th2/Th17 Cytokine Kit.

Additionally, in order to determine the phenotype of T cells in the spleen and lungs, the samples were stained with: anti-CD4-PercP antibody (clone: RM4-5, BD Pharmingen™) and anti-CD3-APC.Cy7 antibody (clone: 17A2, BD Pharmingen™) for 30 min. Then, the cells were washed, fixed, and permeabilized using the Mouse Cytofix/Cytoperm Kit (BD). The cells were further incubated for 30 min with anti-TNF-α-PE (clone: MP6-XT2, BD Pharmingen™), anti-IFN-γ-APC (clone: XMG1.2, BD Pharmingen™), anti-IL-17-BV421 (clone: TC11-18H10, BD Pharmingen™), and anti-IL-10-PE.Cy7 (clone: JESS-16E3, BD Pharmingen™).

Spleen and lung cells were also evaluated for their T regulatory phenotype by staining with Mouse Th17/Treg Phenotyping Kit (BD Pharmingen™). The cells were incubated with anti-CD4-PercP antibody (clone: RM4-5) andanti-CD25-PE antibody (clone: PC619) (BD Pharmingen™) for 30 min. Then, the cells were washed, fixed, and permeabilized using the Mouse Foxp3 Cytofix/Cytoperm Kit (BD). The cells were further incubated for 50 min withanti-FoxP3-AlexaFluor647 antibody (clone: MF23, BD Pharmingen™). Data were acquired on a FACSCanto II flow cytometer (BD Pharmingen™) and analyzed using the FlowJo 8.7 software.

Immunopathological evaluation of the lungs

After infection and treatments, the right caudal lung lobes of mice were collected and fixed in 10% paraformaldehyde (Labsynth®, Diadema, SP). Fixed tissues (5 µm thick) were placed onto glass slides and stained with hematoxylin and eosin (H&E). The intensity of lung inflammation was evaluated according to (17). In brief, H&E-stained sections were photographed at 40 x magnification using a microscope (Axio Imager M2 Zeiss) coupled to a digital camera (Axiocam MRm Zeiss). Image analysis software (ImageJ, National Institutes of Health, USA) was used to determine the pulmonary area affected. Briefly, five images at 40 x magnification per lung lobule, totaling 25 images per group, were randomly selected, and analyzed for the qualitative evaluation of the cell infiltrate and intra-alveolar regions (17–19). To measure the areas of interest, the images were transformed into 8-bit and treated with threshold and percentage of the measured area. For leukocyte counting, the Color Deconvolution 2 plugin was used to visualize and separate nuclei from the cytoplasm. For cell counting, the Cell Counter plugin was used. This analysis is used to facilitate the differential counting of segmented and mononuclear nuclei.

Statistical analysis

The data were imported to Excel (version 14.3.4, 2011) and analyzed using Graphpad Prism Software 6.0. Statistical analysis was performed by one-way ANOVA followed by Bonferroni test; p values < 0.05 was considered statistically significant. Values are reported as the mean ± SD.

Results

rBCG-LTAK63 immunotherapy reduces *Mtb* bacillary load

To determine the immunotherapeutic potential of rBCG-LTAK63, BALB/c mice were infected with *Mtb* and treated with a single dose of BCG or rBCG-LTAK63 administered *via* the SC, IN, or IV routes after 4 weeks of infection. The infection of Mtb was performed using the intranasal route with 500 CFU/mouse to mimic the natural infection route, as previously described (20) (Supplementary Figure 1). Four weeks after treatment with rBCG-LTAK63, either by the IN or IV routes, showed significantly reduced bacillary load (Figures 1A, C). Furthermore, the treatments also induced reduced bacterial load in the spleens (Supplementary Figure 2). The complete chemotherapy with INH (50 mg/kg) and RIF (20 mg/kg) administered daily by gavage for 4 weeks was used as positive control. Neither BCG treatment by any route nor rBCG-LTAK63 administered SC were able to reduce the bacillary load (Figure 1B). Additionally, we investigated whether this reduction would persist for longer periods after the treatment. At eight weeks after treatment the immunotherapy with rBCG-

10.3389/fimmu.2022.943558

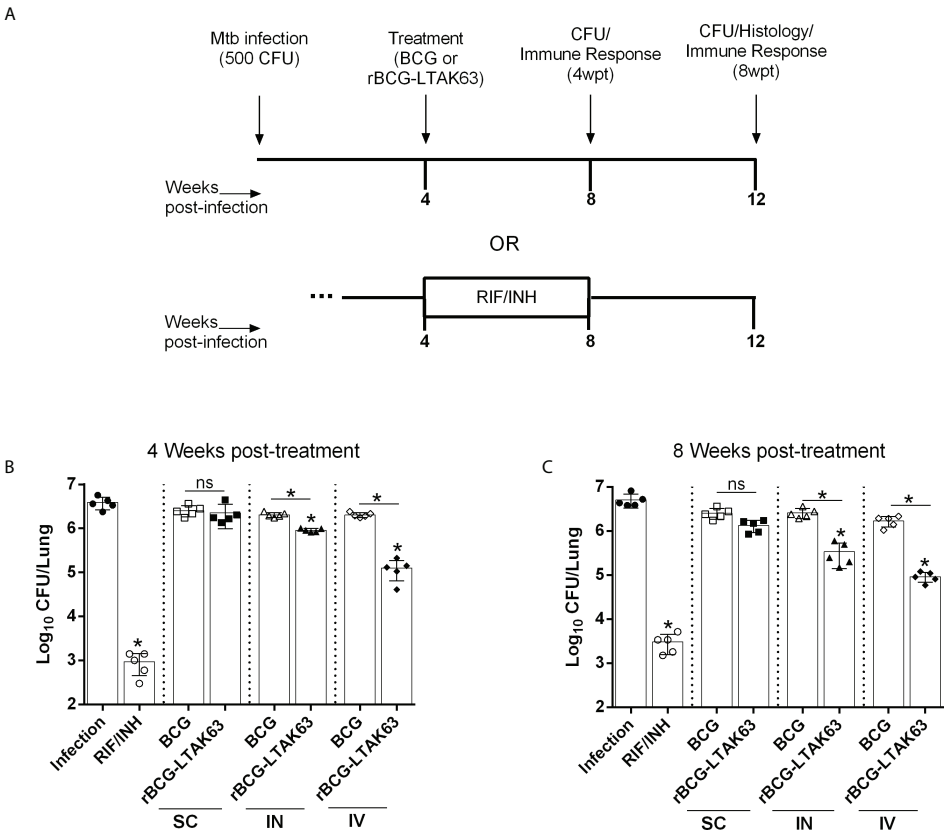

FIGURE 1
Therapeutic effect of rBCG-LTAK63 vaccine in Mtb-infected mice. **(A)** BALB/c mice were infected with Mtb (500 CFU/IN) and treated 4 weeks later with a single of BCG or rBCG-LTAK63 vaccine delivered by the subcutaneous (SC), intranasal (IN) or intravenous (IV) route. As a control, one group received rifampicin and isoniazid daily given by gavage for 4 weeks (RIF/INH). Four weeks **(B)** or eight weeks **(C)** post-treatment (4wpt or 8wpt), the lungs of these animals were collected and homogenized. Serial dilutions were plated onto 7H10 agar plates containing TCH (a BCG growth inhibitor) to assess Mtb CFU. Statistical differences were determined by one-way ANOVA with a Bonferroni test. *p values ≤ 0.05 were considered statistically significant and ns, not significant. Asterisks over the columns refer to the comparison with the infection group. Results are represented by the means $\pm$ SD of the CFU recovered in the cranial and median lung lobes from the groups of mice (n=5/group).

LTAK63 *via* IN or IV also showed a reduced *Mtb* bacillary load (Figures 1C, D). Again, neither rBCG-LTAK63 administered SC nor BCG by any route showed reduction in bacillary load. Comparison of rBCG-LTAK63 administered by different routes demonstrate that the IV route resulted in a greater reduction in the bacillary load than the IN route (Figures 1B, D). On the other hand, two doses of rBCG-LTAK63 did not show therapeutic effectiveness in any administration route (IV, IN, or SC) (Supplementary Figure 3).

Notably, the group treated with antibiotics exhibited reduced effectiveness over time, which is not observed in the rBCG-LTAK63 vaccine-treated group; that is, in the lungs of animals treated with antibiotics, there is a small increase in bacillary load with time that is not observed in the group treated with rBCG-LTAK63 (Supplementary Figure 4).

To evaluate the degree of inflammation, the lungs of infected mice treated with BCG or rBCG-LTAK63 were processed for histopathological examination. Mice infected with *Mtb* (Infection group) developed widespread and diffuse pneumonia, as well as an inflammatory infiltrate surrounding the blood vessels and airways (Figure 2A). In comparison, mice treated with the BCG vaccine (IN and IV routes) developed pneumonia patches and had more severe perivascular and peribronchiolar inflammatory infiltrates than animals treated with rBCG-LTAK63 or conventional antibiotics (RIF/INH) (Figure 2A). Surprisingly, mice treated rBCG-LTAK63 (IN and IV routes) showed decreased lung inflammation (Figure 2B) with reduced neutrophils, macrophages and lymphocytes efflux when compared with the infected animals or mice that received BCG (Figures 2C–E).

rBCG-LTAK63 therapy modulates the inflammatory response induced by *Mtb*

Since the immunotherapy with rBCG-LTAK63 decreased bacillary load and the cellular infiltrate in the lungs of *Mtb*-

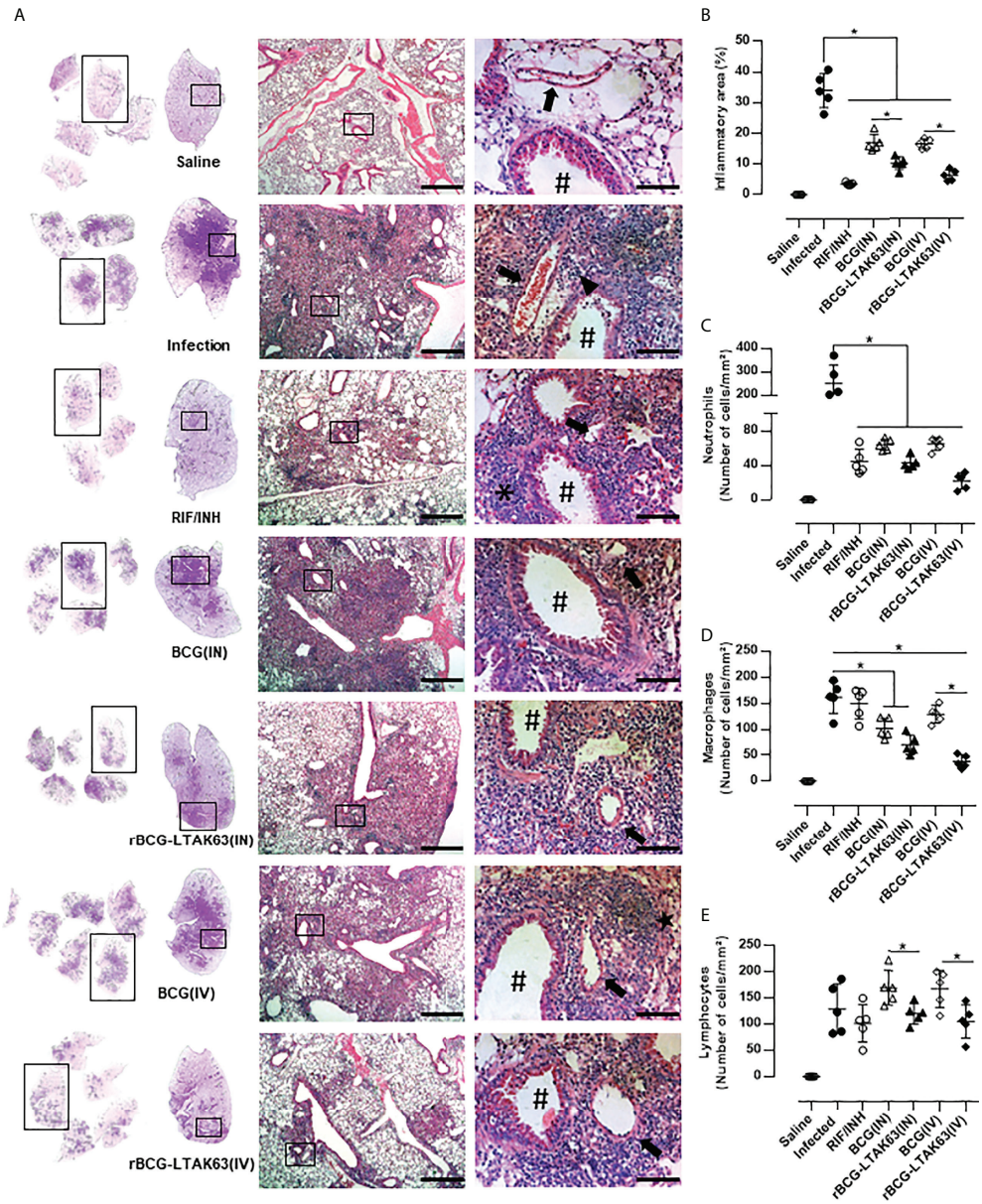

FIGURE 2
Immunotherapy with rBCG-LTAK63 vaccine decreases cellular infiltration in the lungs of *Mtb*-infected mice. **(A)** Representative histopathology of lungs from naïve mice (Saline), infected with *Mtb* and not treated (Infection), treated with antibiotics for 4 weeks (RIF/INH) or treated with BCG or rBCG-LTAK63 delivered intranasally (IN) or intravenously (IV), at 1x, 5x and 20x magnification. Representative images at 40x magnification show the difference in inflammatory process between treatments, neutrophilic infiltrate (arrowhead), interalveolar macrophage (star) and lymphocyte (asterisk), arteriole (arrow) and bronchioles (hashtag). **(B)** Lung inflammation scores are presented as the mean percentage of inflammation area (mm^2) for each mouse (n=5/group). The cellular infiltrate in the lung sections was classified in neutrophils **(C)**, macrophages **(D)** and lymphocytes **(E)** and presented as cell counts per mm^2. Lung sections were stained with H&E (bar, 200 µm (5x) and/20 µm (20x). Statistical differences were determined by one-way ANOVA with a Bonferroni test. *p < 0.05.

infected mice, we evaluated the profile of inflammatory and regulatory $CD4^+$ T cells in the lungs and spleens following the IN or IV treatment with rBCG-LTAK63 (the gating strategy is shown in Supplementary Figure 5). Four and eight weeks after treatment, the mice that received rBCG-LTAK63 IV showed an increased presence of splenic $CD4^+$ $IL\text{-}17^+$ (Figure 3A) and $CD4^+$ $TNF\text{-}\alpha^+$ (Figure 3B). The increase of $CD4^+IFN\text{-}\gamma^+$ in the spleen was not statistically significant (Figure 3C). At the same time, a reduced presence of these cells was observed in the lungs. This was observed at four (Figures 3F–H) and eight weeks after

treatment (Figures 3L, M), as determined by IL-17$^+$ (Figures 3F, L), TNF-α$^+$ (Figures 3G, K) and IFN-γ$^+$ (Figures 3H, M) CD4$^+$ T cells. Interestingly, the lower inflammatory response in the lungs from the rBCG-LTAK63 IV treatment was accompanied by an increased number of regulatory T cells (CD4$^+$CD25$^+$FoxP3$^+$) in the spleen and lungs (Figures 3E, J, O). Furthermore, increased CD4$^+$IL-10$^+$ was observed in the lungs in comparison to the Infection group (Figures 3D, I, N). These findings show that the IV treatment with rBCG-LTAK63 increases the inflammatory response in the spleen and decreases inflammation in the lungs, which may be correlated with the increase in regulatory T cell response.

When two doses of rBCG-LTAK63 were administered the main effect observed was in IL-17 production through the IN and IV routes. Additionally, the IN route showed a significant increase in IFN-γ produced by lung cells (Supplementary Figure 6). The lung mucosal route will induce mostly IL-17, due to the Lung associated Lymphoid Tissue which produces more IL-6 and TGF-b.

Association of chemotherapy and immunotherapy with rBCG-LTAK63

The antibiotic therapy for TB can last several months and is one of the most common reasons for its discontinuation. After showing that rBCG-LTAK63 may be effective in reducing bacillary load and lung inflammation associated with the infection, we tested whether its combination with a reduced regimen of antibiotic therapy could improve the resolution of the infection (e.g., lower bacillary loads and/or disease-related inflammation).

To test this hypothesis, antibiotics were administered for only 2 weeks (half treatment) and two weeks after the end of chemotherapy, they received a single dose of rBCG-LTAK63 (SC, IN or IV route) (Figure 4A). Bacillary load in the spleen (Figure 4B) and lungs (Figure 4C) was determined 8 weeks later. As expected, the reduced chemotherapy decreased the bacillary load (~1.5 $\log_{10}$ reduction), but less efficiently than the full 4 weeks regimen (~ 3 $\log_{10}$ reduction). As hypothesized, the combination of antibiotic and immunotherapy with rBCG-LTAK63 (SC and IV routes) exhibited a substantial decrease in bacillary load in the spleen and lungs, as compared to the group that received only antibiotics (Figures 4B, C). Surprisingly, chemotherapy plus rBCG-LTAK63 administered *via* the IN route did not show any further reduction in comparison to chemotherapy only.

The immune response assessed by the production of inflammatory cytokines by spleen cells from these groups revealed higher levels of TNF-α when rBCG-LTAK63 was delivered by any route, higher IFN-γ when SC and IV was used and higher IL-17 through SC delivery (Figures 5A, C, E). In lung cells, a decrease in the production of these cytokines was observed especially when rBCG-LTAK63 was administered *via* SC and IV (Figures 5B, D, F). Interestingly, one combination (antibiotics and rBCG-LTAK63 SC route) induced an increase in the number of regulatory T cells in both the spleen and lungs (Figures 5G, H). The intravenously treated group also exhibited an increase in the number of regulatory T cells in the lungs. Accordingly, the lungs of these animals (chemotherapy plus rBCG-LTAK63 SC or IN route) showed reduced pneumonia and had fewer perivascular and peribronchiolar inflammatory infiltrates when compared to the Infection group or to the group treated with antibiotics (half regimen) (Figure 6A). Moreover, the cellular infiltrate was less prominent as demonstrated by the reduced lung inflammatory area (Figure 6B). The shorter chemotherapy regimen plus rBCG-LTAK63 (all 3 routes) induced lower inflammatory area also in comparison to the antibiotic group. Moreover, different routes of administration appear to recruit distinct numbers of neutrophils, macrophages, and lymphocytes. rBCG-LTAK63 administered IV resulted in higher number of neutrophils and macrophages in comparison to SC (Figures 6C, D). On the other hand, the number of lymphocytes was higher in the IN group in comparison to SC (Figure 6E). These results suggest that the immunotherapy with rBCG-LTAK63 can complement a reduced regimen of chemotherapy resulting in lower bacillary loads and lung inflammation.

Discussion

In this study, we showed the immunotherapeutic potential of rBCG-LTAK63 in a *Mtb*-infected murine model. rBCG-LTAK63 induces an inflammatory response in the spleens combined with a regulatory response in the lungs, and results in reduced bacillary loads. A second dose of rBCG-LTAK63 increased the immune response but did not reduce bacterial burden. This result is expected since most live vaccines are administered in only one dose due to persistence in the organism. BCG is not effective, probably due to the previous presence of *Mtb* before treatment. The differential effect seen with rBCG-LTAK63 could be due to the adjuvant effects of the toxin derivative.

The immunotherapy with rBCG-LTAK63 can be further combined with conventional antibiotics aiming at reducing the time of chemotherapy required. Other immunotherapeutic strategies commonly used include vaccines in association with chemotherapy (5–7, 21–23). Importantly, these candidates demonstrate increased Th1 responses also as prophylactic vaccines (24–26). The *M. vaccae*, RUTI, MIP and VPM1002 are candidates in clinical trials as prophylactic and therapeutic vaccines. They can activate the Th1-related immune response and work in synergy with antibiotics to reduce the bacterial burden. A common feature in these vaccines is the requirement of two or more doses to control the *Mtb* infection.

In our studies, we did not combine immunotherapy and chemotherapy at the same time. Since rBCG-LTAK63 is a live vaccine, this feature is important for the protection obtained and concomitant use of antibiotics could compromise its efficacy.

10.3389/fimmu.2022.943558

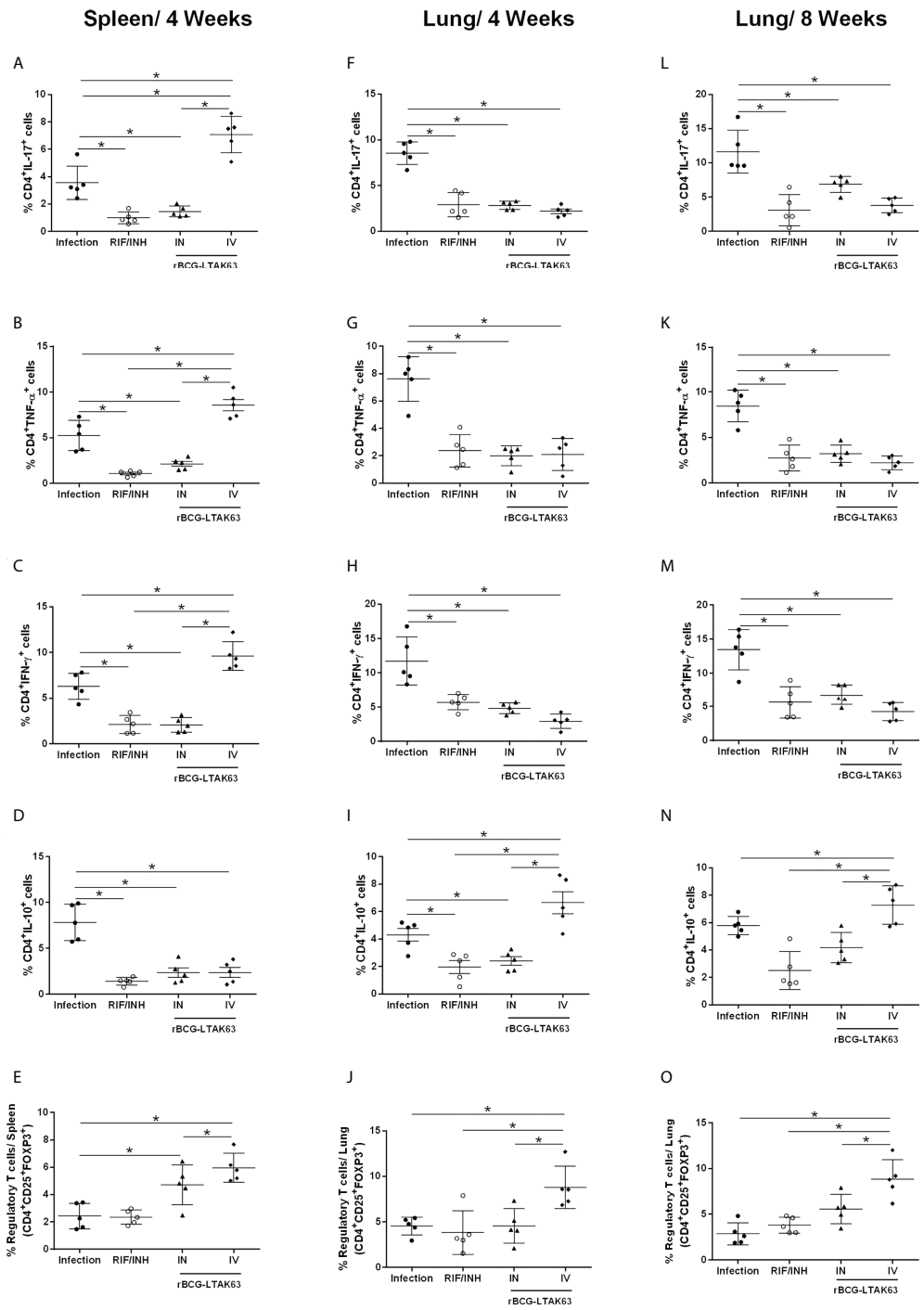

FIGURE 3
Immunotherapy with rBCG-LTAK63 modulates proinflammatory and regulatory immune responses in *Mtb*-infected mice. BALB/c mice were infected with *Mtb* (Infection) and treated with RIF/INH (*via* gavage for 4 weeks) or a single dose of rBCG-LTAK63 delivered intranasally (IN) or intravenously (IV). The immune response in the spleen and lungs was evaluated four and eight weeks post-treatment (4wpt and 8wpt). The number of $CD4^+$ T cells producing IL-17, **(A, F, L)** TNF-α **(B, G, K)**, IFN-γ **(C, H, M)** and IL-10 **(D, I, N)** in these organs was determined by staining with mouse monoclonal antibodies anti-CD3-APC.CY7, anti-CD4-PercP and anti-IL17-BV421, anti-TNF-PE, anti-IFN-APC or anti-IL-10-PE.Cy7. The percentage the regulatory T cells was determined by staining with mouse monoclonal antibodies anti-CD4-PercP and anti-CD25-PE and anti-FoxP3-APC **(E, J, O)**, and analyzed using Flow Cytometer FACS Canto II and FlowJo 8.7 software. Statistical differences were determined by one-way ANOVA with a Bonferroni test. **p* values ≤ 0.05 were considered statistically significant. Asterisks over the columns refer to the comparison with the infection group. Results are represented by the means ± SD of the percentage of CD4+ T cells (for IL-17, TNF-α, IFN-γ and IL-10) or the percentage of regulatory T cells in the $CD4^+$ population (n=5/group).

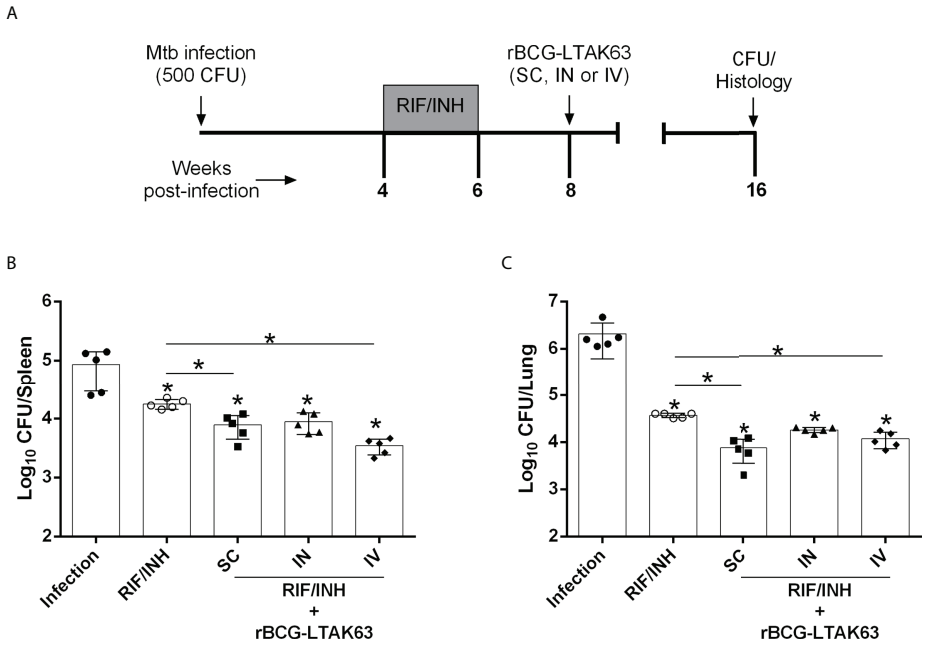

FIGURE 4
Combination of chemotherapy and rBCG-LTAK63 in the treatment of Mtb infection. **(A)** Schematical representation of the combination of chemotherapy with rBCG-LTAK63. BALB/c mice were infected with Mtb (500 CFU/IN) and treated 4 weeks later with rifampicin and isoniazid (RIF/INH) for 2 weeks. After two weeks interval rBCG-LTAK63 was given *via* SC, IN or IV routes. Eight weeks after treatment, the spleens and lungs of these animals were collected and homogenized. Serial dilutions were plated onto 7H10 agar plates containing TCH (a BCG growth inhibitor) to assess Mtb CFU. Bacillary load in the spleens **(B)** and lungs **(C)** of Mtb-infected mice treated with combination chemotherapy (RIF/INH) and rBCG-LTAK63. Statistical differences were determined by one-way ANOVA with a Bonferroni test. *p values ≤ 0.05 were considered statistically significant. Asterisks over the columns refer to the comparison with the infection group. Results are represented by the means $\pm$ SD of the CFU recovered in the cranial and median lung lobes from the groups of mice (n=5/group).

Striking differences of live and killed BCG have been reported (27, 28). Here, after a shorter use of conventional antibiotics, a single dose of rBCG-LTAK63 was administered. Through this approach, an additional reduction in *Mtb* bacillary load was observed suggesting that this scheme may compensate treatment abandonment; the long time required to cure a patient is regarded as one of the major obstacles to the success of TB treatment (29, 30). This may be especially important since the immunotherapy alone with rBCG-LTAK63 prevented the expansion of *Mtb* bacillary load. When only the antibiotic was used, there was an increase in CFU after cessation of treatment. On the other hand, rBCG-LTAK63 maintained the CFU stable for at least 8 weeks after treatment. This is probably related to its activity on the immune system cells that will continue to act even if the treatment is interrupted, while the antibiotic needs a minimum concentration (bioavailability) to maintain its therapeutic effect. Further investigation will determine whether the vaccine can impair the replication of *Mtb* for a longer time.

The immunotherapy with rBCG-LTAK63 resulted in a considerable increase of pro-inflammatory cytokines, such as TNF-α, IL-17 and IFN-γ, in the spleens. On the other hand, there was a decrease of these in the lungs. Immunotherapy of TB is based on the induction of immune activity and suppression of immune responses, e.g., excessive inflammation, which otherwise may cause tissue damage (31). When vitamin D (1α, 25-dihydroxy-vitamin D3) is administered in the immunotherapy of TB, there is a regulation of the pro-inflammatory response associated with bacterial clearance and decrease of pathological lesions in the lungs (32, 33). Anti-inflammatory cytokines, such as IL-10 and TGF-β counteract pro-inflammatory-mediated effects. Interestingly, we observed an increased number of the regulatory T cells and $CD4^+IL\text{-}10^+$ in the lungs of mice treated IV with rBCG-LTAK63. Coincidently, as a prophylactic vaccine, the immunization with rBCG-LTAK63 also induces an increase in IL-10 and TGF-β in the lungs of mice after *Mtb* challenge (12). Furthermore, a balance of pro and anti-inflammatory responses is associated with the differentiation of T helper subsets during the *Mtb* infection and with disease outcome (34, 35).

Our findings demonstrate that immunotherapy with rBCG-LTAK63 reduces both bacterial burden and pathology in the lungs when administered *via* parenteral (IV) or respiratory routes (IN), while the combination with chemotherapy was effective when administered SC or IV. Several studies reported that parenteral immunotherapies or immunizations fail to control TB, a fact related to poorly induced Ag-specific T cells in the lungs (36, 37). This indicates that Ag-specific immune responses may be induced by either route of administration with rBCG-LTAK63. Accordingly,

10.3389/fimmu.2022.943558

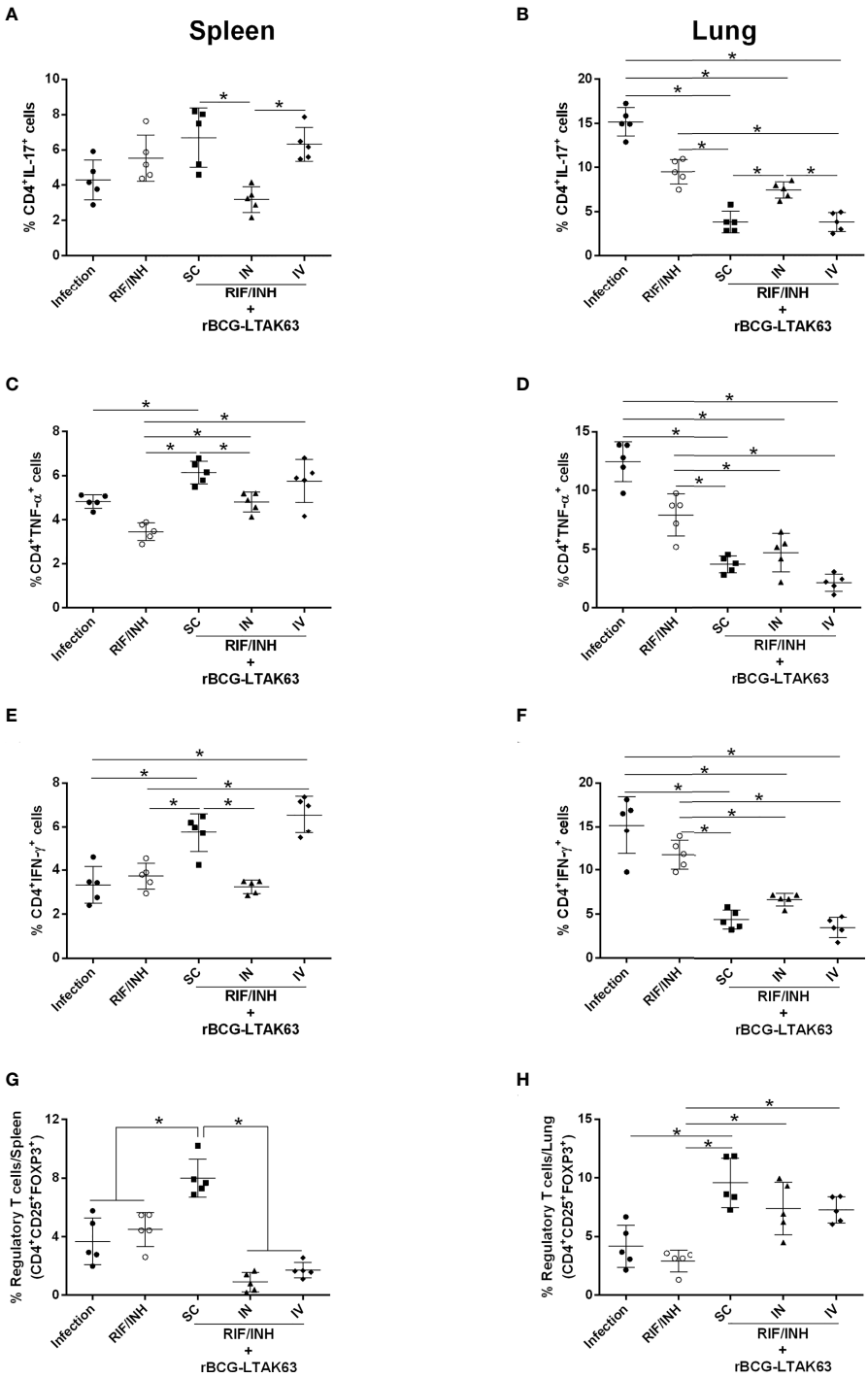

FIGURE 5
Reduced chemotherapy in combination with rBCG-LTAK63 modulates the immune response in the spleen and lungs of *Mtb*-infected mice. BALB/c mice were infected with *Mtb* (500 CFU/IN) and treated 4 weeks later with rifampicin and isoniazid (RIF/INH) for 2 weeks. After two weeks interval, rBCG-LTAK63 treatment was administered *via* SC, IN or IV routes. Eight weeks after treatment, spleens and lungs were recovered, and the number of CD4+ T cells producing IL-17 **(A, B)**, TNF-α **(C, D)** and IFN-γ **(E, F)** in these organs was determined by staining with mouse monoclonal antibodies antiCD3-APC.CY7, anti-CD4-PercP and anti-IL17-BV421, anti-TNF-PE, anti-IFN-APC. Regulatory T cells **(G–H)** were stained using mouse monoclonal antibodies anti-CD4-PercP, anti-CD25-PE and anti-FoxP3-APC, and analyzed using Flow Cytometer FACS Canto II and FlowJo 8.7 software. Statistical differences were determined by one-way ANOVA with a Bonferroni test. **p* values ≤ 0.05 were considered statistically significant. Asterisks over the columns refer to the comparison with the infection group. Results are represented by the means ± SD (n=5/group).

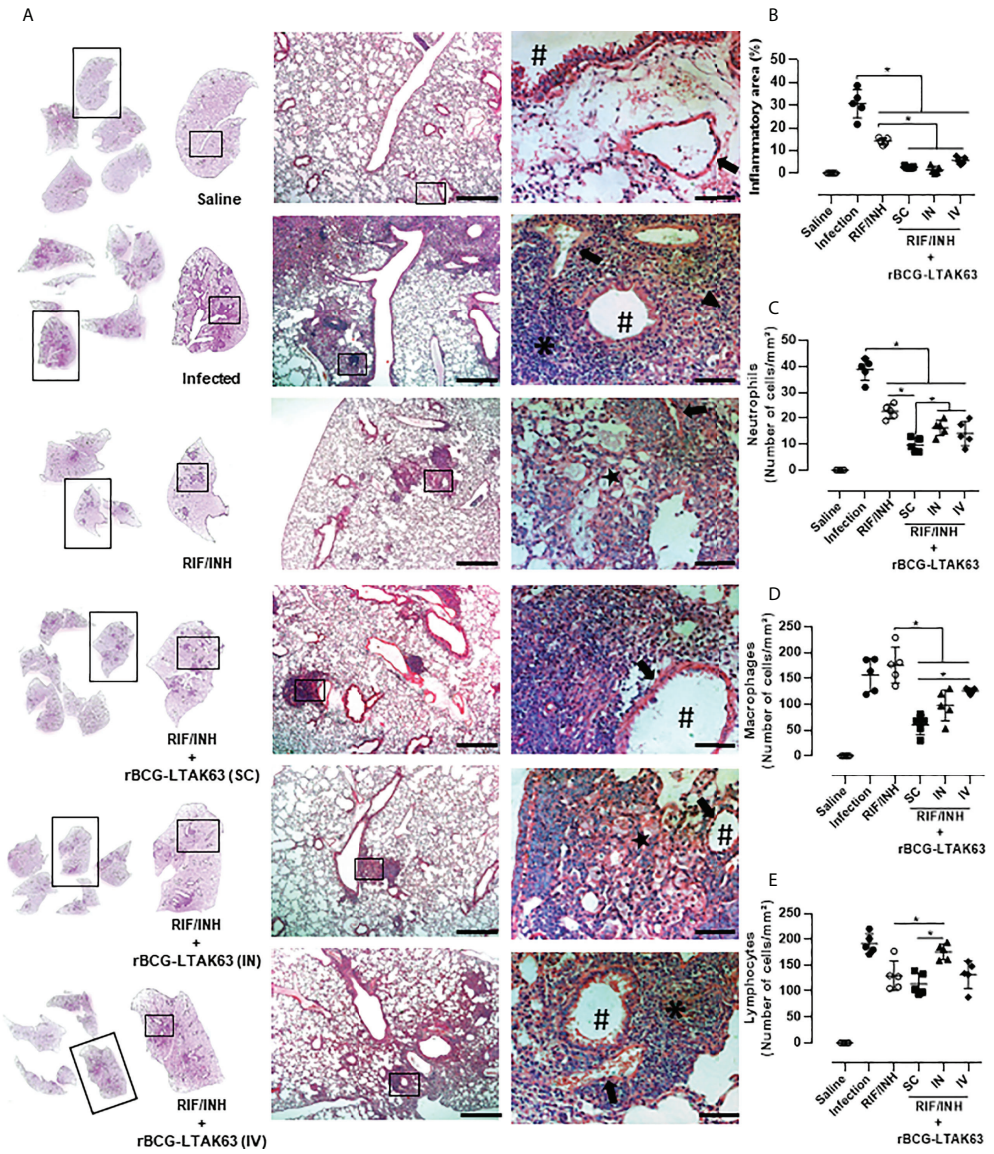

FIGURE 6
Histopathological analysis of the lungs of mice treated with combination antibiotics (RIF/INH) and rBCG-LTAK63 by different inoculation routes. **(A)** Representative histopathology of lungs from naïve mice (Saline), infected with Mtb and not treated (Infection), treated with antibiotics for 2 weeks (RIF/INH) or treated with combination antibiotics and rBCG-LTAK63 delivered subcutaneously (SC), intranasally (IN) or intravenously (IV) at 1x, 5x and 20x magnification. Representative images at 40x magnification show the difference in inflammatory process between treatments, neutrophilic infiltrate (arrowhead), interalveolar macrophage (star) and lymphocyte (asterisk), arteriole (arrow) and bronchioles (hashtag). **(B)** Lung inflammation scores are presented as the mean percentage of inflammation area (mm^2) for each mouse (n=5/group). The cellular infiltrate in the lung sections was classified in neutrophils **(C)**, macrophages **(D)** and lymphocytes **(E)** and presented as cell counts per mm^2. Lung sections were stained with H&E (bar, 200 µm (5x) and/20 µm (20x). Statistical differences were determined by one-way ANOVA with a Bonferroni test. *$p < 0.05$.

previous studies have shown a high number of Ag-specific T cells in the spleen and lungs of rBCG-LTAK63-immunized mice (12, 13).

In our results, the sole use of rBCG-LTAK63 through the IN and IV routes (without chemotherapy) was more efficient in reducing the TB burden than SC. It's known that immune responses are compartmentalized and the IN administrations may benefit from direct stimulation of local immune response, while IV would benefit from its faster (IV facilitating delivery to several organs including the lungs) and stronger stimulation (inducing systemic and local immune responses). On the other hand, although the SC route will induce systemic responses, the priming process is slower when compared to the IV route (38).

When we combined immunotherapy and chemotherapy, IV and SC, but not IN, reduced even further the bacterial load. Our data showed that the immune response (IL-17, TNF-α, and IFN-γ) in the lungs directly correlates with the Mtb load, while in the spleens it correlates better with the immunotherapy. This divergence may be due to the chemotherapy effect, which boosts systemic T cell responses (as dead bacilli may be processed and properly presented to lymphocytes) and may explain why systemic immunotherapy works better than the local approach.

Severe TB pathology is associated with the uncontrolled secretion of pro-inflammatory cytokines and chemokines, extensive neutrophilic infiltration, and intensified T cell responses, especially Th1 responses (39, 40). In this study, we demonstrated that immunotherapy with rBCG-LTAK63 results in neutrophil efflux control with smaller inflammatory foci mainly constituted by mononuclear/lymphocytic cells. This may be important in reducing tissue damage, enabling enough influx to generate a lymphocytic-enriched granuloma and could reduce intracellular *Mtb* niches in the lungs (41, 42). Here we show that rBCG-LTAK63 immunotherapy induced a timely modulation of the pro and anti-inflammatory responses and was effective in reducing *Mtb* bacillary loads. Although histology highlights the effect of treatment in the control of inflammation/pathology by rBCG-LTAK63, it is not possible to identify cell subsets. Future studies (with more specific techniques such as immunohistochemistry of flow cytometry) can further clarify the specific mechanism by which rBCG-LTAK63 decreases the progression of TB pathogenesis, and whether immunotherapy with rBCG-LTAK63 would also be effective in previously immunized recipients or those exposed to environmental mycobacteria. Ultimately, immunotherapy can be combined with conventional antibiotics being especially relevant to tackle non-adherence to conventional chemotherapy.

Data availability statement

The original contributions presented in the study are included in the article/Supplementary Material. Further inquiries can be directed to the corresponding author.

Ethics statement

The animal study was reviewed and approved by Ethical Committee on Animal Use of Butantan Institute (Protocol number: 5135010819).

Author contributions

MT, DR, AK and LL conceived and designed the experiments; MT, LM-N and SE performed the experiments and collected data; MT, LM-N, DR, AK, SE, AC-T and LL processed and analyzed the data; MT, LM-N, DR, AK, SE and LL wrote the manuscript, and all authors critically revised the manuscript. All authors contributed to the article and approved the submitted version.

Funding

We acknowledge the support from FAPESP (Projects 2017/24832-6, 2019/06454-0 and 2019/02305-0) and Fundação Butantan.

Conflict of interest

LL has a patent application on the use of rBCG-LTAK63 as vaccine against Mtb.

The remaining authors declare that the research was conducted in the absence of any commercial or financial relationships that could be construed as a potential conflict of interest.

Publisher's note

Supplementary material

The Supplementary Material for this article can be found online at: https://www.frontiersin.org/articles/10.3389/fimmu.2022.943558/full#supplementary-material

References

1. World Health O. *Global tuberculosis report 2021*. Geneva: World Health Organization (2021).

2. Tiberi S, du Plessis N, Walzl G, Vjecha MJ, Rao M, Ntoumi F, et al. Tuberculosis: Progress and advances in development of new drugs, treatment regimens, and host-directed therapies. *Lancet Infect Dis* (2018) 18:e183–98. doi: 10.1016/S1473-3099(18)30110-5

3. Sable SB, Posey JE, Scriba TJ. Tuberculosis vaccine development: Progress in clinical evaluation. *Clin Microbiol Rev* (2022) 33:e00100–19. doi: 10.1128/CMR.00100-19

4. Gong W, Liang Y, Wu X. The current status, challenges, and future developments of new tuberculosis vaccines. *Hum Vaccin Immunother* (2018) 14:1697–716. doi: 10.1080/21645515.2018.1458806

5. Stanford JL, Bahr GM, Rook GAW, Shaaban MA, Chugh TD, Gabriel M, et al. Immunotherapy with mycobacterium vaccae as an adjunct to chemotherapy in the treatment of pulmonary tuberculosis. *Tubercle* (1990) 71:87–93. doi: 10.1016/0041-3879(90)90002-P

6. Cardona P-J. RUTI: A new chance to shorten the treatment of latent tuberculosis infection. *Tuberculosis* (2006) 86:273–89. doi: 10.1016/j.tube.2006.01.024

7. Gupta A, Ahmad FJ, Ahmad F, Gupta UD, Natarajan M, Katoch V, et al. Efficacy of mycobacterium indicus pranii immunotherapy as an adjunct to chemotherapy for tuberculosis and underlying immune responses in the lung. *PloS One* (2012) 7:e39215. doi: 10.1371/journal.pone.0039215

8. Coler RN, Bertholet S, Pine SO, Orr MT, Reese V, Windish HP, et al. Therapeutic immunization against mycobacterium tuberculosis is an effective adjunct to antibiotic treatment. *J Infect Dis* (2013) 207:1242–52. doi: 10.1093/infdis/jis425

9. Nell AS, D'lom E, Bouic P, Sabaté M, Bosser R, Picas J, et al. Safety, tolerability, and immunogenicity of the novel antituberculous vaccine RUTI: Randomized, placebo-controlled phase II clinical trial in patients with latent tuberculosis infection. *PloS One* (2014) 9:e89612. doi: 10.1371/journal.pone.0089612

10. Huang CY, Hsieh WY. Efficacy of mycobacterium vaccae immunotherapy for patients with tuberculosis: A systematic review and meta-analysis. *Hum Vaccines Immunother* (2017) 13:1960–71. doi: 10.1080/21645515.2017.1335374

11. Barber DL. Vaccination for mycobacterium tuberculosis infection: reprogramming CD4 T-cell homing into the lung. *Mucosal Immunol* (2017) 10:318–21. doi: 10.1038/mi.2016.110

12. Nascimento IP, Rodriguez D, Santos CC, Amaral EP, Rofatto HK, Junqueira-Kipnis AP, et al. Recombinant BCG expressing LTAK63 adjuvant induces superior protection against mycobacterium tuberculosis. *Sci Rep* (2017) 7:2109. doi: 10.1038/s41598-017-02003-9

13. Carvalho Dos Santos C, Rodriguez D, Kanno Issamu A, Cezar De Cerqueira Leite L, Pereira Nascimento I. Recombinant BCG expressing the LTAK63 adjuvant induces increased early and long-term immune responses against mycobacteria. *Hum Vaccin Immunother* (2020) 16:673–83. doi: 10.1080/21645515.2019.1669414

14. Rodrigues RF, Zárate-Bladés CR, Rios WM, Soares LS, Souza PRM, Brandão IT, et al. Synergy of chemotherapy and immunotherapy revealed by a genome-scale analysis of murine tuberculosis. *J Antimicrob Chemother* (2014) 70:1774–83. doi: 10.1093/jac/dkv023

15. Liang Y, Zhao Y, Bai X, Xiao L, Yang Y, Zhang J, et al. Immunotherapeutic effects of mycobacterium tuberculosis rv3407 DNA vaccine in mice. *Autoimmunity* (2018) 51:417–22. doi: 10.1080/08916934.2018.1546291

16. Trentini MM, de Oliveira FM, Kipnis A, Junqueira-Kipnis AP. The role of neutrophils in the induction of specific Th1 and Th17 during vaccination against tuberculosis. *Front Microbiol* (2016) 7:898. doi: 10.3389/fmicb.2016.00898

17. Kim WS, Kim JS, Cha SB, Han SJ, Kim H, Kwon KW, et al. Virulence-dependent alterations in the kinetics of immune cells during pulmonary infection by mycobacterium tuberculosis. *PloS One* (2015) 10:1–20. doi: 10.1371/journal.pone.0145234

18. Mukundan R. Analysis of image feature characteristics for automated scoring of HER2 in histology slides. *J Imaging* (2019) 5(3):35. doi: 10.3390/jimaging5030035

19. Moraes L, Trentini MM, Fousteris D, Eto SF, Chudzinski-Tavassi AM, Leite LC de C, et al. CRISPR/Cas9 approach to generate an auxotrophic BCG strain for unmarked expression of LTAK63 adjuvant: A tuberculosis vaccine candidate. *Front Immunol* (2022) 13:867195. doi: 10.3389/fimmu.2022.867195

20. Logan KE, Gavier-Widen D, Hewinson RG, Hogarth PJ. Development of a mycobacterium bovis intranasal challenge model in mice. *Tuberculosis* (2008) 88:437–43. doi: 10.1016/j.tube.2008.05.005

21. Vilaplana C, Cardona PJ. Tuberculin immunotherapy: Its history and lessons to be learned. *Microbes Infect* (2010) 12:99–105. doi: 10.1016/j.micinf.2009.10.006

22. Sharma SK, Katoch K, Sarin R, Balambal R, Kumar Jain N, Patel N, et al. Efficacy and safety of mycobacterium indicus pranii as an adjunct therapy in category II pulmonary tuberculosis in a randomized trial. *Sci Rep* (2017) 7:1–12. doi: 10.1038/s41598-017-03514-1

23. Dlugovitzky D, Stanford C, Stanford J. Immunological basis for the introduction of immunotherapy with mycobacterium vaccae into the routine treatment of TB. *Immunotherapy* (2011) 3:557–68. doi: 10.2217/imt.11.6

24. Skinner MA, Yuan S, Prestidge R, Chuk D, Watson JD, Tan PL. Immunization with heat-killed mycobacterium vaccae stimulates CD8+ cytotoxic T cells specific for macrophages infected with mycobacterium tuberculosis. *Infect Immun* (1997) 65:4525–30. doi: 10.1128/iai.65.11.4525-4530.1997

25. Das S, Chowdhury BP, Goswami A, Parveen S, Jawed J, Pal N, et al. Mycobacterium indicus pranii (MIP) mediated host protective intracellular mechanisms against tuberculosis infection: Involvement of TLR-4 mediated signaling. *Tuberculosis* (2016) 101:201–9. doi: 10.1016/j.tube.2016.09.027

26. Gengenbacher M, Nieuwenhuizen N, Vogelzang A, Liu H, Kaiser P, Schuerer S, et al. Deletion of nuoG from the vaccine candidate mycobacterium bovis BCG ΔureC::hly improves protection against tuberculosis. *MBio* (2016) 7:e00679–16. doi: 10.1128/mBio.00679-16

27. Haile M, Schröder U, Hamasur B, Pawlowski A, Jaxmar T, Källenius G, et al. Immunization with heat-killed mycobacterium bovis bacille calmette–guerin (BCG) in Eurocine™ L3 adjuvant protects against tuberculosis. *Vaccine* (2004) 22:1498–508. doi: 10.1016/j.vaccine.2003.10.016

28. Whelan AO, Wright DC, Chambers MA, Singh M, Hewinson RG, Vordermeier HM. Evidence for enhanced central memory priming by live mycobacterium bovis BCG vaccine in comparison with killed BCG formulations. *Vaccine* (2008) 26:166–73. doi: 10.1016/j.vaccine.2007.11.005

29. Karumbi J, Garner P. Directly observed therapy for treating tuberculosis. *Cochrane Database Syst Rev* (2015) 2015(5):CD003343. doi: 10.1002/14651858.CD003343.pub4

30. Munro SA, Lewin SA, Smith HJ, Engel ME, Fretheim A, Volmink J. Patient adherence to tuberculosis treatment: A systematic review of qualitative research. *PloS Med* (2007) 4:1230–45. doi: 10.1371/journal.pmed.0040238

31. Doherty TM. Immunotherapy for TB. *Immunotherapy* (2012) 4:629–47. doi: 10.2217/imt.12.52

32. Coussens A, Timms PM, Boucher BJ, Venton TR, Ashcroft AT, Skolimowska KH, et al. 1α,25-dihydroxyvitamin D3 inhibits matrix metalloproteinases induced by mycobacterium tuberculosis infection. *Immunology* (2009) 127:539–48. doi: 10.1111/j.1365-2567.2008.03024.x

33. Kolloli A, Subbian S. Host-directed therapeutic strategies for tuberculosis. *Front Med* (2017) 4:171. doi: 10.3389/fmed.2017.00171

34. Kumar R, Singh P, Kolloli A, Shi L, Bushkin Y, Tyagi S, et al. Immunometabolism of phagocytes during mycobacterium tuberculosis infection. *Front Mol Biosci* (2019) 6:105. doi: 10.3389/fmolb.2019.00105

35. Dwivedi VP, Bhattacharya D, Yadav V, Singh DK, Kumar S, Singh M, et al. The phytochemical bergenin enhances T helper 1 responses and anti-mycobacterial immunity by activating the MAP kinase pathway in macrophages. *Front Cell Infect Microbiol* (2017) 7:149. doi: 10.3389/fcimb.2017.00149

36. Jeyanathan M, Yao Y, Afkhami S, Smaill F, Xing Z. New tuberculosis vaccine strategies: Taking aim at un-natural immunity. *Trends Immunol* (2018) 39:419–33. doi: 10.1016/j.it.2018.01.006

37. Beverley PCL, Ruzsics Z, Hey A, Hutchings C, Boos S, Bolinger B, et al. A novel murine cytomegalovirus vaccine vector protects against mycobacterium tuberculosis. *J Immunol* (2014) 193:2306–16. doi: 10.4049/jimmunol.1302523

38. Power CA, Wei G, Bretscher PA. Mycobacterial dose defines the Th1/Th2 nature of the immune response independently of whether immunization is administered by the intravenous, subcutaneous, or intradermal route. *Infect Immun* (1998) 66(12):5743–50. doi: 10.1128/IAI.66.12.5743-5750.1998

39. Lyadova IV. Neutrophils in tuberculosis: Heterogeneity shapes the way? *Mediators Inflammation* (2017) 2017:8619307. doi: 10.1155/2017/8619307

40. Lyadova IV, Tsiganov EN, Kapina MA, Shepelkova GS, Sosunov VV, Radaeva TV, et al. In mice, tuberculosis progression is associated with intensive inflammatory response and the accumulation of gr-1dim cells in the lungs. *PloS One* (2010) 5(5):e10469. doi: 10.1371/journal.pone.0010469

41. Sia JK, Rengarajan J. Immunology of mycobacterium tuberculosis infections. *Microbiol Spectr* (2019) 7(4). doi: 10.1128/microbiolspec.GPP3-0022-2018

42. Ehlers S, Schaible U. The granuloma in tuberculosis: Dynamics of a host–pathogen collusion. *Front Immunol* (2013) 3:411. doi: 10.3389/fimmu.2012.00411

frontiers | Frontiers in Immunology

TYPE Original Research
PUBLISHED 07 December 2022
DOI 10.3389/fimmu.2022.1025931

OPEN ACCESS

EDITED BY
Hao Li,
China Agricultural University, China

REVIEWED BY
Bingdong Zhu,
Lanzhou University, China
Wanyan Deng,
Chongqing Medical University, China

*CORRESPONDENCE
Ying Xu
yingxu2520@fudan.edu.cn
Wenhong Zhang
zhangwenhong@fudan.edu.cn

SPECIALTY SECTION
This article was submitted to Vaccines and Molecular Therapeutics, a section of the journal Frontiers in Immunology

RECEIVED 23 August 2022
ACCEPTED 18 November 2022
PUBLISHED 07 December 2022

CITATION
Weng S, Zhang J, Ma H, Zhou J, Jia L, Wan Y, Cui P, Ruan Q, Shao L, Wu J, Wang H, Zhang W and Xu Y (2022) B21 DNA vaccine expressing ag85b, rv2029c, and rv1738 confers a robust therapeutic effect against latent *Mycobacterium tuberculosis* infection. *Front. Immunol.* 13:1025931. doi: 10.3389/fimmu.2022.1025931

B21 DNA vaccine expressing ag85b, rv2029c, and rv1738 confers a robust therapeutic effect against latent *Mycobacterium tuberculosis* infection

Shufeng Weng[1], Jinyi Zhang[1], Huixia Ma[1], Jingyu Zhou[2], Liqiu Jia[2], Yanmin Wan[1,2], Peng Cui[1,2], Qiaoling Ruan[2], Lingyun Shao[2], Jing Wu[2], Honghai Wang[1], Wenhong Zhang[2,3,4]* and Ying Xu[1,5]*

[1]State Key Laboratory of Genetic Engineering, Institute of Genetics, School of Life Science, Fudan University, Shanghai, China, [2]Department of Infectious Diseases, Shanghai Key Laboratory of Infectious Diseases and Biosafety Emergency Response, National Medical Center for Infectious Diseases, Huashan Hospital, Fudan University, Shanghai, China, [3]National Clinical Research Center for Aging and Medicine, Huashan Hospital, Fudan University, Shanghai, China, [4]Key Laboratory of Medical Molecular Virology (MOE/MOH), Shanghai Medical College, Fudan University, Shanghai, China, [5]Shanghai Huashen Institute of Microbes and Infections, Shanghai, China

Latent tuberculosis infection (LTBI) treatment is known to accelerate the decline in TB incidence, especially in high-risk populations. *Mycobacterium tuberculosis* (*M. tb*) expression profiles differ at different growth periods, and vaccines protective and therapeutic effects may increase when they include antigenic compositions from different periods. To develop a post-exposure vaccine that targets LTBI, we constructed four therapeutic DNA vaccines (*A39*, *B37*, *B31*, and *B21*) using different combinations of antigens from the proliferation phase (Ag85A, Ag85B), PE/PPE family (Rv3425), and latent phase (Rv2029c, Rv1813c, Rv1738). We compared the immunogenicity of the four DNA vaccines in C57BL/6j mice. The *B21* vaccine stimulated the strongest cellular immune responses, namely Th1/Th17 and $CD8^+$ cytotoxic T lymphocyte responses. It also induced the generation of strengthened effector memory and central memory T cells. In latently infected mice, the *B21* vaccine significantly reduced bacterial loads in the spleens and lungs and decreased lung pathology. In conclusion, the *B21* DNA vaccine can enhance T cell responses and control the reactivation of LTBI.

KEYWORDS

DNA vaccine, immunotherapy, *Mycobacterium tuberculosis*, LTBI, *B21* DNA

Introduction

Despite years of widespread use of the tuberculosis (TB) vaccine Bacillus Calmette-Guerin (BCG), TB still ranks among the deadliest infectious diseases (1, 2). HIV and *Mycobacterium tuberculosis* (*M. tb)* co-infection and the emergence of multidrug-resistant strains of *M. tb* is a worldwide concern (3, 4). About 10% of people who are infected go on to have active disease, usually within 1-2 years of exposure (5). The remaining people enter a latent phase (latent TB infection [LTBI]), and *M. tb* can be reactivated at a later stage, especially when the individual has impaired immune system (6). About 25% of the world's population is thought to be latently infected with *M. tb* (7, 8). Therefore, the control of latent *M. tb* infection is essential in TB outbreak investigations and disease control (9).

Patients with latent *M. tb* infections, which can express antigens different from those of active TB, are the main populations for which therapeutic TB vaccines are applied (10). *M. tb* mainly exists in the form of dormant bacilli during latent infections (11). In this condition, bacilli upregulate a 48-gene regulon known as the DosR regulon, which causes a reduction in RNA and protein synthesis (12, 13). Specific immune responses to latent antigens can be detected in patients with latent *M. tb* infection but not in the population vaccinated with BCG (14). A previous study proposed that a vaccine with the *M. tb* incubation period antigen as the target antigen would obtain a protective immune response to latent period TB infection, eliminate dormant bacilli, and prevent TB recurrence (15). DNA vaccines expressing latent antigens have also been shown to effectively induce Th1-type immune responses (16, 17). Additionally, it has been discovered that immunotherapy using plasmid DNA is an efficient adjuvant therapy in mice when combined with chemotherapy (18, 19). Antigen fusion in various TB-containing latency-related antigens has also been explored as a vaccine target. Baldwin et al. reported that *M. tb* fusion protein (ID83) expressing virulence-associated *M. tb* protein (Rv3620), PE/PPE (Rv2608) and latency-associated antigen (Rv1813) bound to a synthetic Toll-like receptor agonist induced Th1 immune response and protected mice from TB (20). The TB subunit vaccination H56, which contained the proliferative antigens Ag85B and ESAT-6 as well as the latent antigen Rv2660c, protected against both pre- and post-*M. tb* infection in nonhuman primates (21).

Among the many vaccines explored, Ag85A and Ag85B have been widely used as acute phase antigens, and related DNA vaccines have been demonstrated to have immunotherapeutic effects in mice (19, 22). Rv2029c (pfkB) is a member of the DosR regulator family and is upregulated during hypoxia and in macrophages (23). Antigen Rv2029c induces a higher frequency of $CD4^+$ and $CD8^+$ T cells producing IFN-γ and TNF-α in patients with long-term LTBI compared to that in patients with TB (24, 25). For the other two DosR-regulated antigens, Rv1813c stimulated the production of the pro-inflammatory cytokines IL-1β and IL-12 in mice (17), and Rv1738 is a potent cell-activated T antigen (26). In a previous study, the authors of the present study found that Rv3425 is sufficient to induce Th1 immunity (27).

In this study, we combined fragments of the aforementioned antigens to construct four DNA vaccines expressing three fusion proteins and compared the immunogenicity of several groups of vaccines in mouse models. One of the vaccines that we screened showed valid immunotherapeutic effects.

Materials and methods

Mice

All mice were housed under specific pathogen-free conditions at the Animal Center of the School of Life Sciences of Fudan University. All experimental procedures conformed to the Guidelines for the Care and Use of Laboratory Animals of the National Institutes of Health and were approved by the Animal Care and Use Ethical Committee of Fudan University. The animal ethical license number was 2019JS016.

In strict accordance with Fudan University biosafety rules, BCG vaccination and infection experiments were carried out in ABSL-2 laboratory, and *M. tb*-related investigations were carried out in ABSL-3 laboratory.

Bacteria and cell lines

The *Escherichia coli* DH5α strain was grown in LB media and used for the cloning and purification of plasmids, and the BL21 strain was used for protein purification. The rBGC30 for vaccination that overexpresses Rv3425 was constructed using the BCG Danish strain. *M. tb* H37Rv and BCG cultures were grown in 7H9 medium (Cat#271310, Difco, USA) supplemented with 10% OADC (oleic acid, albumin, dextrose, and catalase), 0.05% Tween 80, and 0.5% glycerol, and cultures were grown to mid-log phase. Aliquots of the cultures in 20% glycerol were preserved at -80°C, and these cryopreserved stocks were used for infections. HEK293T and RAW264.7 cells, used for transfection, were cultured in DMEM + 10% FBS.

Construction of latency DNA vaccines

The method of enzymatic ligation was used to construct pVAX1-*ag85a-rv3425-rv2029c* (*A39*), pVAX1-*ag85b-rv2029c-rv1738* (*B21*), pVAX1-*ag85b-rv3425-rv1813c* (*B31*), and pVAX1-*ag85a-rv3425-1738* (*B37*) DNA vaccines. Sequences

encoding Ag85A, Ag85B, Rv2029c, Rv3425, and Rv1738 were amplified from *M. tb* H37Rv by PCR using five pairs of primers (Supplementary Table 1, synthesized by Sangon Biotech Co., Ltd., Shanghai, China). Recombinant plasmid was constructed by ligating the first amplified fragment digested with restriction endonucleases (NheI, HindIII) to the linearized plasmid, the second fragment using HindIII and EcoRI, and the third fragment using EcoRI and NotI, respectively, to enable fusion expression of the three selected genes on the pVAX1 vector using the CMV promoter. DNA was sequenced by Shanghai Sangon and was found to conform to the designed sequences using BLAST analysis. An EndoFree Plasmid Purification Kit (Cat#12391, Qiagen, USA) was used to purify the DNA vaccines.

Preparation of recombinant fusion proteins

Three *M. tb* recombinant fusion proteins, the *A39*, *B31*, and *B21*-pET28a plasmids, were constructed, and the target proteins were obtained by affinity purification using Ni-nitrilotriacetic acid.

Transfection of HEK293T and RAW264.7 cells with DNA vaccines plasmid

In brief, HEK293T cells were cultured in 12-well plates at a density of 5×10^5 cells per well the day before transfection. When the cell growth reached 60%-70%, 2 μg of purified *A39*, *B21*, *B31*, *B37*, or pVAX1 plasmids were transfected into HEK293T cells using Lipofectamine 2000 (Cat#11668019, Invitrogen, USA). The 48h after transfection, the cells were lysed with NP-40 (with PMSF) to obtain whole cell lysate (WCL). RAW264.7 cells were transfected with jetPRIME (Cat#101000046, Polyplus, France) under the same conditions, and the cell supernatants were collected at 24, 48, and 72 h after transfection for cytokine detection.

Western blotting

WCL containing 10 μg of total protein was separated by SDS-PAGE (10% acrylamide gels) and then transferred onto a PVDF membrane (Cat# IPVH00010, Millipore, USA). After blocking with 5% skim milk for 2 h, the membrane was incubated with Ag85B (Cat#ab43019, Abcam, USA) or Rv3425 (in-house)-specific monoclonal antibody at a concentration of 1 μg/mL. After washing, membranes were incubated with HRP-conjugated goat anti-rabbit IgG antibody (Cat#SA00001-2, Proteintech, China) or HRP-conjugated goat anti-mouse IgG antibody (Cat#SA00001-1, Proteintech, China) diluted 1:8000 in TBST (Tris-buffered saline, pH8.0, 0.05% Tween 20) containing 5% skim milk. After washing, the bands were developed using an ultrasensitive ECL substrate (Cat#SQ201, Epizyme, China).

Immunization of DNA vaccines and acquisition splenic lymphocytes

Female C57BL/6j mice were divided into five groups (1): PBS as a negative control (100 μL); (2) vector pVAX1 as a negative control (50 μg/100 μL); (3) *A39* DNA (50 μg/100 μL); (4) *B21* DNA (50 μg/100 μL); and (5) *B31* DNA (50 μg/100 μL). Mice were immunized intramuscularly three times at 2-week intervals. At 16 weeks after immunization, ~1×10^7 CFU of BCG was injected *via* the tail vein, and at 4 weeks after the challenge, animals were sacrificed for bacterial counts in the spleens and lungs. PBMC and splenic lymphocytes were separated using lymphocyte separation medium (Cat#7211011, Dakewe, China), according to the manufacturer's instructions.

Detection of specific antibodies by enzyme-linked immunosorbent assay (ELISA)

An ELISA was used to detect the levels of specific antibodies in the sera of immunized mice. High-binding 96-well EIA plates (Cat# 9018, Corning, USA) were coated with purified A39, B21, and B31 proteins at a final concentration of 2 μg/mL in coating buffer (30 mM $NaHCO_3$,10 mM Na_2CO_3, pH 9.6), which was then washed with PBS and blocked with 5% bovine serum albumin in PBS for 1 h at 37°C. After washing with PBS, the plate was treated with serum derived from the immunized mice as the primary antibody (1:1000) and HRP-conjugated goat anti-mouse IgG (1:10000; Cat#SA00001-1, Proteintech, China) as the secondary antibody. 3,3′,5,5′-Tetramethylbenzidine (Cat#PR1200, Solarbio, China) as the substrate was added to each well for 10 min, and H_2SO_4 (2M) was added to stop the reaction. The optical density was measured at a wavelength of 450 nm. To evaluate the titers of IgG1 and IgG2b, IgG2b (Cat#ab97250, Abcam, USA) and IgG1(Cat#ab97240, Abcam, USA) were used as secondary antibodies.

Detections of fusion protein-specific cellular immune responses

Fusion protein-specific IFN-γ secreting cells were measured using enzyme-linked immunosorbent spot (ELISPOT) assays, according to the manufacturer's instructions (Cat#CT317-PR2, U-CyTech, Netherlands). Spots representing IFN-γ-producing cells were enumerated using an automated ELISPOT plate reader (ChampSpot III Elispot Reader; Saizhi). Additionally, the supernatants in the wells of ELISPOT plates were collected

to detect secreted cytokines using a Mouse IL-2 ELISA array kit (Cat#1210203, Dakewe, China), TNF-α ELISA array kit (Cat#1217202, Dakewe, China), and IL-1β ELISA array kit (Cat#1210122, Dakewe, China).

Flow cytometry

Live cells were discriminated using a live/dead fixable aqua-dead cell stain (Cat# 423107, BioLegend, USA). To stain T cells, splenocytes (2×10^6 cells/well) were cultured in 96-well U-bottom plates with RPMI+10% FBS for 16 h, with or without fusion protein (5 μg/mL). Cells stimulated for 6 h with phorbol myristate acetate (Cat#P1585, Sigma-Aldrich, USA) and ionomycin (Cat#I3909, Sigma-Aldrich, USA) were used as positive controls. Brefeldin A (BFA, final concentration: 5μg/mL; Cat# HY-16592, MCE, China) was added during the last 5 h of culture.

After washing, anti-CD3ϵ PerCP-Cy5.5 (Cat#155615, BioLegend, USA), anti-CD4 BV510 (Cat#100559, BioLegend, USA), anti-CD8a FITC (Cat#100705, BioLegend, USA), anti-CD154 PE-Cy7 (Cat#106511, BioLegend, USA), anti-CD44 BV605 (Cat#103047, BioLegend, USA), and anti-CD62L PE-Cy7(Cat#104417, BioLegend, USA) were used to stain surface markers. Murine anti-CD107a AF700 (Cat#121627, BioLegend, USA), anti-IL-4 APC (Cat#504105, BioLegend, USA), anti-IFN-γ BV605 (Cat#505840, BioLegend, USA), anti-IL-17A PE (Cat#506903, BioLegend, USA), and anti-Ki-67 BV421 (Cat#652411, BioLegend, USA) were stained intracellularly with Cyto-Fast™ Fix/Perm (Cat#426803, BioLegend, USA) or True-Nuclear™ Transcription Factor Buffer Set (Cat#424401, BioLegend, USA), according to the manufacturer's instructions. To aid in data processing, FMO controls and isotype controls were applied.

Staining for cell-surface markers was performed by resuspending in 100μL of PBS with 2% FBS containing the antibody mixture at 4°C for 30 min and then washing with PBS containing 2% FBS. Data were immediately acquired using a BD Fortessa flow cytometer (BD Biosciences). The data were analyzed using FlowJo V10 software (BD Biosciences).

Treatment of TB-infected mice

Latent infection models were established as previously described (28). Thirty 6-week-old female BALB/c mice were immunized subcutaneously with ~5×10^6 CFU rBCG30 and 6 weeks after immunization were infected with ~100 CFU *M. tb* H37Rv intranasally. They were subsequently randomly divided into three groups, and then injected intramuscularly twice after 5 weeks, with a time interval of 2 weeks as follows: (1) the treatment group was injected with 60 μg *B21* DNA in 60 μL of PBS, and (2) the negative control group was injected with 60 μL of PBS or 60 μg pVAX1 DNA. Bacterial burden was estimated by plating serial dilutions of lungs and spleens homogenates on 7H10 agar (Cat#262710, Difco, USA) plates as indicated. The CFU were counted after 21 days. Selected lung tissues were fixed with 4% paraformaldehyde, embedded in paraffin, and evaluated histologically using H&E staining. Pathological evaluation of pulmonary parenchymalization, alveolar wall thickening, and inflammatory cell infiltration was performed using a four-level grading system.

Statistical analysis

All statistical analyses were performed using GraphPad Prism 8 (GraphPad Software Inc., La Jolla, CA, USA). Comparisons between two groups were conducted using *t* tests. Comparisons between three or more groups were performed using one-way ANOVA. $P<0.05$ was considered to indicate statistical significance.

Results

Preparations of latency DNA vaccine

The nucleotide sequences of the four recombinant plasmids expressing antigens pVAX1-*ag85a-rv3425-rv2029c* (*A39*), pVAX1-*ag85b-rv3425-rv1738* (*B37*), pVAX1-*ag85b-rv3425-rv1813c* (*B31*), and pVAX1-ag85b-rv2029c-rv1738 (*B21*) were identical to the designed H37Rv gene sequences (Figure 1A). Restriction enzyme-digested recombinant plasmids *A39*, *B37*, *B31*, and *B21* were resolved by electrophoresis on a 1.0% agarose gel, and the fragment sizes corresponded to the expected 2560 bp, 1786 bp, 1933 bp, and 2283 bp products, respectively (Figure S1). This result confirmed that the recombinant plasmids of the four fusion proteins were successfully constructed. WB recognition reactions were performed with antibodies against Rv3425 and Ag85B for the expression of recombinant proteins after transfecting the constructed vaccines into HEK293T cells. These results demonstrated that all four constructed DNA vaccines expressed complete recombinant proteins (Figure 1B). The ability of the candidate vaccine to activate the macrophages was evaluated *in vitro*. After the transfection of the plasmid into RAW264.7 cells, the contents of TNF-α and IL-6 in the supernatant were detected at 24, 48, and 72 h (Figure 1C). The secretion of TNF-α and IL-6 from B21-, B31-, and A39-transfected cells was significantly increased and higher than that of B37- and vector-transfected cells at 72 h. The results illustrated that the *B21*, *B31*, and *A39* vaccines, but not for the *B37* vaccine, can significantly activate macrophages; therefore, *B37* was discarded in the subsequent immunogenicity evaluation.

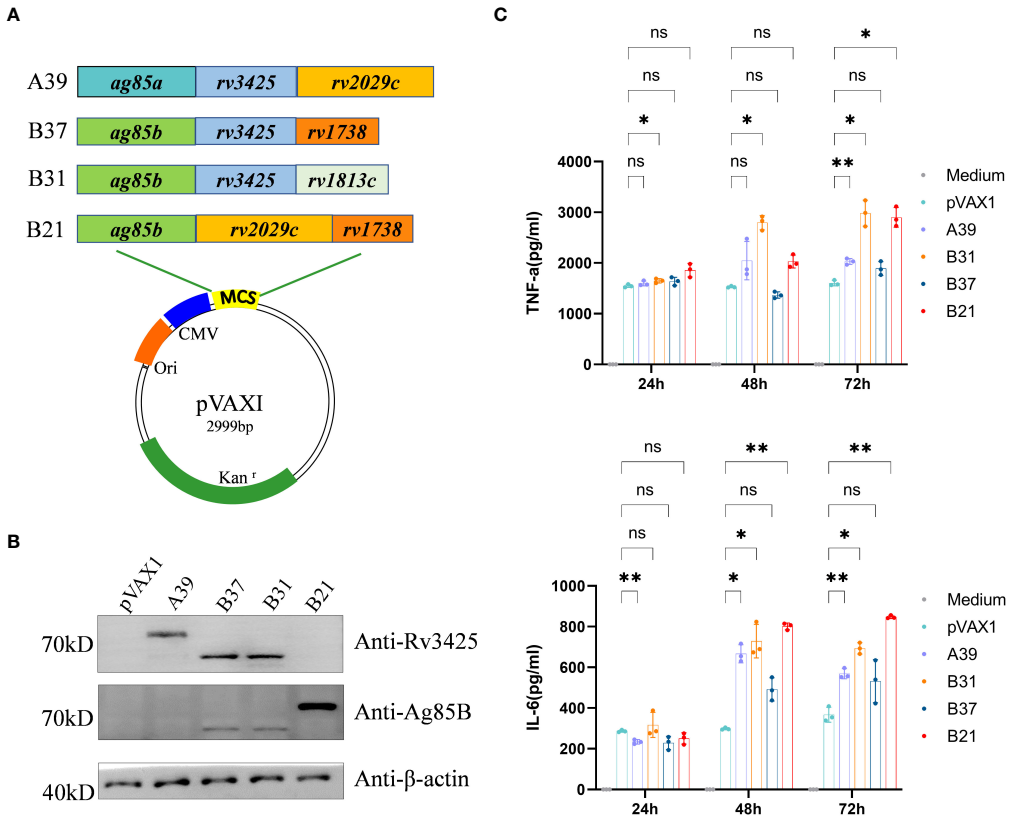

FIGURE 1
Construction of vaccine plasmids that can express fusion proteins. **(A)** Schematic of the candidate DNA vaccine construction strategy. Enzymatic ligation was used to introduce the matching pre-defined *M. tb* antigen fragment into the multiple cloning site (MCS) of the *pVAXI* plasmid. **(B)** HEK293T cells were transfected with the indicated plasmids, and the expression of fusion proteins was detected by Western blot. **(C)** RAW264.7 cells were transfected with recombinant plasmids, and secretion of TNF-α and IL-6 was detected by ELISA. Data are shown as mean±SD, n = 3. Statistical analyses performed by two-way ANOVA (ns, No significance; *$P < 0.05$; **$P < 0.01$).

DNA vaccine stimulated specific antibody production in mice

Using a mouse model, we examined the vaccine's immunogenicity (Figure 2A). Protective antibodies may promote and increase the death of intracellular bacteria through FcR-mediated phagocytosis and improve immune responses through the rapid adsorption and processing of antigens (29). Therefore, we purified the fusion protein for the evaluation of serum antibody levels in mice after immunization (Figure S2). Compared with the vector group, the anti-A39 protein, anti-B31 protein, and anti-B21 protein IgG (Figures 2B–D), IgG1 (Figures 2E–G), and IgG2b (Figures 2H–J) antibody levels in the *A39* DNA, *B31* DNA, and *B21* DNA groups were significantly increased. All antibodies, except for the anti-A39 protein IgG antibody, exhibited higher levels at 4 weeks post-immunization than at 2 weeks post-immunization. We found the IgG level of a single protein in the serum of immunized mice in addition to the fusion protein (Figure S3). According to the findings, vaccination also causes unique antibodies that can identify each fusion protein component. The ratio of IgG2b/IgG1 was calculated to determine the induction of Th1/Th2 responses in animals. The IgG2b/IgG1 ratio was higher in the *A39* and *B21* vaccine groups than in the *B31* vaccine group, and for *A39* and *B21*, the Th1 response based on antibody levels was stronger in *A39* than in *B21*(Figure S4).

Cytokine response was induced by DNA vaccines in mouse splenocytes

In addition to the antibody assay, we also compared the fusion protein-specific T cell response in each group at 2 and 4 weeks after the end of immunization. Splenic lymphocytes were isolated and stimulated *in vitro* with fusion proteins A39, B21, B31, PBS (negative control), or P/I (positive control) for 16 h. The results showed that the candidate DNA vaccine could

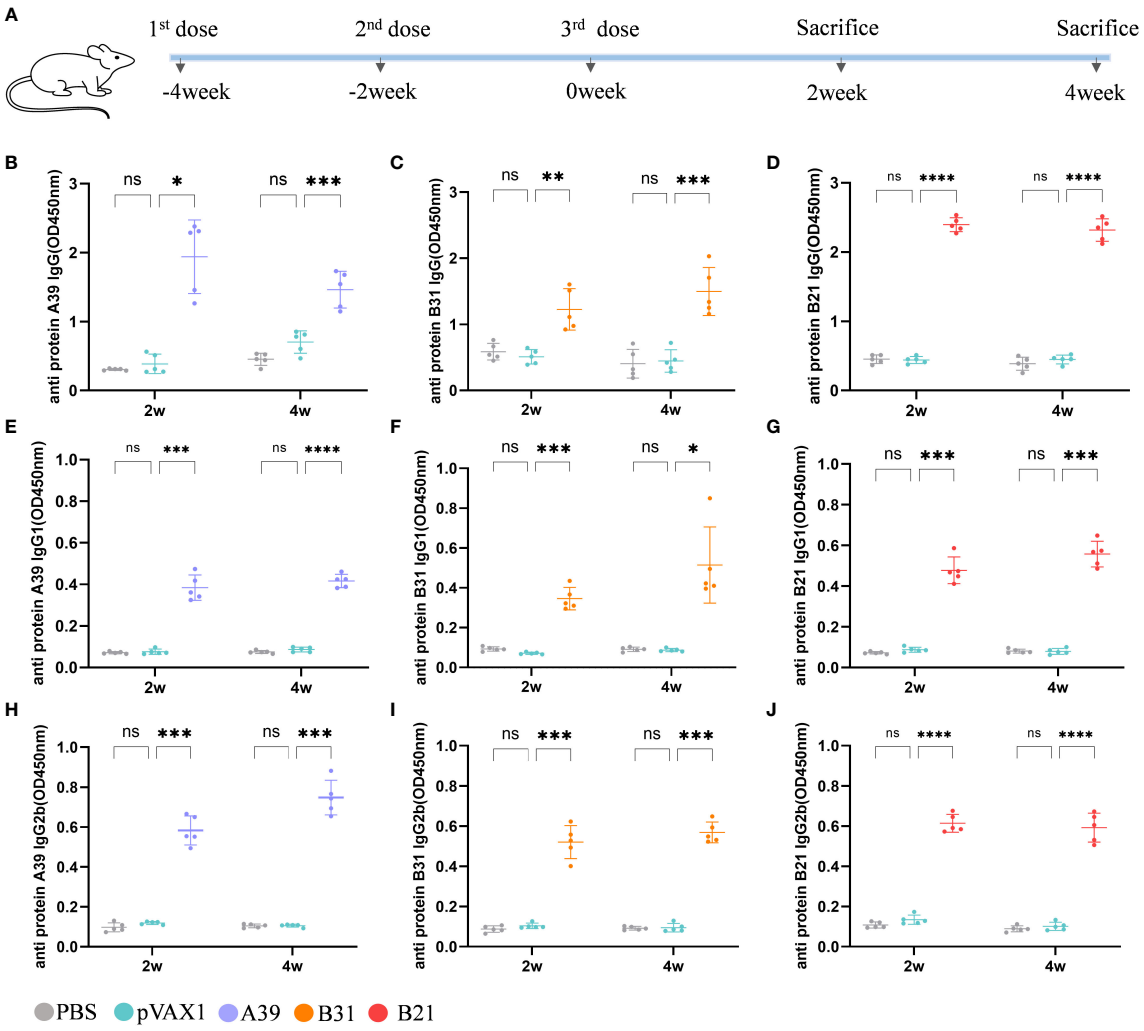

FIGURE 2
Analysis of antibodies in the serum of immunized mice. Levels of antibody detected by ELISA at 2 and 4 weeks after immunization. Samples were diluted 1/1000 in PBS buffer. **(A)** Schedule for DNA vaccine immunization in mice. **(B-D)** Anti A39, B31, B21 protein IgG antibody; **(E-G)** Anti A39, B31, B21 protein IgG1 antibody; **(H-J)** Anti A39, B31, B21 protein IgG2b antibody. Data are shown as mean±SD, n = 5. Statistical analyses performed by two-way ANOVA (ns, No significance; *$P < 0.05$; **$P < 0.01$; ***$P < 0.001$; ****$P < 0.0001$).

induce a strong fusion protein-specific T cell response. Among the candidate vaccines, the *B21* vaccine showed the best immune response. First, *B21*-immunized mice produced the strongest protein-specific IFN-γ^+ T cell responses (Figures 3A, B), and second, mouse splenocytes immunized with *B21* released more TNF-α, IL-2, and IL-1β, and showed a stronger T cell response to B21 protein. The specific responses of *A39* and *B31* were also significantly stronger than those of the control group but slightly weaker than those of *B21* (Figure 3C). Mice in the PBS and vector groups showed no fusion protein-specific T cell responses. When stimulated with a single protein, the same results were obtained as for the fusion protein stimulation that the immunized mouse splenocytes showed a strong immune response against the antigen (Figure S5).

DNA vaccines elevated adaptive immunity in the mouse spleens

To further characterize the host cellular immune response generated by vaccination, the T cell subsets of splenic lymphocytes were assessed using flow cytometry (Figure S6). Because the type I immune response generated after vaccination is essential for the prevention of TB, we first assessed the ratios of Th1 and Th2 cells. The results showed that the response rate of $CD4^+$T cells expressing IFN-γ (Th1) in the spleen lymphoid tissue of the candidate DNA groups to the fusion protein was significantly higher than that of the PBS and vector groups. The *B31* vaccine induced the production of a higher proportion of $CD4^+$IFN-γ^+ cells (Figure 4A), and for $CD4^+$T cells expressing

10.3389/fimmu.2022.1025931

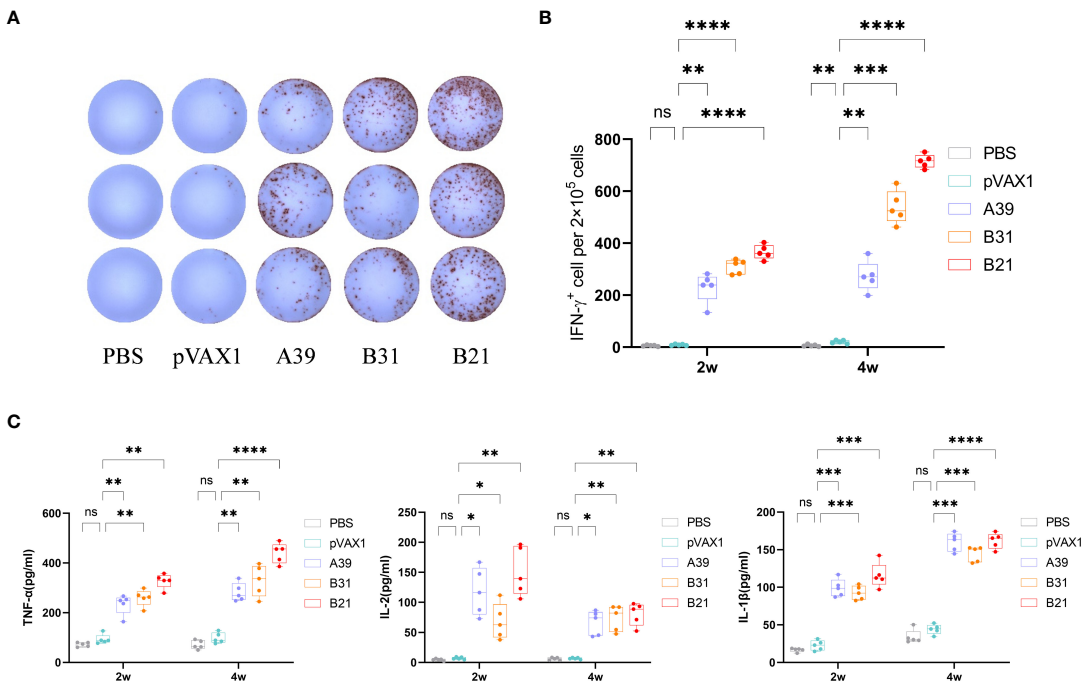

FIGURE 3
Measurement of cytokine production. Two weeks after immunization, mouse splenocytes were stimulated *in vitro* with fusion proteins A39, B31, B21 (5 μg/mL), P/I or PBS for 16 h. Antigen-specific IFN-γ secreting cells were measured by ELISPOT; cytokines in the supernatant were detected using ELISA. **(A)** Display of IFN-γ specific spot forming cells. Three representative samples from each group were selected for the showcase. **(B)** IFN-γ responses between groups were compared. **(C)** Specific release of TNF-α, IL-2, and IL-1β between groups. Data are shown as mean±SD, n = 5. Statistical analyses performed by one-way ANOVA (ns, No significance; *$P < 0.05$; **$P < 0.01$; ***$P < 0.001$; ****$P < 0.0001$).

IL-4 (Th2), no significant difference was observed between the vaccine and control groups (Figure S7A).

In addition, IL-17 and Th17 responses have become important factors in protective immunity against TB (30), with the proportion of Th17 cells being significantly higher in the *B21* vaccine group than in the other groups (Figure 4B). Furthermore, the CD40-CD40L (CD154) pathway is vital for enhancing the adaptive immune response to TB (31), and all vaccine candidates showed significantly increased CD154 expression on the surface of $CD4^+$T cells (Figure 4C). TB is a cellular immune response-mediated disease that includes antigen-specific IFN-γ and $CD8^+$ T cell-mediated cytotoxic responses. Additionally, *in vitro* and *in vivo* data support that $CD8^+$ T cells can produce an antigen-specific CTL function to inhibit bacterial growth. The results of this study showed a significant increase in the percentage of detected and $CD8^+$IFN-γ^+ T cells when the vaccine was immunized compared with that in control animals (Figure 4D).

Also evaluated was the cytotoxic potential of specific $CD8^+$ T cells amplified by immunization. Candidate vaccine immunization induced $CD8^+$ T lymphocytes to express CD107a, it may encourage CTL and target cell interaction and fusion. Similarly, the *B21* vaccine induced greater specific CTL activity (Figure 4E). Furthermore, when the percentage of induced $CD8^+$IFN-$\gamma^+$$CD107a^+$ cells in immunized mice was analyzed, a strengthened immune effect induced by *B21* was also observed (Figure 4F). We obtained results comparable to this proportion 4 weeks after vaccination (Figure S7). In summary, these results demonstrated that the *B21* vaccine was relatively more potent in activating helper T cells (Th1 and Th17) and CTLs than the *A39* and *B31* vaccines to provide superior immune protection.

DNA vaccines established a long-term immune reaction

Specific memory T cells are important for the long-term effects of vaccines. For spleen lymphocytes, after restimulation *in vitro*, the proportions of $CD4^+$ central memory T cells (T_{CM}, $CD44^+CD62L^+$) and effector memory T cells (T_{EM}, $CD44^+CD62L^-$) in the *B21* vaccine group were significantly increased, whereas there was a

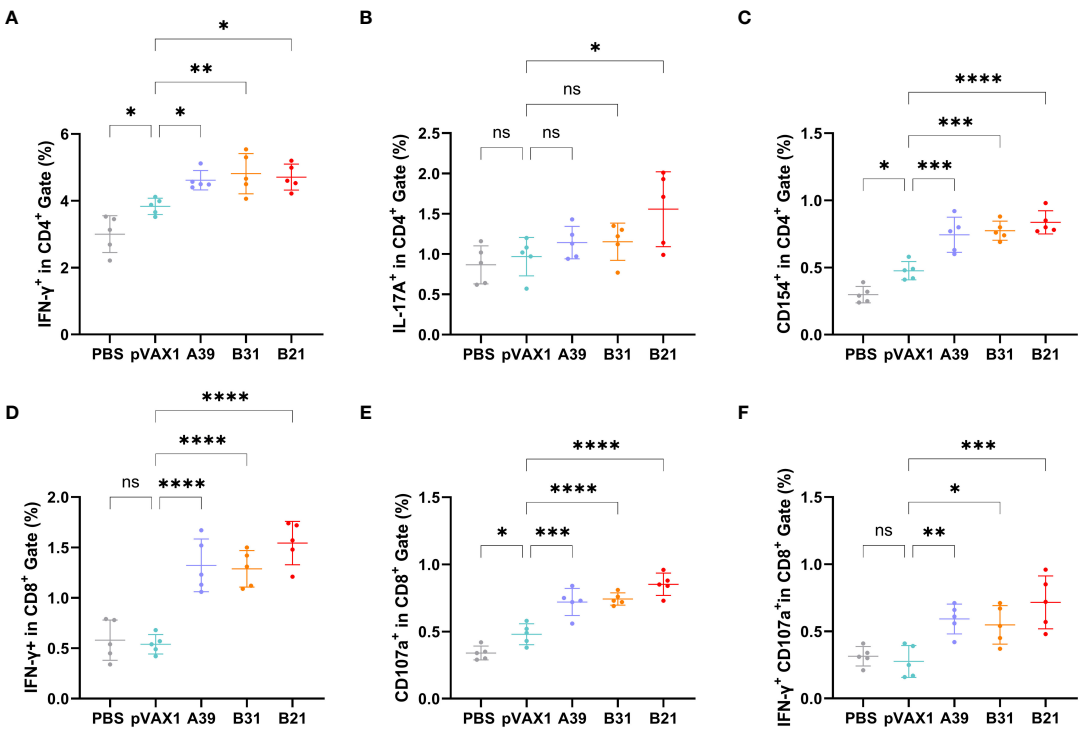

FIGURE 4
Frequency of T cell subsets in splenocytes assessed by flow cytometry. Two weeks after immunization, spleen lymphocytes isolated from vaccine and control mice were stimulated *in vitro* with the fusion protein for 16 h. Representative dot plots are shown for **(A)** % IFN-γ^+ cells in $CD4^+$ T cell subset, **(B)** % IL-$17A^+$cells in $CD4^+$ T cell subset, **(C)** % $CD154^+$cells in $CD4^+$ T cell subset, **(D)** % IFN-γ^+ cells in CD8+ T cell subset, **(E)** % $CD107a^+$ cells in $CD8^+$ T cell subset, and **(F)** % IFN-$\gamma^+CD107a^+$cells in $CD8^+$ T cell subset. Data are shown as mean±SD, n = 5. Statistical analyses were performed by one-way ANOVA (ns, No significance; *$P < 0.05$; **$P < 0.01$; ***$P < 0.001$; ****$P < 0.0001$).

trend for elevated proportions in the *A39* and *B31* groups, but the difference was not significant (Figure 5A). In the $CD8^+$ T cell population, only the central memory T cells in the *B21* group were significantly increased, and the effector memory T cells showed an increasing trend; however, there was no significant difference (Figure 5B). Additionally, we used the expression of Ki-67 as an indicator to evaluate T cell proliferation, in which the proliferative capacity of the *A39* and *B21* groups were significantly increased than that in the PBS and vector groups, and the *B31* group showed no significant change (Figure 5C).

To assess whether three vaccine strains could induce long-term immune responses against Mycobacterium spp., mice were infected with BCG at 16 weeks post-immunization and performed bacterial counts of the spleens and lungs tissues at 4 weeks post-infestation. The *B21* vaccine showed a considerable decrease in the lungs (Figure 5D) and spleens (Figure 5E) bacterial burdens among the vaccine candidates, which is comparable to the effects of cellular vaccination. The findings demonstrated that all of the candidate vaccines induced the development of memory T cells and destroyed Mycobacterium.

Therefore, the *B21* vaccine increased the proportion of memory T cells and established long-term immune protection.

The *B21* vaccine can effectively treat LTBI mice

We considered our findings demonstrating that vaccination with the *B21* vaccine induces a systemic immune response and then evaluated its therapeutic effect in latently infected mice (28, 32). To construct a latent infection model, at 6 weeks after immunization of mice with rBCG, the mice were administered *M. tb* by intranasal infection with approximately 100 CFU (Figure 6A). Six weeks after *M. tb* infection, we monitored the number of viable bacteria in the spleens and lungs to determine the successful establishment of the LTBI model, the data was largely consistent with previous reports (Figure 6B) (32). Colony counts were performed on the spleens and lungs at 2 and 4 weeks after intramuscular injection of the *B21* vaccine twice. In the spleens, *B21*-immunized mice showed a 0.52 and 0.95 $\log_{10}$ decrease in colony count compared with the PBS group at 2 and 4 weeks (Figure 6C); in the lung, it was decreased by 0.43 and 0.61 $\log_{10}$, respectively (Figure 6D). We also evaluated the pathological changes in the lungs using hematoxylin and eosin (H&E) staining (Figure 6E). Consistent with our expectations, lung sections showed clearly visible parenchyma and loss of

10.3389/fimmu.2022.1025931

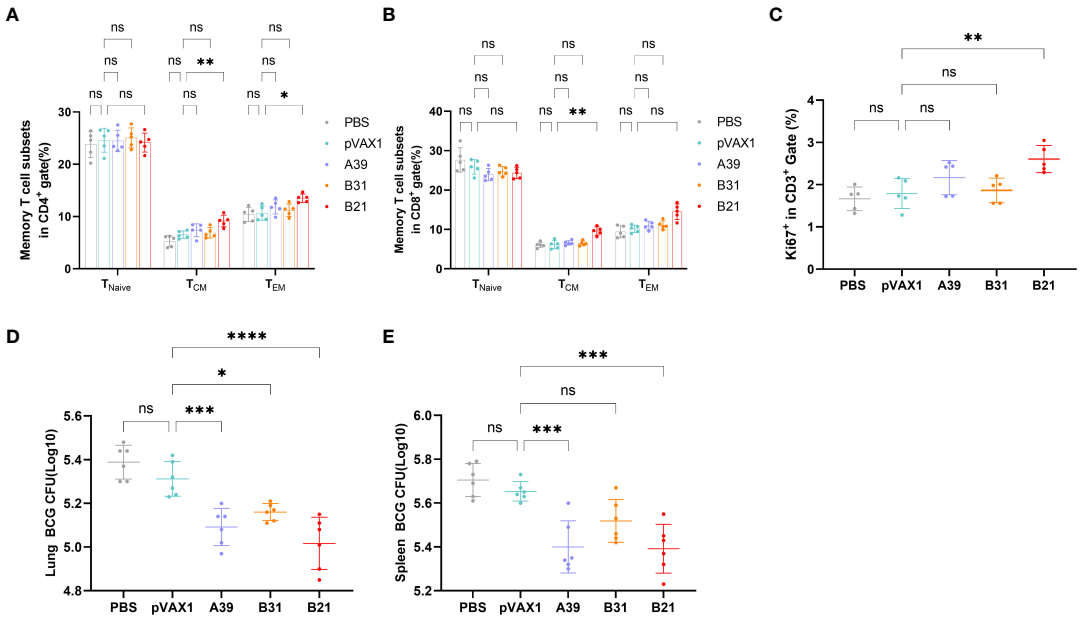

FIGURE 5
Specific memory T cells in Spleens detected by flow cytometry. **(A)** Proportion of T_{EM}($CD44^+CD62L^-$) and T_{CM} ($CD44^+CD62L^+$) in $CD4^+$ T cells. **(B)** Proportion of T_{EM}($CD44^+CD62L^-$) and T_{CM} ($CD44^+CD62L^+$) in $CD8^+$ T cells. Statistical analyses were performed by the method of two-way ANOVA. **(C)** Proportion of Ki-67^+ cells (one-way ANOVA). **(D, E)** Bacterial counts in the spleens and lungs of mice (one-way ANOVA). Data are shown as the mean±SD, n =5 /6. (ns, No significance; *$P < 0.05$; **$P < 0.01$; ***$P < 0.001$; ****$P < 0.0001$).

alveoli in the control lungs with numerous lymphocytes (red arrows), macrophages (green arrows), and neutrophils (yellow arrows) infiltrates; lung tissue from *B21*-treated mice showed mild focal alveolar wall thickening with individual neutrophil infiltrates (yellow arrows) and occasional small lymphocyte infiltrates around blood vessels (red arrows), indicated that animals given the *B21* booster vaccine had less inflammatory damage to their lungs than mice given the BCG vaccine alone. Pathology scores of the lungs also indicate that the *B21* vaccine was able to help the host resist bacterial infection (Figure 6F). Thus, the *B21* vaccine can control the reactivation of LTBI.

Discussion

Over the past ten years, significant progress has been made in the development of TB vaccines, and candidates for the first-generation TB vaccine are now in advanced clinical trials, diversifying the vaccine pipeline to maximize access to improved TB vaccines is necessary (33–35). Secreted proteins of *M. tb* play a critical role in the induction of protective immune responses during TB infection; this diversity can occur in the form of antigen composition, delivery vectors, and/or immune response function (36, 37). *M. tb* changes the expression of the repertoire of antigens from replication to dormancy in response to host immune pressure, and antigens expressed during different growth periods have different roles in activating effective immune protection (38, 39). A post-exposure vaccine that targets LTBI should include dominant antigens to protect against reactivation and early-stage secreted antigens to prevent bacilli replication and limit activity against dormant bacilli. Thus, finding the dominant antigen or optimal combination of antigens is an important part of vaccine construction (17). In this study, we used combinations of antigens from different growth periods of different *M. tb*, secretory proteins (Ag85A, Ag85B), PE/PPE family protein (Rv3425), and latency-associated proteins (Rv2029c, Rv1738, Rv1813c) to construct vaccine candidates with protective and therapeutic effects.

A change in the balance between host natural immunity and the pathogen can induce the development of active TB from latent infection and result in massive bacterial replication and reactivation of TB. For host natural immunity, one hypothetical reason for reactivation is that the T cell response is shifted from the Th1 pole toward the Th2 pole. An efficient post-exposure vaccine is required to lock specific T cells in the Th1 mode and suppress Th2 cell activity (40). IFN-γ, TNF-α, and IL-2 are produced by Th1 cells, and these molecules encourage the growth, maturation, and activation of macrophages and granulocytes. In our study, the *B21* vaccine promoted significantly more IFN-γ production than *A39* and *B31* did, and the levels of TNF-α and IL-2 secretion were also significantly increased at 2-and 4-weeks post-immunization in

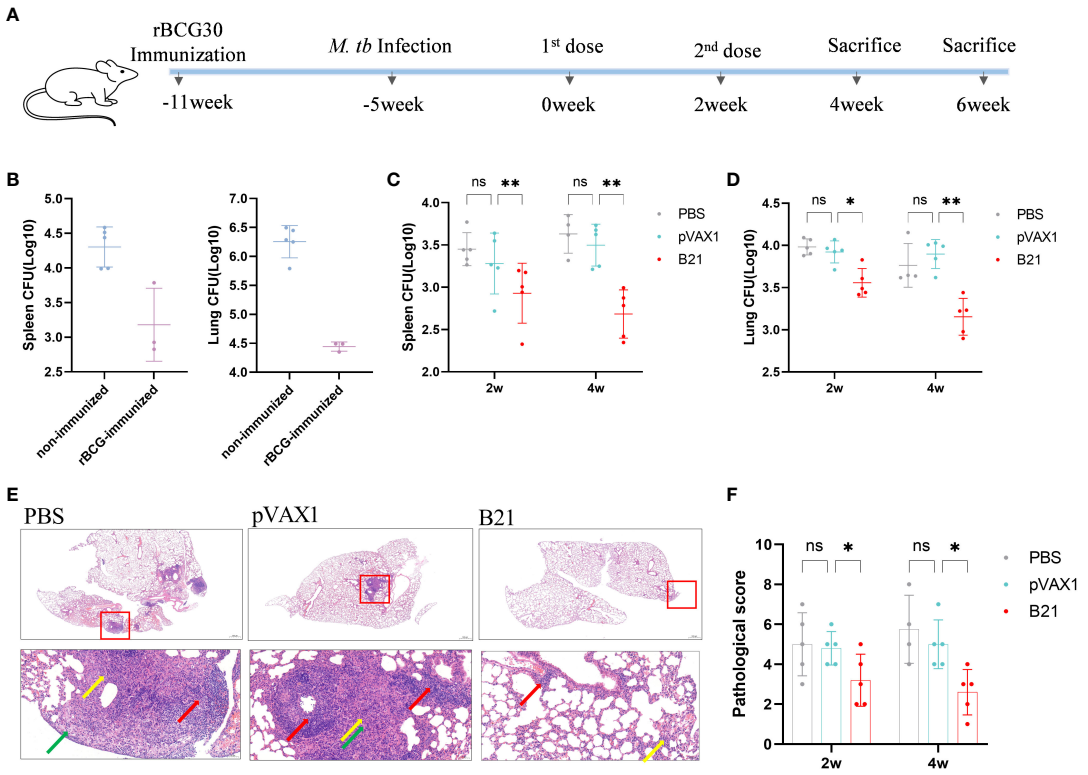

FIGURE 6
Detection of bacterial counts in the spleens and lungs tissues of mice after treatment. 2 and 4 weeks after the last treatment in the LTBI model, mice were sacrificed for tissue load counts. **(A)** Schedules of the preparation and treatment of mouse LTBI model. **(B)** non-immunized and rBCG-immunized mice were sacrificed 5 weeks after *M. tb* challenge, and lungs and spleens bacterial counts were measured. n=3/5. **(C, D)** Bacterial counts in the spleens and lungs of mice (two-way ANOVA). n = 4/5. Data are shown as mean±SD (ns, No significance; $^{*}P < 0.05$; $^{**}P < 0.01$). Lungs were collected 2 and 4 weeks after treatment, preserved in 4% paraformaldehyde, and processed for sectioning and staining with H&E. **(E)** Representative lung pathological changes from the different groups. Arrows mark lymphocytes (red arrows), macrophages (green arrows), and neutrophils (yellow arrows). Original magnification, 2x and 20x. **(F)** Pathological scoring of the lungs.

the *B21* vaccine group, which induced the response of T cells to Th1 polarization (Figure 3). Likewise, we used the antigen-specific IgG2b/IgG1 ratio as an indicator of the Th1 or Th2 response. The results showed that antigen-specific antibody response induced by *B31* and *B21* immunization was directed toward IgG2b, which is a Th1-type antibody isotype. Notably, IL-1β secretion was enhanced, and the percentage of IL-17A^{+}CD4^{+} cells was higher in *B21* mice than in the other groups. IL-1β contributes to Th17 differentiation (41), and the IL-17 family of proteins, which are secreted by Th17 cells, have a role in the recruitment of protective Th1 cells to the lungs following M. tuberculosis infection. Furthermore, the CD40-CD40L (CD154) pathway was shown to promote the proliferation of Th1 and Th17 cells (31, 42), and the *B21* vaccine had a significantly higher percentage of CD154^{+} cells (Figures 4D, E). Consequently, the B21 vaccine could enhance the Th1/Th17 response, which is necessary for vaccine-induced protection.

Mycobacterium tuberculosis is a typical intracellular pathogen, and T cell-mediated immune responses, comprising CD4^{+} T cells, CD8^{+} T cells, or both T cell subsets, are crucial for controlling the infection and postponing the onset of the disease (43, 44). The ability of CD4^{+} T cells to produce IFN-γ, which activates phagocytes to engulf intracellular pathogens, is central for protection. CD8^{+} T cells may modulate phagocyte activity or produce molecules, such as perforin, which mediate the killing of target cells and reduce bacterial survival (45).The results of this study demonstrated that *B21* and *B31* induced a significant increase in the CD3^{+} CD4^{+} IFN-γ^{+} population compared with the other groups. In assays with CTLs, the proportion of IFN-γ^{+} and CD107a^{+} cells were significantly increased in the *B21* immunized group of CD8^{+} cells. Throughout the infection, when a chronic infection is established, the role of the CD8^{+} T cell response increases is importance (46). Therefore, our results suggest that *B21* could elicit *M. tuberculosis*-specific CD4^{+} T cell responses, potentially increasing the protective efficacy and

enhancing $CD8^+$ CTLs. These reactions may reduce the bacterial load during chronic infection. This speculation was confirmed in the therapeutic study, and *B21* immunization induced a significant decrease in the bacterial load in both the spleens and lungs compared with the vector vaccination.

Another hypothesis for the reactivation of TB is that the persistence of *M. tuberculosis* could continuously drive naive T cells to differentiate into effector T cells, with no generation of immunological memory. For the clearance of latent infection, reactive T cells are expected to develop into memory T cells. CD44 is essential for the generation and maintenance of memory T cells (47). The present study illustrated that *B21*-immunized mice showed a significant increase in the number of $CD44^+$ T cells and exhibited the greatest capacity for the development of memory T cells. Additionally, long-term security depends on the development of immunological memory, and at 16 weeks after immunization, the *B21* vaccine still significantly reduced the bacterial count when BCG was used as a substitute strain of *M. tb* to challenge the mice. Therefore, the *B21* vaccine can induce long-lasting immune effects.

Based on the excellent immunogenicity demonstrated by the *B21* vaccine, we evaluated the therapeutic effect of the *B21* vaccine on LTBI. *B21*-treated mice showed a significant decrease in bacterial load in the spleens and lungs and exhibited less severe histopathology than control mice. These results suggest that the *B21* vaccine could limit *M. tb* reactivation and provide a significant therapeutic effect in LTBI mice. Neonatal BCG vaccination has been used to prevent tuberculosis in nations with a high tuberculosis burden, and BCG has been a part of the Expanded Program on Immunization since 1974, according to the World Health Organization. Accordingly, endemic LTBI in adolescents and adults invariably occurs after BCG immunization at birth. Mice were infected with *Mycobacterium tuberculosis* after BCG vaccination to create a mouse model of LTBI, mimicking the occurrence of LTBI (32, 48, 49). This model may also help us consider the possibility of combining the BCG and *B21* vaccines to increase the protective effects of the former. Furthermore, due to the limitations of this study, further investigation of the therapeutic effects of the *B21* vaccine on LTBI reactivation models and the validation of the protective effect in guinea pigs, and nonhuman primate models, is necessary. Exploring the mechanism of action of the vaccine in depth to improve the optimization of current vaccine design ideas is also necessary.

In conclusion, in this study, we provide evidence that the *B21* DNA vaccine containing coding sequences for Ag85B, Rv2029c, and Rv1738 enhances the Th1/Th17 and $CD8^+$CTL immune responses and increases the development of memory T cells. The *B21* vaccine provided a significant therapeutic effect in LTBI mice, as indicated by the significantly reduced bacterial loads and histological damage in the lungs. Our study suggests that *B21* is an excellent potential fusion antigen target, with better prospects for development as a multi-antigen vaccine, especially as a therapeutic vaccine against LTBI.

Data availability statement

The original contributions presented in the study are included in the article/Supplementary Material. Further inquiries can be directed to the corresponding author.

Ethics statement

All mice were housed under specific pathogen-free conditions at the Animal Center of the School of Life Sciences of Fudan University. All experimental procedures conformed to the Guidelines for the Care and Use of Laboratory Animals of the National Institutes of Health and were approved by the Animal Care and Use Ethical Committee of Fudan University.

Author contributions

YX, and WHZ designed the study. SFW, JYZha, HXM, JYZho, LQJ, YMW, and PC conducted the experiments. YX and SFW analyzed the data and drafted the manuscript. YX, QLR, LYS, JW, and WHZ revised the manuscript. All authors read and approved the final manuscript.

Funding

This work was supported by National Natural Science Foundation of China Grant 81971900; Grant from the major project of Study on Pathogenesis and Epidemic Prevention Technology System (2021YFC2302500) by the Ministry of Science and Technology of China; Shanghai Municipal Science and Technology Major Project (HS2021SHZX00, 21NL260010); National Science and Technology Major Project 2018ZX10302302-002 and 2018ZX10731301-004.

Conflict of interest

The authors declare that the research was conducted in the absence of any commercial or financial relationships that could be construed as a potential conflict of interest.

Publisher's note

All claims expressed in this article are solely those of the authors and do not necessarily represent those of their affiliated organizations, or those of the publisher, the editors and the reviewers. Any product that may be evaluated in this article, or claim that may be made by its manufacturer, is not guaranteed or endorsed by the publisher.

Supplementary material

The Supplementary Material for this article can be found online at: https://www.frontiersin.org/articles/10.3389/fimmu.2022.1025931/full#supplementary-material

References

1. Zwerling A, Hanrahan C, Dowdy DW. Ancient disease, modern epidemiology: A century of progress in understanding and fighting tuberculosis. *Am J Epidemiol* (2016) 183(5):407–14. doi: 10.1093/aje/kwv176

2. Harding E. WHO global progress report on tuberculosis elimination. *Lancet Respir Med* (2020) 8(1):19. doi: 10.1016/S2213-2600(19)30418-7

3. Matteelli A, Roggi A, Carvalho AC. Extensively drug-resistant tuberculosis: epidemiology and management. *Clin Epidemiol* (2014) 6:111–8. doi: 10.2147/CLEP.S35839

4. O'Donnell MR, Padayatchi N, Kvasnovsky C, Werner L, Master I, Horsburgh CRJr. Treatment outcomes for extensively drug-resistant tuberculosis and HIV co-infection. *Emerg Infect Dis* (2013) 19(3):416–24 doi: 10.3201/eid1903.120998

5. Dinnes J, Deeks J, Kunst H, Gibson A, Cummins E, Waugh N, et al. A systematic review of rapid diagnostic tests for the detection of tuberculosis infection. *Health Technol Assess* (2007) 11(3):1–196. doi: 10.3310/hta11030

6. Manabe YC, Bishai WR. Latent *mycobacterium tuberculosis*-persistence, patience, and winning by waiting. *Nat Med* (2000) 6(12):1327–9. doi: 10.1038/82139

7. Houben RM, Dodd PJ. The global burden of latent tuberculosis infection: A re-estimation using mathematical modelling. *PloS Med* (2016) 13(10):e1002152. doi: 10.1371/journal.pmed.1002152

8. Kasprowicz VO, Churchyard G, Lawn SD, Squire SB, Lalvani A. Diagnosing latent tuberculosis in high-risk individuals: Rising to the challenge in high-burden areas. *J Infect Dis* (2011) 204(Suppl 4):S1168–78. doi: 10.1093/infdis/jir449

9. Rangaka MX, Cavalcante SC, Marais BJ, Thim S, Martinson NA, Swaminathan S, et al. Controlling the seedbeds of tuberculosis: Diagnosis and treatment of tuberculosis infection. *Lancet* (2015) 386(10010):2344–53. doi: 10.1016/S0140-6736(15)00323-2

10. Barry CE3rd, Boshoff HI, Dartois V, Dick T, Ehrt S, Flynn J, et al. The spectrum of latent tuberculosis: Rethinking the biology and intervention strategies. *Nat Rev Microbiol* (2009) 7(12):845–55. doi: 10.1038/nrmicro2236

11. Parrish NM, Dick JD, Bishai WR. Mechanisms of latency in mycobacterium tuberculosis. *Trends Microbiol* (1998) 6(3):107–12. doi: 10.1016/S0966-842X(98)01216-5

12. Voskuil MI, Visconti KC, Schoolnik GK. Mycobacterium tuberculosis gene expression during adaptation to stationary phase and low-oxygen dormancy. *Tuberc (Edinb)* (2004) 84(3-4):218–27. doi: 10.1016/j.tube.2004.02.003

13. Leyten EM, Lin MY, Franken KL, Friggen AH, Prins C, van Meijgaarden KE, et al. Human T-cell responses to 25 novel antigens encoded by genes of the dormancy regulon of *mycobacterium tuberculosis*. *Microbes Infect* (2006) 8 (8):2052–60. doi: 10.1016/j.micinf.2006.03.018

14. Andersen P. Vaccine strategies against latent tuberculosis infection. *Trends Microbiol* (2007) 15(1):7–13. doi: 10.1016/j.tim.2006.11.008

15. Dannenberg AMJr. Perspectives on clinical and preclinical testing of new tuberculosis vaccines. *Clin Microbiol Rev* (2010) 23(4):781–94. doi: 10.1128/CMR.00005-10

16. Sefidi-Heris Y, Jahangiri A, Mokhtarzadeh A, Shahbazi M-A, Khalili S, Baradaran B, et al. Recent progress in the design of DNA vaccines against tuberculosis. *Drug Discovery Today* (2020) 25(11):1971–87. doi: 10.1016/j.drudis.2020.09.005

17. Liang Y, Zhang X, Bai X, Yang Y, Gong W, Wang T, et al. Immunogenicity and therapeutic effects of latency-associated genes in a mycobacterium tuberculosis reactivation mouse model. *Hum Gene Ther Methods* (2019) 30(2):60–9. doi: 10.1089/hgtb.2018.211

18. Liang Y, Wu X, Zhang J, Yang Y, Wang L, Bai X, et al. Treatment of multi-drug-resistant tuberculosis in mice with DNA vaccines alone or in combination with chemotherapeutic drugs. *Scand J Immunol* (2011) 74(1):42–6. doi: 10.1111/j.1365-3083.2011.02538.x

19. Liang Y, Cui L, Xiao L, Liu X, Yang Y, Ling Y, et al. Immunotherapeutic effects of different doses of mycobacterium tuberculosis ag85a/b DNA vaccine delivered by electroporation. *Front Immunol* (2022) 13:876579. doi: 10.3389/fimmu.2022.876579

20. Baldwin SL, Bertholet S, Kahn M, Zharkikh I, Ireton GC, Vedvick TS, et al. Intradermal immunization improves protective efficacy of a novel TB vaccine candidate. *Vaccine* (2009) 27(23):3063–71. doi: 10.1016/j.vaccine.2009.03.018

21. Lin PL, Dietrich J, Tan E, Abalos RM, Burgos J, Bigbee C, et al. The multistage vaccine H56 boosts the effects of BCG to protect cynomolgus macaques against active tuberculosis and reactivation of latent mycobacterium tuberculosis infection. *J Clin Invest* (2012) 122(1):303–14. doi: 10.1172/JCI46252

22. Zhai J, Gao W, Zhao L, Lu C. Integrated transcriptomic and quantitative proteomic analysis identifies potential RNA sensors that respond to the Ag85A DNA vaccine. *Microb Pathog* (2020) 149:104487. doi: 10.1016/j.micpath.2020.104487

23. Shi L, Sohaskey CD, Pheiffer C, Datta P, Parks M, McFadden J, et al. Carbon flux rerouting during *mycobacterium tuberculosis* growth arrest. *Mol Microbiol* (2016) 99(6):1179. doi: 10.1111/mmi.13350

24. Riaño F, Arroyo L, París S, Rojas M, Friggen AH, van Meijgaarden KE, et al. T Cell responses to DosR and rpf proteins in actively and latently infected individuals from Colombia. *Tuberc (Edinb)* (2012) 92(2):148–59. doi: 10.1016/j.tube.2011.12.005

25. Roupie V, Romano M, Zhang L, Korf H, Lin MY, Franken KL, et al. Immunogenicity of eight dormancy regulon-encoded proteins of *mycobacterium tuberculosis* in DNA-vaccinated and tuberculosis-infected mice. *Infect Immun* (2007) 75(2):941–9. doi: 10.1128/IAI.01137-06

26. Zvi A, Ariel N, Fulkerson J, Sadoff JC, Shafferman A. Whole genome identification of *mycobacterium tuberculosis vaccine* candidates by comprehensive data mining and bioinformatic analyses. *BMC Med Genomics* (2008) 1(1):18. doi: 10.1186/1755-8794-1-18

27. Wang J, Qie Y, Zhang H, Zhu B, Xu Y, Liu W, et al. PPE protein (Rv3425) from DNA segment RD11 of mycobacterium tuberculosis: A novel immunodominant antigen of *mycobacterium tuberculosis* induces humoral and cellular immune responses in mice. *Microbiol Immunol* (2008) 52(4):224–30. doi: 10.1111/j.1348-0421.2008.00029.x

28. Pedroza-Roldan C, Flores-Valdez MA. Recent mouse models and vaccine candidates for preventing chronic/latent tuberculosis infection and its reactivation. *Pathog Dis* (2017) 75(6):ftx079. doi: 10.1093/femspd/ftx079

29. Carpenter SM, Lu LL. Leveraging antibody, b cell and fc receptor interactions to understand heterogeneous immune responses in tuberculosis. *Front Immunol* (2022) 13:830482. doi: 10.3389/fimmu.2022.830482

30. Shen H, Chen ZW. The crucial roles of Th17-related cytokines/signal pathways in m. tuberculosis infection. *Cell Mol Immunol* (2018) 15(3):216–25. doi: 10.1038/cmi.2017.128

31. Sia JK, Bizzell E, Madan-Lala R, Rengarajan J. Engaging the CD40-CD40L pathway augments T-helper cell responses and improves control of *mycobacterium tuberculosis* infection. *PloS Pathog* (2017) 13(8):e1006530. doi: 10.1371/journal.ppat.1006530

32. Ma J, Teng X, Wang X, Fan X, Wu Y, Tian M, et al. A multistage subunit vaccine effectively protects mice against primary progressive tuberculosis, latency and reactivation. *EBioMedicine* (2017) 22:143–54. doi: 10.1016/j.ebiom.2017.07.005

33. Voss G, Casimiro D, Neyrolles O, Williams A, Kaufmann SHE, McShane H, et al. Progress and challenges in TB vaccine development. *F1000Res* (2018) 7:199. doi: 10.12688/f1000research.13588.1

34. Rodo MJ, Rozot V, Nemes E, Dintwe O, Hatherill M, Little F, et al. A comparison of antigen-specific T cell responses induced by six novel tuberculosis vaccine candidates. *PloS Pathog* (2019) 15(3):e1007643. doi: 10.1371/journal.ppat.1007643

35. Hatherill M, White RG, Hawn TR. Clinical development of new TB vaccines: Recent advances and next steps. *Front Microbiol* (2019) 10:3154. doi: 10.3389/fmicb.2019.03154

36. Aagaard C, Hoang T, Dietrich J, Cardona P-J, Izzo A, Dolganov G, et al. A multistage tuberculosis vaccine that confers efficient protection before and after exposure. *Nat Med* (2011) 17(2):189–94. doi: 10.1038/nm.2285

37. Govender L, Abel B, Hughes EJ, Scriba TJ, Kagina BM, de Kock M, et al. Higher human CD4 T cell response to novel *mycobacterium tuberculosis* latency associated antigens Rv2660 and Rv2659 in latent infection compared with tuberculosis disease. *Vaccine* (2010) 29(1):51–7. doi: 10.1016/j.vaccine.2010.10.022

38. Rakshit S, Adiga V, Nayak S, Sahoo PN, Sharma PK, van Meijgaarden KE, et al. Circulating *mycobacterium tuberculosis* DosR latency antigen-specific, polyfunctional, regulatory IL10(+) Th17 CD4 T-cells differentiate latent from active tuberculosis. *Sci Rep* (2017) 7(1):11948. doi: 10.1038/s41598-017-10773-5

39. Esaulova E, Das S, Singh DK, Choreño-Parra JA, Swain A, Arthur L, et al. The immune landscape in tuberculosis reveals populations linked to disease and latency. *Cell Host Microbe* (2021) 29(2):165–78.e8. doi: 10.1016/j.chom.2020.11.013

40. Abebe F. Synergy between Th1 and Th2 responses during mycobacterium tuberculosis infection: A review of current understanding. *Int Rev Immunol* (2019) 38(4):172–9. doi: 10.1080/08830185.2019.1632842

41. Zielinski CE, Mele F, Aschenbrenner D, Jarrossay D, Ronchi F, Gattorno M, et al. Pathogen-induced human TH17 cells produce IFN-gamma or IL-10 and are regulated by IL-1beta. *Nature* (2012) 484(7395):514–8. doi: 10.1038/nature10957

42. Li L, Qiao D, Fu X, Lao S, Zhang X, Wu C. Identification of *mycobacterium tuberculosis*-specific Th1, Th17 and Th22 cells using the expression of CD40L in tuberculous pleurisy. *PloS One* (2011) 6(5):e20165. doi: 10.1371/journal.pone.0020165

43. Bussi C, Gutierrez MG. Mycobacterium tuberculosis infection of host cells in space and time. *FEMS Microbiol Rev* (2019) 43(4):341–61. doi: 10.1093/femsre/fuz006

44. Mayer-Barber KD, Barber DL. Innate and adaptive cellular immune responses to *mycobacterium tuberculosis* infection. *Cold Spring Harb Perspect Med* (2015) 5(12):a018424. doi: 10.1101/cshperspect.a018424

45. de Martino M, Lodi L, Galli L, Chiappini E. Immune response to *mycobacterium tuberculosis*: A narrative review. *Front Pediatr* (2019) 7:350. doi: 10.3389/fped.2019.00350

46. Carpenter SM, Nunes-Alves C, Booty MG, Way SS, Behar SM. A higher activation threshold of memory CD8+ T cells has a fitness cost that is modified by TCR affinity during tuberculosis. *PloS Pathog* (2016) 12(1):e1005380. doi: 10.1371/journal.ppat.1005380

47. Chen J, Meng J, Li X, Li X, Liu Y, Jin C, et al. HA/CD44 regulates the T helper 1 cells differentiation by activating annexin A1/Akt/mTOR signaling to drive the pathogenesis of EAP. *Front Immunol* (2022) 13:875412. doi: 10.3389/fimmu.2022.875412

48. Ma J, Tian M, Fan X, Yu Q, Jing Y, Wang W, et al. *Mycobacterium tuberculosis* multistage antigens confer comprehensive protection against pre- and post-exposure infections by driving Th1-type T cell immunity. *Oncotarget* (2016) 7(39):63804–15. doi: 10.18632/oncotarget.11542

49. Zhang T, Zhang M, Rosenthal IM, Grosset JH, Nuermberger EL. Short-course therapy with daily rifapentine in a murine model of latent tuberculosis infection. *Am J Respir Crit Care Med* (2009) 180(11):1151–7. doi: 10.1164/rccm.200905-0795OC

frontiers | Frontiers in Immunology

TYPE Original Research
PUBLISHED 09 December 2022
DOI 10.3389/fimmu.2022.992062

OPEN ACCESS

EDITED BY
Jianping Xie,
Southwest University, China

REVIEWED BY
Javeed Ahmad,
National Institute of Allergy and Infectious Diseases (NIH), United States
Stephen Crooke,
Centers for Disease Control and Prevention (CDC), United States

*CORRESPONDENCE
Xin He
hexin59@mail.sysu.edu.cn
Hui Zhang
zhangh92@mail.sysu.edu.cn

†These authors have contributed equally to this work

SPECIALTY SECTION
This article was submitted to Vaccines and Molecular Therapeutics, a section of the journal Frontiers in Immunology

RECEIVED 12 July 2022
ACCEPTED 23 November 2022
PUBLISHED 09 December 2022

CITATION
Qiao Y, Zhan Y, Zhang Y, Deng J, Chen A, Liu B, Zhang Y, Pan T, Zhang W, Zhang H and He X (2022) Pam2CSK4-adjuvanted SARS-CoV-2 RBD nanoparticle vaccine induces robust humoral and cellular immune responses.
Front. Immunol. 13:992062.
doi: 10.3389/fimmu.2022.992062

Pam2CSK4-adjuvanted SARS-CoV-2 RBD nanoparticle vaccine induces robust humoral and cellular immune responses

Yidan Qiao[1†], Yikang Zhan[1†], Yongli Zhang[1], Jieyi Deng[1], Achun Chen[1], Bingfeng Liu[1], Yiwen Zhang[1], Ting Pan[1,2], Wangjian Zhang[3], Hui Zhang[1,4*] and Xin He[1*]

[1]Institute of Human Virology, Department of Pathogen Biology and Biosecurity, Key Laboratory of Tropical Disease Control of Ministry of Education, Zhongshan School of Medicine, Sun Yat-sen University, Guangzhou, China, [2]Center for Infection and Immunity Study, School of Medicine, Sun Yat-sen University, Shenzhen, Guangdong, China, [3]Department of Medical Statistics, School of Public Health, Sun Yat-sen University, Guangzhou, Guangdong, China, [4]Guangzhou National Laboratory, Guangzhou, Guangdong, China

As the global COVID-19 pandemic continues and new SARS-CoV-2 variants of concern emerge, vaccines remain an important tool for preventing the pandemic. The inactivated or subunit vaccines themselves generally exhibit low immunogenicity, which needs adjuvants to improve the immune response. We previously developed a receptor binding domain (RBD)-targeted and self-assembled nanoparticle to elicit a potent immune response in both mice and rhesus macaques. Herein, we further improved the RBD production in the eukaryote system by *in situ* Crispr/Cas9-engineered CHO cells. By comparing the immune effects of various Toll-like receptor-targeted adjuvants to enhance nanoparticle vaccine immunization, we found that Pam2CSK4, a TLR2/6 agonist, could mostly increase the titers of antigen-specific neutralizing antibodies and durability in humoral immunity. Remarkably, together with Pam2CSK4, the RBD-based nanoparticle vaccine induced a significant Th1-biased immune response and enhanced the differentiation of both memory T cells and follicular helper T cells. We further found that Pam2CSK4 upregulated migration genes and many genes involved in the activation and proliferation of leukocytes. Our data indicate that Pam2CSK4 targeting TLR2, which has been shown to be effective in tuberculosis vaccines, is the optimal adjuvant for the SARS-CoV-2 nanoparticle vaccine, paving the way for an immediate clinical trial.

KEYWORDS

SARS-CoV-2, nanoparticle vaccine, adjuvant, tuberculosis vaccine, TLR2 agonist, Pam2CSK4

Introduction

Coronavirus disease 2019 (COVID-19), caused by SARS-CoV-2 virus infection, has been spreading around the world with more than 633 million positive infection cases and 6.6 million deaths (by the middle of November 2022, https://covid19.who.int/). The vaccine is considered an essential strategy for preventing the epidemic of infectious diseases (1). In the design of SARS-CoV-2 vaccines, full-length S1 subunit or Receptor Binding Domain (RBD) of Spike (S) protein is often chosen as the immunogen for most current vaccines. The S protein also plays a necessary role in mediating virus entry into host cells *via* interactions with angiotensin-converting enzyme-2 (ACE2) (2). Further studies have found that neutralizing monoclonal antibodies against Spike/RBD elicited by virus infection or vaccination can potently prevent the transmission of SARS-CoV-2 (3, 4). So far, more than thirty vaccines have been approved for clinical use worldwide (5).

Due to the low immunogenicity of inactivated or subunit vaccines, adjuvants are applied to benefit the immune response by improving antigen presentation, recognition, immune reaction type, immune cell activation, proliferation, and so on (6–9). In the early stage of adjuvant development, alum and emulsion were majorly used to enhance vaccine efficacy by controlled release, improving antigen-presentation, and modulating the adaptive immune system. Lately, adjuvants targeting the key innate immune signals, such as Toll-like receptor (TLR), NLRP3 inflammasome, and cGAS, also showed great superiority in enhancing the immune response to vaccines (8). TLR is one of the major pathogen recognition receptors for regulating innate and adaptive immune responses, and cognate agonists have been extensively employed as adjuvants for vaccine development (10). For example, AS04, monophosphatidyl lipid A (MPL)-containing TLR4 agonist adjuvant, was approved for the human papillomavirus (HPV) vaccine Cervarix, which showed high efficacy against cervical intraepithelial neoplasia 2+ (CIN2+) (11). The "1018 ISS adjuvant", a synthetic nucleic acid-based CpG oligonucleotides (CpG ODNs) as TLR9 agonist, was FDA -approved for the hepatitis B vaccine Heplisav-B in 2017, which generated a potent immune response with high titers and durable antibody protection (12). Activation of the TLR2 pathway also plays an important role in tuberculosis vaccine development (13–16). In addition, several other TLR adjuvants, such as TLR3 agonist poly I: C12U, TLR5 agonist VAX102, TLR7/8 agonists Resiquimod and Imiquimod, are also undergoing clinical trials, showing enormous potential for clinical application (17–22).

Nanoparticle vaccine, as a novel and promising carrier and delivery system, can not only be used for enhancing the valence and stability of vaccines but also promote the uptake and presentation of antigens by antigen-presenting cells, thus potently regulating the immune response and improving the efficiency of vaccines (23). In the previous study, we developed a novel nanoparticle vaccine by conjugating receptor binding domain (RBD) and heptad repeats (HR) of Spike onto a Ferritin-based 24-mer particle, which elicited potent immunogenicity in rhesus macaques and protected hACE2-mice from virus infection. However, we used a mixture adjuvant purchased from Sigma company which has never been used in the clinic (24). Alternatively, the aluminum adjuvant was often used in prophylactic vaccination (25). It remains to be determined what type of adjuvants is the most suitable for self-assembled nanoparticle vaccine to enhance its efficacy.

In this study, by screening the toll-like receptor agonists, we identified that a TLR2/6 ligand analog Pam2CSK4 is the most potent adjuvant to enhance the immune response of the SARS-CoV-2 nanoparticle vaccine. We further found that Pam2CSK4 stimulates the secretion of cytokines, such as IL2 and TNF family members, and improves lymphocyte proliferation.

Materials and methods

Ethics statement

The Ethics Review Board of Sun Yat-sen University approved this study. Mice experiments were carried out in concert with the guidelines and regulations of the Laboratory Monitoring Committee of Guangdong Province of China. The animal experiments were also approved by the Ethics Committee of Zhongshan School of Medicine (ZSSOM) of Sun Yat-sen University on Laboratory Animal Care (Assurance Number: 2017-061). All efforts were made to avoid animal suffering.

Cell line

HEK293T and CHO-K1 cell lines were obtained from ATCC, and the HEK293T-hACE2 cell line was established according to our previous work (24). HEK293T and HEK293T-hACE2 cell lines were cultured in Dulbecco's modified Eagle medium (DMEM; Gibco) supplemented with 10% fetal bovine serum (FBS; Gibco) and 1% penicillin-streptomycin (Gibco) at 37°C with 5% CO2. The CHO-K1 cell line was cultured in Media C Plus (DUONING) supplemented with 1% GlutaMAX^{TM} (Gibco) and 1% penicillin-streptomycin (Gibco) at 37°C with 5% CO2. CHO-GS-/- cell and RBD-GS-CHO cell lines were constructed by CRISPR/Cas9-mediated targeted gene integration system.

CRISPR/Cas9-mediated targeted gene integration system

The detailed construction method of the system is in our published work (26). sgRNA sequences targeting the sixth exon

of the human GLUL gene and GAPDH 3′ UTR were designed by the online tool CRISPR Design from Dr. Feng Zhang's laboratory (https://zlab.bio/guide-design-resources). sgRNA was constructed into lentiCRISPR v2 plasmid (Addgene) with the Cas9 gene. Homologous arms with a length of 800bp were designed at both sides of the cleavage site ("GAPDH 3′ UTR") and connected to the target fragment of gene editing, then constructed into lentiviral vector pCPPT-IRES-mStrawberry (27). Cas9/sgRNA and Target fragment with homologous arms were respectively delivered to cells *via* an integrase-deficient lentiviral vector (IDLV) for gene integration. The related sequences are in Supplementary Table 1.

T7 endonuclease I assay

Cells' genomic DNA edited by Cas9/sgRNA system was extracted and used as the template to design primers downstream and upstream of the cutting site, amplifying the mutant fragments by Polymerase Chain Reaction (PCR). The reaction system of the T7E1 digestion method: 300ng PCR product, 2 μl 10×NEB buffer2 (NEB), and ddH2O constant volume to 20 μl. It was heated at 95°C for 5 minutes and cooled naturally to room temperature. Then 0.5 μl T7E1 enzyme (NEB) was added to each reaction system and digested at 37°C for 45 minutes. Add 1 μl 0.25M EDTA stop solution to stop the reaction, and immediately detect the cutting efficiency by 1% agarose gel electrophoresis. T7E1 cleavage efficiency was analyzed and quantified using ImageJ (28). (Primer sequence in Supplementary Table 1)

Cell counting kit-8 assay

Every 100 μl cell suspension was inoculated in a 96-well plate (Corning) at a density of 5×105/ml. 12 to 16 hours later, when the confluence of cells reached 70% to 80%, add 10 μl CCK-8 (DOJINDO) and incubate at 37 °C for 1 to 2 hours. measure absorption at 450 nm. Cell viability (%) = [(absorbance of experimental well - absorbance of blank well)/(absorbance of control well - absorbance of blank well)] × 100%.

BALB/c mice experiment

Six-week-old female BALB/c mice were purchased from Guangdong Medical Laboratory Animal Center. All mice were housed and vaccinated in Specific-pathogen-free (SPF) facilities at the Laboratory Animal Center of Sun Yat-sen University. The RBD-nanoparticle (RBD-NP) vaccine was constructed and purified as previously described (24). Briefly, we purified and conjugated SARS-CoV-2 spike protein receptor binding domain (RBD) (Genbank: QHD43416.1) to 24-mer Ferritin (UniProt: Q9ZLI1) nanoparticles by SpyTag/SpyCatcher (PDB: 4MLI) (ST/SC) system. ST-RBD protein purified from RBD-GS-CHO cells and SC-Ferritin core purified from *E.coli* was covalently bound in a molar ratio of 6:5 and then collected by Size-Exclusion Chromatography (SEC). The concentration was measured by BCA assay, and the purity and homogeneity of RBD-NP were determined by Coomassie blue staining, western blotting, SEC, and transmission electron microscopy (TEM). Mice were immunized subcutaneously with 5.6 ug RBD-NP vaccine alone or in combination with different adjuvants at week 0. Mice were immunized again at week 4. The dosage of various adjuvants was different (Supplementary Table 2). All mice were euthanized at week 10.

Enzyme-linked immunosorbent assay

Recombinant ST-RBD protein at a concentration of 2 ug/ml in coating buffer was coated on high-binding 96-well plates (Corning) respectively, overnight at 4°C. After coating, drain the liquid and block the plates with 5% non-fat milk/PBS at room temperature for 1 hour. Diluted Immunized mice serum into eight different concentrations with PBS at a 3-fold concentration gradient and added them into the well plates each well in duplicate followed by incubating at room temperature for 1 hour. After washing with PBS/T (containing 1% Tween-20), the detection of RBD-specific IgG and RBD-specific IgM in the serum of BALB/c mice was conducted by adding HRP-conjugated goat anti-mouse secondary antibody (Invitrogen) at dilution of 1:6000 and incubating at 37°C for 1 hour. After washing with PBS/T, add HRP substrate TMB solution (eBioscience) to each well, quench reaction with stop solution (Solarbio), and measure absorption at 450 nm.

Enzyme-linked immune absorbent spot assay

The detailed protocol was developed by following previous procedures with minor modifications (29). Briefly, multiScreen$_{HTS}$ IP filter plates of 0.45 μm (Millipore Sigma) were coated with 2.5 mg/mL SARS-CoV-2 RBD protein at 4 °C for 12 hours. Then plates were washed three times with PBS and blocked with DMEM at 37 °C for 1 hour. One million mice bone marrow cells were harvested and incubated inside each well at 37 °C overnight. After washing with PBS/T three times, plates were incubated with anti-IgG-HRP antibody (Jackson ImmunoResearch) at room temperature for 2 hours. Plates were washed with PBS/T three times, RBD-specific spots were then counted using an S6 ultra immunoscan reader (Cellular Technology Ltd.).

Pseudotyped virus neutralization assay

The serum neutralizing antibody titers in immunized mice were measured as previously described. Briefly, pseudotyped SARS-CoV-2 viruses were obtained by co-transfection of packaging plasmid psPAX2 (Addgene), luciferase-expressing lentivirus plasmid pHIV-Luciferase (Addgene) and plasmid expressing SARS-CoV-2 spike protein (isolate Wuhan-Hu-1, GenBank: QHD43416.1) into HEK293T cells. Then serially diluted serum of BALB/c mice were mixed with pseudotyped SARS-CoV-2 viruses and incubated at 37°C for 1 hour. Serum/virus mixtures were added into wells which were seeded with hACE2-HEK293T cells and went on culturing for 48 h. After 48 h, cells were lysed with lysis buffer (Promega) and were measured for relative luminescence units in luminometer (Promega).

Flow cytometry and intracellular cytokine staining

The cell phenotypes were analyzed by FACS Aria II flow cytometer (BD Bioscience), and data were analyzed with the FlowJo V10.0.7 (FlowJo, OR, USA). Cells were collected and washed in PBS, then the single-cell suspensions were labeled with various fluorochrome-conjugated antibodies for 30 minutes within PBS containing 0.5% BSA on ice. The gating strategies for CD4+ central memory T cells, CD8+ central memory T cells, CD4+ effector memory T cells, Tfh cells were CD4+CD62L+CD44+, CD8+CD62L+CD44+, CD4+CD62L-CD44+, CD4+CXCR5+PD-1+, respectively. The following antibodies were used: anti-mouse CD4-AF700 (clone RM4-5, eBioscience), anti-mouse CD8a-BV510 (clone 53-6.7, BD Horizon), anti-mouse CD62L-PE (clone MEL-14, Biolegend), anti-mouse CD44-Percp/Cy5.5 (clone 1M7, Biolegend), anti-mouse CXCR5-APC (clone SPRCL5, eBioscience) and anti-mouse PD-1-PE/Cy7 (clone J43, eBioscience). For ICCS, mice splenocytes were collected and co-stimulated with anti-CD3 antibody and anti-CD28 antibody (Biolegend) for 1 hour at 37 °C, then Cells were incubated with 5 mg/mL brefeldin A (Topscience), 2 mM monensin (Topscience). Cells were then harvested, stained with indicated antibodies with a Fixation/Permeabilization Solution Kit (BD Bioscience). We used these antibodies to detect cytokine secretion of T cells: anti-IFN-γ (clone XMG1.2, Biolegend) and anti-IL-2 (clone JES6-5H4, Biolegend).

RNA-sequencing and transcriptional profiling

BALB/c mice were injected with SARS-CoV-2 RBD Nanoparticle vaccine with or without Pam2CSK4. The peripheral blood mononuclear cells were isolated with the Ficoll method on day 3 and day 7 after the immunization as previously [Luo, B et al., 2020 CDD]. For RNA-sequencing analysis, total RNAs were extracted by TRIzol Reagent (Thermo Fisher Scientific) according to the manufacturer's instructions. The quality of RNA samples was evaluated by Nanodrop 2000 (Thermo Fisher). The RNA-Seq library was built with TruSeq Stranded mRNA Library Prep Kit (Illumina) and sequenced with Hiseq X Ten (Illumina) at BioMarker (Beijing, China) under the PE150 protocol. RNA-Seq reads were trimmed, filtered, and quality-controlled by the FastQC tool. Followed by calculating the reads per kilobase per million mapped reads (RPKM), the reads were aligned with human reference genome NCBI build 38 (GRC38) by Hisat268. The cutoff of fold-change (FC) ≥2 and FDR values <0.05 was used as the criterion. Through z-score normalization, the transcriptional profile data of differentially expressed genes were presented in a heatmap with MEV software.

Statistical analysis

Experiments were conducted independently at least three times, and mice were tested with at least five mice in each group. Software GraphPad Prism 8.0 and OriginPro 8.0 (OriginLab) were used to process and analyze the data, and data were represented as mean ± SEM. Two-tailed student's t-test was used to compare Two independent groups, and one-way ANOVA was used in Tukey's multiple comparisons test. Data are considered statistically significant when $p < 0.05$.

Results

Generation of SARS-CoV-2 RBD immunogen from CRISPR/Cas9-engineered CHO-K1 cells

Chinese Hamster Ovary (CHO) cells are widely used for protein expression and production in eukaryotic systems in biopharmaceuticals (30, 31). Traditional CHO cell production pipeline is always heavy workload and time-consuming. However, a glutamine synthetase (GS) system was introduced into the CHO cell platform for skipping the amplification before screening and enhancing yielding with fewer gene copies to integration (32). Therefore, we intended to construct a CHO-GS cell line by inserting ST(SpyTag)-RBD-GS at the GAPDH site for steadily producing RBD protein (Figure 1A). To this end, we first constructed the CHO-GS cell line to abolish the function of GLUL in CHO-K1 cells, which encoded glutamine synthetase (Figure 1A). Four sgRNA candidates were designed on both sides of exon 6 of the GLUL gene, followed by co-transfection with a Cas9-expressing plasmid. The editing efficiencies of these sg-GLUL RNAs were determined by the T7E1 assay, which could recognize mutations resulting from repair after Cas9 cutting (Supplementary

Figure 1A). The sg-GLUL-1 and sg-GLUL-3 were chosen for subsequent knock-out editing for their high efficiency (Supplementary Figure 1A). The knockdown of the double allele in monoclonal CHO-GS-/- cells was also confirmed by DNA sequencing. Furthermore, CHO-GS-/- cells cannot survive in a glutamine-deficient medium to verify the inactivation of glutamine synthetase by CCK-8 assay (Supplementary Figure 1B). Taken together, the CHO-GS-/- cells were successfully constructed and confirmed from multiple aspects, which could be used for subsequent screening experiments.

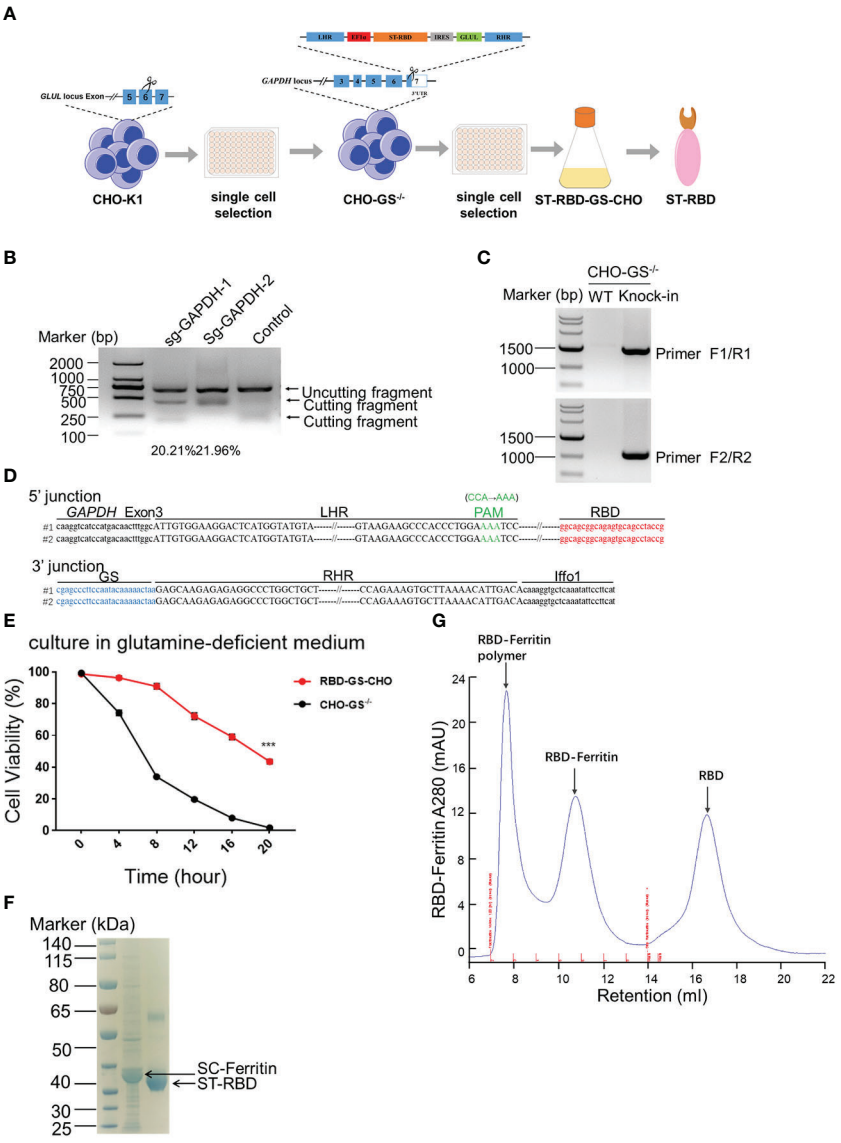

FIGURE 1
Construction of CHO-GS cells stably expressing RBD protein using CRISPR/Cas9 system for the assembly of the SARS-CoV-2 RBD NP Vaccine. **(A)** ST-RBD-GS-CHO cell construction strategy: CHO-K1 cells were transfected with Cas9/sgRNA targeting the GLUL gene, and 24 hours later, CHO-GS-/- cells were screened with puromycin for 3 days and subjected to single-cell screening with amplification. The ST-RBD-GS gene was then knocked into the GAPDH locus by the CRISPR/Cas9 system to consecutively express the RBD protein. **(B)** CHO-GS-/- cells were transfected with Cas9/sgRNA and donor DNA targeting the GAPDH gene by IDLV infection, and the editing efficiency of sgRNA was detected by the T7E1 assay as previously. Negative control was an unrelated sgRNAs. **(C, D)** Single cells were seeded and amplified, and then genomic DNA was extracted and amplified by PCR using primers F1/R1 and F2/R2, primer sites were shown in Figure 1A, respectively. The negative control was CHO-GS-/- cells. C: PCR amplification of fragments to confirm the insertion; D: blast results for DNA sequencing. **(E)**. Cell viability of CHO-GS-/- and RBD-GS-CHO cells was determined by CCK-8 assay in the glutamine-free medium. **(F)** 10 μg of purified ST-RBD and SC-ferritin samples were analyzed by SDS-PAGE electrophoresis and stained with Coomassie Blue. **(G)** Purification and concentration of RBD-Ferritin nanoparticles by size exclusion chromatography. The UV absorption value at 280 nm indicates the abundance of protein molecules. The X-axis indicated the retention volume. All the experiments were performed at least 3 times independently.

We then constructed a plasmid expressing ST-RBD-GS, which is the receptor-binding domain (RBD) immunogen of the SARS-CoV-2 original strain connected with an ST-tag, leading to its covalent conjugation onto the nanoparticle surface *via* the interaction between SpyTag and SpyCatcher (24). The 3' UTR region of the GAPDH was chosen for ST-RBD-GS insertion, which allowed high-yield expression of exogenous proteins, as described in our previous work (26). The homologous arms of LHR and RHR of the target locus were put on both sides of ST-RBD-GS, which would be integrated into the CRISPR/Cas9-mediated cleavage site by homologous recombination (Figure 1A). The sgRNAs candidates were also screened by the T7E1 assay as previously, in which sg-GAPDH-2 was a high editing effect, and it was selected to assist the insertion of ST-RBD-GS (Figure 1B). The site-specific integration of ST-RBD-GS was further confirmed by sequencing (Figures 1C, D). The resulting CHO cell line, named RBD-GS-CHO cells, grew much better in the glutamine-free medium than CHO-GS-/- cells, verifying the successfully constructed screening system and the right cell line with anaplerosis of GS (Figure 1E). Furthermore, the expression and purification of ST-RBD in the medium were confirmed by the analysis of SDS-PAGE electrophoresis (Figure 1F). To assemble the SARS-CoV-2 nanoparticle vaccine, the SC-Ferritin fusion protein was effectively purified from E.coli as previously (Figure 1F) (24). Protein expression, purification, assembly, and molecular sieve enrichment were performed sequentially to obtain RBD-nanoparticle (RBD-NP) vaccines (Figure 1G and Supplementary Figure 2).

The preliminary screening of the TLR agonists-adjuvanted SARS-CoV-2 RBD nanoparticle vaccine on the humoral immune response

To search for the optimal adjuvants for SARS-CoV-2 RBD-NP vaccines, nine adjuvant candidates that are TLR agonists used in clinical trials were respectively used in combination with the RBD-NP vaccines (Supplementary Table 2). The Sigma Adjuvant System (SAS), although not used in clinical trials so far, served as the positive control to compare the immune response. The prime-boost strategy was implemented to elicit the immune response in the BALB/c mice, which were vaccinated at week 0 and week 4 (Figure 2A). To evaluate the humoral immunity induced by the adjuvanted RBD-NP vaccine, we monitored the titers of RBD-specific IgG by ELISA at multiple time points. After boost immunization, the IgG antibodies in the groups of Pam2CSK4, Pam3CSK4, and RS09 were significantly elevated more than that in other adjuvanted groups (Figure 2B). The Pam2CSK4-adjuvanted groups produced approximately ten times higher IgG titers than those in the non-adjuvant group after boost immunization ($p<0.0001$) (Figure 2B). Furthermore, the IgG titers in the Pam2CSK4, Pam3CSK4, and RS09 groups were effectively maintained at higher levels for a long time (Figures 2C, D). Long-lived plasma cells (LLPCs) could produce specific antibodies for a long time, which play key role in eliciting durable humoral responses (33). In our study, the Pam2CSK4 group induced more LLPCs producing RBD-specific antibody than the other groups by Enzyme-Linked Immune Absorbent Spot (ELISpot) (Supplementary Figure 3). Since IgM is the earliest type of antibody produced after infection or vaccination, we examined the titers of RBD-specific IgM in the Pam2CSK4, Pam3CSK4, and RS09 groups and found that they were much higher than the non-adjuvant group in the early time (Figure 2E). The above data suggest that these three adjuvants could potently boost and maintain higher levels of protective antibodies including both IgG and IgM.

To further determine whether these adjuvants could improve the generation of neutralizing antibodies elicited by the RBD-NP vaccine, which reflected the capability of the antibodies to block the virus entry through the interaction between Spike and ACE2, we constructed a SARS-CoV-2 Spike protein-expressing plasmid for packaging the pseudotyped SARS-CoV-2 S/HIV-1 virus as described previously (24). The luciferase gene was inserted into the HIV-1 vector and can be expressed after infection with the pseudotyped viruses. We incubated the sera with pseudotyped SARS-CoV-2 S/HIV-1 virus, followed by the infection of HEK293T-ACE2 cells and the detection of luciferase. The results showed that neutralizing antibodies were produced at week 4 after prime immunization, without any differences between the adjuvant and control groups (Figure 3A). However, the titers of neutralizing antibodies in mice peaked at week 4 after boost immunization. Compared to the non-adjuvant group, the Pam2CSK4, Pam3CSK4, and RS09 groups produced approximately 70-fold higher neutralizing antibodies titers than the non-adjuvant group (Figures 2B, C). Taken together, the adjuvants, including Pam2CSK4, Pam3CSK4, and RS09 can contribute to a higher protective humoral immune response to the RBD-NP vaccine by eliciting higher titers of serum neutralizing antibodies, RBD-specific IgM, and IgG. Importantly, Pam2CSK4 is superior to the other two adjuvants in helping to maintain high IgG potency, leading to substantial durability of antibody protection.

Evaluate the cellular immune responses of the TLR agonists-adjuvanted SARS-CoV-2 RBD nanoparticle vaccine

To explore whether these three adjuvants could also enhance the cellular immune responses, we analyzed the percentage of central memory T cells (Tcm) in the spleen of mice by flow cytometry ten weeks after the initial vaccination. Pam2CSK4

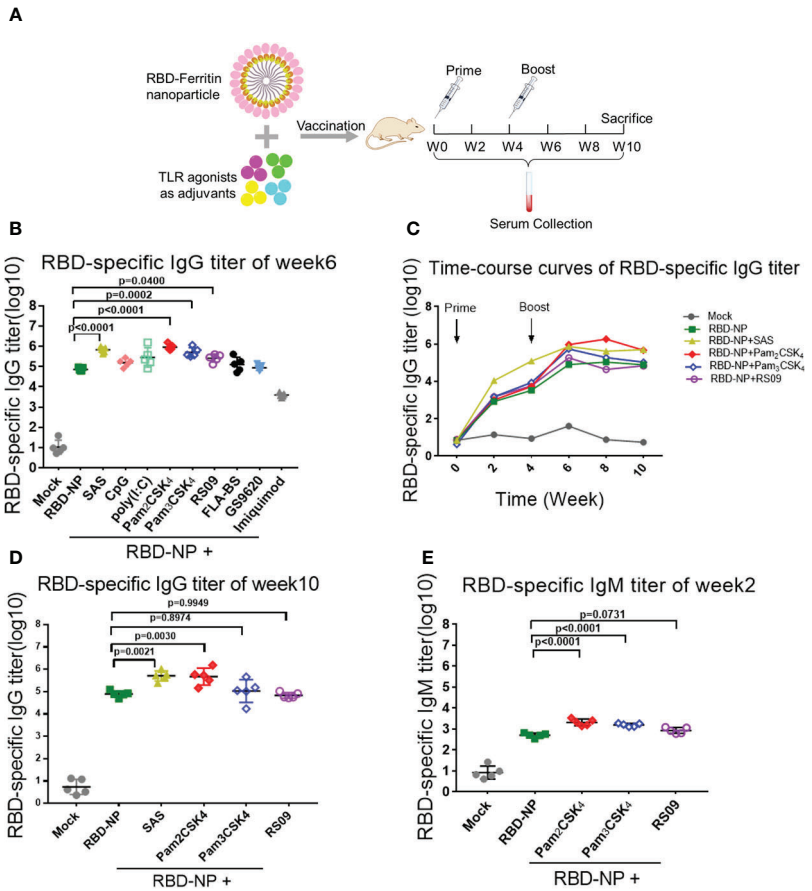

FIGURE 2
Screening of TLR agonist adjuvant to enhance humoral immune response elicited by SARS-CoV-2 nanoparticle vaccine. **(A)** Schematic design of BALB/c mice immunized with the Prime-Boost strategy. Sera were collected every two weeks after the initial immunization. **(B–D)** Monitor SARS-CoV-2 RBD-specific IgG titers in immunized mice by ELISA from week 0 to week 10. IgG titers of sera were measured by serial dilution and represented as the reciprocal of the endpoint serum dilution (n = 5). B: IgG titers of sera at week 6; c: RBD-specific IgG titers were calculated every two weeks and plotted as a time-course curve; D: IgG titers of sera at week 10. **(E)** RBD-specific IgM titers of immunized mice were collected by ELISA at week 2 (n = 5). One-way ANOVA was used in Tukey's multiple comparison test. Experimental data are expressed as Mean ± SEM.

significantly promoted the production of more CD4+Tcm cells (CD4+CD62L+CD44+T cells) and CD8+Tcm cells (CD8+CD62L+CD44+T cells) than Pam3CSK4 and RS09, indicating a potential long-term protection from the immune memory (Figures 4A, B). Moreover, T cells in Pam2CSK4-adjuvanted group were more responsive to the re-stimulation ten weeks post prime vaccination, in accordance with the more expression of the IFN-γ and IL-2 (Supplementary Figure 4).

Safety is as equally important as efficacy in the vaccine and adjuvant development. The type 2 T helper (Th2)-biased immune response is potentially associated with vaccine-associated enhanced respiratory disease (VAERD) and hypersensitivity (34, 35). In addition, it was reported that the Th1-biased immune response could enhance the resistance to SARS-CoV-2 infection (35, 36). In the mouse model, the IgG2a/IgG1 ratio was usually used to indicate the type bias of the Th1/Th2 response, in which IgG2a had a high correlation with the Th1-biased immune response. Through analyzing the antibodies in the sera of mice 6 weeks after initial immunization, only Pam2CSK4 could induce Th1-type immune responses, indicating superior and safer protection compare to another two adjuvants (Figure 4C, Supplementary Figure 5). The above data suggested that Pam2CSK4 has a positive effect on improving the efficacy and safety of the immune response induced by the RBD-NP vaccine.

To further investigate whether Pam2CSK4 could promote the differentiation of fast-acting and protective effector memory T cells (Tem), lymph node cells were extracted from mice 10 days after vaccine immunization. Compared to the non-adjuvanted group, there were more antigen-stimulated CD4+Tem cells (CD4+CD62L-CD44+ T cells) in the Pam2CSK4-adjuvanted group, indicating a boosting role of Pam2CSK4 in

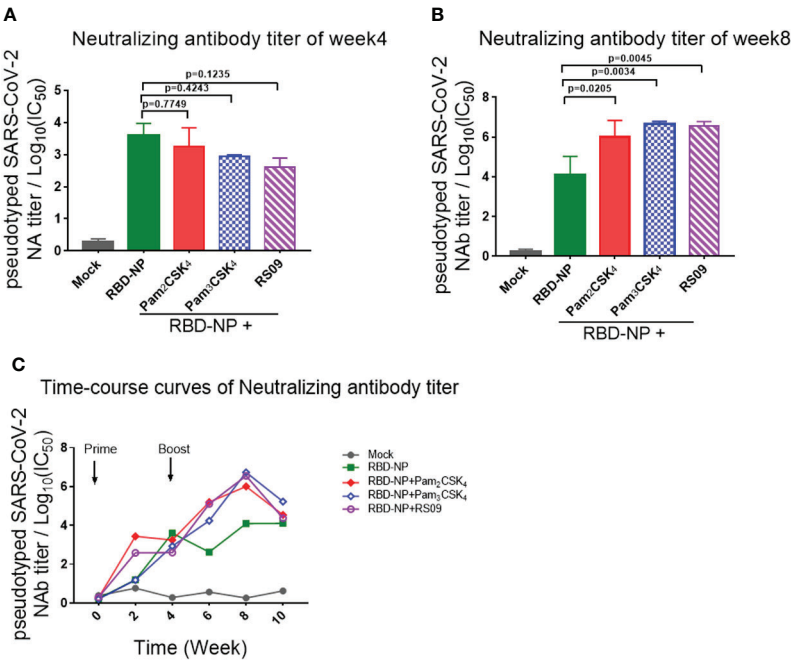

FIGURE 3
Detection and comparison of the neutralizing antibodies titer elicited by TLR agonist-adjuvanted SARS-CoV-2 nanoparticle vaccine. **(A–C)** Mice were immunized with the Prime/Boost strategy. Neutralizing antibody titers were detected by pseudotyped SARS-CoV-2 virus neutralization assay, which reflected the capability of antibodies to block the virus entry (n=5). Log_{10}(IC50) indicates neutralizing antibody titers. **(A)** Time course curve from week 0 to week 10; **(B)** Neutralizing antibody titer at week 4; **(C)** Neutralizing antibody titer at week 8. Experiments were performed independently at least 3 times. One-way ANOVA was used in Tukey's multiple comparison test. Experimental data are expressed as Mean ± SEM.

antigen presentation and T cell activation (Figure 4D). In addition, it was reported that nanoparticle vaccines were more readily captured and presented by APC, which facilitated follicular helper T (Tfh) cells to participate in the synergistic regulation between T cells and B cells (37, 38). Indeed, Pam2CSK4 significantly increased the Tfh cells in mouse lymph nodes ten days after immunization (Figure 4E). Taken together, our results suggested that Pam2CSK4 enhanced the immune response elicited by the RBD-NP vaccine, by promoting protective Th1-biased reaction, improving antigen presentation, and facilitating both memory and follicular T cell differentiation.

The molecular signatures of Pam2CSK4-adjuvanted SARS-CoV-2 nanoparticle vaccine

Upon immunization, the immune system responds with changes associated with cell activation and the coordination of various cellular subpopulations and pathways (39). To further explore the regulatory mechanisms of how Pam2CSK4 enhanced the protective immune response of the RBD-NP vaccine against SARS-CoV-2, we compared the molecular characteristics of peripheral blood leukocytes in the Pam2CSK4-adjuvanted RBD-NP group with those in the non-adjuvant group. Three days after vaccination, gene set enrichment analysis (GSEA) showed that Pam2CSK4 promoted the SARS-CoV-2 nanoparticle vaccine with significant changes in ribosomal and cell adhesion pathways, consistent with cell activation and migration. Moreover, the metabolic levels of the immune system were significantly elevated to provide energy for immune response at different time points, such as the glutathione metabolic pathway (Figures 5A, B, Supplementary Figure 6). Meanwhile, the transcriptional analysis revealed significant upregulation of genes involved in extracellular matrix (ECM)-receptor interactions and RAS signaling pathways, such as *Itgb5*, *Itga6*, *Calml3*, and *Gp6*, in Pam2CSK4-adjuvanted SARS-CoV-2 nanoparticles (Figures 5C–E). Compared to the non-adjuvant group, these genes were more involved in leukocyte adhesion in the Pam2CSK4 group. Furthermore, the transcriptional profile also showed Pam2CSK4 promoted RAP1 signaling pathways activation, including *Mapk3*, *Rac1*, *Pdgfa*, and *Gng11* (Figures 5D, E). Taken together, our results suggested that Pam2CSK4 can effectively promote cell differentiation and proliferation through multiple cell activation-associated pathways.

GSEA was also carried out for comparing the differences on day 7 after vaccination between Pam2CSK4-adjuvanted and

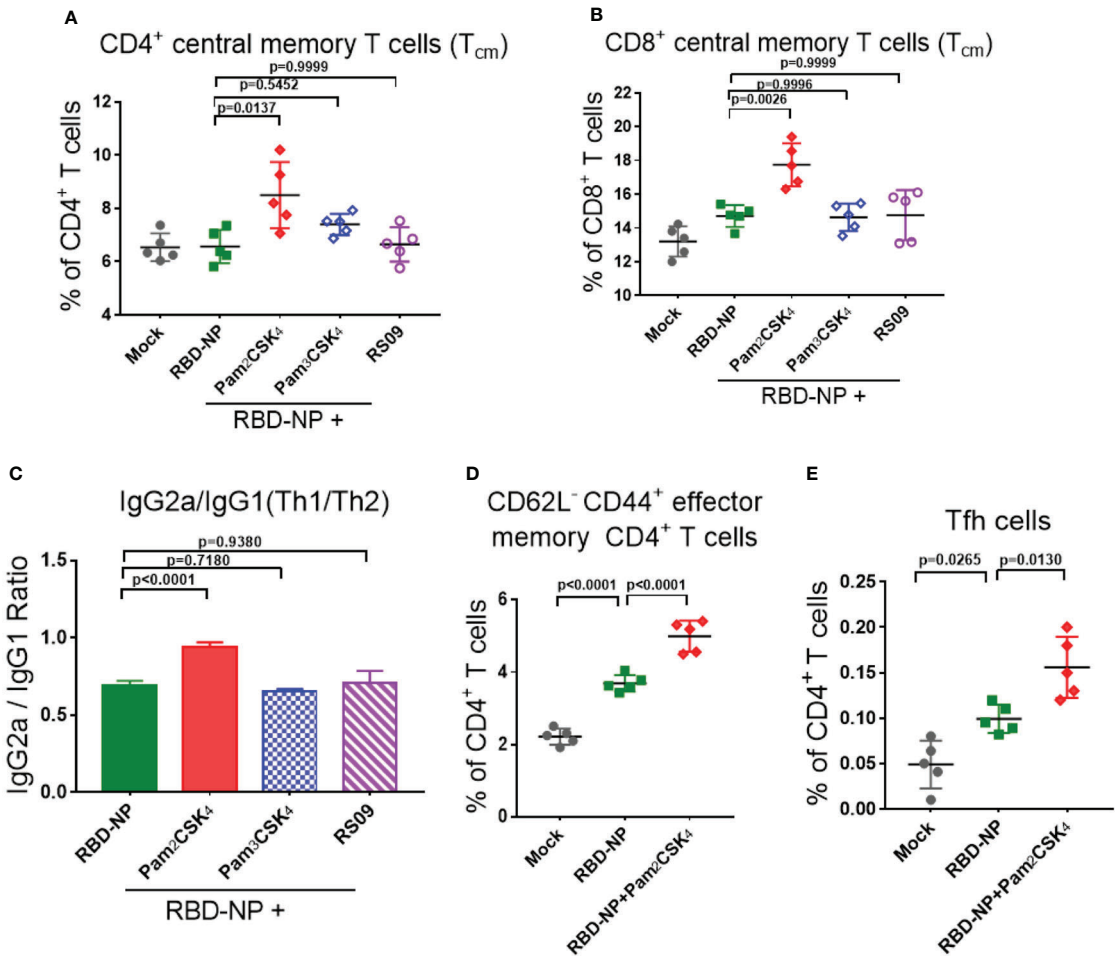

FIGURE 4
Evaluate the cellular immune responses of the adjuvanted SARS-CoV-2 nanoparticle vaccine *in vivo*. **(A, B)** Splenocytes were collected at week 10 and the central memory T cells were detected by flow cytometry. **(A)** CD4+CD62L+CD44+ Tcm cells; **(B)** CD8+CD62L+CD44+ Tcm cells (n=5). **(C)** IgG2a and IgG1 titers in sera were measured by ELISA at week 6, and the ratio of IgG2a/IgG1 represented a trend of Th1/Th2 response (n=5). **(D)** Mandibular lymph nodes were collected and the central memory CD4+ T cells (CD4+CD62L-CD44+ T cells) were analyzed 10 days after immunization (n=5). **(E)** Tfh cells (CD4+CXCR5+PD-1+) were collected from lymph nodes and analyzed 10 days after immunization (n=5). Experiments were performed at least three times independently. One-way ANOVA was used for Tukey's multiple comparison test. Experimental data are expressed as Mean ± SEM.

non-adjuvanted groups. Pam2CSK4 increased more expression of genes associated with chemokine signaling and cytokine-cytokine receptor for the SARS-CoV-2 NP vaccine (Figure 5B). The upregulation of related genes involved mediates leukocyte activation and leukocyte migration, including *Il2*, *Ccl2*, *Ccl6*, *Ccl9*, *Cxcl2*, *Cx3cr1*, *Il1r1*, *Cxcr1*, *Ccr1*, *Ccr2*, and importantly, *Tnfsf13* (*April*) (Figures 5F, G). Remarkably, the upregulation of *Il2*, *Ccl2*, *Csf3r*, and the downregulation of *Il4* were consistent with the Th-1-biased immune response, further suggesting that Pam2CSK4 could induce a potent and safe immune response (Figures 5G and 4C) (40). Overall, the transcriptional profiling analysis revealed a positive molecular signature induced by Pam2CSK4-adjuvanted SARS-CoV-2 nanoparticle vaccination.

Discussion

The massive requirement for vaccines against the COVID-19 pandemic has also driven the urgent demand for adjuvant development (41). Based on previous work, CHO cells were genetically edited by the CRISPR/Cas9 system to efficiently and continuously secrete RBD protein, facilitating the production of the nanoparticle vaccine in the clinical standard. Meanwhile, by screening and comparing all TLR agonists in clinical trials, we found that Pam2CSK4 can significantly enhance both humoral and cellular immune responses of RBD-based nanoparticle vaccines. Furthermore, Pam2CSK4 induced a much safer and more potent Th1-bias reaction and showed advantages in maintaining immune memory and T-B cell coordination, which was also demonstrated

10.3389/fimmu.2022.992062

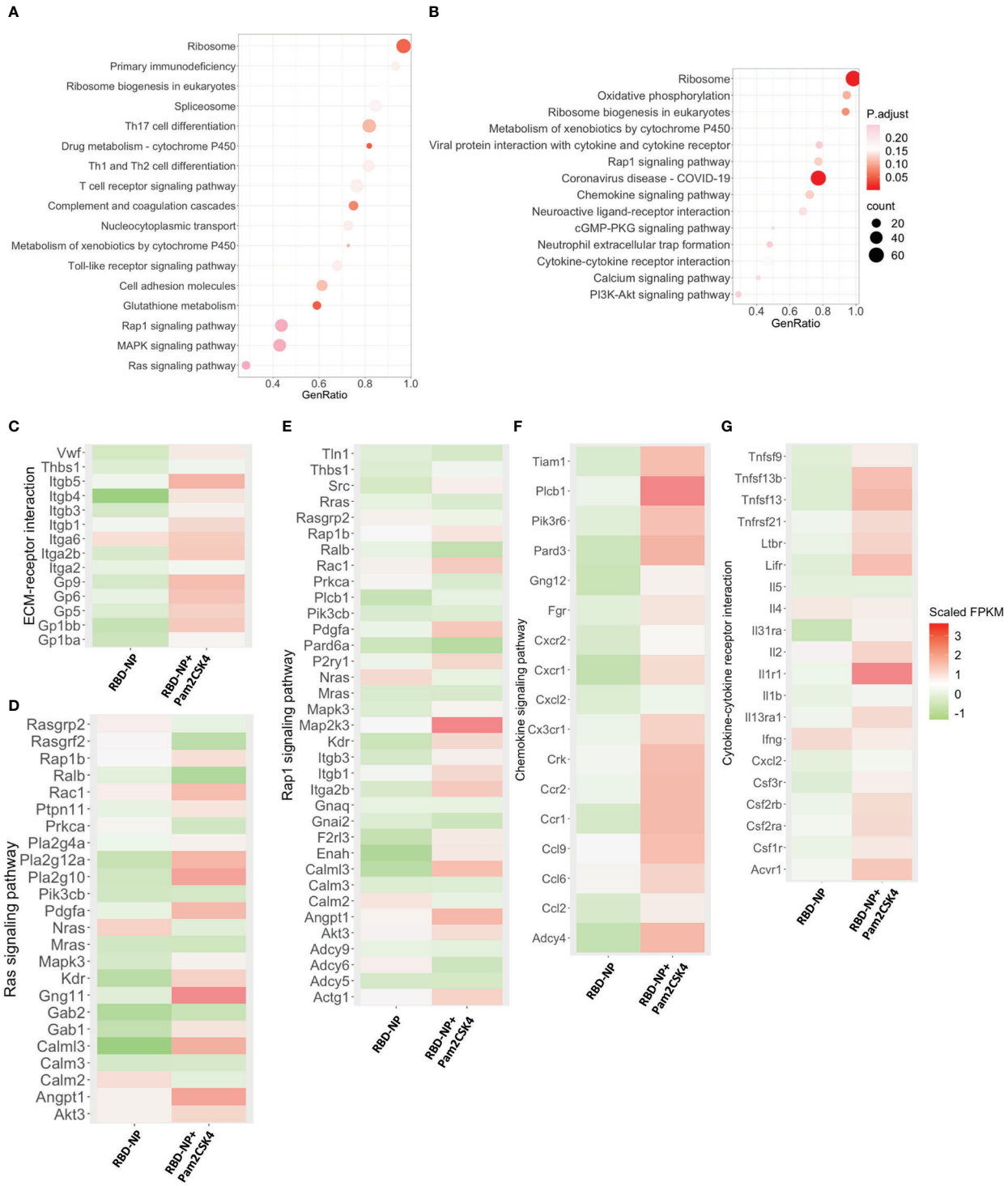

FIGURE 5
Transcriptional characterization of Pam2CSK4-adjuvanted SARS-CoV-2 nanoparticle vaccine. **(A, B)** Major gene enrichment maps of GSEA for peripheral leukocytes in the RBD-NP and RBD-NP+Pam2CSK4 groups of mice, respectively. Circles represent the number of genes involved in the gene pathway. **(A)** three days after immunization; **(B)** 7 days after immunization. **(C–E)**. Heat map of genes associated with ECM-receptor interactions, Ras, and Rap1 signaling pathways showing the activation enrichment in the Pam2CSK4 + RBD-NP group compared to the RBD-NP group at day 3 post-immunization. **(F, G)** A heat map of genes associated with chemokine signaling and cytokine-cytokine receptor interactions pathways shows activation enrichment in the Pam2CSK4 + RBD-NP group compared to the RBD-NP group at day 7 post-immunization. Color changes represent Scaled FPKM. RNA expression levels are indicated by red/green Scaled FPKM for high and low expression levels, respectively.

by the transcriptional profiles of mouse peripheral leukocytes. Taken together, Pam2CSK4, targeting TLR2/6, is a potent adjuvant that can enhance the efficacy of SARS-CoV-2 nanoparticle vaccines by boosting the protective immune response.

The launch of mRNA-1273 and NVX-CoV2373 has drawn attention to nanoparticle vaccines (42–44). The RBD-Ferritin nanoparticle vaccine developed in our early stage has played an excellent advantage with the assistance of the SAS (24). To further promote the clinical translation of this nanoparticle vaccine, we used the CHO system commonly used in clinical biological products to further optimize it. There are three advantages to employing the CHO system for RBD protein preparation. First, CHO cells could endow the Spike/RBD with the natural folding confirmation and glycosylation modification compared to the prokaryotic bacterial system. Second, the CHO system has been a proven production standard for the pharmaceutical industry and is widely applied in protein production. Third, the CHO system could produce large-scale protein in a high density in the serum-free medium (31, 45, 46). In combination with the site-specific genetically engineered CRISPR/Cas9 technology, the CHO system got further improvement in efficiency and standardization (47).

In addition, adjuvants played an essential role in improving immunogenicity and boosting efficacies and we tried to find a clinically relevant adjuvant match for this nanoparticle vaccine. Since alum adjuvant was first shown to improve diphtheria vaccine protection in 1926, it has become the most commonly used adjuvant to persistently activate the adaptive immune response by the slow release of antigens and the prolonged interaction with APC (48, 49). Other emulsion adjuvants, such as AS01, AS03, and MF59, have also been shown to enhance vaccine immune response *via* the mechanisms that induce cell immigration and improve APC activation by increasing the secretion of related cytokines (50–52). NVX-CoV2373, a recent FDS-approved SARS-CoV-2 nanoparticle vaccine, is composed of a trimeric full-length Spike protein, adjuvanted with Matrix-M1, a saponin-based compound (42, 53). It remains to be elucidated the combination principle for the vaccines and various adjuvants. Along with the in-depth understanding of the immune regulation post-vaccination, it has been found that the recognition and activation mediated by pattern recognition receptors (PRRs) are essential to bridge the innate immune to adaptive immune. Because TLR agonists have been widely used in vaccine studies and showed extensive safety and efficacy, we performed the screening of all the TLR agonists to look for a potent adjuvant to boost the immune response of the SARS-CoV-2 nanoparticle vaccine. We demonstrated that TLR2/6-targeted Pam2CSK4 played a potent role in inducing high and more durable titers of antibody production than any other TLR agonist (Figure 2). Pam2CSK4 also accelerated the immune reaction to produce a protective effect *in vivo*, showing its superiority (Figure 3).

It's reported that there was a significant decrease in serum neutralizing antibody levels after recovery in some COVID-19 patients (54, 55). Therefore, it is remarkable that Pam2CSK4 can also play a key role in long-term protection by inducing more memory T cells and Tfh cells (Figure 4). Furthermore, molecular signatures of transcriptional profiles showed the pathways related to cell migration, activation, proliferation, and adhesion were most activated during immunization of Pam2CSK4-adjuvanted nanoparticles vaccine, contributing to the potent and long-lasting immune protection (39, 56). Importantly, the upregulated expression of *APRIL*, which is a key ligand for the differentiation of long-lived plasma cells, could lead to a durable production of nAbs against SARS-CoV-2 (57–59). Together, we provide an important theoretical principle of the combination of SARS-CoV-2 NP vaccine and adjuvant for clinical transformation.

The safety of the adjuvants is the priority for vaccine development. It has been shown that Pam2CSK4 is a Th2 polarizing adjuvant in Chlamydia vaccine, Leishmania major and Brugia malayi murine vaccine in clinical trials (60, 61). However, other studies have shown that TLR2 agonist-adjuvanted tuberculosis vaccine can induce a Th1-biased immune response (13, 16). Our data indicate that the Pam2CSK4-adjuvanted SARS-CoV-2 NP vaccine induced a Th1-biased immune response in our results (Figure 4C), which was also confirmed by the analysis of transcriptional profiling that *IL2* and *TNF* family genes were significantly elevated in the Pam2CSK4-adjuvanted group (Figure 5G). In addition, previous studies on SARS-CoV believed that a Th1-biased immune response is also considered as much safer than a Th2-biased one, reducing the risk of VAERD and contributing to the safety assessment (34, 35).

In summary, we engineeringly modified the RBD preparation to produce the SARS-CoV-2 nanoparticle vaccine, paving the way for rapid transformation. We also demonstrated that Pam2CSK4, a TLR2/6 agonist already used in clinical trials with other vaccines, was the most potent adjuvant to boost the immune response of the RBD-NP vaccine. This adjuvanted-nanoparticle vaccine has the potential advantages of high antibody titers, durable efficacy, and safety for further clinical use to prevent COVID19.

Data availability statement

The datasets presented in this study can be found in online repositories. The names of the repository/repositories and accession number(s) can be found below: All RNA-seq data have been deposited in the Sequence Read Archive (SRA) under accession number PRJNA857815.

Ethics statement

The animal study was reviewed and approved by the Ethics Committee of Zhongshan School of Medicine (ZSSOM) of Sun Yat-sen University.

Author contributions

Conceptualization, HZ and XH. Methodology, YQ, YKZ, YLZ and JD. Investigation, BL, AC, YWZ, TP and WZ. Writing – original draft, YQ and YKZ. Writing – Review & editing, HZ and XH. Supervision, HZ and XH. All authors contributed to the article and approved the submitted version.

Funding

This work was supported by National Natural Science Foundation of China (NSFC, 32100743, 82171825, 82141205) Guangdong Basic and Applied Basic Research Foundation (2022B1111020004, 2022A1515010132) Science and Technology Planning Project of Guangzhou (202201011469) to XH, the Important Key Program of Natural Science Foundation of China (NSFC) (92169201, 81730060), the Exchange Program of NSFC (82150710553), the Emergency Key Program of Guangzhou National Laboratory (EKPG21-24), and the Special Research and Development Program of Guangzhou (202008070010) to HZ.

Conflict of interest

The authors declare that the research was conducted in the absence of any commercial or financial relationships that could be construed as a potential conflict of interest.

Publisher's note

All claims expressed in this article are solely those of the authors and do not necessarily represent those of their affiliated organizations, or those of the publisher, the editors and the reviewers. Any product that may be evaluated in this article, or claim that may be made by its manufacturer, is not guaranteed or endorsed by the publisher.

Supplementary material

The Supplementary Material for this article can be found online at: https://www.frontiersin.org/articles/10.3389/fimmu.2022.992062/full#supplementary-material

References

1. Lurie N, Saville M, Hatchett R, Halton J. Developing covid-19 vaccines at pandemic speed. *N Engl J Med* (2020) 382:1969–73. doi: 10.1056/NEJMp2005630

2. Verdecchia P, Cavallini C, Spanevello A, Angeli F. The pivotal link between ACE2 deficiency and SARS-CoV-2 infection. *Eur J Internal Med* (2020) 76:14–20. doi: 10.1016/j.ejim.2020.04.037

3. Chen XY, Li R, Pan ZW, Qian CF, Yang Y, You RR, et al. Human monoclonal antibodies block the binding of SARS-CoV-2 spike protein to angiotensin converting enzyme 2 receptor. *Cell Mol Immunol* (2020) 17:647–9. doi: 10.1038/s41423-020-0426-7

4. Wrapp D, Wang NS, Corbett KS, Goldsmith JA, Hsieh CL, Abiona O, et al. Cryo-EM structure of the 2019-nCoV spike in the prefusion conformation. *Science* (2020) 367:1260–+. doi: 10.1126/science.abb2507

5. (2022). Available at: https://vac-lshtm.shinyapps.io/ncov_vaccine_landscape.

6. Dupuis M, Murphy TJ, Higgins D, Ugozzoli M, Van Nest G, Ott G, et al. Dendritic cells internalize vaccine adjuvant after intramuscular injection. *Cell Immunol* (1998) 186:18–27. doi: 10.1006/cimm.1998.1283

7. Sun H, Pollock KG, Brewer JM. Analysis of the role of vaccine adjuvants in modulating dendritic cell activation and antigen presentation *in vitro*. *Vaccine* (2003) 21:849–55. doi: 10.1016/S0264-410X(02)00531-5

8. Kool M, Soullie T, Van Nimwegen M, Willart M, Muskens F, Jung S, et al. Alum adjuvant boosts adaptive immunity by inducing uric acid and activating inflammatory dendritic cells. *J Exp Med* (2008) 205:869–82. doi: 10.1084/jem.20071087

9. Calabro S, Tritto E, Pezzotti A, Taccone M, Muzzi A, Bertholet S, et al. The adjuvant effect of MF59 is due to the oil-in-water emulsion formulation, none of the individual components induce a comparable adjuvant effect. *Vaccine* (2013) 31:3363–9. doi: 10.1016/j.vaccine.2013.05.007

10. O'hagan DT, Lodaya RN, Lofano G. The continued advance of vaccine adjuvants - 'we can work it out'. *Semin Immunol* (2020) 50:101426. doi: 10.1016/j.smim.2020.101426

11. Paavonen J, Naud P, Salmeron J, Wheeler CM, Chow SN, Apter D, et al. Efficacy of human papillomavirus (HPV)-16/18 AS04-adjuvanted vaccine against cervical infection and precancer caused by oncogenic HPV types (PATRICIA): final analysis of a double-blind, randomised study in young women. *Lancet* (2009) 374:301–14. doi: 10.1016/S0140-6736(09)61248-4

12. Barry M, Cooper C. Review of hepatitis b surface antigen-1018 ISS adjuvant-containing vaccine safety and efficacy. *Expert Opin Biol Ther* (2007) 7:1731–7. doi: 10.1517/14712598.7.11.1731

13. Byun EH, Kim WS, Kim JS, Jung ID, Park YM, Kim HJ, et al. Mycobacterium tuberculosis Rv0577, a novel TLR2 agonist, induces maturation of dendritic cells and drives Th1 immune response. *FASEB J* (2012) 26:2695–711. doi: 10.1096/fj.11-199588

14. Doddam SN, Peddireddy V, Ahmed N. Mycobacterium tuberculosis DosR regulon gene Rv2004c encodes a novel antigen with pro-inflammatory functions and potential diagnostic application for detection of latent tuberculosis. *Front Immunol* (2017) 8:712. doi: 10.3389/fimmu.2017.00712

15. Rai PK, Chodisetti SB, Maurya SK, Nadeem S, Zeng W, Janmeja AK, et al. A lipidated bi-epitope vaccine comprising of MHC-I and MHC-II binder peptides elicits protective CD4 T cell and CD8 T cell immunity against mycobacterium tuberculosis. *J Transl Med* (2018) 16:279. doi: 10.1186/s12967-018-1653-x

16. Khan A, Bakhru P, Saikolappan S, Das K, Soudani E, Singh CR, et al. An autophagy-inducing and TLR-2 activating BCG vaccine induces a robust protection against tuberculosis in mice. *NPJ Vaccines* (2019) 4:34. doi: 10.1038/s41541-019-0122-8

17. Ichinohe T, Kawaguchi A, Tamura SI, Takahashi H, Sawa H, Ninomiya A, et al. Intranasal immunization with H5N1 vaccine plus poly I: Poly C12U, a toll-like receptor agonist, protects mice against homologous and heterologous virus challenge. *Microbes Infection* (2007) 9:1333–40. doi: 10.1016/j.micinf.2007.06.007

18. Adams S, O'neill DW, Nonaka D, Hardin E, Chiriboga L, Siu K, et al. Immunization of malignant melanoma patients with full-length NY-ESO-1 protein using TLR7 agonist imiquimod as vaccine adjuvant. *J Immunol* (2008) 181:776–84. doi: 10.4049/jimmunol.181.1.776

19. Turley CB, Rupp RE, Johnson C, Taylor DN, Wolfson J, Tussey L, et al. Safety and immunogenicity of a recombinant M2e-flagellin influenza vaccine (STF2.4xM2e) in healthy adults. *Vaccine* (2011) 29:5145–52. doi: 10.1016/j.vaccine.2011.05.041

20. Halperin SA, Mcneil S, Langley JM, Smith B, Mackinnon-Cameron D, Mccall-Sani R, et al. Safety and immunogenicity of different two-dose regimens of an investigational hepatitis b vaccine (hepatitis b surface antigen co-administered with an immunostimulatory phosphorothioate oligodeoxyribonucleotide) in healthy young adults. *Vaccine* (2012) 30:5445–8. doi: 10.1016/j.vaccine.2012.05.074

21. Glavan TM, Pavelic J. The exploitation of toll-like receptor 3 signaling in cancer therapy. *Curr Pharm Des* (2014) 20:6555–64. doi: 10.2174/1381612820666140826153347

22. Apostolico Jde S, Lunardelli VA, Coirada FC, Boscardin SB, Rosa DS. Adjuvants: Classification, modus operandi, and licensing. *J Immunol Res* (2016) 2016:1459394. doi: 10.1155/2016/1459394

23. Smith DM, Simon JK, Baker JRJr. Applications of nanotechnology for immunology. *Nat Rev Immunol* (2013) 13:592–605. doi: 10.1038/nri3488

24. Ma X, Zou F, Yu F, Li R, Yuan Y, Zhang Y, et al. Nanoparticle vaccines based on the receptor binding domain (RBD) and heptad repeat (HR) of SARS-CoV-2 elicit robust protective immune responses. *Immunity* (2020) 53:1315–1330 e1319. doi: 10.1016/j.immuni.2020.11.015

25. Yuan Y, Zhang X, Chen R, Li Y, Wu B, Li R, et al. A bivalent nanoparticle vaccine exhibits potent cross-protection against the variants of SARS-CoV-2. *Cell Rep* (2022) 38:110256. doi: 10.1016/j.celrep.2021.110256

26. Luo B, Zhan Y, Luo M, Dong H, Liu J, Lin Y, et al. Engineering of alpha-PD-1 antibody-expressing long-lived plasma cells by CRISPR/Cas9-mediated targeted gene integration. *Cell Death Dis* (2020) 11:973. doi: 10.1038/s41419-020-03187-1

27. Liu B, Zou F, Lu L, Chen C, He D, Zhang X, et al. Chimeric antigen receptor T cells guided by the single-chain fv of a broadly neutralizing antibody specifically and effectively eradicate virus reactivated from latency in CD4+ T lymphocytes isolated from HIV-1-Infected individuals receiving suppressive combined antiretroviral therapy. *J Virol* (2016) 90:9712–24. doi: 10.1128/JVI.00852-16

28. Guschin DY, Waite AJ, Katibah GE, Miller JC, Holmes MC, Rebar EJ. A rapid and general assay for monitoring endogenous gene modification. *Methods Mol Biol* (2010) 649:247–56. doi: 10.1007/978-1-60761-753-2_15

29. Lederer K, Castano D, Gomez Atria D, Oguin TH3rd, Wang S, Manzoni TB, et al. SARS-CoV-2 mRNA vaccines foster potent antigen-specific germinal center responses associated with neutralizing antibody generation. *Immunity* (2020) 53:1281–1295 e1285. doi: 10.1016/j.immuni.2020.11.009

30. Fan LC, Kadura I, Krebs LE, Hatfield CC, Shaw MM, Frye CC. Improving the efficiency of CHO cell line generation using glutamine synthetase gene knockout cells. *Biotechnol Bioengineering* (2012) 109:1007–15. doi: 10.1002/bit.24365

31. Fischer S, Handrick R, Otte K. The art of CHO cell engineering: A comprehensive retrospect and future perspectives. *Biotechnol Adv* (2015) 33:1878–96. doi: 10.1016/j.biotechadv.2015.10.015

32. Brown ME, Renner G, Field RP, Hassell T. Process development for the production of recombinant antibodies using the glutamine synthetase (GS) system. *Cytotechnology* (1992) 9:231–6. doi: 10.1007/BF02521750

33. Robinson MJ, Webster RH, Tarlinton DM. How intrinsic and extrinsic regulators of plasma cell survival might intersect for durable humoral immunity. *Immunol Rev* (2020) 296:87–103. doi: 10.1111/imr.12895

34. Tseng CT, Sbrana E, Iwata-Yoshikawa N, Newman PC, Garron T, Atmar RL, et al. Immunization with SARS coronavirus vaccines leads to pulmonary immunopathology on challenge with the SARS virus. *PloS One* (2012) 7:e35421. doi: 10.1371/journal.pone.0035421

35. Graham BS. Rapid COVID-19 vaccine development. *Science* (2020) 368:945–6. doi: 10.1126/science.abb8923

36. Capone S, Raggioli A, Gentile M, Battella S, Lahm A, Sommella A, et al. Immunogenicity of a new gorilla adenovirus vaccine candidate for COVID-19. *Mol Ther* (2021) 29:2412–23. doi: 10.1016/j.ymthe.2021.04.022

37. Kelly HG, Tan HX, Juno JA, Esterbauer R, Ju Y, Jiang W, et al. Self-assembling influenza nanoparticle vaccines drive extended germinal center activity and memory b cell maturation. *JCI Insight* (2020) 5:e136653. doi: 10.1172/jci.insight.136653

38. Wang W, Zhou X, Bian Y, Wang S, Chai Q, Guo Z, et al. Dual-targeting nanoparticle vaccine elicits a therapeutic antibody response against chronic hepatitis b. *Nat Nanotechnol* (2020) 15:406–16. doi: 10.1038/s41565-020-0648-y

39. Tsang JS, Schwartzberg PL, Kotliarov Y, Biancotto A, Xie Z, Germain RN, et al. Global analyses of human immune variation reveal baseline predictors of postvaccination responses. *Cell* (2014) 157:499–513. doi: 10.1016/j.cell.2014.03.031

40. Lambert SL, Yang CF, Liu Z, Sweetwood R, Zhao J, Cheng L, et al. Molecular and cellular response profiles induced by the TLR4 agonist-based adjuvant glucopyranosyl lipid a. *PloS One* (2012) 7:e51618. doi: 10.1371/journal.pone.0051618

41. Machhi J, Shahjin F, Das S, Patel M, Abdelmoaty MM, Cohen JD, et al. Nanocarrier vaccines for SARS-CoV-2. *Adv Drug Delivery Rev* (2021) 171:215–39. doi: 10.1016/j.addr.2021.01.002

42. Keech C, Albert G, Cho I, Robertson A, Reed P, Neal S, et al. Phase 1-2 trial of a SARS-CoV-2 recombinant spike protein nanoparticle vaccine. *N Engl J Med* (2020) 383:2320–32. doi: 10.1056/NEJMoa2026920

43. Baden LR, El Sahly HM, Essink B, Kotloff K, Frey S, Novak R, et al. Efficacy and safety of the mRNA-1273 SARS-CoV-2 vaccine. *N Engl J Med* (2021) 384:403–16. doi: 10.1056/NEJMoa2035389

44. Widge AT, Rouphael NG, Jackson LA, Anderson EJ, Roberts PC, Makhene M, et al. Durability of responses after SARS-CoV-2 mRNA-1273 vaccination. *N Engl J Med* (2021) 384:80–2. M, R.N.a.S.G. doi: 10.1056/NEJMc2032195

45. Tihanyi B, Nyitray L. Recent advances in CHO cell line development for recombinant protein production. *Drug Discovery Today Technol* (2020) 38:25–34. doi: 10.1016/j.ddtec.2021.02.003

46. Szkodny AC, Lee KH. Biopharmaceutical manufacturing: Historical perspectives and future directions. *Annu Rev Chem Biomol Eng* (2022) 13:141–65. doi: 10.1146/annurev-chembioeng-092220-125832

47. Louie S, Haley B, Marshall B, Heidersbach A, Yim M, Brozynski M, et al. FX knockout CHO hosts can express desired ratios of fucosylated or afucosylated antibodies with high titers and comparable product quality. *Biotechnol Bioengineering* (2017) 114:632–44. doi: 10.1002/bit.26188

48. Tomljenovic L, Shaw CA. Aluminum vaccine adjuvants: Are they safe? *Curr Medicinal Chem* (2011) 18:2630–7. doi: 10.2174/092986711795933740

49. Hogenesch H. Mechanism of immunopotentiation and safety of aluminum adjuvants. *Front Immunol* (2012) 3:406. doi: 10.3389/fimmu.2012.00406

50. Morel S, Didierlaurent A, Bourguignon P, Delhaye S, Baras B, Jacob V, et al. Adjuvant system AS03 containing alpha-tocopherol modulates innate immune response and leads to improved adaptive immunity. *Vaccine* (2011) 29:2461–73. doi: 10.1016/j.vaccine.2011.01.011

51. Caproni E, Tritto E, Cortese M, Muzzi A, Mosca F, Monaci E, et al. MF59 and Pam3CSK4 boost adaptive responses to influenza subunit vaccine through an IFN type I-independent mechanism of action. *J Immunol* (2012) 188:3088–98. doi: 10.4049/jimmunol.1101764

52. O'hagan DT, Ott GS, De Gregorio E, Seubert A. The mechanism of action of MF59 - an innately attractive adjuvant formulation. *Vaccine* (2012) 30:4341–8. doi: 10.1016/j.vaccine.2011.09.061

53. Tian JH, Patel N, Haupt R, Zhou H, Weston S, Hammond H, et al. SARS-CoV-2 spike glycoprotein vaccine candidate NVX-CoV2373 immunogenicity in baboons and protection in mice. *Nat Commun* (2021) 12:372. doi: 10.1038/s41467-020-20653-8

54. Ibarrondo FJ, Fulcher JA, Goodman-Meza D, Elliott J, Hofmann C, Hausner MA, et al. Rapid decay of anti-SARS-CoV-2 antibodies in persons with mild covid-19. *N Engl J Med* (2020) 383:1085–7. doi: 10.1056/NEJMc2025179

55. Long QX, Tang XJ, Shi QL, Li Q, Deng HJ, Yuan J, et al. Clinical and immunological assessment of asymptomatic SARS-CoV-2 infections. *Nat Med* (2020) 26:1200–4. doi: 10.1038/s41591-020-0965-6

56. Olafsdottir T, Lindqvist M, Harandi AM. Molecular signatures of vaccine adjuvants. *Vaccine* (2015) 33:5302–7. doi: 10.1016/j.vaccine.2015.04.099

57. Bossen C, Schneider P. BAFF, APRIL and their receptors: structure, function and signaling. *Semin Immunol* (2006) 18:263–75. doi: 10.1016/j.smim.2006.04.006

58. Benson MJ, Dillon SR, Castigli E, Geha RS, Xu S, Lam KP, et al. Cutting edge: the dependence of plasma cells and independence of memory b cells on BAFF and APRIL. *J Immunol* (2008) 180:3655–9. doi: 10.4049/jimmunol.180.6.3655

59. Turner JS, Kim W, Kalaidina E, Goss CW, Rauseo AM, Schmitz AJ, et al. SARS-CoV-2 infection induces long-lived bone marrow plasma cells in humans. *Nature* (2021) 595:421–5. doi: 10.1038/s41586-021-03647-4

60. Cheng C, Jain P, Bettahi I, Pal S, Tifrea D, de la Maza LM. A TLR2 agonist is a more effective adjuvant for a chlamydia major outer membrane protein vaccine than ligands to other TLR and NOD receptors. *Vaccine* (2011) 29:6641–9. doi: 10.1016/j.vaccine.2011.06.105

61. Halliday A, Turner JD, Guimaraes A, Bates PA, Taylor MJ. The TLR2/6 ligand PAM2CSK4 is a Th2 polarizing adjuvant in leishmania major and brugia malayi murine vaccine models. *Parasit Vectors* (2016) 9:96. doi: 10.1186/s13071-016-1381-0

Frontiers in Immunology

Explores novel approaches and diagnoses to treat immune disorders.

The official journal of the International Union of Immunological Societies (IUIS) and the most cited in its field, leading the way for research across basic, translational and clinical immunology.

Discover the latest Research Topics

See more →

Frontiers

Avenue du Tribunal-Fédéral 34
1005 Lausanne, Switzerland
frontiersin.org

Contact us

+41 (0)21 510 17 00
frontiersin.org/about/contact